GA Technologies

GA-A16831
UC-77

HTGR APPLICATIONS PROGRAM

SEMIANNUAL REPORT FOR THE PERIOD OCTOBER 1, 1981, THROUGH MARCH 31, 1982

by
PROJECT STAFF

Prepared under
Contract DE-AT03-76SF70046
for the San Francisco Operations Office
Department of Energy

DATE PREPARED: OCTOBER 1982

DISCLAIMER

Printed in the United States of America
Available from
National Technical Information Service
U.S. Department of Commerce
5285 Port Royal Road
Springfield, Virginia 22161
NTIS Price Code: Printed Copy A23; Microfiche A01

GA Technologies

GA-A16831
UC-77

HTGR APPLICATIONS PROGRAM

GA-A--16831

DE84 002956

SEMIANNUAL REPORT FOR THE PERIOD OCTOBER 1, 1981, THROUGH MARCH 31, 1982

by
PROJECT STAFF

Prepared under
Contract DE-AT03-76SF70046
for the San Francisco Operations Office
Department of Energy

GA PROJECT 6000
DATE PREPARED: OCTOBER 1982

DISCLAIMER

ABSTRACT

This report describes progress in the design of and process applications related to the 2240-MW(t) HTGR-SC/C, the monolithic HTGR-PH, and the 250-MW(t) HTGR-MRS/PH and HTGR-SETS plant concepts. The HTGR core design program is reported, including proposed solutions to the thermal-hydraulic core fluctuation phenomena experienced in the FSV HTGR design. Detailed descriptions are presented on improvements in NSSS components, including the PCRV and thermal barrier, reactor internals, steam generator, main and auxiliary circulators, and helium service system and auxiliaries.

The expected performance of the HTGR-SC/C NSSS is presented, and the progress on priority technical issues related to nuclear heat supply integration is discussed. Plant system dynamics, availability, and maintainability studies are reported along with goals and best estimates for achieving them. Licensing, safety investment, and reliability study results are also presented.

A probability risk assessment study for the HTGR-PH concept is described which indicated that the presence of combustible gases in this plant does not present undue public hazard.

Design concept solutions for the intermediate heat exchanger for the HTGR-PH are presented together with cost estimates for indirect cycle and direct cycle PCRVs.

System performance for the HTGR-MRS/PH plant design is also included together with results of a preliminary reliability analysis of core cooling for the HTGR-MRS/PH and the consequence of a loss of forced coolant accident.

Details of the core and reactor internals arrangement for the HTGR-MRS and details of proposed control rod design and operation and refueling system are given.

HTGR-SETS applications include repowering of a large oil refining complex and a SUPERSETS complex incorporating a multi-unit SETS nuclear heat source. Other applications studies discussed are HTGR-PH (VHTR) and HTGR-SC/C to above-ground retorting (AGR) oil shale processes and the investigation of oil field and process complex water recovery treatment for use with the HTGR. Site specific studies in the Port Arthur, Texas, area are discussed as related to the impact of HGTR plants supplying energy to process facilities. Energy transmission options are described and evaluated.

NOMENCLATURE

A/E	architect/engineer
BOP	balance of plant
BORP	balance of reactor plant
CACS	core auxiliary cooling system
CAHE	core auxiliary heat exchanger
CE	Combustion Engineering
C&I	control and instrumentation
GA	GA Technologies Inc.
GCRA	Gas Cooled Reactor Associates
HEU	highly enriched uranium
HPS	helium purification system
HTGR-MRS/PH	high-temperature gas-cooled reactor - modular reactor system/process heat
HTGR-SC/C	high-temperature gas-cooled reactor - steam cycle/cogeneration
HTGR-PH	high-temperature gas-cooled reactor - process heat
HTGR-SETS	high-temperature gas-cooled reactor - sensible energy transport and storage
IFMU	in-flux core mapping unit
IHX	intermediate heat exchanger
ISI	in-service inspection
LEU	low-enriched uranium
LMLC	loss of main loop cooling
LOSP	loss of offsite power
NHS	nuclear heat source
NRC	Nuclear Regulatory Commission
NSSS	nuclear steam supply system
PCRV	prestressed concrete reactor vessel
PLR	plant playout requirement
RSS	reserve shutdown system

SSAR	standard safety analysis report
UHS	ultimate heat sink
UE&C	United Engineers and Constructors
VCS	vessel cooling system

CONTENTS

FIGURES

TABLES

1. INTRODUCTION AND SUMMARY

This report describes the progress achieved during the first half of FY-82 on the technical program for the GA HTGR-SC/C, HTGR-PH, and HTGR-MRS/PH systems together with market definitions and application studies related to the HTGR-SC/C and HTGR-PH.

Summaries of work performed under each of the principal tasks are presented in this section. More detailed descriptions of design progress are given in Section 2 for the HTGR-SC/C, in Section 3 for the HTGR-PH, and in Section 4 for the HTGR-MRS/PH. HTGR-SETS application studies and various application development studies are described in Section 5.

1.1. HTGR-SC/C

1.1.1. HTGR Plant Technical Description

During this reporting period, the HTGR Plant Technical Description was updated to include enhanced safety features, parameters, and descriptions of an updated reactor core, together with related systems and components. The Expected NSSS Performance plant specification was also updated and now contains the current performance for a wide operating range and various operating modes as well as the impact of component uncertainties.

1.1.2. NHS Integration

Important progress was made in those tasks related to the resolution of technical issues:

1. Core Thermal-Hydraulic Phenomena and Uncertainties (previously identified as the Core Region Temperature Fluctuations issue).

2. Fuel Element Graphite Stress Analysis.
3. Water Ingress.
4. Core Support Graphite Stress and Oxidation.
5. Fission Product Transport.
6. Core Heatup.
7. Thermal Barrier.
8. Acoustically Induced Vibration.
9. Variation of Axial Power with Time.

The list of technical issues was prepared and assigned priorities during the previous reporting period.

1.1.3. Plant Availability

The Plant Availability Assessment documentation was revised to focus on a quantitative availability approach considering scheduled and unscheduled downtime and on the areas requiring availability improvement. In order to achieve the 90% plant availability criterion (a goal established by GCRA that was used as a criterion for GA work), a very substantial level of effort will be required, since the current "best estimate" plant availability is about 77% (23%/yr downtime).

The plant availability was allocated to scheduled and unscheduled downtime. The NSSS unscheduled downtime was suballocated to the plant systems. A draft of the availability specification was written and is being reviewed. Interfacing organizations were given an overview of the availability program to establish a common basis for completing system availability status report input.

1.1.4. Plant Dynamics

Plant dynamics activities included updating the plant design data, analysis of key transients, issuance of the plant transient specification, and a preliminary control/protective system evaluation. Estimated target

parameter tolerances were set for control functional requirements, controller setpoints were established, and major functional level BOP requirements were developed.

1.1.5. BOP Interfaces

A special design data package was assembled relative to plant layout and fuel handling within the PCRV to assist UE&C in development of a nuclear island optimization study. The BOP and PLR documents have been updated to include refueling and storage, PCRV, and control and instrumentation requirements. The results of a variable cogeneration plant configuration study presented in a UE&C topical report have been reviewed. This turbine plant design permits the NSSS to be utilized for either all electric generation or ranging degrees of cogeneration at any time depending on demand. Some difficulty is foreseen in turbine operation if process extraction flow is allowed to vary over a wide range.

1.1.6. Licensing Support

Revision of the Nuclear Safety Plant Specification and Safety/Licensing Assessment of the 2240-MW(t) HTGR-SC/C is in progress, with the principal changes being to conform to the current plant design status. The risk analysis is to be completely revised as new information becomes available. A report comparing plant conditions (used in the Nuclear Safety Plant Specification and the NRC's proposed numerical guidelines) was completed.

Some concern has been expressed over conflict with the present methods for treating accidents and possibly rendering presently used methods obsolete. A review of the documents, particularly the recent NRC policy statement on safety goals, confirmed that present rules remain valid and that numerical guidelines and risk assessments to implement them are supplemented.

Consideration by GCRA and the HTGR Project Office of a plan to prepare a Standard Safety Analysis Report (SSAR) in FY-83 has been abandoned on the basis that the objective and schedule are beyond the state of the HTGR design at the present time.

1.1.7. Safety/Investment Reliability

Partial safety reliability criteria and system description documentation reflecting enhanced safety features of major systems was completed. The partial safety reliability criteria include suggested interfacing to aid communication between reliability and systems engineering in order to meet plant safety goals.

A water ingress assessment study of the unavailability due to steam generator leaks was completed. The unavailability from this cause was estimated to be ~0.9/yr, and the estimated unscheduled downtime was estimated to be 400 hr/yr.

Consequence models for the safety assessment of the 2240-MW(t) HTGR-SC/C were developed. A core heatup base case analysis was also performed, and fault and event trees were developed in connection with LOSP and LMLC events.

The results of a study to evaluate UE&C fault tree models for their UHS design did not lead to any significant improvement in system reliability. The UHS should be designed with both independence and diversity rather than redundancy in order to achieve the core heatup probability goal of $<10^{-4}$/yr.

1.1.8. PCRV Design

The PCRV design effort comprised activities in the areas of PCRV, liner, and thermal barrier and included updating word documents and generating general arrangement drawings for developing cost information on

PCRV, liner, and thermal barrier components in support of the Project Decision Package. Detailed sequence drawings of the PCRV and liner erection were prepared to assist the A/E in the preparation of the PCRV construction schedule and coordination for the BOP. Primary activities in the thermal barrier area were to perform design and analytical studies to minimize the effect of moisture on the thermal barrier, resolve the problem of high noise levels on thermal barrier components, and resolve problems associated with the core cavity bottom head design.

As presently conceived and developed for the HTGR pressure vessel, a completely sealed, impermeable fibrous insulation thermal barrier is impractical. However, a water-resistant thermal barrier capable of excluding practically all impinging water can be achieved with some revisions to the seal components of the present design.

1.1.9. Neutron and Region Flow Control

The basic concepts for the equipment in the neutron and region flow control system have not changed significantly since they were initially developed for other HTGR plants several years ago. However, the documents defining these concepts have become increasingly obsolete as systems in the HTGR have evolved, and the primary effort during this period was to update and reissue these documents.

Some of the main factors causing design changes were the adoption of the in-vessel refueling concept, the improved core design to minimize core fluctuations, and the development of the Toshiba fission chamber for use with the in-core flux mapping units (IFMUs).

A new system description document providing a comprehensive summary of the function, design bases, and description for all of the equipment in the system was completed.

1.1.10. Fuel Handling and Reactor Service Equipment

The basic concept for an alternate refueling system, now called the "in-vessel" refueling system, was developed during FY-79. During the present reporting period, the primary effort was directed toward the generation of documents and other data for the HTGR Decision Package.

The adoption of the in-vessel refueling system with its associate dual storage facilities allowed the rearrangement and optimization of the nuclear island by the A/E. As a result of this rearrangement and changes caused by the in-vessel system, most of the available documents for fuel service operations (i.e., receiving, inspecting, storing, shipping) were rendered obsolete. New layouts and other documents were generated during this period to illustrate new conceptual designs for the fuel service operations which are compatible with the proposed plant arrangement and the in-vessel fuel handling equipment.

In the area of reactor service equipment, design layouts and descriptive documentation were completed.

1.1.11. Reactor Internals

In the area of reactor internals, layout drawings were completed for the core peripheral seal (CPS). The structure is supported off the liner primarily by a corrugated web torque box that accommodates thermal expansion and minimizes heat transfer. The structure is designed to be shop-fabricated in segments, thereby reducing site assembly cost while providing greater manufacturing tolerance control. Early analyses indicated that most of the core bypass leakage will occur at interfaces associated with the seal log, and more work is required to reduce this leakage. The core lateral restraint design has undergone modifications as a result of the recent reactor core redesign. In particular, the former disk spring concepts have been replaced by radial keys that provide a positive location for the permanent side reflector during installation and operation. Layout drawings were

also completed for the upper plenum in-vessel refueling structure. Preliminary calculations showed that structure stresses will be low during reactor operation. However, the structure must be designed to provide a solid support for refueling operational equipment.

1.1.12. Reactor Core Design

Activities during this reporting period included completion of an alternate core configuration study and a recommendation for the selected design for the HTGR, preparation of system description documentation for (1) the core and (2) the reactor internal components (including the permanent side reflector, core support structure, core lateral restraint, peripheral seal, and in-vessel refueling bridge). A structural analysis of the recommended core configuration was also performed with emphasis on the fuel element seals and the permanent side reflector. These scoping studies confirmed the feasibility of the design changes to the core elements. Additional detailed analysis is being performed to substantiate the preliminary conclusions. A seismic evaluation of the revised core was made using a number of computer codes to develop interblock forces from seismic input. The new seismic evaluations show substantial (39%) reduction in lateral design loads from those obtained with the previous methods.

An analysis was made to determine the steady-state temperature distribution in a typical permanent side reflector block (at the core mid-plane) at design operating conditions. Temperature gradient analyses were also performed on the lower core support block for selected transient conditions. An axisymmetric model of the lower core support block was constructed, and graphite temperatures were calculated using a thermal analysis computer code. Similar data have been generated for other design transients and are presently being compared to identify a worst case core support floor operating condition.

Preliminary estimates of the fission product and neutron activation products in the primary circuit of the 2240-MW(t) HTGR-SC/C have been

completed. The circulating and plateout criteria for the HTGR-SC/C have been revised upward ~40%, equivalent to 14,000 Ci of Kr-88 (Level B) based on allowable site boundary doses and containment access requirements. The revised limits (1) are less restrictive than previous criteria, (2) allow decoupling of criteria and expected activities, (3) provide a stronger licensing position, and (4) may result in increased plateout levels if circulating activity is allowed to rise.

Various design physics calculations have been carried out for alternate fuel element block concepts to assess their impacts on core performance and safety characteristics for the 2240-MW(t) HTGR-SC/C plant. Studies include fuel cycle and loading requirements, redesigns of the control rod deployment, region pin power distributions, fuel zoning, and burnup effects.

The principal conclusion of these studies is that the redesign concepts considered show no detrimental effects on the core performance, fuel performance, safety margins, and fuel cycle cost for the HTGR-SC/C operating on the current reference LEU/Th cycle. In addition to improving the flow and stability characteristics of the core as intended, the new block designs offer potential improvements in some aspects of core performance, mainly for reductions of power peaking, maximum fuel temperatures, and fast neutron fluences.

1.1.13. Primary Coolant System

The Primary Coolant Chemistry Plant Specification was issued and contains criteria to limit the level of contaminants in the primary coolant and for the design of components and systems in contact with the primary coolant. The primary coolant system description document, which defines the functional requirements and design basis for the pressurized helium volume and its associated components and instrumentation, was also completed.

The identification and evaluation of possible design solutions to the water ingress problem, in conjunction with component design (including the thermal barrier and core graphite qualification activities), were continued.

1.1.14. Main Circulator Design

The aerodynamic design of the main circulator has been revised to satisfy the latest NSSS thermal performance and to provide greater surge margin at its design point, resulting in a blade height reduction. The circulator layout was also modified to optimize the circulator cavity closure plug and liner design configuration.

A revised shutdown seal design was developed that reduces the stresses in the bellows and isolates vortex excitation in the bellows.

An assessment of torsional vibration of the complete drive train was performed using a computer code developed for this purpose and showed the first critical speed (2700 rpm) to be above the operating speed range.

1.1.15. Steam Generator

An initial workscope established in September 1981 and subsequently revised in February 1982 resulted in CE participation in the steam generator and CAHE design effort. During this reporting period, a contractual working basis with CE and agreement on the workscope and schedule for FY-82 were established, and initial transfer of GA steam generator technology to CE was accomplished.

A general arrangement drawing of the steam generator was completed. In addition, investigations into utilization of additional cavity height, water ingress (leak sources and sizes), tube bundle design effectiveness, and tube combined stress levels were completed.

1.1.16. Helium Service System

Description documents for the helium service system and the PCRV pressure relief system were issued, and process flow diagrams for both the helium service system and the PCRV pressure relief subsystems were prepared.

A brief study was also made to characterize the capabilities of the helium purification system to remove the chemical impurities from the PCRV following water ingress. An alternate design approach was proposed that offers shorter cleanup times and involves partial purification by the helium purification system and PCRV pumpdown through the system followed by PCRV repressurization.

1.1.17. CACS Analysis

Additions and improvements to the CACS system description document were made and incorporate expanded descriptions of the CAHE and of the auxiliary circulator service subsystem. A section on preoperational and in-service testing was also added. The section on CACS design cycles was revised, and an enumeration of interfacing systems and services was added.

The most significant work performed on the CACS is the transient analyses of the system. This work, which will be completed by the end of FY-82, will result in design basis transients that will confirm the adequacy of the system as sized to meet performance criteria.

1.1.18. Auxiliary Circulator Design

Based on preliminary CACS system operating parameters, the basic configuration of the auxiliary circulator was confirmed. A general arrangement drawing showing the auxiliary circulator and auxiliary loop isolation valve installed within the PCRV was issued. Component descriptions were also established.

1.1.19. Core Auxiliary Heat Exchanger

Input from the CAHE flow test has been incorporated into both the sizing analysis and the design. Gas side flow maldistribution has been reduced. General arrangement drawings of the CAHE have been reissued to be consistent with recent design and PCRV modifications. The latest optimized plant conditions have favored the CAHE, resulting in higher gas outlet temperature, reducing the surface area requirements, reducing the number of tubes, and resulting in a slight reduction in unit diameter and height. Studies have also been completed to improve CAHE stability, enthalpy margins, and tube support grid and ISI access and to mitigate the consequences of water leaking from the CAHE into the primary system. The latter study indicated the need for a water drain from the shell side of the CAHE. A half-scale CAHE flow test is substantially complete.

1.1.20. Control and Instrumentation

1.1.20.1. Primary Coolant System Controls/Instrumentation. The main circulator service system and plant control system requirements have been updated and issued as input to the BOPR documents. The plant layout criteria for the CACS control system portion of the BOPR manual were reviewed and updated, and the control instrumentation and electrical sections of the CACS control system description were prepared, including discussion of each operational phase.

1.1.20.2. Safety Control and Instrumentation. In the area of safety control and instrumentation, the safety-related C&I system description document has been updated to incorporate the present state of the design and to reflect a new safety-related organization. This new organization of the safety-related C&I system (previously identified as the plant protection system) is introduced to avoid confusion from the use of "safety system," "safety-related systems," and "systems important to safety" topics being included in one large system. The safety-related C&I system is now subdivided into three functional systems: the plant protection system, the safety-related moisture monitor/detection equipment, and the special

safety-related systems. A summary of the functional description of the safety-related C&I is given in Section 2.23.

Investigation into several critical issues is continuing. Addition of an auxiliary feedwater pump to improve feedwater availability and overall plant safety may impose delay in the plant protection system initiation of the CACS.

1.2. HTGR-PH

1.2.1. System Performance

A study of the monolithic 1170-MW(t) HTGR-PH plant NHS was made to identify primary system parameter trends that lead to economic improvement. The study was based on a nuclear-heated chemical process plant for producing hydrogen by steam reforming of methane and included both 850°C indirect cycle and 950°C direct cycle reactor outlet temperatures. Parameters identified for improvement potential included primary system operating pressure, reactor inlet temperature, and core power density. The results of the study showed limited potential for improved economics. For example, increasing the primary pressure from 5.0 to 6.0 MPa (725 to 870 psia), i.e., a 20% increase, results in only a 1% decrease in cost of product. The same economic trends are expected to apply to both indirect cycle and direct cycle systems, and based on this limited potential, it is concluded that the existing parameters (Ref. 1-1) are close to optimum and do not merit change.

1.2.2. Safety Studies

The results of a probabilistic risk assessment for the indirect cycle HTGR-PH concept indicate that the VCEs initiated by compressor failure in the reformer train pose a small additional risk to the public. The risk is considered similar to that associated with the HTGR-SC plant, and thus the presence of combustible gases in the indirect cycle HTGR-PH does not present

an undue hazard to the public. However, additional work is recommended to extend the preliminary study.

Licensing activities during the reporting period were limited to review of program documents and plans.

1.2.3. IHX

Two problem areas in the IHX design (previously identified in Ref. 1-1) involving (1) the tube bundle support and (2) expansion joint design were studied, and conceptual designs were developed.

A comparison study of the helical and straight tube IHX concepts was continued, and it was concluded that the straight tube design is better suited to the IHX application where minimizing the unit diameter is important and length is secondary. A steam generator sizing exercise was completed in sufficient detail to identify major cost items.

1.2.4. Vessel Design

In the area of HTGR-PH vessel design development studies to provide cost reduction and plant parameter optimization, it was shown that the diameter of the indirect and direct cycle PCRVs and the secondary loop PCVs can be reduced by increasing the present concrete and linear tendon capacities. While further diameter reduction can be achieved by reducing the number of reformer or steam generator cavities, the height of the vessels in all cases cannot be reduced since they are controlled by component height considerations.

1.3. HTGR-MRS/PH

1.3.1. Decay Heat Removal

Studies to define the decay heat system requirements for the HTGR-MRS/PH plant have resulted in a prime configuration consisting of one more

safety class main cooling system and one redundant safety class vessel cooling system. This work also included consideration of the applicable guiding criteria needed to satisfy the reliability goals, consideration of transient design requirements on the plant components, and alternate design strategies.

To further reduce the probability of unrestrained core heatup, a brief study was also made of an alternate diverse method of cooling the reactor vessel by means of a forced flow of air over the outer surface of the vessel. The forced air cooling would be diverse from the water cooling coils. The preliminary study results indicated the concept to be feasible with the current confinement geometry. The current estimated heatup probability for the HTGR-MRS/PH design is 3×10^{-4}/module-year, but the safety consequences of such an event are considered negligible. Addition of a non-safety forced air cooling system is only one possible alternative to reduce this probability to less than 10^{-4} /module-year if this is desired.

Based upon these results it was concluded that natural circulation cooling by an external set of cooling coils is feasible for vessel design limits ~450°C (~850°F) and 6.2 MPa (900 psia); that some design flexibility resulted from tradeoff between vessel design temperature and pressure by changing the helium annulus size; and that natural circulation cooling is relatively insensitive to the circulator flow resistance, so a bypass valve around the circulator is not required. As a result of this study, an upper helium annular gap of 127 mm (5 in.) and a lower gap of 76.2 mm (3 in.) were selected for future analyses.

These transient study results are for an early version of the simulation. Effects which should lower the calculated peak vessel temperature and pressure have subsequently been included in the simulation. These include calculation of parallel induced natural circulation flow through both the steam generator and the annular bypass, a more complete simulation of the surface area of the vessel available for decay heat removal, and inclusion of a smaller, though significant, heat transfer mechanism (other than radiation) from the outside surface of the vessel, namely free convection to the

surrounding air. Other effects which should lower the calculated peak vessel temperature and pressure have been added to subsequent simulations. Updated transients with these effects will be reported in the next semi-annual report.

1.3.2. Consequence of Core Heatup Accident

Depressurized core heatup events have been investigated for the 250-MW(t) modular VHTR with various conditions such as with or without vessel cooling system and prior cooldown conditions. Without prior cooldown, the peak core temperatures reach a value of 1982°C (3600°F) at approximately 30 hr into the depressurized core heatup accident. The peak core temperatures are fairly insensitive to vessel-cavity cooling. The maximum failed fuel fraction in the core is only 1% during the core heatup accident. The shortest time of prior cooldown to avoid any core or component damage is roughly 16 days. However, the core graphite and component temperatures would reach a lower peak with longer prior cooldown.

Failures of the components strongly depend on vessel-cavity cooling. No component damage would occur with vessel-cavity cooling available. If vessel-cavity cooling were absent, the steel vessel would experience much higher temperatures: in excess of 1038°C (1900°F) with depressurization and 649°C (1200°F) without immediate depressurization.

1.3.3. Licensing

A review of available design information on the HTGR-MRS/PH concept revealed a number of potentially significant licensing problems. These include the unproven ability to maintain cooling to components within prescribed limits, introduction of the rod drop accident as prescribed for the HTGR, the unproven ability to incorporate two diverse reactivity control systems, the effects of steam generator or reformer leaks, and the potential for a large primary coolant blowdown area. A Bechtel proposal to use confinement rather than containment was reviewed, and comments were provided to the Project Office.

1.3.4. Core Nuclear Studies

Core nuclear design studies have resulted in a preliminary core design for the 250-MW(t) HTGR-MRS/PH with 950°C (1742°F) helium outlet temperature. The design features an initial fuel cycle based on LEU/Th fuel and 4-yr batch loading and, at some later time, a fuel cycle based on HEU/Th fuel with a batch residence time of 4 to 5 yr. The HEU/Th fuel provides significant fuel cycle cost and core performance advantage. Fuel loadings and radial and axial fuel zoning and power distribution studies have been performed for both fuel cycles. Two-dimensional burnup and control rod worth calculations have also been made for the LEU/Th cycle. Both 5- and 4-yr HEU/Th fuel cycles were evaluated in scoping studies; the latter offers a fallback design option should potential problems be revealed in more detailed studies.

An important consideration in core design is the relationship between the fuel cycle length and the core inlet gas temperature. In general, the longer cycle length limits the steepness of the axial fuel zoning and corresponding power profile, which in turn imposes restrictions on the maximum allowable core temperature rise (core ΔT). A core ΔT of 525°C (945°F) was adopted for the reference HTGR-MRS design. For the HEU/Th cycle, the present studies show that a core ΔT of 575°C (1035°F) could be acceptable.

1.3.5. Reactor Internals

A conceptual design for the reactor internals of the HTGR-MRS/PH has been developed. Major features include:

1. A batch-loaded, upflow, prismatic graphite core using standard, unsealed, 10-row HTGR fuel blocks. The active core contains 85 columns and is eight rows high. The active core is surrounded by 1016 mm (40 in.) of reflector radially and 1219 mm (48 in.) of reflectors top and bottom. Because the core is batch-loaded, no regions or flow control orifices are required. Control rods are inserted from below the core.

2. A core barrel that separates the primary coolant flow internal and external to the core.

3. A steel core support plate that supports the core and is in turn supported from the bottom of the vessel by a steel core support cylinder.

4. A system of radial keys that connect the reactor core to the core barrel and the core support to the pressure vessel, thus transmitting the lateral core seismic loads to the pressure vessel.

5. Top lateral restraint of all core columns accomplished either by inter-element keying of the top row of reflector blocks or by special column constraint devices.

6. Bottom-mounted control rods.

Scoping structural analyses were performed for normal operating loads and for seismic and other off-normal events to verify the adequacy of the design.

1.3.6. Refueling and Control Rod Drives

Scoping studies were made of alternate refueling concepts and reactor control rod drive arrangements. Early concepts were based on an original premise that the reformer removal would coincide with the refueling outage and such removal would provide access to the core. Because of the uncertainty of this premise and the certain need to maintain shielding and a helium blanket above the core during removal of the reformer, a concept was developed that includes a large, permanently installed isolation valve between the reformer and reactor vessels. Fuel is transferred from the reactor vessel to the storage area via a vertical chute and conveyer system.

Reactor control is by means of control and shutdown rods inserted from below the reactor; the drive mechanisms are located below and outside the reactor vessel. The CRD design concept follows that already developed and proven for the Peach Bottom HTGR. A supplementary gravity scram feature for driving the rods upward into the core was also studied. The reserve shutdown system consists of absorber balls contained in hoppers located within the top reflector.

1.3.7. Circulator

A circulator configuration and performance definition study for the 250-MW(t) HTGR-MRS/PH was completed. The preferred concept is a two-stage axial flow compresser operating at ~4500 rpm. The rotor is supported by two water-lubricated bearings, and axial thrust bearings are oil lubricated. The circulator is driven by a fully enclosed 3930-kW (5266-hp) variable speed synchronous motor mounted external to the reactor vessel. A preliminary supporting maintenance requirement study was also performed.

1.4. PROCESS APPLICATIONS DEVELOPMENT STUDIES

1.4.1. HTGR-SETS

GA technical input to the HTGR-SETS applications studies report has been completed, and economic evaluation of the results is presently under way. Drafts of the GA contribution to the HTGR-SETS screening report have been initiated. The HTGR-SETS studies included refinery repowering and long-distance energy transmission and are reported elsewhere in this document. The role of SETS in oil shale recovery was also studied and is reported in Section 5.2. The results of this study (performed under Task 6003030001) which examines the SETS compatibility with a Paraho aboveground retorting will also be included in the HTGR-SETS screening report for completeness.

The refinery repowering study considered the coupling of a twin 1170-MW(t) HTGR-SETS nuclear power source to a base-loaded electrical plant

and to a 32-km (20-mi) long molten salt pipeline connecting the nuclear plant to the refinery. A concept known as SUPERSETS (an extension of the refinery study) is also being studied to examine the economic/scale incentives for a large-capacity SETS facility and includes four 1170-MW(t) HTGR-SETS/NHS units. The large-capacity multiple energy sources, improved availability, and remote siting capability make the SUPERSETS ideal for a concentrated industrial area such as the East Houston, Texas, ship channel. Technical work has been completed sufficient to support ongoing economic evaluation.

A third HTGR-SETS refinery concept (Ref. 1-2) presents the HTGR-SETS role as a remote-sited cogenerator of process steam and electric power for a large oil refinery. The economic projections showed that steam and electricity needs could be better met at separation distances of up to 32 km (20 mi) by a remote-sited HTGR-SC/C plant.

1.4.2. HTGR Applications to Above-Ground Retorting (AGR)

Studies were made of the HTGR-PH/HTR and HTGR-SC/C concepts to supply heat for above-ground retorting shale processes. The applications included (1) high-temperature recycle gas heated by an HTGR-PH/VHTR, (b) a conventional low-temperature recycle gas supplied by an HTGR-SC/C plant, and (3) low-pressure superheated steam supplied by an HTGR-SC/C plant.

Since these studies are ongoing. a final assessment cannot be made at this time. However, the data developed so far and preliminary assessment indicate that the steam retorting process has the highest overall plant thermal efficiency followed by the high-temperature and low-temperature gas retorting processes. The steam retorting process also shows the highest Fischer assay (100%). The recycle gas needs to be heated to 704°C (1300°F) in the high-temperature gas retorting process as compared with 510°C (950°F) in the low-temperature gas retorting process and steam to 482°C (900°F) in the steam retorting process. The requirement of 704°C (1300°F) gas in the high-temperature gas process will impact the selection of suitable materials for equipment construction and equipment cost.

Related studies in the process applications area included (1) water treatment concepts and the environmental impact in the heavy oil fields of California as applied to providing a treated water acceptable for use in an HTGR feedwater system and (2) design and cost estimates for reboilers to process untreated water from oil and tar sand fields and chemical plants to make it suitable for an HTGR steam generator. The major finding from the California oil field water treatment study is the need for water treatment filtration and demineralization equipment at an estimated cost of $15 million. The operating cost for treating the water would be 26¢ to 32¢/m^3 ($1 to 1.20/$10^3$ gal). The study also indicated, for steam generator comparison purposes, that effluents from the HTGR were significantly lower than those from conventional fossil fuel units.

1.4.3. Site Specific Studies

Site specific studies during this period included pipeline energy transport design and cost evaluations of the HTGR-SC and HTGR-SETS to process applications, a boiler and feedwater study, a suitability evaluation for sites near Port Arthur, Texas, and an assessment of the external explosion hazard at the Gulf Oil site within the Port Arthur area.

1.4.3.1. Pipeline Transport Studies. Studies were performed to investigate possible design improvements/cost reductions for the systems used to transport energy from HTGR-SC/C and HTGR-SETS plants to process plants located remotely from the reactor plants. This work was an extension of transport system studies performed by UE&C in FY-81.

Cost versus distance trends based on the improved transport system designs indicated that direct transmission of steam from HTGR-SC plants at moderate temperatures and pressures may be economical for much longer distances than previously considered practical. For applications requiring process steam, it appears that the economics favor direct transmission of steam over energy transmission from HTGR-SETS plants at distances up to 32 km (20 mi). The SETS system shows an advantage over direct steam

transmission for higher pressure and temperature process steam at distances greater than 32 km (20 mi).

1.4.3.2. HTGR SC/C Site Suitability - Demographic Evaluation. Four potential sites near Port Arthur, Texas, have been surveyed for compliance with the population density criteria of Regulatory Guide 4.7 and the March 1981 NRC staff recommendations. Acceptable locations were found at three sites: the Gulf Oil site and alternate sites at Big Hill Dome and near the Gulf States Utilities plant near Bridge City, Texas. The Gulf Oil site has been chosen for further safety studies.

1.4.3.3. External Explosion Hazards. A preliminary study was performed to characterize the hazards from external explosions at the Gulf Oil site near Port Arthur, Texas. The study considered several specific conditions of external explosion for the various source types present near the plant site. The source types considered were the tank farm, liners, trucks, and pipelines carrying combustible products. The conclusion from the preliminary study was that the external explosion hazard is more prominent for the pipelines carrying the heavier-than-air combustible products, such as propane. Additional probablistic risk assessment work is recommended to further quantify the hazards from pipelines.

1.4.3.4. Port Arthur Site Suitability. In the site evaluation, the task force concluded that both the Gulf and Texaco sites were sufficiently large to accommodate a nuclear plant. Flood protection and foundation construction are major engineering challenges. A potential alternate site at Sabine Power Station would meet the demographic criteria; however, the economic penalty resulting from the long pipeline might be severe.

REFERENCES

1-1. "HTGR Applications Program Semiannual Report for the Period Ending September 20, 1981," DOE Report GA-A16538, GA Technologies, to be issued.

1-2. Hopwood, G. R., et al., "HTGR Applications Comparative Assessment Study," DOE Report GA-A16525, GA Technologies, April 1982.

2. HTGR-SC/C

2.1. NUCLEAR STEAM SUPPLY SYSTEM (NSSS) PERFORMANCE (6032010100)

2.1.1. Scope

The purpose of this task is to describe the overall NSSS design and establish the steady-state performance with a goal of minimum product cost and acceptable technical risk. The task includes establishing the basic design data, requirements, and criteria for the 2240-MW(t) HTGR-SC/C NSSS. It also encompasses definition and documentation of the steady-state performance requirements (performance envelopes) of the NSSS, including the expected (nominal) performance and off-design performance conditions that the NSSS design and its components must accommodate.

2.1.2. Discussion

Throughout the HTGR-SC/C plant design program, three major steady-state NSSS performance documents are being maintained in an updated status:

1. The "Plant Technical Description of the 2240-MW(t) HTGR-SC/C Plant" (TED), which provides the NSSS design requirements, a description of the overall NSSS design basis, and major physical and performance features of the NSSS design.

2. The "Expected NSSS Performance" plant specification, which provides the steady-state performance of the NSSS at nominal reactor power level and at a number of reduced reactor power levels with and without several main loops out of service and the expected NSSS performance conditions during plant refueling. The performance presented for nominal reactor power is used in sizing all primary loop components and equipment.

3. The "NSSS Thermal Performance Requirements" plant specification, which specifies the complete operating performance envelopes, including both the adverse and expected operating conditions, for all NSSS systems, subsystems, and components.

During this reporting period, the TED was updated. It now incorporates enhanced safety features and the customer requirements given in GCRA's Plant Functional Specification (Ref. 2-1) and includes parameters and descriptions of an updated reactor core and affected systems and components.

The "Expected NSSS Performance" plant specification was also updated and contains the current expected performance data at 100%, 75%, 50%, and 25% feedwater flow with all loops operating, at 75% feedwater flow with three out of four loops operating, and at 50% feedwater flow with two out of four loops operating. Data on the primary coolant operating pressure and the core helium inlet temperature during refueling are included. The expected performance at full-load conditions, which are used in the sizing and optimizing of all the primary loop components and equipment, are presented in Table 2-1 and Fig. 2-1.

A third issue of the "NSSS Thermal Performance Requirements" plant specification, which includes the impact of component performance uncertainties and the steam generator inlet temperatures and the reactor power measurement/instrumentation error, was also prepared and issued.

The performance envelope at 100% (indicated) nominal power (see Fig. 2-2) specifies the range of conditions over which all NSS structural, power conversion, control, and safety systems are required to operate. The overall performance envelope consists of two sub-envelopes: the main helium circulator envelope and the steam generator envelope. The main helium circulator envelope is bounded by maximum circulator power between points 1 and 7, by $\pm 2\sigma$ deviation in primary system flow resistance between points 7 and 5 and points 1 and 6, and by the minimum flow required by the steam generator under extreme conditions between points 6 and 5. The steam generator

TABLE 2-1
MAJOR PLANT/SYSTEM PERFORMANCE AND DESIGN PARAMETERS
FOR THE HTGR-SC/C PLANT

NSSS Heat Balance	
Heat generated by core, MW(t)	2240
Heat added by main circulators, MW(t)	41.31
Heat loss to CACS, MW(t)	1.43
Heat loss to PCRV liner cooling system	
From core cavity, MW(t)	2.75
From steam generator cavities, MW(t)	3.38
From CAHE cavities, MW(t)	0.58
Heat loss (miscellaneous), MW(t)	1.88
NSSS thermal power, MW(T)	2271
NSSS efficiency, %	99.56
Primary Coolant System Performance Parameters	
Number of primary coolant loops	4
Reactor inlet	
Temperature, °C (°F)	319 (607)
Pressure, MPa (psia)	7.233 (1049)
Helium flow rate (total), kg/s (lb/hr)	1165 (9,245,000)
Reactor outlet temperature, °C (°F)	688.9 (1272)
Reactor presure drop (plenum to plenum), kPa (psi)	93.75 (13.59)
Reactor power-to-flow ratio	
Expected kJ/kg (W-hr/lb)	1921 (242)
Maximum kJ/kg (W-hr/lb)	2222 (280)
Steam generator inlet	
Temperature, °C (°F)	685.6 (1266)
Pressure, MPa (psia)	7.129 (1034)
Helium flow rate (total), kg/s (lb/hr)	1173 (9,306,000)
Steam generator outlet temperature, °C (°F)	313 (595)
Steam generator pressure drop, kPa (psi)	52.1 (7.56)
Main circulator inlet	
Temperature, °C (°F)	313 (595)
Pressure, MPa (psia)	7.081 (1027)
Helium flow rate (total), kg/s (lb/hr)	1176 (9,337,000)
Main circulator outlet	
Temperature, °C (°F)	319 (607)
Pressure, MPa (psia)	7.24 (1050)
Main circulator pressure rise, kPa (psi)	160 (23.20)
Main circulator	
Shaft power/unit, MW	10.33
Input motor power/unit, MW	12.04
Helium inventory	
Total (within PCRV), kg (lb)	14,890 (32,820)
Circulating, kg (lb)	11,400 (25,100)
Bypass, buffer, and leakage flows	
Total circulator bypass, kg/s (lb/hr)	3.9 (31,000)
Total steam generator buffer, kg/s (lb/hr)	5.86 (46,500)
Total leakage through standby CACS, kg/s (lb/hr)	1.83 (14,600)

TABLE 2-1 (Continued)

Secondary Coolant System Performance Parameters	
Feedwater	
Temperature at steam generator inlet, °C (°F)	221 (430)
Pressure at steam generator inlet, MPa (psia)	21.19 (3074)
Flow rate (total), kg/s (lb/hr)	930 (7,380,000)
Steam	
Temperature at steam generator outlet, °C (°F)	540.6 (1005)
Pressure at steam generator outlet, MPa (psia)	17.34 (2515)
NSSS Component Design Parameters	
Core	
Core power density, W/cm^2	5.78
Equilibrium segment exposure, yr	4.0
Fuel cycle	Low enrichment thorium (LEU/Th) fuel (20% enriched)
Steam generators	
Type of steam generator bundle	Helical EES[a]/ straight tube superheater
Total installed surface area/loop, m^2 (ft^2)	4,314.8 (46,446)
Type of exhaust	Bottom
Tube plugging method	Manual
Main circulators	
Type	Centrifugal flow
Drive	Electric motor
Orientation	Vertical shaft
Motor power margin, %	9.7
Adiabatic efficiency (overall), %	81.0
Mechanical efficiency, %	97.5
Motor/controller combined efficiency, %	88.0
Auxiliary cooling system	
Total number of loops	3
Type of heat exchanger bundle (CAHE)	Straight-tube bayonet
CAHE heat transfer area, m^2 (ft^2)	234.3 (2522)
Penetration location in PCRV	Bottom
Auxiliary circulator	
Type	Axial flow
Drive	Variable speed induction electric motor
Orientation	Vertical shaft
Motor (design) power, MW(e) (hp)	<0.67 (900)

[a]Evaporator-economizer-superheater.

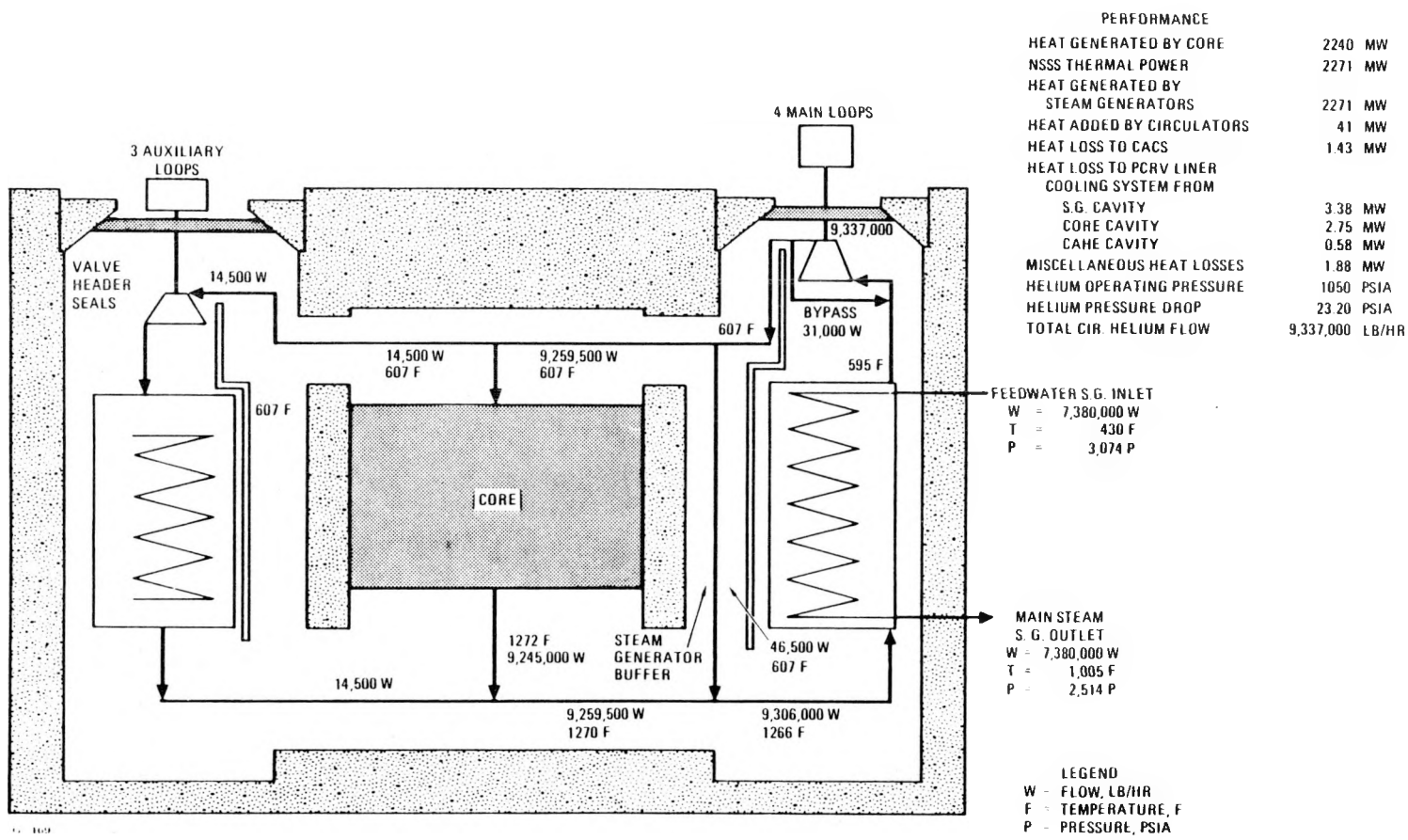

Fig. 2-1. 2240-MW(t) HTGR-SC/C plant heat and mass balance diagram

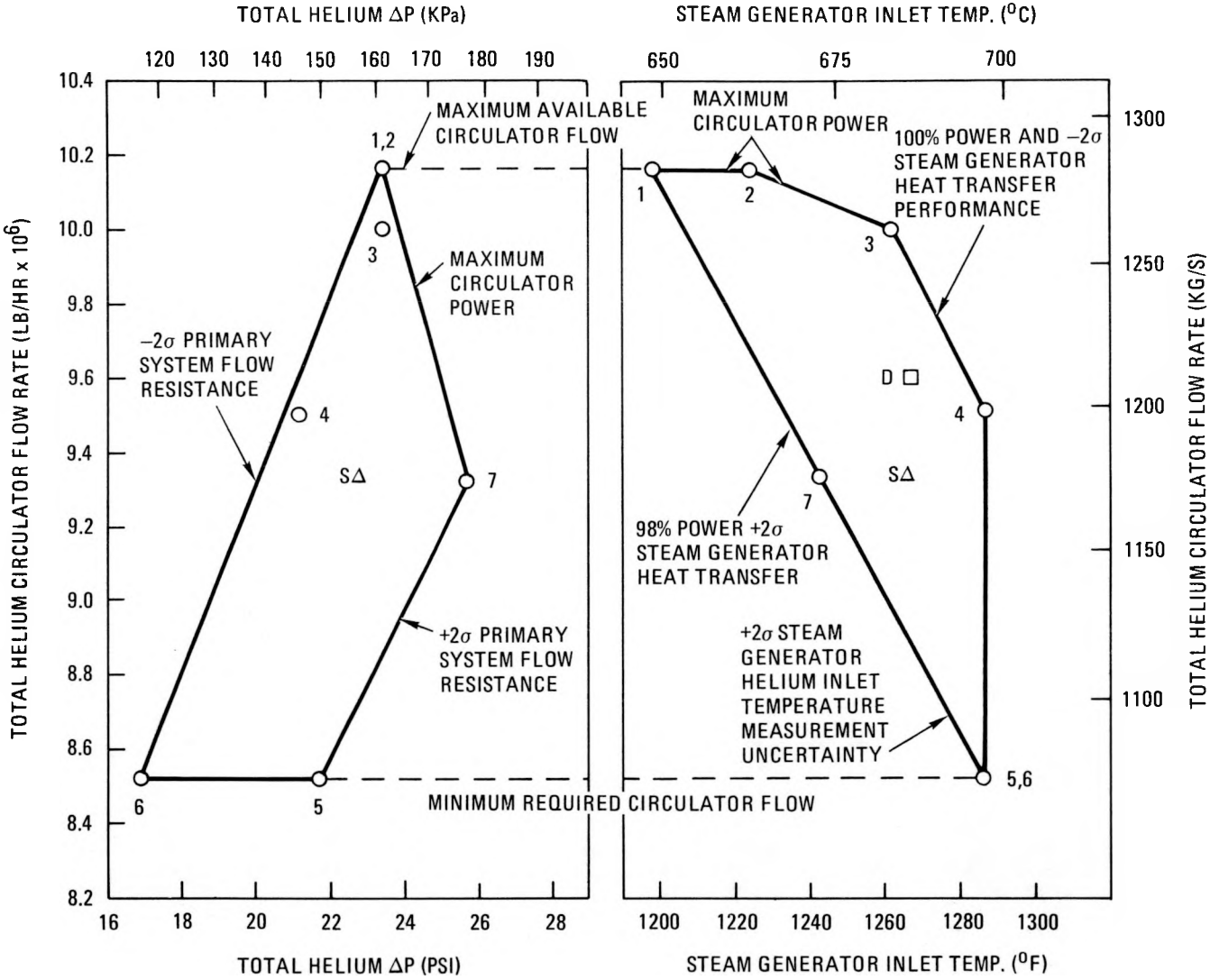

Fig. 2-2. Performance envelope for 2240-MW(t) HTGR-SC/C plant at 100% indicated reactor power

envelope is bounded by maximum circulator power between points 1 and 3, by $\pm 2\sigma$ deviation in steam generator heat transfer coefficients including measurement errors (temperature and power) between points 3 and 4 and 1 and 6, and by a temperature 11°C (20°F) above the expected operating value (accounts for the measurement errors) between points 4 and 6. Table 2-1 gives the system parameter values for the reactor core, main helium circulator, and steam generator at the performance envelope points of Fig. 2-2.

Point "S" and point "D" of Fig. 2-2 are provided for reference. Point "S" is the 100% NSSS expected performance at which the NSSS is sized and optimized. Point "D" is the 102% NSSS expected performance, which is the reference condition for use in "at power" safety-related analyses. In performing component safety analyses, the most adverse condition anywhere within these envelopes must be evaluated.

The reactor core operating conditions pertaining to the Fig. 2-2 performance envelope are given in Table 2-1. A specific performance envelope is not given for the core since no core-performance-related uncertainties have been identified that have not been accounted for by appropriate design margin. Therefore, the core is required to operate satisfactorily for the life of the plant at any point within the Fig. 2-2 envelope.

2.2. NHS INTEGRATION (6032010200)

2.2.1. Scope

The objective of this task is to assure that the design of the NSSS components properly interface from mechanical, thermal-hydraulic, electrical, nuclear, etc., standpoints and are consistent with the requirements of the Plant Technical Description. The workscope includes the review of NSSS technical documents to verify their technical content and applicability and the coordination of efforts to resolve outstanding technical issues.

2.2.2. Discussion

In the previous reporting period, a list of technical issues was prepared, with priorities being assigned to the various issues. During this reporting period, progress toward resolving the major technical issues was made as described below.

2.2.2.1. Core Region Temperature Fluctuations. The name of this technical issue was changed to Core Thermal-Hydraulic Phenomena and Uncertainties to more accurately characterize the problem. Extensive design changes to the core to alleviate this problem were recommended and are being implemented. Analysis of the effect of the changes indicates a strong potential for eliminating the major core thermal-hydraulic uncertainties.

2.2.2.2. Fuel Element Graphite Stress Analysis Uncertainty. Improvements have been made in the ability to calculate in-core seismic loadings. These improvements have lowered the predicted loads and the uncertainty in the loads. This results in lower predicted stresses for the fuel elements for the seismic event.

2.2.2.3. Water Ingress. A primary coolant chemistry plant specification has been issued that establishes acceptable moisture levels compatible with plant availability goals. Calculational methods are being developed to evaluate the moisture ingress and removal rates under transient conditions. A bearing and seal test of the modified circulator design is being assembled to demonstrate improved leakage characteristics. The thermal barrier design is being reevaluated with regard to preventing leakage into the fibrous insulation.

2.2.2.4. Core Support Graphite Stress and Oxidation. The effect of oxidation on the core supports has been found by analysis and by measurements to be less than anticipated. The seismic loading on the core support using the new plant structural response model has also been lowered.

2.2.2.5. Fission Product Transport Prediction. Updated radionuclide design criteria have been adopted which result in lower predictions for circulating activities. Tests in the TRIGA reactor on intentionally punctured particles are continuing. These tests measure gas release as a function of temperature and hydrolysis. Tests on irradiated reference fuel confirmed prior results for gas and metallic release during an accident and showed that propagating failure caused by kernel-coating interaction is not a significant performance risk.

2.2.2.6. Core Heating. Several design modifications are being studied to keep core heatup during postulated events within acceptable temperature limits. These modifications include prevention and mitigation features. The prevention feature was accepted, but mitigation features are still under consideration.

2.2.2.7. Thermal Barrier Class C Design. A design evaluation of candidate ceramic materials was performed, and the most promising materials were identified. The test program to demonstrate fabrication effects is continuing.

2.2.2.8. Acoustically Induced Vibrations. A scale model test of the main circulator for aerodynamic performance and acoustic characteristics, followed by full-scale, full-power tests, is being planned. The effect of acoustic vibration on samples of Saffil and Kaowool fibrous insulation has been tested. It has become clear that acoustic vibration governs the sizing of thermal barrier coverplates.

2.2.2.9. Variation of Axial Power Distribution with Time. Stable forms of axial power distributions are obtainable using a 4-4 axial fuel zoning.

2.3. PLANT AVAILABILITY/MAINTAINABILITY (6032010400)

2.3.1. Scope

The purpose of this task is to develop an availability/maintainability program that will meet the plant availability criteria. Current work is

directed toward an availability assessment, unavailability allocations, the initial specification, and a plant availability status report.

2.3.2. Discussion

The Plant Availability Assessment document was revised with particular emphasis on the quantitative unavailability of plant systems and on the areas requiring improvement to achieve the plant criterion of 90% availability. This goal was subdivided by GCRA into goals for scheduled and unscheduled downtime per Table 2-2. The goal for scheduled downtime is 23 days per year, or 63% of the downtime. The goal for unscheduled downtime (due to unplanned events such as equipment failure, operator error, or external events) is 13.5 days per year, or 37% of the downtime. Assuming that a typical equipment failure might require a week to repair, only two such failures would be tolerable per year. Therefore, it is important that equipment reliability, access, and ease of maintenance be given considerable attention during the plant design process. In addition, a continuing availability program must follow the design phase to assure that plant availability is not compromised during manufacture, shipping, installation, or operation.

The availability assessment examined current nuclear plant performance, for both water- and gas-cooled reactors, and determined the HTGR-SC/C availability using this data base. Current pressurized water reactor (PWR) plants have achieved an availability of approximately 74%. The preliminary results of the HTGR-SC/C plant quantitative availability assessment are summarized in Table 2-3. The resulting assumptions used for a "best estimate" plant value are given in the footnotes of Table 2-3. This value is expected to be conservative and allows for unknowns at this stage of design.

An optimistic estimate of plant availability is 88.5% (Table 2-4). The major assumptions used in determining this value are given in the footnotes of Table 2-4. If assumptions (b) and (c) in Table 2-4 are not applied, the overall plant availability decreases to 84%. The major differences in the optimistic results (Table 2-4) and the availability goal (Table 2-2) are

TABLE 2-2
HTGR-SC/C PLANT DOWNTIME GOALS FOR 90% AVAILABILITY (PER GCRA)

	Downtime	
	Days/Year	%/Year
Scheduled (Planned Outages)		
Refueling	15	4.1
Other (not including turbine-generator maintenance)	8	2.2
Subtotal	23	6.3
Unscheduled (Forced Outages)	13.5	3.7
Total	36.5	10.0

TABLE 2-3
HTGR-SC/C PLANT DOWNTIME BEST ESTIMATE

	Downtime		
	Hours/Year	Days/Year	%/Year
Scheduled (Planned Outages)[a]	466	19.4	5.3
Unscheduled (Forced Outages)			
NSSS[b]	555	23.1	6.3
BOP[c]	500	20.9	5.8
Allowance[d]	528	22.0	6.0
Total	2049	85.4	23.4

[a] With allowance for turbine-generator maintenance.
[b] Assumes 4 out of 4 primary loops are operating.
[c] An allowance based on 90% of NSSS unscheduled downtime.
[d] An allowance based on 50% of all unscheduled downtime.

TABLE 2-4
HTGR-SC/C PLANT DOWNTIME OPTIMISTIC ESTIMATE[a]

	Downtime		
	Hours/Year	Days/Year	%/Year
Scheduled (Planned Outages)[b]	294	12.2	3.3
Unscheduled (Forced Outages)			
NSSS[c]	376	15.7	4.3
BOP[d]	338	14.1	3.9
Total	1008	42.0	11.5

[a] With no allowance for items that have not been considered (e.g., administrative downtime for greater training).

[b] With no allowance for turbine-generator maintenance.

[c] Assuming 3 out of 4 primary loops are operating.

[d] An allowance based on 90% of NSSS unscheduled downtime.

very significant. The availability goal has 23 days/yr (7.3%/yr) for scheduled downtime versus a "best estimate" value of 23.1 days and an optimistic value of 12.2 days (~77% and 88% availability respectively). Based on light water reactor (LWR) experience, the average total refueling outage (refueling plus other activities) has been taking 13.1% of the year, or 47.8 days/yr. From these results, it can be seen that the scheduled downtime is less than half of what has been achieved by operating LWRs. The goal of 13.5 days/yr (3.6% of the year) for unscheduled downtime compares with a best estimate value of 66 days/yr (18% of the year) and an optimistic value of 29.8 days/yr (8.2% of the year). The LWR experience shows unscheduled downtime (capacity factor) of 10.2%/yr for the NSSS and 6.2%/yr for the BOP. Since plant capacity factors are about 10% lower than plant availability, estimated plant unscheduled downtime would be 9.2% for the NSSS and 5.6% for the BOP, or a total of 14.8% of the year. Therefore, the availability goal is four times better than that achieved by mature LWR nuclear plants. From these brief comparisons, it can be seen that achieving 90% plant availability will require a very high level of effort.

As part of the support for availability assessment, a file is being developed to include all the system availability assessments which have been made in the past few years. Most NSSS's have not been assessed in detail recently. Only a few BOP systems have been assessed, using a simplified approach of counting major components and adding the component failure rates. This file will be kept up to date to reflect the latest assessment information. For this file the FSV historical availability data base and its associated programs were retrieved and programming modifications were made (to enable changes to be made more easily). The data base was reviewed and re-classification of some events was initiated.

The availability procedure (developed during the last fiscal year) was released for use as HTGR Engineering Division Instruction HED-2, "HTGR Engineering Division Procedure for Flow of Information for Quantitative Availability Assurance." An availability specification is being prepared for the guidance of system and component designers. This specification will include

(1) the purpose and scope, (2) availability definitions and concepts, and (3) the design criteria. The primary purpose of this specification is to present availability design criteria for the HTGR-SC/C plant. These design criteria are presented as unavailability (in hours/year) for unscheduled outages and all scheduled outages for each NSSS.

The plant availability was allocated to scheduled and unscheduled downtime. The unscheduled downtime was further subdivided between the NSSS and BOP. Nuclear industry experience has been that the total unavailability is about 54% due to scheduled downtime and 46% due to unscheduled downtime. This compares with the GCRA goal (Table 2-2) of 63% scheduled downtime and 37% unscheduled downtime. A recommended revision to the downtime allocation for the HTGR-SC/C plant is as follows:

	Days/Year	% of Total
Scheduled	18.25	50
Unscheduled		
NSSS	9.125	25
BOP	9.125	25
Total	36.5	100

These recommended values for downtime reflect recent nuclear plant experience and the goals established for an LWR with high availability as a goal (Sundesert) and for a recent 900-MW(e) HTGR.

Interfacing organizations will use the availability specification and simple availability methods to develop a revised estimate of system availability and to prepare the System Availability Status reports (including system flexibilities, trade-offs, etc.). This will allow the Plant Availability Status report to be completed by the end of FY-82.

2.4. PLANT DYNAMICS (6032010500)

2.4.1. Scope

The scope of this task is to provide plant transient analyses for component design requirements, develop control/protective system functional requirements, develop plant protective system (PPS) functional requirements, and prepare accident analyses for design basis and safety evaluation.

Specific objectives for the first half of FY-82 were:

1. Update plant design data in MLTAP and perform analyses of key transients. Issue plant transient specification.

2. Evaluate preliminary control/protective system functions and analyze plant operations.

2.4.2. Discussion

A majority of the steam flow is to be taken off to the process between the high-pressure and low-pressure turbines, and the need to hold near-constant process conditions is a process requirement. To adequately assess the plant response, significant detailed modeling in the BOP was necessary.

The reference cogeneration plant configuration was modeled, and provisions were developed to meet the functional requirements of the reference plant design. The dynamic model has provided a basis for defining plant control system and BOP functional requirements. The response and requirements of many of the trip events are unique to the cogeneration application.

A first issue of the Plant Transient Specification was produced based on:

1. A functional system configuration developed to meet all required operating conditions.

2. A plant control system functional design developed to satisfy all specified nominal and worst upset case conditions.

Several major transients characteristic of the HTGR-SC/C plant differing from previous HTGR-SC designs were analyzed.

Controls/BOP functional requirements originally informally documented were included for completeness in the initial issue of the transient specifications. Key elements of these requirements and the transient results are presented below.

2.4.2.1. Plant Operational Requirements. Figure 2-3 is a simplified diagram of the steam system configuration developed to satisfy the functional requirements summarized in Table 2-5. The major additions to the configuration defined by the heat balance diagram for the reference HTGR-SC/C design are the bypasses, desuperheaters, flash tanks, and certain piping connections needed to accommodate some of the trip events and startup/shutdown procedures.

The bypass and desuperheater around the HP turbine are needed for limiting main steam pressure and maintaining process/IP turbine conditions following an HP turbine trip and during startup/shutdown when below the conditions necessary for HP turbine operation. A water separation is necessary since large desuperheating flows exist under some conditions and some of the desuperheated steam is supplied to the IP turbine, which should be in close proximity. A flash tank was chosen for the water separation since it will enhance startup/shutdown operation. The bypass for the IP/LP turbine trip (and startup/shutdown) is split to provide the steam-driven boiler feedpump (BFP) steam and feedwater heating. A flash tank is included for water

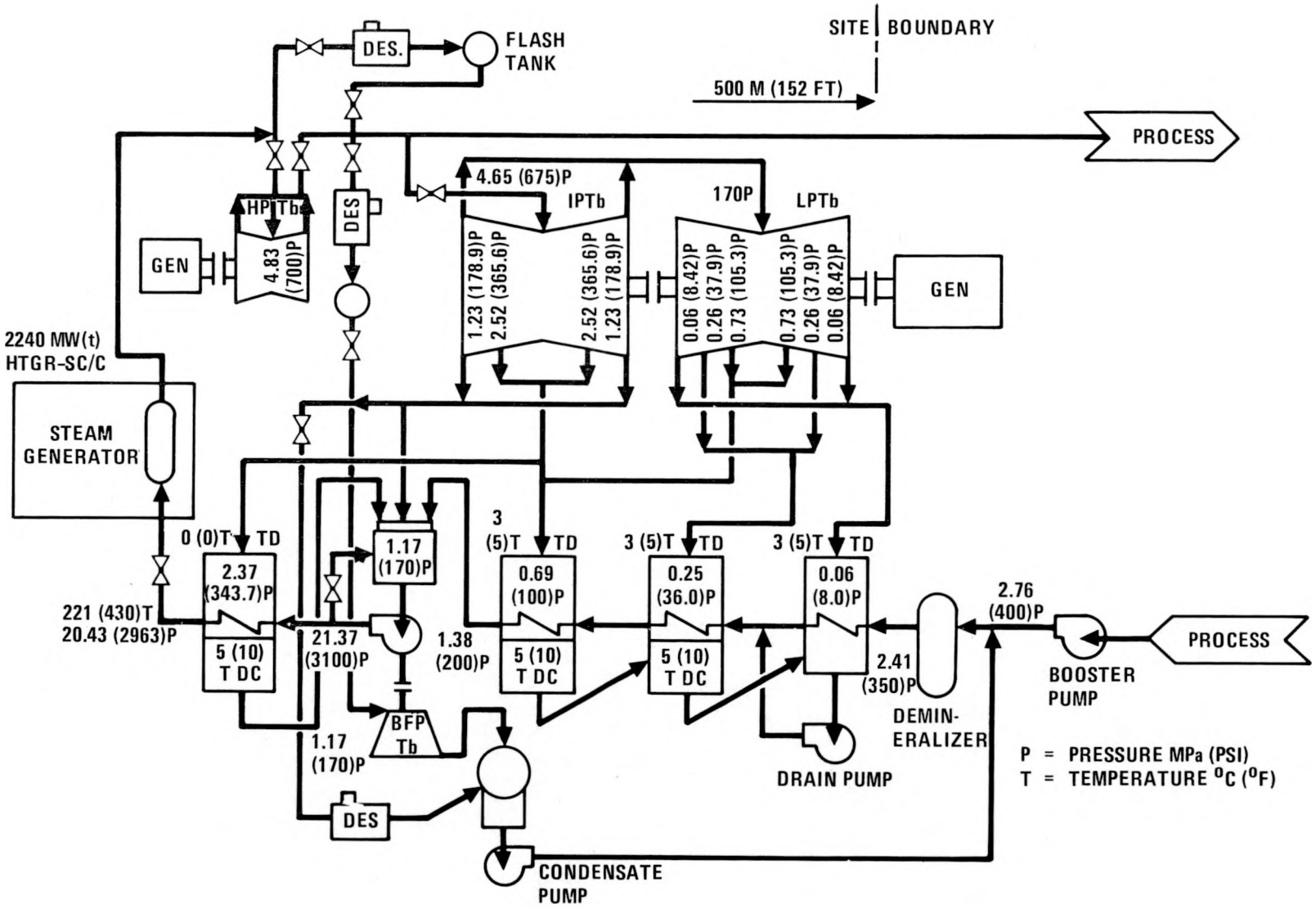

Fig. 2-3. 2240-MW(t) HTGR-SC/C multipurpose application

TABLE 2-5
HTGR-SC/C PLANT OPERATION REQUIREMENTS FOR TRIPS[a]

1. HIGH-PRESSURE (HP) TURBINE TRIP

   - Process steam conditions shall be maintained within +22°, -8°C (+40°, -15°F) and ±172 kPa (±25 psia).[b]
   - The intermediate pressure/low pressure (IP/LP) turbine shall continue to provide electrical generation.

2. IP/LP TURBINE TRIP

   - Process steam conditions shall be maintained within +22°, -8°C (+40°, -15°F) and ±172 kPa (±25 psia).
   - The HP turbine shall continue to provide electrical generation.

3. HP AND IP/LP TURBINE TRIP

   - Process steam conditions shall be maintained within +39°, -8°C (+70°, -15°F) and ±344 kPa (±50 psia).[b]

4. PROCESS TRIP

   - No specific requirement except continued safe operation of the NSSS.

5. REACTOR TRIP

   - Shall provide for safe shutdown and aftercooling.
   - Shall provide the ability to accept main steam from an alternative source and provide essentially normal process operation using the externally supplied steam [up to a maximum of (later)% of nominal process steam flow].

---

[a] Though not required, it is desirable that electrical generation be maintained on loss of process. This is feasible with the provisions made to meet the other requirements.

[b] Tolerances presented are target values used in preliminary analysis in lieu of top level requirements.

separation during startup operation and to accommodate the high desuperheating (attemperation) flows that occur under certain upset conditions. The LP bypass and desuperheater system limits the IP/LP junction pressure and discharges, through a desuperheater, to the condenser.

In addition to the turbine bypasses and desuperheating, throttling pressure control of the deaerator/BFP-turbine header and a bypass around the first feedwater heater are shown in Fig. 2-3. The pressure control for the deaerator/BFP-turbine is needed for all operations of the HTGR-SC/C because of the imbalances in turbine and feedwater conditions at reduced loads. The bypass/desuperheater around the first feedwater heater is also provided to accommodate the part-load turbine/feedwater imbalance and prevent overheating in the feedwater system. The use of the heater bypass reduces IP/LP turbine backpressure and maximizes the electrical output of the IP/LP turbine at part-load conditions.

Another provision is shown by the process line isolation valve and alternate source isolation valve in the upper right-hand corner of Fig. 2-3. This configuration provides the ability to supply the process from an alternate source (per the functional requirement) while maintaining the integrity of main loop cooling for afterheat removal. The combination of the 5-min full-flow storage in the deaerator, the fairly large anticipated on-site treated water storage, and the large reservoir of untreated water at the process will significantly enhance main loop aftercooling capability.

The multiple-level bypass system with flash tanks will maximize steam utilization during startup/shutdown operations and allow maximum process supply during startup while bringing up the IP/LP turbine-generator and subsequently the HP turbine-generator. In addition, the bypass system and the deaerator/BFP turbine header (deaerator header) pressure control can mitigate feedwater thermal transients during certain transient events. For example, a trip of the IP/LP turbine would remove feedwater heating (as a turbine trip does in the HTGR-SC). However, excess steam can be supplied via the deaerator header to the feedwater to limit the decrease in steam generator inlet feedwater temperature.

Initial analyses were performed on the basis of not allowing venting to atmosphere to establish the data needed for the tradeoff of added bypass and heat rejection versus transient atmospheric venting. One case assessed indicates the significant reduction in the severity of bypass system requirements and condenser capacity that can be achieved by allowing some transient venting.

The HTGR-SC/C can be controlled to meet the functional requirements, and in general the transient impact on the NSSS can be maintained at less than or equal to the conditions seen by the HTGR-SC plant.

2.4.2.2. Overall Plant Control System Used in Analysis. To enable operational and transient evaluation, control functions were developed and modeled. A brief discussion of these functions is presented below.

Figure 2-4 is an overall plant control system diagram in block form. The diagram is divided into reactor system controls, feedwater system controls, turbine system controls, and the process feedback. Block 1 of the reactor controls is the control of individual steam generator module outlet steam temperature to match the average steam outlet temperature of all modules. This is accomplished by trim of the circulator speed away from the reference speed, set by module feedwater flow.

Block 2 of the reactor controls is the control of main steam temperature by adjusting the power demand setpoint from the reference set by plant feedwater flow. The power, in turn, is controlled to match demand via control rod position adjustment.

Block 3 is the IP turbine throttle temperature (process tap-off junction temperature) control. This control adjusts the setpoint for the main stem temperature control to compensate for changes in HP turbine temperature drop with varying steam flow.

Block 4 of the reactor controls is the runback logic. In certain events this logic will initiate runback at predetermined rates of reactor

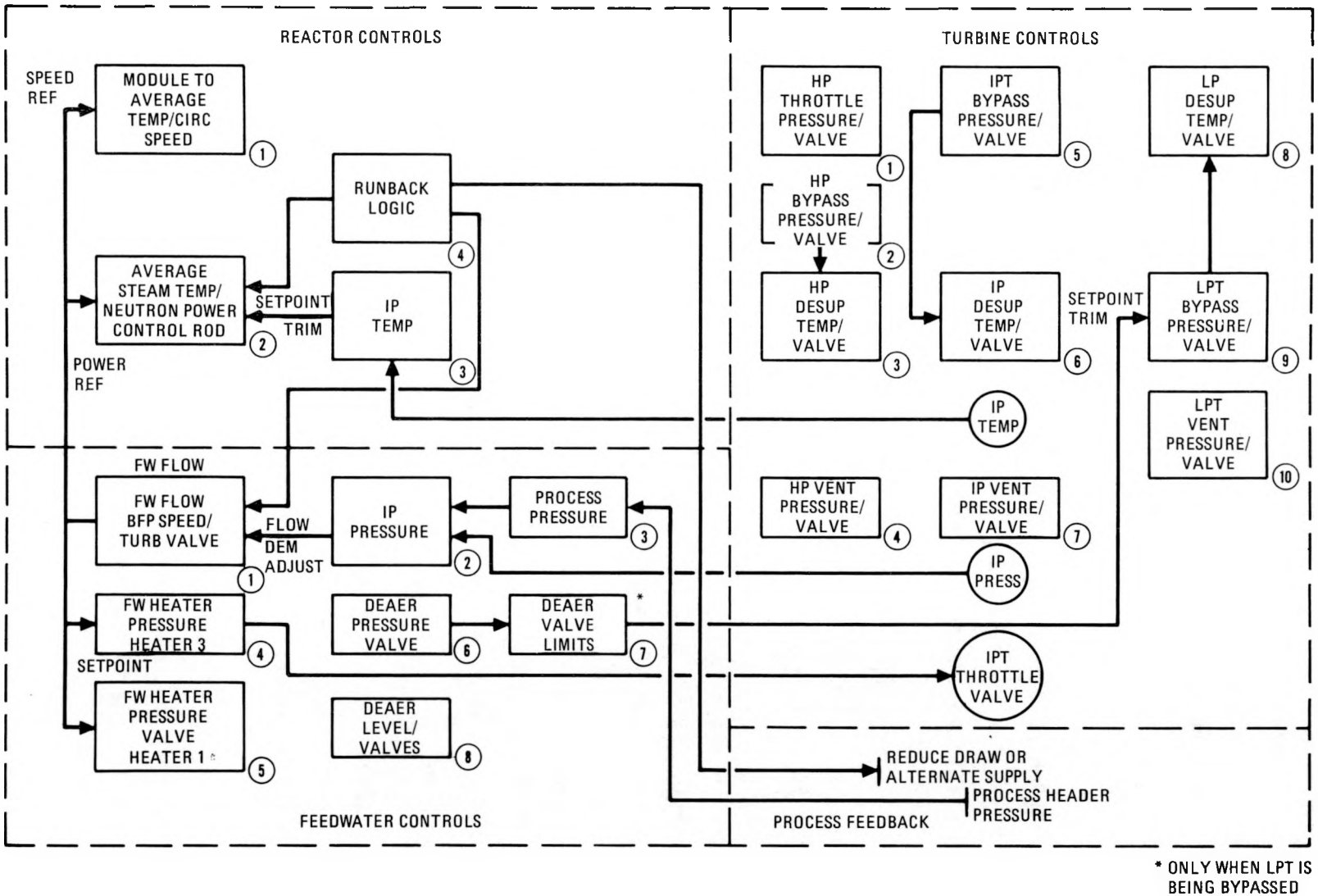

Fig. 2-4. HTGR-SC/C overall plant controls

power and/or feedwater flow. The logic will also supply a signal to the process and/or alternate steam supply to either reduce process steam draw or supply makeup steam from the alternate source. The runbacks are initiated by trips and/or inhibits initiated by either the control system or the PPS. The runback signal overrides the control signals upstream of its point of insertion so that the runback setpoint can be achieved.

Block 1 of the feedwater controls is the feedwater flow control. The feedwater setpoint, which is a sum of a reference and adjustment from block 2 that acts to control IP turbine inlet pressure, is controlled by adjusting feedpump speed demand. The feedpump speed, in turn, is controlled by adjusting the BFP turbine admission valve.

Block 2 of the feedwater controls holds the IP turbine throttle pressure to a setpoint which is the sum of a reference plus a trim from the much longer term control of pressure at the process header (Block 3). The controller adjusts feedwater flow demand to effect a steam flow which will supply the desired pressure.

Block 4 of the feedwater controls is used to control the heater 3 pressure if it exceeds a programmed setpoint. The control output adjusts the IP turbine throttle valve in order to adjust IP turbine steam flow and thereby heater system steam flow.

Block 5 of the feedwater controls is used to limit total feedwater system heating which becomes excessive at part load. The control initiates a bypass from the steam inlet to heater 1 to the condenser if the pressure exceeds the programmed setpoint.

Block 6 of the feedwater controls is used to control the deaerator pressure by adjusting a throttle valve in the line beween the IP turbine extraction and the deaerator/BFP-turbine header.

Block 7 of the feedwater controls ensures that the throttle valve of Block 6 is not driven out of its control range when the LP turbine is in

bypass (control is otherwise inactive). This action is accomplished by trim of the LP bypass pressure setpoint, which changes the pressure available to the throttle valve.

Block 1 of the turbine controls is used to control the HP turbine throttle pressure to a setpoint by adjustment of the throttle valve. This is the "initial pressure regulator mode" of HP throttle valve control used in the FSV and subsequent HTGR-SC designs.

Block 2 of the turbine controls is the turbine bypass control, which regulates HP throttle pressure to the bypass pressure setpoint by means of a throttle valve around the HP turbine, through a desuperheater to the flash tank at the HP/IP turbine junction. The output of the control also supplies, through a characterizer, the reference for the desuperheater valve to minimize required temperature control action.

Block 3 of the turbine controls maintains the steam temperature downstream of the desuperheater in the HP bypass line to a setpoint. The temperature control is accomplished by control of the desuperheater water spray by adjustment of the water supply throttle valve.

Block 4 of the turbine controls is the pressure control for atmospheric vent. This control maintains the HP throttle pressure to a limit above the bypass pressure setpoint of Block 1. The control will operate only in the event of malfunction of the turbine/turbine-bypass systems.

Block 5 of the turbine controls is the IP turbine bypass-pressure/bypass-valve control. This control acts as described in the HP bypass. Flow is through a desuperheater to a flash tank at the IP/LP turbine junction (deaerator/BFP-turbine header extraction point).

Block 6 of the turbine controls is the IP bypass desuperheater temperature/desuperheater spray valve control, which operates as described for Block 3.

Block 7 of the turbine controls is the IP turbine inlet pressure/atmospheric vent control. This control acts if the IP turbine/turbine-bypass flows become limited and increase the pressure a set amount above the bypass setpoint pressure.

Block 8 of the turbine controls is the LP superheater temperature/spray valve control, which acts as described for similar HP and IP controllers.

Block 9 of the turbine controls is the LP turbine bypass pressure control. This control acts as described for the HP and IP bypass pressure controllers. The setpoint, however, is the sum of a reference and the output of the feedwater controller (Block 7) as previously discussed. The bypass flow is through a desuperheater to the condenser.

Block 10 of the turbine controls is the LP atmospheric vent control, which acts as described for the IP turbine (Block 7).

2.4.2.3. Control System Functional Requirements. Preliminary control functions for the overall plant control system were developed and exercised for the major trip events which differ from those of the HTGR-SC plant.

Table 2-6 gives the best estimate and target parameters for the initial analysis in lieu of the specific top level requirements. The tolerances are given in terms of the controllers, that is, in terms of deviation of measured signal from demand (setpoint). The tolerances specified in Table 2-6 are for steady state (static) and for the worst case among the spectrum of normal and upset events (but not necessarily for emergency or faulted events). The exceptions are that not all parameters will be maintained in the event of reactor trip or of the uncontrollable loss of ability to produce steam (such as feedwater limiting) unless one of the following is guaranteed:

1. The process will reduce steam draw to the available level.

TABLE 2-6
TARGET PARAMETER TOLERANCES - MEASUREMENT FROM SETPOINT

Measurement	Static	Transient Normal/Upset[a]
Process steam temperature, °C (°F)	+17, -3 (+30, -5)	+39, -8 (+70, -15)
Reactor power	1% of design	Later
Circulator speed, %	0.5	2
Module to average temperature trim, °C (°F)	5 (10)	14 (25)[b]
Main steam temperature, °C (°F)	3 (5)	+33, -8 (+60, -15)
Feedwater flow,[c] kg/s (lb/sec	18 (40)	90 (200)
BFP turbine speed	Later	Later
IP inlet pressure, kPa (psi)	34 (5)	172 (25)
Process header pressure, kPa (psi)	69 (10)	206 (30)
Deaerator pressure, kPa (psi)	34 (5)	172 (25)
Deaerator level	Later	Later
Feedwater heater 3 pressure,[d] kPa (psi)	34 (5)	138 (20)
Feedwater heater 1 pressure, kPa (psi)	3.4 (0.5)	14 (2)
HP throttle pressure, kPa (psi)	103 (15)	689 (100)
HP bypass pressure, kPa (psi)	69 (10)	345 (50)
HP desuperheat temperature, °C (°F)	8 (15)	17 (30)
IPT bypass pressure, kPa (psi)	20.5 (3)	138 (20)
IPT desuperheat temperature °C (°F)	8 (15)	17 (30)
LPT bypass pressure, kPa (psi)	6.8 (1)	+172, -79 (+25, -2)
LPT desuperheat temperature,°C (°F)	8 (15)	17 (30)

[a] Exclusive of reactor trip or of uncontrollable steam loss such as loop trip if process response is not guaranteed.

[b] Exclusive of loop failure events (such as loop trip).

[c] Above 140.6 kg/s (310 lbm/sec).

[d] When active (works in conjunction with heater 1 pressure control).

2. An alternate source of steam will provide the supplementary steam flow in accordance with NSSS timing requirements.

Analyses for one controller concept that is planned was not included in the Plant Transient Specification because there was insufficient time to implement and evaluate the controller prior to the required issuance of the Plant Transient Specification. This controller is a switch of the IP throttle valve control to an "initial pressure regulator" mode if the IP turbine inlet pressure falls a set amount below the setpoint. The control will close down on the throttle valve if the pressure tries to decrease, which will cut down on the IP/LP steam flow and make more flow available to the process. The purpose of the control is to maximize steam flow to the process in events where the NSSS may be steam flow limited.

Table 2-7 gives the controller setpoint data. Included in the table are the design setpoint values, the expected setpoint range (or variation) over the automatic load control range, and the total range expected. The last column includes operation for startup and shutdown as well as upsets for controls which operate under those conditions. For controllers whose setpoints are a function of another controller output (i.e., inner loop controllers), the range includes overshoot of the outer loop controller.

2.4.3.4. Major Functional Level BOP Requirements. These requirements were developed from an NSSS evaluation for overall plant operation. The final detailed BOP provisions/configuration will be determined by the customer and the architect-engineer.

In order to meet the functional requirements, a system design/analyses effort was undertaken, and a reference plant configuration was developed which would meet both the top level requirements and certain restrictions of components of the plant. The plant configuration developed is, of course, not the only possible solution for meeting all the requirements. The data should therefore be considered representative, depending on the final plant configuration. In this section, those requirements that are essentially independent of the design solution (configuration and/or control scheme) and

TABLE 2-7
CONTROLLER SETPOINTS AND SETPOINT RANGES

Controller	Nominal Setpoint	Expected Range	
		Auto. Control	Maximum
Module/average steam temperature, °C (°F)	540 (1005)	449-549 (840-1020.5) [476-549 (890-1020.5)][(b)]	800-1020.5
Neutron power	100% of nominal	10%-110%	0%-110%
Main steam temperature, °C (°F)	538 (1000)	460-538 (860-1000) [488-538 (910-1000)][(b)]	426-538 (800-1000)
IP turbine temperature, °C (°F)	375 (675.5)	355-357 (671.2-675.5)	355-357 (671.2-675.5)
BFP turbine speed	NA[(a)]	NA	NA
Feedwater flow, kg/s (lb/sec)	925 (2040)	208-971 (459-2142)	37-971 (82-2142)
IP turbine pressure, MPa (psia)	4.74 (687.5)	4.48-4.9 (651-713)	4.49-4.9 (651-713)
Process header pressure, MPa (psia)	4.5 (650)	None	None
Deaerator pressure, MPa (psia)	1.17 (170)	0.14-1.17 (20-170)	0.14-1.17 (20-170)
Deaerator valve position limiter	20, 80% of stroke	None	None
FW heater 3 pressure, MPa (psia)	0.76 (110)	0.83-0.75 (120.7-109.3)	0.83-0.75 (120.7-109.3)
FW heater 1 pressure, kPa (psia)	62 (9)	15.4-65.2 (2.24-9.45)	13.7-65 (2.0-9.45)
HP turbine throttle pressure MPa (psia)	16.6 (2415)	None	None
HP turbine bypass pressure, MPa (psia)	17.6 (2550)	None	4.13-17.58 (600-2550)
HP bypass desuperheat temperature, °C (°F)	357 (675.5)	355-357 (671.2-675.5)	149-357 (300-675.5)
HP vent pressure, MPa (psia)	18.27 (2650)	None	None
IP bypass pressure, MPa (psia)	4.9 (713)[(c)]	4.7-4.9 (690-713)	0.41-4.9 (60-713)
IP bypass desuperheat temperature, °C (°F)	204 (400)	246-204 (475-400)	132-246 (270-475)
IP vent pressure, MPa (psia)	5.0 (725)	None	None
LP bypass pressure, MPa (psia)	1.38 (200)	1.24-1.62 (180-235)	0.276-1.62 (40-235)
LP bypass desuperheat temperature, °C (°F)	180 (356)	None	120-180 (248.4-356)
LP vent pressure, MPa (psia)	1.55 (225)	None	None

(a)Not available.
(b)For proportional only IP inlet temperature control and 25% steam flow and minimum load.
(c)Reset to 4.76 MPa (690 psia) on turbine trip signal (either turbine-generator).

those which are primarily dependent on the configuration and/or control scheme are identified.

The major functional requirements can be divided into four basic functional control groups:

A. Feedwater flow control per the NSSS requirement and as required to maintain pressures at the IP/process header.

B. Control of feedwater train heating and deaerator pressure/level.

C. Bypass desuperheating and vent system to maintain steam flows and pressures as required for various operating conditions including turbine trips.

D. Control of the HP turbine throttle valve bypass and vent systems such that pressure excursions seen by the steam generators are limited.

The control requirements for Group A are listed in Table 2-8. Requirement 1 is straightforward. Requirement 2 is necessary to enable a match of feedwater, helium flow, and power for events such as loop trips or reactor trips. Requirement 3 results from the need to hold process header pressure within a tolerance of nominal which will not drive the user admission valves to their stops. This is combined with the need to hold sensible conditions in the turbine/feedwater steam source area to prevent upset and the potentially large separation of the turbine plant and process header (long steam transmission line). Requirement 4 limits steam dump.

Table 2-9 presents the requirements for Group B. Requirement 1 reflects the need to limit feedwater thermal shock of the steam generators and the desirable feature of minimizing any such shocks. Requirement 2 is standard, and no specific requirements were developed in the initial studies. Requirement 3 is a function of the design source of deaerator steam and could be modified by design change. Requirement 4 results from

TABLE 2-8
FEEDWATER FLOW REQUIREMENTS

Function	Requirement	
	Any Solution	Solution Dependent
1. Feedwater flow must be controlled to a manual/programmed setpoint independent of other parameters (such as in startup/shutdown).	X	
2. Feedwater flow must permit an NSSS commanded runback which will override/reset any outer loop control setpoint.	X	
3. Feedwater must respond to maintain the process steam/transmission line inlet pressure compatible with existing flow and process header pressure (fast response) and provide longer-term adjustment to trim out process header pressure offset (slow response).		X
4. Provision must be made to enable overall flow reduction to eliminate vent flows and to reduce excessive bypass flows.[a]	X	

[a] Appropriate criteria for excess bypass flow reduction have not yet been fully developed.

TABLE 2-9
FEEDWATER TRAIN HEATING AND DEAERATOR REQUIREMENTS

	Function	Requirement: Any Solution	Requirement: Solution Dependent
1.	The deaerator pressure (enthalpy, temperature) must be maintained within reasonable bounds and should be controlled to minimize steam generator thermal transients.(a)	X	
2.	The deaerator level must be controlled (no requirements developed in this report).	X	
3.	Under some conditions the deaerator pressure control valve may be driven out of its control range (when the LP turbine is in bypass), and a source pressure adjustment should be made to bring it back into range.		X
4.	Feedwater train overheating must be prevented at reduced process steam flow.	X	
	a. To attain the "best" operation, heat should be bypassed around part of the feedwater heaters.	X	
	b. The simple bypass of part of the feedwater heating steam is insufficient to control overheating and some IP turbine throttling is necessary.		X
5.	Feedwater heater drain controls must provide for proper feedwater heater performance (no specific requirements developed in the initial studies).	X	

(a) Holding deaerator pressure under some conditions can require as much as five times design steam flow. If such high flows are prohibitive to the deaerator design, feed of some of the deaerator header steam to one or more of the LP heaters should be evaluated.

the fact that the HTGR-SC/C plant inherently causes excessive feedwater train heating at reduced process steam (feedwater) flow. The purpose of requirement 4.a is to maintain reasonable flow through the turbines without allowing too much heat to the feedwater heaters. Requirement 4.b is a solution to the fact that bypass around only the first heater cannot quite limit the feedwater overheating. Requirement 5 is also standard but will be pushed beyond normally expected conditions due to the peculiar conditions of feedwater overheating just discussed.

Table 2-10 gives the requirements for Group C. The requirements for maintenance of process conditions in the event of trip of either or both turbine-generators and the need to bypass at least the HP unit during startup are reflected in requirement 1. Requirement 2 results from the fact that the bypass flows will be re-inserted into points in the normal flow stream and must be cooled to temperatures at or near those existing at the insertion points. Requirement 3 results from the 34-kPa (5-psig) minimum pegging point for the deaerator, the desirability of higher pegging steam for limiting feedwater thermal transients, and the need, with a steam-driven BFP, to continue steam to maintain feedwater flow. Requirement 4 for atmospheric relief valves will exist for protection in any event, but is stated here in terms of the need relative to limiting bypass flows.

Group D is the requirement for limiting pressure changes seen by the steam generator.

Secondary more detailed BOP requirements were also generated from the reference configuration supplied in the initial issue of the Plant Transient Specification. The type of information supplied included:

1. Peak bypass flows.
2. Peak/minimum heater 1 bypass and deaerator steam flows.
3. Control valve characteristics and response.

2.4.3.5. Transient Results. Much of the information developed in the transient analyses for the Plant Transient Specification document has been

TABLE 2-10
TURBINE BYPASS, DESUPERHEATING, AND VENT REQUIREMENTS

	Function	Requirement: Any Solution	Requirement: Solution Dependent
1.	Turbine steam flow bypass must be provided for both the HP and IP/LP units to enable continued operation with turbines tripped and for startup/shutdown operations.	X	
2.	The bypass flows must be thermally conditioned to values commensurate with the point of re-entry to the system.	X	
3.	The bypass system must provide steam for continued feedpump operation and at least minimum pegging of the deaerator.	X	X[a]
4.	It appears impractical to handle all potential bypass flow via bypass/desuperheating self-contained clear to the condenser; if the bypasses are flow limited, atmospheric vents will be needed. In any event, vents will be required for protection.	X	

[a]The system could use motor-driven BFPs, thus eliminating part of the requirement.

indicated by summary requirements presented in the preceding subsections. Typical information derived from the transients includes controlled parameter peak deviations (range), peak bypass flows, required valve characteristics/response, and feedwater heating limits. The remainder of the information presented is in the form of time history parameter plots. While such data are too voluminous to even summarize in this report, selected parameters from five transients that differ significantly from previous HTGR-SC results are presented in Figs. 2-5 through 2-9. In the figure for each event, frame A shows the major steam flows, frame B the process steam transmission line inlet conditions, and frame C the gross electric output of the two turbogenerators.

Figure 2-5 presents the data for a steam load reduction at the maximum required rate of 5%/min. The analysis was run from 100% to 30% of nominal steam load per the candidate process minimum load requirement. The run was made by controlling the process valve at the equivalent of the site boundary to attain a flow at that location which would ramp down from design to 30% at the desired rate. All other response to this action is automatic based on the closed-loop controls described. The process header pressure control trim of IP turbine pressure setpoint was not in play since the steam transmission line length, size, equivalent process volume, etc., data have not become available (hence the choice of throttle at site boundary for evaluation).

The significant aspects of this event are:

1. The main steam temperature drop required to maintain process line inlet temperature.

2. The major decrease in HP electric generation (due to total flow decrease - see HP inlet in frame A of Fig. 2-5).

3. The actions necessary to limit feedwater heating [heater 1 bypass flow (frame A, Fig. 2-5)] and throttling [process line in versus IP stage 1 in (frame B, Fig. 2-5)].

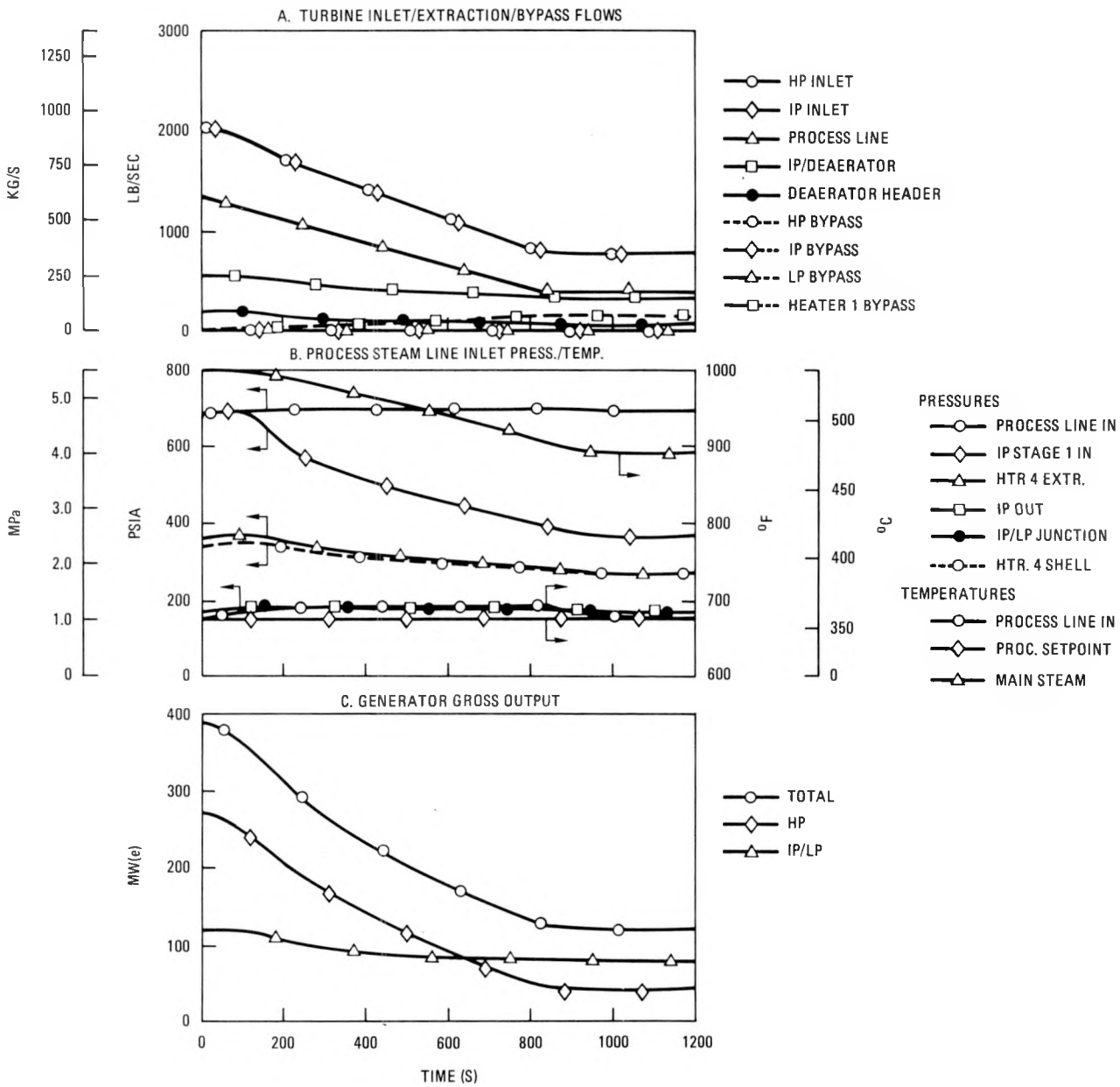

Fig. 2-5. Parameters for rapid steam load decrease at 5%/min (100% to 30%)

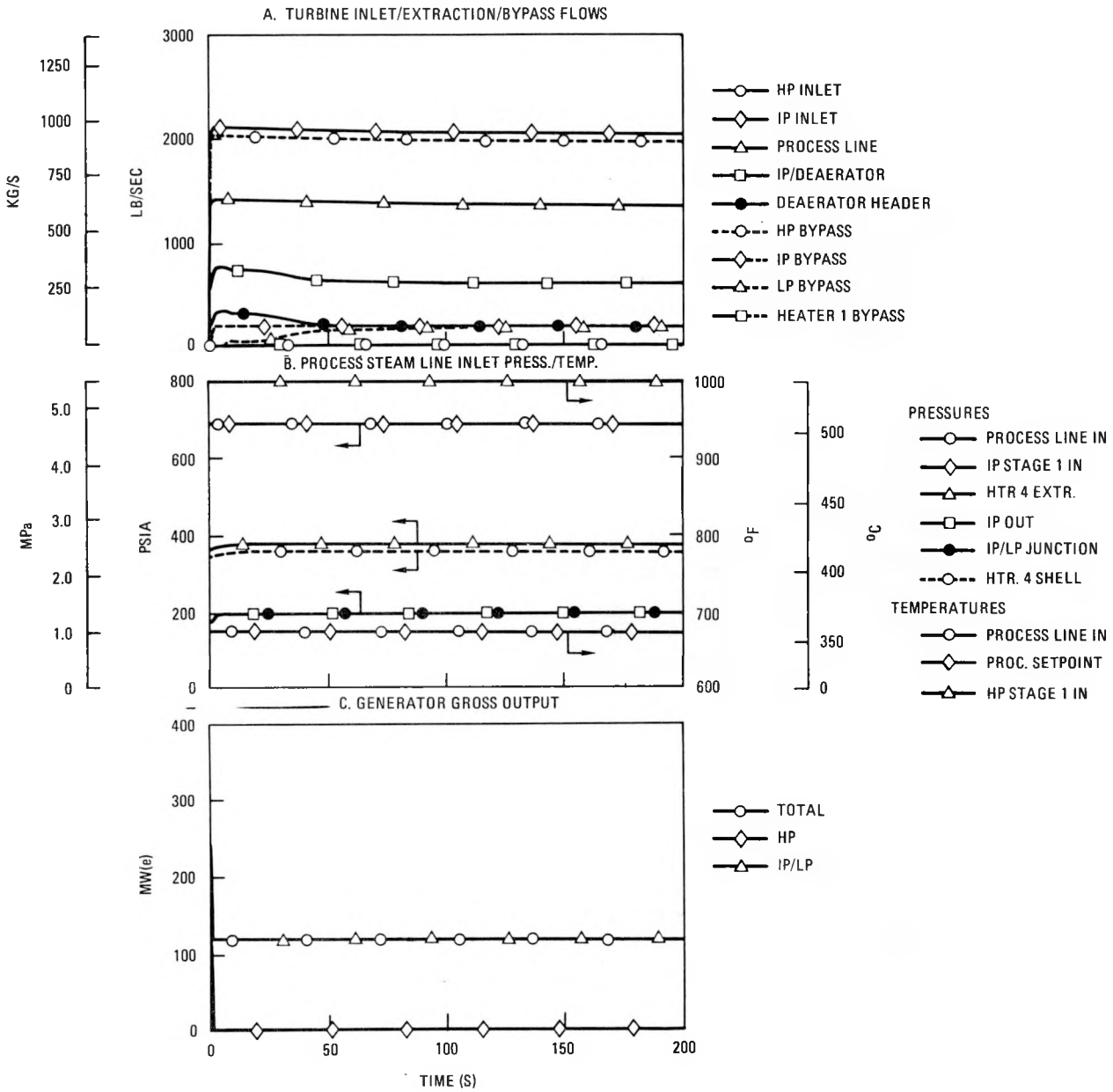

Fig. 2-6. Parameters for HP turbine trip

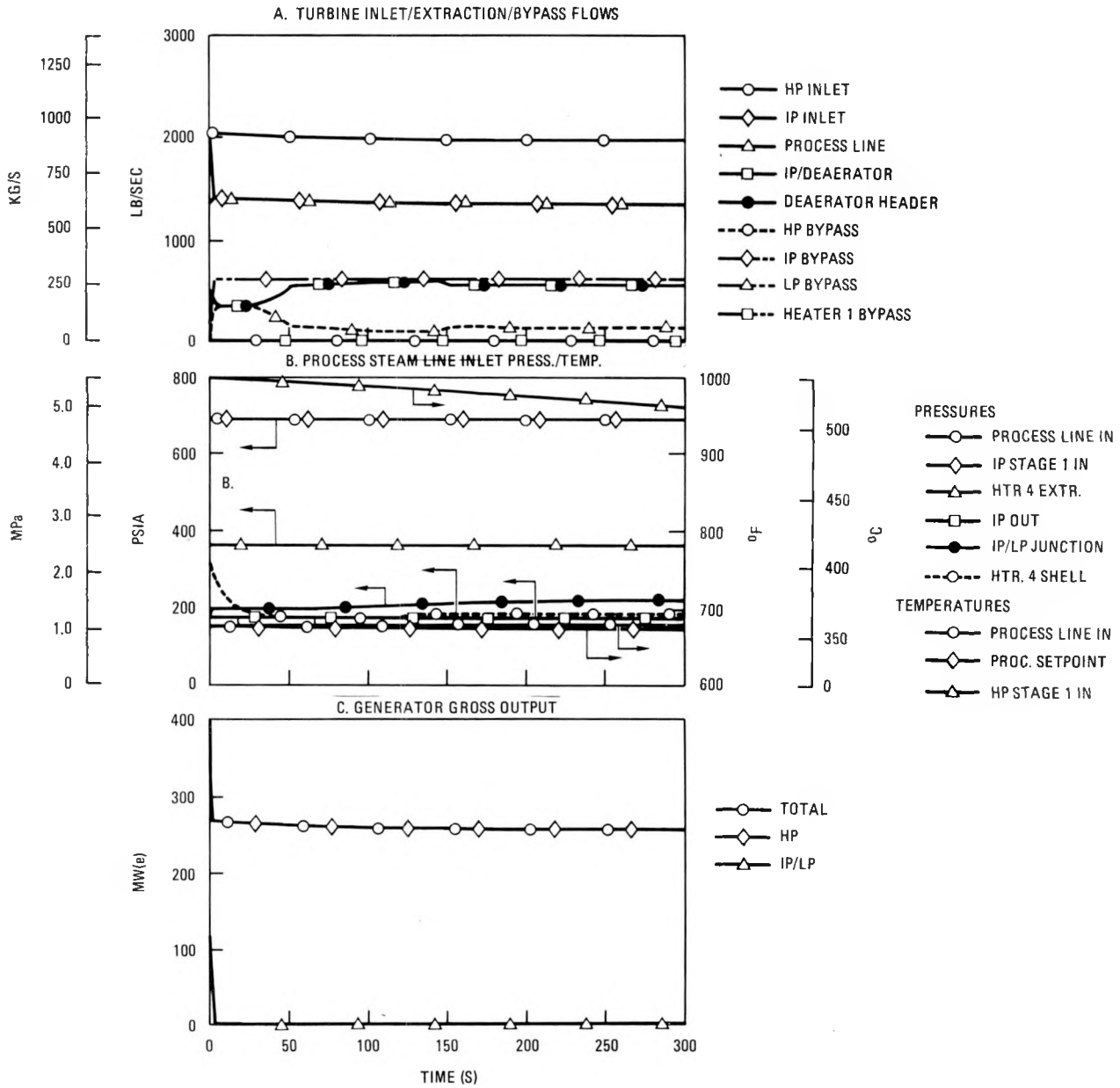

Fig. 2-7. Parameters for IP/LP turbine trip

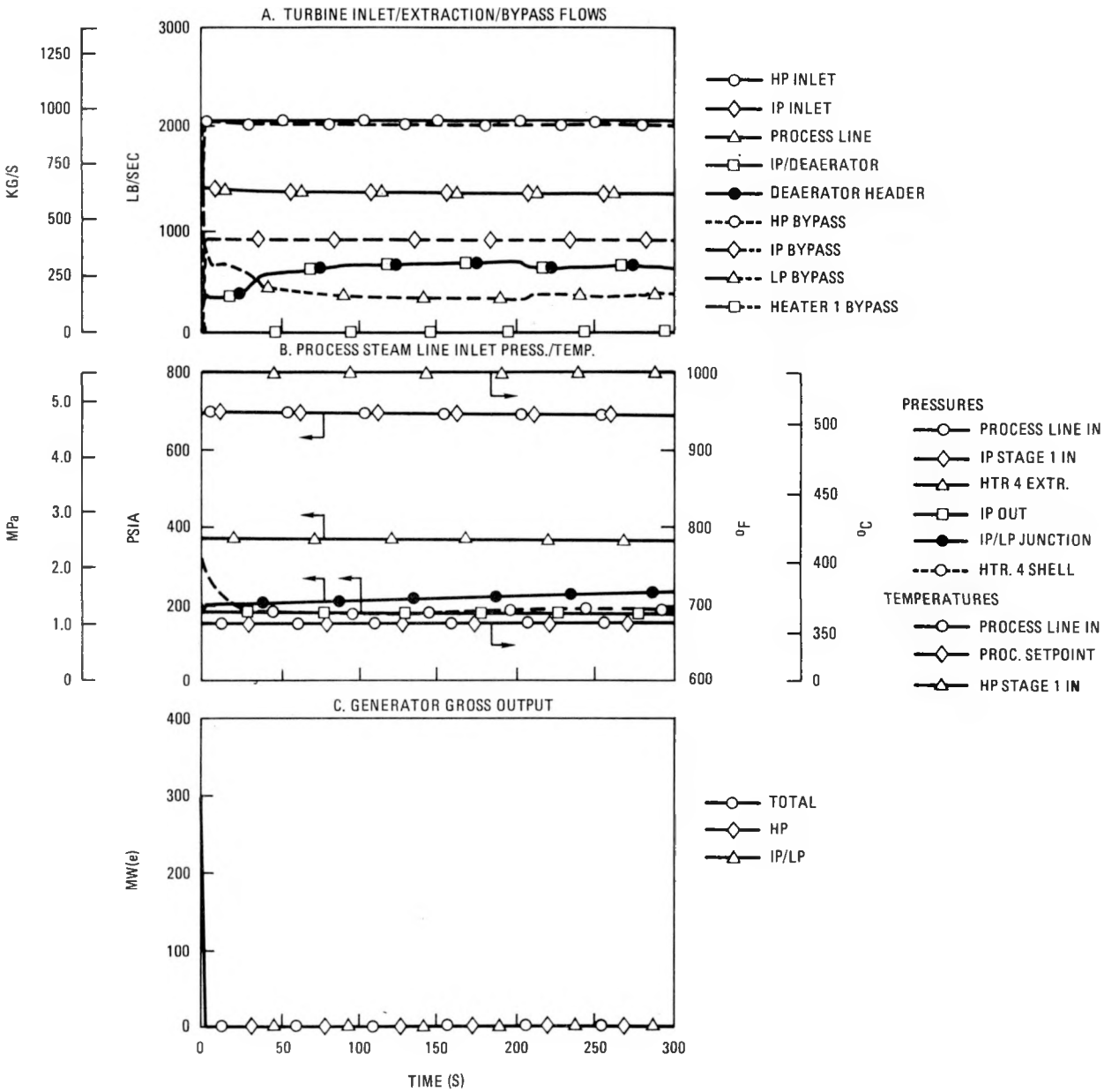

Fig. 2-8. Parameters for simultaneous trip of all turbines

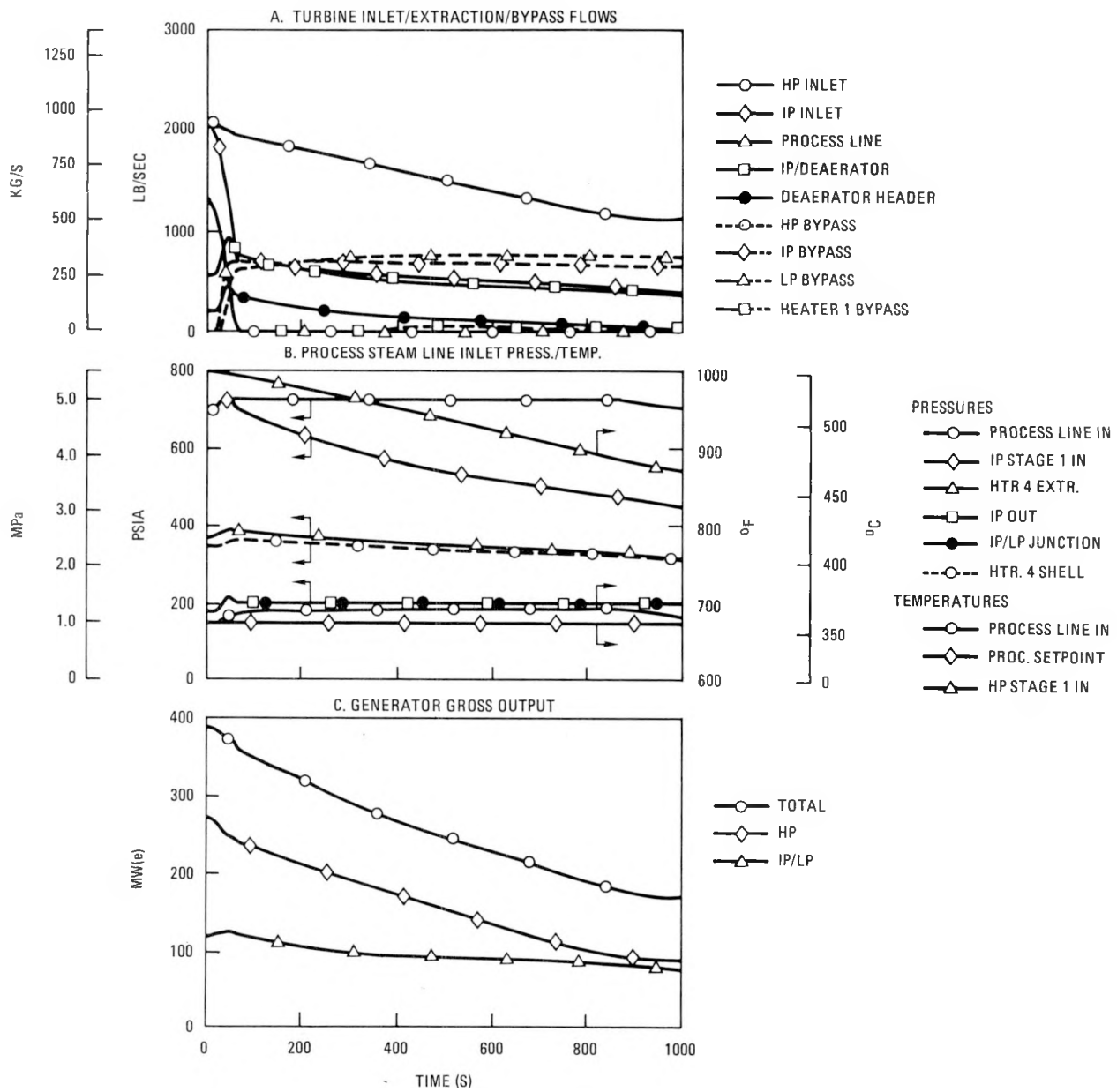

Fig. 2-9. Parameters for rapid process load cutoff

Figure 2-6 presents the results of an HP turbine trip with the process and IP/LP turbine operation being maintained via the HP bypass/desuperheater/flash-tank system. The bypass is set to operate at 17.58 MPa (2550 psia) [16.65-MPa (2415-psia) design throttle pressure], and a pressure-controlled throttle valve has been assumed versus a pressure-regulating valve. The pressure control was chosen to enable bypass at lower pressures during startup operations via bypass setpoint adjustment.

Electric load on the HP essentially steps to zero (frame 6, Fig. 2-6) at 1 s when the trip occurs. High-pressure bypass flow comes on immediately, followed in about 1 s by IP bypass and at about 8 s by LP bypass. The IP and LP bypasses occur owing to the buildup of pressure caused by the desuperheat flow for the HP bypass. Little other disturbance occurs in the system. The IP and LP bypasses would be backed off if the plant were going to continue to operate for a significant time with the HP turbine tripped.

Figure 2-7 presents the results of an IP/LP turbine trip with the IP/LP bypass systems maintaining the process flow/pressure conditions. When the turbine trips (at 1 s), the flow that had been going to the turbine tries to divert to the process. For a turbine trip the IP turbine bypass setpoint is reduced from 4.9 to 4.76 MPa (713 to 690 psia). The extra flow to the process (frame A, Fig. 2-7) rapidly raises the process/IP junction (IP throttle) pressure to bypass setpoint, and the high IP bypass/desuperheat flow and LP intercept valve closure immediately cause the LP bypass/desuperheat system to come on.

From frame A of Fig. 2-7 it can be seen that although the bypasses limit the excess of flow to the process, some increase occurs which is subsequently removed by the process/IP junction pressure control via reduction of total steam (feedwater) flow. The deaerator header flow initially essentially steps up in the first few seconds after trip [from 81.5 kg/s (180 lbm/sec) to a little over 181 kg/s (400 lbm/sec)] owing to the higher pressure, then is cut back by the system and subsequently is raised to over 272 kg/s (600 lbm/sec). This action results from the fact that right after the trip, the condensate coming to the deaerator is at essentially the same

temperature as before the trip owing to the heat in the water in the heaters and heat stored in the metal mass of the heaters. Therefore, the extra deaerator header flow, driven by the increase in pressure from a design value of 1.24 MPa (180 psia) to slightly above the LP bypass setpoint pressure of 1.38 MPa (200 psia), tends to raise the deaerator pressure. The control initially cuts back on deaerator steam flow; then the heater temperatures start to fall since steam heating has been cut off. As the deaerator inlet temperature falls, the deaerator pressure starts to drop and the deaerator pressure control opens the header control valve until it is wide open at 55 s.

The control is set to maintain the deaerator at design pressure to minimize the drop in feedwater temperature associated with a loss of feedwater heating. Subsequently, the system conditions are shifted so that more than enough steam is available for the deaerator and the control brings the valve back into the control range. The LP bypass to waste heat rejection is cut back as steam is used to maintain the deaerator pressure (frame A, Fig. 2-7). Again, if the plant were going to operate for a significant period with the turbogenerator tripped, the IP and LP bypasses would be backed off.

Figure 2-8 presents the data for a simultaneous trip of all turbines. This should be a very rare event, since specific design measures will be taken to ensure that house load can be held on grid separation and that inability to hold load with one of the units does not seriously compromise the ability to hold load with the other unit. The event is a composite of the actions described individually for the HP trip and the IP/LP trip cases.

Numerical values of some of the parameters change since all bypasses are on at once, and the bypasses all come on essentially simultaneously so that little runback of total flow occurs. While the cutback of heat rejection noted in the IP/LP trip case owing to the need of steam to maintain deaerator pressure does occur, both the initial peak and steady heat

rejection loads (LP bypass flow) are significantly higher due to the HP turbine bypass.

Figure 2-9 presents the data for a rapid process load cutoff. While current indications are that total sudden loss of all of a multiple user process is extremely unlikely, the HTGR-SC/C single line delivery makes the event at least possible. Further, the need to isolate the process and be able to supply it from an alternate source forces an isolation valve into the process line which could inadvertently close. Since the process isolation valve closure is both more rapid and more effective than anything that conceivably could result from any foreseeable event at the other end of a long steam transmission line, the isolation valve closure was chosen for analysis. The event shown is the bypass-flow-limited (with atmospheric vent) case.

A valve stroke time of less than 7 s and a linear Cv versus stroke characteristic were assumed. Process line flow cutoff as seen by the process/IP junction, including volumetric effects, occurs in 7.5 s (frame A, Fig. 2-9). The IP throttle pressure increases very rapidly to above the 4.9-MPa (713-psia) nominal bypass relief pressure setpoint as the bypass controller tries to accommodate the rapidly increasing flow. The pressure rise tries to force a rapid increase in flow to the deaerator header and through the IP and LP turbines. The IP and LP turbine bypass flows rapidly climb to values equivalent to the reduction in process flow, and the process/IP junction pressure control cuts back on total flow as indicatd by the HP turbine inlet flow.

As can be seen, when the IP bypass reaches 317.5 kg/s (700 lbm/sec), the IP vent comes on, limiting the bypass. An automatic cutback to eliminate the atmospheric vent flow has been implemented which acts by adding a signal to the IP inlet pressure control of feedwater flow so that feedwater is run back. The reduction in feedwater continues until the vent flow goes to zero and removes the signal from the IP pressure controller.

Electrical generation (frame C, Fig. 2-9) decreases with the reduction of total steam flow. When the atmospheric vent flow has been eliminated (85 s), the electric output is roughly 1/2 of design, with the HP at about 1/3 of its design point output.

2.5. BOP INTERFACES (6032010800)

2.5.1. Scope

The scope of this task is to prepare and convey NSSS requirements and information (BOP, PLR) to the BOP designer (architect-engineer) in order to obtain an efficient, integrated overall plant design, to provide a focal point for NSSS/BOP interfacing to properly coordinate the exchange of technical information within GA between the NSSS and BOP designers, and finally to review the BOP designs to ensure their compliance with the interface criteria.

2.5.2. Discussion

A special NSSS design data package was compiled to assist UE&C in the development of a nuclear island optimization study which was being conducted to a limited schedule. The package comprised information related to plant layout requirements, mainly in the PCRV and fuel handling system areas, together with some updated BOPR data. In addition, recommendations were submitted regarding the key areas subject to change as a result of converting the plant from a steam cycle mode to the cogeneration configuration.

Discussions held with the architect-engineer resulted in a revised layout of the PCRV top head to provide greater design flexibility in the development of the nuclear island reconfiguration study. The CAHEs were relocated to permit a revised routing of the fuel handling equipment transporter tracks. The work was coordinated with the PCRV and Mechanical Design groups. A key factor that permitted increased freedom in the design of the nuclear island was the introduction of the in-vessel refueling scheme, which

eliminated some constraints regarding servicing, fuel handling, and storage facility locations.

The results of the nuclear island reconfiguration study, presented in a UE&C topical report, were reviewed. The overall conceptual approach was endorsed, with some recommendations being made to improve serviceability and maintenance in the auxiliary reactor service building. These latter features would be accommodated in subsequent, more detailed design of the plant structures.

An NSSS/BOP interface meeting was held, primarily to present the results of the plant control system transient analysis which had been performed at GA. The control system philosophy for the cogeneration plant and the division of responsibility for the system between the NSSS and BOP were discussed. Other topics briefly covered during the same session were:

1. Definition of responsibility for control and instrumentation systems, particularly in the areas of post-accident monitoring, plant diagnostics, emergency response, and the NRC nuclear data link system.

2. General Atomic review comments on the nuclear island reconfiguration study.

3. Layout of the fuel sealing and inspection facility.

The results of a Variable Cogeneration Plant Configuration Study, presented in a topical report by UE&C, were reviewed. This concept presents a turbine plant design which permits the NSSS to be used for either all electrical generation or varying degrees of cogeneration at any time, depending on the relative demands for process steam or electricity. Three separate LP turbines are included in this concept, with two automatic extraction points. Some difficulty in turbine operation may result when process extraction flow is allowed to vary over a wide range. GA recommends that this scheme be reviewed by a turbine supplier before adoption.

A proposed method for the removal of a CAHE from the PCRV was submitted to UE&C for their review. The approach requires a trench arrangement to be provided in the containment base mat beneath the CAHE cavities.

Two issues of both the BOPR and PLR documents have been made. The first issue was based on a partial update of the requirements which had been specified for the 900-MW(e) HTGR-SC plant. The second issue included further provisions for the cogeneration application plus additional update and requirements related to the refueling and storage systems, PCRV, and control and instrumentation systems.

2.6. LICENSING SUPPORT (6032020001)

2.6.1. Scope

The scope of this task consists of (1) revising the Nuclear Safety Plant Specification, (2) updating the report on the safety/licensing assessment of the HTGR-SC/C plant, and (3) providing support and guidance on matters related to regulatory requirements.

2.6.2. Discussion

Revision of the "Nuclear Safety Plant Specification - HTGR-SC/C 2240 MW(t)" document was initiated. Aside from bringing the list of regulatory guides up to date, the main changes will involve modifying sections on NSSS's so as to conform to current design descriptions.

"Safety/Licensing Assessment of the 2240 MW(t) HTGR Steam Cycle/Cogeneration Plant" (Ref. 2-2) is also in the process of being updated. This work has been limited to updating the design descriptions and incorporating the latest program planning into the discussion of issues. It is intended to completely revise the risk analysis as new information becomes available.

Consideration by GCRA and the HTGR Project Office of a plan to prepare a Standard Safety Analysis Report (SSAR) in FY-83 led to the development of information needed to implement such an activity. This included a list of proposed ground rules, a detailed SSAR outline consistent with Rev. 3 of Regulatory Guide 1.70 (format and content of SARs), preparation and review assignments, and a proposed schedule. However, the SSAR plan was abandoned after HTGR Engineering concluded that the objective and schedule are beyond the state of the design at this time.

Other tasks included review of design documents, including the Functional Specification and the Plant Technical Description, review of HTGR and LWR technical specifications, and the development of a list of specifications that could affect the availability of an HTGR and updating of the system and component safety classes in the Balance-of-Plant Requirements document.

A report comparing plant conditions (used in the Nuclear Safety Plan Specification) and the NRC's proposed numerical safety guidelines was prepared. Some concern has been expressed that the safety goals would conflict with present methods for treating accidents, and perhaps even make the presently used acceptance criteria obsolete. However, review of the pertinent documents, particularly the recent NRC policy statement on safety goals, confirms that present rules remain in place and that numerical guidelines and the risk assessments needed to implement them are supplemental.

2.7. SAFETY/INVESTMENT/RELIABILITY STUDIES (6032070001)

2.7.1. Scope

The scope of this task is to investigate safety risk, investment risk, and reliability criteria for the 2240-MW(t) HTGR-SC/C plant and to support the water ingress issue through reliability assessments of the circulator service system.

2.7.2. Discussion

2.7.2.1. Partial Safety Reliability Criteria. Partial safety reliability criteria were developed and documented. Major system descriptions reflecting enhanced safety features were prepared together with plant safety goals used to determine system reliabilities. Adequate margins are imposed on the conceptual design safety reliability criteria. The purpose and size of these margins are to cover expected increases in accident frequencies and consequences as the design proceeds from the conceptual to the final stage and to prevent accident sequences from exceeding values that may not meet final plant safety goals. A table of conceptual design safety reliability criteria has been compiled showing all NSSS's which dominate plant compliance with the safety goals of the final plant design. An excerpt from this table is shown in Fig. 2-10.

In the partial safety reliability criteria, several interfacing approaches are suggested as an aid for communicating the design requirements between the reliability and the system engineers so that the plant safety goal imposed by the reliability criteria can be met. These interface tools include fault tree methodology as well as defenses against redundant system common mode failures and intersystem common mode failures.

2.7.2.2. Water Ingress Assessment. The preliminary assessment of unavailability due to steam generator leaks was completed. From the unavailability event tree for steam generator leak initiated outages, the total outage frequency due to steam generator leaks is estimated to be ~0.9/yr. It is also estimated that steam generator leaks will, on the average, cause unscheduled downtime of about 400 hr/yr.

The event tree also discloses a new investment risk scenario consisting of:

1. A steam generator leak occurs.
2. The reactor is tripped.

TABLE 1
EVENT (EXOGENOUS) CONDITIONS

System	Response	Description	System Parameter	Median Reliability Value
Core Auxiliary Cooling System (CACS)	Failure to start on demand (all three loops)	LMLC, and the reactor is tripped with control rods.	Failure probability	3.5×10^{-5}
		LOSP, and the reactor is tripped with control rods.	Failure probability	1.5×10^{-3}
	Failure to operate (each loop)	LMLC, and the CACS starts on demand.	Failure rate	2.7×10^{-4}/hr
			Common mode factor	3.0×10^{-2}
		LOSP, and the CACS starts on demand.	Failure rate	8.6×10^{-4}/hr
			Common mode factor	7.2×10^{-2}
	Restoration (each loop)	LMLC, CACS starts on demand, CACS fails prior to MLCS restoration.	Prob. the failed components are accessible	0.76
			Mean repair time (accessible components)	24 hours

NOTES: LMLC Loss of Main Loop Cooling
LOSP Loss of Off-Site Power
MLCS Main Loop Cooling System

Fig. 2-10. Excerpt from conceptual design safety reliability criteria table

3. The helium circulator in the leaking loop fails to trip during loop isolation.

4. The steam generator is dumped.

The mean frequency of this occurrence is ~1 x 10^{-3}/yr, and the consequence of circulating hot helium through a dry steam generator is approximately 2 yr of downtime. Further analysis has disclosed that installing interlocks that prevent a steam generator dump if the circulator fails to trip will reduce the investment risk contribution from this scenario to a negligible level with respect to proposed investment risk goals.

2.7.2.3. Consequence Model Revision. Consequence models for the safety assessment of the 2240-MW(t) HTGR were prepared. In the course of this work the RATSAM and SORS computer programs were modified and input data were included.

A new version of RATSAM that contains a quasi-steady solution algorithm was added. This new version can be used as an alternative to the transient equation integration scheme of prior versions and allows a much more rapid solution of slow transients because larger time steps (by a factor of 100 to 1000) can be taken. Additional changes include modifications to the circulator operating characteristics [2240-MW(t) plant conditions] and the option to switch the liner cooling system on or off as well as means to calculate the liner temperature.

Besides having increased the number of available options, the SORS computer program can now perform fission product transport analysis using the geometric factors for the 2240-MW(t) composite fuel element block. SORS has been modified to use the new TRISO fuel failure model.

2.7.2.4. Safety Assessment. A core heatup base case analysis was performed on the RATSAM computer program. The analysis was initiated at full-power operation and assumed total loss of forced circulation and liner cooling. The results show that the ensuing upper plenum heating will lead to a rather

rapid rise in system pressure. The pressure rises to about 8.3 MPa (1200 psia), at about 3 hr after reactor scram, before the pressure relief valve lifts.

Fault trees for the loss of offsite power (LOSP) and loss of housepower were revised. A preliminary LOSP event tree for the 2240-MW(t) plant was also completed. The point estimate median frequency for core heatup (category CH-5) was calculated at 5×10^{-8} per reactor year. This is about three orders of magnitude (a factor of 800) less than core heatup from the loss of main loop cooling (LMLC) event tree.

An amended LMLC event tree was also developed. It indicates that HTGR target limits for frequency and consequences are exceeded for the containment failure category of core heatup accidents if core auxiliary cooling water service system (CACWS) redesign for diversity is not accomplished. Main contributors were identified as accidents leading to containment failure by gas accumulation and overpressurization.

A Markov model was completed simulating simultaneous repair and operation of three CACS loops during LMLC accident conditions. Results indicate a factor of four to five reduction in CACS failure probability (assuming the CACS has operated for a minimum of 100 hr). A Runga-Kutta based program was developed for solving the sets of simultaneous differential equations found in Markov models.

2.7.2.5. Ultimate Heat Sink Capability Assessment. A study was performed to evaluate UE&C's fault tree models for their modified ultimate heat sink (UHS) design, which incorporates three identical but separate systems. Each system contains one of the following: nuclear service water system (NSWS), CACWS, or reactor plant cooling water system (RPCWS) and associated electrical systems.

The results of the analysis indicate that UE&C's modified UHS design does not lead to a significant improvement in system reliability; i.e., current values are not acceptable. In order to maintain the probability of

core heatup at or below the 10^{-4}/yr goal, the UHS should be designed with both independence and diversity (rather than redundancy).

2.8. PCRV DESIGN (6032110100, 6032110200, 6032110300)

2.8.1. Scope

The scope of this task is to develop the PCRV layout and provide design and analytical support for the Design Decision Package, develop cavity liner and closure component design and perform analytical studies, and develop thermal barrier components by performing design and analytical studies, including studies concerning moisture ingress into and removal from the thermal barrier.

2.8.2. Discussion

2.8.2.1. PCRV and Liner. The system description document for the PCRV; liner, penetrations and closures; cooling water system; thermal barrier; and PCRV instrumentation and pressure relief system was revised to provide an updated function description, design bases, and interface requirements reflecting comments from the Baseline Review Meeting.

General arrangement drawings for the PCRV and liner were generated with sufficient details for cost development. These drawings, as shown in Fig. 2-11, incorporated a core cavity diameter change as a result of implementation of HTGR-SC/C core design improvements. The core cavity diameter was increased by 0.79 m (31 in.) from 11.51 m (37 ft 9 in.) to 12.29 m (40 ft 4 in.). This cavity diameter change resulted in a PCRV size increase from 31.10 m (102 ft 0 in.) O.D. to 32.00 m (105 ft 0 in.) O.D. and a height increase from 30.18 m (99 ft 0 in.) to 30.86 m (101 ft 3 in.). The PCRV layout includes four cylindrical steam generator/main helium circulator cavities grouped asymmetrically on one side and three CAHE/auxiliary circulator cavities grouped together on the opposite side. The center of the core cavity is offset from the geometric center of the PCRV. This offset was increased from 1.52 m (5 ft 0 in.) to 1.98 m (6 ft 6 in.). The resulting

PCRV diameter is governed by stresses in the inner and outer ligaments through the steam generator cavity. The requirements for circumferential and linear prestressing steels were established, and quantities of concrete and reinforcing bars were determined and included in the general arrangement drawings (Fig. 2-11) to provide a basis for updating the PCRV cost estimate.

The design basis for PCRV penetrations and closures was reviewed during this period. General Atomic maintains the position that catastrophic failure of ASME Code, Section III, Division 1, Class 1 penetrations and closures need not be postulated as a design basis event. Exceptions are penetrations and closures that perform at operating temperatures requiring design to high-temperature Code cases. Provisions are made in the PCRV penetration design to accommodate incorporation of flow restrictors with minimal impact on PCRV configuration should they be required by future safety and/or design criteria changes. For the CACS cavity, a secondary closure/zero leakage flow restrictor has been included as backup to the primary closure to ensure that any leakage through such a primary closure will not prevent the affected CACS loop from performing its safety function. Conceptual design details of closures for the steam generator and CACS cavities are also shown in Fig. 2-11.

Detailed PCRV and liner erection sequence drawings were generated to assist the architect-engineer in preparing the PCRV construction schedule and coordinating BOP efforts for the HTGR-SC/C plant. These drawings show details of the PCVRV concrete placement sequence and core and side cavity liner installation with notes indicating step-by-step procedures.

2.8.2.2. Thermal Barrier.

General Arrangement

A general arrangement drawing was completed that provided a technical basis for updating the cost estimate for the revised 2240-MW(t) HTGR-SC/C.

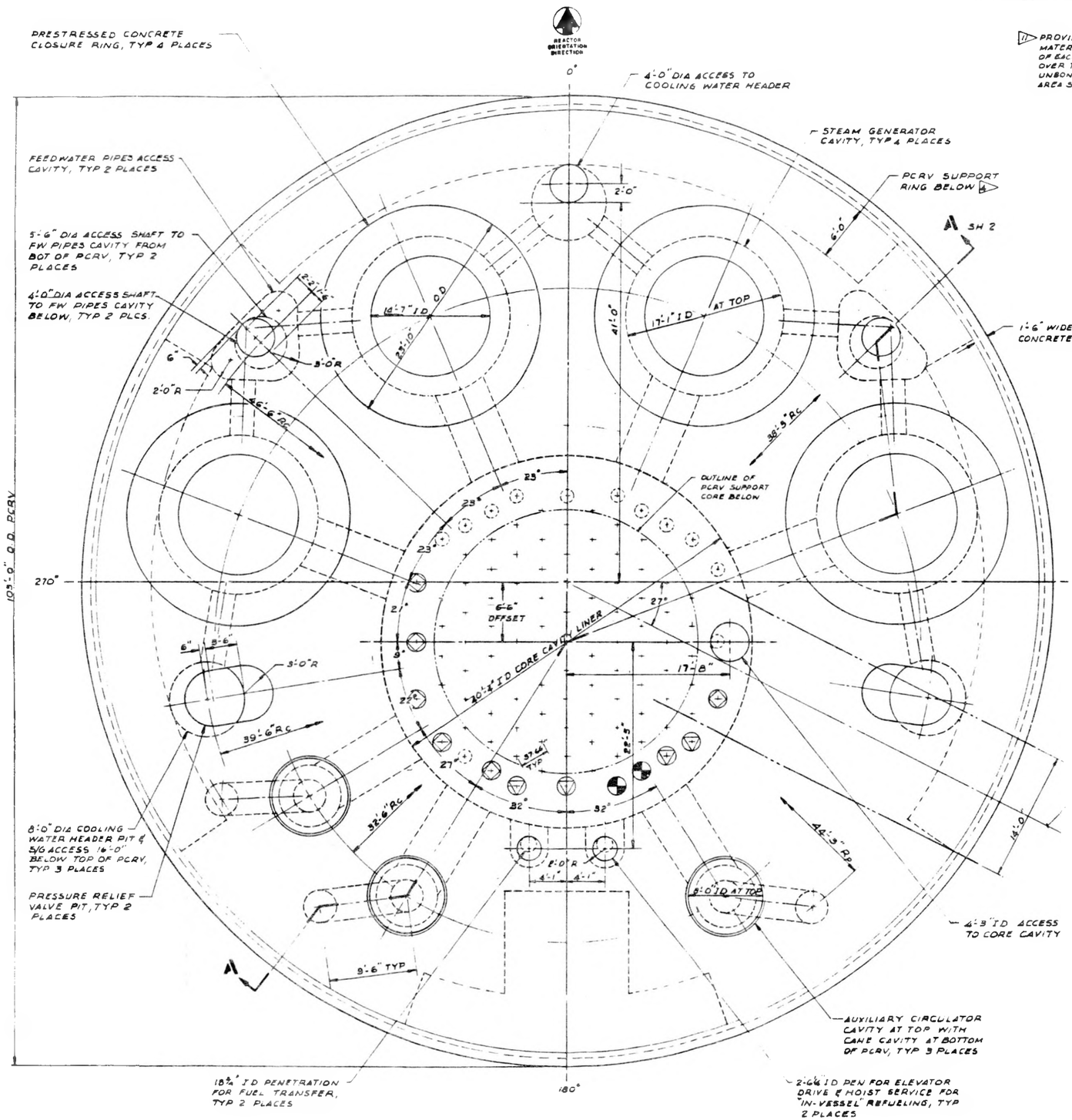

PLAN-PCRV TOP HEAD

Fig. 2-11. PCRV general arrangement (sheet 1 of 2)

PROVIDE ¼" MIN OF COMPRESSIBLE MATERIAL ON THE OUTER SURFACE OF EACH REFUELING PENETRATION OVER THE LENGTH INDICATED (FOR UNBONDING OF THE CONCRETE IN THE AREA SHOWN)

GENERAL NOTES

1. PCRV SIZING AND LAYOUT ARE CONCEPTUAL AND REQUIRES VERIFICATION BY ANALYSIS. THE DESIGN IS IN COMPLIANCE WITH THE REQUIREMENTS OF ASME BOILER & PRESSURE VESSEL CODE, SEC III, DIV 2 AND GA SYSTEM DESCRIPTION DOCUMENT 905857.
2. MATERIAL PROPERTIES AND MAXIMUM CAVITY PRESSURE USED IN THE DESIGN OF THE PCRV COMPONENTS ARE AS FOLLOWS:
   a. SPECIFIED CONCRETE COMPRESSIVE STRENGTH AT 60 DAYS = 8000 PSI FOR PCRV, PRECAST PANELS AND CLOSURES.
   b. BONDED REINFORCEMENT PER ASTM A 615, GR 60
   c. LINEAR PRESTRESSING: 72-½ϕ, 7-WIRE STRAND TENDONS, CAPACITY = 8374 KIPS @ GUTS
   d. CIRCUMFERENTIAL PRESTRESSING
      PCRV-½ϕ 7-WIRE STRAND, CAP = 41.3 KIPS @ GUTS
      CLOSURE - ⅜ϕ 7-WIRE STRAND; CAP = 23 KIPS @ GUTS
   e. MAXIMUM CAVITY PRESSURE FOR PCRV AND LINER DESIGN = 1130 PSIG
3. THIS PCRV LAYOUT DOES NOT SHOW THE REQUIRED CORE REGION OUTLET THERMOCOUPLE PENETRATIONS AND OTHER MINOR ISI PENETRATIONS. HOWEVER ALLOWANCE HAS BEEN MADE IN THE LAYOUT FOR SUCH REQUIREMENTS AND WILL BE SHOWN WHEN THE INFORMATION IS AVAILABLE.
4. THE LAYOUT DETAILS, DIMENSIONS AND CUTOUTS SHOWN AS PER THIS FLAG ARE PART OF THE BOP DESIGN.
5. MATERIALS FOR LINERS SHALL BE AS FOLLOWS:
   - PLATE TO CONFORM TO ASME SA-537, CLASS 2
   - FORGINGS TO CONFORM TO ASME SA-508, CLASS 2A
6. LINER THICKNESS TO BE ½ INCH EXCEPT WHERE NOTED OTHERWISE.
7. ALL LINER STUDS TO BE ⅝ INCH IN DIAMETER TIMES THE LENGTH SHOWN ON THE DRAWING. PROVIDE ONE STUD PER 60 SQUARE INCHES OF LINER SURFACE WHERE SHOWN ON THE DRAWING.
8. COOLING TUBE PITCH TO BE 5¾ INCHES EXCEPT WHERE NOTED OTHERWISE.
9. CAVITY ENVELOPES USED IN THIS PCRV AND LINER LAYOUT ARE OBTAINED FROM THE FOLLOWING DRAWINGS:

MARK II-A STEAM GENERATOR	000838
MAIN CIRCULATOR	026952
AUXILIARY CIRCULATOR	027027
CORE AUX HEAT EXCHANGER	026765
IN-VESSEL REFUELING	025499
CANE REMOVAL PROCEDURE STUDY	027034

10. EMBEDDED COOLING AND INTERCONNECTING PIPING TO CONSIST OF 10,000 LF OF 1½ SCH 40 PIPE.

QUANTITIES:

1. CONCRETE (8000 PSI):

PCRV	23,350 C.Y.
PRECAST PANELS	1,050 C.Y.
STEAM GENERATOR CLOSURES	
PLUGS (4)	140 C.Y.
RINGS (4)	380 C.Y.

2. REINFORCEMENT (ASTM A 615, GR 60)

PCRV	875 TONS
PRECAST PANELS	15: TONS
STEAM GENERATOR CLOSURES	
PLUGS (4)	24 TONS
RINGS (4)	65 TONS
NO. OF MECHANICAL SPLICES IN THE PCRV	2,000

3. LINEAR PRESTRESSING (ASTM A 416 GR 270):
   NO. OF 72-½ϕ STRAND TENDONS — 327

	QUANTITY	LENGTH*
CORE CAVITY (X-DUCTS	173	102'-0"
AUX CIRC CAVITIES	18	102'-0"
STEAM GEN CAVITIES	112	110'-0"
PERIPHERALS	24	102'-0"

   *LENGTH GIVEN BETWEEN CONC SURFACES, ALLOW 5'-0" ADDITIONAL PER TENDON FOR TENSIONING

4. CIRCUMFERENTIAL PRESTRESSING (ASTM A 416 GR 270):
   ½ϕ STRAND TOTAL LENGTH — 8.97×10^6 FT
   ⅜ϕ STRAND TOTAL LENGTH — 4.81×10^6 FT
   TOTAL NO. OF ½ϕ STRAND LAYERS — 313
   TOTAL NO. OF ⅜ϕ STRAND LAYERS — 312
   NO. OF 20" PRECAST FULL PANELS — 228
   NO. OF 20" PRECAST HALF PANELS — 16
   NO OF LOAD MONITOR PANELS (STEEL) — 6
   PANEL SURFACE AREA — 37,450 SQ FT

5. INSTRUMENTATION
   NO. OF CPE LOAD MONITORS — 6
   NO. OF LPS LOAD CELLS — 17
   NO OF PCRV SENSORS — 450
   NO OF LINER SENSORS — 400
   NO. OF PCRV SPARE SENSORS — 45
   NO. OF LINER SPARE SENSORS — 40

LEGEND:

- + REFUELING PENETRATIONS - 85
- ELEMENT TRANSPORTER PENETRATIONS - 6
- HELIUM PURIFICATION HIGH TEMPERATURE FILTER - 4
- HELIUM PURIFICATION HIGH TEMPERATURE ADSORBER - 2
- COLUMN SUPPORT FOR FUEL HANDLING MACHINE - 12

HTGR SC/C 2240 MWt

027024 SH 1 OF 2

ITEM	PART NO	DESCRIPTION	MAT'L/MATL SPEC
REQD/ASSEMBLY	ALT. ITEM NO. / SUPERSEDED DOCUMENT 905857	PARTS LIST	
	DSG SYSTEM 5 / TYP 11 / PROJECT DLO 6654		
2240 MW (t) HTGR-SC/C	DIST	GENERAL ATOMIC COMPANY	

REVISIONS									
NO	ZONE	DESCRIPTION	DATE	BY	CHK	DES	APPD	APPD
1		REVISED CAVE CAVITY CONCEPTUAL						

UNLESS OTHERWISE SPECIFIED DIMENSIONS ARE IN INCHES. NO BURRS OR SHARP EDGES. DIMENSIONS PER ANSI Y 14.5 TOLERANCE DECIMAL XX = ± XXX = ± ALL MACHINED SURFACES. DO NOT SCALE PRINT. FRACTION ± ANGLE ±

TITLE: PCRV GENERAL ARRANGEMENT FOR 4-LOOP PLANT

SIZE E | CODE IDENT NO 32334 | DWG NO 027024 | REV 1/2

SCALE 1/10 | WEIGHT | SHEET 1 OF 2

027024 SH 1 OF 2

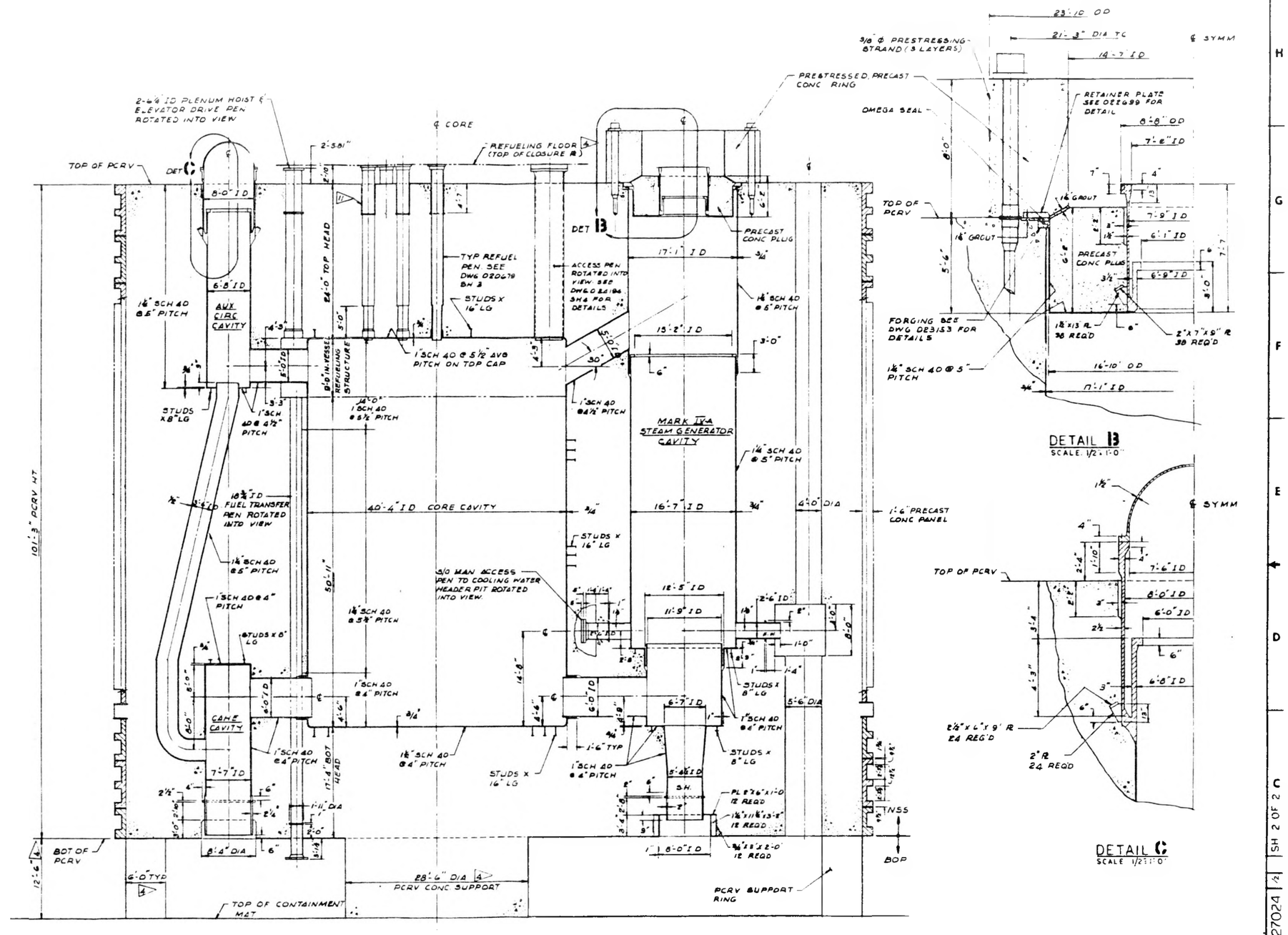

VERTICAL SECTION A-A
SCALE 3/16"=1'-0"

DETAIL B
SCALE: 1/2"=1'-0"

DETAIL C
SCALE 1/2"=1'-0"

Fig. 2-11. PCRV general arrangement (sheet 2 of 2)

ITEM	PART NO	DESCRIPTION	MAT'L/MATL SPEC
REQD/ASSEMBLY		PARTS LIST	

2240 MW(t) HTGR-SC/C — GENERAL ATOMIC COMPANY

UNLESS OTHERWISE SPECIFIED DIMENSIONS ARE IN INCHES. NO BURRS OR SHARP EDGE. DIMENSIONS PER ANSI Y 14.5 TOLERANCE DECIMAL .XXX = ± .01 .X = ± ALL MACHINED SURFACES

TITLE: PCRV GENERAL ARRANGEMENT FOR 4 LOOP PLANT

SIZE E | CODE IDENT NO 32334 | DWG NO 027024 | ISSUE ½

SCALE NONE | SHEET 2 OF 2

LTR | DATE | ISSUE DESCRIPTION | DR | CHK | DES | APPR | APPR

SEE SHEET 1

HTGR SC/C 2240 MW(t)

027024 SH 2 OF 2

027024 | ½ | SH 2 OF 2

As shown in Figs. 2-12 and 2-13, the thermal barrier is divided into 17 zones, which are dictated by geometry or temperature regime. Table 2-11 presents the component sizes and quantities used for costing.

Excluding the top and bottom heads of the core cavity, virtually all of the coverplates will be curved. Of the curved plates, 85% are expected to have the same general dimensions [e.g., 508 x 508 mm (20 x 20 in.)]. These plates represent about 75% of the total area covered by thermal barrier. Efforts are being made to minimize the number of different curvatures of the plates and plate dimensions in the various cavities. For example, the 13 zones employing curved plates will require only four different radii of curvature. These can probably be shaped using progressive dies, thereby minimizing tooling cost.

Thermal Barrier Water Ingress Effects

Failure or malfunction of NSSS components or systems could cause water, in either liquid or vapor form, to be introduced into the primary coolant. While such incidents would have no impact on safety, protracted plant downtime becomes a major economic concern if dryout and removal of contaminants are prolonged.

Under certain circumstances, removal of entrapped water from the thermal barrier insulation can be time consuming. To assure that specified plant availability is achieved, several avenues have been explored:

1. Preventing or limiting potential leak paths through the thermal barrier seal sheets.

2. Collecting or containing water before it can enter the thermal barrier.

3. Preventing impinging water from reaching the fibrous insulation.

TABLE 2-11
2240-MW(t) HTGR-SC/C THERMAL BARRIER SIZES AND QUANTITIES[a]

Zone	Class	Coverplate[b] Size (mm) t x l x w	Coverplate[b] Qty	Coverplate[b] Area (m^2)	Seal Sheet[b] Size (mm) t x l x w	Seal Sheet[b] Qty	Blanket Size (mm) l x w	Blanket Qty	Total Insulation Reqd. (m^2) Saffil (25 mm)	Total Insulation Reqd. (m^2) Kaowool (25 mm)	Total Insulation Reqd. (m^2) Kaowool (13 mm)	Composition of Blanket Layers and Thickness (mm) Saffil	Composition of Blanket Layers and Thickness (mm) Kaowool
1	A	13 x 508 x 508	3600	929	0.64 x 711 x 711	3600	610 x 610	3600	929	2786		1 at 25 mm	3 at 25 mm
2	A	19 x 508 x 508	1672	431	0.64 x 711 x 711	1672	610 x 610	1672	431	1294		1 at 25 mm	3 at 25 mm
3	A	19 x 508 x 508	276	71	0.64 x 711 x 711	276	610 x 610	276	71	213		1 at 25 mm	3 at 25 mm
4	A	13 x 508 x 508	260	68	0.64 x 711 x 711	260	610 x 610	260	68	203		1 at 25 mm	3 at 25 mm
5[c]	A	Hex. 13 x 940 A/F and	111	103	Hex. 0.64 x 1143 A/F and irreg.	111	1016 x 1016 and irreg.	111	103	309		1 at 25 mm	3 at 25 mm
		irreg. polygons	45		polygons	45	polygons	45				1 at 25 mm	3 at 25 mm
6	A	16 x 914 x 1067 and irregular	288 432	441	0.64 x 1118 x 1270 and irregular	288 432	1016 x 1016 and irregular	288 432	441	1324		1 at 25 mm	3 at 25 mm
10	A	13 x 508 x 508	120	32	0.64 x 711 x 711	120	610 x 610	120		95	32		3 at 25; 1 at 13
12	A	13 x 508 x 508	153	39	0.64 x 711 x 711	153	610 x 610	153		118	39		3 at 25; 1 at 13
13	A	13 x 508 x 508	630	163	0.64 x 711 x 711	630	610 x 610	630		489	163		3 at 25; 1 at 13
14	A	13 x 508 x 508	801	207	0.64 x 711 x 711	801	610 x 610	801		620	207		3 at 25; 1 at 13
6	B	16 x 914 x 1067	144	141	0.64 x 1118 x 1270	144	1016 x 1168	144	282	282		2 at 25 mm	2 at 25 mm
7	B	13 x 508 x 508	340	88	0.64 x 711 x 711	340	610 x 610	340	263	263		3 at 25 mm	3 at 25 mm
9[c]	B	13 x 508 x 508	360	94	0.64 x 711 x 711	360	610 x 610	360	282	282		3 at 15 mm	3 at 25 mm
10	B	13 x 508 x 508	250	65	0.64 x 711 x 711	250	610 x 610	250	196	196		3 at 25 mm	3 at 25 mm
11	B	13 x 508 x 508	768	206	0.64 x 711 x 711	768	610 x 610	768	617	617		3 at 25 mm	3 at 25 mm
15	B	13 x 508 x 508	669	173	0.64 x 711 x 711	669	610 x 610	669	519	519		3 at 25 mm	3 at 25 mm
16	B	13 x 508 x 508	180	49	0.64 x 711 x 711	180	610 x 610	180	146	146		3 at 25 mm	3 at 25 mm
8[c]	C	Hex. 13 x 965 A/F and irreg.	111	114	Hex. 0.64 x 1219 A/F and irreg.	111	1473 x 610	102	683	683		6 at 25 mm	6 at 25 mm
		polygon	45		polygon	45	635 x 635	350					
							864 dia.	111					
							991 x 991	111					

[a] To be used in conjunction with Fig. 2-13.

[b] Class A metallic materials to be carbon steel, Class B metallic material to be Hastelloy X; all coverplates are with single attachment fixture.

[c] Special parts required: Zone 5 - 2 mid-edge retainers shared per coverplate.
Zone 9 - 4 each inlet fairing; inlet omega, support, and thermal shield.
Zone 16 - 3 each inlet fairing and support ring.
Zone 8 - 2020 graphite: 111 each hexagons 114 mm t x 965 A/F; 45 each irregular polygons 114 mm t; 936 each alumina pads 38 mm t x 216 mm dia; 468 each alumina pads 76 mm t; 468 each silica pads 51 mm t; 468 each alumina dowels 83 mm h x 76 mm dia; 468 each alumina dowels 146 mm h x 76 mm dia; 468 carbon steel cups; 468 carbon steel shims.

As shown in Figs. 2-12 and 2-13, the thermal barrier is divided into 17 zones, which are dictated by geometry or temperature regime. Table 2-11 presents the component sizes and quantities used for costing.

Excluding the top and bottom heads of the core cavity, virtually all of the coverplates will be curved. Of the curved plates, 85% are expected to have the same general dimensions [e.g., 508 x 508 mm (20 x 20 in.)]. These plates represent about 75% of the total area covered by thermal barrier. Efforts are being made to minimize the number of different curvatures of the plates and plate dimensions in the various cavities. For example, the 13 zones employing curved plates will require only four different radii of curvature. These can probably be shaped using progressive dies, thereby minimizing tooling cost.

Thermal Barrier Water Ingress Effects

Failure or malfunction of NSSS components or systems could cause water, in either liquid or vapor form, to be introduced into the primary coolant. While such incidents would have no impact on safety, protracted plant downtime becomes a major economic concern if dryout and removal of contaminants are prolonged.

Under certain circumstances, removal of entrapped water from the thermal barrier insulation can be time consuming. To assure that specified plant availability is achieved, several avenues have been explored:

1. Preventing or limiting potential leak paths through the thermal barrier seal sheets.

2. Collecting or containing water before it can enter the thermal barrier.

3. Preventing impinging water from reaching the fibrous insulation.

TABLE 2-11
2240-MW(t) HTGR-SC/C THERMAL BARRIER SIZES AND QUANTITIES[a]

Zone	Class	Coverplate[b] Size (mm) t x l x w	Coverplate[b] Qty	Coverplate[b] Area (m^2)	Seal Sheet[b] Size (mm) t x l x w	Seal Sheet[b] Qty	Blanket Size (mm) l x w	Blanket Qty	Total Insulation Reqd. (m^2) Saffil (25 mm)	Total Insulation Reqd. (m^2) Kaowool (25 mm)	Total Insulation Reqd. (m^2) Kaowool (13 mm)	Composition of Blanket Layers and Thickness (mm) Saffil	Composition of Blanket Layers and Thickness (mm) Kaowool
1	A	13 x 508 x 508	3600	929	0.64 x 711 x 711	3600	610 x 610	3600	929	2786		1 at 25 mm	3 at 25 mm
2	A	19 x 508 x 508	1672	431	0.64 x 711 x 711	1672	610 x 610	1672	431	1294		1 at 25 mm	3 at 25 mm
3	A	19 x 508 x 508	276	71	0.64 x 711 x 711	276	610 x 610	276	71	213		1 at 25 mm	3 at 25 mm
4	A	13 x 508 x 508	260	68	0.64 x 711 x 711	260	610 x 610	260	68	203		1 at 25 mm	3 at 25 mm
5[c]	A	Hex. 13 x 940 A/F and	111	103	Hex. 0.64 x 1143 A/F and irreg.	111	1016 x 1016 and irreg.	111	103	309		1 at 25 mm	3 at 25 mm
		irreg. polygons	45		polygons	45	polygons	45				1 at 25 mm	3 at 25 mm
6	A	16 x 914 x 1067 and irregular	288 432	441	0.64 x 1118 x 1270 and irregular	288 432	1016 x 1016 and irregular	288 432	441	1324		1 at 25 mm	3 at 25 mm
10	A	13 x 508 x 508	120	32	0.64 x 711 x 711	120	610 x 610	120		95	32		3 at 25; 1 at 13
12	A	13 x 508 x 508	153	39	0.64 x 711 x 711	153	610 x 610	153		118	39		3 at 25; 1 at 13
13	A	13 x 508 x 508	630	163	0.64 x 711 x 711	630	610 x 610	630		489	163		3 at 25; 1 at 13
14	A	13 x 508 x 508	801	207	0.64 x 711 x 711	801	610 x 610	801		620	207		3 at 25; 1 at 13
6	B	16 x 914 x 1067	144	141	0.64 x 1118 x 1270	144	1016 x 1168	144	282	282		2 at 25 mm	2 at 25 mm
7	B	13 x 508 x 508	340	88	0.64 x 711 x 711	340	610 x 610	340	263	263		3 at 25 mm	3 at 25 mm
9[c]	B	13 x 508 x 508	360	94	0.64 x 711 x 711	360	610 x 610	360	282	282		3 at 15 mm	3 at 25 mm
10	B	13 x 508 x 508	250	65	0.64 x 711 x 711	250	610 x 610	250	196	196		3 at 25 mm	3 at 25 mm
11	B	13 x 508 x 508	768	206	0.64 x 711 x 711	768	610 x 610	768	617	617		3 at 25 mm	3 at 25 mm
15	B	13 x 508 x 508	669	173	0.64 x 711 x 711	669	610 x 610	669	519	519		3 at 25 mm	3 at 25 mm
16	B	13 x 508 x 508	180	49	0.64 x 711 x 711	180	610 x 610	180	146	146		3 at 25 mm	3 at 25 mm
8[c]	C	Hex. 13 x 965 A/F and irreg.	111	114	Hex. 0.64 x 1219 A/F and irreg.	111	1473 x 610 635 x 635	102 350	683	683		6 at 25 mm	6 at 25 mm
		polygon	45		polygon	45	864 dia. 991 x 991	111 111					

[a] To be used in conjunction with Fig. 2-13.

[b] Class A metallic materials to be carbon steel, Class B metallic material to be Hastelloy X; all coverplates are with single attachment fixture.

[c] Special parts required: Zone 5 - 2 mid-edge retainers shared per coverplate.
Zone 9 - 4 each inlet fairing; inlet omega, support, and thermal shield.
Zone 16 - 3 each inlet fairing and support ring.
Zone 8 - 2020 graphite: 111 each hexagons 114 mm t x 965 A/F; 45 each irregular polygons 114 mm t;
936 each alumina pads 38 mm t x 216 mm dia; 468 each alumina pads 76 mm t;
468 each silica pads 51 mm t; 468 each alumina dowels 83 mm h x 76 mm dia;
468 each alumina dowels 146 mm h x 76 mm dia; 468 carbon steel cups; 468 carbon steel shims.

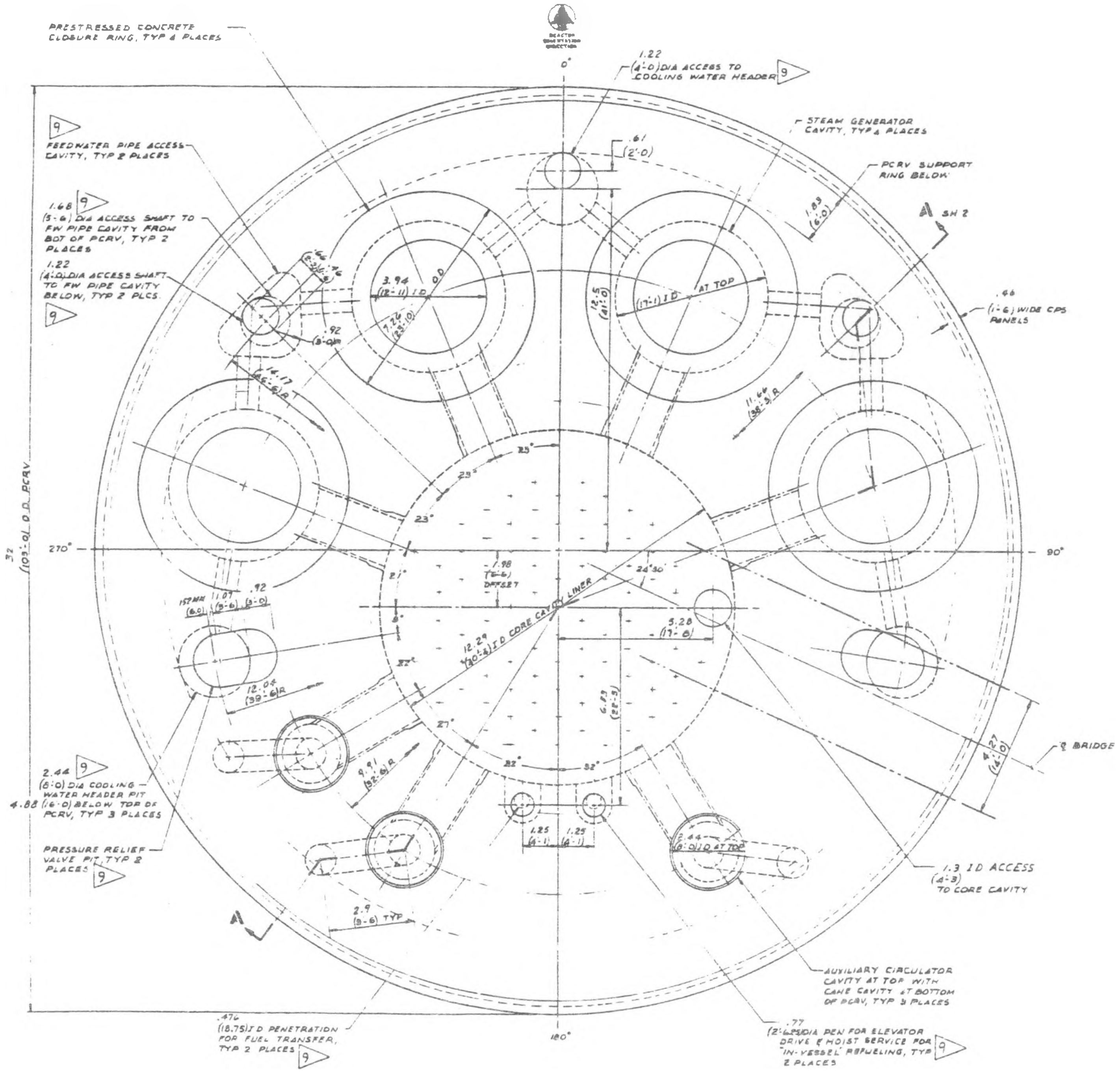

PLAN-PCRV TOP HEAD

SCALE : 1/64 (3/16 : 1 FT)

NOTES.

1. INSTALLATION PER GA SPEC NO. 900008
2. SYMBOL : [X] INDICATES THERMAL BARRIER ZONE NO.
3. INLET FAIRING FOR ZONE 9 & ZONE 16 TO BE INSTALLED AFTER ZONE 7 IS INSTALLED.
4. TOTAL AREA PER REACTOR (MEASURED AT LINER SURFACE).
5. CLASS A : ASTM A-36. CARBON STEEL COVER PLATES. ASTM A-606 SEAL SHEETS. KAOWOOL INSULATION. (SAFFIL USED SELECTIVELY)
   CLASS B : HASTELLOY-X COVERPLATES & SEAL SHEETS. KAOWOOL & SAFFIL INSULATION.
   CLASS C : 2020 GRAPHITE FOR FLOOR BLOCKS. ALUMINA AND FUSED SILICA FOR SUPPORT PADS. STAINLESS STEEL COVERPLATES AND CONTAINERS. KAOWOOL & SAFFIL INSULATION.
6. BLANKET SET CONSISTS OF LAYERS OF INSULATION MATERIAL AND IS NOT IN A COMPRESSED STATE.
7. ALL CLASS A & B COVERPLATES ARE TO BE DESIGNED FOR A SINGLE CENTRAL FIXTURE ONLY.
8. DIMENSIONS ARE SHOWN IN METERS WITH FEET & INCHES SHOWN ENCLOSED THUS (XX'-X).
9. NO THERMAL BARRIER REQUIRED IN THIS CAVITY.
10. ALL LINER & PCRV DIMENSIONS ARE REF ONLY. SEE DWG NO. 027024 FOR LINER & PCRV DIMENSIONS.

ZONE	CLASS (5)	QTY	INSTALLED THICKNESS IN MM (IN.)	AREA M² (FT²)	DRAWING NO.	DESCRIPTION
1	A	4	76 (3.00)	928.8 (9,998)		STEAM GENERATOR CAVITY, UPPER
2		4	76 (3.00)	431.5 (4,644)		MAIN CIRCULATOR CAVITY
3		4	76 (3.00)	70.9 (763)		CLOSURE, MAIN CIRCULATOR CAVITY
4		4	76 (3.00)	67.6 (728)		UPPER MAIN CROSS DUCT
5	A	1	76 (3.00)	103 (1108)		TOP HEAD, CORE CAVITY.
6	A	1	76 (3.00)	441.5 (4752)		UPPER SIDEWALL, CORE CAVITY.
	B		76 (3.00)	141.2 (1520)		
7	B	1	127 (5.00)	87.6 (943)		LOWER SIDEWALL, CORE CAVITY.
8	C	1	356 (14.00)	113.8 (1225)		BOTTOM HEAD, CORE CAVITY.
(3) 9	B	4	152 (6.00)	94 (1012)		LOWER MAIN CROSS DUCT.
10	A	4	76 (3.00)	31.7 (341)		SUPERHEAT PENETRATION.
	B		127 (5.00)	65.5 (705)		
11	B	4	127 (5.00)	205.8 (2215)		STEAM GENERATOR CAVITY, LOWER.
12	A	3	76 (3.00)	39.5 (424)		UPPER AUXILIARY CROSS DUCT
13	A	3	76 (3.00)	163 (1755)		AUXILIARY CIRCULATOR CAVITY
14	A	3	76 (3.00)	206.5 (2222)		AUXILIARY CIRCULATOR DUCT
15	B	3	127 (5.00)	173 (1862)		CAHE CAVITY
(3) 16	B	3	127 (5.00)	48.6 (523)		LOWER AUXILIARY CROSS DUCT
17	B	1	N/A	SEE DWG 027022		PERIPHERAL SEAL.

(4) TOTAL AREA: 3413 (36,740)

		M²	FT²	%
CLASS	A :	2484	26,735	73
CLASS	B :	816	8,780	24
CLASS	C :	114	(1225)	3

PARTS LIST

2240 MW(t) HTGR-SC/C

GENERAL ATOMIC COMPANY

THERMAL BARRIER GENERAL ARRANGEMENT

E 32334 027025 /2

027025 1/2 SH 1 OF 2

Fig. 2-12. Thermal barrier general arrangement: plan view

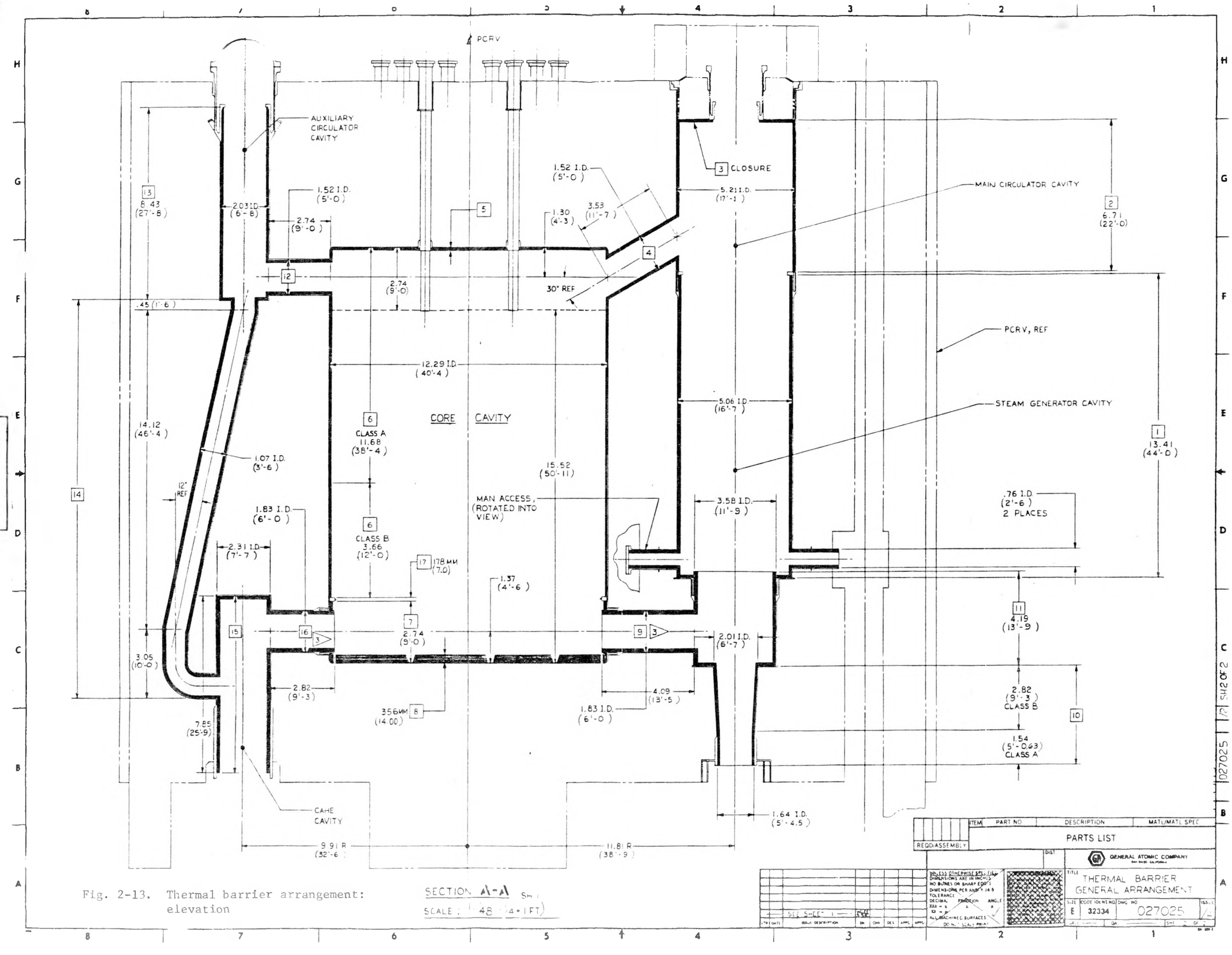

Fig. 2-13. Thermal barrier arrangement: elevation

SECTION A-A SH 1
SCALE : 1/48 (1/4" = 1FT)

ITEM	PART NO	DESCRIPTION	MATL/MATL SPEC
REQD/ASSEMBLY		PARTS LIST	

GENERAL ATOMIC COMPANY

TITLE: THERMAL BARRIER GENERAL ARRANGEMENT

SIZE E | CODE IDENT NO 32334 | DWG NO 027025 | REV

SEE SHEET 1

UNLESS OTHERWISE SPECIFIED DIMENSIONS ARE IN INCHES. NO BURRS OR SHARP EDGES. DIMENSIONS PER ANSI Y14.5 TOLERANCE DECIMAL XXX = ± XX = ± FRACTION ± ANGLE ± ALL MACHINED SURFACES 125

027025 SH 2 OF 2

Prevention of significant degrees of permeation in order to prevent unacceptable overheating of the liner by convection heat flow is one of the basic premises of the thermal barrier concept. Permeation is limited by continuous, overlapping seals, and such restricted permeation can occur only when localized differential pressures induce bypass flow.

It is possible that the same permeation flow paths that may induce vapor deposit within the insulation can work equally as well in reverse to remove moisture with permeation of dry helium. It is concluded that dryout of the thermal barrier will be excessively time consuming only in locations where water can enter the thermal barrier by mechanisms other than permeation.

Design of a water-resistant fibrous insulation thermal barrier thus needs to contend principally with areas that may be exposed to impinging water or pools of standing water on horizontal surfaces or cavities. A proposed method of modifying the thermal barrier design locally to permit run-off and containment of impinging water is shown in Fig. 2-14. The catch basin, in this case shown with a maximum capacity of 0.45 m^3 (898 gal), is located at the lower end of the steam generator cavity, sitting above the lower horizontal surface thermal barrier. This arrangement was devised as a possible secondary backup to the main catch basin within the steam generator, which would have a similar capacity.

As presently conceived and developed for the HTGR pressure vessel, a completely sealed, impermeable fibrous insulation thermal barrier is impractical. However, a water-resistant thermal barrier that will exclude practically all impinging water can probably be achieved with some revisions to the seal components of the present design. Such changes to the present basic design, which would assure shedding of impinging water, will probably affect the sequence and procedures of installation. It is likely that a fixed procedural pattern of sequential installation within each zone would have to be employed. Figure 2-15 shows an example of progressive layup of the thermal barrier that is similar to the reference design but has seal

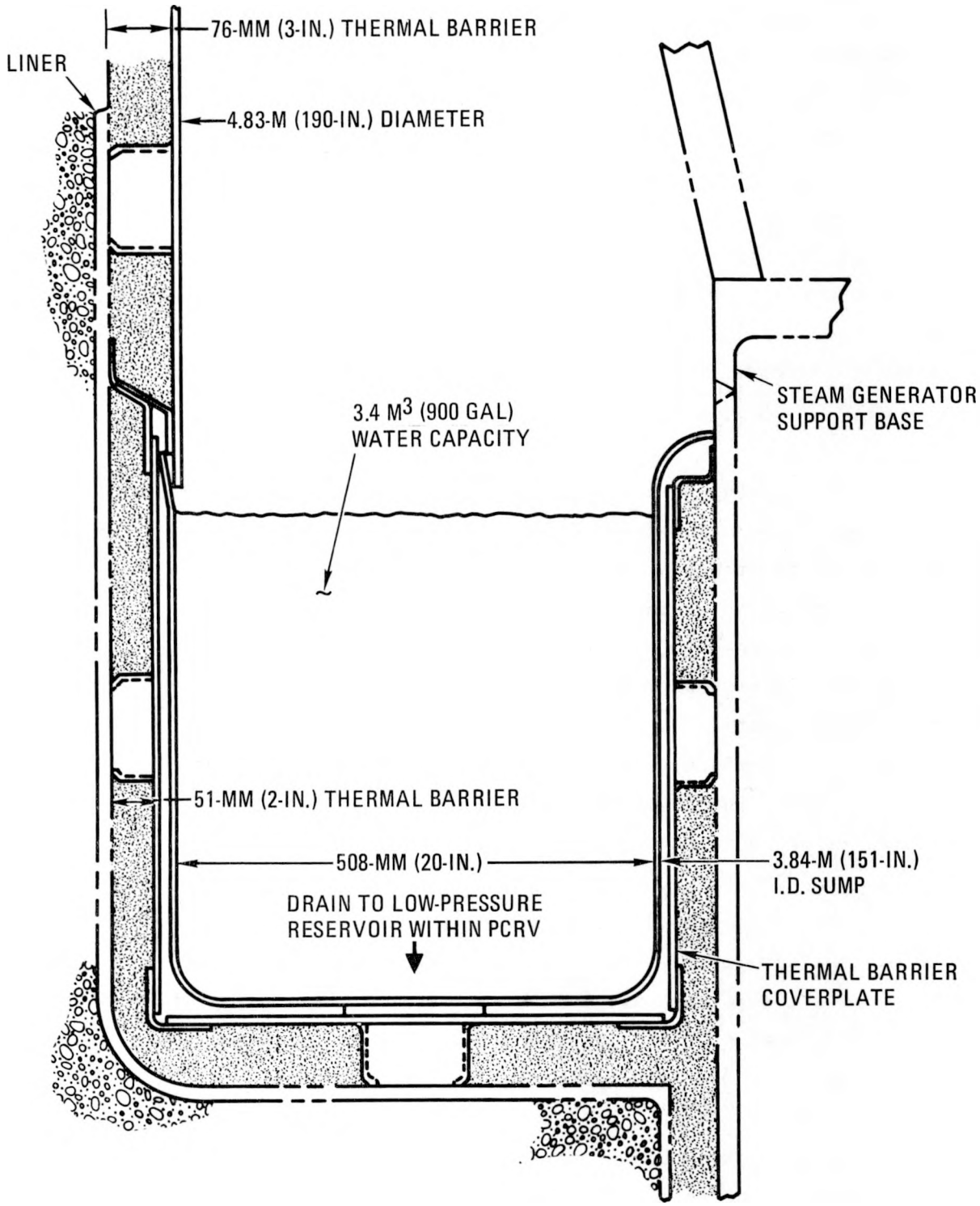

Fig. 2-14. Proposed thermal barrier design for handling water ingress

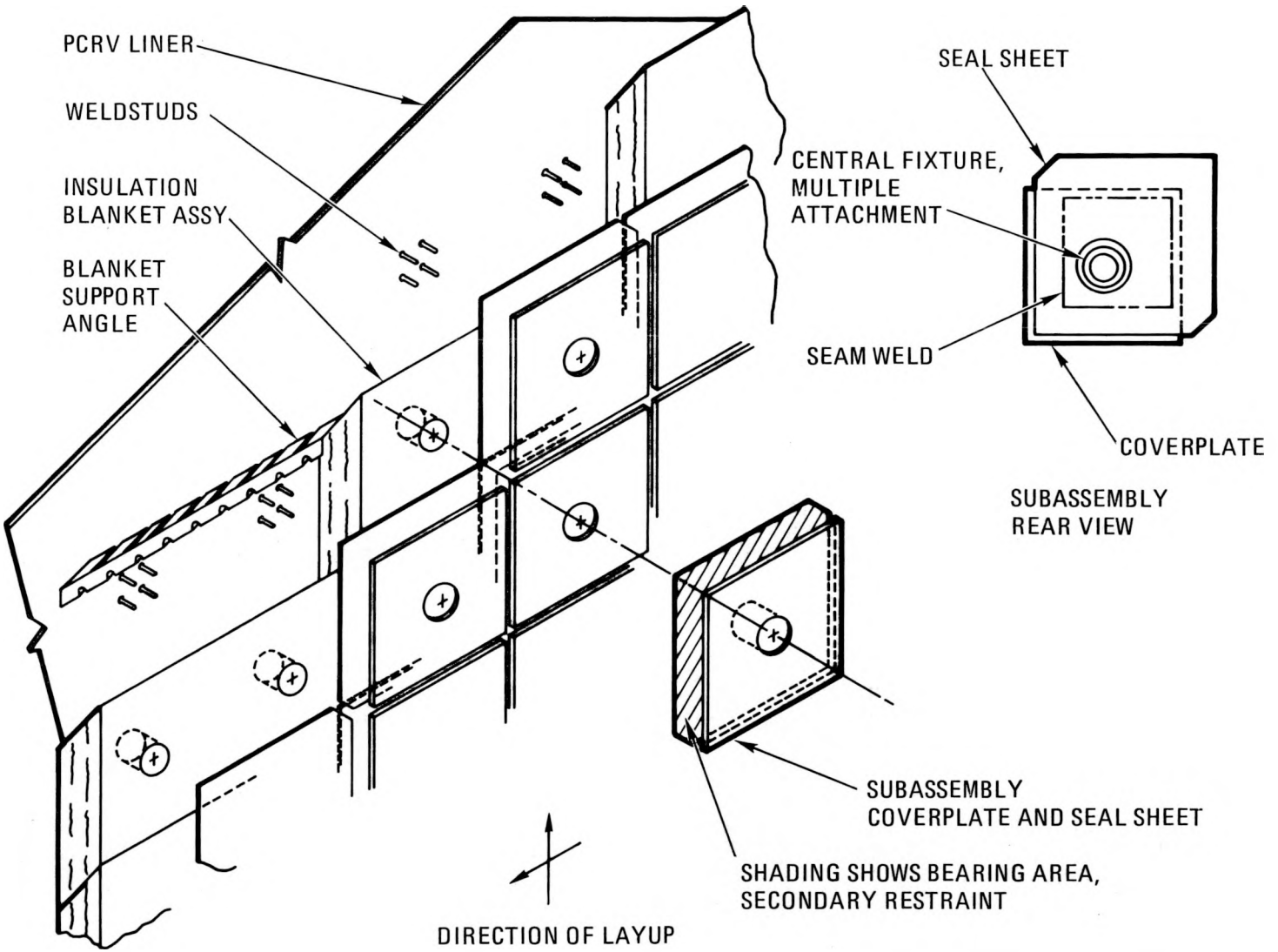

Fig. 2-15. Thermal barrier progressive layup with single fixture coverplate

sheets joined to the coverplates. The combined seal sheet/coverplate/fixture assemblies would be installed counterclockwise, starting from the bottom. Special "starter" and "closing" seal sheets are necessary in each row. This arrangement with the seal sheets being secured (pre-assembled) to the coverplate and installed in a fixed sequence is very similar to the FSV thermal barrier design, where the seal sheets were spot welded to the coverplates at the factory.

Acoustic Influence Studies

The thermal barrier is subjected to cyclic pressure loads resulting from noise generated mainly by the circulators and from turbulence within the flowing primary coolant. Past analyses have considered only the design acoustic pressure loads.

Based on these analyses, the allowable size of a thermal barrier coverplate has been determined to be a strong function of the following three parameters:

1. $\dot{y}$ = the design allowable peak velocity of the coverplate.
2. ξ = the damping ratio.
3. P_p = the design peak acoustic pressure.

During this reporting period, the values of these parameters have changed as follows:

1. $\dot{y}$ was reduced by a factor of 0.4 for Class A coverplates with Kaowool as the reference fibrous insulation. $\dot{y}$ remains unchanged for Class B coverplates. For this reason it was believed to be cost effective to change the reference Class A fibrous insulating material in most zones from Kaowool to a composite blanket assembly of Saffil and Kaowool.

2. ξ remains unchanged owing to lack of additional data on the reference coverplate design. However, testing scheduled later during FY-82 should help quantify ξ with more confidence.

3. P_p values have been determined to be conservatively high and will need further refinement in order to represent the current reference circulator design.

During the first half of FY-82, a study was completed which estimated the magnitude (P_p') and frequency (f) of turbulence-induced pressure fluctuations and evaluated their effect on the thermal barrier. The estimates show that locally, in at least eight thermal barrier zones, the magnitude (P_p') could be high compared with the acoustically induced fluctuations that are now controlling the thermal barrier design. The eight thermal barrier zones are (see Figs. 2-12 and 2-13):

1. Zone 7 (lower core cavity sidewall), especially near the inlet to the lower main cross duct.

2. Zone 9 (lower main cross duct).

3. Zone 11 (lower steam generator cavity).

4. Zone 2 (main circulator cavity), especially near where primary coolant exits the circulators and enters the upper main cross duct.

5. Zone 1 (steam generator cavity), especially where primary coolant exits the steam generator.

6. Zone 4 (upper main cross duct).

7. Zone 5 (top head of core cavity).

8. Zone 6 (sidewall of core cavity), especially near the exit of the upper main cross ducts.

While the magnitude of P_p' could be high, it is estimated that the associated frequency (f) will be low compared with the first fundamental frequency of the coverplates. As a result, the turbulence-induced pressure fluctuations are not as controlling as the pressure fluctuations that are acoustically induced. Testing with suitable models is recommended to quantify P_p' and f with more confidence. Tests with such models have been included in the overall planning of the 2240-MW(t) HTGR-SC/C plant.

Bottom Head Thermal Barrier Configuration Studies

The design function of the bottom head thermal barrier is to support the core while insulating the PCRV liner and concrete from the hot primary coolant. The reference bottom head thermal barrier (Fig. 2-16) incorporates stacks of ceramic support pads along with fibrous insulation material sandwiched between the liner and graphite cover blocks. As shown in Fig. 2-17, the ceramic materials selected for the pads are fused silica and alumina.

This ceramic pad design is an extension of FSV technology. Ceramics were selected for the FSV design primarily because of their ability to withstand high temperatures during loss of main loop cooling conditions. For such a postulated event, the reactor would be scrammed and the core residual heat removed via the liner cooling water system. This scenario would result in primary coolant temperatures substantially above 1093°C (2000°F) at the bottom head.

For a loss of main loop cooling, the reference HTGR-SC/C plant uses a CACS which maintains the primary coolant temperature at substantially lower temperatures. These lower temperatures introduce the possibility of replacing the ceramic pad design with a metallic design. Two bottom head thermal barrier designs which rely on metallic components to support the core have been evaluated. In both these design concepts, metallic (either

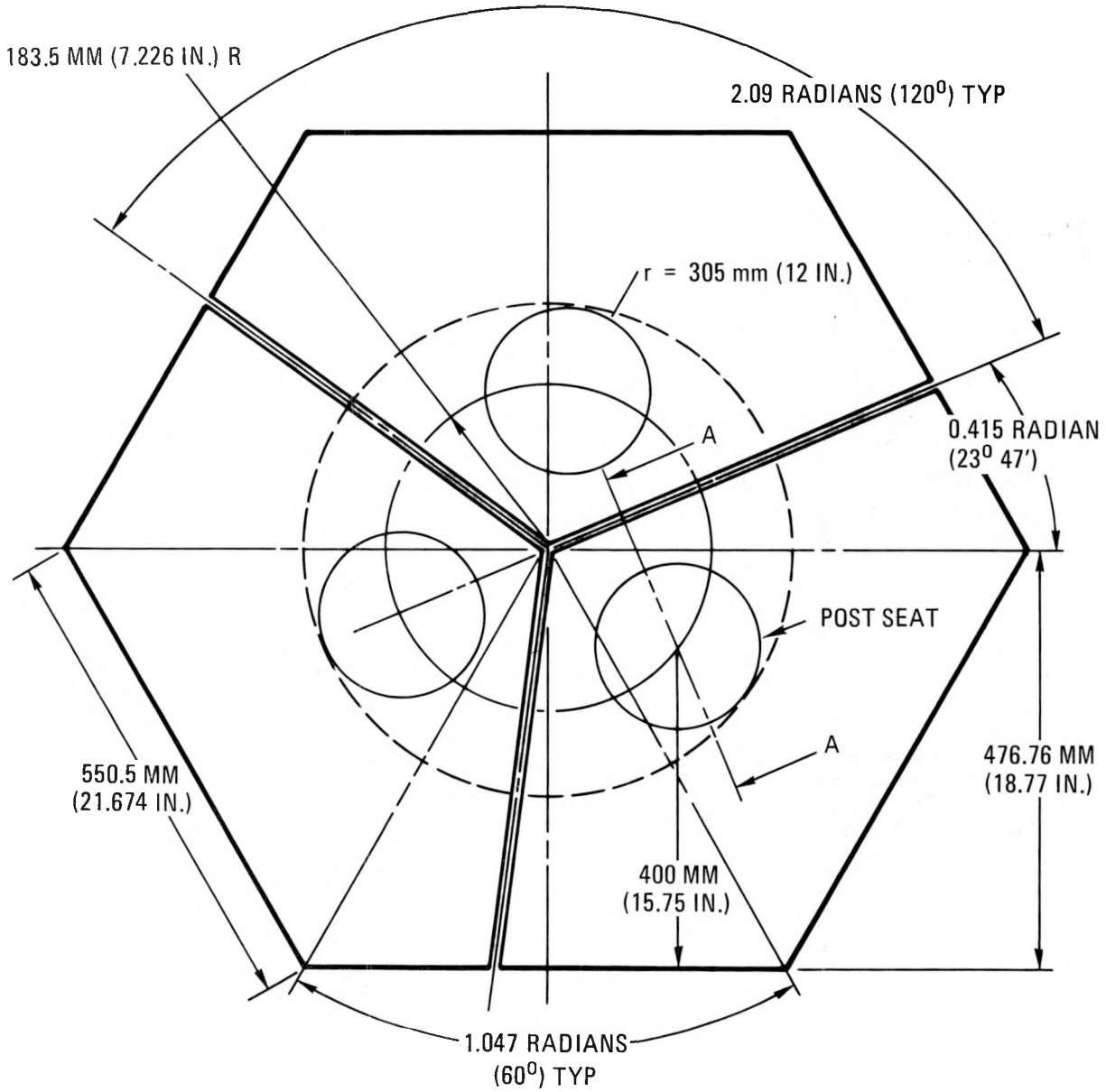

Fig. 2-16. Reference Class C thermal barrier for HTGR-SC/C plant

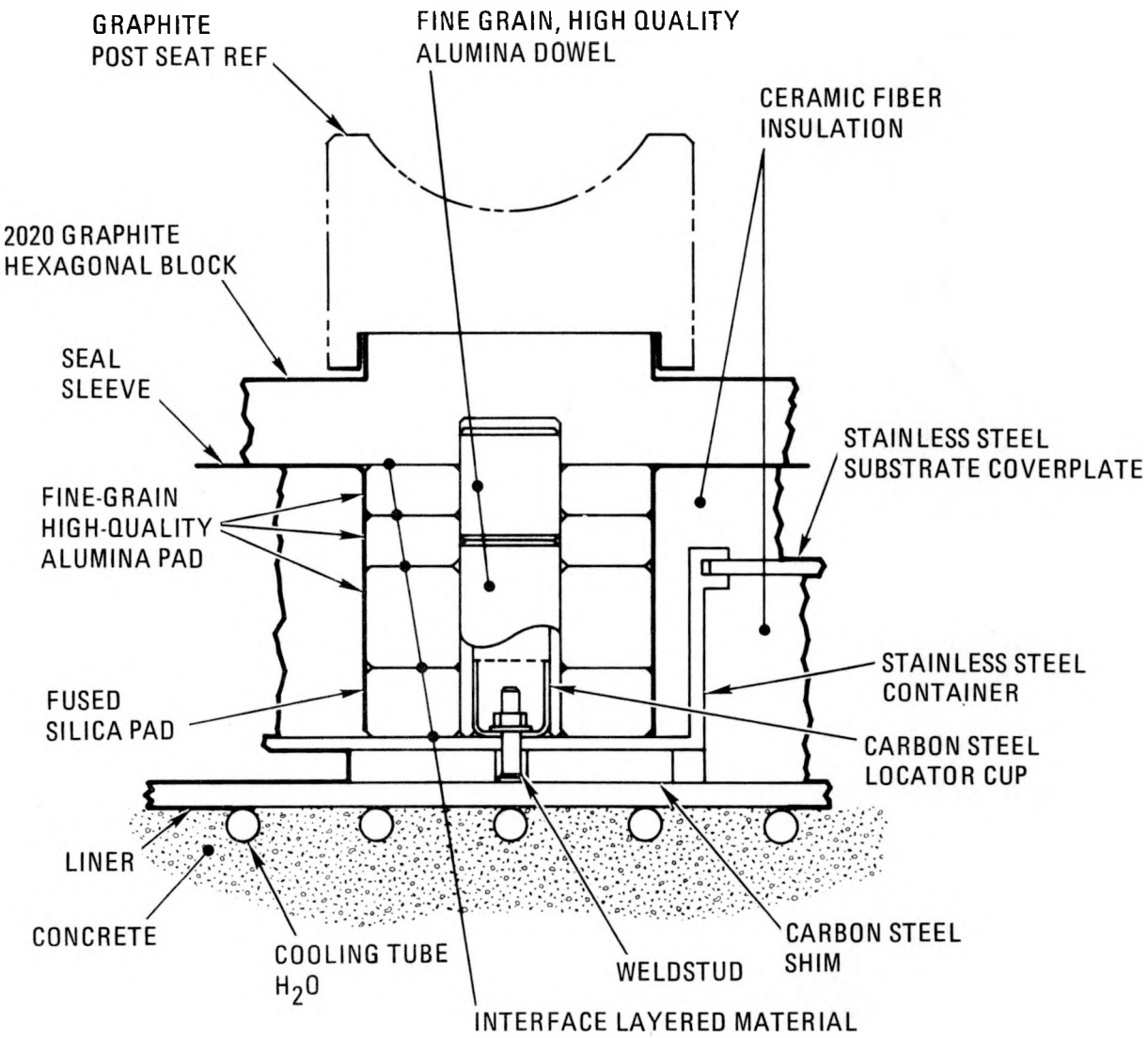

Fig. 2-17. Reference Class C thermal barrier for HTGR-SC/C plant (Section A-A of Fig. 2-16)

Hastelloy X or Alloy 713LC) components would replace the three alumina and one fused silica pads as well as the alumina dowels.

Figure 2-18 shows a conceptual design using Hastelloy X. It consists of a top cap supported by a cylinder filled with fibrous insulation. The top cap could be machined out of plate material, while the cylinder could be manufactured by forming plate material into a cylindrical shape and then seam welding the edges together. Figure 2-19 shows a similar design using Alloy 713LC. In this case the top cap and cylinder would be cast into an integral part. Both designs incorporate a hold-down mechanism that positions the graphite cover blocks and metallic support structure prior to installing the reactor core. Without a hold-down mechanism the compressed fibrous insulation could force the cover blocks and metallic support structures out of position.

Both metallic design alternatives are viable replacements for the ceramic pad design in the 2240-MW(t) HTGR-SC/C plant. The metallic design using Hastelloy X is the primary candidate to replace the ceramic pad design because of its strength and the fact tht Hastelloy X is the reference Class B thermal barrier metallic. However, there are still unresolved issues which require additional material data and design work prior to a formal recommendation of design change and implementation in the HTGR-SC/C program. Further design evaluation and a formal recommendation are scheduled for the end of FY-82.

2.9. NEUTRON AND REGION FLOW CONTROL (6032120001)

2.9.1. Scope

The scope of this task is to refine the conceptual design of the neutron and region flow control system as required to support the HTGR Decision Package through the preparation of a preliminary system description document, updating of the BOP interface data, and updating of equipment cost estimates.

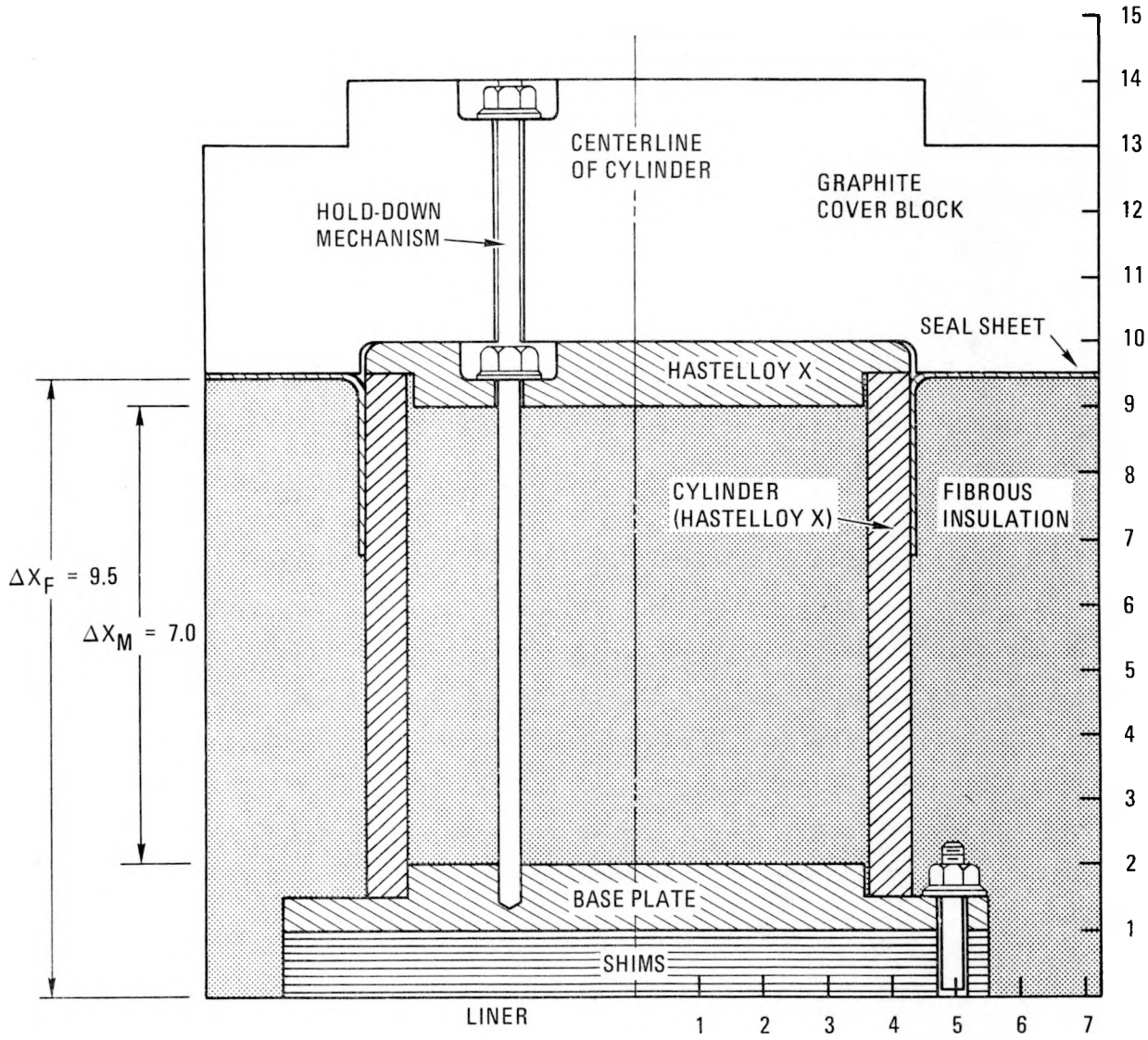

Fig. 2-18. Hastelloy X bottom head thermal barrier configuration

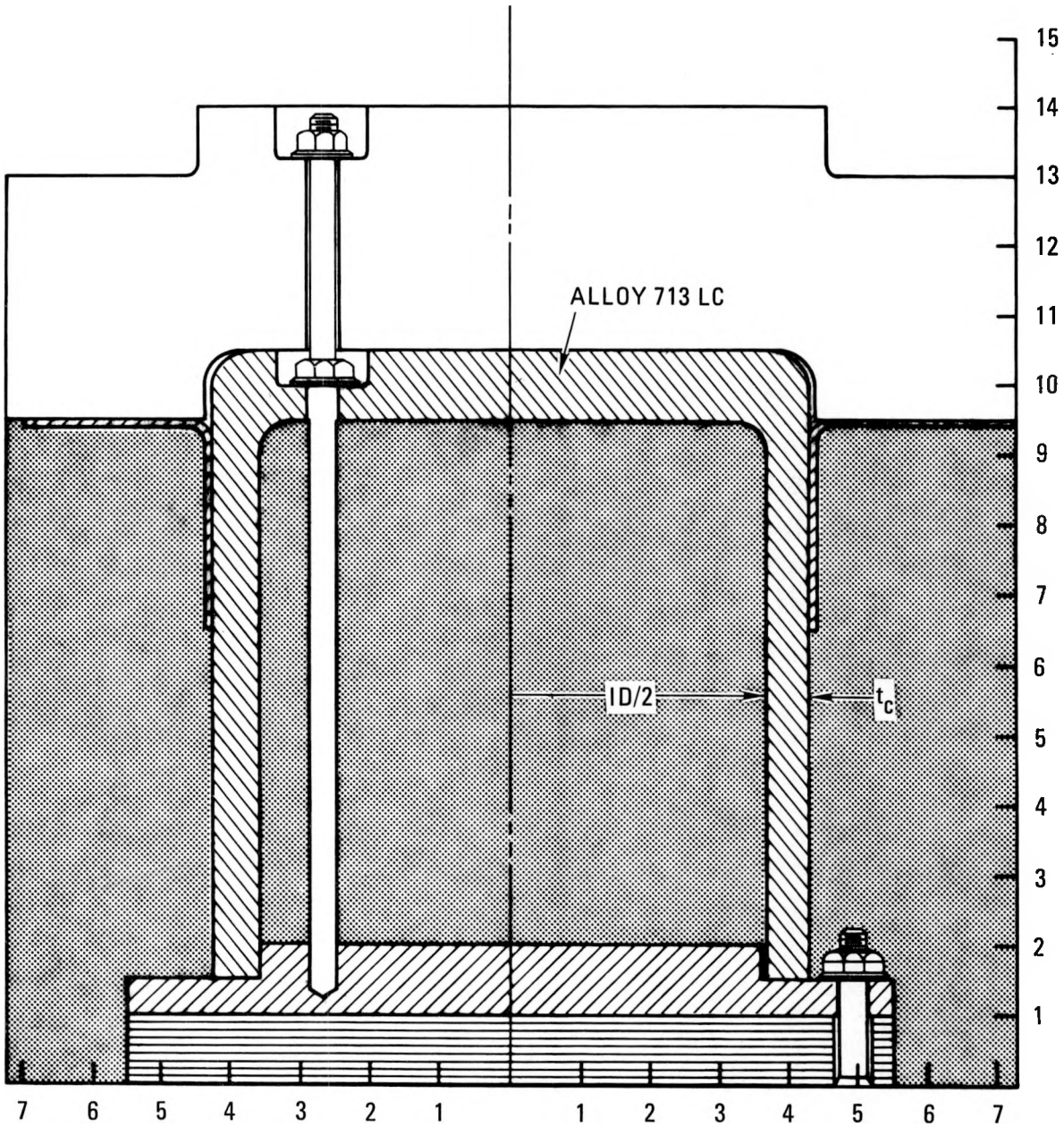

Fig. 2-19. Alloy 713LC bottom head thermal barrier configuration

2.9.2. Discussion

Some of the main factors causing design changes in the neutron and region flow control system were the adoption of the in-vessel refueling concept, the improved core design to minimize core fluctuations, and the development of the Toshiba fission chamber for use with the in-core flux mapping units (IFMUs). Approximately 15 layouts were updated to reflect the current design of the control and orifice assemblies which are installed in penetrations in the top head of the PCRV.

The neutron and region flow control system consists of two major subsystems: The neutron control subsystem and the primary coolant flow control subsystem. The neutron control subsystem comprises (1) the normal flux control and reactor shutdown system, which includes neutron detectors, power rods, and control rod pairs, (2) the reserve shutdown system (RSS), (3) the movable IFMU system, and (4) the movable startup detector system. The primary coolant flow control subsystem consists of variable orifices and drives and helium outlet temperature thermocouples for each core region.

Each of the above subsystems includes equipment as appropriate for shielding, penetration flow restriction, actuation, control, and indication. The rod drives, actuators, and mechanical components of these sybsystems are integrated into control and orifice assemblies (see Fig. 2-20) which normally are housed in refueling penetrations in the top head of the PCRV.

The neutron control subsystem uses ex-core flux detectors, the power rods, the control rods, and/or the reserve shutdown material to adjust core reactivity as required to meet the demands of the plant control system, the plant protection system, or the plant operator.

The region flow control subsystem adjusts the helium flow through regions of the core to match region power by incrementally positioning each adjustable core region inlet orifice valve when commanded by the plant operator on the basis of the core region outlet helium temperature measurements.

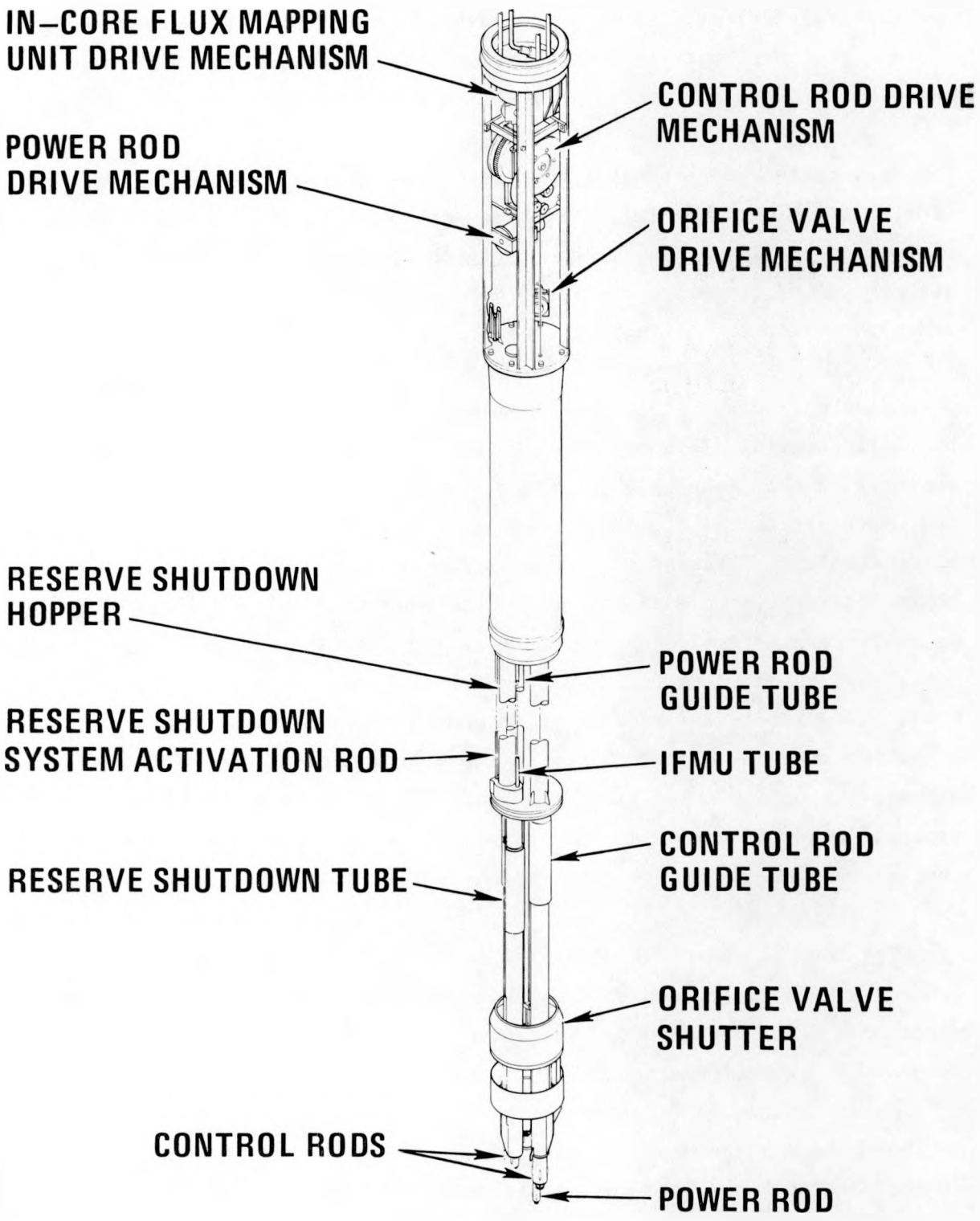

Fig. 2-20. Isometric view of control and orifice assembly

Reactor in-core flux distribution and startup range neutron measurements are also determined by using movable detectors in selected core locations. The core instrumentation system also measures core region outlet temperatures with thermocouples inserted through sidewall penetrations.

Appropriate controls together with indications of individual rod position, rod motion, rod limit of travel and abnormal cable tension, reactor power (flux), helium flow control orifice valve position, reserve shutdown system status, in-core and startup detector position and flux measurements, and core region outlet temperatures are provided in the control room.

Figure 2-20 shows an overall view of the control and orificing assembly, illustrating all subsystems and their locations. The basis of the assembly is the gamma shield/upper structure/neutron shield subassembly. The upper structural frame, which is bolted to the gamma shield, supports all mechanisms. Because of the gamma shield, the neutron shield, and the thermal barrier, the environment in this area is relatively mild. The assembly remains inside the concrete of the PCRV down to the thermal barrier. The guide tubes for control and power rods, reserve shutdown material, and orifice valve actuation extend through the upper plenum to the interface with the plenum blocks on top of the active core. The orifice valve rests on the upper plenum blocks. The lower guide tubes have telescoping joints to compensate for height variation and thermal movement of the core as well as lateral offset due to tolerances or seismic events.

The control rod drive mechanism is located in the upper part of the control and orificing assembly as shown in Fig. 2-20. The mechanism consists of a dc torque motor, which drives the dual cable storage drums through 10:1 gear reduction. The control rods are lowered and raised through a flexible, aircraft-quality stainless steel cable which is taken up on the cable storage drums. Small guide rollers locate the cable in the proper position above the gamma shield penetrations.

The motor, gears, and drums are mounted inside a frame attached to the control and orifice upper support structure by means of a pivoting support

shaft. The rotation of the mechanism is resisted by a redundant load cell, which monitors the cable load that the weight of the control rods causes in the support cables. This device is used to detect a stuck control rod or a broken control rod cable.

The control rod position is monitored by dual potentiometers, which are driven through a reduction gear from the drum shaft.

Load resistors are provided to slow down the control rods in case of power failure and free wheeling of the dc drive motor.

Two electrical systems provide power and signals to the mechanism for redundancy. One load cell and one position indicator are grouped together, and their wires are separated from the other system, which supplies the other load cell, the other position indicator, and the drive motor.

Motor and drum shaft bearings are lubricated with a special grease developed for this type of low-radiation and moderate-temperature application. The lubricant has been subjected to long-duration tests in helium, which show that the possibility of bearing seizure from deterioration of the lubricant is minimal. Relubrication of all bearings at maintenance intervals is planned.

The power rod drive mechanism and its location in the control and orifice assembly is shown in Fig. 2-20. The mechanism is compact and is mounted just above the support ledge in the refueling penetration.

The drive train utilizes several components that are also specified for the orifice valve drive system. The output shaft of the speed reducer drives a storage drum which raises the power rod by wrapping a small stainless steel cable in precut grooves on the outer surface of the drum.

The mechanism is mounted on a frame attached to the control rod drive upper support structure through the load cell and two guide pins. The load

cell carries the weight of the mechanism, cable, and power rod, and the guide pins provide proper alignment.

Two guide rollers direct the power rod support cable to the correct location of the power rod channel.

The reserve shutdown system consists of a storage hopper containing the cylindrical boronated graphite shutdown material, the fuse link actuator, which will open the hopper gate upon operator action by means of the actuation rod, and the reserve shutdown tubes, which guide the reserve shutdown material from the hopper into a special channel within the active core control column. Figure 2-21 shows the arrangement of the reserve shutdown system within the control and orificing assembly.

The reserve shutdown hopper is a stainless steel tube within the control rod guide tube system, extending through the refueling plenum from below the thermal barrier to the circular plate on top of the lower guide tubes. The hopper is filled with cylindrical boronated graphite neutron absorber pellets. A gate at the lower end of the hopper retains the material. After the gate is opened, the reserve shutdown system material is channeled through a funnel into the reserve shutdown system guide tube, which is telescoping and capable of following lateral core movements by means of an articulating joint just like the lower guide tubes of the control rod system. The guide tube directs the reserve shutdown system material into the channel provided within the control column. The general arrangement of the reserve shutdown system hopper is shown in Fig. 2-22.

The redundant fuse link actuator is shown in Fig. 2-23. Redundancy is required because the system is safety related. Therefore, two fuse link actuators and a small cable routed over the rollers support the actuation rod for the hopper gate. The fuse link actuator proper is a braided multistrand aluminum wire rope. Each aluminum wire is surrounded by a thin palladium jacket. Whenever sufficient electric energy is sent through the fuse link wire, an exothermic chemical reaction between the palladium and the aluminum takes place, melting the wire and severing the fuse link. This

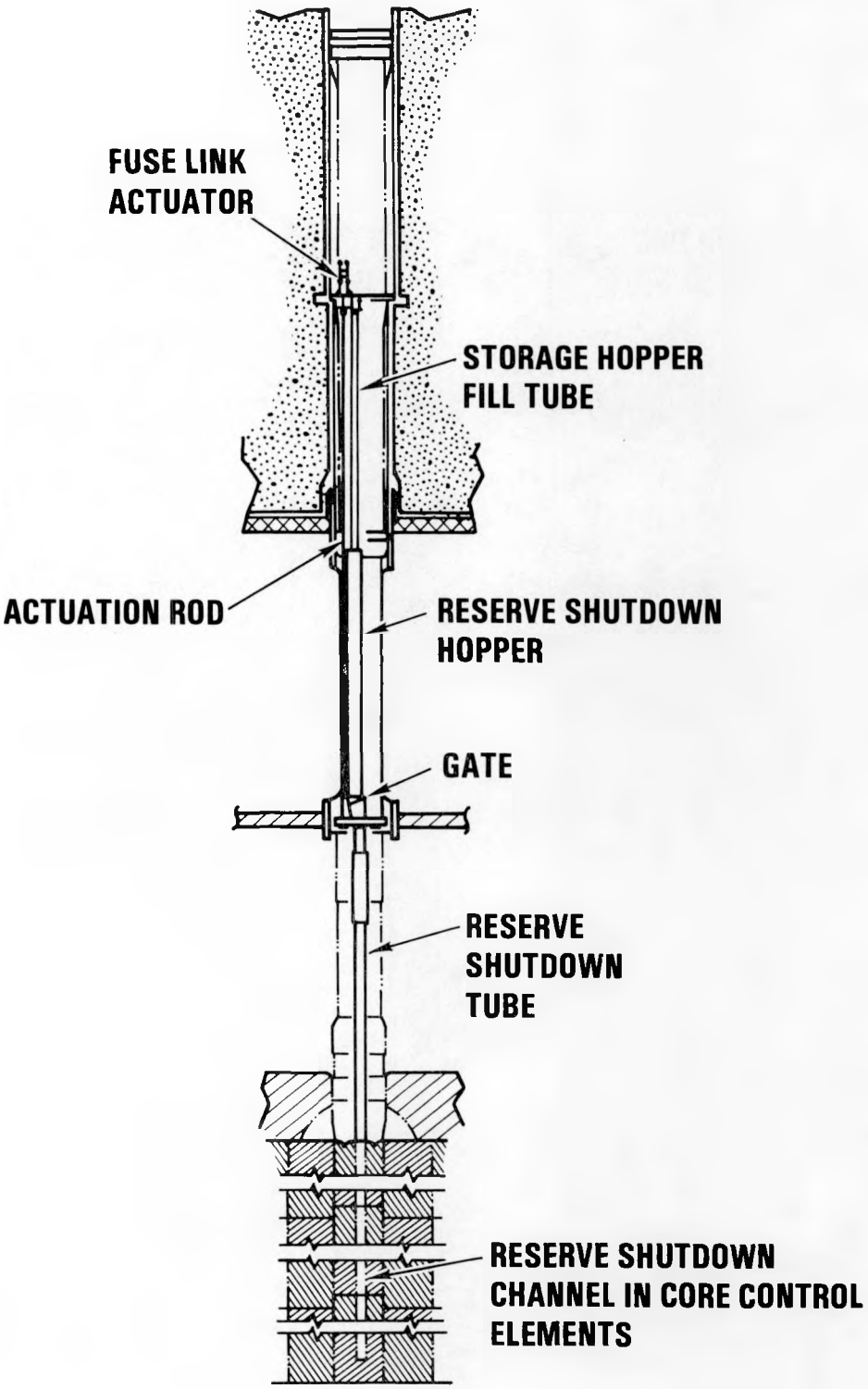

Fig. 2-21. Reserve shutdown system

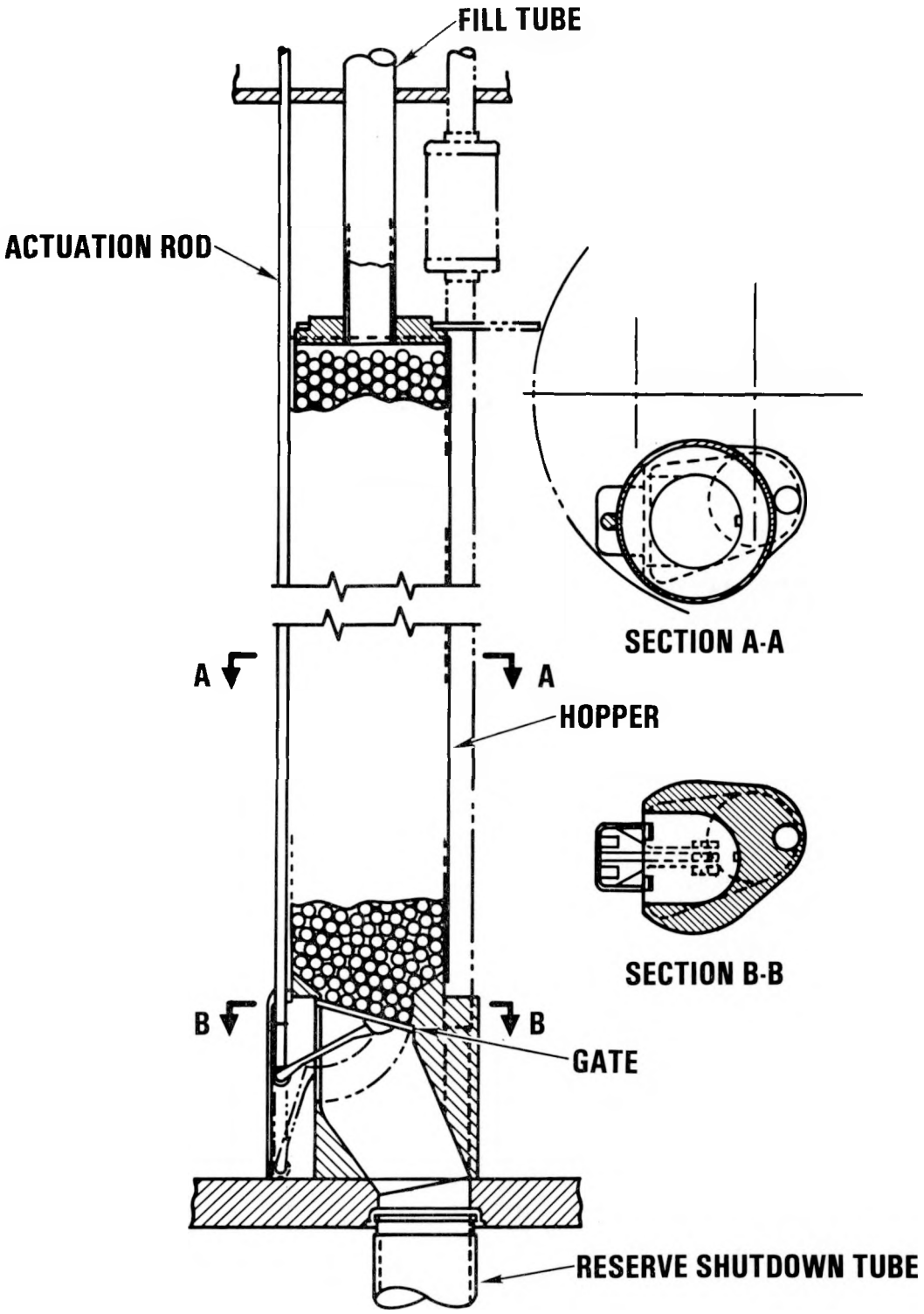

Fig. 2-22. Reserve shutdown system hopper

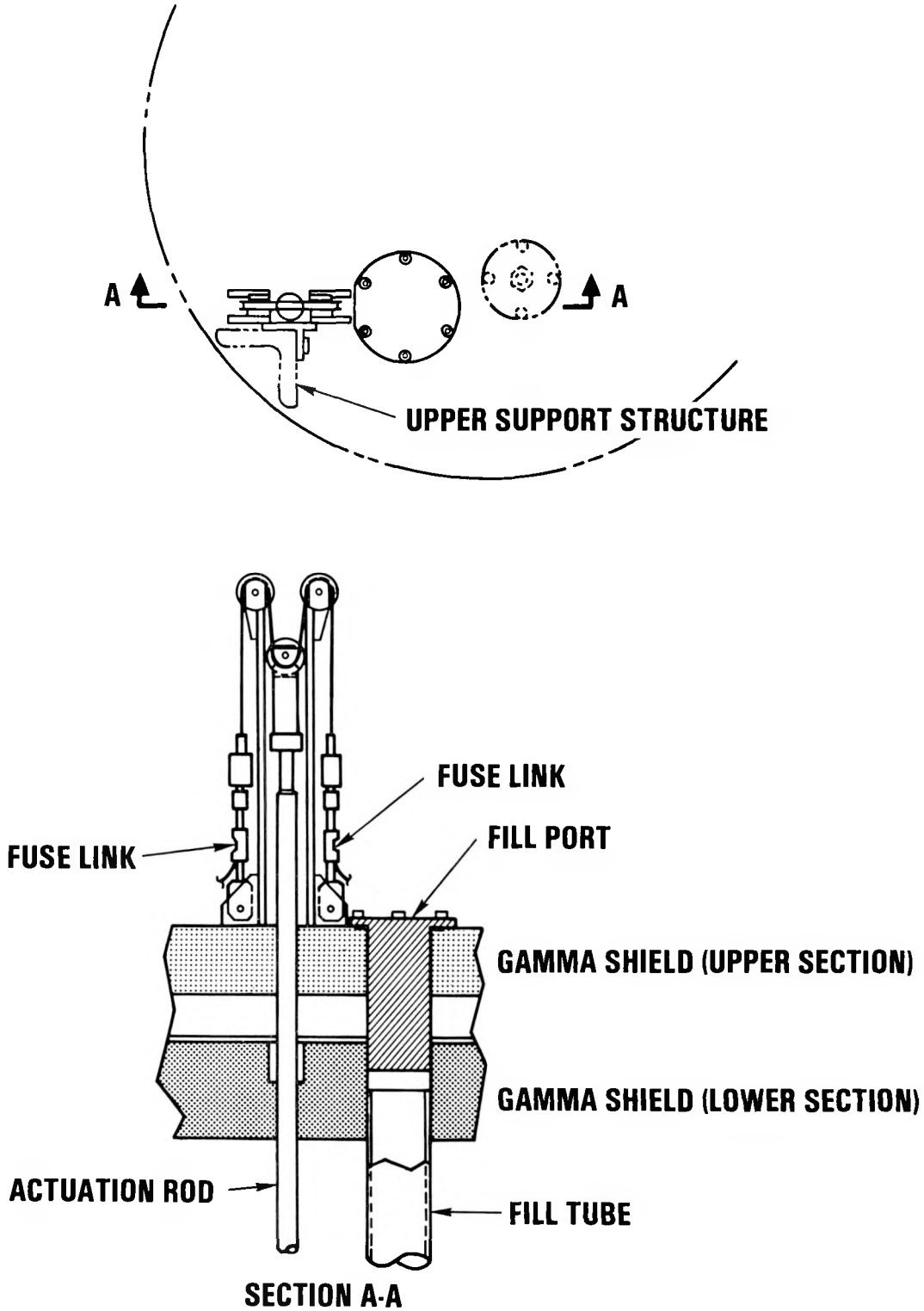

Fig. 2-23. Reserve shutdown system fuse link actuator

allows the actuation rod to drop and the hopper gate to open, subsequently releasing the reserve shutdown system material into the core.

In order to avoid creep problems, the fuse link itself is designed with a large margin of safety. Since this would require an excessive amperage to start the reaction, a small starter wire of only six strands is provided and wrapped tightly around the load-carrying strands of the fuse link. Upon actuation, a small amount of current is sufficient to start the reaction in the starter wire, which carries it over to the main link.

The flow control orifice system is shown in Fig. 2-24. The drive mechanism is located within the protected area of the control and orifice assembly, while the valve sits within the core plenum elements. The valve shutter is actuated from the mehanism through a stainless steel cable.

The orifice valve drive mechanism is supported by a hollow shaft, which extends down along the centerline of the control and orifice assembly to the orifice valve structure. The valve structure, in turn, is supported by the central plenum element in the core region. This arrangement enables the entire flow control orifice system to follow core movements without disrupting the position of the valve shutter. Guide rollers running on the angle irons of the upper structure prevent the drive mechanism from rotating.

The drive mechanism consists of an electric stepping motor which rotates a cable pulley through a harmonic drive speed reducer. The actuating cable is attached to the cylindrical gate of the orifice valve and moves the gate between the "open" and "closed" positions. Mechanical stops limit the valve stroke. The motor can be driven against the stops and stalled for an indefinite time without detrimental effects; therefore, no limit switches are provided. The position of the valve is indicated by a single-turn potentiometer that is coupled to the cable pulley.

The general arrangement of the orifice valve is shown in Fig. 2-25. The valve is supported by the center plenum block. It fits closely into a round opening of the upper plenum blocks. A movable cylindrical shutter is

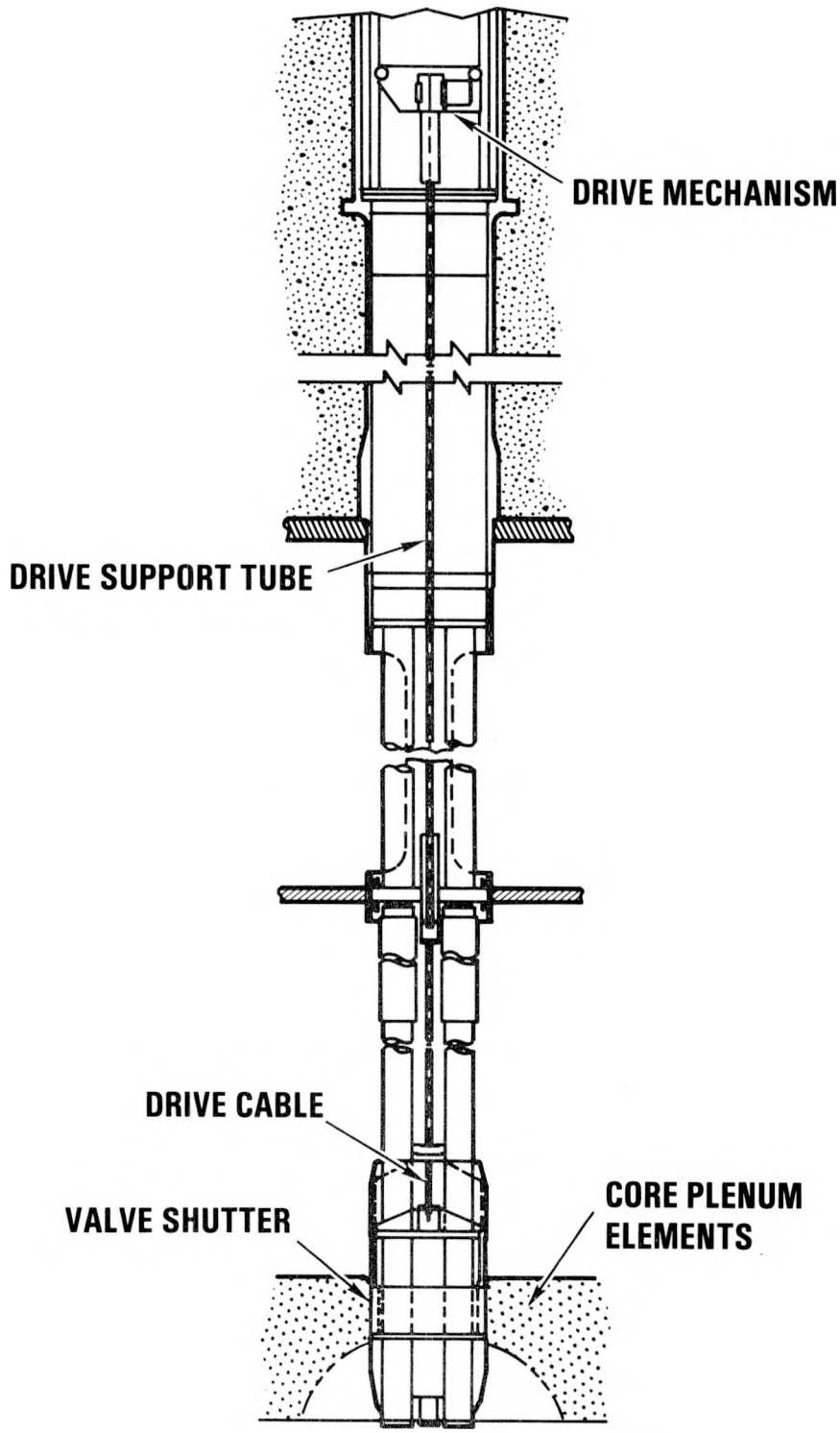

Fig. 2-24. Flow control orifice system

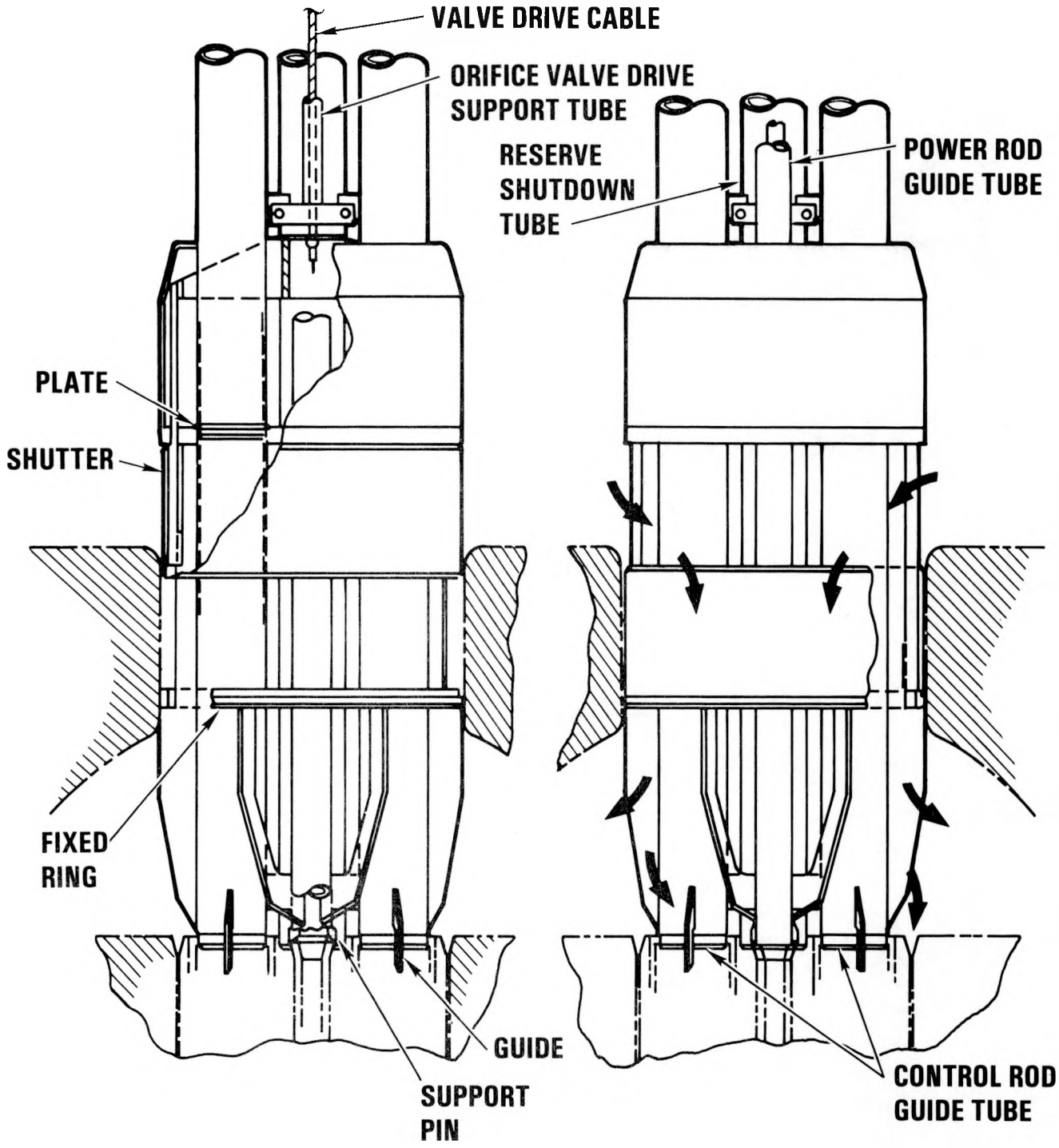

Fig. 2-25. Orifice valve

used to open or close the flow path for the cooling gas. Therefore, no additional forces from pressure differential act on the shutter and the shutter control cable. The fixed valve structure is attached to the control and power rod guide tubes and the reserve shutdown guide tube. These connections allow the valve some freedom of movement, which is needed when the control and orifice assembly is installed in the reactor. All metal surfaces that can slide relative to each other are protected from self-welding by a flame-sprayed coating of chromium carbide.

Twelve IFMUs are used to determine the axial thermal neutron flux profile of an HTGR operating between 5% power and 125% rated power. Each IFMU consists of a Toshiba Type FS-3 fission chamber detector attached to the end of a hollow helically wire wrapped drive cable containing the detector electrical leads. The drive mechanism is located in the upper portion of a control and orifice assembly as illustrated in Fig. 2-26. The drive mechanism inserts the fission chamber into the active core, positions it to measure the flux at several axial points, and withdraws it to its storage position.

Three start-up-detector assemblies are used to monitor core flux at lower power levels. The detectors are high-sensitivity fission chambers, and their drive mechanism is very similar to the IFMU drive mechanism except that a shorter stroke is required to insert the detector (see Fig. 2-27).

2.10. FUEL HANDLING (6032130001)

2.10.1. Scope

The scope of work during this reporting period was to support the HTGR Decision Package through the preparation of a preliminary system description document for the fuel handling system, updating of the BOP interface data, and updating of equipment cost estimates. Several new layouts were required to illustrate the proposed interfaces with the fuel storage and shipping facilities.

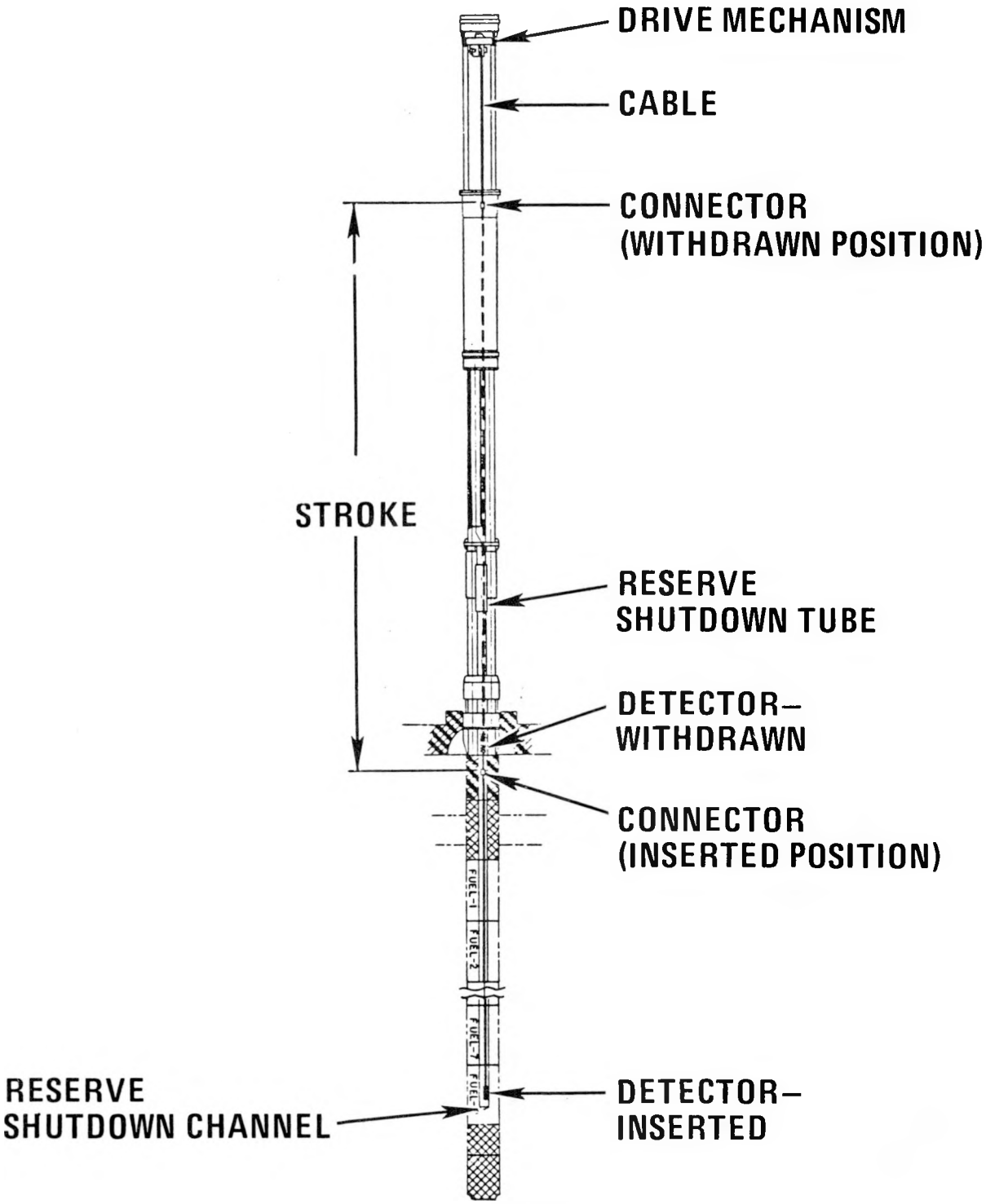

Fig. 2-26. In-core flux mapping unit

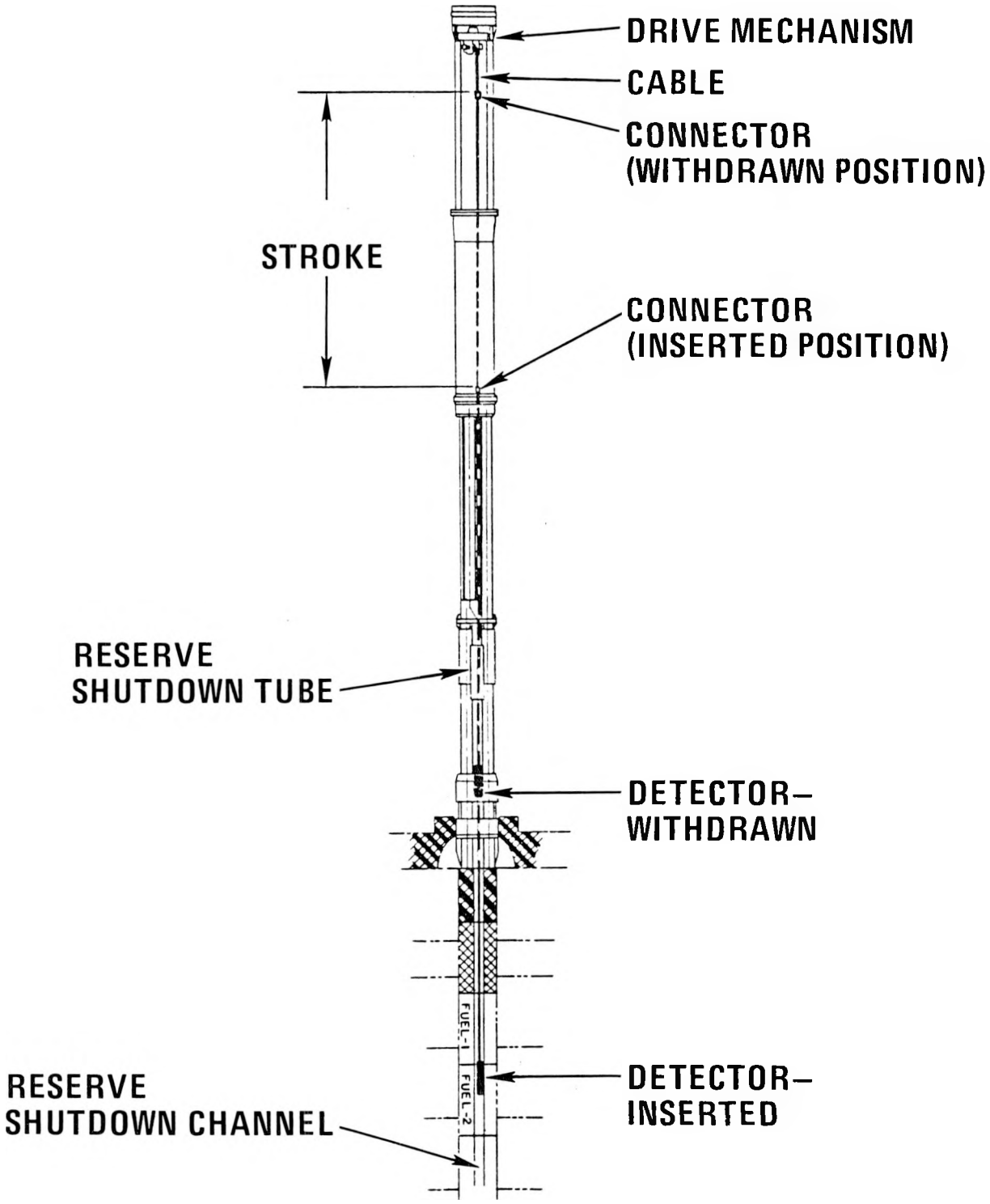

Fig. 2-27. Startup detector

2.10.2. Discussion

The adoption of the "in-vessel" refueling system with its associated dual storge facilities allowed the rearrangement and optimization of the nuclear island by the architect-engineer. As a result of this arrangement and the direct changes caused by the in-vessel system, most of the available documents for fuel service operations (i.e., receiving, inspecting, storing, shipping, etc.) were rendered obsolete. The new layouts and other documents generated during this period present new conceptual designs for the fuel service operations that are compatible with the proposed plant arrangement and the in-vessel fuel handling equipment.

There are now a total of eleven design layouts that illustrate the new equipment in the fuel handling system and seven design studies that define various interfaces and clearances.

The new system description document is a comprehensive summary of the function, design bases, and description of all the equipment in the system and how it is used during fuel handling operations.

A brief description of the in-vessel fuel handling system and additional data on the BOP interface data developed during this period are given below.

2.10.2.1. In-Vessel Reactor Refueling Concept. The basic function of the fuel handling system is to accomplish the periodic, remote replacement of core fuel and reflector elements in a safe and efficient manner. Refueling operations are predicated on a 4-yr fuel residence time whereby one quarter of the fuel elements are replaced each year with new fuel. Replaceable reflector elements adjacent to the active core are replaced at 8-yr intervals.

The basic procedure for replacing fuel or replaceable reflector elements is illustrated in Figs. 2-28 and 2-29 and involves the exchange of new hexagonal elements from the temporary fuel storage facility beside the PCRV

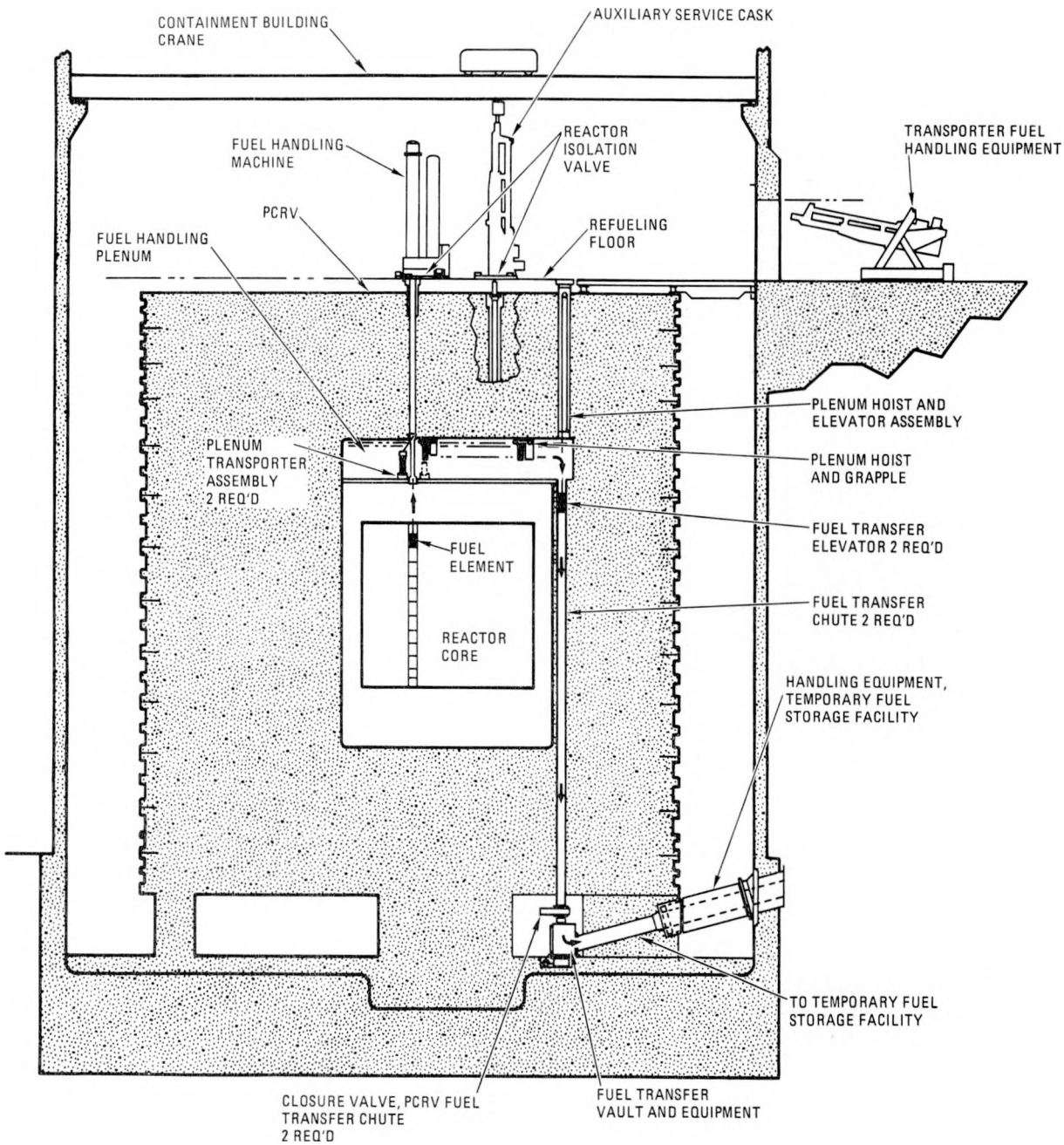

Fig. 2-28. In-vessel fuel handling concept

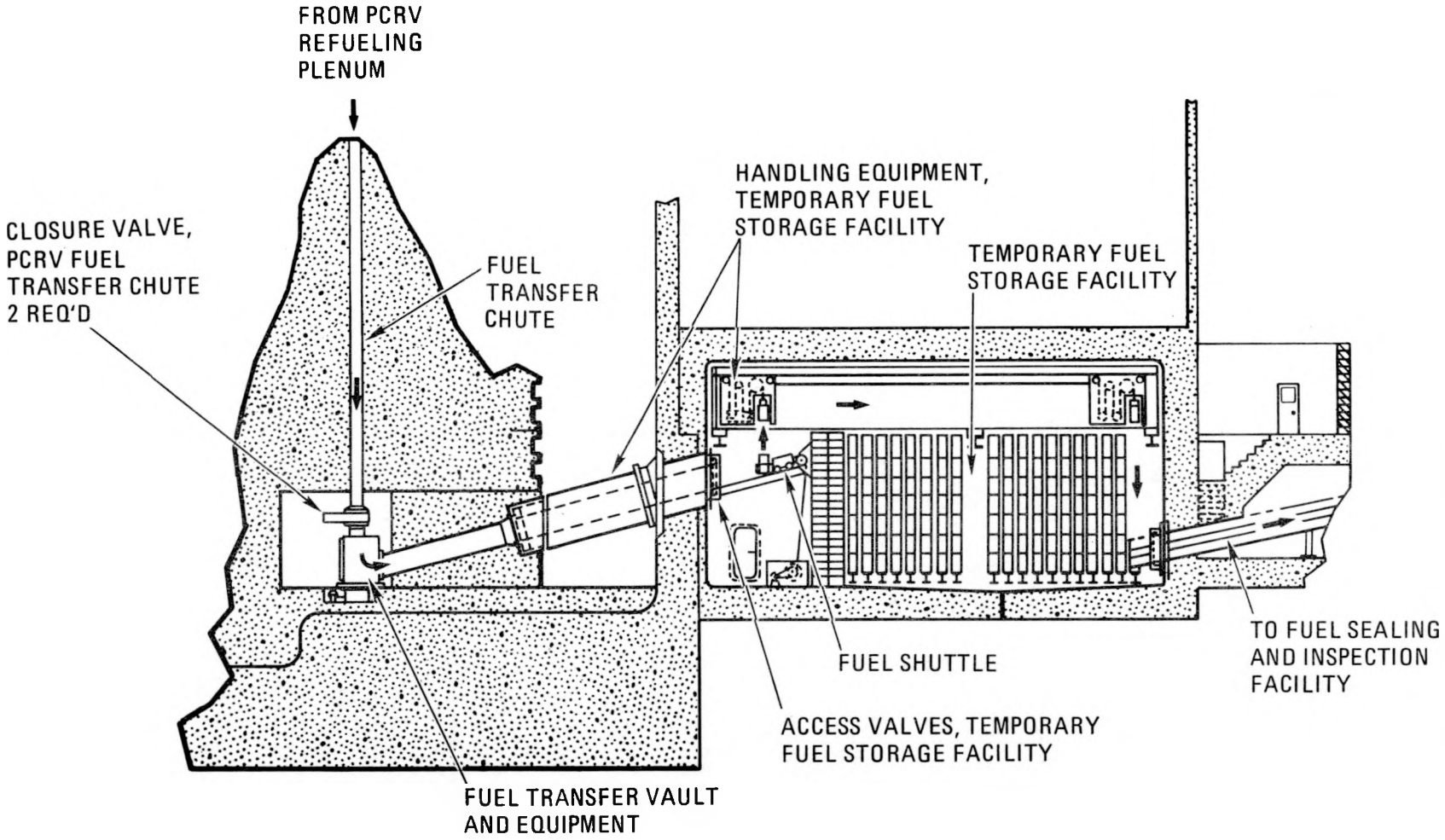

Fig. 2-29. Fuel transfer vault and temporary fuel storage facility

for selected spent core elements. This exchange occurs after the reactor has been shut down and depressurized.

Fuel handling machine access to the various core regions is achieved through the sequential removal of control and orifice assemblies from their penetrations in the top head of the PCRV with the auxiliary service cask. A reactor isolation valve is used to maintain the helium environment in the PCRV during the installation of the fuel handling machine. The plenum transporter assembly and the plenum hoist and elevator assembly are installed in their respective penetrations in similar fashion.

The fuel handling machine lifts each spent element to the plenum at the top of the core cavity. The plenum equipment either stores the element temporarily in the upper plenum structure or translates the element horizontally to the side of the core, where it is lowered through the PCRV into the fuel transfer vault (see Fig. 2-30). Handling equipment in the temporary fuel storage facility receives elements from the transfer vault and places them in storage wells. New elements are moved from the temporary storage facility into the empty core region by the reverse process. Each refueling region, consisting normally of seven columns of fuel and removable reflector elements, is entirely emptied of spent fuel before the insertion of new fuel.

All refueling equipment is removed from the PCRV upon the completion of refueling. Therefore, only fixed structures (i.e., guide rails and their supports) are exposed to reactor operating conditions and the refueling equipment is accessible for maintenance and checkout in the reactor service building in preparation for the next refueling.

The fuel handling system utilizes a digital computer to control all critical refueling operations and monitor related refueling activities. Refueling of a region is normally accomplished in an "automatic" mode with a minimum of operator involvement after initiation of the refueling cycle. The computer assures that the machines are operated within acceptable limits and in a predetermined sequence.

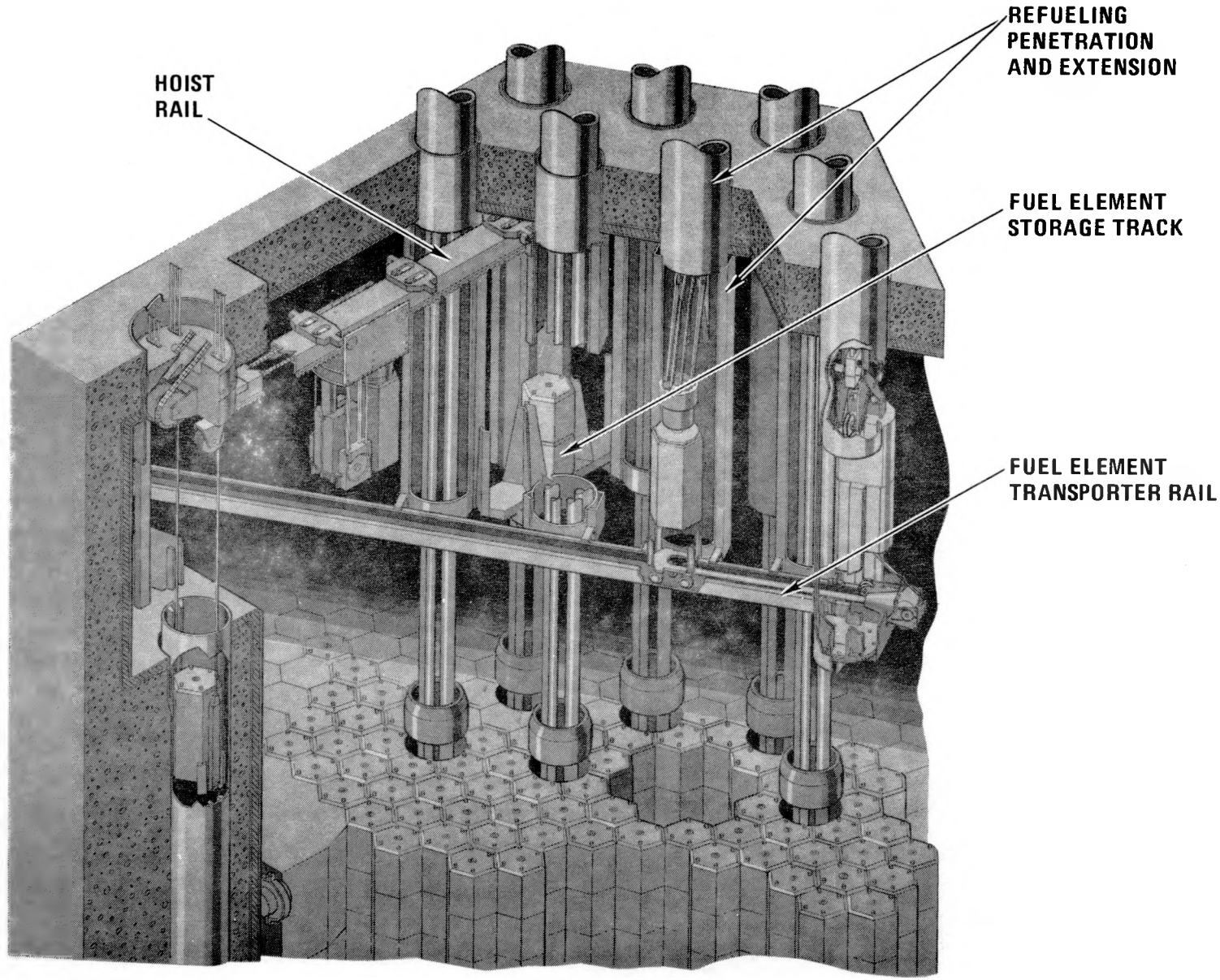

Fig. 2-30. In-vessel refueling equipment

The spent elements remain in the temporary storage facility for several months and are cooled by water circulating through redundant cooling coils attached to the exterior surface of the individual storage tubes in the storage vault. When the decay heat generation rate has dropped to an acceptable level, the facility atmosphere is changed from helium to air and the individual elements are moved from the facility to the fuel sealing and inspection facility with the spent fuel transporter.

2.10.2.2. Fuel Service Operations. The fuel sealing and inspection facility (FSIF) is the focal point for fuel handling operations which occur while the reactor is in operation (see Figs. 2-31 and 2-32). This facility is strategically located in the fuel service building and performs the following functions. New fuel and replaceable reflector elements enter the handling cycle at the FSIF, where they are inspected and subsequently moved remotely to the temporary fuel storage facility. Spent fuel that has decayed to acceptable heat generation rates is moved remotely from the temporary fuel storage area into the FSIF, where one of two possible events occurs. The spent elements may be placed in disposable canisters holding three elements each or placed directly into fuel shipping containers holding six elements per container. The disposable containers are used for elements which are to be placed in long-term on-site storage, and the shipping containers are used for elements to be shipped immediately to the reprocessing plant. The disposable containers may also be retrieved from long-term storage and deposited into shipping containers for shipment to reprocessing or off-site storage.

The FSIF is a shielded vault located above grade. It houses the fuel sealing and inspection equipment and has shielded windows and closed-circuit television systems for viewing the operations in the facility. Access penetrations are provided in the floor for moving fuel and other components into and out of the facility.

The handling of components is accomplished with two cable-supported grapple assemblies positioned by a common bridge crane structure. One grapple handles fuel elements and similar items by their central handling

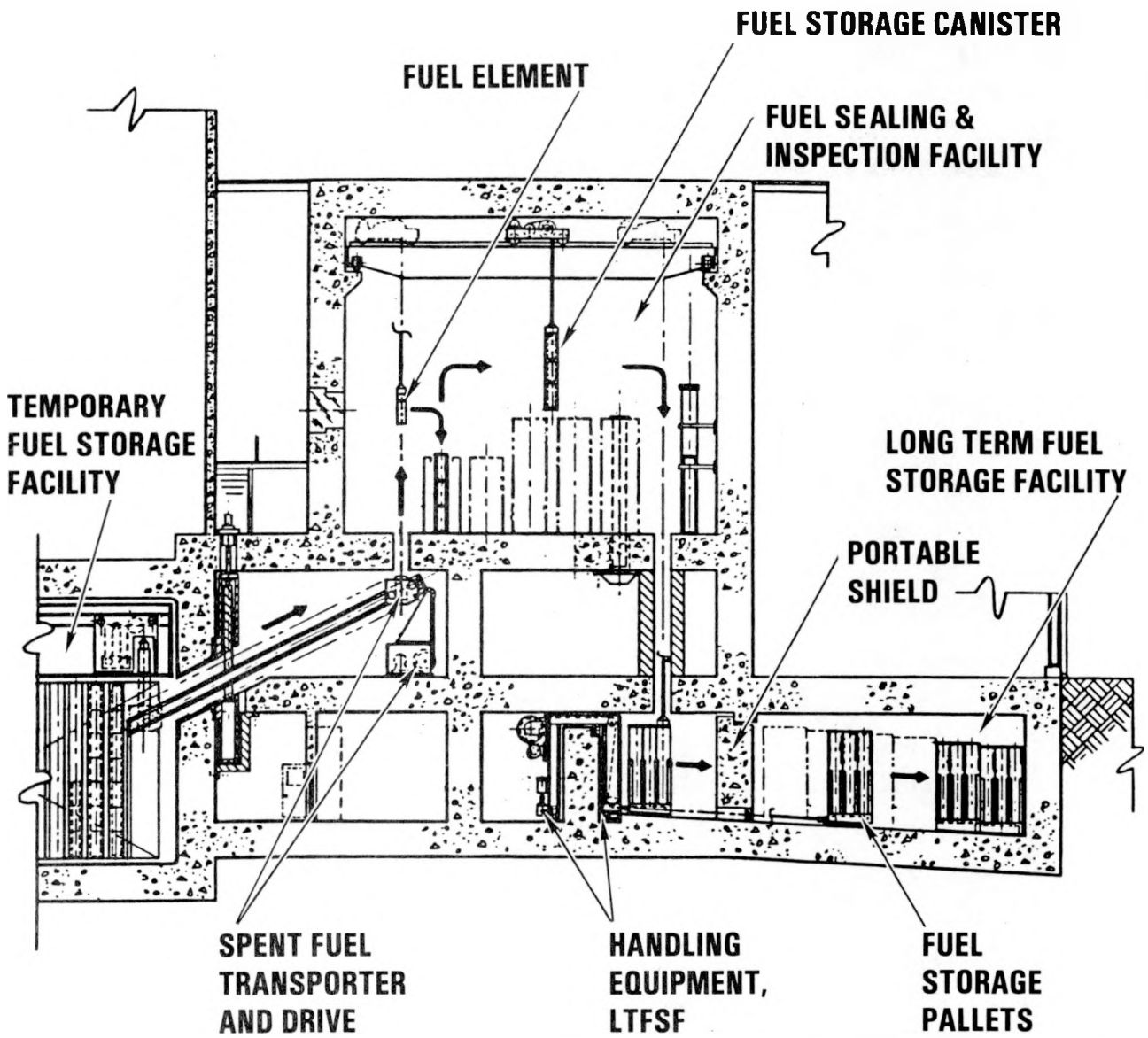

Fig. 2-31. Preparation of fuel elements for long-term storage

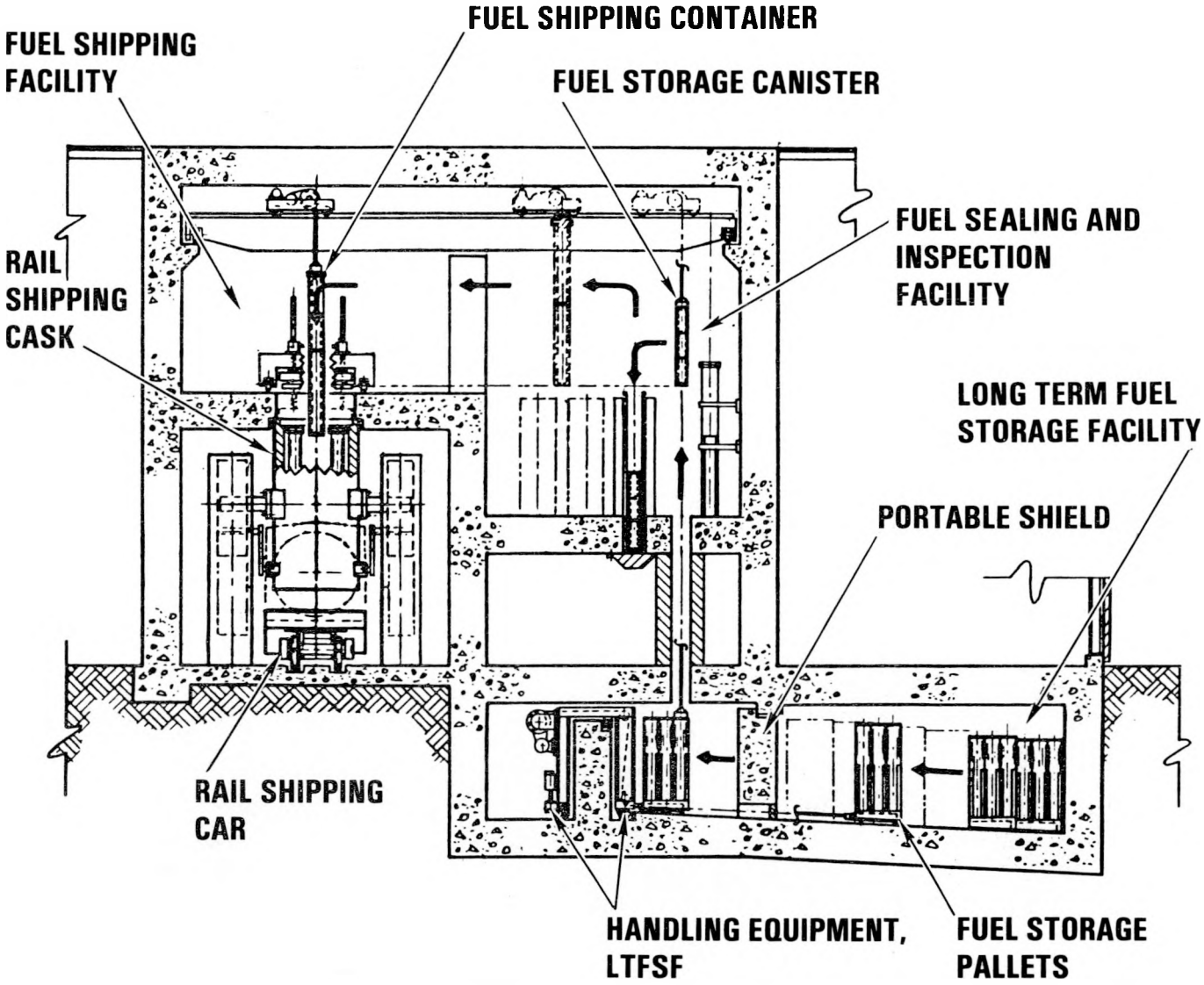

Fig. 2-32. Preparation of fuel elements for shipment

hole. The other grapple handles fuel storage canisters and fuel shipping containers.

The elevation and location of the FSIF are influenced by the fuel shipping cask, which is transported by a special railroad car (see Fig. 2-32). The railroad tracks are routed beneath the FSIF, where the cask is mated to the bottom surface of the vault structure. The shielded cask lid is lifted up into the vault and moved to one side by a remotely operated mechanism.

The loading of spent fuel into the shipping cask is accomplished with the bridge crane and shipping container grapple. The same equipment could be used to unload reprocessed fuel if necessary. Storage racks provided within the facility will hold a complete load of shipping containers to facilitate rapid loading of the shipping cask.

The shipping containers have a bolted lid with redundant gaskets and are reusable. The containers will hold six bare elements or two sealed storage canisters or five reprocessed elements with protective packing. Equipment within the facility bolts the lids to the shipping containers and checks them for leaks in preparation for shipping.

As noted earlier, spent fuel may also be placed in long-term storage from the FSIF. The spent elements are placed in disposable canisters holding three elements each, and a closure is placed over the elements. Sealing of the closure to the canister by brazing is optional, depending upon the rate of release of radioactive gases from the elements. The bridge crane lowers the loaded canister through a shielded port into the long-term fuel storage facility. Sixteen loaded canisters are placed in each fuel storage pallet. The handling equipment in the long-term fuel storage facility places the storage pallets in shielded storage bays. The long-term storage facility is initially sized to hold four reload segments with design provisions for expansion.

2.11. REACTOR SERVICE EQUIPMENT (6032160001)

2.11.1. Scope

The scope of work during this reporting period included refinement of the conceptual design of the reactor service equipment as needed for interfacing systems, plant definitions, and cost estimating in support of the HTGR preliminary system description documentation and BOP interfacing.

2.11.2. Discussion

The reactor service equipment system encompasses a group of subsystems or components, each comprising equipment and tools that facilitate in- and ex-vessel service and maintenance operations as well as handling and storage of a number of reactor components.

The components and subsystems within this system have somewhat unrelated functions and are categorized as follows primarily for organizational purposes:

1. Circulator handling equipment.
2. Core outlet thermocouple service equipment.
3. Core service tools.
4. Service facility tools.
5. Control and orifice assembly storage equipment.
6. Equipment storage wells.
7. Plenum hoist penetration shield plug.
8. Wire winding equipment.
9. In-service inspection equipment (as required).

The basic design concepts for most of the equipment in the reactor service equipment system have not changed significantly since they were initially developed for other HTGR plants several years ago. The exceptions are discussed below.

2.11.2.1. Circulator Handling Equipment. The circulator handling cask (see Figs. 2-33 and 2-34) has become larger with the adoption of the electric-motor-driven circulators and is now the heaviest component that is routinely lifted with the cranes in the containment and reactor service buildings. A new criterion requiring the ability to service the loop isolation valves has also added weight to this equipment.

Additional conceptual design and shielding studies will be needed to assure that the assumed source strengths for plateout and activation are accurate and that the shielded volume within the cask is optimized. The results of these studies will confirm the adequacy of the maximum loads specified for the building cranes and may permit cost reductions for these expensive components.

2.11.2.2. Control and Orifice Assembly Storage Equipment. The control and orifice assembly storage equipment component consists of a turntable structure containing the storage positions arranged in two concentric circles. A single access port (normally closed with a shield plug) for each storage circle permits loading and unloading of the facility with the auxiliary service cask.

The equipment is primarily used to store spare control and orifice assemblies. However, it is also designed to hold any components normally handled with the auxiliary service cask, including penetration shield plugs, the plenum transporter assemblies used for fuel handling, the reserve shutdown vacuum tool, and spare high-temperature filters and adsorbers from the purification system.

When the control and orifice assemblies are installed in the turntable, all radioactive portions of the control and orifice assembly are beneath the turntable and the gamma shielding built into each assembly plugs the opening in the turntable. Portable shield plugs fill any unoccupied locations. This arrangement permits personnel access into the upper portion of the storage facility for direct maintenance of the control and orifice assembly mechanisms.

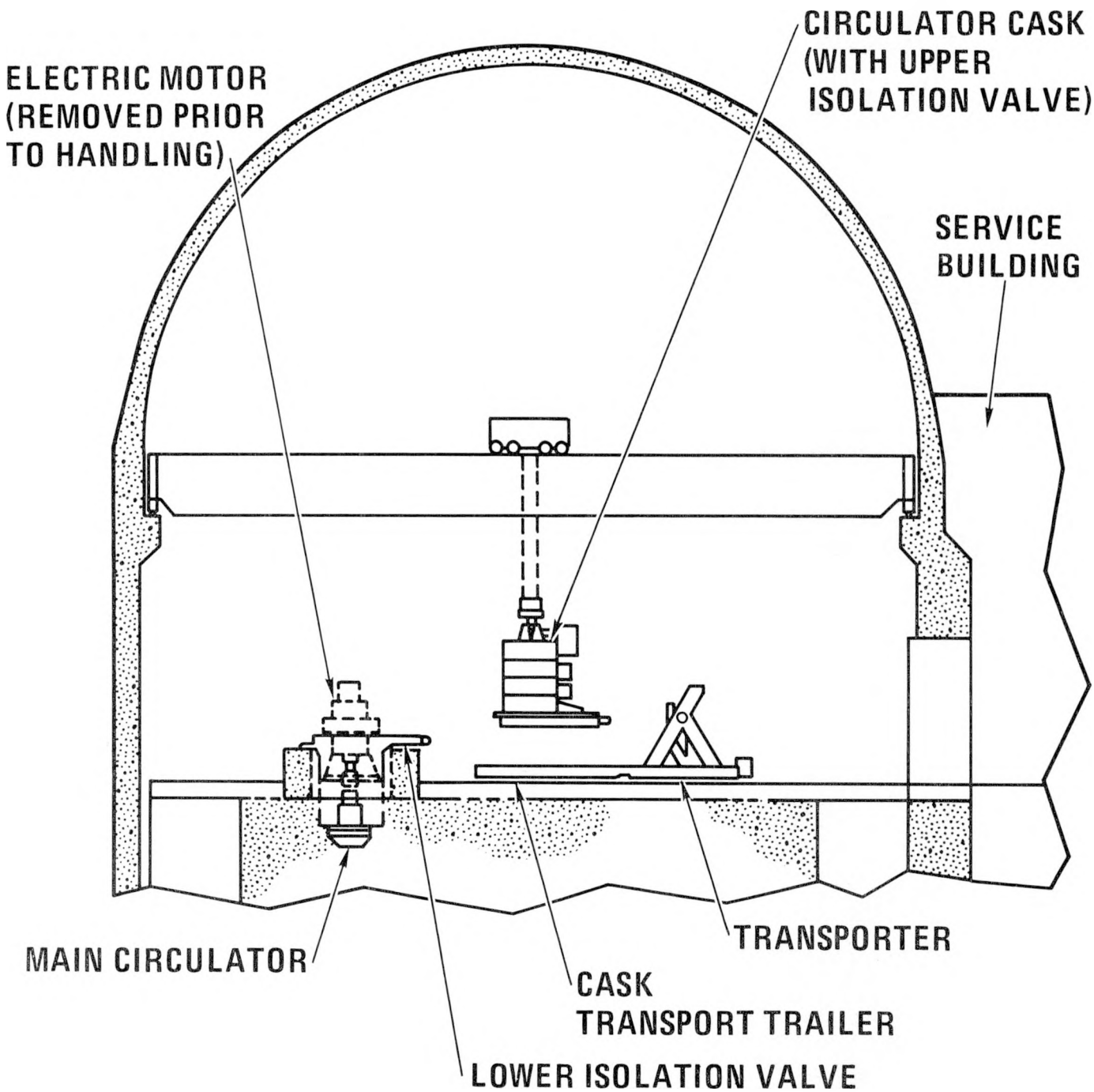

Fig. 2-33. Circulator handling concept

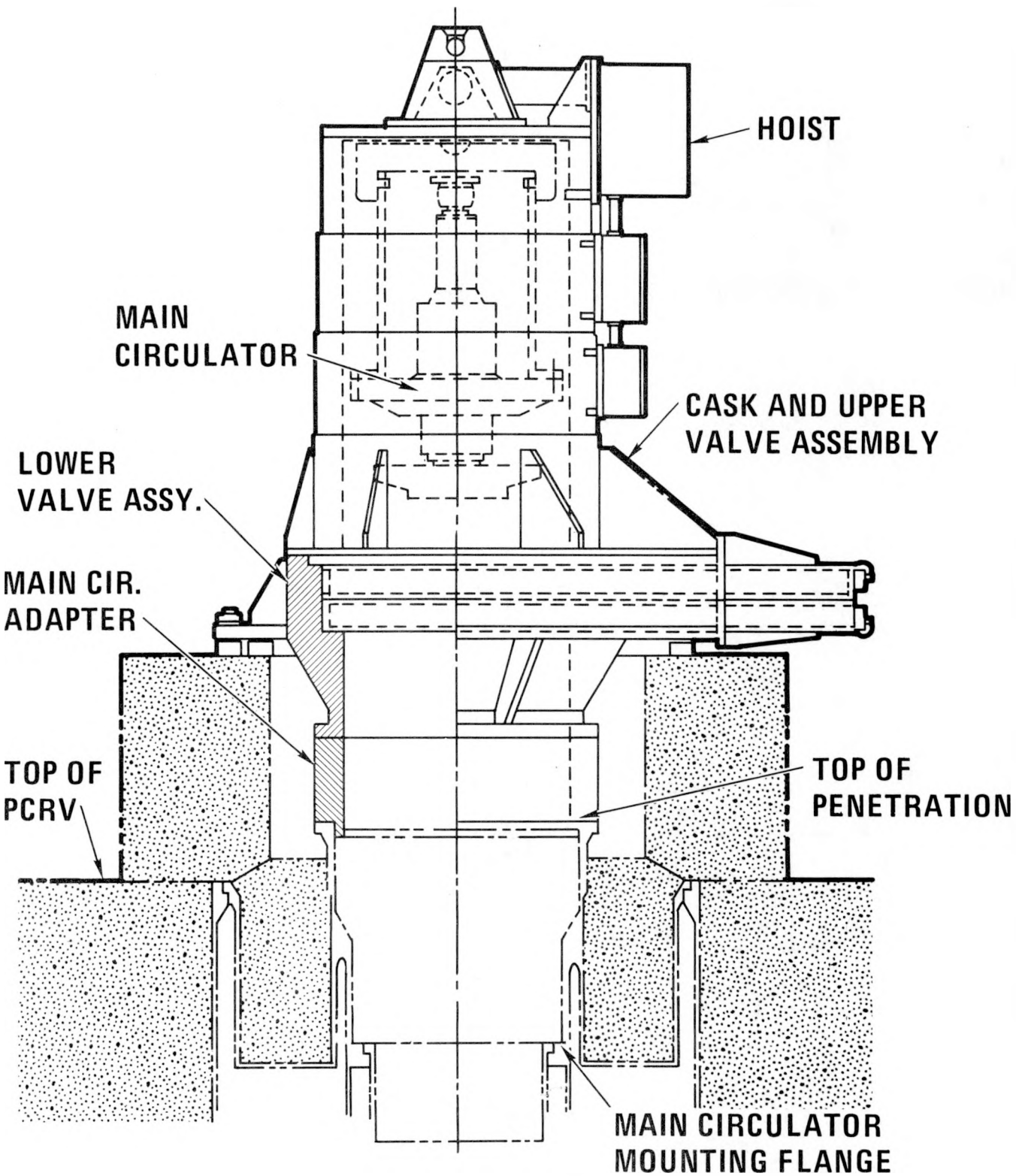

Fig. 2-34. Circulator handling equipment

A cylindrical shield wall is provided between the inner and outer storage circles. Components that are contaminated or do not contain sufficient shielding to plug the opening in the turntable are stored in the inner circle. Maintenance of these components is accomplished at the reactor equipment service facility.

Operation of the equipment during loading and unloading is performed remotely from a control console external to the facility. Visual monitoring is provided via a closed-circuit video system.

The atmosphere in the facility is monitored to assure that it is clean and free of radioactive particulate matters, undesirable gases, etc., and that the pressure is maintained slightly below atmospheric.

2.11.2.3. Equipment Storage Wells. Two circulator storage wells are provided in the reactor service building to permit the exchange of a spare main or auxiliary circulator or loop isolation valve for a defective component. Each well is capable of holding two components and is provided with an adjustable support feature to adapt to the items to be stored. The upper flange of the circulator storage wells mates with the circulator handling equipment. Closures are not required since the circulator handling equipment is normally stored over the storage wells. The reactor service building ventilation system maintains a slightly negative pressure in the storage wells and prevents the release of any radioactive gases or particulates into inhabited areas of the service building. The wells are embedded in the concrete structure of the reactor service building for structural support and shielding.

Three plenum hoist and elevator assembly storage wells are required to store two plenum hoist and elevator assemblies used during refueling or two plenum hoist penetration shield plugs which are removed for refueling. The upper end of the plenum hoist and elevator assembly storage wells mates with the plenum hoist service equipment. Bolted closures are provided for these storage wells. These wells are also embedded in the concrete structure of the service building for structural support and shielding.

2.11.2.4. Plenum Hoist Penetration Shield Plugs. Two plenum hoist penetration shield plugs are required as a result of the change to the in-vessel refueling system. They are similar in function to the refueling penetration shield plugs provided with gamma, neutron, and thermal protection for the two plenum hoist and elevator assembly penetrations during reactor operation. These passive components are removed with the plenum hoist service equipment to provide access for the plenum hoist and elevator assemblies which must be installed for refueling.

2.11.2.5. In-Service Inspection (ISI) Equipment (As Required). It has been recently acknowledged that special-purpose ISI equipment will be needed for inaccessible areas of the HTGR. The reactor service equipment system will be expanded as the needs for this equipment are identified and conceptual designs for gaining access and performing the inspections evolve.

2.12. REACTOR INTERNALS

2.12.1. Scope

The scope of this task included preparing conceptual design layout drawings and supporting analyses for the core peripheral seal, the core lateral restraint, and the upper plenum refueling structure.

2.12.2. Discussion

2.12.2.1. Core Peripheral Seal. With the goal of reducing leak paths and improving overall performance, a new approach to the design of the support structure for the core peripheral seal was studied and developed.

The primary loads applied to the seal support structure are a consequence of those imposed by the pressure difference between the upper and lower plena of the core cavity. Another major factor that influences the design approach is the need to accommodate the relative thermal expansion between the hot inner edge (seal seat) and cold outer edge attached to the vessel liner. To achieve this accommodation (see Fig. 2-35), two sine wave

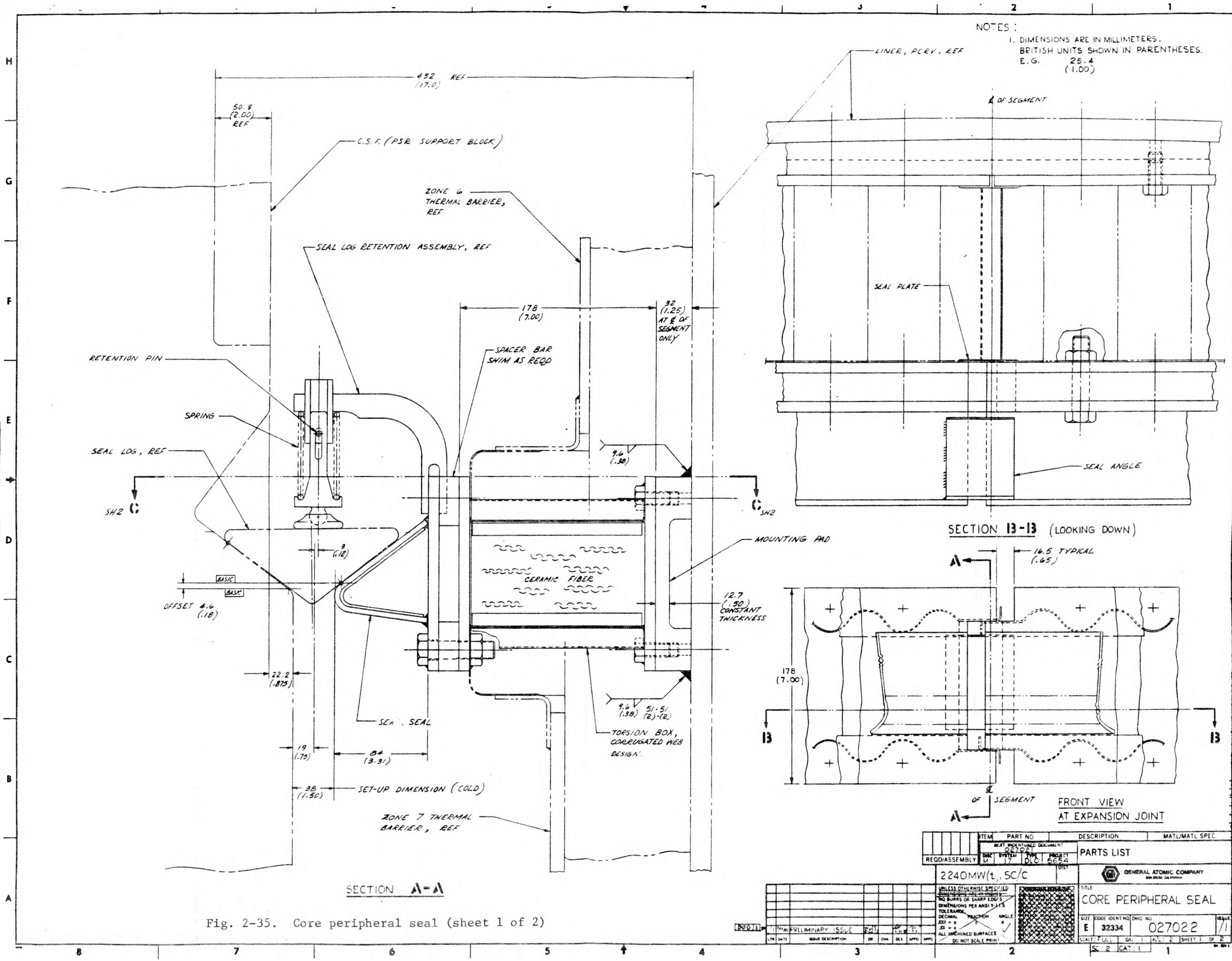

Fig. 2-35. Core peripheral seal (sheet 1 of 2)

LENGTH OF INSIDE ARC — 1073 (42.24)
LENGTH OF CHORD = 1071 (42.18)
ARC = 10°

LINER I.D. = 12.29 M REF (40'-4)

℄ OF SEGMENT

4.8 GAP (.19)

12.7 DIA BOLTS, 28 PL (.50)

5° TYP

16.5 REF (.65)

15.88 DIA BOLTS, 28 PL (.625)

SEAL LOG RETENTION ASSEMBLY, 2 PL

SECTION C-C SH 1

℄ SEAL LOG (REF)

4.8 (.19)

SLOTTED HOLE 28 PLACES

PITCH 115.8 (4.56)

1.27 THK (.050) TYP

33 (1.30) TYP

66 (2.60) PITCH, TYP

19 R, TYP (.75)

SECTION D-D

ITEM	PART NO.	DESCRIPTION	MAT'L/MAT'L SPEC
REQD/ASSEMBLY			

PARTS LIST

GENERAL ATOMIC COMPANY

TITLE: CORE PERIPHERAL SEAL

SIZE	CODE IDENT NO.	DWG NO.	ISSUE
E	32334	027022	/1

SCALE — SHEET 2 OF 2

SEE SHEET 1

DO NOT SCALE PRINT

SH 2 OF 2

027022 /1 SH2OF2

Fig. 2-35. Core peripheral seal (sheet 2 of 2)

corrugated webs are employed between the inner (hot) and outer (cold) cap plates to form a stiff shear-resistant torque box which transmits all loads to the liner.

As shown in Section C-C of Fig. 2-35, this support structure will be fabricated in the factory in 0.174-rad (10-deg) segments that are coincident with the length of each of the 36 graphite seal logs which circle the core support floor. Lateral circumferential movements of the structural support components caused by thermal expansions are accommodated at the center of each segment with overlapping slip joints designed to limit leakage (see Section B-B of Fig. 2-35). This seal support design also permits final on-site adjustments of seal seat alignment without disturbing the protective thermal barrier.

To prevent possible displacement or misalignment of the seal logs during a seismic event, both ends of each log are firmly held down with a spring-loaded log retention assembly as shown in Section A-A of Fig. 2-35.

Preliminary analysis of the potential rate of flow through the core peripheral seal shows that approximately 70% of the total leakage will occur across the seal logs. This includes leak areas at the log/log end abutment and the log/seat interfaces. The major portion of the remaining leakage will be through the thermal expansion joints of the support structure.

2.12.2.2. Core Lateral Restraint. As a result of numerous design and testing investigations made for the HTGR-SC/C core, several design improvements have been approved for further development. One of these involves the core lateral restraint assembly. The disk springs used in the original concept for seismic load attenuation have been replaced by radial keys. These radial keys provide the shear connection to the PCRV core cavity liner and also, in conjunction with the face plate, provide a positive means of locating the permanent side reflector during both installation and operation. In addition, the permanent side reflector will be firmly preloaded by the core lateral restraint, thereby limiting the displacement of the core during seismic events. The preload will also maintain the sealing function of the

permanent side reflector by keeping the gaps between elements of the permanent side reflector outer ring tight during all operating conditions.

A preliminary issue of the core lateral restraint layout drawing (Fig. 2-36) was produced as the technical basis for cost updating of this component. Stress analysis of the redesigned structure has commenced.

2.12.2.3. Upper Plenum In-Vessel Refueling Structure. This design consists of fuel transporter rails, hoist rails, and fuel storage racks attached to support structures extending from the top of the core cavity in the upper plenum. A plenum hoist mechanism that rides on the hoist rail moves the fuel blocks from the core and deposits them in a temporary storage rack or in the elevator assembly. The elevator lowers the block through a vertical penetration that extends out the bottom of the PCRV into a storage vault. This procedure is reversed for placing a block in the core.

Design calculations indicate that the structure is subjected to very low stresses during operation. A lateral force of 1.5 $\bar{g}$ applied to the structure in combination with other mechanical loads again resulted in low stresses. The primary reason for such conservatism in the design is to provide a rigid structure that will prevent unwanted displacement or offset of the fuel handling mechanisms during refueling.

The structure is designed as a life-of-plant component. However, the subcomponents of the structure can be replaced, although with difficulty.

2.13. REACTOR CORE DESIGN (6032180102, 6032170203)

2.13.1. Scope

The scope of this task is to investigate alternate core design configurations and their performance to respond to the core thermal-hydraulic priority issue. Included in this effort are (1) an alternate core configuration study, (2) thermal-hydraulic flow analyses of the core support floor and permanent side reflector, (3) seismic and structural analysis of core

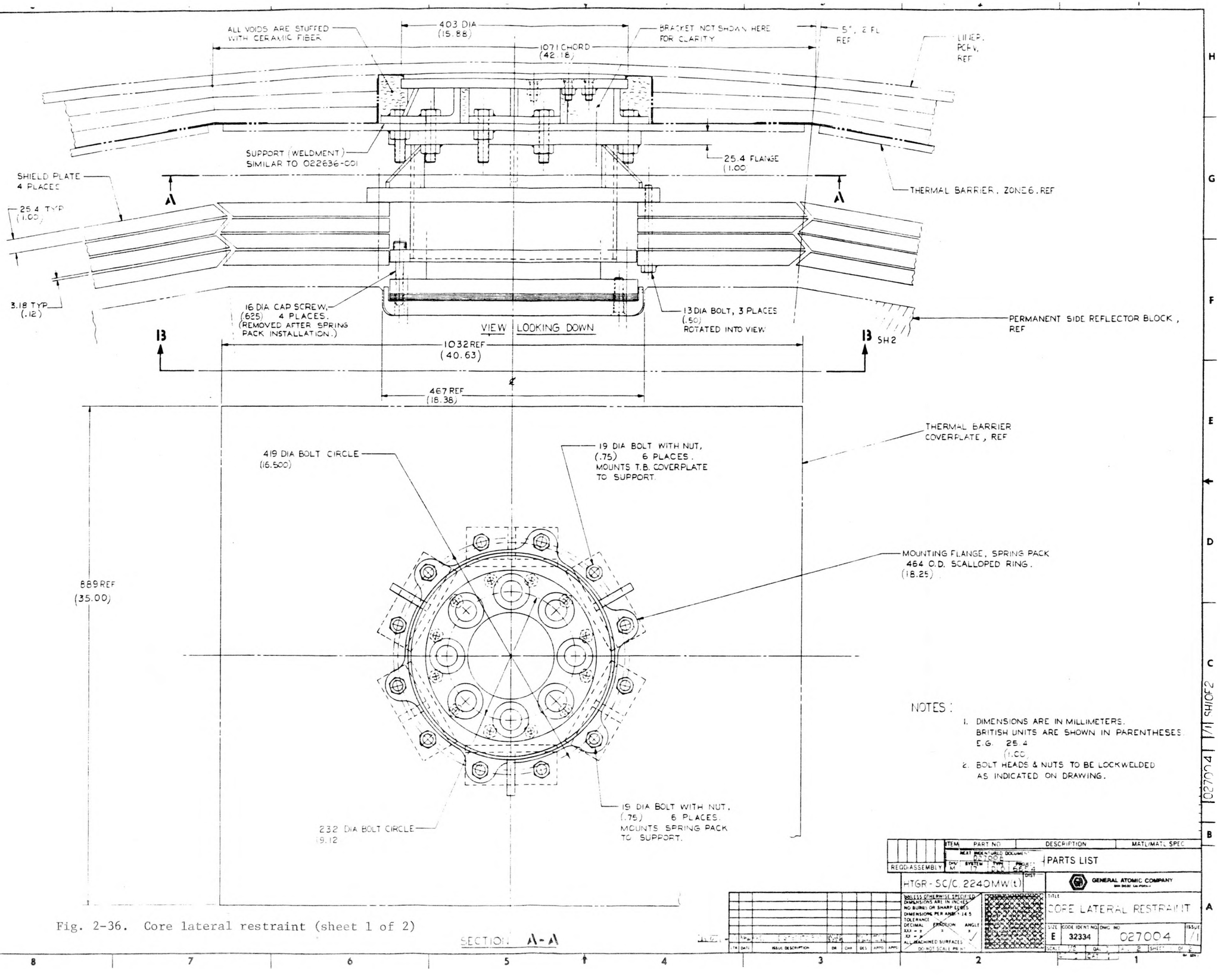

NOTES:

1. DIMENSIONS ARE IN MILLIMETERS. BRITISH UNITS ARE SHOWN IN PARENTHESES. E.G. 25.4 (1.00)
2. BOLT HEADS & NUTS TO BE LOCKWELDED AS INDICATED ON DRAWING.

ITEM	PART NO.	DESCRIPTION	MAT'L/MAT'L SPEC
NEXT HIGHER ASSY	027005		
REQD/ASSEMBLY	QTY/M 17	SYSTEM 027	TYPE 001

PARTS LIST

HTGR-SC/C 2240MW(t)

GENERAL ATOMIC COMPANY

UNLESS OTHERWISE SPECIFIED DIMENSIONS ARE IN INCHES. NO BURRS OR SHARP EDGES. DIMENSIONS PER ANSI Y14.5. TOLERANCE DECIMAL XXX = ±, XX = ±, FRACTION ±, ANGLE ±. ALL MACHINED SURFACES. DO NOT SCALE PRINT.

LTR	DATE	ISSUE DESCRIPTION	DR	CHK	DES	APPD	APPD

TITLE: CORE LATERAL RESTRAINT

SIZE	CODE IDENT NO.	DWG NO.	ISSUE
E	32334	027004	1/1

SCALE 1/8 QA SHEET OF

027004 1/1 SH OF 2

Fig. 2-36. Core lateral restraint (sheet 1 of 2)

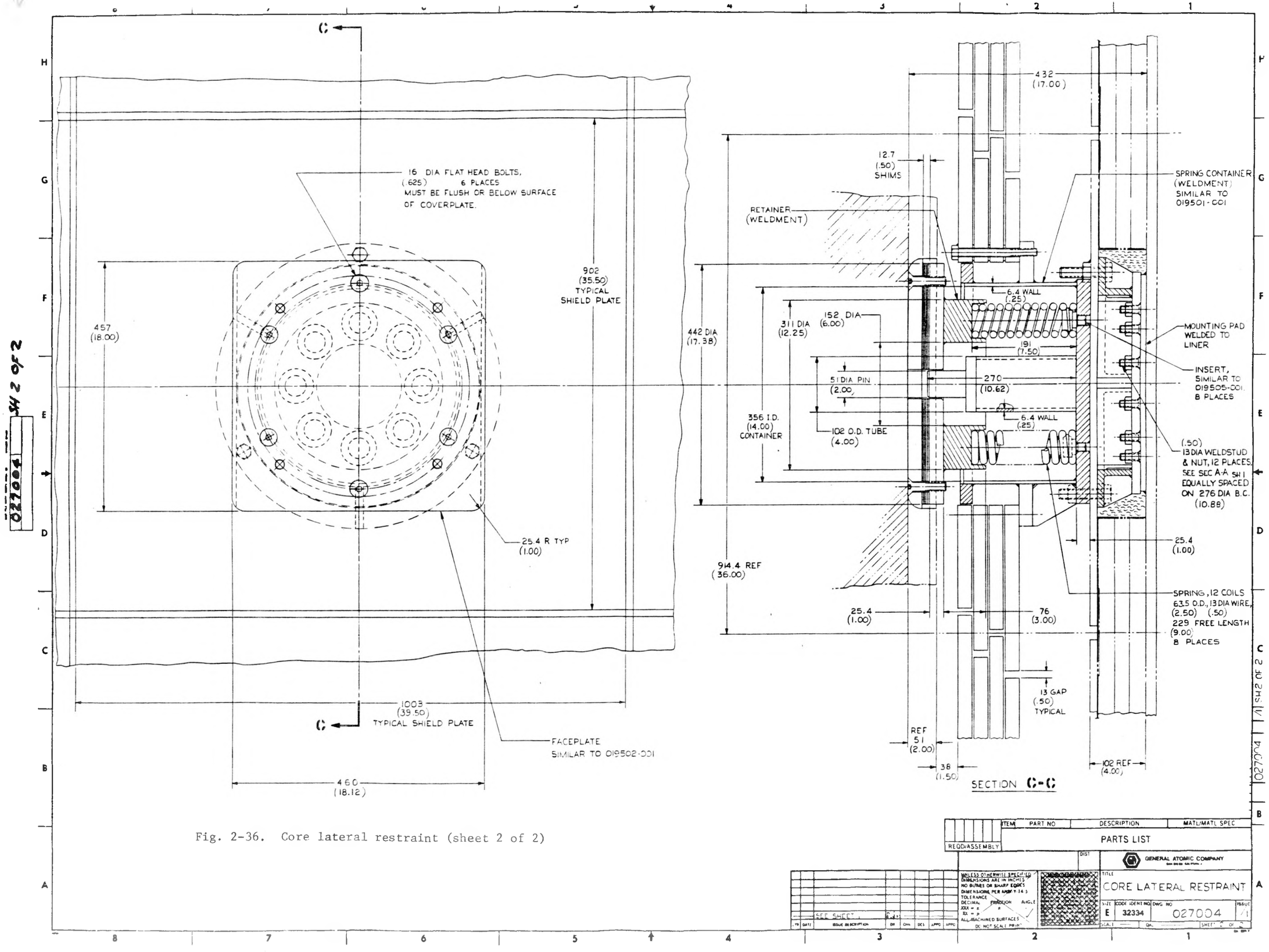

Fig. 2-36. Core lateral restraint (sheet 2 of 2)

support, (4) fuel performance analysis (fission product transport), and (5) nuclear calculations for alternate core designs.

2.13.2. Discussion

2.13.2.1. Alternate Core Configuration Study. The recommended core design changes are the result of a concentrated study during the last quarter of CY-81 augmented by follow-up thermal-hydraulic and stress analysis in the present reporting period. The primary purpose of the core redesign study was to resolve the fundamental thermal-hydraulic priority issue associated with the core.

The priority issue combines the problems of fluctuations, temperature redistribution, uncertain temperature measurements, and crossflow, all of which had been experienced in the FSV plant. For this reason, an expedient resolution was considered important to a successful continuation of the HTGR program, and a task force was formed to undertake a core redesign study.

The groundrule established for the task force was to primarily resolve the thermal-hydraulic issue, while being cognizant of the two other priority issues related to the core: fuel element stresses and the reactor internals adequacy. Preferably, any recommended design modifications would also improve these two other issues, or at least not make them worse.

In order to avoid any adverse effect on the two other issues, it became necesary to address them in some detail, particularly the fuel element stress issue. The fuel element stresses develop from three major sources: temperature differences, irradiation-induced shrinkage, and seismic loads. The first two sources are to a large extent controlled by the fundamental coolant and fuel hole pattern, but the thermal stresses are also affected by crossflow, potential local upflow, and other thermal-hydraulic aspects. These latter contributions to the thermal stresses were given considerable attention in the study.

The seismic loads are influenced by the fuel element stiffness, the core arrangement, and the boundary conditions. Since changes to all of these factors were considered as solutions to the thermal-hydraulic problems, a fairly extensive seismic analysis was included in the redesign effort.

Since it would also be necessary to evaluate the role of the permanent side reflector in contributing to the thermal-hydraulic uncertainties, it was decided to address three long-standing permanent side reflector concerns: (1) no known supplier of graphite for the large blocks, (2) lack of positive location during both installation and operation, and (3) marginal structural stability under the radial pressure gradient conditions.

Alternatives Evaluated

The first phase of the study involved screening ideas and identifying candidate design solutions. Some preliminary work in this area had already been completed toward the end of FY-81 (Ref. 2-3). The screening phase produced 14 different candidates for further evaluation, and the key design features of these candidates are shown in a matrix form in Table 2-12. The 14 cases are arranged in ascending order of deviation from the reference design, which is labeled Case 0 in the table.

Following an evaluation by the task force and steering committee, the 14 cases were reduced to the following three for the final selection.

Final Case 1. This is the initial Case 1 (which was identical to the reference design with the addition of sealing flanges at the ends of the element) but extended to include external grooves in the side faces at the fuel elements and the permanent side reflector modifications. Sealing the gaps at the top of the core and venting at the bottom were also included. The case was divided into three variants, depending on how the sealing flange was incorporated into the fuel elements.

TABLE 2-12
CANDIDATES EVALUATED IN ALTERNATE CORE CONFIGURATION STUDIES

Design Features	0 Ref. Design	1 Ref. Design With Sealed Fuel Elements	2 Ref. Design With Sealed Fuel Elements	3 Light Spring Clamping, Unsealed Permanent Side Reflector	4 Light Spring Clamping, Sealed Permanent Side Reflector	5 Region-alized Brick Wall	6 Self-Tightening Regions	7 Keyed Layers(s), Conventional Fuel Elements	8 Keyed Layers(s), Sealed Fuel Elements	9 Keyed Fuel Elements, Large and Small Elements	10 Keyed Fuel Elements, Flanged Elements	11 Active Mechanical Core Clamping	12 Active Mechanical Clamping	13 Active Mechanical Clamping	14 Active Mechanical Clamping
Lateral Restraint															
Current spring packs	X	X	X												
Clamping spring packs				X	X										
Tangential restraint						X	X	X	X	X	X				
Active mechanical clamping												X	X	X	X
Permanent Side Reflector															
Tight ring	X	X	X			X	X	X	X	X	X				
Clamping				X	X							X	X	X	X
Region															
Conventional	X	X	X	X	X			X	X	X	X	X	X	X	X
Brick wall						X									
Self-tightening							X								
Fuel Elements															
Plain hexagonal, uniform size	X			X				X	X			X	X		
End seal, flanged end		X			X						X			X	
End seal, large and small			X							X					X
Irregular shapes						X	X								
Keyed elements										X	X				
Keyed layer(s)								X	X						
Clamped layer							X								
Top of Core Restraint	X	X	X			X	X	X	X	X	X				

- In Variant A, a solid rim of graphite was added to the outside of the reference element, increasing the across flats dimension to 391 mm (15.4 in.).

- In Variant B, the outermost row of holes was removed, maintaining the outside dimension at 360 mm (14.17 in.). To compensate for the lost fuel, 102 new fuel columns were added. (Ultimately this became the recommended design.)

- In Variant C, both fuel and outside dimension were retained. This is achieved through a high-efficiency design in which the holes of the outermost row stop short of the sealing flange from where they are "dog-legged" toward the center.

Final Case 2. This is the initial Case 4, having light spring pack clamping and a sealed permanent side reflector.

Final Case 3. This is the initial Case 10 which uses 391-mm (15.4-in.) wide elements to make room for the keys and the keyways while retaining the standard 10-row hole pattern. For the purpose of fuel handling, the keys extend only along a part of the height of the element. The permanent side reflector modifications described above are included in this case.

The major reasons for rejecting the other cases were as follows:

- Case 2 was found to be a greater deviation than Case 1 from the reference design without offering any additional advantages.

- Case 3 was unacceptable because of the excessive radial inflow through an unsealed permanent side reflector.

- Cases 5 and 6 represented unacceptably drastic deviations from the established designs and also would require extensive development.

- Cases 7 through 9 were found to be less attractive variants of the selected keyed core concept (Case 10).

- Cases 11 through 14 were rejected because a feasible clamp design which was considered acceptable from a practical standpoint could not be found.

Having reduced the candidates to the three cases described, a "Must/Want" list was used for the final selection. Final Case 2 was found to have excessive crossflow owing to the gradual "hour-glassing" of a clamped core and consequent opening of "jaws," and thus failed a "Must" criterion of predictable temperature measurements. Final Cases 1 and 3 met all the "Must" requirements. The "Want" criteria were then used for a quantified comparison of the merits of the remaining cases. Final Case 1, Variant B, received the highest rating and became the recommended design.

Component Descriptions

Major components of the recommended design are described below. The core general arrangement is shown in Figs. 2-37 and 2-38.

Fuel Elements. The graphite fuel elements that constitute the active core are hexagonal right prisms containing arrays of fuel and coolant holes (Fig. 2-39). Holes are also provided in certain locations for neutron sources, control rods, reserve shutdown material, and instrumentation (Fig. 2-40). In the center of the top end is a pickup hole for remote fuel handling. The elements are 360 mm (14.17 in.) across the hexagonal flats and 793 mm (31.22 in.) tall. The following features are provided to mitigate temperature fluctuations. The sides have 18 vertical grooves (three on each face) consisting of shallow scallops with a 9.5-mm (0.375-in.) radius. The six vertical edges are machined down to provide additional vertical vents around each column. The top end of each hexagonal element incorporates a sealing flange that forms a socket connection with the element above. The column weight and lateral seismic loads are carried by the raised edge of the flange. The flange is designed to be a close fit around the outside of

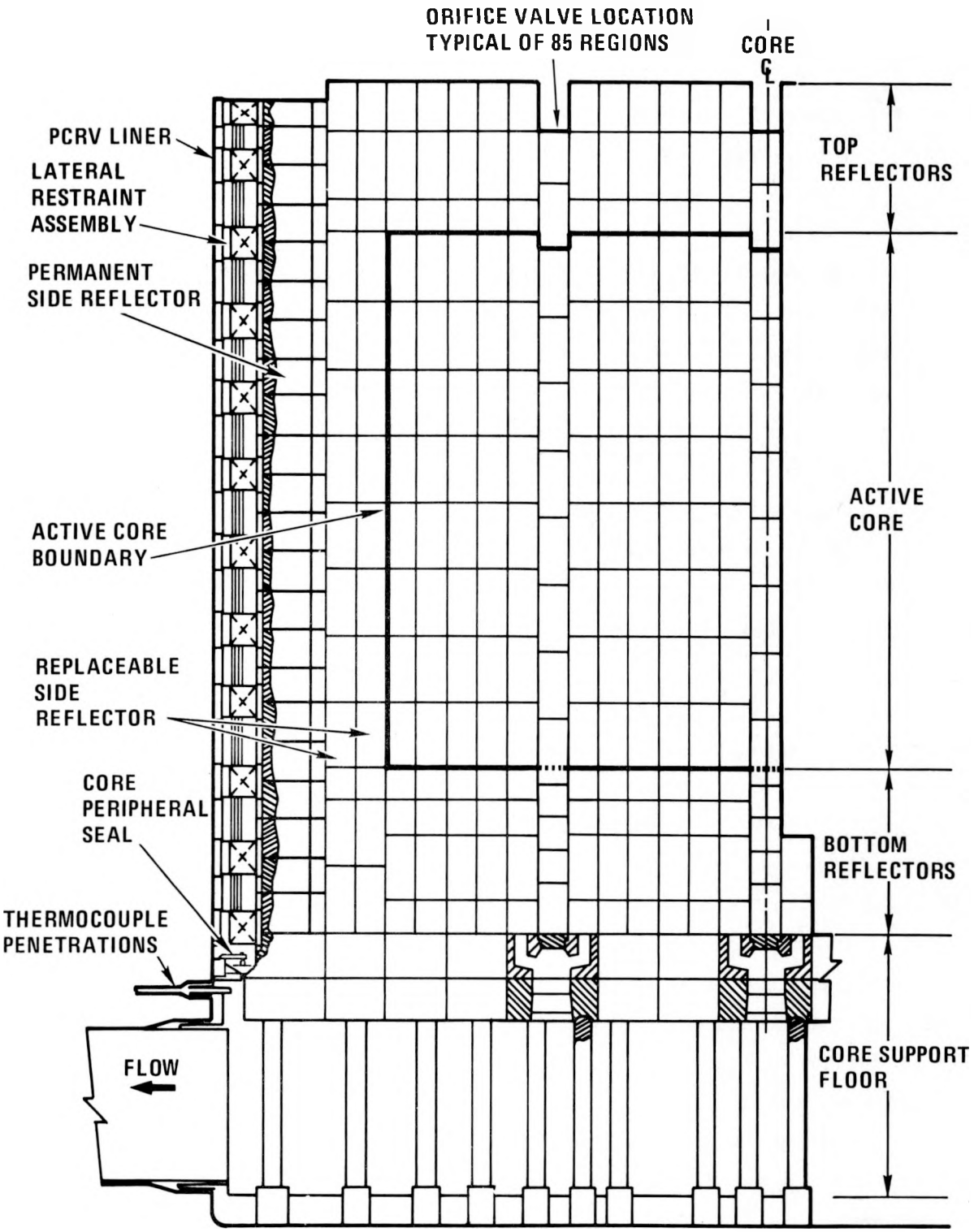

Fig. 2-37. Core and reactor internals assembly, elevation view

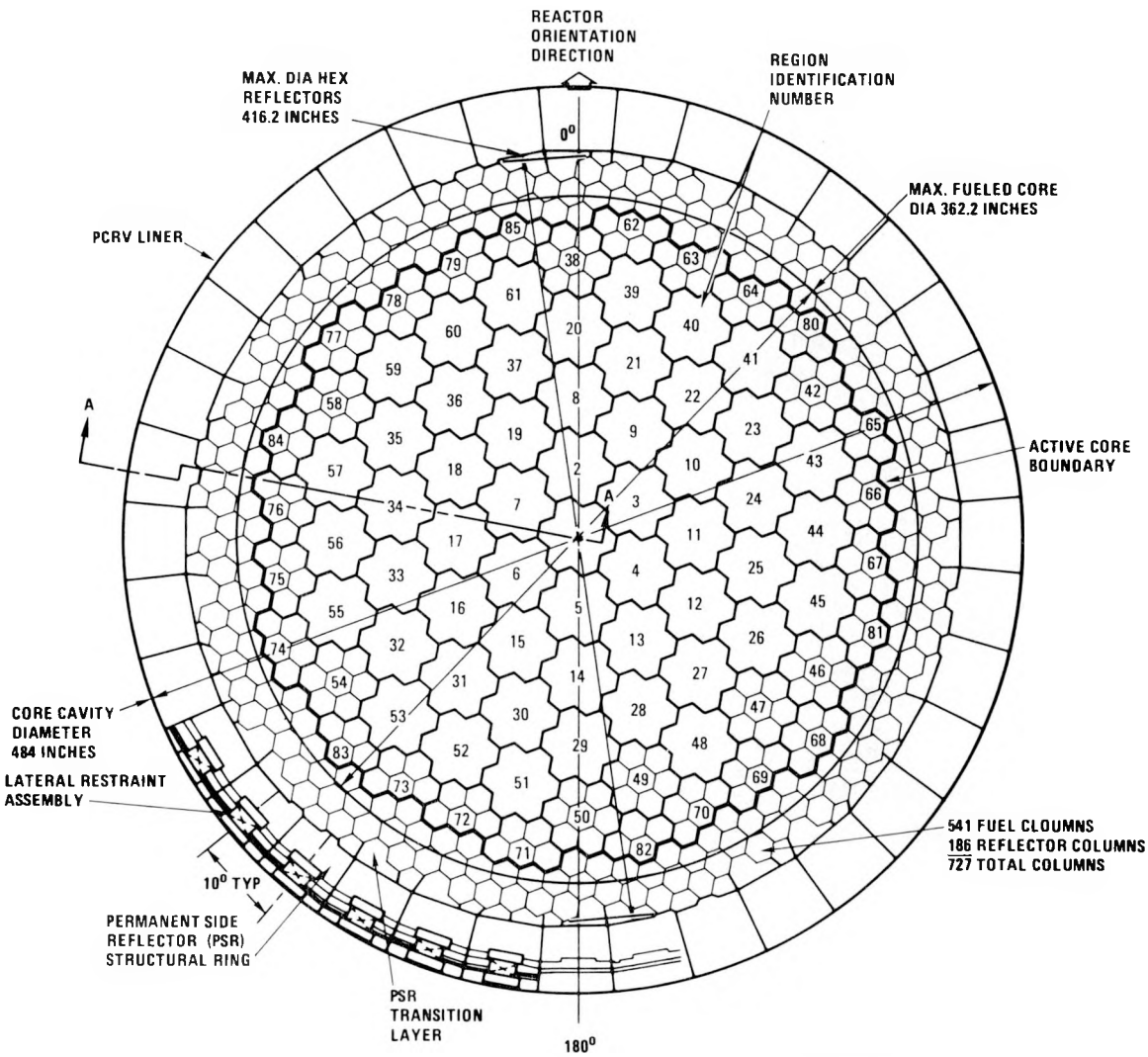

Fig. 2-38. Plan view of core and internals for 2240-MW(t) HTGR-SC/C reference design

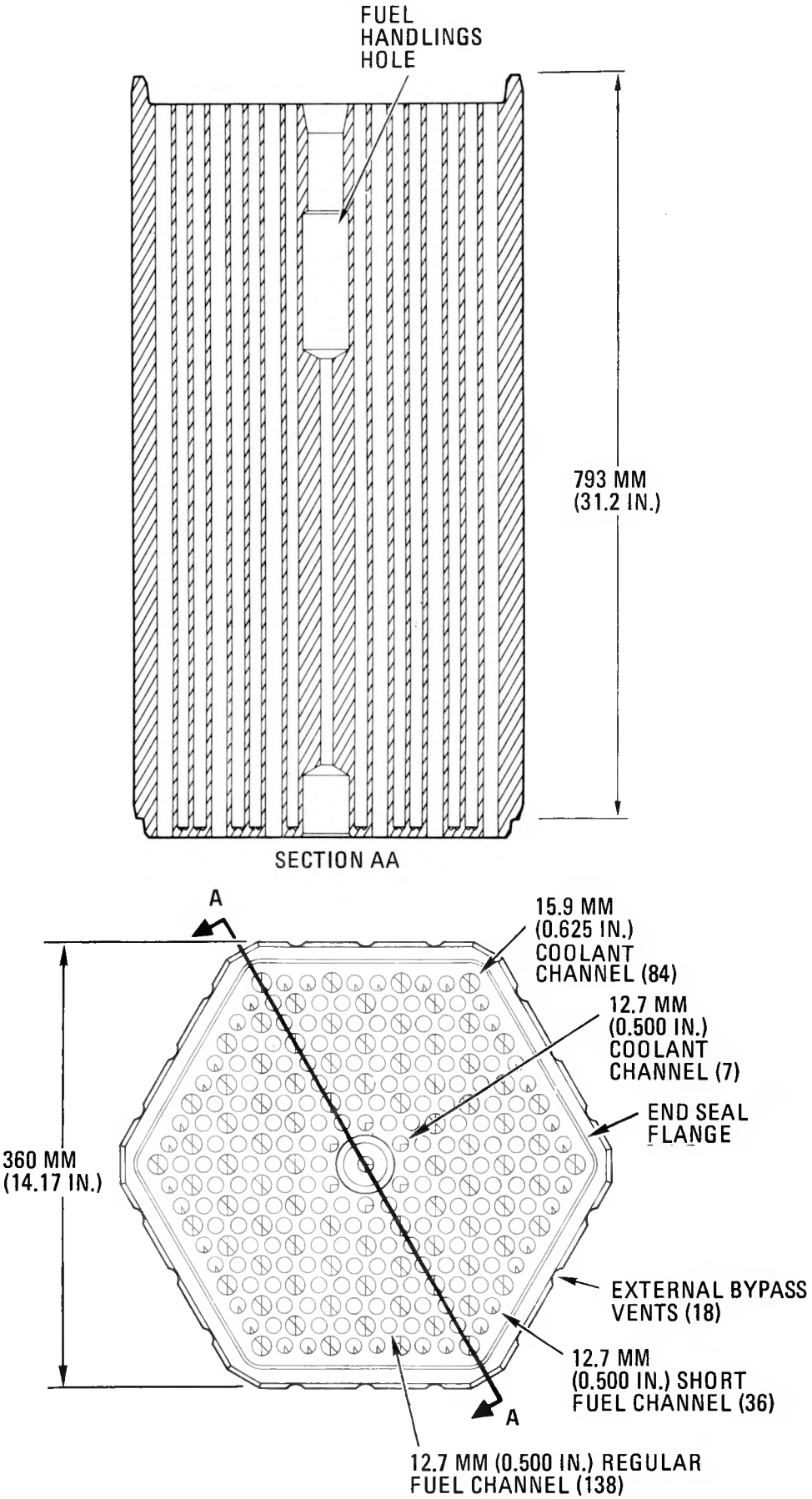

Fig. 2-39. Standard 2240-MW(t) HTGR-SC/C fuel element

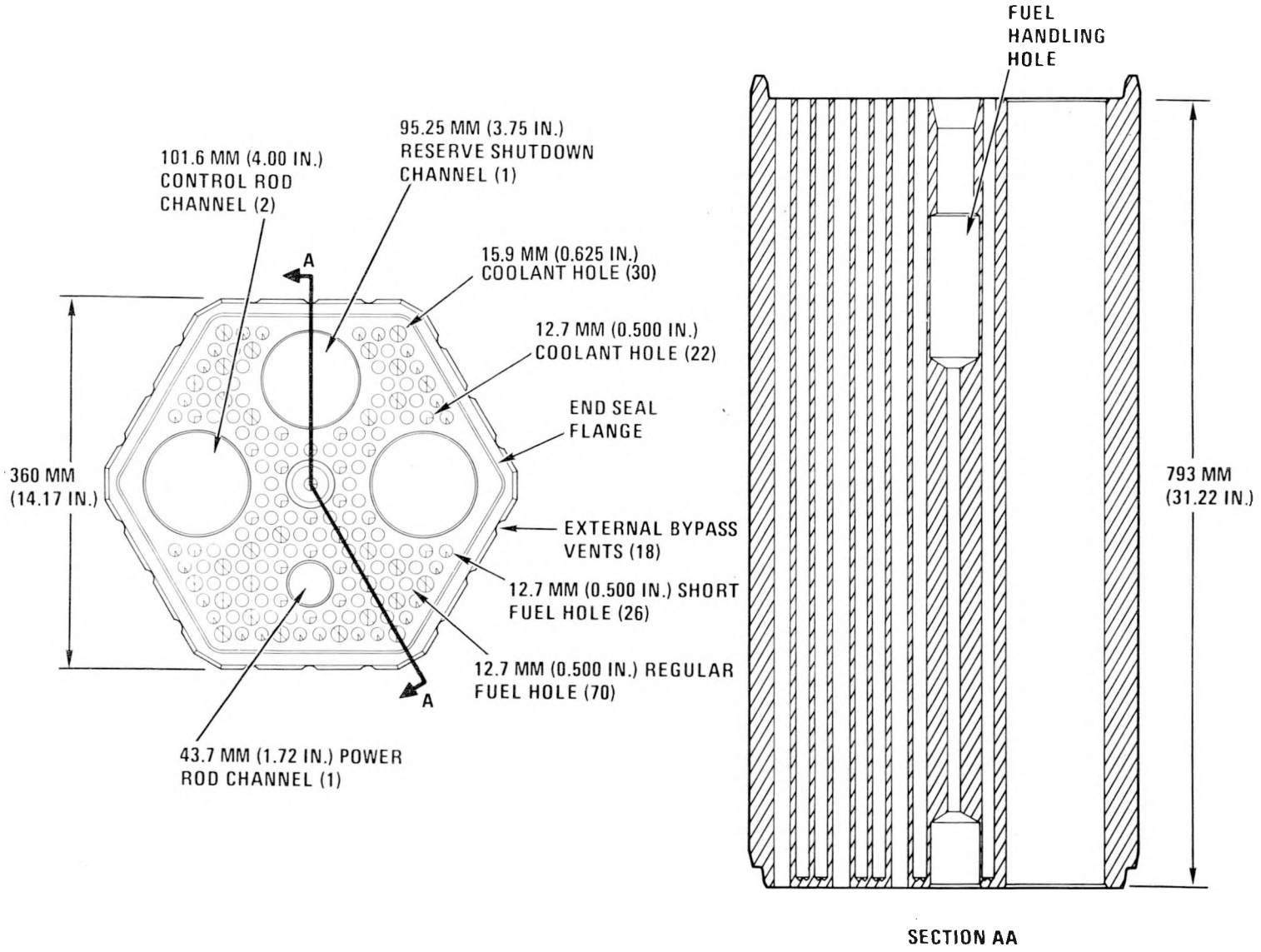

Fig. 2-40. 2240-MW(t) HTGR-SC/C control fuel element

the element to minimize coolant leakage between elements. However, the flange maintains a small gap between the ends of elements in the central area around coolant holes to provide a flow equalization plenum.

The center column of each seven-column region is a control column. These fuel elements have two 102-mm (4-in.) diameter holes for control rods. A single 95-mm (3.75-in.) diameter hole is for reserve shutdown pellets. The power-regulating rod is accommodated by a 50-mm (2-in.) diameter hole (approximate size). Fuel and coolant holes are distributed on an 18.8-mm (0.74-in.) triangular pitch around the larger holes, leaving sufficient ligaments of graphite to satisfy design loads. The 96 fuel holes are 12.7 mm (0.5 in.) in diameter, and 30 coolant holes are 15.9 mm (0.625 in.) in diameter. To maintain sufficient graphite ligaments, 23 coolant holes in certain locations are 12.7 mm (0.5 in.) in diameter. The fuel holes are drilled to near the bottom of the element, and the holes are filled with a stack of fuel rods. The holes are closed at the top by cemented graphite plugs.

The control column is surrounded by six standard fuel columns. These fuel element blocks contain an integral array of fuel and coolant holes of the same sizes as in the control fuel elements. The only interruption in the hole pattern is for the center pickup hole (no holes for control rods or reserve shutdown material). There are 174 fuel holes, 84 large coolant holes, and 7 small coolant holes. Standard and control elements have the same external bypass vents and sealing flanges.

The fuel rods consist of coated fissile and fertile particles bonded in a close-packed array with a carbonaceous matrix to form the cylindrical rods. The rods are 62.9 mm (2.476 in.) long and 12.4 mm (0.49 in.) in diameter. The rod matrix optimizes heat transfer and prevents fuel mechanical interaction with the graphite fuel element. Different fuel loadings in the fuel rod can be achieved by use of controlled amounts of graphite shim particles, which displace a proportionate amount of standard fuel particles.

Burnable poison wafers are placed between all the rods in the fuel rod stack. The wafers are 1.52-mm (0.06-in.) thick disks with a monolayer of BISO-coated natural B_4C particles. These wafers are placed in every fuel hole throughout the core.

The fissile and fertile fuel particles contain spherical kernels of UCO and ThO_2, respectively. The 350-μm-diameter fissile kernel contains 20% enriched uranium and is a chemical blend of about 15% uranium carbide (UC_2) and 85% uranium oxide (UO_2). The fertile ThO_2 kernel is about 500 μm in diameter. Each kernel is surrounded by a porous pyrolytic carbon buffer, which provides void volume for fission gas accumulation and fission fragment trapping. The buffer layer is overcoated with three separate dense coating layers, consisting of a silicon carbide layer sandwiched between two layers of pyrolytic carbon. The buffer and the inner pyrolytic carbon, silicon carbide, and outer pyrolytic carbon layers form the standard TRISO particle.

Reflector Elements. The reflector elements make up the top, bottom, and hexagonal side reflector arrays (in addition to the non-hexagonal permanent side reflector). The core graphite reflector elements are the same size, i.e., 360-mm (14.17-in.), hexagonal right prisms as the fuel elements. Some are full height, 793 mm (31.22 in.) and others are half-height, 396 mm (15.61 in.). All have sealing flanges similar to fuel elements. The elements nearest the fuel elements are replaced on a regular schedule and others have a 40-yr lifetime. The top reflector elements have the same coolant holes as the fuel elements. The control column top reflector elements have holes for two control rods and one power rod and a hole for reserve shutdown material. However, only the bottom reflector has the external vents as described for fuel elements. Coolant holes in the two upper layers of half-height bottom reflector elements match those in fuel elements. The full-height bottom reflector layer provides a coolant flow transition from all the holes into a mixing chamber for that column. Two layers in the bottom reflector contain pins filled with boronated graphite for neutron shielding.

Hexagonal side reflector elements do not have coolant holes. However, they have pickup holes and sealing flanges similar to those of the other elements. Lateral seismic loads are carried by these sealing flanges.

Plenum Elements. The top layer elements are stainless steel hexagonal right prisms. Their functions are region inlet flow distribution, alignment and lateral restraint, and shielding. Three types are used depending on location. Each is basically a heavy-wall hexagonal can with internals for the flow distribution and shielding functions.

The control column plenum elements have holes for the control rods, power rods, and reserve shutdown material. The center pickup hole also is the positioning seat for the orifice valve. Guide tubes for the control rods and reserve shutdown material fit into the appropriate holes at the top. Holes in the bottom plate correspond to the fuel coolant hole positions. These holes and the internal structure are designed to direct the correct portion of the region flow to the center column. The remaining volume is filled with boronated graphite for neutron shielding.

The standard fuel column plenum elements have large internal flow baffles to direct coolant to the outer coolant channels in the region. A pattern of holes in the bottom plate equalizes the flow per channel. The volume above the flow baffle is filled with boronated graphite shielding. The six standard plenum elements in a region are keyed together with rectangular keys, one key and one keyway per element. The keys have tapers on both ends to facilitate engagement. Contact surfaces are coated with chromium carbide. Both types of plenum elements over fuel columns have bottom flanges to match the sealing flange on top of the graphite elements below.

The third type of plenum element is located above hexagonal side reflector columns. There is no coolant flow in these columns. They have the same structural stiffness as other plenum elements and are filled with boronated graphite shielding. A unique feature of the plenum element is T-shaped keys to the permanent side reflector to stabilize these columns during refueling. The bottom plate is designed to fit over the sealing

flanges of the graphite reflector elements. All types of plenum elements have center pickup holes for use during refueling.

Startup Neutron Sources. Neutron sources are installed in the reactor and to provide a sufficient flux of neutrons so that significant changes in the reactivity of the subcritical core will provide an observable change in the output signal of the neutron detectors. Several sources are distributed across the core in the top layer of fuel. The source material is Cf-252, double encapsulated in stainless steel. The small cylindrical sources fit into the lower part of the fuel element pickup hole.

Permanent Side Reflector. The permanent side reflector consists of stacked graphite blocks forming a cylinder surrounding the outer hexagonal reflector columns of the reactor core. The outer structural ring contains 36 blocks per layer, each block being about 1000 mm (40 in.) wide to extend around the circumference. There are 22 layers, each with height and thickness of 457 mm (18 in.). Pairs of adjacent layers are doweled together so that two blocks (one above the other) act together. A 51-mm (2-in.) deep recess spans the separation between these pairs of blocks to accept the spring pack face plates. Thus, there are recesses for spring packs in every column of permanent side reflector structural ring blocks. The spring packs preload the blocks into a tight-fitting structural ring for seismic support and minimize coolant leakage into the sides of the core. Thermal neutron shielding is installed to protect the PCRV liner, thermal barrier cover-plates, and spring packs. Nuclear heating in the concrete is also reduced.

The inner ring of transition blocks fills the space between the near-circular structural ring and the irregular hexagonal shapes of the hexagonal side reflector columns. The transition blocks are not preloaded by the spring packs. There are from one to three transition blocks for each outer block in the structural ring. Transition blocks are thinner but have the same 457-mm (18-in.) height as the structural blocks. Vertical gaps between transition blocks are about 1.5 mm (0.06 in.), similar to the gaps between fuel columns.

At the top of the permanent side reflector, metal caps fit over the 36 segments of the structural and transition elements. Keyways on the inner faces accept the T-shaped keys on the outer reflector column plenum elements.

Core Support Structure. The core support structure consists of two layers of graphite blocks supported by graphite posts, which in turn are supported on graphite seats atop ceramic bases on the PCRV bottom liner (Fig. 2-41). The upper core support blocks have the same hexagonal size as the fuel columns. These blocks are hollowed out to collect the coolant flow from the column above and direct it out through the center of the lower core support block. A single lower support block (having the same star shape as the region) supports each seven-column region. Permanent side reflector blocks are supported on one or two smaller peripheral lower core support structure blocks. The upper peripheral blocks also provide the inner face for the core peripheral seal and the recessed area to accept the bottom ring of spring packs. The upper block is doweled to the bottom block in the permanent side reflector structural ring, and the spring pack spans the horizontal separation between these two blocks.

Every lower core support structure block is supported by three graphite support posts arranged in an equilateral triangle pattern. The interior posts are 229 mm (9 in.) in diameter and about 1.9 m (6 ft) tall. Some of the outer posts are 279 mm (11 in.) in diameter. Peripheral blocks are supported by three posts with irregular spacing due to the different transition shapes. The ends of the core support posts are spherical and fit into similarly shaped recesses in post seat inserts in the core support structure blocks and post supports at the bottom of the core cavity.

The tops of the upper core support structure blocks are doweled into the hexagonal bottom reflectors to provide lateral restraint. The coolant passages through the core support blocks direct the core exit gas streams into a central mixing and temperature measurement chamber inside the lower

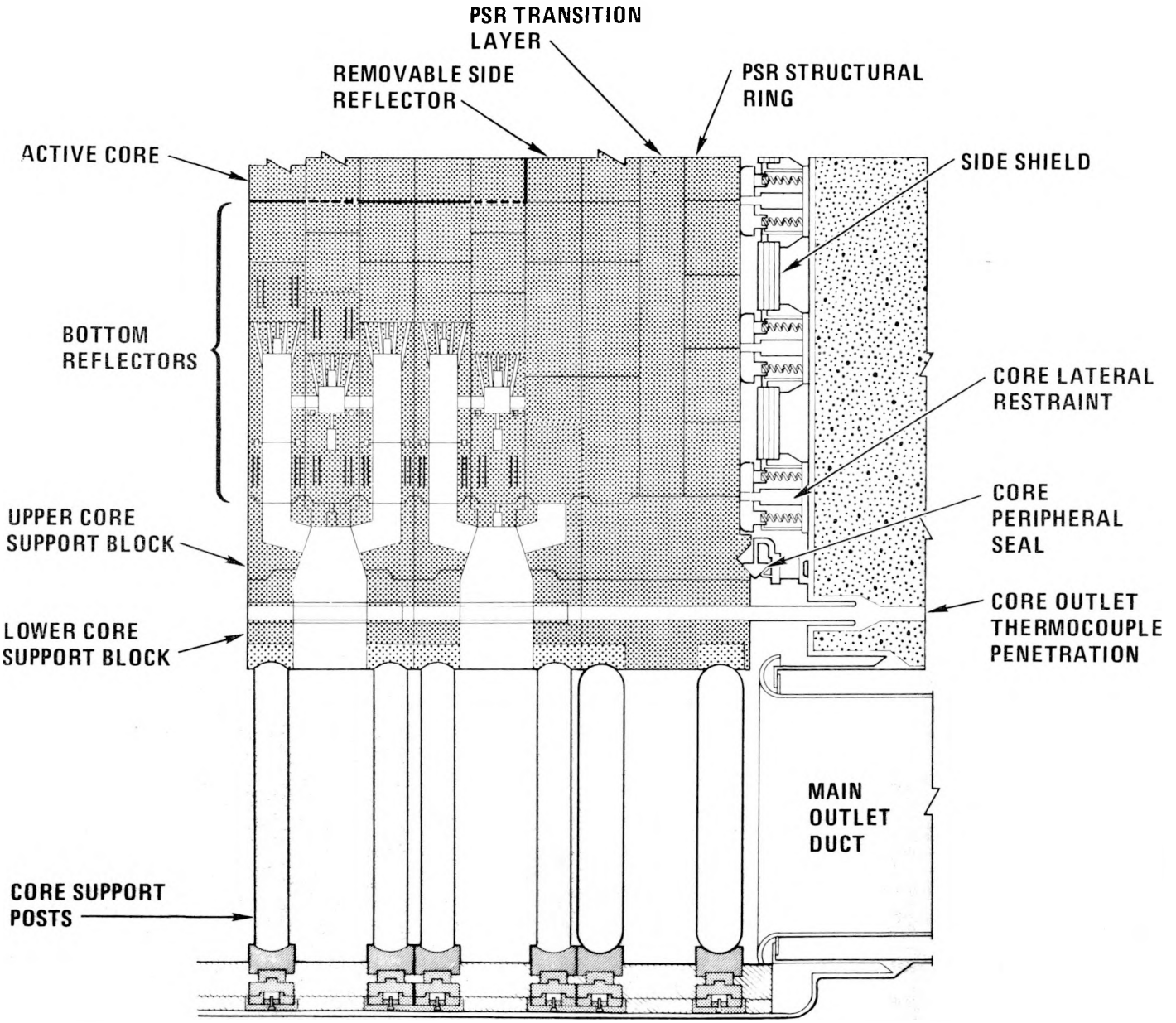

Fig. 2-41. Core support for 2240-MW(t) HTGR-SC/C, elevation view

blocks. Graphite sleeves across the mixing chambers provide a heat-conducting housing for the thermocouples while protecting them from direct, high-velocity coolant impingement.

Core Lateral Restraint. The core lateral restraint structure (see Fig. 2-36) consists of metal support assemblies located in regular array between the permanent side reflector and PCRV liner and includes the thermal neutron side shield. There are 432 identical, radially oriented spring pack assemblies attached to the PCRV through the thermal barrier. These spring packs are spaced so that there is one at every other horizontal intersection of permanent side reflector blocks, located on the vertical centerline. This results in 12 horizontal rows of spring packs with 36 units in each row. The spring packs transfer lateral and tangential core loads from the permanent side reflector into the liner, and they support the steel plates which form the side shield.

Each spring pack contains a group of eight helical coil springs arranged in parallel inside a cylindrical spring housing. A face plate attached to the inner ends of the coil springs interfaces with the permanent side reflector and transfers loads into the springs. The springs are compressed at installation to provide a substantial preload on the permanent side reflector in order to create a continuous permanent side reflector ring structure, thereby resulting in the seismic loads being resisted in shear. The preload also improves the sealing function of the permanent side reflector structure by maintaining the small radial gap clearances. Location of the permanent side reflector structure at installation is also improved by the preloading. Axial and lateral deflections of the coil springs are limited by physical limit stop features built into the face plate and coil spring housing. Thus, slow relative movements due to thermal expansion and PCRV shrinkage and creep are accommodated by the coil springs without developing excessive static loads. The clearance between the radial key and face plate controls the maximum tangential deflection of these springs. The radial keys provide positive location for the permanent side reflector during both installation and operation.

The thermal neutron side shield consists of sandwich layers, up to 100 mm (4 in.) thick, of 25.4-mm (1-in.) thick low-carbon steel plates. A central hole which is in each plate fits over the coil spring housing for support, and the shield assembly is bolted to the housing with standard flat washers as spacers between plates to allow room for relative thermal bowing. The edges of the shield plates are bevelled and, on assembly, interleave with those of adjacent plates to eliminate gaps in the shield through which neutrons or gamma rays could stream. There are 1728 plates in the side shield.

Core Peripheral Seal. The core peripheral seal is formed by 36 triangular-cross-section graphite logs which fit in the annular space between the core support structure and the thermal barrier. A sloping shelf in the outer face of each peripheral core support structure block provides the inner seal set. The outer seat is provided by a metal structure extending from the PCRV liner and enclosed within the thermal barrier. A sine wave web oriented radially prevents bypass coolant flow through the fibrous insulation. The sine wave configuration accommodates the relative thermal expansion resuling from the large thermal gradient between the inner and outer edges of the web.

As relative motion occurs between the core support structure and the PCRV, the seal logs slide up or down the sides of the V-shaped trough formed by the seal seats to maintain its sealing function. During reactor operation the core pressure drop acts across the seal to force the seal logs down against the seats. Coil spring retainers are installed from brackets above each log to prevent its being dislodged should an earthquake occur during an unpressurized condition.

A small amount of bypass coolant flow is permitted in order to keep the core peripheral seal, core lateral restraint, side shield, and sidewall thermal barrier temperatures within design limits.

In-Vessel Refueling Bridge. The in-vessel refueling bridge (see Fig. 2-30) consists of fuel transporter rails, hoist rails, and fuel storage

racks attached to support structures extending down from the top of the core cavity. The refueling mechanism deposits a fuel block on a dolly that rides in the transporter rail. The transporter dolly places the fuel block under a hoist rail. A plenum hoist mechanism, which rides in the hoist rail, removes the block from the transporter dolly and deposits the block in a temporary storage rack or in the elevator assembly. The elevator lowers the block through a penetration that extends out the bottom of the PCRV into a storage vault. This procedure is reversed when placing a block in the core. The elevator and hoist mechanism are housed in two penetrations, one at the end of each hoist rail, that extend out the top of the PCRV. The transporter mechanism is housed in a penetration located at one end of each transporter rail. These penetrations extend out of the top of the PCRV.

During reactor operation the structure is not in use and is supporting only its own weight. During the refueling operation the structure is subjected to the forces applied by the refueling mechanisms and the fuel blocks.

The transporter and hoist rails are welded to a support structure at one end only. They are simply supported at all other locations to allow for thermal growth.

Structural Analysis of Recommended Core Configuration. Structural analysis of the recommended core focused primarily on the two areas where the most significant structural changes from the previous design were made. These areas are the element end seals, which were added to reduce leakage of coolant at the interfaces between elements of a column, and the permanent side reflector, which was redesigned to provide better sealing and to provide core lateral restraint via a system of radial keys. The scoping calculations confirm the feasibility of the design changes and are described below.

Element End Seal. During the course of the alternate core design study, it was found necessary to limit the amount of flow that could bypass the normal coolant channel flow path and leak into and out of openings

developed at the element interfaces. Several methods for accomplishing this were considered. The final configuration of the element end seal consists of a hexagonal flange machined into the top of the fuel elements that mates with a hexagonal recess machined into the bottom of the elements. The inner surfaces of the flange and the outer surface of the recess form a flow restriction that limits the leakage flow into or out of the element. For the seal to be an adequate flow restrictor, the mating surfaces must be accurately machined to achieve a close fit. In the present design a nominal gap of about 0.4 mm (0.016 in.) is used. This is close to the minimum gap that can be practically achieved with graphite in a production environment.

Because of the close clearances involved with the end seal parts, it would be impossible to design dowels and sockets to carry the lateral seismic loads imposed on the blocks. Instead it is necessary for the flange and recess to carry these loads, eliminating the need for dowels. The seismic strength of the flange was evaluated using simple hand calculations. It was assumed that the allowable total stress was 70% of the minimum ultimate strength of the graphite, with half of the allowable allocated to thermal and irradiation stress and the other half allocated to seismic stress. It was found that the seismic strength of the flange was about 4450 N (1000 lb).

Mechanical interference between the mating parts of the end seal is also a concern. The possibility that this might occur as a result of differential irradiation shrinkage of the mating graphite parts was evaluated. Even if the mating parts were exposed to identical temperatures and irradiation doses, the variability in the irradiation shrinkage of graphite (which may amount to ±15% from block to block) is sufficient to result in a worst case differential change in the across-flats dimension of the end seal parts of about 1.1 mm (0.043 in.). Since this is greater than the nominal clearance initially provided between the seal parts, it appears that mechanical interference between the seal parts is a possibility. Analyses were performed to evaluate whether such interference was acceptable.

There were three major concerns regarding mechanical interference between the mating parts of the end seal. The first was concern that interference could lead to difficulties during refueling. The second was that continued operation beyond the time of initial interference might lead to high stress buildup and eventual failure of the flange. Finally, there was a concern that even if steady-state operation with interference were shown to be acceptable, thermal transients imposed on an end seal in an interference condition might cause its failure. The present design of the end seal was evaluated with regard to all three of these concerns and was shown to be acceptable.

Permanent Side Reflector/Core Lateral Restraint. The permanent side reflector and the core lateral restraint were significantly changed during the course of the alternate core design study. The permanent side reflector is divided into two regions: an outer uniform structural ring, which is kept in compression and which seals the core from the gas outside the permanent side reflector, and a transition layer, which makes the transition from the irregular outer boundary of the core to the more regular inner surface of the permanent side reflector structural ring. The core lateral restraint was changed to a system in which springs are used to compress the core and radial keys are used to resist seismic loads.

The amount of preload was calculated based on the radial force required to keep the permanent side reflector under compression during an operating basis earthquake (OBE). This is required to assure tht the radial keys function properly. Based on an estimated OBE ZPA for the core of 0.3 $\bar{g}$, the required spring force was found to be about 31,000 N (7000 lb) at cold shutdown.

The spring rate of the spring pack is designed to be high enough so that the fundamental frequency of lateral vibrations of the permanent side reflector and the core is well into the rigid range. A value of the spring pack spring rate of 87.50 N/mm (5000 lb/in.) was selected, resulting in a fundamental frequency of lateral vibrations of the core and permanent side reflector of about 20 Hz, which should be adequate. This spring rate is

achieved with eight coil springs per spring pack. Each coil spring consists of 12 coils of 12.7-mm (0.5-in.) spring steel rod, with a coil diameter of 63.5 mm (2.5 in.) and a free length of 229 mm (9 in.). With this spring pack design the highest load exerted by a spring pack on the permanent side reflector is about 44,480 N (10,000 lb), and the highest stress in the spring is about 531 MPa (77 ksi), which is acceptable for high-strength spring steel.

The radial keys will consist of circular tubes, 305 mm (12 in.) long, 102 mm (4 in.) in outside diameter, with a 6.35-mm (0.25-in.) wall, which mate with recesses provided in the permanent side reflector blocks. The theoretical largest load on the keys during an OBE was calculated to be about 22,240 N (5,000 lb). For conservatism, the radial keys are designed for a load of 44,480 N (10,000 lb). The resulting stress in the keys is about 262 MPa (38 ksi), which should be acceptable. The bottom disk, to which the radial keys are attached, was also evaluated for seismic loading. With the disk 305 mm (12 in.) in diameter and 25.4 mm (1 in.) thick, the OBE stress is about 227 MPa (33 ksi).

The permanent side reflector structural ring is designed to withstand the loading from the spring packs and from an external pressure loading which varies from nothing to the full core pressure drop of 89 kPa (13 psi). The thickness of the permanent side reflector structural ring is selected to prevent buckling. (A large safety factor is included in this calculation to account for the difficulty in calculating the buckling load of the segmented structure.) Considering the permanent side reflector as a cylinder subjected to an external pressure loading and assuming a cylinder thickness of 457 mm (18 in.), the critical buckling pressure of the cylinder is calculated to be 931 kPa (135 psi). This is nearly a factor of 6 greater than the sum of the actual maximum pressure load [89 kPa (13 psi)] plus the equivalent pressure load of the spring packs [68 kPa (10 psi)] and therefore should be adequate to assure stability of the permanent side reflector structural ring.

2.13.2.2. Core Seismic Analysis. New seismic evaluations using the soil/structural interaction analysis of the FLUSH code show substantial reduction in the lateral design loads from those obtained with previous methods. The resultant design loads are reduced to 39% of previous evaluations, and the resultant maximum predicted load is 66,700 N (15,000 lb) for the fuel elements.

Dynamic analyses of the reactor core are required to determine the magnitude of seismic design loads on its components. In order to establish the design loads, it is necessary to determine first the seismic excitations the core will experience. This is done by a computer code that uses an analytical model of the plant. The plant model includes the PCRV, containment building, auxiliary building, etc., and the substructures that support them. The plant model uses the Nuclear Regulatory Commission (NRC) specified seismic excitations (Ref. 2-4) for an OBE and a safe shutdown earthquake (SSE) for nuclear power plants. The code determines the excitations that the reactor core will experience based on the soil conditions simulated. The NRC has defined five types of soil compositions that are used to bracket the magnitude of the excitation spectra of the construction site:

Soil Type	Description
1	Competent rock
2	Soft rock
3	Firm soil
4	Intermediate soil
5	Soft soil

Each type of soil will influence the excitation magnitude and spectra at the reactor core. The seismic analyses were limited to OBE events.

Until recently the HTGR plant model was analyzed by a computer program that could not account for the attenuating effects of re-radiation of the seismic energy back into the soil. These plant analyses are termed "surface

founded" data because little credit was given to the damping effects of the subsoil due to the normal plant embedment.

GA is now using a three-dimensional finite element computer code, called FLUSH (Ref. 2-5), that does account for normal embedment with soil damping. The plant analyses performed with this code are termed "embedded" data. The embedded data maximum values are approximately 39% of the surface founded horizontal g-loads and 89% of the vertical g-load.

Core Models

A number of computer codes are used to develop inter-block forces from the seismic excitation input. These codes include CRUNCH-1D, which uses a one-dimensional model of one layer of blocks across the diameter of the core. The CRUNCH-2D code uses a two-dimensional model of the core and can include all the hexagonal blocks in the x and y plane (which is the plan view of the core). This code also analyzes only one layer of blocks. A third computer code called MCOCO is also a two-dimensional code but in a different plane than CRUNCH-2D. It simulates the excitations in the core and the x and z plane, where x and y are the coordinates in the plan view of the core and z is the elevation. The core model is based on all the blocks in a one-layer thickness from top to bottom of the core.

CRUNCH-1D Evaluation. The core seismic excitations developed from previous surface founded analyses were used to simulate the five soil conditions on a CRUNCH-1D core model. The core model was based on the reference spring-pack design reactions for a 2240-MW(t) core size. This previous spring pack design is composed of two spring mechanisms. One is a relatively soft spring which permits about 12.7-mm (0.5-in.) lateral movement of the core before the second spring is engaged. The second spring has a much higher spring rate.

A new spring pack concept was also simulated for comparative analyses. This spring pack concept used a radial key that absorbs the tangential forces of the permanent side reflector during a seismic event. It also

utilizes a spring that provides a radial force and an initial preload condition to the permanent side reflector blocks. This concept model cannot be directly included in a CRUNCH-1D model because the one-dimensional approach cannot simulate the radial key effect.

CRUNCH-2D Evaluation. A CRUNCH-2D core model of the 1170-MW(t) HTGR was used to determine the effects of the radial key type spring pack design. This model is based on one layer of core blocks across the core in the x and y directions. It can simulate the effects of the radial key type spring pack and a preload condition on the core. The core model analysis is based on only one inter-block gap dimension, which is 2.3 mm (0.090 in.). The maximum inter-block force is 44,900 N (10,100 lb.).

MCOCO Evaluation. The MCOCO model uses the core input excitation spectra based on the results produced from the FLUSH code model of the 2240-MW(t) reference HTGR plant. These FLUSH code results are based on OBE input excitation spectra with a Type 3 soil condition. The MCOCO model is based on an 1170-MW(t) HTGR core size since as yet there is no core model for the 2240-MW(t) HTGR. It is believed that the difference in core size should not significantly affect the 1170-MW(t) version results.

The conceptual design loads are based on conservative estimates basically from MCOCO analyses and are shown in Table 2-13 both for the seismic excitation spectra for a surface founded plant and the new seismic excitation spectra, which account for soil damping by the normal embedment structure of the plant.

All future seismic evaluations during the later design phases will be based on the FLUSH code, which reduces the seismic input excitation due to soil damping. Taking credit for soil damping reduces the design load to approximately 39% of those based on surface founded plant criteria. The conceptual lateral impact design load is 66,700 N (15,000 lb) and the block-to-block shear load is 4448 N (1000 lb) for active core fuel elements.

TABLE 2-13
PREDICTED SEISMIC DESIGN LOADS

Core Element Condition	Previous Load[a] [N (lb)]	New Load [N (lb)]
Lateral impact force	169,500 (38,100)	66,700 (15,000)
Dowel shear force	12,000 (2,700)	4448 (1000)

[a]The previous loads are based on surface founded excitation spectra.

[b]The new loads are based on soil damping excitation spectra from the FLUSH code based on normal plant embedment.

2.13.2.3. Thermal/Flow Analysis of Core Support Floor and Permanent Side Reflector Components. Work continued on the conceptual design of the HTGR core support floor and permanent side reflector components to meet core thermal/flow requirements. Thermal analyses of permanent side reflector and core support floor graphite blocks were performed, and the worst case core support floor operating condition was identified.

Permanent Side Reflector Block Analysis

The permanent side reflector consists of a cylinder of large, segmented graphite block columns that completely surround the core. Although the blocks are currently designed without coolant holes, helium flows vertically in the gaps between columns, horizontally through crossflow gaps between individual blocks, and between the outer radius of the permanent side reflector and the thermal barrier. Neutron and gamma ray attenuation results in a low level of volumetric heating within the blocks.

An analysis was performed to determine the steady-state temperature distribution in a permanent side reflector block at design operating conditions. The block at the core midplane was selected for analysis because that is the axial location of peak power and peak power-to-flow ratio. Helium flow rates and temperatures in the vertical and horizontal gaps were estimated and served as boundary conditions for detailed finite element thermal analysis of the block.

An example of the resulting graphite temperature calculations is shown in Fig. 2-42. Owing to circumferential symmetry, only one-half of the block was analyzed. The dotted isotherms are separated by a temperature difference of approximately 1°C (1.8°F). The right-hand side of the model represents the vertical midplane of the block, an assumed adiabatic boundary. The low heat transfer coefficient on the outer radius (top) results in a nearly adiabatic condition at that face. The largest temperature gradient of 0.5°C/mm (228°F/in.) occurs on this same outer face.

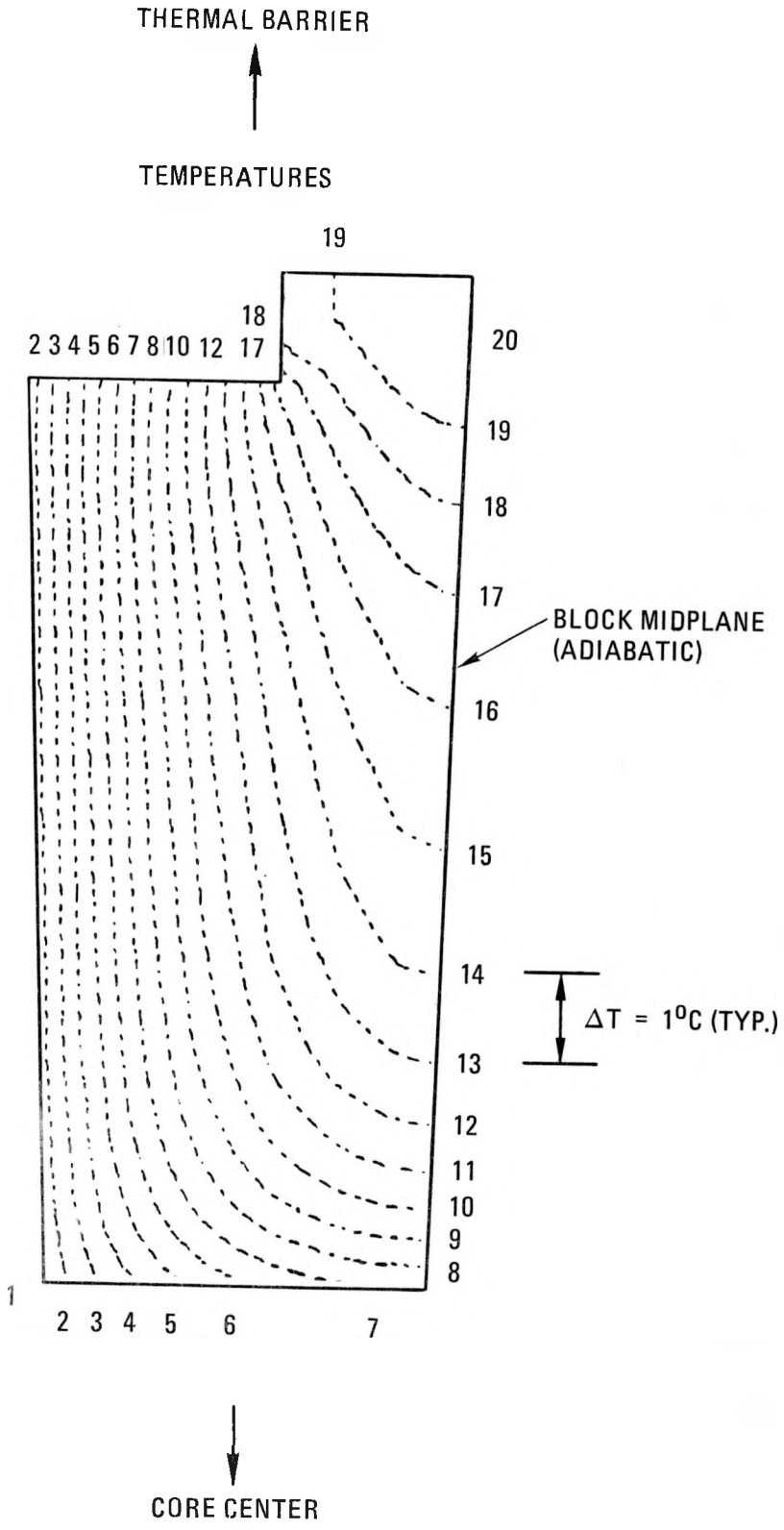

Fig. 2-42. Permanent side reflector temperature profiles

Although the radial temperature gradients in the permanent side reflector blocks do not appear to be significant, these calculations will be repeated after the flow and temperature boundary conditions have been better defined.

Core Support Block Analysis

The core support floor consists of an upper and a lower layer of graphite blocks that support all of the fuel and reflector blocks (Fig. 2-43). The upper layer blocks are similar in size to the fuel elements, while the larger lower blocks have the same outer configuration as a seven-column refueling region. The upper blocks channel the flow into a single 480-mm (19-in.) diameter hole that passes through the large lower block. The new HTGR-SC/C core design incorporates venting the bulk of the core gap flow directly to the outlet plenum through vent gaps or channels located at the interfaces of the lower blocks.

Analyses were performed to determine the temperature gradients in a lower core support block for selected transient operating conditions. Temperature gradients in the graphite are primarily influenced by the rate of change of the coolant temperature and the instantaneous local heat transfer coefficient. Plant control system response to the operational transients is such that the core outlet temperature decreases monotonically with time, either immediately or after a brief period between initiation and detection of an event. As reactor power is run back during a reactor trip, for example, helium circulator speed is programmed to follow feedwater flow as it is automatically reduced at a rate of 0.5%/s to 15% of design flow. Although the mass flow transient will have terminated in approximately 3 min, the core outlet temperature will continue to fall for over an hour.

An axisymmetric model of the lower core support block was constructed, and graphite temperatures during the transients were calculated with a transient thermal analysis computer code. At each time point the mean temperature of a vertical cross section through the block was calculated. This value was compared with the local maximum and minimum point temperatures to

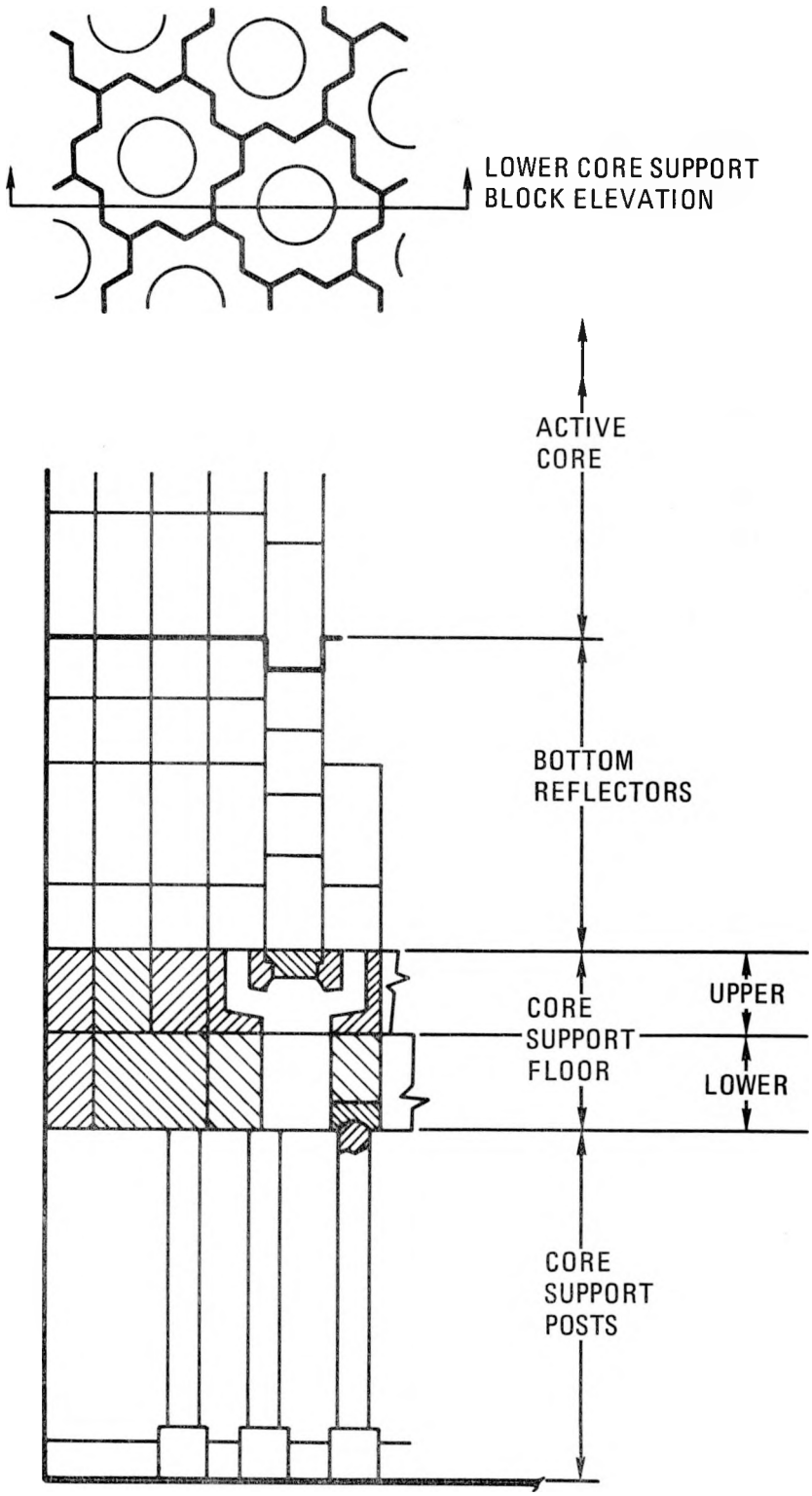

Fig. 2-43. Core outlet region

obtain an indication of the relative tensile and compressive thermal stresses the block experiences during the transients.

Figure 2-44 shows the differences between each temperature extreme and the mean temperature as a function of time for the reactor trip transient. The curve for mean temperature minus minimum temperature, the more important because it represents the more critical tensile stress in the block, peaks at 98°C (208°F) at 2000 s.

Figure 2-45 shows the temperature profiles near the inlet and outlet of the block as a function of time. Near the inlet, the larger surface temperature gradients occur on the outer (vent flow) face, while the opposite is true near the outlet of the block. The larger heat transfer coefficient and much lower mass flow rate on the block periphery cause the vent gas temperature to rise substantially between the inlet and outlet. This results in different axial temperature gradients on the inner and outer faces.

Similar data have been generated for other design transients and are presently being compared to identify a worst case core support floor operating condition.

2.13.2.4. Fuel Performance Analysis. This analysis is directed to the resolution of Priority Issue 1125, Fission Product Transport Uncertainty.

The criteria for circulating and plateout activity in the primary circuit of the 2240-MW(t) HTGR-SC/C have been reviewed, and the circulating activity criteria have been increased 40%, equivalent to 14,000 Ci of Kr-88 (Level B) based on allowable site boundary doses and containment access requirements. To ensure that weaker doses are as low as reasonably achievable (ALARA), a factor of 4 reduction in circulating activity (3500 Ci) is used as the Level A criteria. It is a goal of core design that the predicted fission product release be in close agreement with the Level A design activities. The revised limits in circulating activity (1) are less restrictive than previous criteria, (2) allow decoupling of criteria and "expected" activities, (3) provide a stronger licensing position, and

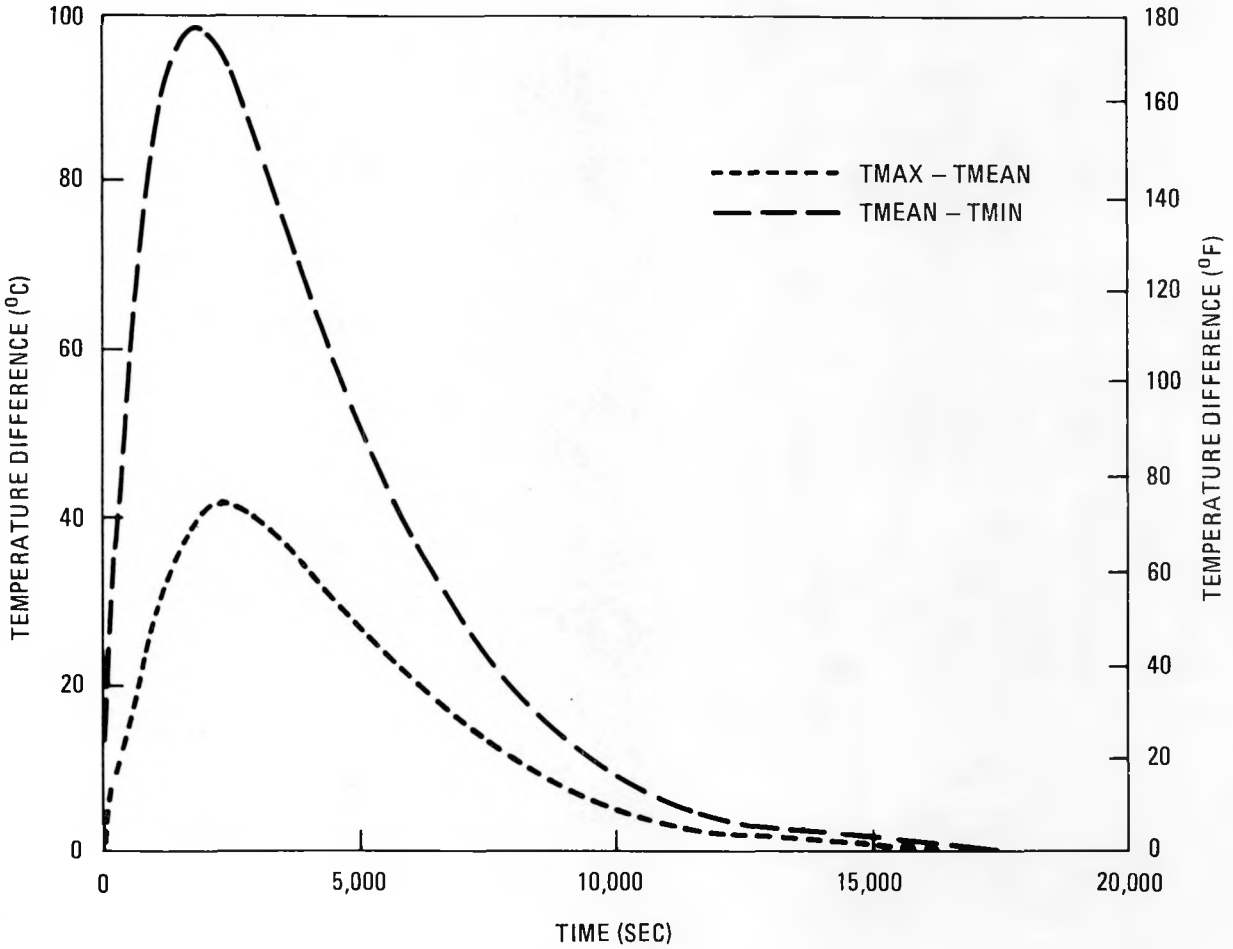

Fig. 2-44. Temperature differences for reactor trip transient

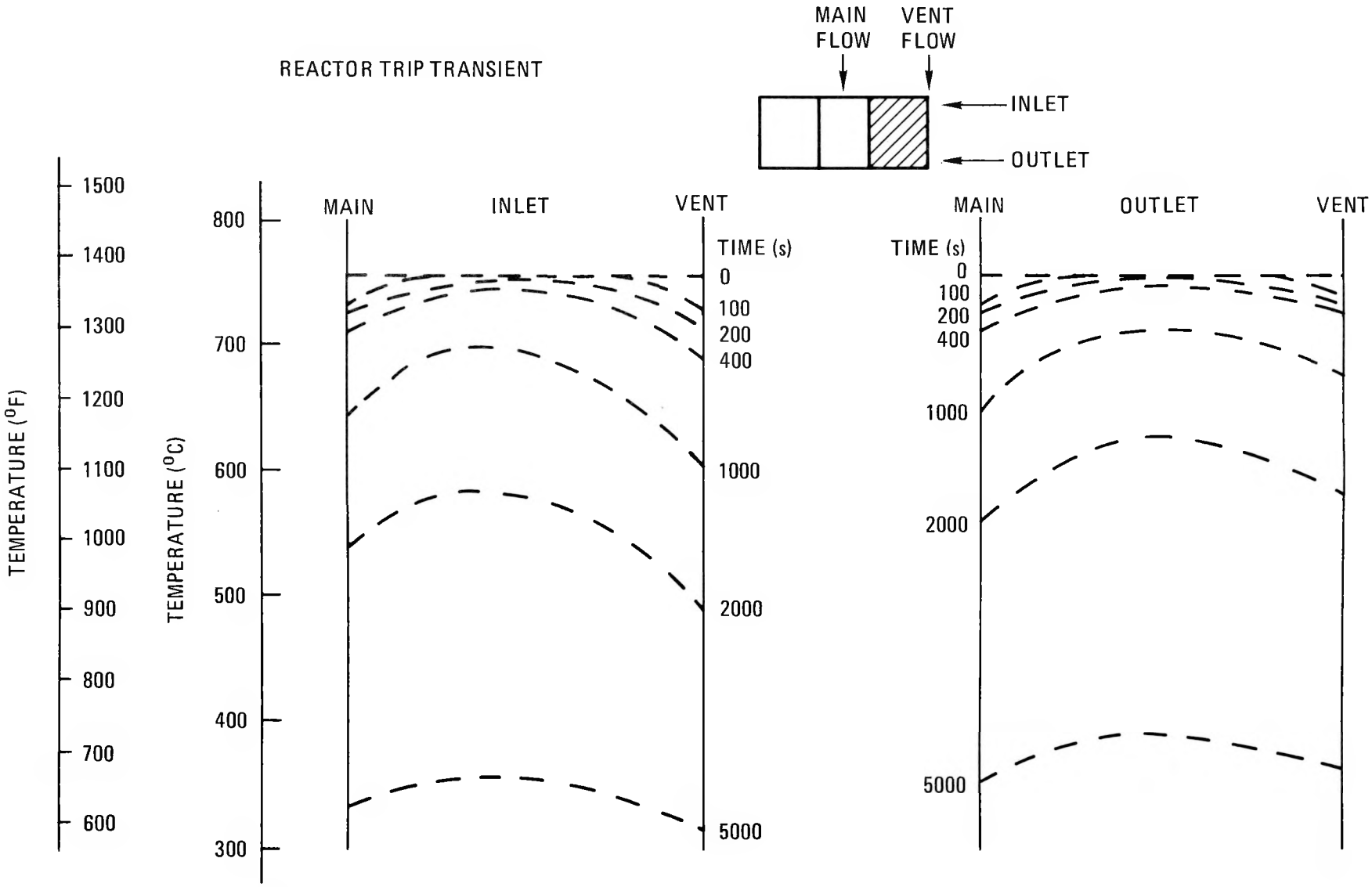

Fig. 2-45. Temperature profiles near inlet and outlet of lower core support block

(4) may result in increased plateout levels if circulating activity is allowed to rise.

The previous plateout criteria for Cs-137 and Sr-90 are retained on an interim basis, since an analogous treatment of plateout criteria has not been performed for the HTGR-SC/C. Plateout of radionuclides is principally a maintenance and ISI issue impacting projected worker doses. It is not a safety issue per se, since plateout activity released via primary circuit blowdown during a design basis depressurization accident would be contained within the isolated containment. Thus, evaluation of acceptable plateout levels becomes principally an economic issue defined by plant ALARA dose requirements. A cost-benefit study is being initiated to evaluate acceptable worker doses as a function of NSS/BOP component layouts and configuration, time and motion studies of maintenance and ISI tasks, and the presence of permanent or temporary shielding.

Preliminary estimates of fission products and neutron activation products in the primary circuit of the 2240-MW(t) HTGR-SC/C have been completed. The data base and methodology are largely equivalent to those used in earlier calculations, with corrections for power level and LEU/Th fission yields. Table 2-14 presents the Level B primary circuit circulating and plateout activity. Analogous results have been calculated for the Level A activity and fuel activity. The results are used in planning studies of helium purification and radwaste system designs, associated plant equipment and shielding, component removal and maintenance procedures, and siting and safety studies. The tables will be updated for the Ref. (0) design using the most recent criteria (i.e., revised values of Level B and Level A) and core design parameters.

2.13.2.5. Nuclear Calculations for Alternate Core Design. Design alternates for the fuel element blocks for the 2240-MW(t) HTGR-SC/C are under consideration with the prime objective of eliminating the problems experienced with the FSV core, involving coolant gas crossflow at block axial interfaces and thermal/flow induced power instabilities. Nuclear calculations applicable to the candidate designs were performed and evaluated.

TABLE 2-14
2240-MW(t) HTGR-SC/C LEVEL B CIRCUIT ACTIVITY (Ci)

NUCLIDE	HALFLIFE	GAS BORNE WITH PURIFICATION SYSTEM OPERATIVE	GAS BORNE WITH PURIFICATION SYSTEM INOPERATIVE	PLATEOUT AFTER 40 YEARS OPERATION INITIAL	PLATEOUT AFTER 40 YEARS OPERATION 1 DAY DECAY	PLATEOUT AFTER 40 YEARS OPERATION 10 DAY DECAY
H3	12.3-Y	4.68+00	5.02+03	0.00	0.00	0.00
C14	5730-Y	0.00	0.00	0.00	0.00	0.00
AR37	34.4-D	7.04-01	8.04+01	0.00	0.00	0.00
GE79	43.0-S	9.20-01	9.22-01	9.86-01	0.00	0.00
AS79	9.0-M	1.05+00	1.06+00	2.06+00	0.00	0.00
SE79M	3.89-M	2.37+01	2.39+01	3.39+01	0.00	0.00
*SE79	STABLE	9.37-05	9.59-05	1.09+02	1.09+02	1.09+02
SE80	STABLE	2.37-04	2.38-04	2.72+02	2.72+02	2.72+02
SE81	18.5-M	8.67+01	8.80+01	2.47+02	0.00	0.00
BR81	STABLE	3.42-04	3.50-04	4.01+02	4.01+02	4.01+02
SE82	STABLE	5.72-04	5.86-04	6.68+02	6.68+02	6.68+02
SE83M	70.-S	7.29+01	7.31+01	8.14+01	0.00	0.00
SE83	22.5-M	1.12+02	1.14+02	3.64+02	0.00	0.00
BR83	2.4-H	1.33+02	1.36+02	2.31+03	2.33+00	0.00
KR83M	1.86-H	3.15+03	3.96+03	0.00	0.00	0.00
KR83	STABLE	4.24-02	2.86+01	0.00	0.00	0.00
SE84	3.3-M	3.64+02	3.66+02	4.84+02	0.00	0.00
BR84	31.8-M	4.56+02	4.65+02	2.03+03	0.00	0.00
KR84	STABLE	7.66-02	5.15+01	0.00	0.00	0.00
BR85	2.87-M	4.82+02	4.85+02	6.21+02	0.00	0.00
KR85M	4.48-H	4.03+03	6.52+03	0.00	0.00	0.00
KR85	10.73Y	8.77+00	5.75+03	0.00	0.00	0.00
RB85	STABLE	1.92-04	2.32-04	2.25+02	2.25+02	2.25+02
KR86	STABLE	1.48-01	9.93+01	0.00	0.00	0.00
KR87	76.-M	5.14+03	6.04+03	0.00	0.00	0.00
RB87	STABLE	4.57-04	4.72-04	5.34+02	5.34+02	5.34+02
KR88	2.8-H	8.97+03	1.24+04	0.00	0.00	0.00
RB88	17.7-M	3.26+03	4.57+03	9.03+03	0.00	0.00
SR88	STABLE	5.23-05	5.98-05	9.26+01	9.26+01	9.26+01
KR89	3.16-M	2.12+03	2.14+03	0.00	0.00	0.00

TABLE 2-14 (Continued)

NUCLIDE	HALFLIFE	GAS BORNE WITH PURIFICATION SYSTEM OPERATIVE	GAS BORNE WITH PURIFICATION SYSTEM INOPERATIVE	PLATEOUT AFTER 40 YEARS OPERATION INITIAL	PLATEOUT AFTER 40 YEARS OPERATION 1 DAY DECAY	PLATEOUT AFTER 40 YEARS OPERATION 10 DAY DECAY
RB89	15.2-M	8.76+02	8.95+02	2.21+03	0.00	0.00
SR89	50.5-D	1.54+00	1.58+00	1.25+04	1.24+04	1.09+04
Y89	STABLE	4.12-07	4.22-07	6.97+01	6.97+01	6.98+01
KR90	32.3-S	9.32+02	9.33+02	0.00	0.00	0.00
RB90M	4.28-M	8.85+01	8.92+01	1.26+02	0.00	0.00
RB90	2.7-M	7.19+02	7.23+02	9.15+02	0.00	0.00
SR90	29.-Y	8.06-03	8.25-03	6.70+03	6.70+03	6.70+03
Y90	64.-H	1.23-02	1.26-02	6.70+03	6.70+03	6.70+03
ZR90	STABLE	2.27-08	2.32-08	3.75+01	3.75+01	3.75+01
KR91	9.0-S	3.20+02	3.20+02	0.00	0.00	0.00
RB91	58.5-S	3.80+02	3.81+02	4.17+02	0.00	0.00
SR91	9.48-H	8.35+00	8.56+00	5.21+02	9.02+01	1.25-05
Y91	58.6-D	1.33-02	1.36-02	6.25+02	6.21+02	5.59+02
ZR91	STABLE	4.98-07	5.10-07	4.11+00	4.11+00	4.11+00
SR92	2.71-H	6.10+00	6.24+00	1.05+02	2.27-01	0.00
Y92	3.53-H	5.06+00	5.18+00	2.12+02	4.26+00	0.00
ZR92	STABLE	5.45-07	5.59-07	1.82+00	1.82+00	1.82+00
SR93	7.5-M	6.45+01	6.52+01	1.13+02	0.00	0.00
Y93	10.2-H	2.90+00	2.98+00	2.29+02	4.51+01	1.90-05
ZR93	STABLE	5.87-07	6.01-07	1.99+00	1.99+00	1.99+00
SR94	1.29-M	9.64+01	9.67+01	1.09+02	0.00	0.00
Y94	19.0-M	7.37+01	7.50+01	2.26+02	0.00	0.00
ZR94	STABLE	9.59-07	9.87-07	2.01+00	2.01+00	2.01+00
Y95	10.5-M	5.73+01	5.80+01	1.18+02	0.00	0.00
ZR95	65.5-D	1.87-02	1.92-02	2.37+02	2.34+02	2.13+02
NB95M	3.61-D	2.21-03	2.26-03	3.52+00	3.32+00	2.40+00
NB95	35.1-D	2.33-02	2.39-02	3.56+02	3.54+02	3.32+02
MO95	STABLE	5.95-07	6.09-07	2.79+00	2.79+00	2.79+00
Y96	6.0-S	1.08+02	1.08+02	1.09+02	0.00	0.00
ZR96	STABLE	1.14-06	1.17-06	1.34+00	1.34+00	1.34+00

TABLE 2-14 (Continued)

NUCLIDE	HALFLIFE	GAS BORNE WITH PURIFICATION SYSTEM OPERATIVE	GAS BORNE WITH PURIFICATION SYSTEM INOPERATIVE	PLATEOUT AFTER 40 YEARS OPERATION INITIAL	PLATEOUT AFTER 40 YEARS OPERATION 1 DAY DECAY	PLATEOUT AFTER 40 YEARS OPERATION 10 DAY DECAY
ZR97	16.8-H	1.10+00	1.12+00	1.12+02	4.15+01	5.59-03
NB97	73.6-M	1.35+01	1.38+01	2.24+02	4.47+01	6.03-03
MO97	STABLE	6.48-07	6.64-07	2.02+00	2.02+00	2.02+00
NB98	51.0-M	1.20-01	1.22-01	7.33-01	2.32-09	0.00
MO98	STABLE	5.77-07	5.90-07	6.77-01	6.77-01	6.77-01
NB99M	2.5-M	3.23+01	3.24+01	4.03+01	0.00	0.00
NB99	14.0-S	7.34+01	7.34+01	7.51+01	0.00	0.00
MO99	66.02H	5.59-01	5.73-01	2.32+02	1.80+02	1.87+01
TC99M	6.02-H	2.77+00	2.84+00	3.07+02	1.80+02	1.81+01
TC99	STABLE	6.28-07	6.43-07	2.77+00	2.77+00	2.77+00
NB100M	7.0-S	5.80+01	5.80+01	5.86+01	0.00	0.00
NB100	2.9-M	4.54+01	4.57+01	5.86+01	0.00	0.00
MO100	STABLE	8.72-07	8.93-07	1.10+00	1.10+00	1.10+00
MO101	14.6-M	3.98+01	4.03+01	9.79+01	0.00	0.00
TC101	14.2-M	5.69+01	5.79+01	1.96+02	0.00	0.00
RU101	STABLE	8.30-07	8.55-07	1.84+00	1.84+00	1.84+00
MO102	11.1-M	4.03+01	4.08+01	8.50+01	0.00	0.00
TC102M	4.3-M	8.76+01	8.86+01	1.70+02	0.00	0.00
RU102	STABLE	9.36-07	9.63-07	1.62+00	1.62+00	1.62+00
MO103	60.-S	6.18+01	6.19+01	6.80+01	0.00	0.00
RU103	39.6-D	2.30-02	2.36-02	1.38+02	1.35+02	1.15+02
RH103M	56.-M	1.04+01	1.06+01	2.05+02	1.34+02	1.14+02
RH103	STABLE	4.37-07	4.48-07	1.76+00	1.76+00	1.76+00
MO104	1.6-M	4.04+01	4.05+01	4.69+01	0.00	0.00
TC104	18.-M	3.19+01	3.24+01	9.59+01	0.00	0.00
RU104	STABLE	4.47-07	4.61-07	9.35-01	9.35-01	9.35-01
TC105	8.0-M	1.87+01	1.89+01	3.36+01	0.00	0.00
RU105	4.44-H	1.90+00	1.95+00	6.74+01	1.61+00	0.00
RH105	35.5-H	1.67-01	1.71-01	1.01+02	6.91+01	1.02+00
PD105	STABLE	1.89-07	1.94-07	8.79-01	8.79-01	8.79-01

TABLE 2-14 (Continued)

NUCLIDE	HALFLIFE	GAS BORNE WITH PURIFICATION SYSTEM OPERATIVE	GAS BORNE WITH PURIFICATION SYSTEM INOPERATIVE	PLATEOUT AFTER 40 YEARS OPERATION INITIAL	PLATEOUT AFTER 40 YEARS OPERATION 1 DAY DECAY	PLATEOUT AFTER 40 YEARS OPERATION 10 DAY DECAY
RU106	369.-D	4.23-04	4.33-04	2.25+01	2.24+01	2.21+01
PD106	STABLE	9.25-08	9.47-08	2.56-01	2.56-01	2.56-01
RU107	4.2-M	1.07+01	1.08+01	1.52+01	0.00	0.00
RH107	21.7-M	8.20+00	8.35+00	3.05+01	0.00	0.00
PD107	STABLE	1.33-07	1.37-07	3.04-01	3.04-01	3.04-01
RU108	4.5-M	6.63+00	6.69+00	9.62+00	0.00	0.00
PD108	STABLE	5.69-08	5.82-08	6.64-02	6.64-02	6.64-02
RH109	1.5-M	6.42+00	6.44+00	7.38+00	0.00	0.00
PD109M	4.69-M	4.71+00	4.75+00	7.40+00	0.00	0.00
PD109	13.46H	1.87-01	1.92-01	1.85+01	5.39+00	7.99-05
AG109	STABLE	6.51-03	6.67-03	7.61+03	7.61+03	7.61+03
PD110	STABLE	1.74-08	1.78-08	2.03-02	2.03-02	2.03-02
AG110M	252.-D	1.00+00	1.02+00	3.63+04	3.62+04	3.53+04
RH111	63.-S	1.33+00	1.33+00	1.47+00	0.00	0.00
PD111	22.-M	9.00-01	9.15-01	3.02+00	0.00	0.00
AG111M	74.-S	2.18+00	2.20+00	4.55+00	0.00	0.00
AG111	7.47-D	2.21+02	2.26+02	2.38+05	2.17+05	9.41+04
CD111	STABLE	1.31-06	1.37-06	1.64+03	1.64+03	1.64+03
PD112	20.1-H	6.46-03	6.61-03	7.87-01	3.44-01	2.00-04
AG112	3.13-H	4.01-02	4.10-02	1.57+00	4.11-01	2.37-04
PD113	1.5-M	4.65-01	4.66-01	5.35-01	0.00	0.00
AG113	5.3-H	2.74-02	2.81-02	9.63-01	4.18-02	0.00
CD113	STABLE	2.86-09	2.93-09	8.93-03	8.93-03	8.93-03
SN119M	245.-D	1.35-07	1.38-07	4.78-03	4.76-03	4.64-03
SN119	STABLE	2.02-09	2.07-09	2.40-03	2.40-03	2.40-03
SN123	129.-D	3.69-06	3.78-06	6.86-02	6.83-02	6.50-02
SB123	STABLE	3.10-07	3.18-07	3.63-01	3.63-01	3.63-01
SN125	9.65-D	2.63-04	2.69-04	3.66-01	3.40-01	1.78-01
SB125	2.73-Y	8.12-04	8.31-04	1.17+02	1.17+02	1.16+02
TE125M	58.-D	1.28-02	1.31-02	1.34+02	1.32+02	1.21+02

TABLE 2-14 (Continued)

NUCLIDE	HALFLIFE	GAS BORNE WITH PURIFICATION SYSTEM OPERATIVE	GAS BORNE WITH PURIFICATION SYSTEM INOPERATIVE	PLATEOUT AFTER 40 YEARS OPERATION INITIAL	PLATEOUT AFTER 40 YEARS OPERATION 1 DAY DECAY	PLATEOUT AFTER 40 YEARS OPERATION 10 DAY DECAY
TE125	STABLE	5.37-05	5.49-05	6.44+01	6.44+01	6.44+01
SN126	STABLE	1.37-08	1.40-08	1.60-02	1.60-02	1.60-02
SB126M	19.0-M	7.07-01	7.18-01	2.05+00	2.07-04	2.07-04
SN127M	4.4-M	5.21-01	5.24-01	7.50-01	0.00	0.00
SN127	2.12-H	2.46-01	2.52-01	3.39+00	1.32-03	0.00
SB127	3.8-D	9.39-03	9.63-03	8.52+00	7.17+00	1.39+00
TE127M	109.-D	7.12-02	7.29-02	1.12+03	1.11+03	1.05+03
TE127	9.4-H	8.61+00	8.81+00	1.60+03	1.18+03	1.03+03
I 127	STABLE	6.12-04	6.26-04	7.27+02	7.27+02	7.27+02
SN128	59.-M	1.14+00	1.16+00	7.84+00	3.53-07	0.00
SB128M	10.4-M	4.48+00	4.54+00	1.58+01	4.27-07	0.00
SB128	9.0-H	8.93-03	9.13-03	5.05-01	7.98-02	4.77-09
TE128	STABLE	1.23-03	1.26-03	1.44+03	1.44+03	1.44+03
SN129M	2.5-M	6.69+00	6.72+00	8.36+00	0.00	0.00
SN129	7.5-M	3.27+00	3.31+00	5.73+00	0.00	0.00
SB129	4.34-H	9.58-01	9.82-01	3.01+01	6.57-01	0.00
TE129M	33.4-D	6.36-01	6.51-01	3.07+03	3.01+03	2.49+03
TE129	70.-M	8.63+01	8.81+01	2.67+03	1.92+03	1.59+03
I 129	STABLE	2.60-03	2.66-03	3.07+03	3.07+03	3.07+03
SN130	3.7-M	1.54+01	1.55+01	2.11+01	0.00	0.00
SB130M	6.6-M	2.38+01	2.40+01	4.46+01	0.00	0.00
SB130	37.-M	2.07+00	2.07+00	1.01+01	0.00	0.00
TE130	STABLE	5.27-03	5.39-03	6.16+03	6.16+03	6.16+03
SN131	63.-S	1.57+01	1.58+01	1.74+01	0.00	0.00
SB131	23.-M	1.96+01	1.99+01	6.62+01	0.00	0.00
TE131M	30.-M	1.22+01	1.25+01	2.21+03	1.27+03	8.65+00
TE131	25.-M	3.47+02	3.53+02	1.65+03	2.32+02	1.58+00
I 131	8.041D	2.61+01	2.67+01	3.33+04	3.07+04	1.42+04
XE131M	11.99D	2.39+01	9.72+02	0.00	0.00	0.00
XE131	STABLE	3.89-01	2.62+02	0.00	0.00	0.00

TABLE 2-14 (Continued)

NUCLIDE	HALFLIFE	GAS BORNE WITH PURIFICATION SYSTEM OPERATIVE	GAS BORNE WITH PURIFICATION SYSTEM INOPERATIVE	PLATEOUT AFTER 40 YEARS OPERATION INITIAL	PLATEOUT AFTER 40 YEARS OPERATION 1 DAY DECAY	PLATEOUT AFTER 40 YEARS OPERATION 10 DAY DECAY
SN132	40.0-S	9.62+00	9.63+00	1.03+01	0.00	0.00
SB132M	4.1-M	1.79+01	1.80+01	2.55+01	0.00	0.00
SB132	2.1-M	3.02+01	3.03+01	3.69+01	0.00	0.00
TE132	78.-H	5.97+01	6.06+01	2.78+04	2.25+04	3.30+03
I 132	2.285H	3.40+02	3.48+02	3.28+04	2.32+04	3.40+03
XE132	STABLE	5.68-01	3.82+02	0.00	0.00	0.00
SB133	2.4-M	3.24+01	3.26+01	4.02+01	0.00	0.00
TE133M	55.4-M	3.95+02	4.03+02	2.59+03	3.89-05	0.00
TE133	12.5-M	4.69+02	4.75+02	1.35+03	6.54-06	0.00
I 133	20.8-H	1.80+02	1.84+02	2.54+04	1.15+04	8.58+00
XE133M	2.23-D	2.00+02	1.74+03	0.00	0.00	0.00
XE133	5.29-D	4.20+03	7.92+04	0.00	0.00	0.00
CS133	STABLE	1.86-03	2.45-03	2.17+03	2.17+03	2.17+03
TE134	42.-M	7.24+02	7.38+02	3.77+03	0.00	0.00
I 134M	3.6-M	6.88+01	6.92+01	9.36+01	0.00	0.00
I 134	52.6-M	9.35+02	9.56+02	8.93+03	1.37-04	0.00
XE134	STABLE	9.57-01	6.43+02	0.00	0.00	0.00
CS134	2.06-Y	4.30-01	4.40-01	4.66+04	4.66+04	4.62+04
I 135	6.585H	2.84+02	2.90+02	1.15+04	9.20+02	0.00
XE135M	15.3-M	2.07+03	2.14+03	0.00	0.00	0.00
XE135	9.17-H	6.22+03	1.16+04	0.00	0.00	0.00
CS135	STABLE	1.91-03	1.99-03	2.23+03	2.23+03	2.23+03
I 136	85.-S	2.88+02	2.89+02	3.29+02	0.00	0.00
XE136	STABLE	8.21-01	5.51+02	0.00	0.00	0.00
CS136	13.0-D	8.29+00	8.48+00	1.55+04	1.47+04	9.12+03
XE137	3.84-M	1.11+03	1.12+03	0.00	0.00	0.00
CS137	30.1-Y	1.62-01	1.66-01	1.34+05	1.34+05	1.34+05
BA137M	2.55-M	4.34+00	4.36+00	1.27+05	1.27+05	1.27+05
BA137	STABLE	4.93-06	5.05-06	1.14+03	1.14+03	1.14+03
XE138	14.2-M	2.08+03	2.14+03	0.00	0.00	0.00

TABLE 2-14 (Continued)

NUCLIDE	HALFLIFE	GAS BORNE WITH PURIFICATION SYSTEM OPERATIVE	GAS BORNE WITH PURIFICATION SYSTEM INOPERATIVE	PLATEOUT AFTER 40 YEARS OPERATION INITIAL	PLATEOUT AFTER 40 YEARS OPERATION 1 DAY DECAY	PLATEOUT AFTER 40 YEARS OPERATION 10 DAY DECAY
CS138M	2.9-M	3.67+00	3.69+00	4.74+00	0.00	0.00
CS138	32.2-M	5.22+02	5.47+02	2.20+03	0.00	0.00
BA138	STABLE	1.16-04	1.19-04	1.50+02	1.50+02	1.50+02
XE139	39.7-S	3.79+02	3.79+02	0.00	0.00	0.00
CS139	9.3-M	2.57+02	2.61+02	4.97+02	0.00	0.00
BA139	83.3M	4.06+01	4.18+01	6.18+02	4.25-03	0.00
LA139	STABLE	1.20-06	1.23-06	6.38+00	6.38+00	6.38+00
XE140	13.6-S	1.79+02	1.79+02	0.00	0.00	0.00
CS140	63.8-S	2.57+02	2.57+02	2.84+02	0.00	0.00
BA140	12.79D	7.95+00	8.14+00	1.47+04	1.39+04	8.55+03
LA140	40.23H	5.28-01	5.41-01	1.48+04	1.46+04	9.80+03
CE140	STABLE	8.98-07	9.19-07	1.30+02	1.30+02	1.30+02
BA141	18.3M	3.92+01	3.98+01	1.11+02	0.00	0.00
LA141	3.87-H	6.23+00	6.40+00	2.23+02	3.16+00	0.00
CE141	32.53D	2.52-02	2.58-02	3.35+02	3.29+02	2.72+02
PR141	STABLE	8.38-07	8.58-07	3.91+00	3.91+00	3.91+00
BA142	10.7-M	5.27+01	5.33+01	1.09+02	0.00	0.00
LA142	92.4-M	1.61+01	1.65+01	2.22+02	4.81-03	0.00
CE142	STABLE	9.71-07	9.97-07	2.94+00	2.94+00	2.94+00
LA143	14. -M	4.56+01	4.62+01	1.09+02	0.00	0.00
CE143	33.0-H	7.82-01	8.03-01	2.20+02	1.33+02	1.42+00
PR143	13.58D	5.66-02	5.80-02	3.30+02	3.22+02	2.13+02
ND143	STABLE	8.36-07	8.56-07	3.90+00	3.90+00	3.90+00
CE144	284.4D	2.42-03	2.47-03	9.90+01	9.88+01	9.66+01
PR144	17.28M	2.79+01	2.83+01	1.75+02	9.88+01	9.66+01
ND144	STABLE	7.97-07	8.18-07	2.25+00	2.25+00	2.25+00
CE145	3.3-M	5.41+01	5.44+01	7.20+01	0.00	0.00
PR145	5.98-H	3.42+00	3.50+00	1.44+02	8.96+00	0.00
ND145	STABLE	5.81-07	5.96-07	1.94+00	1.94+00	1.94+00
CE146	14.2-M	2.27+01	2.30+01	5.50+01	0.00	0.00

TABLE 2-14 (Continued)

NUCLIDE	HALFLIFE	GAS BORNE WITH PURIFICATION SYSTEM OPERATIVE	GAS BORNE WITH PURIFICATION SYSTEM INOPERATIVE	PLATEOUT AFTER 40 YEARS OPERATION INITIAL	PLATEOUT AFTER 40 YEARS OPERATION 1 DAY DECAY	PLATEOUT AFTER 40 YEARS OPERATION 10 DAY DECAY
PR146	24.2-M	2.28+01	2.33+01	1.10+02	0.00	0.00
ND146	STABLE	6.07-07	6.25-07	1.50+00	1.50+00	1.50+00
CE147	70.-S	3.61+01	3.62+01	4.03+01	0.00	0.00
PR147	12.-M	3.56+01	3.61+01	8.26+01	0.00	0.00
ND147	10.99D	4.91-02	5.06-02	1.25+02	1.17+02	6.65+01
PM147	2.623Y	3.07-04	3.14-04	1.67+02	1.67+02	1.67+02
SM147	STABLE	3.85-05	3.94-05	4.65+01	4.65+01	4.65+01
PR148	2.0-M	2.63+01	2.64+01	3.16+01	0.00	0.00
ND148	STABLE	4.57-07	4.68-07	5.82-01	5.82-01	5.82-01
PM148M	41.3-D	2.32-04	2.37-04	1.38+00	1.36+00	1.17+00
PM148	5.37-D	7.52-03	7.69-03	5.83+00	5.12+00	1.60+00
PR149	2.3-M	1.64+01	1.65+01	2.02+01	0.00	0.00
ND149	1.73-H	3.28+00	3.36+00	4.12+01	2.77-03	0.00
PM149	53.1-H	7.58-02	7.78-02	6.21+01	4.64+01	2.77+00
SM149	STABLE	1.17-05	1.16-05	1.35+01	1.35+01	1.35+01
ND150	STABLE	1.08-07	1.11-07	1.27-01	1.27-01	1.27-01
ND151	12.4-M	4.09+00	4.14+00	9.17+00	0.00	0.00
PM151	28.4-H	7.79-02	8.01-02	1.84+01	1.03+01	5.29-02
SM151	93.-Y	2.28-04	2.33-04	2.40+02	2.40+02	2.40+02
EU151	STABLE	8.89-06	9.09-06	1.26+01	1.26+01	1.26+01
ND152	11.5-M	2.79+00	2.82+00	6.00+00	0.00	0.00
PM152	4.1-M	6.34+00	6.41+00	1.22+01	0.00	0.00
SM152	STABLE	6.17-06	6.32-06	7.26+00	7.26+00	7.26+00
EU152	13.-Y	1.36-07	1.40-07	7.63-02	7.63-02	7.62-02
ND153	67.5-S	2.89+00	2.90+00	3.22+00	0.00	0.00
PM153	5.4-M	4.37+00	4.41+00	7.06+00	0.00	0.00
SM153	45.5-H	2.94-02	3.02-02	1.09+01	7.64+00	3.05-01
EU153	STABLE	3.76-06	3.85-06	4.50+00	4.50+00	4.50+00
ND154	7.73-D	1.24-03	1.27-03	1.39+00	1.27+00	5.65-01
PM154	2.8-M	1.38+00	1.38+00	3.15+00	1.27+00	5.66-01

TABLE 2-14 (Continued)

NUCLIDE	HALFLIFE	GAS BORNE WITH PURIFICATION SYSTEM OPERATIVE	GAS BORNE WITH PURIFICATION SYSTEM INOPERATIVE	PLATEOUT AFTER 40 YEARS OPERATION INITIAL	PLATEOUT AFTER 40 YEARS OPERATION 1 DAY DECAY	PLATEOUT AFTER 40 YEARS OPERATION 10 DAY DECAY
SM154	STABLE	2.17-06	2.18-06	2.50+00	2.50+00	2.50+00
EU154	8.6-Y	5.67-05	5.80-05	2.37+01	2.37+01	2.36+01
SM155	22.2-M	3.48-01	3.54-01	1.12+00	0.00	0.00
EU155	4.8-Y	2.54-05	2.60-05	7.11+00	7.11+00	7.08+00
GD155	STABLE	8.89-09	9.10-09	7.84-02	7.84-02	7.85-02
SM156	9.4-H	1.14-02	1.17-02	6.56-01	1.12-01	1.36-08
EU156	15.2-D	3.62-02	3.71-02	8.01+01	7.65+01	5.08+01
GD156	STABLE	5.78-09	5.93-09	7.81-01	7.81-01	7.82-01
SM157	83.-S	3.40-01	3.41-01	3.87-01	0.00	0.00
EU157	15.2-H	8.04-03	8.24-03	7.89-01	2.64-01	1.39-05
GD157	STABLE	1.95-09	1.99-09	6.60-03	6.60-03	6.60-03
	TOTALS	5.55+04	1.58+05	8.45+05	7.31+05	5.18+05

* - STAPLE NUCLIDES ARE GIVEN IN GRAMS

EXPONENTIAL NOTATION IS EMPLOYED (1.23+01 REPRESENTS 12.3)

Design Options Studied

Four options were considered in the alternate core design selection for the 2240-MW(t) HTGR-SC/C:

1. The 10-row block. The current reference design uses a 10-row block in a 439-column layout, yielding a power density of 7.12 W/cm^3.

2. The 9-row block. The selected alternative is a 9-row block in a 541-column layout, giving 5.78 W/cm^3. The 9-row block is a modified 10-row block, lacking the outer row of holes and having a graphite sleeve to reduce bypass flow.

3. The 381-mm (15-in.) block. This rejected option adds a 12.7-mm (0.5-in.) graphite sleeve to a 356-mm (14-in.), 10-row block, creating a 381-mm (15-in.) block.

4. Alternate rod pattern. Another rejected option was a different control rod pattern in the reference block design. Instead of having a pair of rods central to each region of seven columns, this alternative uses a single control rod in every fourth column in a regular array.

Each option is described in Tables 2-15 and 2-16 by block type and core layout, respectively. Each 9-row block contains about 80% of the fuel volume of the 10-row reference block. However, the 541-column core is 23% larger than the 439-column core, resulting in the selected alternative having 97.2% of the total fuel volume of the reference design, with a power density of only 5.8 W/cm^3 compared with the 7.1 W/cm^3 reference design.

The 380-mm (15-in.) block uses the same core layout as the reference 14-in. block, but since this block is 18.7% larger, the power density is only 6.0 W/cm^3. For purposes of comparison, this alternative was assumed to have the same heavy metal loading as the reference 10-row design. The

TABLE 2-15
FUEL AND CORE BLOCK DESIGN ALTERNATIVES

	10-Row	9-Row	381-mm (15-in.)	Alt. Rod Pattern
Fuel Block				
Fuel rods	2568	2052	2568	2520
Holes				
Fuel, 12.7 mm	216	174	216	216
Coolant, 15.9 mm	102	84	102	102
Coolant, 12.7 mm	6	7	6	6
Burnable poison rods, 12.7 mm	0	0	0	0
Fuel volume fraction	0.2185	0.1750	0.1840	0.2144
Coolant area fraction	0.1867	0.1561	0.1571	0.1867
Initial core fueled weight [kg (lb)]	123.8 (273)	129.1 (285)	153.0 (337)	124.1 (274)
Control Block				
Fuel rods	1344	1037	1344	2232
Holes				
Fuel, 12.7 mm	114	88	114	192
Coolant, 15.9 mm	45	31	45	90
Coolant, 12.7 mm	15	20	15	6
Control rod, 101.6 mm	2	2	2	1
Reserve shutdown system, 95.25 mm	1	1	1	0
Power rod, 43.28 mm	1	1	1	0
Burnable poison rods, 12.7 mm	0	0	0	6
Fuel volume fraction	0.1143	0.0884	0.0963	0.1899
Coolant area fraction	0.0963	0.0773	0.0810	0.1655
Initial core fueled weight [kg (lb)]	104.4 (230)	106.9 (235.7)	133.6 (294.6)	116.2 (256.2)

TABLE 2-16
CORE LAYOUTS FOR FUEL ELEMENT BLOCK ALTERNATIVES

	10-Row	9-Row	381-mm (15-in.)	Alt. Rod Pattern
Columns				
Standard	378	456	378	169
Control/reserve shutdown system	61	85	61	109/61
Blocks				
Standard	3,024	3,648	3,024	2,152
Control/reserve shutdown system	427	595	427	853/446
Short control/reserve shutdown system	61	85	61	19/42
Total	3,512	4,328	3,512	3,512
Fuel rods	8,402,106	8,170,031	8,402,106	8,423,424
Volume (m^3)	314.5	386.5	373.4	314.5
Power density (W/cm^3)	7.12	5.78	6.00	7.12
Fuel fraction	0.2044	0.1617	0.1722	0.2050
Coolant area fraction	0.1706	0.1417	0.1443	0.1785

381-mm (15 in.) block was rejected owing to lack of commonality with FSV for testing and concern about the effect on shutdown margin. Thus, calculations were not extensive for this option.

The alternative rod pattern for the 439-column core uses a rod layout that differs from the reference. Instead of one control column surrounded by six standard columns in a refueling region, every fourth column is a control column, and every refueling region contains in addition one column of blocks having a reserve shutdown system hole. This simpler alternative gains fuel volume by eliminating power rods and handling holes (power rods are not needed with the control rods more spread out). Handling is accomplished by a modification to the coolant holes through the dowels. The major disadvantage of this alternative, which led to its rejection, is the requirement for many more PCRV penetrations.

Typical block and total core fuel loadings derived from fuel cycle calculations are listed for the four options in Table 2-17.

Neutronic Calculations for the 9-Row Block

Fuel Cycle Survey. A study was made of the 9-row block design with varied heavy metal loadings to compare this alternative with the reference design. The zero-dimensional GARGOYLE depletion code was used to calculate annual makeup requirements for the initial core and the reloads to equilibrium. Following the 1-1/2 yr initial core at C/Th = 375, searches at each annual reload determined thorium makeup requirements to provide criticality at the end of cycle for specified uranium loadings. Figures 2-46 through 2-50 show plots of the results.

From these results, an equilibrium C/Th atom ratio of 610 was selected (compared with C/Th = 790 for the 10-row block design) to achieve an end-of-cycle age peaking factor of 1.30. The choice was based upon experience with the 10-row design, which has an end-of-cycle age peaking factor of 1.26.

TABLE 2-17
HEAVY METAL LOADINGS FOR FUEL ELEMENT BLOCK ALTERNATIVES

	10-Row	9-Row	381-mm (15-in.)	Alt. Rod Pattern
Initial Core				
Total				
kg Th	19,654.2	25,344.8	19,654.2	19,654.2
kg U	10,685.6	8,632.9	10,685.6	10,685.6
Standard block				
kg Th	6.01	6.37	6.01	5.88
kg U	3.27	2.17	3.27	3.20
g/rod				
Th	2.34	3.10	2.34	2.33
U	1.27	1.06	1.27	1.27
Particle packing fraction				
Fertile	0.193	0.257	0.193	0.193
Fissile	0.204	0.169	0.204	0.203
Total	0.397	0.426	0.397	0.396
C/Th	372	375	473	372
C/U	701	1,127	890	700
C/heavy metal	243	281	309	243
Equilibrium Reload				
Total				
kg Th	2,713.9	3,340.5	2,713.9	2,713.9
kg U	3,165.8	2,793.8	3,165.8	3,165.8
Standard block				
kg Th	3.27	3.44	3.27	3.21
kg U	3.82	2.88	3.82	3.74
g/rod				
Th	1.27	1.68	1.27	1.27
U	1.49	1.40	1.49	1.48
Particle packing fraction				
Fertile	0.106	0.139	0.106	0.105
Fissile	0.238	0.225	0.238	0.238
Total	0.344	0.364	0.344	0.343
C/Th	687	699	871	686
C/U	603	855	764	602
C/heavy metal	321	385	407	321

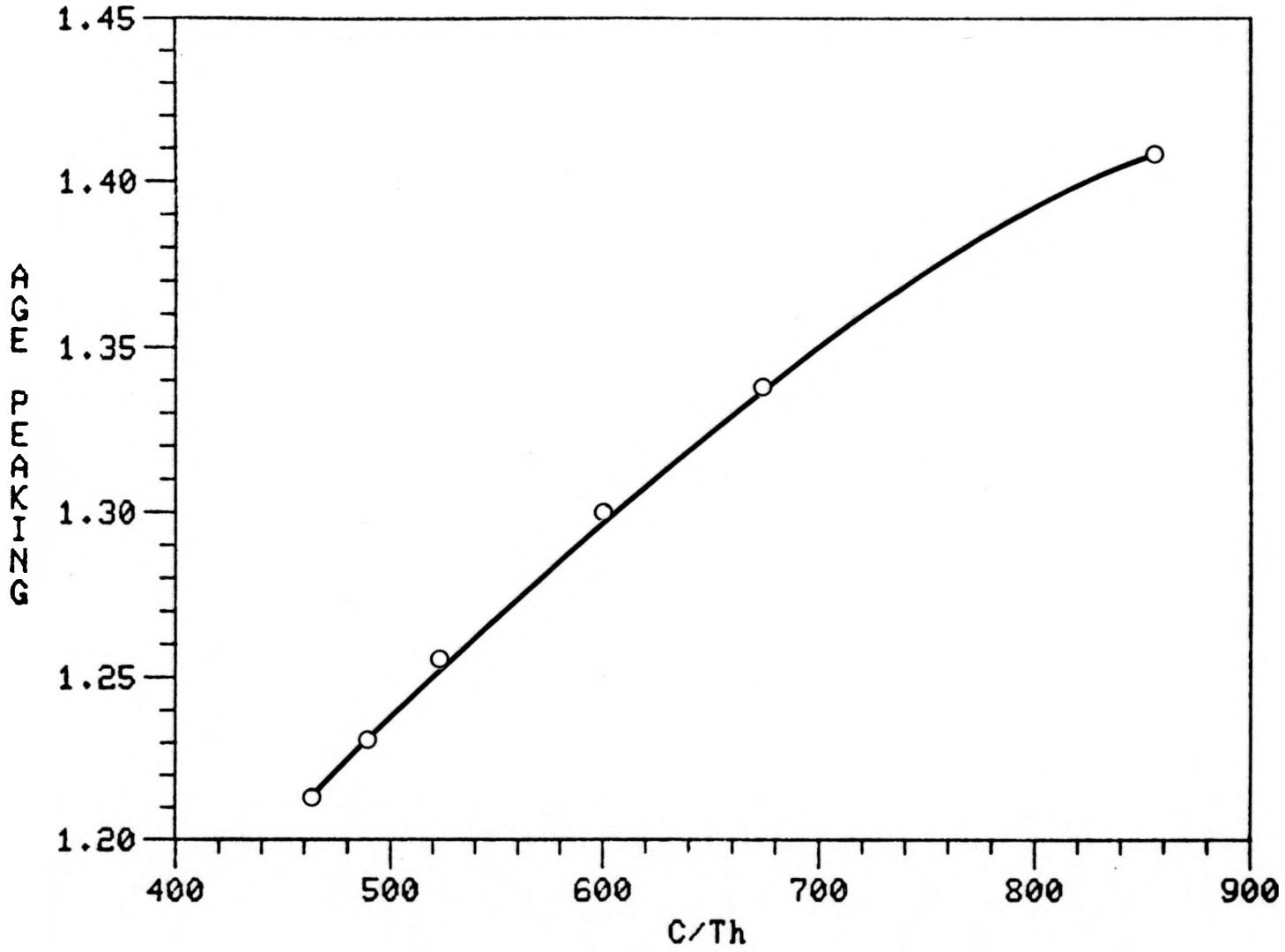

Fig. 2-46. Equilibrium age peaking versus C/Th atom ratio

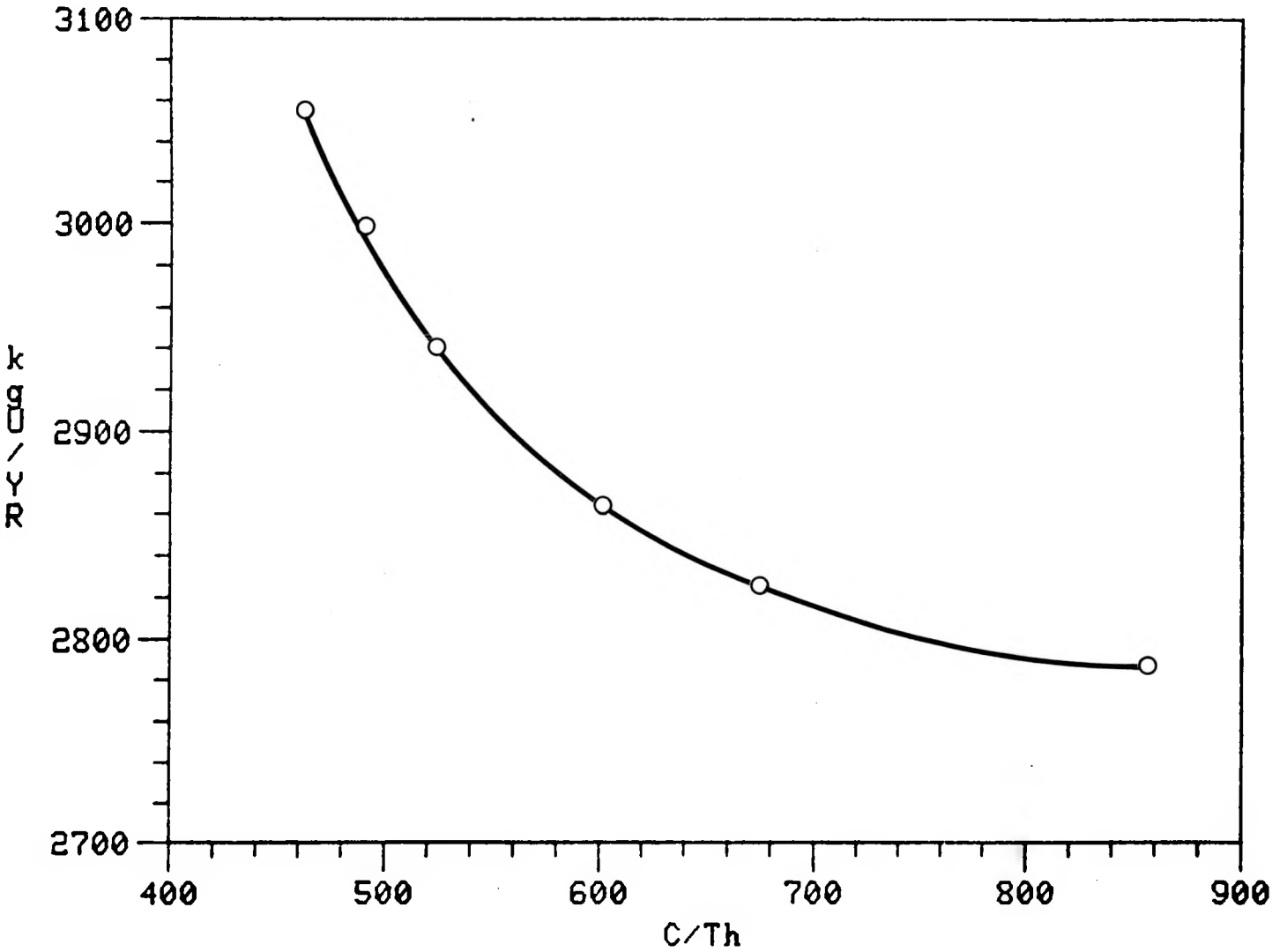

Fig. 2-47. Annual makeup versus C/Th atom ratio

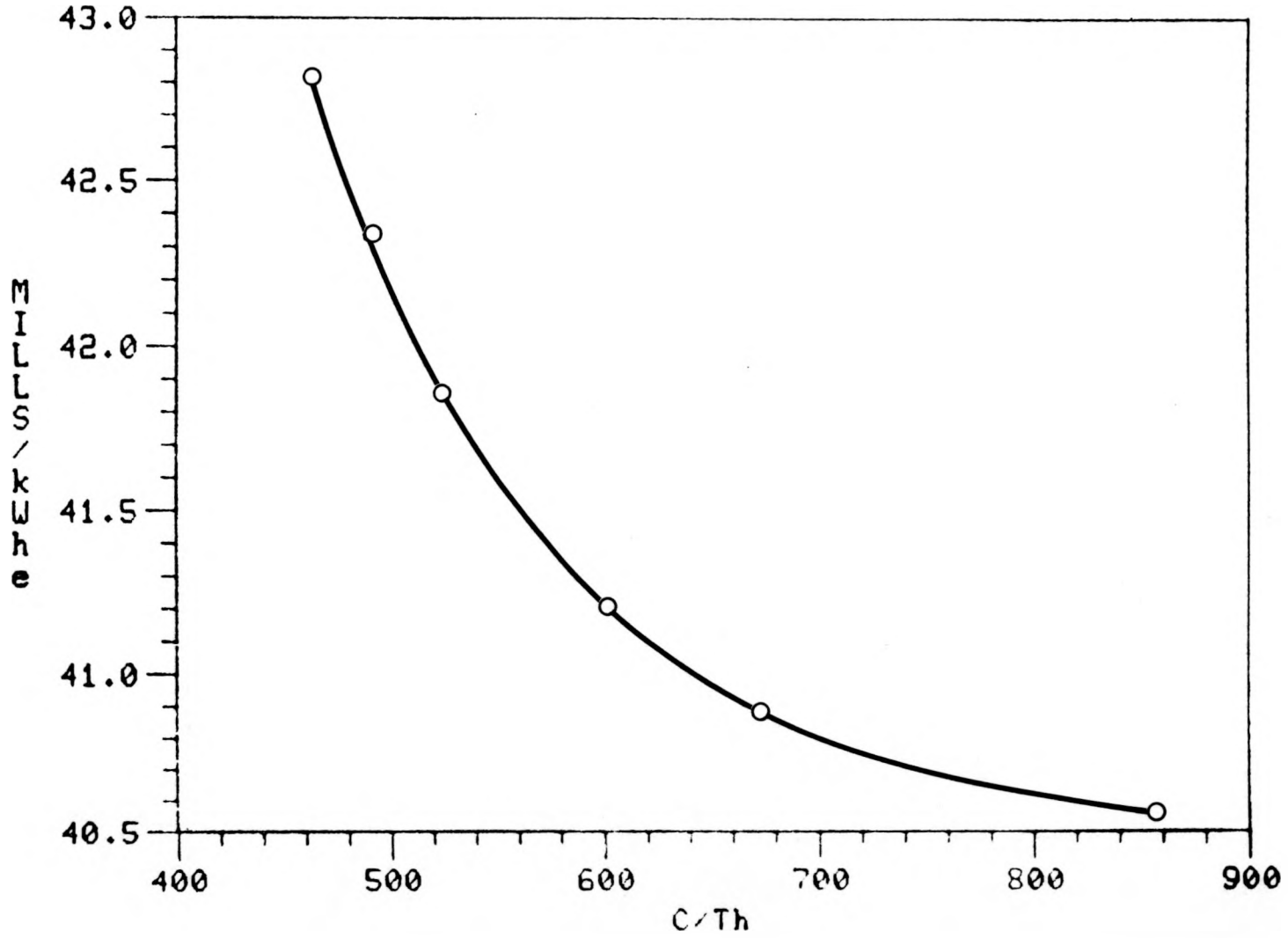

Fig. 2-48. 30-yr levelized cost versus C/Th atom ratio

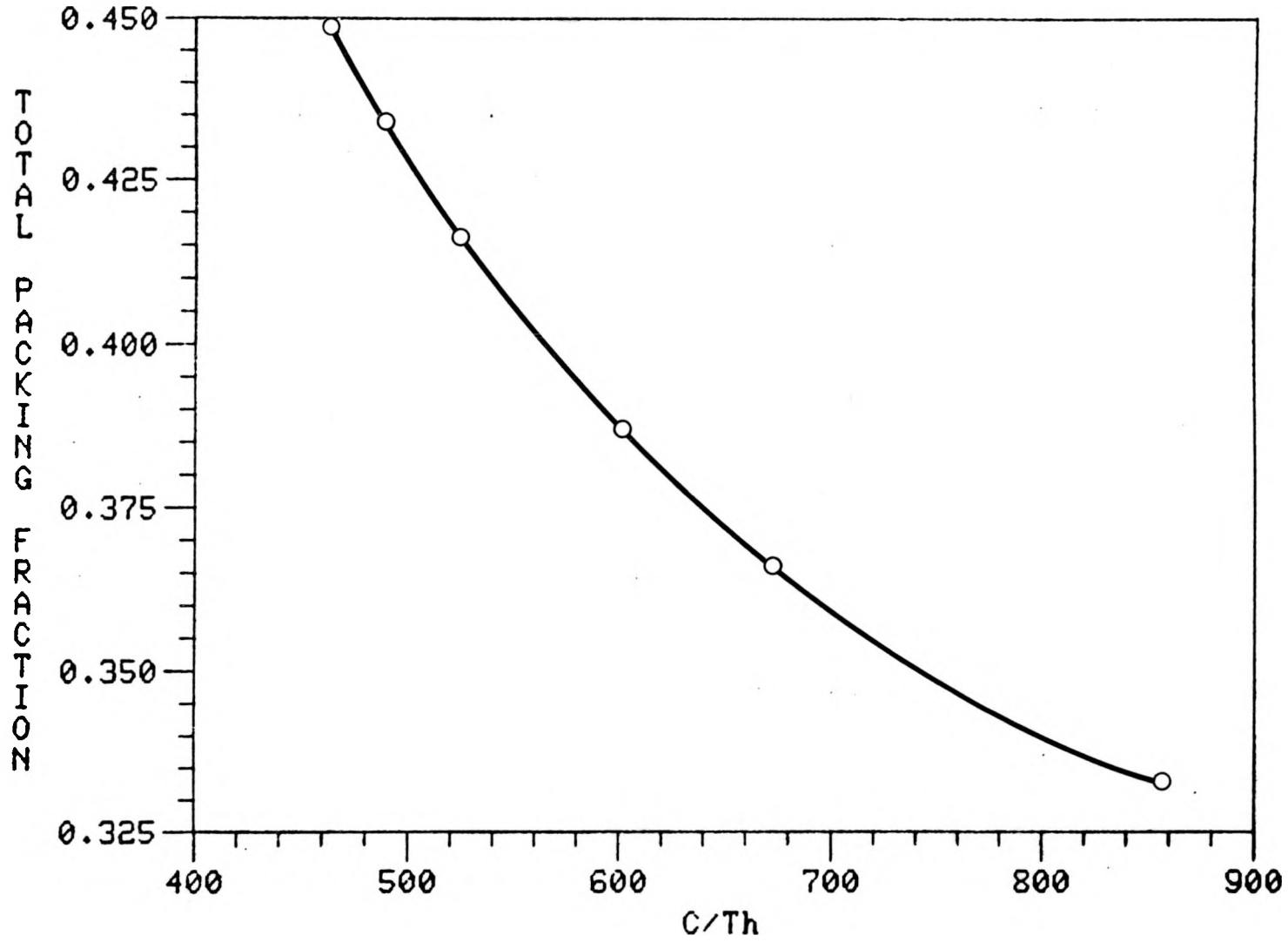

Fig. 2-49. Particle packing fraction versus C/Th atom ratio

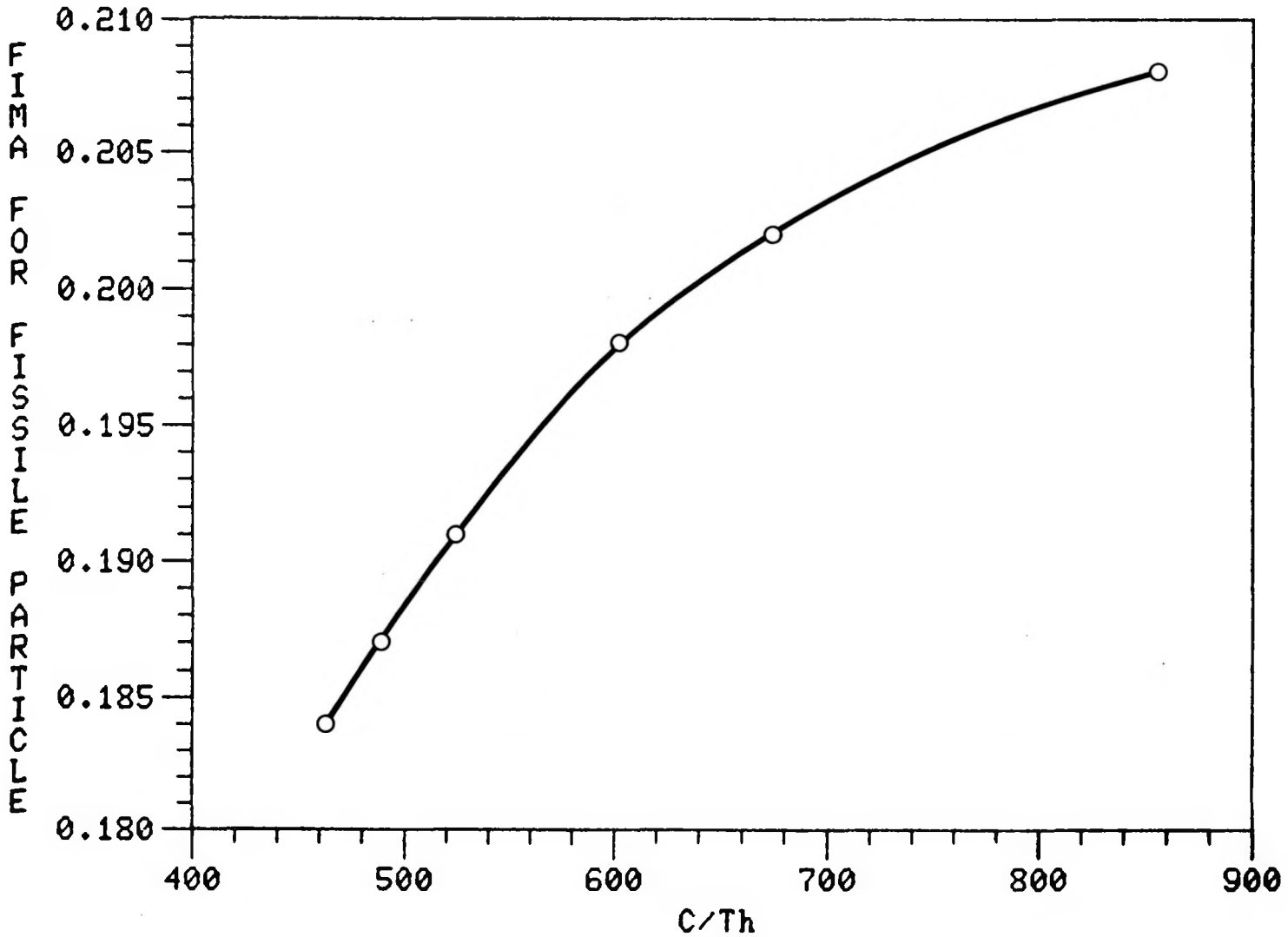

Fig. 2-50. Burnup versus equilibrium C/Th atom ratio

Some of the block design details used for these survey calculations have been modified since the adoption of the 9-row block. Table 2-18 presents the results of a later GARGOYLE calculation that correted for minor changes which occurred during the selection. Table 2-19 presents the same data for the previous 10-row block reference design. Tables 2-18 and 2-19 allow comparison of the adopted 9-row design with the 10-row design. The 9-row design differs mainly in having a physically larger core with more graphite, a slightly lower total fuel volume, and a lower power density. At equilibrium, annual uranium requirements are lower by 8.4% and thorium requirements are higher by 67%. End-of-cycle age peaking is 1.30 compared with 1.26 and fissile particle FIMA is 19.8% compared with 19.6% for the 10-row design. Burnup is about 9.24 x 10^6 MJ/kg (97,000 MWd/T) compared with 11.4 x 10^6 MJ/kg (120,000 MWd/T) for the 10-row design.

Fuel Cycle Cost. The fuel cycle cost for the 9-row block design was evaluated in detail for the LEU/Th once-through cycle. New fresh fuel fabrication cost assumptions were used. With these assumptions the benefit of the lower annual uranium requirements at 5.8 W/cm^3 more than compensated for the ~20% increase in fuel handling costs, and the net result was a 4% reduction in total fuel cycle costs for the modified design. About 1.5% of the gain is directly attributable to the 6% increase in the core graphite density.

The modified 9-row block design has not yet been evaluated in detail for use in HEU/Th cycle designs. However, it is known that fuel cycle costs for HEU/Th designs will increase as the power density is lowered. Some method, such as adding additional fuel and coolant channels into the outer graphite region of the block, will be required for achieving a higher power density, and thus lowering these costs, for future HEU/Th designs.

Fuel Zoning for Power Distributions. As part of the initial calculations, radial and axial zoning calculations were carried out for the 9-row block design. The objective of the power zoning is to minimize radial power peaking and shape the axial power profile in order to minimize fuel temperature peaks. The axial 4-4 scheme from the reference HTGR-SC/C design was

TABLE 2-18
NEUTRONIC CHARACTERISTICS OF 9-ROW BLOCK

DATE OF THIS RUN: 03 MAR 82 SUBMITTED BY: ST2100 ABSOLUTE NAME/VERSION: GARGYL /MAP COMPILED ON 021882 AT 144347
POWER LEVEL: 2240 MW(T) POWER DENSITY: 5.78 W/CM**3 EQUIL. EOC LEAKAGE: 3.93%
RUN TITLE: 2240MWT 5.78W/CM**3 4YR IC=1.5YRS C/TH=375/SEARCH 9-ROW BLOCK

SUMMARY TABLE

REL	C/TH	C/U	C/HM	DAYS	AGE PEAKING BOC	AGE PEAKING EOC	CONVERSION RATIO BOC	CONVERSION RATIO EOC	K-EFF BOC	K-EFF EOC	ETA BOC	ETA EOC	<----LOADED----> URANIUM KG	<----LOADED----> THORIUM KG	<---------DISCHARGED---------> BURNUP MWD/T	<-PART.1-> FIMA	<-PART.1-> FIFA	<-PART.2-> FIMA	<-PART.2-> FIFA
0	375	1127	281	438	1.00	1.00	.535	.685	1.209	1.010	1.989	2.013	8632.9	25344.8					
1	880	857	434	292	1.37	1.26	.555	.658	1.144	1.010	2.004	2.021	2857.6	2721.1	28637	.104	.522	.005	.000
2	620	854	359	292	1.36	1.30	.532	.635	1.150	1.010	2.004	2.015	3005.8	4042.5	45758	.152	.758	.013	.000
3	653	854	370	292	1.36	1.32	.511	.615	1.154	1.010	1.996	2.007	2793.9	3568.9	61334	.187	.934	.023	.000
4	595	853	351	292	1.37	1.35	.494	.599	1.157	1.010	1.987	1.997	2793.9	3914.1	76044	.215	1.075	.034	.000
5	740	856	397	292	1.36	1.31	.500	.603	1.155	1.010	1.990	1.999	2857.6	3230.1	111825	.200	1.000	.033	.000
6	540	852	331	292	1.34	1.33	.506	.607	1.153	1.010	1.989	1.998	3005.8	4631.9	97899	.200	1.001	.032	.000
7	669	854	375	292	1.34	1.31	.505	.607	1.152	1.010	1.989	1.999	2793.9	3488.9	99965	.200	1.001	.032	.000
8	646	854	368	292	1.35	1.32	.502	.604	1.154	1.010	1.989	1.998	2793.9	3608.2	96066	.200	.999	.032	.000
9	677	855	378	292	1.34	1.30	.505	.606	1.152	1.010	1.990	1.999	2857.6	3523.9	104595	.200	.998	.032	.000
10	507	851	318	292	1.34	1.33	.508	.609	1.152	1.010	1.987	1.997	3005.8	4934.1	91869	.199	.996	.031	.000
11	678	855	378	292	1.33	1.30	.508	.609	1.151	1.010	1.989	1.999	2793.9	3442.8	100291	.199	.996	.032	.000
12	674	855	377	292	1.33	1.30	.506	.607	1.152	1.010	1.990	1.999	2793.9	3462.8	98845	.199	.995	.032	.000
13	648	854	368	292	1.33	1.30	.508	.608	1.151	1.010	1.990	1.999	2857.6	3683.0	100603	.199	.994	.032	.000
14	492	851	312	292	1.33	1.33	.509	.610	1.152	1.010	1.987	1.997	3005.8	5079.0	89019	.199	.994	.030	.000
15	683	855	380	292	1.33	1.29	.509	.610	1.151	1.010	1.989	1.999	2793.9	3417.1	100522	.199	.993	.032	.000
16	688	855	381	292	1.33	1.29	.508	.609	1.151	1.010	1.990	2.000	2793.9	3392.3	100240	.199	.993	.031	.000
17	633	854	363	292	1.32	1.30	.509	.609	1.150	1.010	1.990	2.000	2857.6	3769.3	98586	.199	.993	.031	.000
18	485	850	309	292	1.33	1.33	.509	.610	1.151	1.010	1.987	1.997	3005.8	5146.6	87709	.198	.992	.030	.000
19	686	855	381	292	1.33	1.29	.510	.610	1.150	1.010	1.989	1.999	2793.9	3402.6	100669	.198	.992	.031	.000
20	695	855	383	292	1.32	1.29	.509	.610	1.150	1.010	1.990	2.000	2793.9	3357.6	100936	.198	.992	.031	.000
21	625	854	361	292	1.32	1.30	.510	.610	1.150	1.010	1.990	2.000	2857.6	3816.1	97538	.198	.992	.031	.000
22	482	850	308	292	1.33	1.33	.509	.610	1.151	1.010	1.986	1.997	3005.8	5177.8	87105	.198	.992	.030	.000
23	688	855	381	292	1.32	1.29	.510	.610	1.150	1.010	1.989	1.999	2793.9	3394.4	100764	.198	.992	.031	.000
24	699	855	384	292	1.32	1.29	.510	.610	1.150	1.010	1.991	2.000	2793.9	3340.5	101284	.198	.991	.031	.000

TABLE 2-18 (Continued)

DATE OF THIS RUN: 03 MAR 82 SUBMITTED BY: ST2100 ABSOLUTE NAME/VERSION: GARGYL /MAP COMPILED ON 021882 AT 144347
POWER LEVEL: 2240 MW(T) POWER DENSITY: 5.78 W/CM**3 EQUIL. EOC LEAKAGE: 3.93%
RUN TITLE: 2240MWT 5.78W/CM**3 4YR IC=1.5YRS C/TH=375/SEARCH 9-ROW BLOCK

MASS FLOW SUMMARY TABLE

	DISCH. PTL. 1 U -235	DISCH. PTL. 1 U -236	DISCH. PTL. 1 U -238	DISCH. PTL. 1 NP-239 PU-239	DISCH. PTL. 1 PU-241	DISCH. PTL. 2 PA-233 U -233	DISCH. PTL. 2 U -234	DISCH. PTL. 2 U -235	DISCH. PTL. 2 U -236	LOADED PTL. 1 U -235	LOADED PTL. 1 U -238	LOADED PTL. 1 TH-232
0	.0	.0	.0	.0	.0	.0	.0	.0	.0	1709.1	6923.7	25344.8
1	193.0	40.5	1668.5	14.8	4.7	88.6	5.7	.4	.0	565.8	2291.9	2721.1
2	117.6	55.5	1712.4	15.6	7.3	122.8	12.8	1.4	.1	595.1	2410.7	4042.5
3	63.3	57.0	1552.6	14.4	7.4	128.5	18.4	2.6	.3	553.1	2240.7	3568.9
4	36.5	58.7	1514.1	14.2	7.5	135.5	24.7	4.1	.6	553.1	2240.7	3914.1
5	62.5	79.2	2090.5	17.9	9.4	64.7	10.8	1.7	.2	565.8	2291.9	3230.1
6	65.5	83.4	2198.3	19.0	9.9	93.1	15.6	2.4	.3	595.1	2410.7	4631.9
7	61.0	77.4	2043.0	17.9	9.3	82.9	13.8	2.2	.3	553.1	2240.7	3488.9
8	61.5	77.3	2043.1	17.9	9.4	90.1	15.0	2.3	.3	553.1	2240.7	3608.2
9	63.7	79.1	2090.0	18.2	9.6	76.1	12.6	2.0	.2	565.8	2291.9	3523.9
10	67.6	83.2	2198.5	19.3	10.1	165.4	17.4	2.7	.3	595.1	2410.7	4934.1
11	63.0	77.3	2043.5	18.0	9.4	81.4	13.5	2.1	.3	553.1	2240.7	3442.8
12	63.3	77.3	2043.6	18.0	9.4	84.0	13.8	2.2	.3	553.1	2240.7	3462.8
13	65.2	79.1	2090.4	18.4	9.6	82.4	13.6	2.1	.3	565.8	2291.9	3683.0
14	68.8	83.1	2198.8	19.5	10.2	111.6	18.3	2.8	.4	595.1	2410.7	5079.0
15	64.1	77.3	2043.8	18.0	9.5	80.5	13.2	2.1	.3	553.1	2240.7	3417.1
16	64.2	77.3	2043.8	18.1	9.5	81.0	13.3	2.1	.3	553.1	2240.7	3392.3
17	65.9	79.0	2090.6	18.5	9.7	85.8	14.1	2.2	.3	565.8	2291.9	3769.3
18	69.5	83.1	2199.0	19.5	10.2	114.5	18.7	2.9	.4	595.1	2410.7	5146.6
19	64.6	77.2	2044.0	18.1	9.5	80.0	13.1	2.0	.3	553.1	2240.7	3402.6
20	64.7	77.2	2044.0	18.1	9.5	79.5	13.0	2.0	.3	553.1	2240.7	3357.6
21	66.3	79.0	2090.7	18.6	9.7	87.6	14.3	2.2	.3	565.8	2291.9	3816.1
22	69.8	83.1	2199.1	19.6	10.2	115.9	18.9	2.9	.4	595.1	2410.7	5177.8
23	64.9	77.2	2044.0	18.1	9.5	79.7	13.1	2.0	.3	553.1	2240.7	3394.4
24	64.9	77.2	2044.0	18.1	9.5	78.8	12.9	2.0	.2	553.1	2240.7	3340.5
FINAL	699.7	260.1	8672.5	74.3	30.9	299.0	35.1	4.5	.5			
TOTAL	2411.1	2056.0	57002.6	502.2	250.9	2529.5	385.9	57.9	7.1	15311.6	62028.3	116890.4

TABLE 2-19
NEUTRONIC CHARACTERISTICS OF 10-ROW BLOCK

DATE OF THIS RUN: 24 MAR 82 SUBMITTED BY: ST4700 ABSOLUTE NAME/VERSION: GARGYL /MAP COMPILED ON 021882 AT 144347
POWER LEVEL: 2240 MW(T) POWER DENSITY: 7.12 W/CM**3 EQUIL. EOC LEAKAGE: 3.03%
RUN TITLE: 2240MWT 7.12W/CM**3 4YR IC=1.5YRS C/TH=375/SEARCH 10-ROW BLOCK

SUMMARY TABLE

REL	C/TH	C/U	C/HM	DAYS	AGE PEAKING BOC	AGE PEAKING EOC	CONVERSION RATIO BOC	CONVERSION RATIO EOC	K-EFF BOC	K-EFF EOC	ETA BOC	ETA EOC	<----LOADED----> URANIUM KG	<----LOADED----> THORIUM KG	<---------DISCHARGED---------> BURNUP MWD/T	<-PART.1-> FIMA	<-PART.1-> FIFA	<-PART.2-> FIMA	<-PART.2-> FIFA
0	375	689	243	438	1.00	1.00	.534	.674	1.207	1.010	1.964	1.960	10959.9	19509.5					
1	1361	606	419	292	1.15	1.12	.558	.648	1.131	1.010	1.960	1.969	3194.5	1390.0	32255	.087	.437	.005	.000
2	880	604	358	292	1.17	1.19	.534	.623	1.136	1.010	1.962	1.986	3166.9	2182.6	52715	.134	.670	.012	.000
3	663	602	316	292	1.20	1.24	.516	.606	1.140	1.010	1.955	1.959	3166.9	2869.3	72186	.173	.867	.022	.000
4	627	601	307	292	1.23	1.28	.502	.592	1.143	1.010	1.947	1.952	2994.9	2868.9	90714	.207	1.035	.034	.000
5	984	604	374	292	1.21	1.23	.508	.597	1.140	1.010	1.953	1.955	3194.5	1918.4	106776	.193	.967	.034	.000
6	820	603	348	292	1.20	1.23	.509	.598	1.140	1.010	1.953	1.955	3166.9	2276.9	122786	.195	.974	.034	.000
7	685	602	321	292	1.20	1.25	.508	.598	1.141	1.010	1.951	1.954	3166.9	2718.6	112404	.196	.978	.033	.000
8	792	603	342	292	1.22	1.26	.502	.593	1.142	1.010	1.950	1.953	2994.9	2227.8	110323	.196	.979	.033	.000
9	834	604	350	292	1.21	1.24	.506	.596	1.141	1.010	1.952	1.954	3194.5	2280.3	127441	.196	.979	.034	.000
10	774	603	339	292	1.21	1.24	.507	.597	1.141	1.010	1.952	1.954	3166.9	2412.0	120776	.196	.979	.034	.000
11	699	602	324	292	1.21	1.25	.507	.597	1.142	1.010	1.950	1.954	3166.9	2665.7	113968	.196	.980	.033	.000
12	927	604	366	292	1.22	1.24	.504	.594	1.142	1.010	1.951	1.954	2994.9	1907.7	119689	.196	.980	.034	.000
13	763	603	337	292	1.21	1.25	.506	.595	1.142	1.010	1.952	1.954	3194.5	2467.7	121505	.196	.980	.034	.000
14	752	603	335	292	1.21	1.25	.506	.596	1.142	1.010	1.951	1.954	3166.9	2482.1	118694	.196	.980	.034	.000
15	705	602	325	292	1.22	1.26	.506	.596	1.142	1.010	1.950	1.953	3166.9	2643.0	114836	.196	.980	.033	.000
16	1024	605	380	292	1.21	1.23	.505	.594	1.141	1.010	1.952	1.955	2994.9	1728.9	125549	.196	.981	.034	.000
17	727	603	329	292	1.21	1.26	.506	.595	1.142	1.010	1.952	1.954	3194.5	2588.4	118188	.196	.980	.034	.000
18	738	603	332	292	1.21	1.25	.506	.596	1.142	1.010	1.951	1.954	3166.9	2526.8	117634	.196	.980	.034	.000
19	709	602	326	292	1.22	1.26	.506	.596	1.142	1.010	1.950	1.953	3166.9	2630.3	115210	.196	.981	.033	.000
20	1089	605	389	292	1.21	1.23	.505	.595	1.141	1.010	1.953	1.955	2994.9	1626.3	129165	.196	.981	.034	.000
21	707	602	325	292	1.21	1.26	.505	.595	1.142	1.010	1.952	1.954	3194.5	2658.7	116350	.196	.980	.034	.000
22	730	603	330	292	1.22	1.26	.505	.595	1.142	1.010	1.951	1.954	3166.9	2554.4	116960	.196	.981	.034	.000
23	711	602	326	292	1.22	1.26	.505	.596	1.142	1.010	1.950	1.953	3166.9	2622.2	115413	.196	.981	.033	.000
24	1130	605	394	292	1.21	1.23	.505	.595	1.141	1.010	1.953	1.955	2994.9	1567.3	131354	.196	.981	.035	.000

TABLE 2-19 (Continued)

DATE OF THIS RUN: 24 MAR 82 SUBMITTED BY: ST4700 ABSOLUTE NAME/VERSION: QARGYL /MAP COMPILED ON 821882 AT 144347
POWER LEVEL: 2240 MW(T) POWER DENSITY: 7.12 W/CM**3 EQUIL. EOC LEAKAGE: 3.93%
RUN TITLE: 2240MWT 7.12W/CM**3 4YR IC=1.5YRS C/TH=375/SEARCH 10-ROW BLOCK

MASS FLOW SUMMARY TABLE

	DISCH. PTL. 1 U -235	DISCH. PTL. 1 U -236	DISCH. PTL. 1 U -238	DISCH. PTL. 1 NP-239 PU-239	DISCH. PTL. 1 PU-241	DISCH. PTL. 2 PA-233 U -233	DISCH. PTL. 2 U -234	DISCH. PTL. 2 U -235	DISCH. PTL. 2 U -236	LOADED PTL. 1 U -235	LOADED PTL. 1 U -238	LOADED PTL. 1 TH-238
0	.0	.0	.0	.0	.0	.0	.0	.0	.0	2150.0	8710.0	19509.5
1	299.2	46.0	2137.1	28.2	6.9	80.2	4.7	.3	.0	632.4	2562.1	1390.0
2	196.0	61.9	2060.4	29.3	12.0	109.6	9.9	1.1	.1	627.0	2539.9	2122.6
3	127.9	70.9	2002.4	28.7	14.1	127.2	15.8	2.4	.2	627.0	2539.9	2809.3
4	78.0	70.9	1839.4	26.3	13.7	129.3	20.4	3.7	.4	592.9	2402.0	2808.9
5	112.1	86.4	2296.8	30.7	15.9	42.5	6.3	1.1	.1	632.4	2562.1	1918.4
6	107.9	85.8	2274.8	30.7	15.7	63.3	9.5	1.6	.2	627.0	2539.9	2276.8
7	106.5	85.8	2273.9	30.9	15.8	81.9	12.3	2.1	.2	627.0	2539.9	2718.6
8	100.4	81.1	2150.2	29.2	14.9	81.5	12.3	2.1	.2	592.9	2402.0	2827.8
9	107.3	86.6	2293.6	30.7	15.8	57.7	8.7	1.5	.2	632.4	2562.1	2260.3
10	106.1	85.9	2273.6	30.6	15.7	67.6	10.2	1.8	.2	627.0	2539.9	2412.0
11	105.8	85.9	2273.5	30.7	15.7	79.5	12.0	2.1	.2	627.0	2539.9	2665.7
12	99.7	81.2	2150.0	29.0	14.9	66.0	10.0	1.7	.2	592.9	2402.0	1907.7
13	106.6	86.6	2293.4	30.8	15.8	67.2	10.2	1.8	.2	632.4	2562.1	2467.7
14	105.6	85.9	2273.5	30.6	15.7	71.2	10.8	1.9	.2	627.0	2539.9	2482.1
15	105.5	85.9	2273.4	30.6	15.7	78.0	11.8	2.1	.2	627.0	2539.9	2643.0
16	99.6	81.2	2149.9	28.9	14.8	57.2	8.7	1.5	.2	592.9	2402.0	1728.9
17	106.4	86.6	2293.3	30.9	15.8	72.8	11.0	1.9	.2	632.4	2562.1	2588.4
18	105.4	85.9	2273.4	30.6	15.7	73.1	11.1	1.9	.2	627.0	2539.9	2526.8
19	105.4	85.9	2273.4	30.6	15.7	77.4	11.7	2.0	.2	627.0	2539.9	2630.3
20	99.6	81.2	2149.9	28.9	14.8	52.2	7.9	1.4	.1	592.9	2402.0	1626.3
21	106.3	86.6	2293.2	30.9	15.8	76.1	11.5	2.0	.2	632.4	2562.1	2658.7
22	105.4	85.9	2273.4	30.6	15.7	74.3	11.2	2.0	.2	627.0	2539.9	2554.4
23	105.3	85.9	2273.3	30.6	15.7	77.1	11.7	2.0	.2	627.0	2539.9	2622.2
24	99.6	81.3	2149.9	28.8	14.8	49.3	7.5	1.3	.1	592.9	2402.0	1567.3
FINAL	907.9	273.0	9372.3	120.0	46.7	227.8	25.6	3.7	.3			
TOTAL	3705.5	2220.5	62367.8	837.7	403.6	2040.0	282.5	47.3	4.9	17025.5	68973.6	75124.1

retained, including the specified 60%/40% power split previously found to be about optimum for equalizing zone fuel temperature peaks. Radially, a 4-zone scheme was adopted which is similar to that used before except for the larger number of core columns.

Axial Zoning Model. The one-dimensional diffusion theory code GASP was used for the fuel zoning determinations in both axial and radial geometry. Specified zone average relative power densities are achieved in the GASP calculation by iterative adjustments on one fuel constituent (fissile or fertile), and adjustments are then made on the other to assure power shape stability with burnup.

The zone-to-column-average power ratios of 1.20 and 0.80 for the two axial zones were selected on the basis of past zoning studies and are not necessarily optimum for equalizing and minimizing fuel temperature peaks for the most extreme RPF/TILT conditions for the revised fuel cycle. Iterations of GASP calculations and thermal-flow calculations performed by the BACH code were not done because the radial-power history parameters have not yet been generated via GAUGE calculations. Also, revisions to BACH will be required if the 9-row block with block-end gas mixing plena is adopted. Based upon past studies, the 60%/40% zonal power split gives equilibrated fuel temperature peaks for a RPF/TILT combination of about 1.50/1.50 [for a maximum fuel temperature of about 1250°C (2282°F) without engineering corrections].

Radial Zoning Model. Fuel column counts of 133, 126, 198, and 84 were selected for the four radial zones in the alternate core design based on a preliminary layout of the reload segments for GAUGE depletion calculations.

The transverse leakage in radial GASP calculations was represented by input core-average axial bucklings edited from the axial GASP calculations. Similarly, radial bucklings from the radial GASP cases were used in the axial calculations.

Input values for the zone-average power density search were selected by an iterative process. Initially, uniform averages were used (zone-to-core average ratios of 10), and adjustments were then made to yield nearly equalized zone peak-to-core average power ratios.

Burnable Poison Zoning. Burnable poison distributions and lumping parameters were also provided by the GASP calculations. Based on past studies, eigenvalue search values of 1.01 and 1.06, respectively, were input for the initial core and equilibrium cycle cases. Further analyses of fuel cycles and burnup traits might indicate different optimum unburned reactivity excess requirements for the alternate core design.

In the GASP methodology, the distribution of the poison added to reduce the reactivity is based upon equalizing the net change in k-infinity by zone. In theory, this should maintain the same relative zone power densities as before the poison addition. However, with the use of bucklings to represent transverse leakage, the zone power splits and peak-to-average ratios are found shifted up to 5% from designated optimums, and further adjustments to the poison zoning will be required.

Axial Zoning Results. Results of the axial GASP cases for the initial core and equilibrium cycle are listed in Table 2-20, and the output axial power profiles with only fuel zoned (no burnable poison) are plotted in Fig. 2-51. As shown in Table 2-20, the fissile (uranium) loading distribution factors are the same for both cases and require that 68.3% of the uranium be in the top half of the core. The previous HTGR-SC/C studies for LEU loadings, in which the radial leakage was represented by an adjusted fission distribution, indicated a 70% top zone uranium fraction for the 60% power fraction. The thorium zone loading factors for the alternate designs are seen to be sensitive to the core-average thorium-to-uranium ratio: the lower the U-238 contribution to the total fertile content, the higher the thorium fraction in the top zone to provide adequate conversion ratios for maintaining power stability.

TABLE 2-20
AXIAL ZONING PARAMETERS FOR ALTERNATE CORE HTGR-SC/C DESIGN (9-ROW BLOCKS)

Cycle	Initial Core		Equilibrium Reload	
Average C/Th	375		608	
Average C/U	1127		853	
Average fuel rod packing (%)				
Th	25.67		15.90	
U	16.94		22.47	
Total	42.61		38.37	
Calculated k without lumped burnable poison	1.1393		1.2534	
Axial region of core power factor	Zone 1 1.200	Zone 2 0.800	Zone 1 1.200	Zone 2 0.800
Loading factors				
Th	1.096	0.904	0.907	1.093
U	1.366	0.634	1.366	0.634
Packing fraction[a]				
% Th	28.13	23.21	14.42	17.38
% U	23.14	10.74	30.69	14.25
% Total	51.27	33.95	45.11	31.63
Lumped burnable poison search results				
Homogeneous B-10, 10^{-7}/b-cm	4.007	2.015	7.072	3.464
Lumping G-factor	0.879	0.745	0.797	0.687
Ratio/radius	9.549×10^{-3}	2.388×10^{-3}	9.549×10^{-3}	3.267×10^{-3}
Power factor with lumped burnable poison	1.229	0.771	1.249	0.751
k for lumped burnable poison search	1.010		1.060	
Fractional absorption in lumped burnable poison at beginning of cycle	8.32%		11.40%	

[a] Without radial zoning factors.

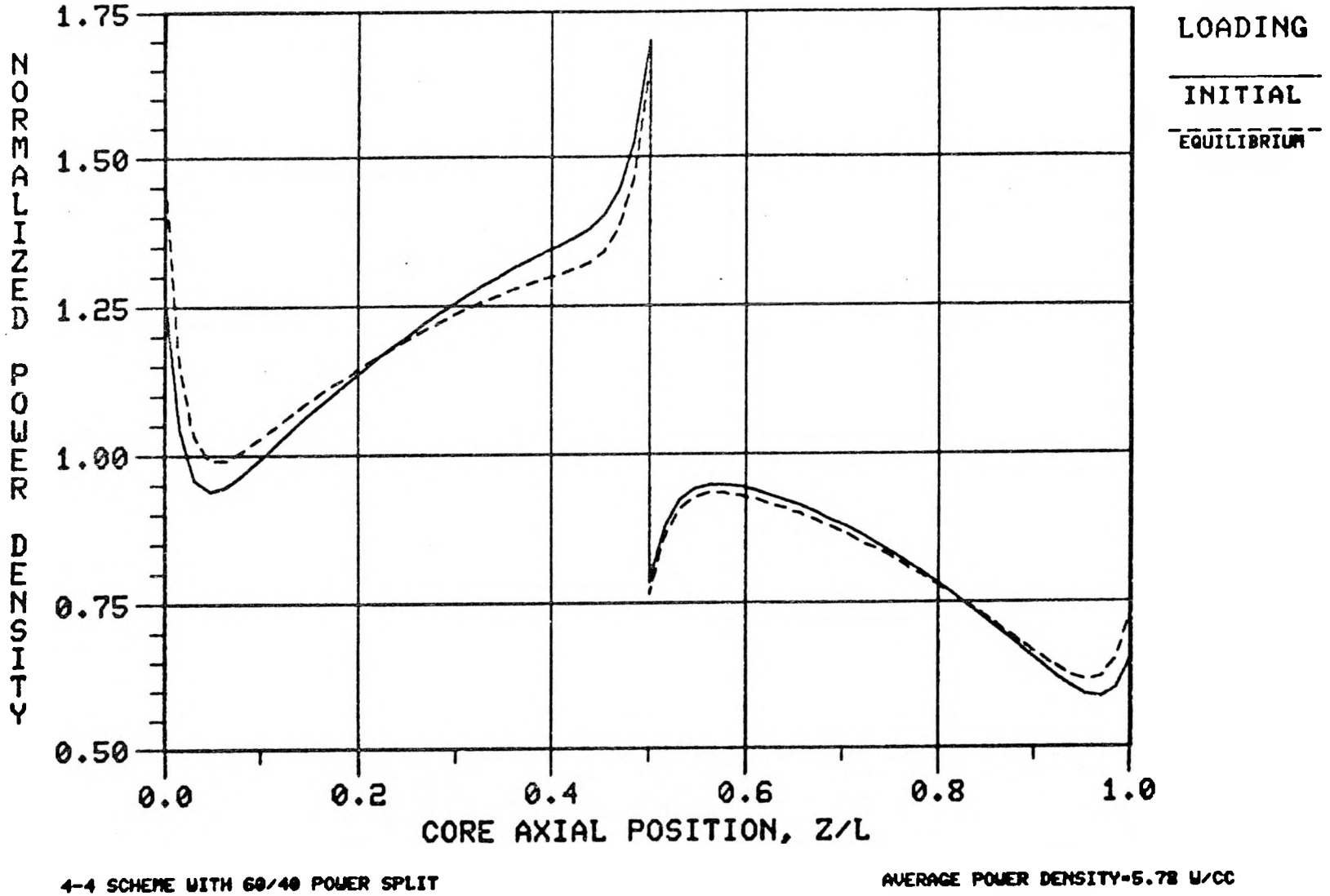

Fig. 2-51. Axial power profiles for alternate core loadings

Comparison of the unpoisoned, unburned axial power distributions in Fig. 2-51 for the two loading cases shows the effects of the harder core-average spectrum for the heavier initial loading on the in-zone power shapes. In Fig. 2-52, the axial power profile for the alternate core, equilibrium loading is compared with the corresponding curve for the reference design HTGR/SC/C core using the 10-row blocks. The close correspondence of the two distributions probably reflects the nearly equal carbon-to-metal ratios for the new and old designs. Also, the agreement supports the preliminary use of the previous thermal-flow analysis predictions on temperature profiles, given the nearly equal core-average fuel rod linear power rates and power-to-flow data.

Radial Zoning Results. Results of the radial GASP calculations are listed in Table 2-21, and Fig. 2-53 shows the derived radial power distributions for the two loading distributions. For the radial zoning, the correlation between zone fissile factors and power factors is seen to be a bit obscure. Calculated eigenvalues in the radial GASP cases are a few percent higher than those of the corresponding axial results, possibly a result of the leakage assumptions for the reflector regions.

The radial power profiles in Fig. 2-53 are relatively flat out to 300 cm, covering the inner two zones adopted for this design. These curves and the loading factor data suggest that the first and second zones could be combined, yielding a 3-radial-zone scheme, without significant increases in the radial power peaks or loading factors. Studies of burnup stability are needed to verify this conclusion.

The bottom lines of Table 2-21 give the maximum fuel particle packing fractions derived from the combined radial and axial zoning analyses for the alternate design. The maximum of 51.85% is only about 3% higher than that found previously for the 10-row reference HTGR-SC/C design.

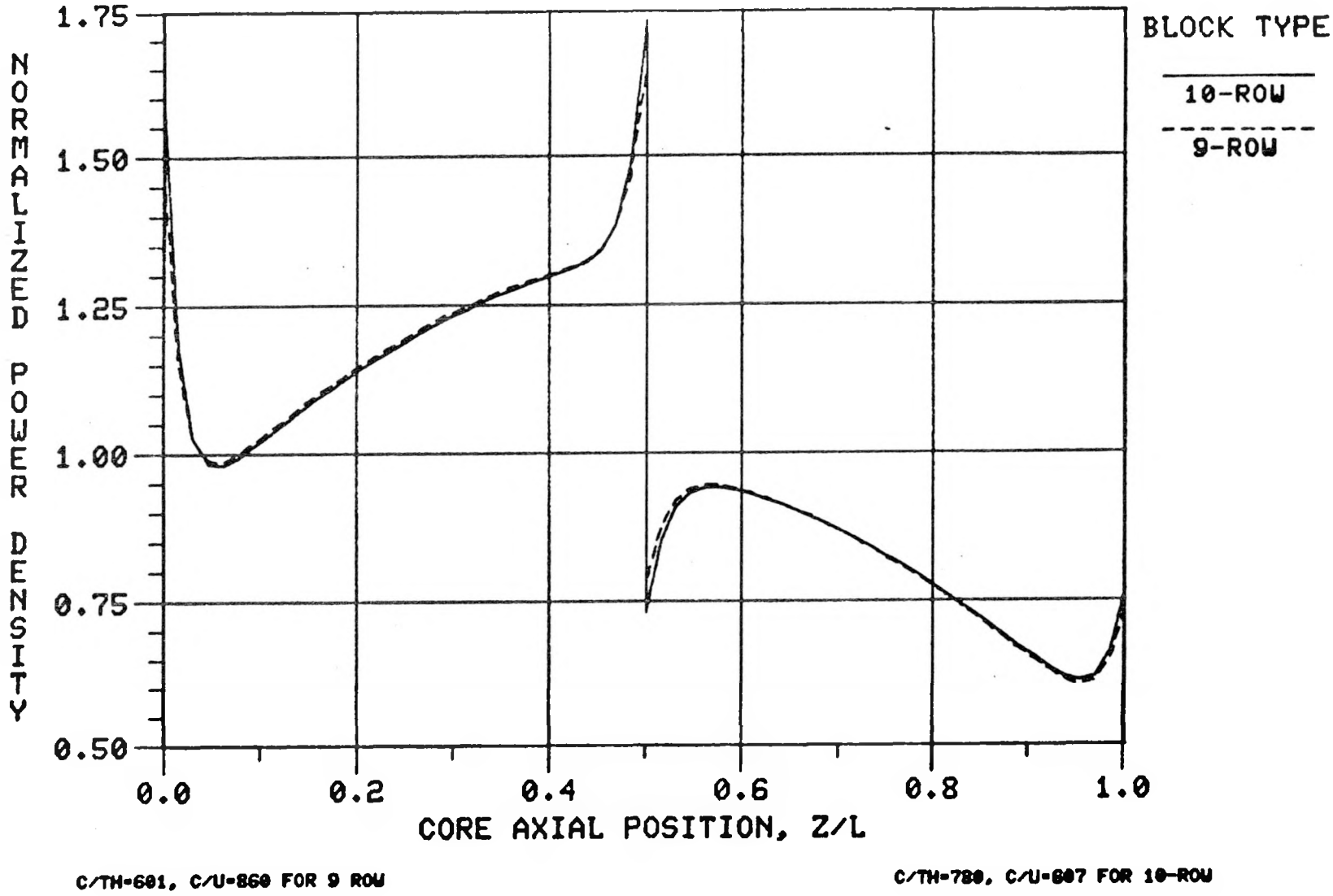

Fig. 2-52. Axial power shapes for reference and alternate cores

TABLE 2-21
RADIAL ZONING PARAMETERS FOR ALTERNATE CORE HTGR-SC/C DESIGN (9-ROW BLOCKS)

Cycle			Initial Core	Equilibrium Reload
Core average: C/Th			375	608
C/U			1127	853
Zone-to-core average power ratios	Radial Zone No.	No. of Columns		
	1	133	1.0562	1.0331
	2	126	1.0429	1.0476
	3	198	0.9781	0.9896
	4	84	0.8984	0.8690
Thorium loading factors:		Zone 1	1.0399	1.0778
		Zone 2	1.0310	1.0669
		Zone 3	0.9814	0.9446
		Zone 4	0.9342	0.9070
Uranium loding factors:		Zone 1	0.9865	1.0212
		Zone 2	0.9885	1.0220
		Zone 3	1.0358	1.0227
		Zone 4	0.9810	0.8680
Zone peak-to-core average power ratios:		Zone 1	1.065	1.0545
		Zone 2	1.064	1.0523
		Zone 3	1.062	1.0461
		Zone 4	1.059	1.0490
Calculated k (without lumped burnable poison)			1.1489	1.2763
Maximum fuel particle packing; top axial zone of radial zone No.			51.85%, Zone 3	46.88%, Zone 1

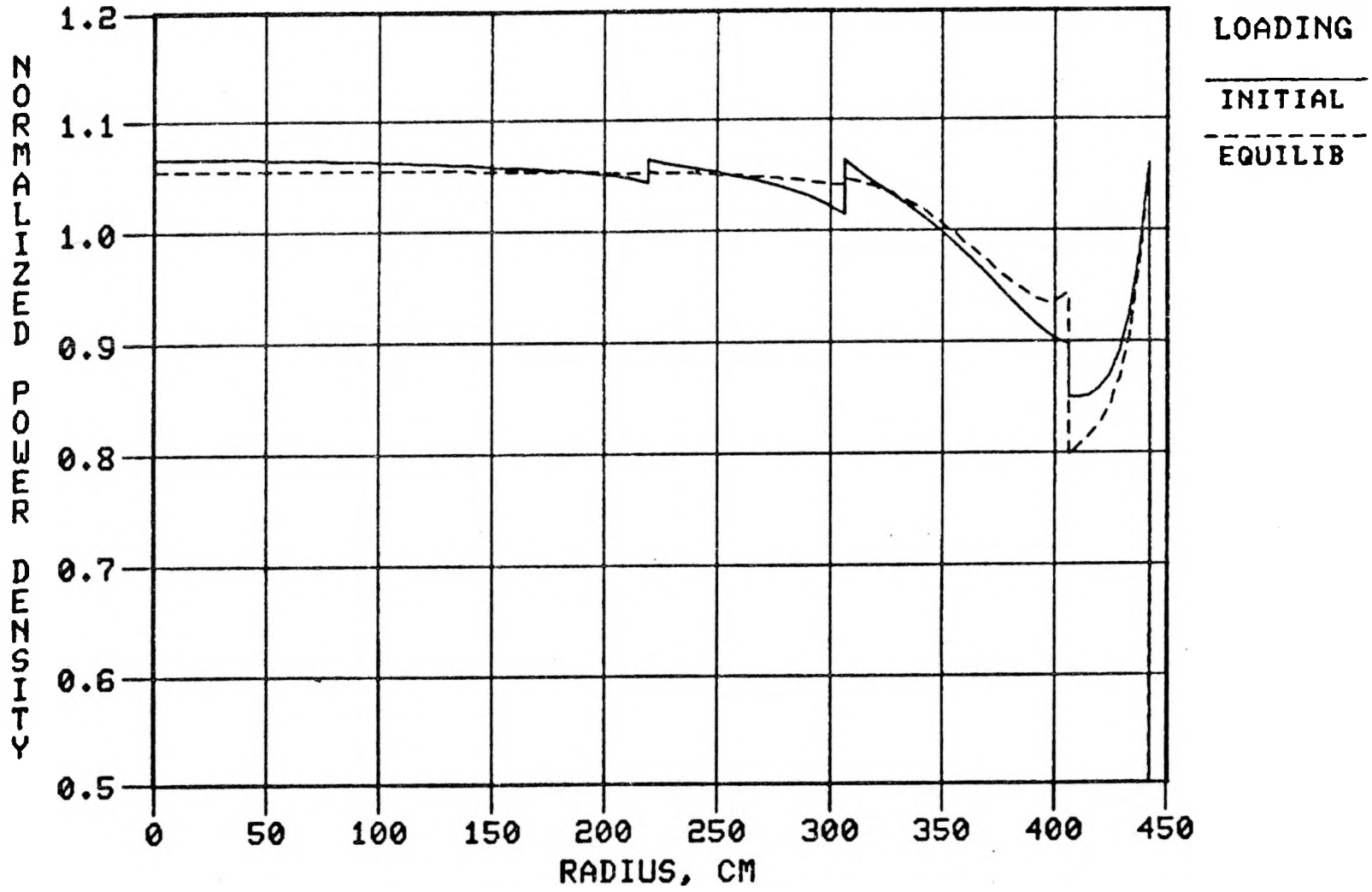

Fig. 2-53. Radial power profiles for alternate core HTGR-SC/C

Pin Power Distributions in Alternative Block Types

A study was made with the prime purpose of quantifying the changes caused by the alternate fuel block designs in the power distributions within the columns and regions. The introduction of the fuel-less bands of graphite around the perimeter of the fuel, to provide for the block-end crossflow seals, increases the thermal flux and thus power in the adjacent edge rows of fuel pins. An assessment of the increased in-column peak-to-average power ratios (on a per-pin basis) then can be factored into the thermal-flow analyses to define the impact of block redesigns on expected fuel temperature peaking. Also, the calculations provide flux advantage factors for the fuel material relative to the column-average area which can be applied to the cross sections used in neutronic calculations for core design and burnup analysis.

One-dimensional transport-theory calculations were run with the DTFX code to determine the radial distributions of the fuel pin power across 7-column cell models of the reference and alternate core fuel block designs. The reference design was the 360.7-mm (14.2-in.) block with 10 rows of fuel/coolant holes. In the alternate designs studied, a 15.8-mm (0.625-in.) thick graphite band was provided around the fuel lattice either by deleting the outermost row of fuel and coolant holes in the 360.7-mm (14.2-in.) block type (to give a 9-row design) or by increasing the block thickness to 391 mm (15.4 in.), retaining the 10-row hole lattice, and fuel rod count. For the 9-row block type, designs with three different counts of fuel rods in the control column were used over the course of the analysis as the engineering details were refined. These variations served to illustrate the impact of control column fuel content.

Relative Power Peaking in Control Column. Table 2-22 presents the results of the cell calculations for a normal patch, with a central control rod column surrounded by six standard columns. The first two cases are for the 9-row design with different assumptions on the number of fuel pins loaded; the different loading (92 versus 74 pins per control rod column) decreases the average power density, on a per-pin basis, by about 6% in the

TABLE 2-22
RESULTS OF DTFX CALCULATIONS FOR POWER DISTRIBUTIONS IN 7-COLUMN CELL MODELS FOR REFERENCE AND ALTERNATE CORE FUEL BLOCK DESIGNS

Block Size [mm (in.) flat-to-flat]	360.7 (14.2)	360.7 (14.2)	360.7 (14.2)	391 (15.4)
Block Type	9-row	9-row	10-row	10-row
Fuel Pins per Control Column	74	92	114	114
Fuel Pins per Standard Column	176	174	216	216
DTFX-calculated k-effective	1.4273	1.4256	1.3466	1.4143
Volumetric power density ratio (column-to-patch)				
Central column	0.527	0.618	0.631	0.637
Outer 6 columns	1.079	1.064	1.062	1.060
Relative pin power densities				
Center column				
Average	1.159	1.100	1.124	1.135
Inner point	1.174	1.103	1.159	1.144
Outer point	1.158	1.110	1.106	1.143
Outer 6 columns				
Average	0.989	0.991	0.989	0.998
Inner point	1.074	1.055	1.072	1.070
Outer point	1.045	1.064	1.008	1.056
Peak-to-average in central column				
Inner point	1.013	1.003	1.031	1.007
Outer point	0.999	1.010	0.984	1.006
Peak-to-average in outer 6 columns				
Inner point	1.085	1.064	1.084	1.083
Outer point	1.057	1.063	1.020	1.069

control rod column (as a result of the decreased C/Th ratio). However, the in-column, peak-to-average factors for the 92-and 74-pin loadings are only 1% different.

Comparison of the 9-row and 10-row cases shows that the added graphite band flattens out the power distribution within the control column, reducing the power peaking factor from 1.031 to 1.003. This is seen in the power profile plots of Fig. 2-54. Also, for the 10-row, widened block the control column power shape is flattened relative to the 10-row reference design block. Figure 2-55 compares the pin power profiles for the two alternate core block designs with the 16-mm (0.625-in.) graphite band around the fuel. As shown in the figure, similar within-column power shapes are produced by the additional moderation at the column edges.

Relative Power Peaking in Standard Columns. In the reference block [10-row, 355.6-mm (14-in.)], the in-column peak-to-average power for the fuel pins of a standard column near the edge adjacent to the control column is a factor of 1.084. For the 9-row block design, this inner-edge peak-to-average power for the standard column is reduced a few percent, to 1.064, by virtue of the increased peaking for the fuel pin power at the outer edges of the patch. In the widened alternate block design [10-row, 391-mm (15.4-in.)], the inner-edge peak-to-average power for the standard columns is increased to 1.08 again, probably because the power in the central column is higher, as shown in Fig. 2-55.

All calculations modeling seven full standard columns were also done to study power peaking at the edges of a standard column adjacent to another standard column. Table 2-23 gives the results. For the reference design, the peaking at the outside edge of the central standard column gives an in-column peak-to-average power of 1.023. The increase of the peak-to-average power within the center column due to adding the graphite band is then about 3% (to 1.054) for the 391-mm (15.4-in.) block design and about 2% (to 1.047) for the 9-row case. Two 9-row cases are given in Table 2-23 where the difference is only in the smear areas assumed for the fuel of the outer six columns. The remodeling shifts the column-average power densities

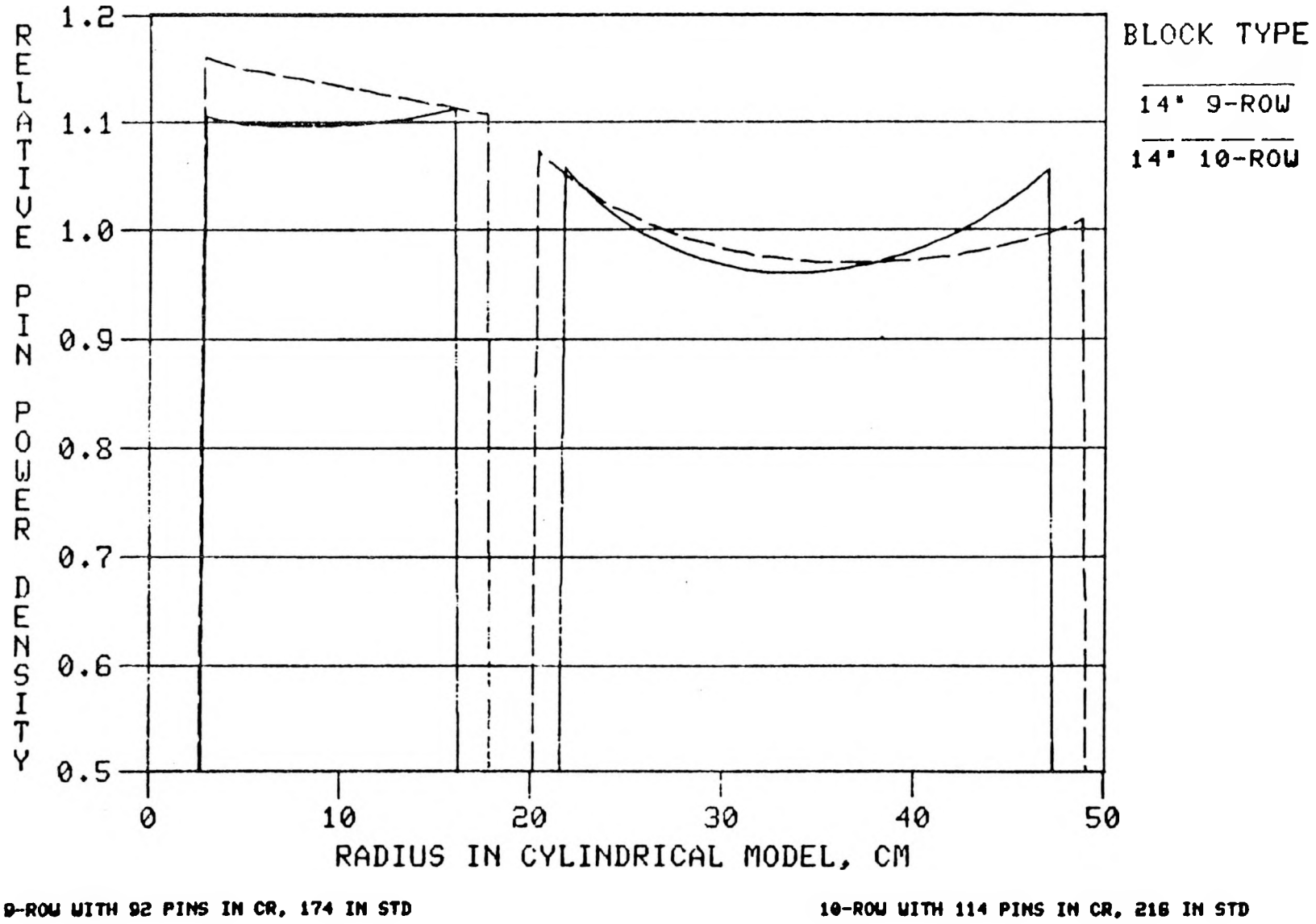

Fig. 2-54. Pin power profiles across regions of 9- and 10-row columns

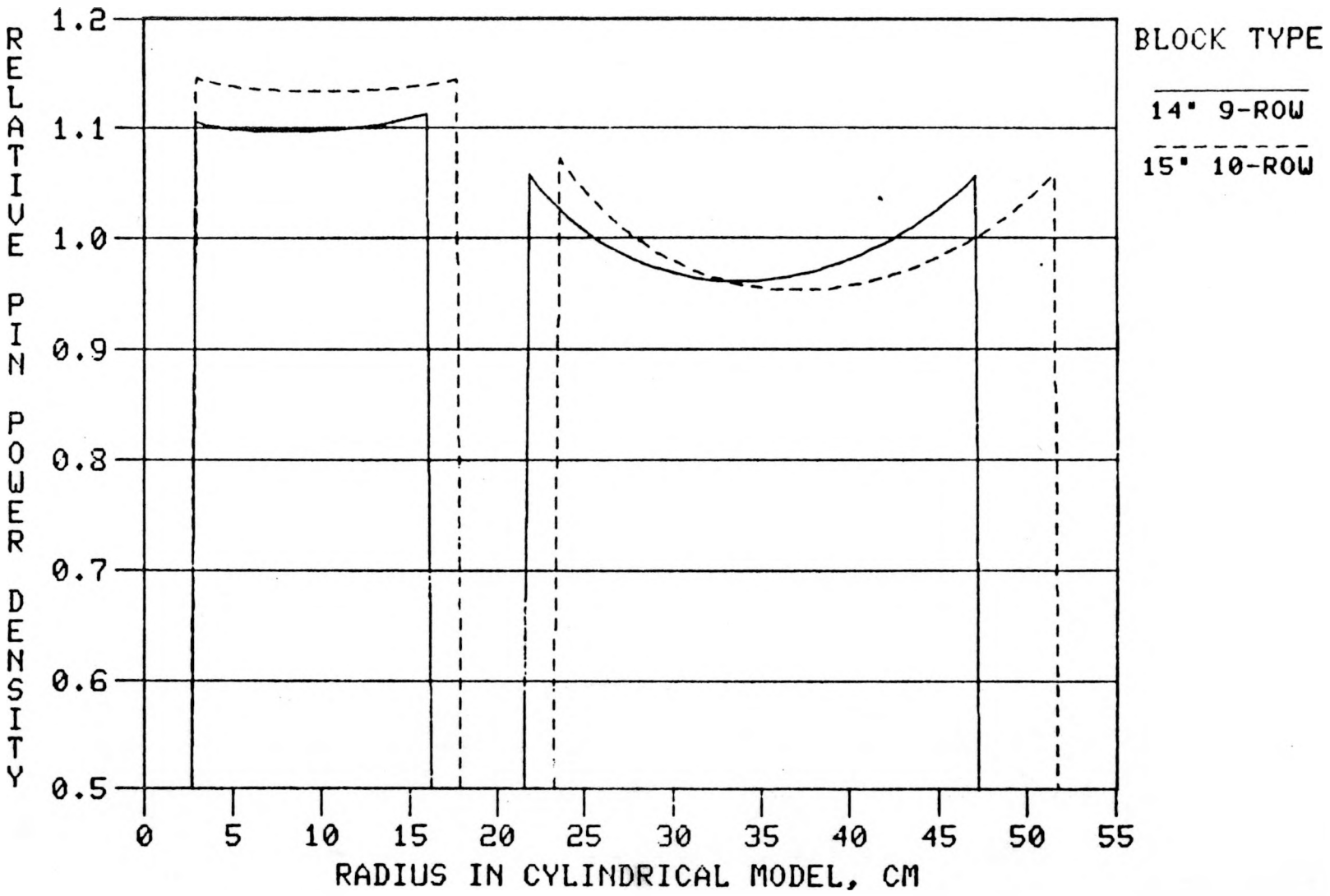

Fig. 2-55. Power profiles across regions of alternate block designs

TABLE 2-23
RESULTS OF DTFX CALCULATIONS FOR POWER PEAKING AT BOUNDARY BETWEEN STANDARD COLUMNS FOR REFERENCE AND ALTERNATE CORE BLOCK DESIGNS

Block Size [mm (in.) flat-to-flat]	360.7 (14.2)	360.7 (14.2)	360.7 (14.2)	391 (15.4)
Block Type	9-row	9-row	10-row	10-row
Fuel Pins per Control Column	216	216	173	174
Smear Area of Outer 6 Columns of Fuel	632,100 mm^2	674,700 mm^2	558,600 mm^2	589,100 mm^2
DTFX-calculated k-effective	1.3299	1.3992	1.4130	1.4119
Volumetric power density ratio (column-to-patch)				
Central columns	0.992	0.997	0.975	0.987
Outer 6 columns	1.001	1.004	1.004	1.002
Relative pin power density				
Central column				
Average	0.992	0.976	0.975	0.987
Inner point	0.987	0.944	0.946	0.961
Outer point	1.015	1.028	0.121	1.033
Outer 6 columns				
Average	1.001	1.004	1.004	1.002
Inner point	1.015	1.030	1.024	1.041
Outer point	1.041	1.092	1.083	1.050
Peak-to-average in central column				
Inner point	0.995	0.967	0.971	0.974
Outer point	1.023	1.054	1.047	1.047
Peak-to-average in outer 6 columns				
Inner point	1.014	1.026	1.020	1.039
Outer point	1.039	1.088	1.079	1.048

and alters the power shape in the outer regions, but the relative power distribution within the central column is little changed. The cylindrical modeling cannot be expected to accurately portray the power shapes near the outer hexagonal patch boundaries.

Figure 2-56 compares the power profiles across the patch of seven standard columns calculated for the reference and 9-row block designs. The added graphite bands increase the power variation across a standard block going from edge to edge when both edges are near other standard blocks. However, the hot spot in the standard column still occurs at the edge adjacent to a control column owing to the higher influx of thermal neutrons there. The net impact of the alternate designs on the power in the standard columns is to shift the power shape, but maintain or reduce a few percent the maximum peak-to-average power from the 1.084 value calculated for the reference design. Also, it is found that this hot-spot factor for the standard columns will depend on the number of fuel pins in the control column.

Evaluation of Alternative Control Block Designs

Among the possibilities considered for improvement of core performance in the HTGR-SC/C was a scheme for redesign of the control rod block and the core layout for the rod deployments. The reference design with the 10-row, 360.7-mm (14.2-in.) block uses a control column with four rod holes at the center of each 7-column patch. The alternate scheme employs single-hole control columns distributed uniformly in a fraction of the total columns of the core, not necessarily at the center of the orificed regions or in a 1/7 core fraction. For a given rod-hole diameter, various control columns could be designated for startup rods, reserve shutdown rods, or power rods, for whatever selection of independent control systems and operating modes is required.

The main advantage of the single control rod concept lies in its use of a considerably stronger control block that has only one central hole. Other significant advantages are the reduced stuck-rod worths and the possibility of eliminating power rods without worsening the power distributions during

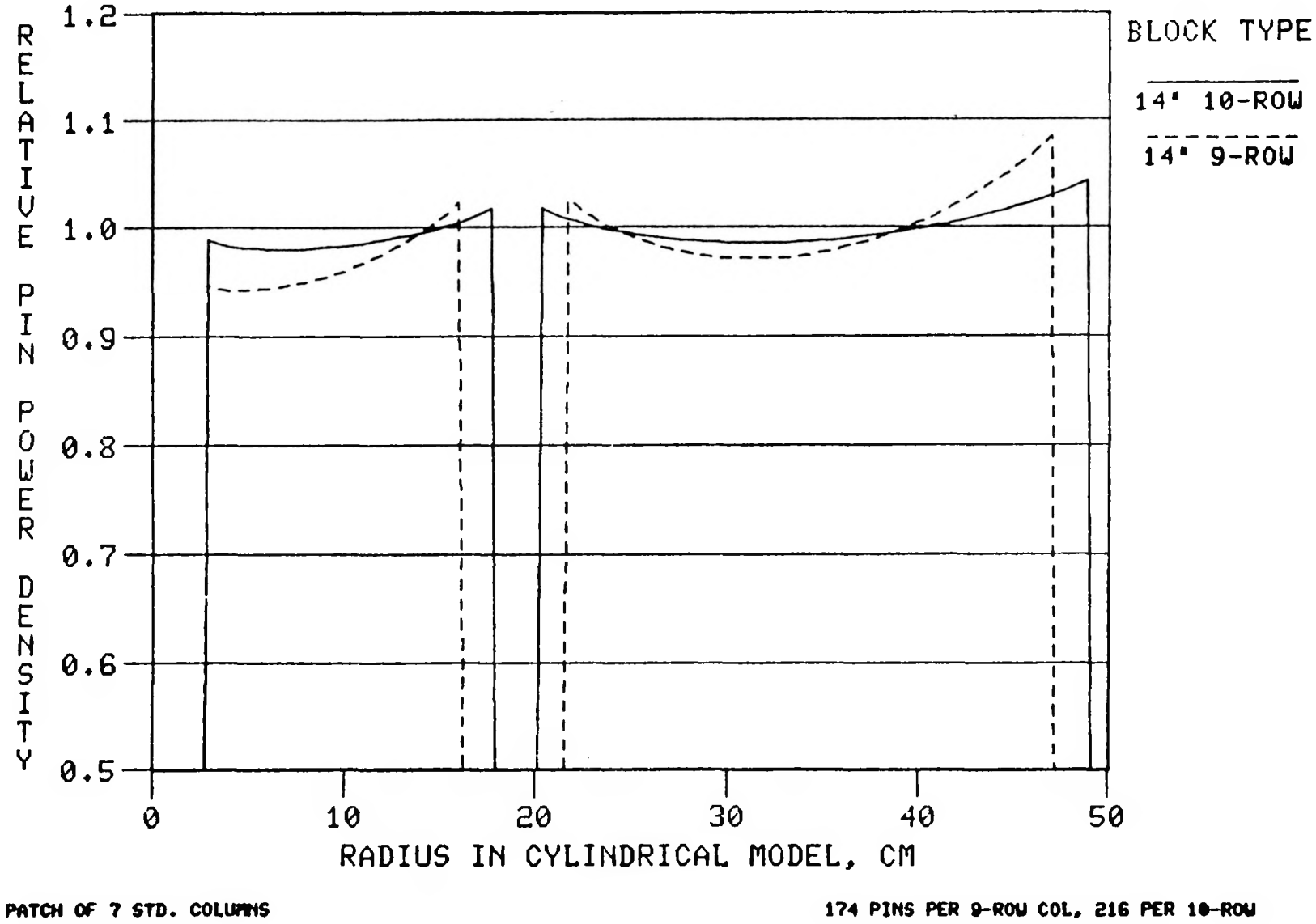

Fig. 2-56. Power peaking between standard blocks, 9-row versus 10-row

normal operations. An evaluation was made of rod worths and effective rod deployment for obtaining reasonable radial power peaking parameters in a representative burnup cycle. For purposes of comparison with previous HTGR-SC/C core evaluations, these calculations were made for the current 2240-MW(t) core design with 439 fuel columns using the reference 10-row, 360.7-mm (14.2-in.) block design. Thus, these rod-column design studies did not include the effects of incorporating a block-end lip seal and added graphite or reduced fuel rod content.

Table 2-15 includes data for the single-rod control column block with a 101.6-mm (4-in.) diameter central hole. Figure 2-57 shows the reference core layout and indicates the location and purpose of holes in the patch-centered control columns. For the single-rod control block design, the control column distribution shown in Fig. 2-58 was selected for study. Here rods designated for control purposes are distributed in a regular triangular array with another uniform distribution for reserve shutdown purposes.

Effective Cross Sections. Previous evaluations of the neutron adsorption cross sections for various control systems in the large HTGR core were carried out for the HEU/Th fueled systems. It was found that the effective macroscopic cross sections of the absorber materials were generally insensitive to core composition and temperature owing largely to the compensatory effects on the microscopic cross sections and the corresponding self-shielding factors. The effective macroscopic cross sections for the absorber materials thus obtained were therefore used in several subsequent studies related to other HEU/Th and LEU/Th core compositions.

The objective of the reported study was two-fold: (1) to obtain more appropriate effective macroscopic absorption cross sections for the conventional control-rod-pair system (Fig. 2-57) to be used in the LEU/Th cores, and (2) to obtain the effective absorption cross sections for the single control rods in the core layout shown in Fig. 2-58.

The calculations for the conventional rod-pair utilized the DTFX one-dimensional transport theory code in nine energy groups for a reactor cell

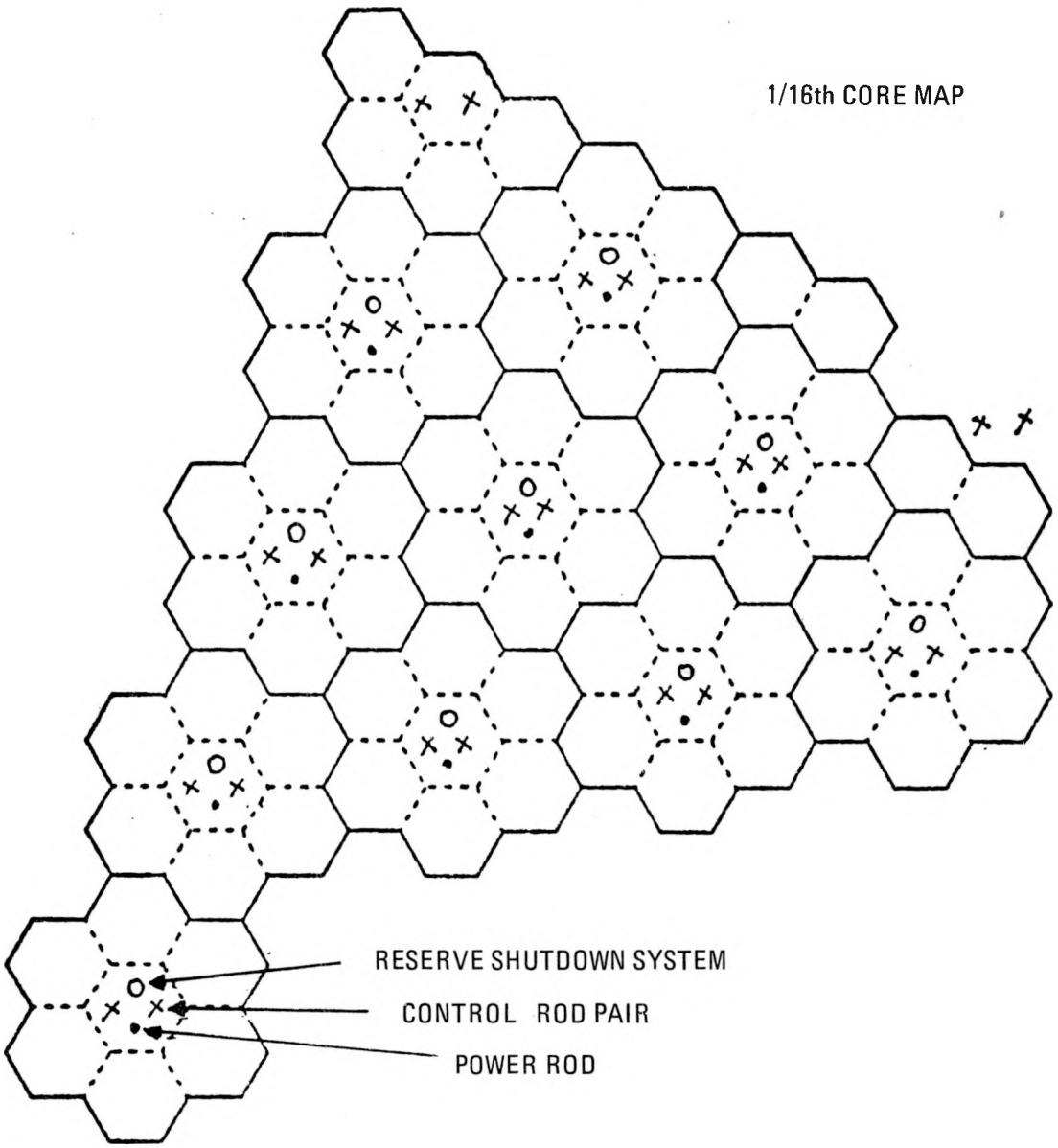

Fig. 2-57. Reference HTGR-SC/C core reactivity control layout using control rod pairs

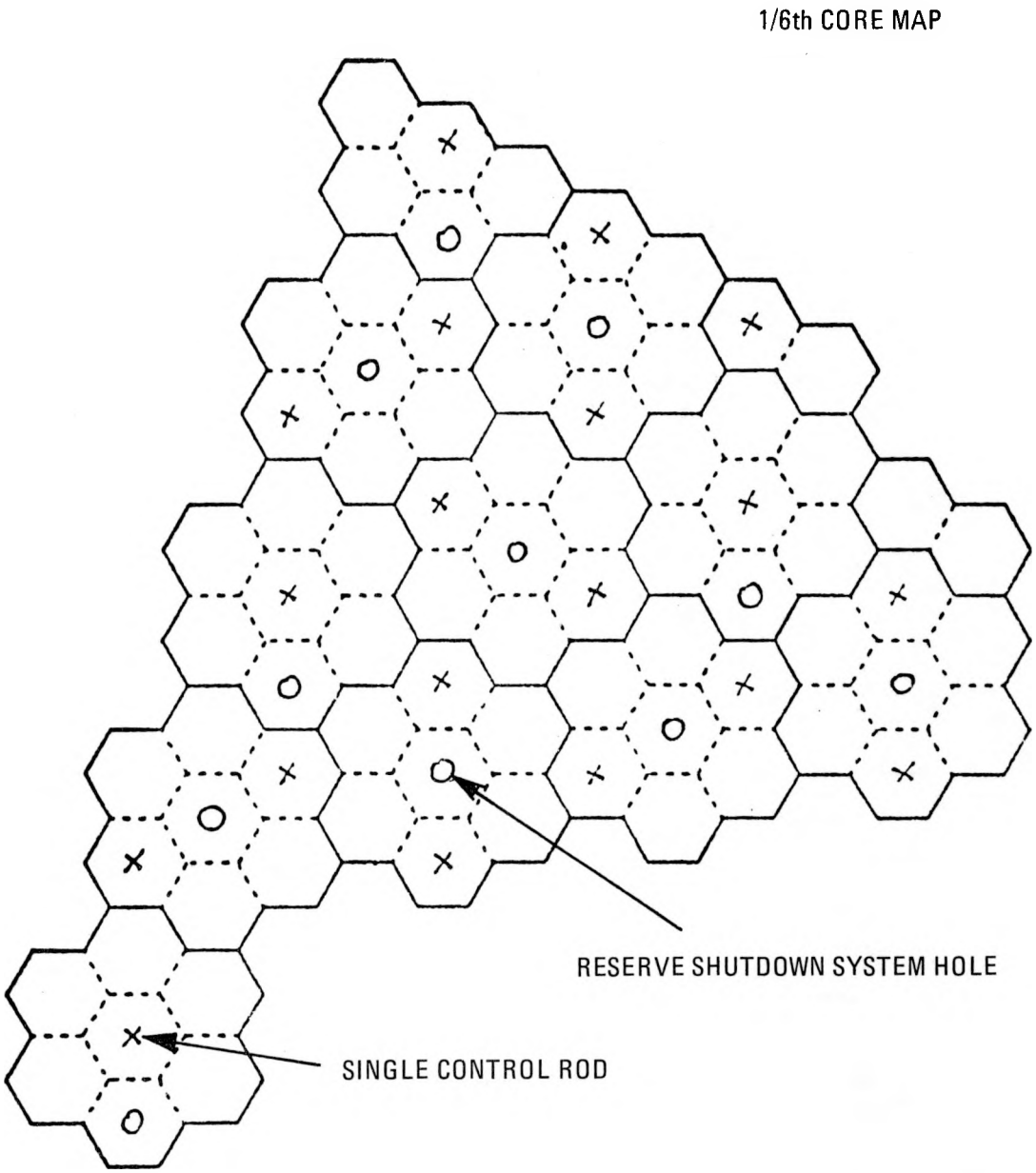

Fig. 2-58. Alternate reactivity control layout using single-rod control columns

comprised of just one of the rod-pairs. The macroscopic cross sections thus obtained were then adjusted to correct for the rod-pair geometry and other effects. The homogenized fuel compositions in the zones representing the control element and the ring of six surrounding standard fuel elements corresponded to the fresh fuel loading at the beginning of an equilibrium cycle for the reference 2240-MW HTGR-SC/C operating on a 4-yr annual LEU/Th cycle with C/Th = 800, C/U = 578. Self-shielding factors were calculated assuming that the control rods are homogenized over the whole control column. Table 2-24 lists the evaluated rod-pair shielding factors and macroscopic cross sections derived in the 9-group structure.

In the case of the single rods, the one-dimensional transport theory cell model is a much closer approximation to the true geometry, so two-dimensional corrections are unnecessary. The outer boundary of the single control rod cell was at 378 mm (14.9 in.) [instead of 504 mm (19.8 in.) for the rod pairs], reflecting the smaller pitch of the rod pattern. However, the average cell composition was the same. Table 2-24 includes the shielding factors and macroscopic cross sections generated for the single rod design control column. The shielding factors for the single-rod design are seen to be lower than those for the rod-pair evaluation, principally because of the smaller unit cell involved. The column-smeared cross section is effectively about 60% less for the single-rod design owing to the combination of the increased shielding and halving of the poison content.

Cell Calculations. For the reference rod-pair control column design, the difference in cell calculation eigenvalues (with and without a rod) gave a reactivity worth of 11.7% (without corrections for axial effects, etc.). Using a previously determined factor of 1.66 to adjust for the rod pairing gives a net reactivity worth of -21.37% for the reference design. This represents the effect of inserting the control rod pairs in all regions of the core at once (61 rods in the HTGR-SC/C model).

With the single-rod cell model, the rodded/unrodded eigenvalue difference yields an uncorrected value of -20.43% for rod worth. In this case, the results represent the insertion of all the triangular pattern of rods in

TABLE 2-24
RESULTS OF DTFX CELL CALCULATIONS FOR EFFECTIVE CONTROL ROD CROSS SECTIONS IN REFERENCE AND ALTERNATE ROD DESIGNS: LEU/TH-FUELED HTGR-SC/C CORE

Group No.	Lower Energy Boundary (eV)	Boron-10 Microscopic Cross Section (barns)	Control Rod Self-Shielding Factors		Column-Smeared Effective Rod Macroscopic Cross Section ($\times 10^3$)	
			Ref. Design Rod Pair	Alt. Design Single Rod	Ref. Design Rod Pair	Alt. Design Single Rod
1	1.830×10^5	0.129	0.8935	0.8730	0.224	0.110
2	9.610×10^2	1.315	0.7972	0.7822	2.040	1.001
3	1.760×10^1	11.88	0.3313	0.2907	7.661	3.434
4	3.930	42.40	0.1236	0.1050	10.192	4.331
5	2.380	69.20	0.07452	0.06239	10.033	4.200
6	1.275	91.57	0.00534	0.04578	9.861	4.078
7	0.825	118.3	0.04189	0.3456	9.641	3.977
8	0.130	229.7	0.2180	0.01773	9.741	3.962
9	0.000	471.0	0.01076	0.00878	9.861	4.022

the core as designated by the X-locations in Fig. 2-58. Thus, based on one-dimensional calculations, the alternate rod scheme offers nearly the same reactivity control as the reference scheme with about 12% fewer rods, but with 1.78 times the requirements for rod drives if individually operated.

It should be pointed out that some of the single-rod control columns would be designated to provide for depletion-reactivity compensation as afforded by the so-called "power rods" in the reference design control block. Based on other calculations for the LEU/Th-fueled HTGR-SC/C core, the total reactivity control for the 61 power rods inserted together would be about 4%. Thus, on the order of 20 or 21 (one fifth) of the rods in the single-rod scheme would be operated in banks for withdrawal during a burn cycle.

Two-Dimensional Depletion Calculations. For two-dimensional depletion calculations using the GAUGE code, the cross sections in Table 2-24 were collapsed to a four-group structure and further adjustments were made, including factors for effects of axial gaps between poison pellets, finite rod length, and diffusion versus transport theory discrepancies. The total correction factors for the rod-pair and single-rod designs were 0.702 and 0.912, respectively.

GAUGE calculations in the presence of rods were then carried out for the first five cycles so that the effect of the different segment age distributions on power distribution were fully accounted for. The analysis was done for the LEU/Th-fueled 2240-MW(t) HTGR-SC/C employing the uniform pattern of single control rods as shown in Fig. 2-58. Some of the region-centered single rods were used to control excess reactivity during depletion, thus eliminating the need for power rods.

The total fuel loading at each reload was obtained from reference GARGOYLE calculations. The LEU/Th fuel cycle is characterized by its 4-yr cycle at 7.12 W/cm^3 with the initial core operating for 1.5 yr (C/Th = 375) and subsequent reloads for 1 yr (equilibrium C/Th ≈ 760). Fuel and lumped burnable poison were zoned into three radial zones, including the buffer

zone comprising a single row of outermost columns, to equalize the powers. Lumped burnable poison pins were assumed to be located in both block types, and the poisoning was adjusted to provide an initial excess reactivity of 4%.

The reactivity control during core depletion was exercised entirely by the use of those single rods which are located centrally within the regions. In all the reloaded cores it was found sufficient to use only 13 of the 19 such control rod locations. The six control rods located in the central block of the partial five-column regions at the core boundary were thus not required for the control of excess reactivity during most of the core depletion.

Power distribution parameters over the first five cycles, expressed in terms of the RPF/TILT envelope, are shown in Fig. 2-59. Included on the graph is the envelope derived from the previous depletion studies for the reference HTGR-SC/C core. The maximum tilts from this single-rod scheme are appreciably lower (1.55 versus 1.7) than before. The isotherm plots included in Fig. 2-59 indicate that the new rod scheme might lower peak fuel temperatures by about 30°C (54°F). The reactivity behavior and two-dimensional power profiles obtained demonstrate the feasibility of the alternate core operating with the limited number of single control rods.

The effect on power distributions of using single rods not centered within the regions was simulated by arbitrarily halving the power during the fourth operational cycle. The use of four additional single control rods that are not region-central gave tilts in some of the regions which were higher by about 15%, although the maximum tilt remains about the same. Thus, the peak fuel centerline temperatures might be somewhat adversely affected. The additional power peaking could be eliminated by a judicious choice of the additional rods and/or the use of both the diametrically opposed single rods in some regions.

Shutdown Margins. To compare shutdown margins, additional GAUGE calculations were done with control bank insertions throughout the depletion

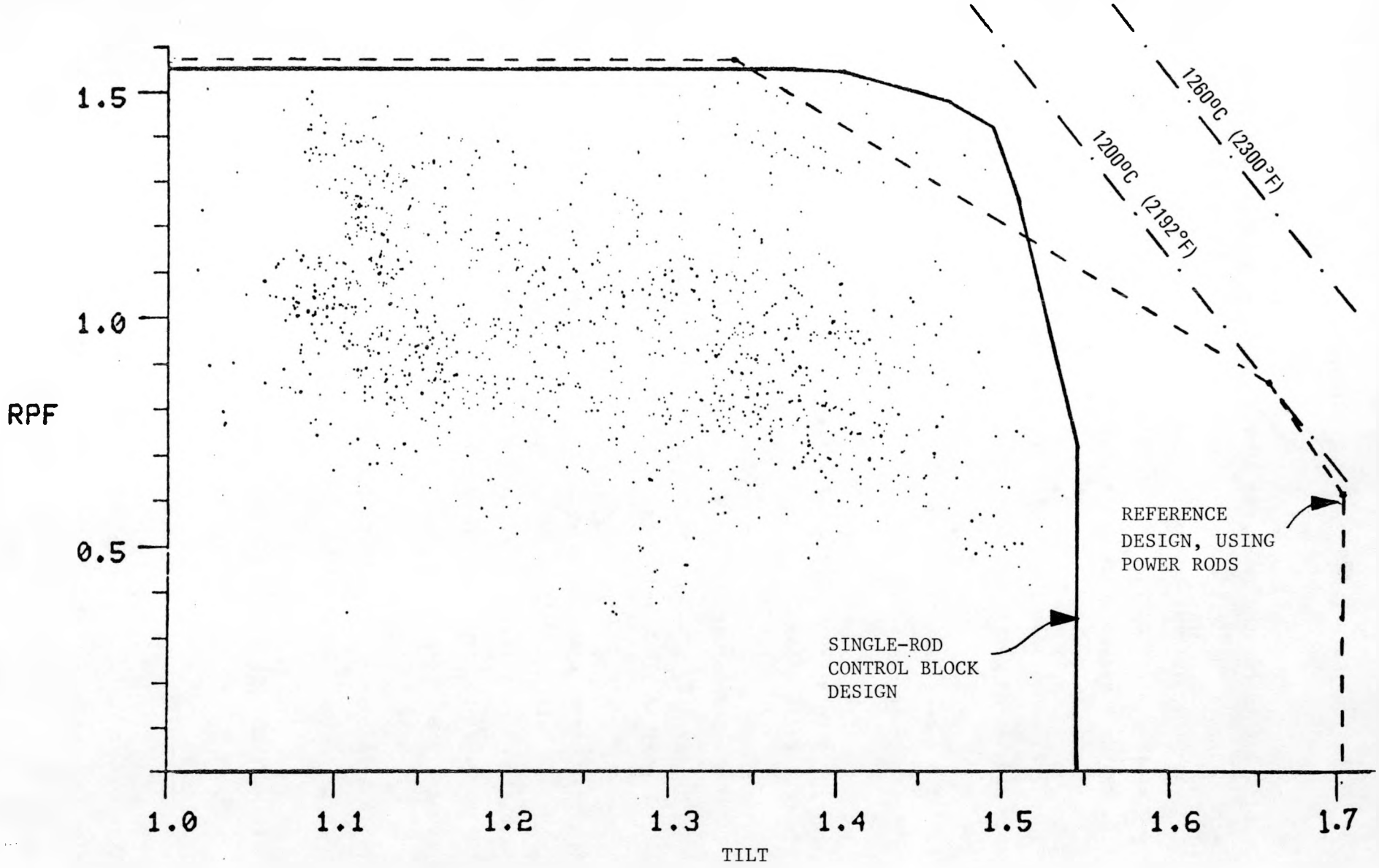

Fig. 2-59. Comparison of radial power envelopes for 439-column HTGR-SC/C core using reference and alternate control block designs

of the initial core for the reference 10-row block design and the alternate single-rod design. The initial core, being a 1.5-yr cycle, should contain the point with the minimum shutdown margin. At the beginning of the initial cycle and at the points during the depletions with the rods most fully inserted, shutdown margin checks were performed for both designs.

Table 2-25 summarizes the results for the two rod patterns. The alternate single-rod design has the following advantages:

1. The excess reactivity controlled by rods is 2.7% versus 4.1% for the reference design.

2. The bank worth of the control rods is 0.209 versus 0.188 for the reference design.

3. The shutdown margins for one, two, and no stuck rods are approximately 0.05 greater than for the reference case for the same number of stuck rod pairs.

Shutdown margin calculations were repeated for modified versions of the reference case using six and 12 reflector shutdown rods. Table 2-26 shows that with six extra rods, the reference design shutdown margins are improved by 0.026 to 0.031 for stuck rod cases, meeting all shutdown margin requirements.

Table 2-27 compares the LEU/Th-fueled reference case with no reflector rods with a previous HEU/Th-fueled case of similar size.

2.14. PRIMARY COOLANT SYSTEM ANALYSIS (6032210100)

2.14.1. Scope

The scope of this task is to define criteria for limiting the amount of contaminants allowed in the primary coolant at various plant operating conditions and for component interfacing the primary coolant, to prepare a

TABLE 2-25
SHUTDOWN MARGIN SUMMARY FOR 10-ROW BLOCK ROD PATTERN

	10-Row Block Rod Pattern	
	Reference	Alternate
Hot, Unrodded k_{eff}	1.041	1.027
Hot, Bank Worth (Δk)	0.188	0.209

Inoperable Rods or Pairs	Temperature [°C (K)]	Nuclides Decayed	Shutdown Margins ($1 - k_{eff}$)	
None	103.8 (377)	None	0.114	0.150
None	103.8 (377)	Xe	0.081	0.120
None	103.8 (377)	Xe and Pa	0.065	0.104
One	103.8 (377)		0.074	0.123
One	103.8 (377)	Xe	0.038	0.092
One	26.8 (300)		0.067	0.117
One	26.8 (300)	Xe	0.031	0.084
Two	103.8 (377)		0.042	0.098
Two	103.8 (377)	Xe	0.004	0.065

TABLE 2-26
EFFECT OF REFLECTOR RODS ON SHUTDOWN MARGINS FOR 10-ROW BLOCK - MIDDLE OF CYCLE 1

Rod Core Position Numbers and Mode	k_{eff} Reflector Rods In		
	0	6	12
1 through 61 in	0.88604	0.87063	0.86356
1 through 61 in, 39 out	0.92598	0.90066	0.88176
1 through 61 in, 39-40 out	0.95827	0.92762	0.91524

	Shutdown Margins (1 - keff) Reflector Rods In		
	0	6	12
One rod stuck, 26.8°C (48°F), 140 days	0.014	0.040	0.058
Two rods stuck, 26.8°C (48°F), 14 days	-0.002	0.029	0.041

TABLE 2-27
COMPARISON OF MIDDLE OF CYCLE SHUTDOWN MARGINS FOR 2240-MW(t) LEU/Th FUELED HTGR-SC/C USING 10-ROW BLOCK WITH 2000-MW(t) HEU/Th FUELED REFERENCE DESIGN (2 CORE)

	2000-MW(t) Case	2240-MW(t) Case
Excess reactivity	0.029	0.041
Bank worth	0.226	0.188
Temperature defect[a] [hot to 104°C (187°F)]	0.043	0.032
Xenon decay	0.030	0.032
Pa-233 decay		
2 weeks	0.012	0.006
4 weeks	0.022	0.009
20 weeks	0.043	0.016
Maximum worth rod and xenon decay	0.028 0.031	0.040 0.036
Maximum worth 2 rods and xenon decay	0.064 0.033	0.072 0.038
Temperature defect [104°C (187°F)]	0.008 0.033	0.007 0.037

[a]Reactivity worth of temperature charge.

system specification including contaminant criteria and a Primary Coolant System Description, and to develop and evaluate cost-effective design solutions to resolve the water ingress technical issue.

2.14.2. Discussion

2.14.2.1. Primary Coolant Chemistry Plant Specification. The initial issue of the primary coolant chemistry plant specification has been completed and published.

The primary coolant in the HTGR is helium, which is inert, has excellent heat transfer properties, does not condense at any temperature in the system, and undergoes an insignificant degree of neutron activation. Because helium is chemically inert, the core components can in theory operate at high temperatures without problems of corrosion or other chemical reactions. In practice, small and sometimes large amounts of contaminants are expected to be introduced into the primary coolant system during the life of the plant.

The presence of these contaminants can have detrimental effects on the performance of several components exposed to the circulating helium. These effects can be minimized by limiting the operating temperatures and/or by keeping the concentrations below specific levels. During normal plant operations, the amount of contaminants introduced by small leaks can be maintained below these levels by the helium purification system. For leakage above the helium purification system capacity, the reactor power must be reduced or the reactor shut down and the sources of impurities eliminated or reduced below maximum acceptable levels.

The primary coolant chemistry plant specification provides criteria for limiting the amount of contaminants allowed in the primary coolant at various plant operating conditions and for designing components and systems that affect the introduction and removal of contaminants. The basis for these criteria is a design that satisfies the plant performance, availability, and safety goals. This specification covers all the chemical

impurites and particulates shown in Table 2-28. These are the contaminants that affect the structural integrity and/or the performance of the components and systems interfacing with the primary coolant. The specification also includes the sources of contaminants shown in Table 2-29 and the components and systems affecting their removal. Not included in the scope of this specification are the fission and the neutron activation products present in the primary coolant system as circulating or plateout impurities. Their sources and their concentrations within the primary coolant are specified in the shielding and source strength plant specification.

The criteria discussed in the primary coolant chemistry specification will be used as design bases for all the affected components normally exposed to the primary coolant and for all the systems handling the primary coolant. The values of the various parameters discussed in the specification are preliminary in nature since the plant design is still in the conceptual phase. As the design of the plant progresses, the plant specification will be updated as required.

2.14.2.2. Primary Coolant System Description. The primary coolant system description has been prepared and issued. This system description defines the functional requirements and the design basis for the entire HTGR pressurized helium coolant volume, its associated instrumentation, and those components associated with transfer of heat from the core to the secondary steam system. Components included in the primary coolant system are:

1. Main helium circulators.
2. Main loop isolation valve.
3. Main helium circulator drives and controllers.
4. Main helium circulator service system.
5. Steam generators.
6. Primary coolant loop instrumentation.

The principal function of the primary coolant system is to transfer heat from the reactor core to the steam generators in order to produce steam for industrial process applications and cogeneration of electricity. While

TABLE 2-28
CHEMICAL IMPURITIES IN PRIMARY COOLANT, THEIR PRIMARY SOURCES, AND THEIR EFFECTS

Chemical Impurities	Primary Sources	Effects on Components
O_2	Air ingress during refueling or from the transfer compressor or adsorbed in fuel or reflector elements	Oxidation of graphite and metallic components
H_2O	Steam generator and CAHE tube leak, circulator bearing leak, graphite outgassing, buffer helium dryer breakthrough, auxiliary circulator cooling coils, thermal barrier outgassing, helium transfer compressors	Oxidation of graphite and metallic components
CO_2	Product of graphite oxidation and outgassing	Oxidation of graphite and metallic components
CO	Product of graphite oxidation, outgassing, and breakthrough of low-temperature adsorber	Carbon deposition and carburization
H_2	Product of graphite oxidation, outgassing, and oil ingress	Carbon deposition and H_2 embrittlement
CH_4	Oil ingress or reaction of $C + H_2$	Carburization
Hydrocarbons	Oil ingress	Carburization
N_2	Air ingress or breakthrough of low-temperature adsorber	Large amount could saturate low-temperature adsorber, requiring regeneration
H_2S,S	Graphite outgassing	Metallic corrosion
Particulates		
Carbon dust	Core graphite	

TABLE 2-29
POTENTIAL SOURCES OF CHEMICAL IMPURITIES AND PARTICULATES

Sources	Contaminants
Chemical Impurities	
Steam generators	H_2O
Main circulator bearings	H_2O
Buffer helium dryers	H_2O
Graphite and thermal barrier insulation outgassing	O_2, H_2O, CO_2, CO, H_2, CH_4, N_2, H_2S, S
Auxiliary circulator cooling coils	H_2O
Air ingress (refueling, maintenance, helium transfer compressor)	O_2, N_2
Breakthrough of helium purification system	H_2O, CO_2, N_2, CH_4
Auxiliary circulator bearings	H_2, CH_4, other hydrocarbons
Purified helium and helium transfer compressors	H_2, CH_4, other hydrocarbons
Contaminated helium charging tanks	N_2, O_2
Particulates	
Core graphite	C

the primary coolant system is not safety class, it is designed to remove stored and decay heat from the core during normal shutdown, upset, emergency, and faulted conditions. In addition, the main loop isolation valve performs a safety function by isolating any shutdown main loops to prevent coolant flow from bypassing the core. Some primary coolant components (steam generator, circulator, and circulator shaft seal) provide a primary coolant pressure boundary to confine radioactive coolant within the PCRV. The steam generator also provides a pressure boundary to prevent the ingress of water and steam into the reactor.

The primary coolant system description also defines functional requirements when the plant is operating at reduced output with one or two main loops isolated. The main loop isolation valve is designed to allow a minimum leakage flow of 3.7 kg/s (30,000 lb/hr) through the steam generator. This flow is required to suppress natural circulation of hot gas from the lower plenum into the isolated steam generator cavity.

2.14.2.3. Water Ingress Design Solutions. The present 2240-MW(t) HTGR-SC/C plant design has the potential for water ingress in the primary and auxiliary cooling systems. The most likely sources of water are the main circulators, the steam generators, and the CAHEs. Water ingress into the PCRV does not directly affect the safety of the reactor but can have a major impact on its availability.

A task is presently in progress to develop cost-effective design features for reducing the risk of a prolonged plant shutdown caused by water ingress. Work is being performed in the areas of (1) prevention, (2) early and selective detection, (3) quick removal, and (4) increased tolerance of the affected components. In principle, a perfect solution in any of the above four areas could solve the problem. However, in practice the design solutions are expected to be a combination of improvements in all four areas.

Most of the recent work in the area of reducing the possibility of water ingress has been concentrated on the steam generators and the main

circulators. The CAHEs are a less frequent potential source of water since when the reactor is at power, their feedwater pressure is always less than the primary coolant pressure.

Work on the steam generator included an analysis of steam generator leak sources and sizes, plant response to steam generator leaks, the frequencies of various classes of steam generator leaks, and the downtime associated with repairing and leak cleanup. Moisture ingress events were analyzed for the plant conditions of 100% power, 25% power, one-loop shutdown, refueling, pressurized startup, and pressurized shutdown. Results of these analyses show that:

1. Small pinhole leaks occur 10 and 50 times more frequently than large single-ended ruptures and offset tube ruptures, respectively.

2. The downtimes associated with each type of leak vary little, at most 13%. Downtime is dominated by the time required to plug the faulty tube.

A main circulator service system design has been developed that promises to be highly reliable in preventing water bearing inleakage. A dynamic model of this system has been developed, and the results of the analyses have confirmed its high resistance to water ingress. With the exception of catastrophic failure of the circulator, water ingress can occur only through very unlikely combinations of multiple failures and malfunctions. Water ingress rates ranging from 300 mm^3/s (0.2 gal/min) to a maximum of 800 mm^3/s (22 gal/min) were calculated for a variety of postulated failure events.

The work on leak detection has shown that next to the helium purification system flow rate, the detection time is the most important parameter affecting plant downtime following a water ingress event. More work is planned on minimizing the vapor and liquid water detection time during plant operation or shutdown. Work has also been planned on improving the

the capability of detecting the right leaking loop when the leak is so small that the difference in moisture concentration from one loop to another is within the moisture monitors' accuracy.

Several design features have been proposed for increasing the rate of water removal. Several locations throughout the primary and auxiliary cooling systems have been identified as prime candidates for catch basins for collecting and draining liquid water. Sensitivity studies have shown that the helium purification system flow rate is one of the most important parameters for decreasing the water removal time. An alternative way of operating the helium purification system during cleanup has been proposed. Instead of running the system at a constant volumetric flow rate, the alternative involves partial purification at a constant volumetric flow rate, followed by PCRV pumpdown to refueling conditions and finally by helium repressurization of the PCRV to operating pressures. This technique can reduce the cleanup time by about 20%.

In many cases, the removal of water trapped beneath the thermal barrier coverplates is the controlling factor during the cleanup process. Areas related to this problem include:

1. The development of design features for preventing liquid water from reaching to thermal barrier coverplates in areas removed from the main coolant flow and for preventing any direct path from potential sources of water to the liner beneath the thermal barriers.

2. The development of drain systems beneath thermal barriers strategically located in stagnant areas. These systems can either suck or blow dry helium through the thermal barrier insulation.

3. Development of a thermal barrier coverplate design that is resistant to impinging water penetration.

Additional information is given on the thermal barrier design in Section 9.2.2 and on the helium purification system in Section 19.

Graphite is the key material for controlling the amount of water allowed at any given time in the primary coolant. Work is also in progress on qualifying new types of graphite and developing new designs for those components affected by oxidation with water.

2.15. MAIN CIRCULATOR DESIGN (6032210201)

2.15.1. Scope

The scope of this task is to complete the main circulator conceptual design, including (1) establishment of the interfaces of the main circulator and circulator auxiliaries with the BOP, (2) development of system description data supporting the project decision package, (3) definition of the electric motor drive requirements, and (4) further development of helium/water shaft seal system features to minimize the possibility of water ingress into the primary coolant.

2.15.2. Discussion

2.15.2.1. Main Circulator Configuration. The aerodynamic design of the main circulator has been recalculated to satisfy the latest NSS thermal performance envelope. To avoid gross changes in the circulator layout, the 1829-mm (72-in.) diameter impeller was retained while changes were made in the blade trim.

The new circulator design point calls for 11.3 MW (15,200 shp) at 2360 rpm. This change is caused by combination of the sum of pressure loss margins throughout the primary loop and the minimum hellum flow value. The operating point for the circulator when the NSS is at its design point remains the same. However, the extreme points in the envelope must have the surge margin that will ensure stable operation for those conditions. As a

result, the blade height at the tip has been decreased from 130.2 mm (5.125 in.) to 119.9 mm (4.72 in.).

The main circulator layout was modified in several other areas. A change in thermal sleeve/mounting flange configuration has resulted in a steeper primary closure cone. This change was needed to optimize the concrete plug and liner configuration. The loop isolation valve assembly was modified to improve the remote handling removal and replacement of the valve assembly. A new 0.523-rad (30-deg) inclined cross-duct was incorporated. Since this increases the direct radiation from the top plenum, a 3.14-rad (180-deg) segment neutron shield was added to limit the activation of the valve assembly. Figure 2-60 shows the latest circulator layout incorporating the above changes.

2.15.2.2. Main Circulator Helium/Water Shaft Seals. This area was redesigned to accommodate an improved configuration of bellows-actuated static shutdown seals. The functional characteristics of the helium buffer flow and the helium return flow labyrinths remain unchanged, although the overall seal arrangement has changed.

The main circulator static shutdown seals have been redesigned, as shown in Fig. 2-61. The seals are actuated by pressurizing metal bellows, thus moving a sealing ring against a shoulder on the shaft after a circulator has been shut down. Two seals are provided for redundancy to ensure isolation of the bearing cartridge from the primary coolant circuit.

The revised shutdown seal design lowers the bellows stresses for a given stroke and also isolates the turbulent vortex excitation to the bellows caused by rotation of the shaft. The compactness of the design minimizes the overhang between the journal bearing and the compressor wheel. The alignment of the two seals permits the use of the same bellows configuration for both seals, simplifying tooling and reducing fabrication costs.

2.15.2.3. Electric Motor Drive Interface. An assessment of torsional vibration was made for a complete drive train, as shown in Fig. 2-62. The

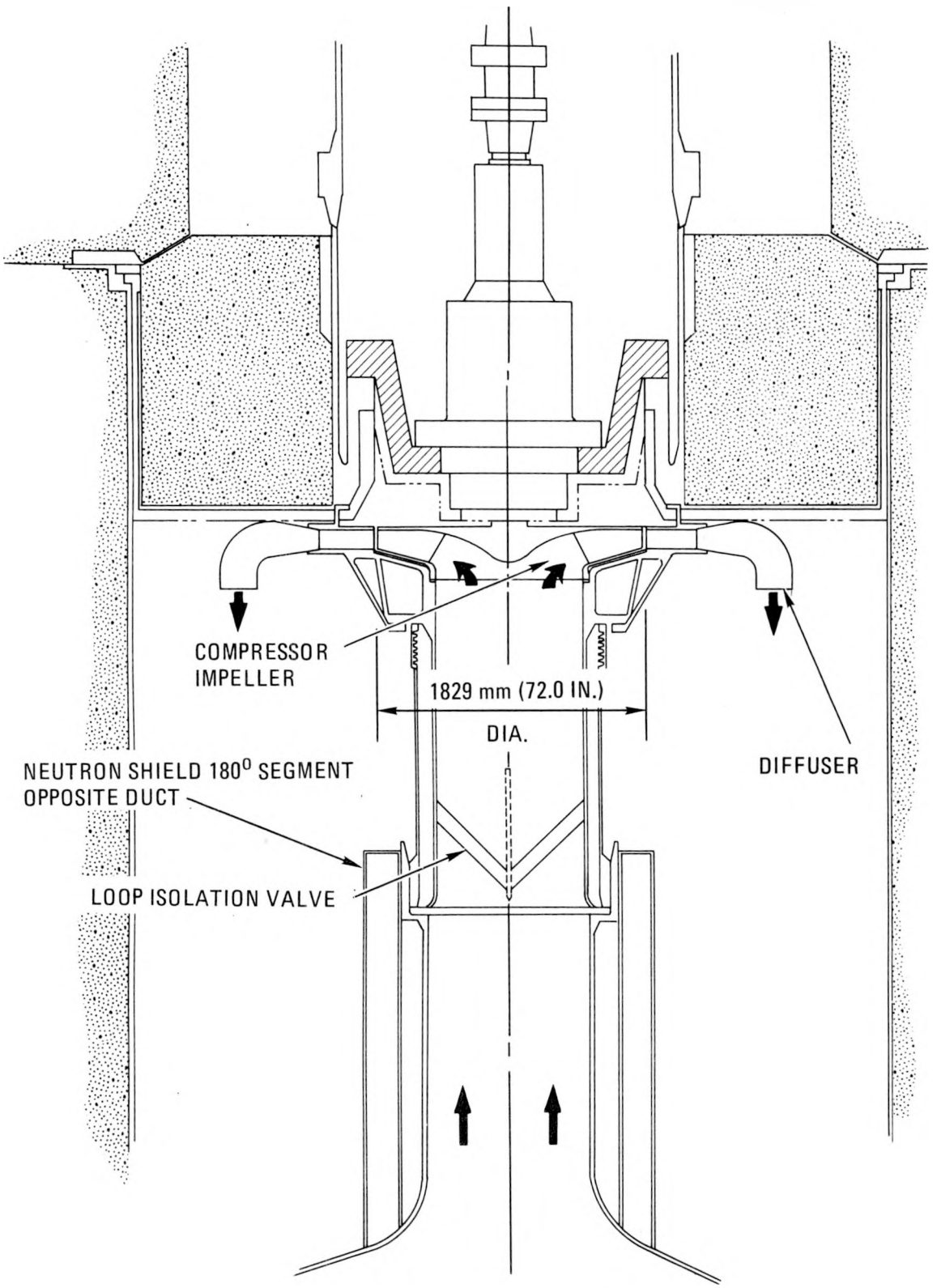

Fig. 2-60. Modified main circulator layout

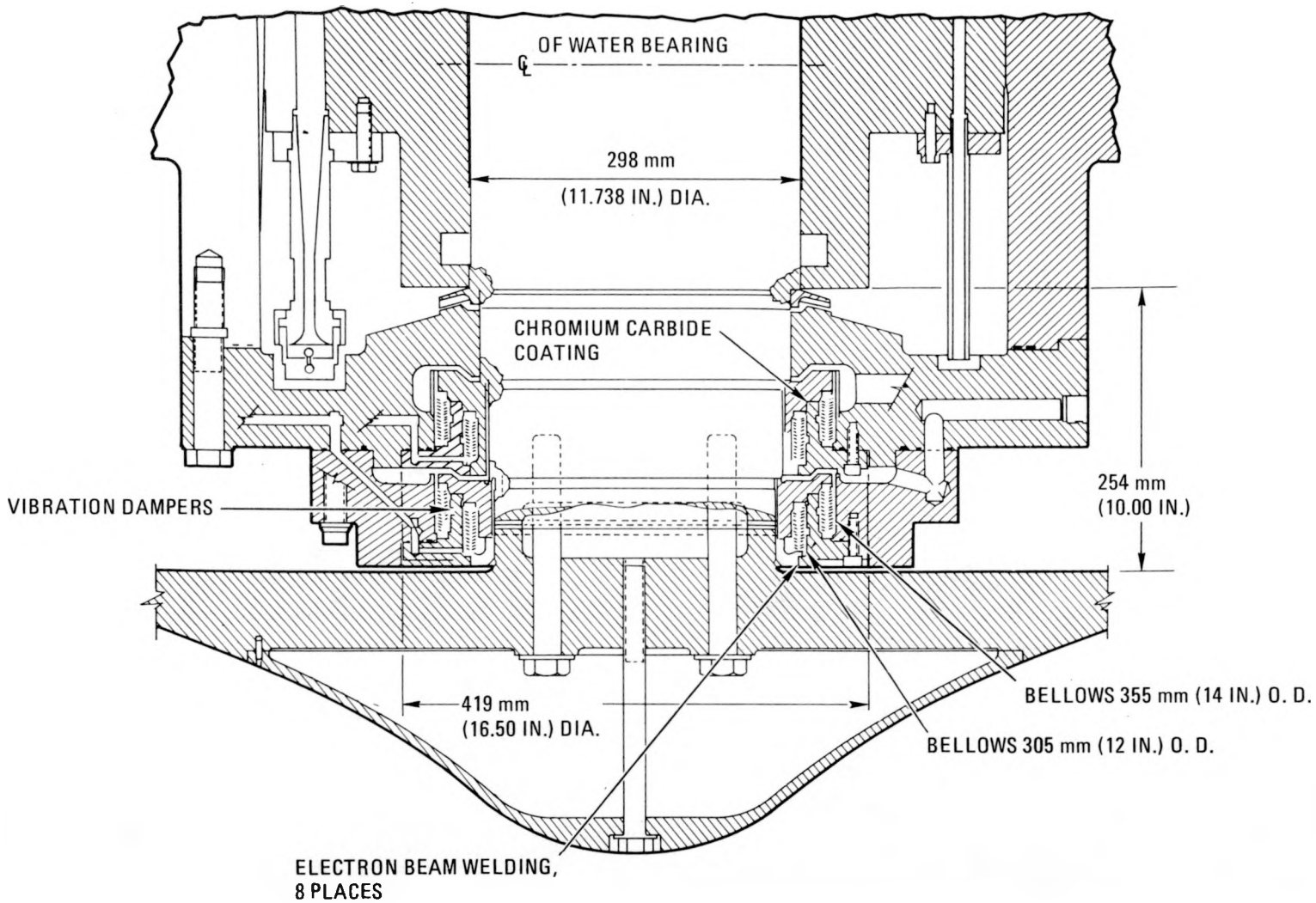

Fig. 2-61. Main circulator shutdown seals

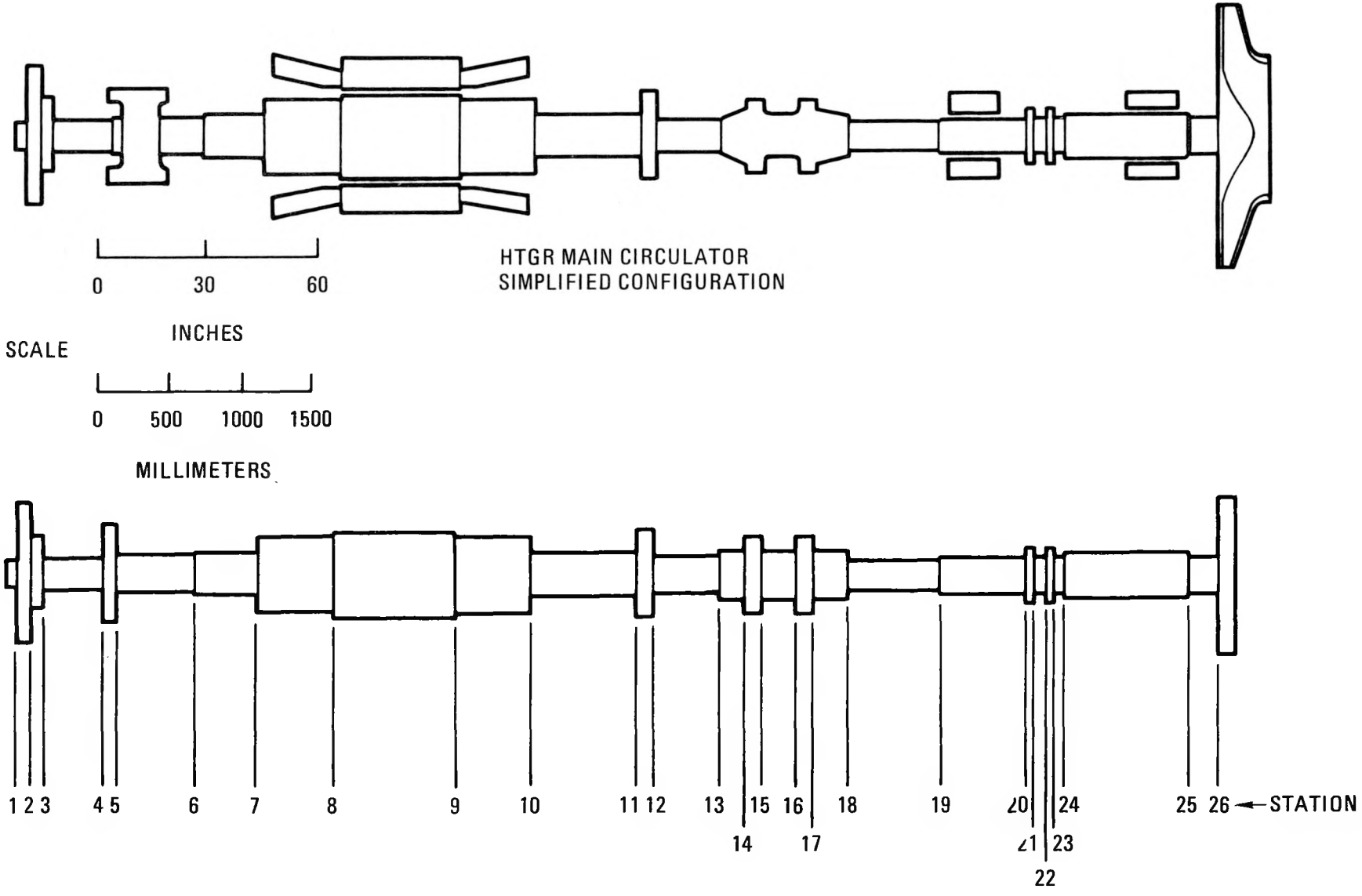

Fig. 2-62. Results of torsional vibration analysis of circulator and drive motor rotor

purpose of this study was to generate data on values of motor rotor polar moments of inertia that, when combined with a given shaft torsional stiffness, may cause torsional resonance within the operating speed range. A computer program using multimass/spring capability was developed for this purpose.

An analysis of torsional vibration was conducted on the complete circulator and drive motor rotor. The results show that the first critical speed (2700 rpm) is above the operating speed range of zero to 2360 rpm. The assumption here was a conservatively large polar moment of inertia.

Figure 2-62 shows the rotor configuration, and Fig. 2-63 is a plot of residual torque versus speed obtained from the analysis using a computer program of the Holzer method. The torsional critical speeds are at zero residual torque values. Since the polar moment of inertia of the motor rotor has a strong influence on the torsional critical speed, these values will be used in designing the electric motor.

2.16. STEAM GENERATOR (6032210300)

2.16.1. Scope

The scope of this task is the design and analysis of the steam generator by GA and CE. The primary objectives of this task are to advance the design of the steam generator and to transfer design responsibility to the steam generator subcontractor (CE).

2.16.2. Discussion

2.16.2.1. Subcontracting Work to CE. In September 1981 a work scope was agreed upon under which CE began participating in the steam generator design effort. This work scope (subsequently revised in February 1982) identified technical and program support tasks to be performed by CE on the HTGR-SC/C steam generator and the CAHE. A general review meeting was held at GA

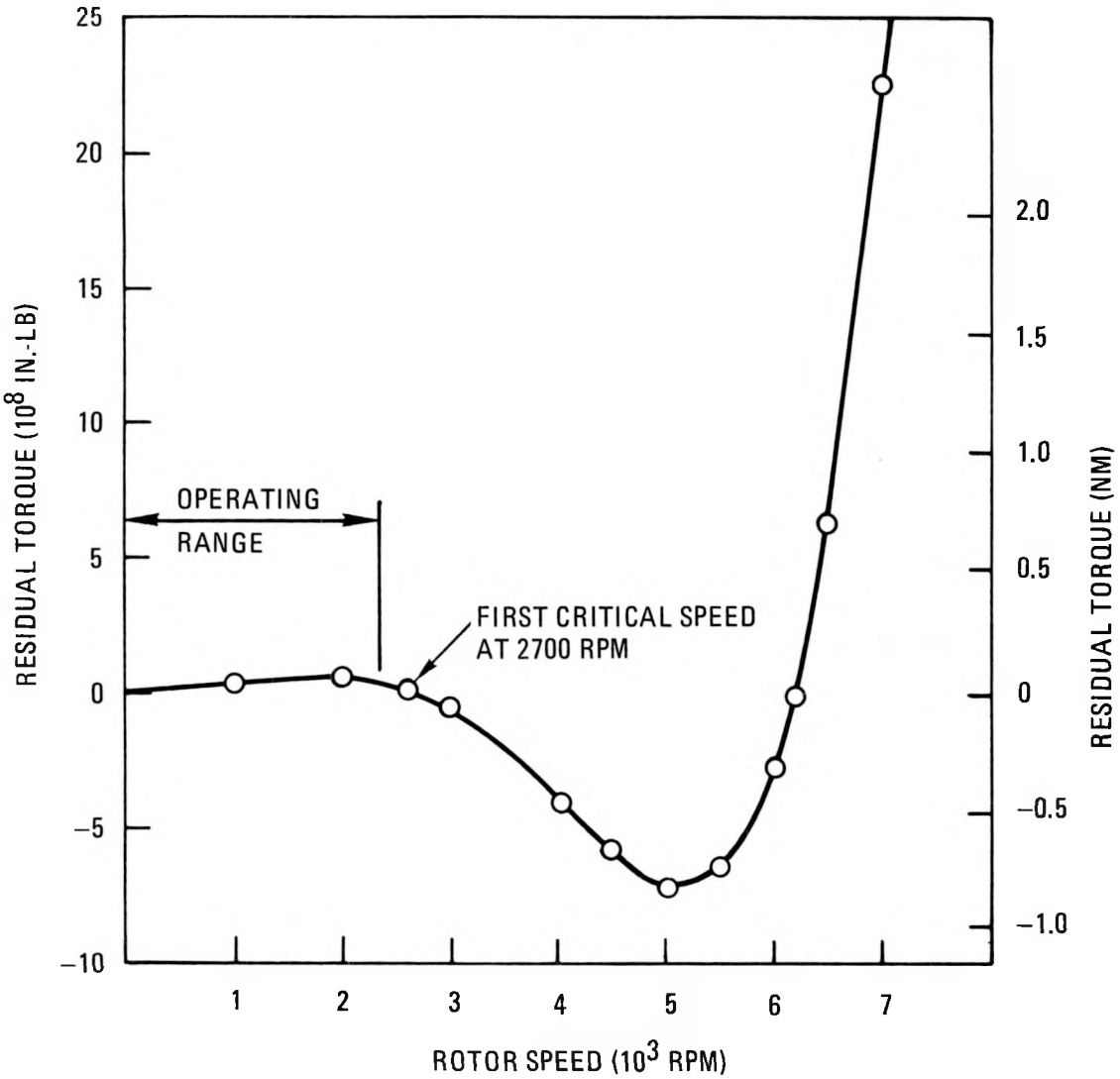

Fig. 2-63. Residual torque versus rotor speed for HTGR-SC/C main circulator. Points of zero torque represent critical speeds.

between GA and CE personnel to identify detailed responsibilities and assign action items and schedules for FY-82.

Technology Transfer

During this reporting period technological information was transferred to CE, including: (1) the "Steam Generator Design Guide" (Ref. 2-6), (2) the "Steam Generator Design Basis" (Ref. 2-7), (3) structural design documents, (4) the thermal sizing code NUSIZE, (5) the helical bundle thermal stress code C-STRES, (6) a steam generator general arrangement drawing, and (7) CAHE general arrangement drawings.

In addition, engineering personnel from CE spent several weeks at GA participating in modification and operation of the transferred computer codes.

Water Ingress

A study of the probability of various sizes of water leaks into the primary coolant from the steam generators and the time required to detect and plug them was completed. The results of this study, including steam generator leak sources and sizes, plant response, frequencies of various classes of steam generator leaks, and the plant downtime associated with subsequent repair, were documented.

Use of Extra Cavity Height

An investigation into the possible use of excess cavity height that has resulted from core redesign studies was initiated by both GA and CE personnel. The steam generator thermal sizing was explored using NUSIZE, new tube bundle diameters being developed for incremental height increases up to 3 m (118 in.). At the same time, analyses of the additional expansion loop requirements and the additional seismic support requirements were made. The results of these analyses indicate that expansion loops that incorporate

254-mm (10-in.) vertical legs will accommodate the additional thermal expansion imposed by the 3-m (118-in.) additional steam generator height.

The tube bundle size analysis indicated a saving of about 140 mm (5.5 in.) on the bundle or cavity diameter with the 3-m (118-in.) increase in height. With these new dimensions, the requirements for seismic support were found to cause an increase in the outer shroud thickness of 95 mm (3.75 in.), resulting in a total thickness of almost 178 mm (7 in.). This was judged to be excessive and will not be pursued.

Straight Tube Bundle Performance Code STRUBE

The straight tube superheater (STSH) performance code STRUBE was used to examine the overall effectiveness of the STSH. It became evident that the bundle was about 8% undersurfaced owing to the eddy- and separation-producing effects of the radial flow inlet and exit sections. Several measures were considered to regain the lost performance: increasing the surface area by lengthening the STSH, increasing the STSH tube diameters, and decreasing the tube pitch to increase the shell-side film coefficient. The last option was shown to effectively overcome the problem at the cost of a slight increase in STSH helium pressure loss.

EES Tube Stress Problem Resolution

A more detailed examination of the stresses in the EES bundle was carried out in conjunction with the development of a version of the NUSIZE code that includes tube stress data. During this effort it was learned that an incorrect EES helium inlet velocity distribution had been included in the early conceptual design of the steam generator. Correcting this error resulted in the calculation of higher tube wall temperatures than previously calculated, which effectively lowered the allowable stress level. With these conditions the calculated combined stresses at the hot end of the 2-1/4 Cr-1 Mo EES bundle were somewhat higher than the allowable stress. This was due in part to the fact that initially a conservative, simplified method was used to determine the bundle-tube support differential thermal

expansion stress ("bear-hug" stress). It was therefore decided that a detailed analysis of this stress, which constitutes a major contributor to the combined stress level, should be performed using the C-STRES code. It was found that the combined stress using the more realistic "bear-hug" stress was back within the allowable stress at the higher tube wall temperature.

2.17. PRIMARY COOLANT SYSTEM CONTROLS/INSTRUMENTATION (6032210400)

2.17.1. Scope

The scope of this task during this reporting period was the preparation of the main circulator service system control and instrumentation system conceptual design.

2.17.2. Discussion

Main circulator service system requirements to the Balance of Plant Requirements (BOPR) document has been completed and issued. The BOP interfaces at this point in the conceptual design are as follows:

1. Non-Class 1E electrical power to the main circulator drive motors.

2. Reactor plant cooling water for main circulator drive motor cooling.

3. A radioactive liquid waste system to accept liquid waste from the main circulator service module.

4. A feedwater and condensate system to supply treated condensate for the main circulator bearing water system.

5. A main control room area to house main circulator control cabinets and service system control cabinets.

The control and instrumentation input to the primary coolant system description has been updated to include the present state of the design. A brief summary of the functional description of the main circulator service system is given below.

The principal function of the main circulator service system is to provide water to the integral pump on the circulator shaft. This water is used for circulator bearing lubrication and cooling. Another function is to provide the circulator labyrinth seals with purified buffer helium to prevent inleakage of bearing water to the primary coolant and outleakage of primary coolant to the service system. The system also provides high-pressure helium to actuate the circulator static seals and air to actuate the main circulator brakes.

The services required for the circulator drive motor are supplied by the motor manufacturer and are not included in the main circulator service systems.

The main circulator service system conceptual design instrument block diagrams have been issued. The instrument block diagrams reflect the present system design. A main circulator service module for each circulator is provided and contains all the service system equipment associated with one circulator. Major equipment includes a surge tank, two bearing water boost pumps (one standby), two bearing water filters (one standby), a bearing water cooler, a helium/water drain cooler, an auxiliary jet supply water cooler, a helium/water drain cooler, an auxiliary jet supply pump, a bearing water make-up pump, two helium dryers (one being regenerated), and a regeneration heater.

2.18. AUXILIARY SYSTEMS DESIGN (6032230001)

2.18.1. Scope

The scope of this task is to develop a helium purification system design that can satisfactorily meet water, air, and oil removal criteria for

a helium bleed flow from the PCRV and to update conceptual designs for the helium purification, the PCRV service, and the PCRV pressure relief subsystems of the 2240-MW(t) HTGR-SC/C plant.

2.18.2. Discussion

2.18.2.1. Helium Services System. A brief study was carried out to characterize the capability of the helium purification system to remove chemical impurities from the PCRV following a water ingress event. The study assumed a helium purification sytem (see Fig. 2-64) operating at 0.277 kg/s (2200 lb/hr) at full PCRV pressure following a 362.8-kg (800-lb) water ingress. It was further assumed that all water was in the vapor phase or was entrained as droplets in the helium. That is, no water was formed by release from the thermal barrier, nor was water depleted by entrapment in the thermal barrier or by condensation during PCRV cooldown. Additional assumptions were that there was complete impurity removal in the helium purification system as well as perfect mixing of the helium being returned from the helium purification system with that in the PCRV.

The results of this study (Fig. 2-65, solid curves) show that under the above criteria, an impurity level of less than 10 ppmv total oxidants in the PCRV can be attained in less than 4 days. These findings are not realistic, because all water does not remain in the vapor phase and, in fact, cleanup will be much longer since water is only slowly removed from the thermal barrier and only slowly vaporized from condensed water in the PCRV. An alternate approach was proposed which can reduce cleanup times. This concept involves partial helium purification system purification, the PCRV pumpdown through the helium purification system to refueling conditions, followed by PCRV repressurization to 100% operating conditions. This approach (see Fig. 2-66) can reduce impurity cleanup times by more than 21 hr.

The system description document for the 2240-MW(t) HTGR-SC/C plant has been issued. Its principal revisions, compared with the previous document for the prior 900-MW(e) HTGR-SC plant, include:

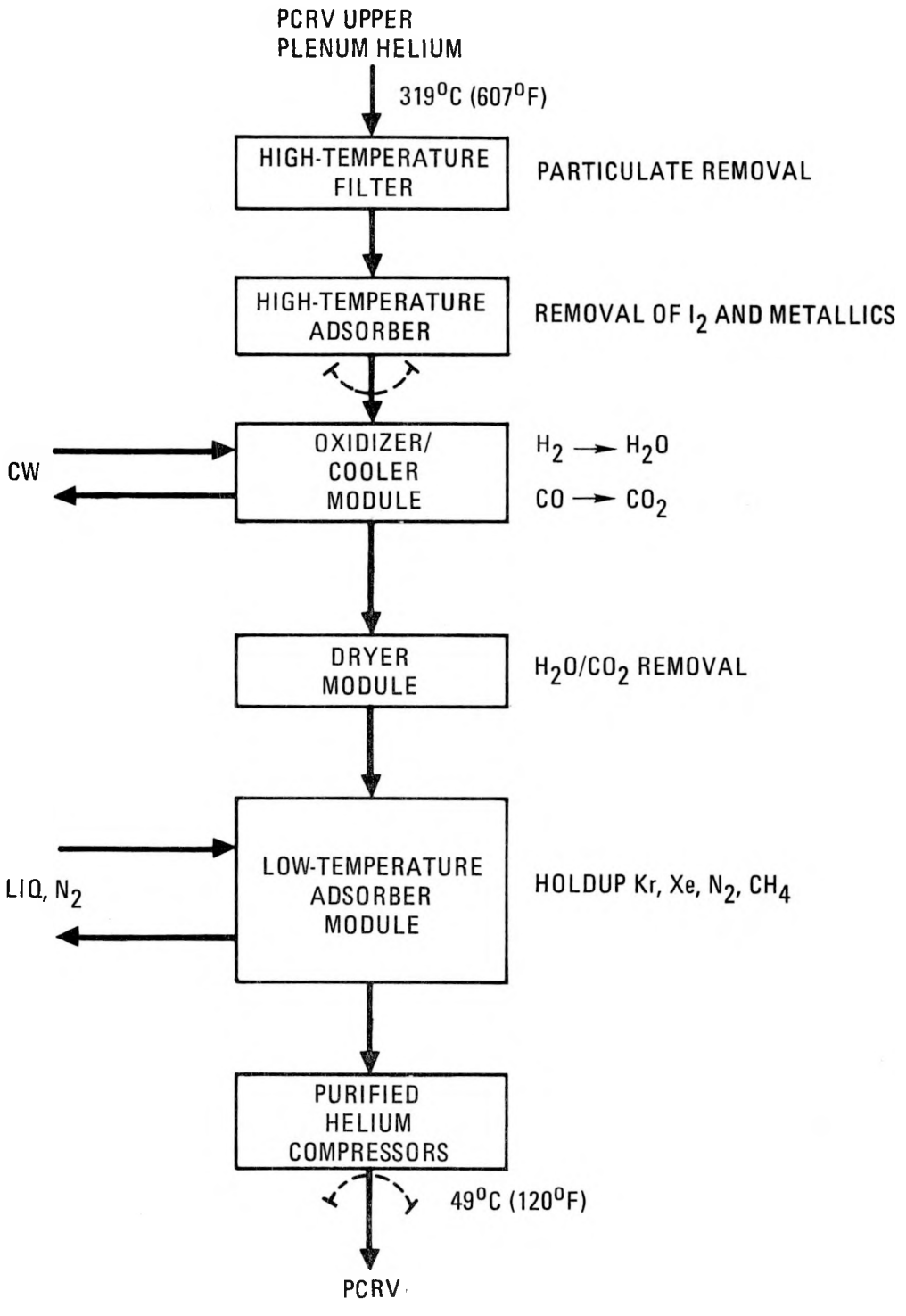

Fig. 2-64. Flow schematic of simplified helium purification system

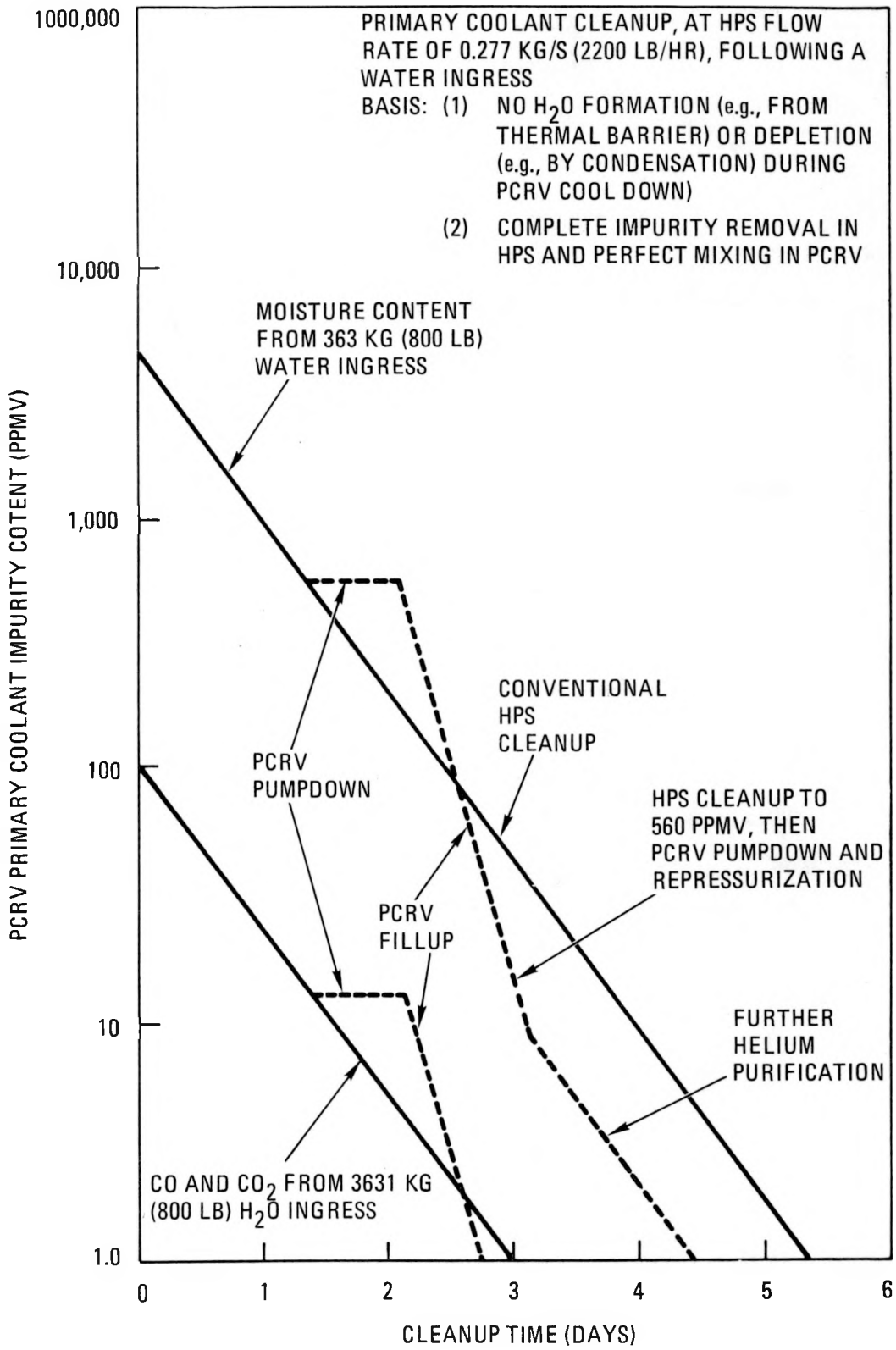

Fig. 2-65. Primary coolant cleanup following a 363-kg (800-lb) water ingress

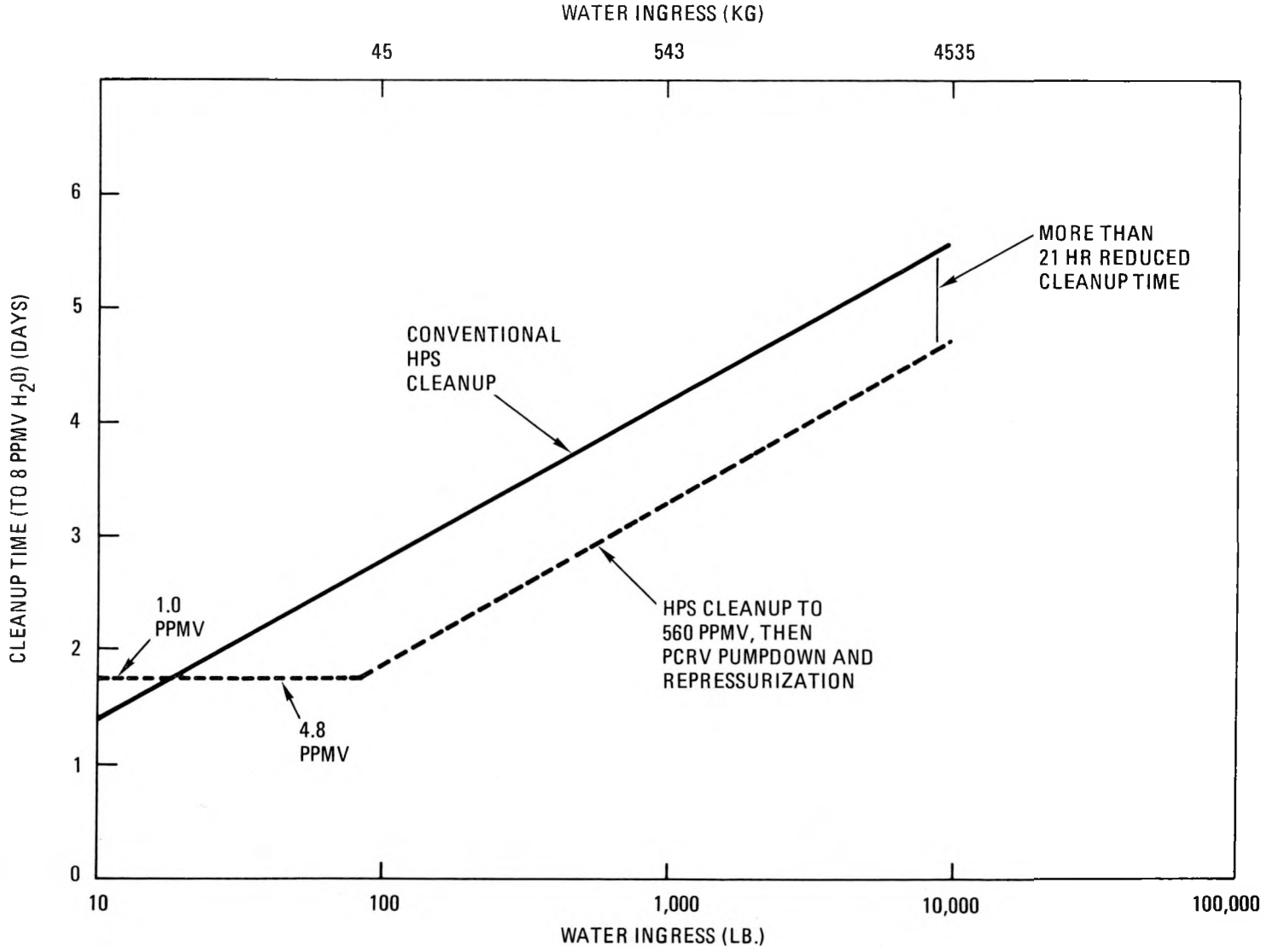

Fig. 2-66. Helium service system cleanup times for various water ingresses

1. An adjustment for the redesigned core.

2. An increase in the helium purification system helium flow requirement from 0.277 to 0.328 kg/s (2200 to 2600 lb/hr), owing to a difference in the buffer helium treatment for the main circulator service system (none of its buffer helium is now recycled back to the helium purification system purified helium compressor).

3. Because of potential ingestion or inhalation by workers at the process plant, a criterion to limit tritium levels in the PCRV to assure that secondary coolant dose levels (from tritium diffusion at the steam generators) will be below regulatory limits.

4. Interfacing with the new plant specification on primary coolant chemistry related to PCRV impurity concentrations and the size of the maximum water, air, or oil ingresses into the PCRV.

5. Inclusion of simplified flow schematics for the helium purification and the PCRV service systems.

6. Addition of nominal frequencies for helium purification system equipment regeneration or replacement.

7. Minor additions to the seals serviced by the PCRV service system.

2.18.2.2. PCRV Pressure Relief Subsystem. Input on the PCRV pressure relief subsystem was submitted for inclusion in the PCRV system description document for the 2240-MW(t) HTGR-SC/C plant.

2.18.2.3. Moisture Monitoring Subsystem. Input on the safety-related moisture monitor/detection equipment was submitted for inclusion in the safety-related control and instrumentation system description document for the 2240-MW(t) HTGR-SC/C plant. The principal revisions to the prior document [for the 900-MW(e) HTGR-SC plant] were:

1. Treating four individual steam generator loops, rather than two double-loop headers, because of moisure monitoring/steam generator dump considerations.

2. Addressing CAHE/CACWS leakage more specifically, i.e., for moisture detection/CACS loop isolation, as a safety-related control and instrumentation criterion.

2.19. CORE AUXILIARY COOLING SYSTEM ANALYSIS (6032280100)

2.19.1. Scope

The scope of this task is to provide system input to the conceptual design of the CACS components and control system.

The system design basis transients and other transients that reflect expected CACS performance will be prepared for use by the NSS component designers and the CACWS designers and will be published in a third issue of the system documentation. This information will then be used in NSS component and CACWS design.

2.19.2. Discussion

The CACS is the principal engineered safety system of the HTGR. Its design has developed generically through various HTGR plant designs since the initial larger reactors following FSV. The FSV reactor has no CACS.

The overall performance of the CACS is shown in Table 2-30. It should be noted that this information is given here as a guide for the present 2240-MW(t) HTGR-SC/C.

The safety requirements of 10CFR50, Appendix A, "General Design criteria for Nuclear Power Plants," criteria (GDS) 34 and 35, require inclusion in the reactor plant design of a system or systems to provide "Residual

TABLE 2-30
OVERALL CACS PERFORMANCE AT THREE DESIGN POINTS CORRESPONDING TO PEAK DUTIES IN TRANSIENT CASES[a]

	Depressurized PCRV		Pressurized PCRV with Water Ingress
	Pure Helium	Air Ingress	
CACS loops operating	2	2	1
Primary coolant pressure [MPa (psia)]	0.163 (23.6)	0.163 (23.6)	7.24 (1050)
Primary coolant molecular weight	4	12	5.6
Heat duty per CACS [MW (Btu/hr)]	25.6 (87.3 x 10^6)	21.9 (74.6 x 10^6)	78.4 (267.7 x 10^6)
Primary coolant circuit flow per CACS loop [kg/s (lb/hr)]	7.45 (59,100)	17.6 (140,000)	35.8 (284,000)
CAHE inlet temperature [°C (°F)]	952 (1746)	952 (1746)	860 (1580)
Core inlet temperature [°C (°F)]	292 (557)	349 (660)	352 (666)
Pressure drop [kPa (psi)]			
CAHE	Later	5.0 (0.72)	Later
Core	Later	0.62 (0.09)	Later
Ducts and plena	Later	1.1 (0.16)	Later
Secondary water (CACWS) circuit			
Flow per CACS loop [kg/s (lb/hr)]	141 (1.12 x 10^6)	141 (1.12 x 10^6)	141 (1.12 x 10^6)
CAHE inlet temperature [°C (°F)]	78 (172)	73 (163)	167 (333)
Air blast heat exchanger inlet temperature [°C (°F)]	123 (254)	112 (233)	284 (544)
Pressure drop [kPa (psi)]			
CAHE	Later	Later	190 (28)
Piping and air blast heat exchanger	Later	Later	1270 (184)

[a] Information for auxiliary cooling loop performance is for the 900-MW(e) reference plant and is presented as a guide for the present 2240-MW(t) HTGR-SC/C plant.

Heat Removal" and "Emergency Core Cooling." In the HTGR the CACS is provided to meet these functional requirements.

The CACS is called upon for cooling the reactor core whenever main loop cooling is not available and is designed to function with the PCRV either pressurized or depressurized. The CACS cooling capability is sufficient to maintain the temperatures of all components in the PCRV within safe limits.

Except in the reactor core cavity, the CACS is entirely separate from the main loops of the HTGR, through which power is normally delivered from the core to the turbine plant and/or user process. The main and auxiliary loops function independently, with the exception that the main loop primary coolant isolation valves must close in order for the CACS to cool the core.

The CACS is designed to the following specific performance criteria, which are appropriate to such an engineered safety system:

1. The CACS is capable of providing adequate cooling for all credible accident events in all plant operating modes.

2. In all events this capability includes assumption of either a single active failure disabling one CACS loop or failure of one main loop isolation valve in the full open position. (The former establishes that there must be three independent CACS loops, since a failure in one CACS loop is a potential initiating event for a pressurized CACS core cooldown and a second CACS loop would be lost to the single failure criterion.)

3. The cooling function of the CACS is completely independent of the main primary coolant loops and the normal core heat removal path.

4. The CACS will be operable from either on-site or off-site power, and it will sustain a loss of off-site power at any time during a cooldown following an initiating event.

5. The design accounts for most extreme environmental conditions at the time of CACS operation, including effects of an SSE.

6. Sufficient redundancy, multiplicity, and diversity will be included in the CACS design to assure that the probability of occurrence of combined permanent loss of main loop core cooling and failure of the CACS to operate as required will be less than 10^{-4} per reactor-year.

The identification of credible accident sequences and the superposition of the above criteria related to coincident failures and occurrences lead to selection of three design basis transients for the CACS. All subsystems and components of the CACS are designed and physically sized so that the CACS will cool the core in accordance with these transients while maintaining significant margin on appropriate safety limits for all plant components, such as core, PCRV, and reactor internal temperature and pressure limits. All analyses demonstrating these margins account conservatively for uncertainties and allowances for variations in performance parameters. Other steady-state or transient operations impose less severe requirements on the CACS. The three transients are described below:

1. Loss of main loop cooling. This transient is the cooldown of the reactor core with one CACS loop following ingress of a CAHE inventory of water with the primary coolant pressure below the PCPV relief valve setpoint value. In this transient the primary coolant flow through the core is maintained at a level 10% greater than the value required to suppress any reverse flow in a core region, which might occur owing to the buoyancy of heated helium. In this transient the CACS is subjected to the greatest heat duty.

2. Depressurized cooldown with helium. For this transient the reactor core is cooled with two CACS loops. The primary coolant inventory is initially depressurized to equilibrium pressure with the containment volume, and all flow is assumed to be out of the

reactor vessel. In this transient the lower thermal barrier temperature is at least 38°C (100°F) below the safety limit. For this transient the auxiliary circulator must deliver maximum volumetric flow.

3. Design basis depressurization accident (DBDA). In the DBDA the reactor core is cooled with two CACS loops. The primary coolant inventory is initially depressurized to equilibrium pressure with the containment volume, and it is postulated that the vessel and containment volume communicate through a breach between the reactor inlet plenum and the containment. Helium and air mix through convection via that breach. In this transient the lower thermal barrier temperature is at least 38°C (100°F) below the safety limit. The CACS power requirements are greatest in this transient.

2.20. AUXILIARY CIRCULATOR DESIGN (6032280200)

2.20.1. Scope

The scope of this task covers the initial conceptual design of the auxiliary circulator, the auxiliary circulator service system, and the auxiliary loop isolation valves, which are all components of the plant CACS.

2.20.2. Discussion

Based on the preliminary CACS operating parameters, the basic configuration of the auxiliary circulator was confirmed. Component descriptions as detailed below were established during this reporting period.

2.20.2.1. Compressor, Motor, and Housing. The auxiliary circulator is a vertically oriented axial flow compressor, driven with an integral electric motor. Parts of the auxiliary circulator which retain reactor coolant pressure are classified as Code Class 1 nuclear vessels. The design and

material specifications for pressure parts and direct attachments thereto (including welding filler material) are in accordance with the requirements of Section III of the ASME Code for the designated material. Fabrication methods, procedures, and practices used in the manufacturing of these parts meet the requirements of the ASME Code, Section III for Class 1 nuclear vessels. The circulator support structure adjacent to or associated with the primary closure is provided with stops and aligning features to ensure proper installation.

The circulator and its motor are removable using remote handling methods. The compressor, motor, and housing general arrangement is shown in Fig. 2-67. The compressor tip diameter is 1199 mm (47.2 in.).

The circulator drive motor is a 6711-kW (900-hp), 3600-rpm, four-pole squirrel-cage induction motor. In order to meet the wide range of required operating conditions, the electric motor is driven by a variable-frequency speed controller to a maximum frequency of 120 Hz. The motor stator and rotor are of typical standard vertical motor construction. The motor operates in a cool helium environment at the same pressure as the primary coolant system.

The rotor is supported on oil-lubricated rolling element bearings that carry the axial and radial loads; the bearings are located on each side of the motor rotor and the compressor is overhung. Each bearing is mounted on the shaft through an inverted U-shaped extension, and the oil is prevented from escaping down the shaft by a stationary dam. A cross-sectional drawing of the auxiliary circulator motor is shown in Fig. 2-68. Oil vapor is prevented from entering the primary coolant loop by means of a labyrinth seal buffered by purified helium flow. Purified helium is introduced into the center of the labyrinth and flows out each end. The helium that flows down the shaft enters the primary coolant system. The helium that flows up the shaft mixes with oil vapor in the motor compartment and is then routed to external oil separation equipment.

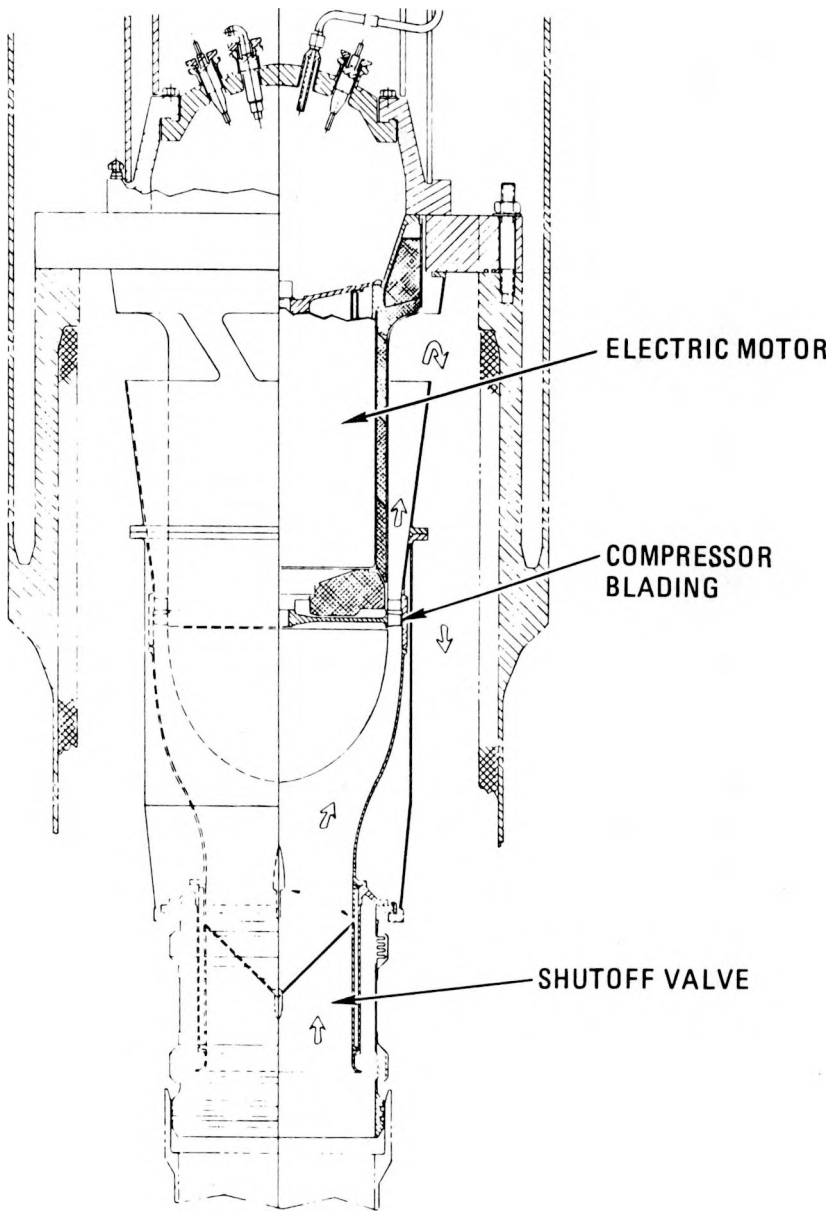

Fig. 2-67. Cross section through auxiliary circulator

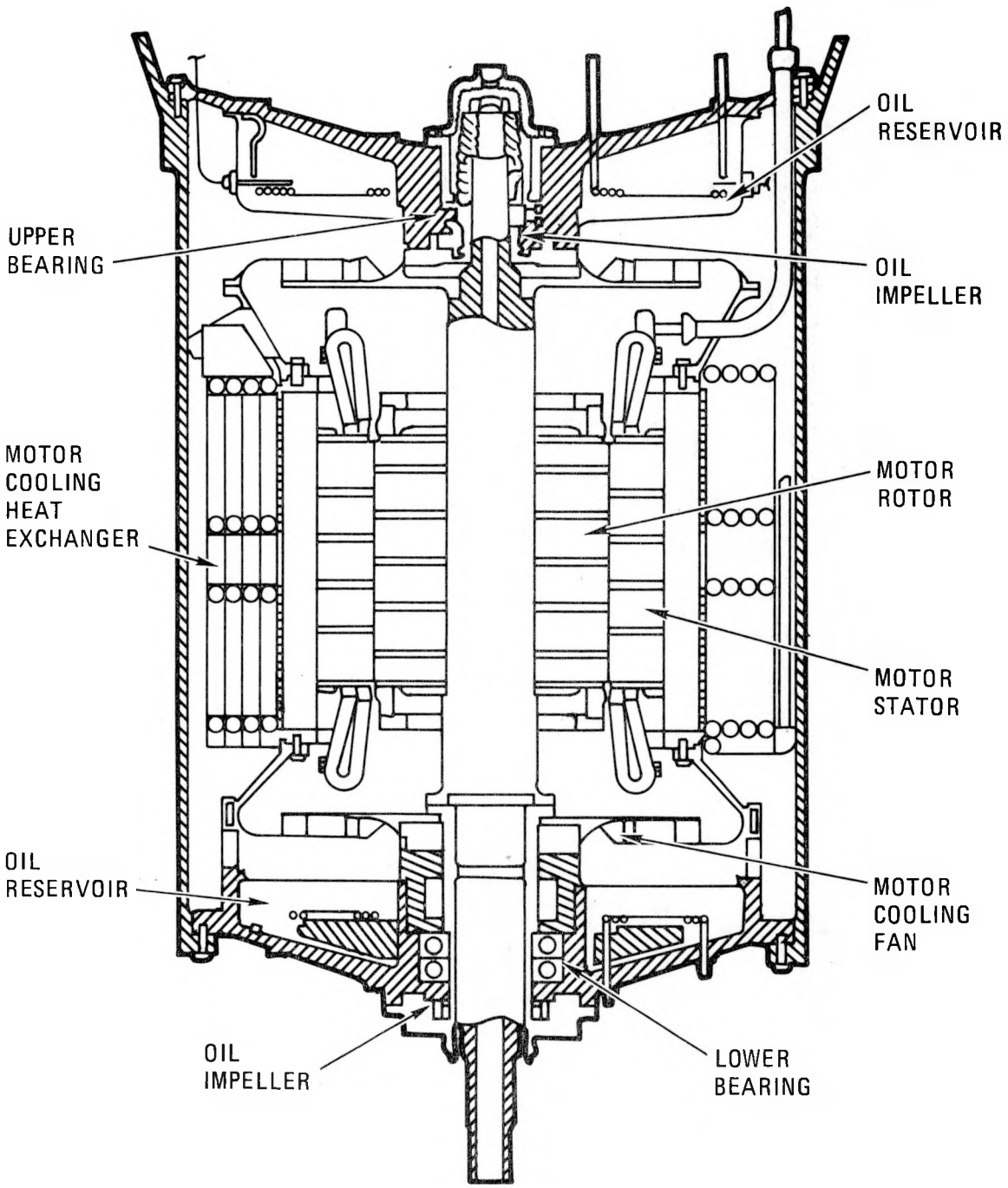

Fig. 2-68. Auxiliary circulator drive motor

Motor cooling is performed by circulating cool helium through the rotor and stator windings with shaft-mounted cooling fans. Heat is removed from the cooling circuit with an internal helim-to-water heat exchanger. The cooling water is also used to cool the housing and bearing oil reservoirs. The cooling arrangement is shown in Fig. 2-68.

The auxiliary circulator motor is designed in accordance with applicable IEEE standards for Class 1E components.

2.20.2.2. Auxiliary Loop Isolation Valve. The function of this valve is to limit backflow through an auxiliary coolant loop when the associated circulator is shut down. The valve is installed in the vertical duct directly below the compressor. Coolant leakage flow is vertically downward through the closed valve during normal plant operation or when other CACS loops are operating.

The valve consists of two semi-elliptical plates which are at an angle of 0.78 rad (45 deg) to the vertical centerline [1.57 rad (90 deg) to each other] when the valve is closed and at a small angle to the duct centerline when the valve is fully open. Closure of the valve is effected by gravity and pressure forces generated by reverse flow from the operating circulators.

When the valve is closed, the valve plates rest on support struts inclined at 0.78 rad (45 deg), which permits the use of small thin valve plates that are still capable of withstanding the pressure differential produced by the operating circulators. To ensure that the valve plates will open under all circumstances, the rubbing and touching parts of the valve are hard-faced with materials that have been shown to exhibit a low coefficient of friction in hot helium. Opening of the valve automatically results from operation of the associated auxiliary loop when sufficient aerodynamic forces have been generated by the auxiliary circulator. The flow generated by the auxiliary circulator is sufficient to maintain the lightweight valve plates in the open position during all operating conditions. An override

mechanism to assist opening and closing the valve is included in the design.

The valve may be removed from the penetration by remote handling methods following removal of the auxiliary circulator.

2.20.2.3. Auxiliary Circulator Services. The auxiliary circulator services provide the following:

1. A supply of purified buffer helium for preventing inleakage of motor bearing lubricant to the primary coolant system or leakage of primary coolant into the motor casing.

2. Removal of oil vapor carried over in purge helium from the auxiliary circulators.

3. Removal and replacement of motor bearing lubricant when an auxiliary circulator is shut down.

The circulator services to all CACS loops are provided by components mounted on a single, separate module.

Buffer Helium and Oil Adsorption

During reactor plant operation, buffer helium is supplied to the motor cavity of each circulator at a flow rate of about 2.8×10^{-3} m^3/s (6 acfm). The flow rate will be controlled at this value regardless of fluctuations in the primary coolant system pressure. The helium purge is withdrawn from the two bearing-oil cavities in each motor and purged at a controlled flow rate of 2.13×10^{-3} m^3/s (4.5 acfm) (at approximately reactor pressure). The control system thus adjusts the helium flow to effect a split so that approximately one quarter of the flow leaks into the primary coolant system and the remaining three quarters leaks out through the vents of the motor bearing-oil cavities. This controlled leakage of buffer helium also prevents leakage of lubricating oil vapor into the primary coolant system.

Helium purging from the motor bearing-oil cavities is piped first to the oil adsorber and from there to the helium purification system. The module incorporates two adsorber columns, each of which contains a non-regenerable bed of adsorbent. Each column is rated to pass the combined helium purge from the auxiliary circulators and is designed to permit adsorbent removal and replacement over the complete range of system operating pressures during auxiliary circulator standby or operating modes. The purge helium is supplemented by makeup at the helium compressor section; following compression, it is piped to the auxiliary circulator buffer helium inlet cavity for reuse. Auxiliary circulator functional capability is not affected by the failure or unavailability of the oil adsorber.

The auxiliary circulator is designed to operate continuously without buffer helium. The use of buffer helium improves the cleanliness and maintainability of the system and auxiliary circulator internals in accordance with the 40-yr design life objective.

Motor Lubricant

The bearing-oil reservoirs within the circulator assembly are normally isolated from the oil service system. Oil is maintained within the reservoirs except during the removal and replacement servicing operation. Removal and replacement are achieved by helium pressure displacement. A pressure differential of 170 kPa (10 psi) is required to overcome line friction losses for removal or replacement of the oil. Since the reactor primary coolant is the pressure source for oil removal, this operation must be performed at reactor primary coolant pressures of 0.17 MPa (10 psig) or greater. Bearing-oil replacement can be accomplished at any pressure within the reactor operating range. The bearing-oil replacement and removal tanks have a capacity of 0.045 m^3 (10 gal) and are designed for a pressure of 8.37 MPa at 149°C (1200 psig at 300°F). A predetermined quantity of oil is supplied for each bearing cavity. The replacement interval will be determined later, based on the amount of oil removed by the continual helium purge within the motor cavity and the radiation tolerance capability of the oil.

Instrumentation and Controls

Each auxiliary circulator service system is instrumented to provide an indication in the control room of buffer helium flow to the auxiliary circulator motor. Low buffer helium flow is alarmed in the control room. Instrumentation is provided to show an indication in the control room of the flow in the buffer helium/oil vapor return line from the auxiliary circulator motor. High or low flow in this line is alarmed in the control room.

Motor and Bearing Lubricant Cooling

The cooling water for the motor, motor housing, and motor bearing lubricant reservoirs is supplied separately to each auxiliary circulator from the reactor plant cooling water system and is not part of the auxiliary circulator service system.

2.21. CORE AUXILIARY HEAT EXCHANGER (CAHE) (6032280301)

2.21.1. Scope

The scope of this task covers the conceptual design and analysis of the CAHE in support of the Design Decision Package.

2.21.2. Discussion

Significant design progress was made in the CAHE design during this reporting period, resulting in the changes shown in Fig. 2-69.

2.21.2.1. Enthalpy Margin. In the past there has been some concern regarding the adequacy of the enthalpy margin (the additional heat required to initiate boiling). Because the unit has a very small water-side pressure drop, minor differences in tube circuits would affect water flow rates; a lower flow rate in a tube circuit could initiate boiling. Should boiling begin, the pressure drop in that particular circuit would rise slightly; because normal pressure drop is low, the slight increase reduces flow rate

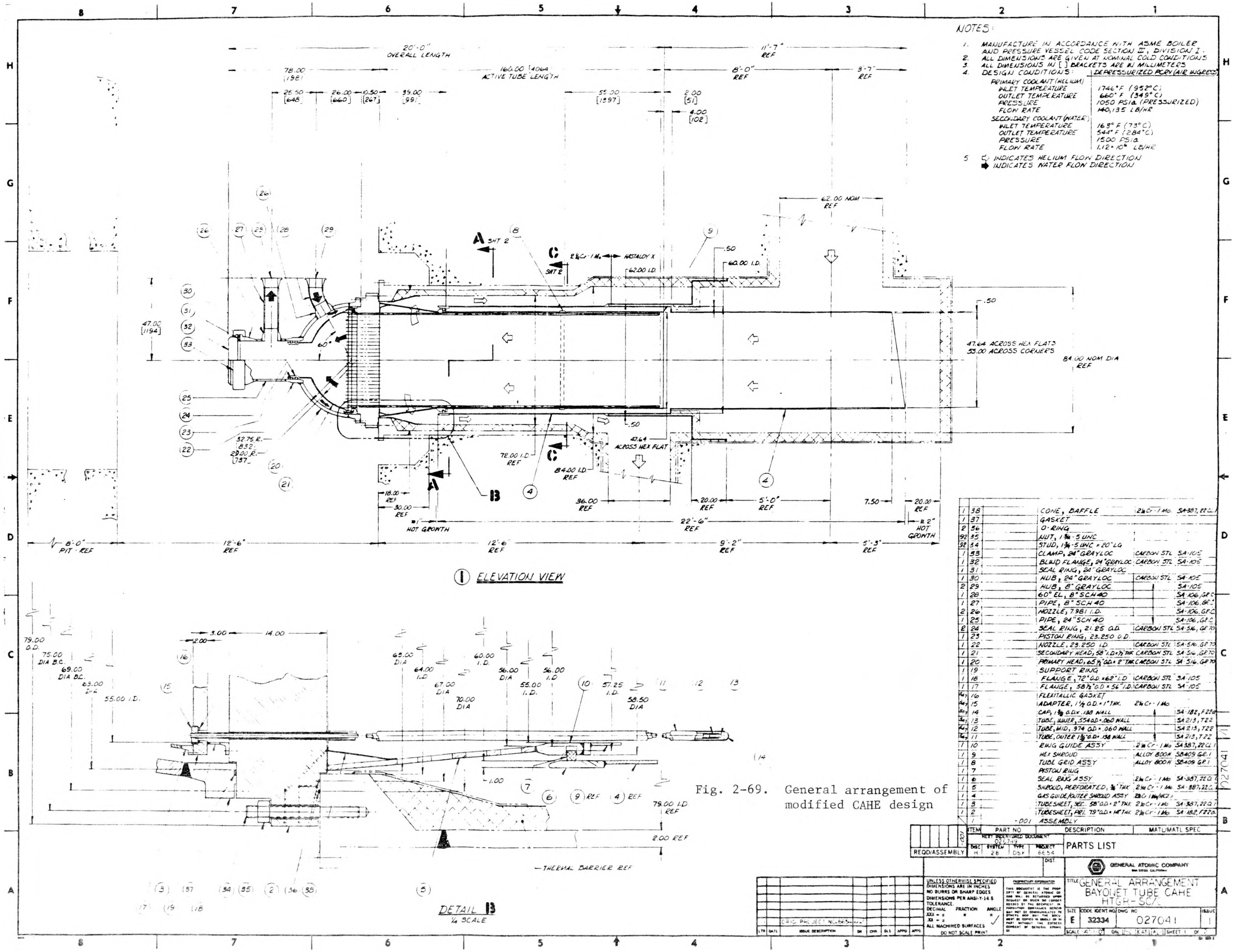

Fig. 2-69. General arrangement of modified CAHE design

further, until the tube boils dry. Boiling thus occurs in a non-stable mode.

A dual approach is being used to alleviate these concerns. First, the water mass flow has been increased while inlet temperature is maintained, thus lowering outlet temperature from 286°C (547°F) to 262°C (504°F) and increasing enthalpy margin. The increase in mass flow also increases pressure drop. Second, the annulus between sheath and bayonet tubes has been reduced from 2.5 to 0.8 mm (0.10 to 0.03 in.), also increasing pressure drop.

As a result of the increased enthalpy margin, no reasonable combination of events, including partial tube inlet blockage (up to 70%), gas-and water-side flow maldistribution (limited as shown by flow tests), and hot streaks [maximum 38°C (100°F)] will initiate boiling. Also, because of the increase in water-side ΔP from 70 to 180 kPa (10 to 26 psi), stability has been increased to a point that should boiling occur, the tube would boil in a stable mode; because the tube would not boil dry, the high heat transfer rate from the water/steam mixture would maintain acceptable tube temperatures.

The effect of these modifications is to slightly decrease the CAHE surface and significantly increase the air blast heat exchanger surface. The change in water mass flow requires a larger pump and larger piping. The total cost increase of these design changes for the plant is about $\$1 \times 10^6$.

2.21.2.2. Waterbox and Tubesheet Modifications. The waterbox and tubesheet have been modified to facilitate installation and ISI. The tubesheet is now bolted to the liner and the waterbox is bolted to the tubesheet as shown in Fig. 2-69; previously they were welded. The new arrangement requires a minimum amount of headroom below the PCRV for installation--just the total of the tube bundle and tubesheet. Installation is relatively quick and easy.

The waterbox can now be completely removed, allowing excellent access to both high-pressure and low-pressure tubesheets. It is not necessary to

remove the waterbox to examine the main primary or secondary pressure boundary welds. Also, the tubes near the center of the bundle may be examined by removing the man-access flange rather than removing the waterbox.

The seal between the tubesheet and liner is expected to be double metallic O-rings, with a "telltale" between the O-rings. In the event the "telltale" detects a leak through the inner O-rings, the space between the O-rings will be pressurized with purified helium. The seal between the water bonnet and tubesheet will be a single spiral wound gasket.

The impact of these changes is that fabrication costs are increased and installation costs are decreased. There is probably little net change.

2.21.2.3. Modifications Based on Results from Air Flow Test. A half-scale CAHE air flow test has been substantially completed. Test results indicate that best gas-side flow distribution is achieved by extending the shroud up to the top of the cross duct, forcing the gas to flow around and over the shroud as it enters the unit. A maximum gas-side flow maldistribution of 1.2:1 appears achievable with this configuration with almost no increase in pressure drop.

Test results for the outlet screen indicate the screen height can be reduced from 914 to 610 mm (36 to 24 in.), improving flow distribution without significantly increasing pressure drop.

An unexpected unstable flow condition at the inlet indicated a need for a partial splitter on the outside of the shroud at the top and 3.14 rad (180 deg) from the inlet duct. This has been incorporated.

2.21.2.4. New System Conditions. The latest optimized plant conditions* (Table 2-31) have had a favorable impact on the CAHE. The higher gas outlet temperature has raised the log mean temperature difference at the cold end

*Changes in water mass flow and temperature to increase enthalpy margin have also been incorporated.

TABLE 2-31
CAHE SYSTEM CONDITIONS[a]

	Old			New[b]		
		Depressurized			Depressurized	
	Pressurized	Pure He	Air Ingress	Pressurized	Pure He	Air Ingress
Gas Side						
Flow rate [kg/s (lb/hr)]	35.9 (285,029)	7.46 (59,205)	17.78 (141,164)	33.94 (269,457)	8.47 (67,224)	18.2 (144,463)
Inlet temperature [°C (°F)]	860 (1580)	952 (1746)	952 (1746)	860 (1580)	952 (1746)	952 (1746)
Outlet temperature [°C (°F)	362 (684)	306 (588)	262 (504)	409 (768)	351 (664)	319 (606)
Water Side						
Flow rate [kg/s (lb/hr)]	141.4 (1.122×10^6)	141.4 (1.122×10^6)	141.4 (1.122×10^6)	172.36 (1.36×10^6)	186.25 (1.478×10^6)	187.1 (1.478×10^6)
Inlet temperature [°C (°F)]	165 (329)	79 (174)	74 (162	176 (349)	91 (196)	83 (181)
Outlet temperature [°C (°F)]	284 (543)	122 (252)	116 (241)	262 (504)	124 (255)	112 (234)

[a] Gas inlet temperature is unchanged.

[b] Not yet confirmed.

and made the unit more effective, thus reducing surface requirements. The number of tubes has been reduced from 721 to 547, with slight reductions in unit length and diameter.

2.21.2.5. New Grid Concept. A new grid concept has been developed (Fig. 2-70) for the CAHE. This concept consists of a tri-axis egg-crate grid with each tube supported on three sides. The concept can be considered to be an endless truss, providing great strength for very small web thickness. As a result of thin webs and minimal tube contact, the concept has very low blockage and pressure drop; the web thickness used is 0.8 mm (0.03 in.), which provides 17.3% blockage. The calculated blockage is

$$B = \frac{3Pt}{0.866\ P^2 - \pi D^2/4} \quad ,$$

where t = thickness = 1.5 mm (0.06 in.),
P = pitch = 52 mm (2.05 in.),
D = tube O.D. = 35 mm (1.38 in.).

Manufacturing cost is expected to be lower than for most systems previously considered. The pressure drop is also low, and in fact a second grid can be added without exceeding pressure drop limits.

2.22. CACS CONTROL AND INSTRUMENTATION (6032280400)

2.22.1. Scope

The scope of the control, instrumentation, and electrical engineering effort during this reporting period was (1) to provide NSSS input for the BOPR document on the CACS controls and the CACWS and (2) to prepare the control, instrumentation, and electrical portion of the system description for the CACS.

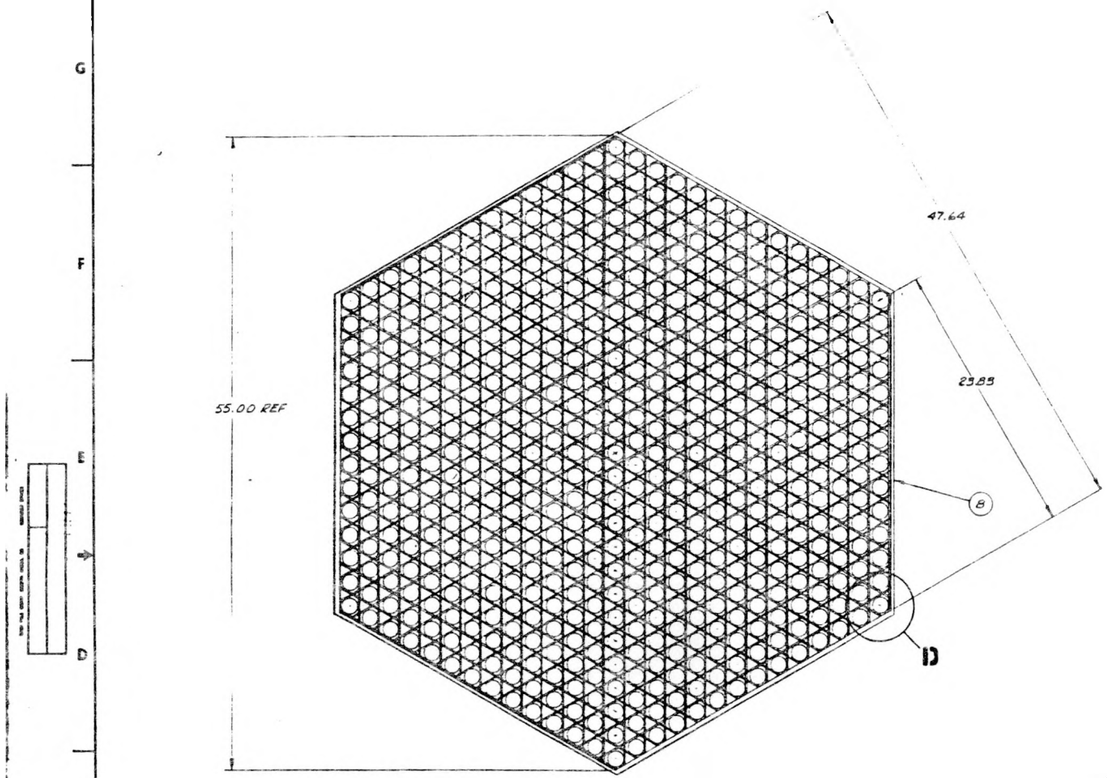

SECTION **C-C**
1/4 SCALE
INNER HEX SHROUD (ITEM 9) NOT SHOWN THIS VIEW

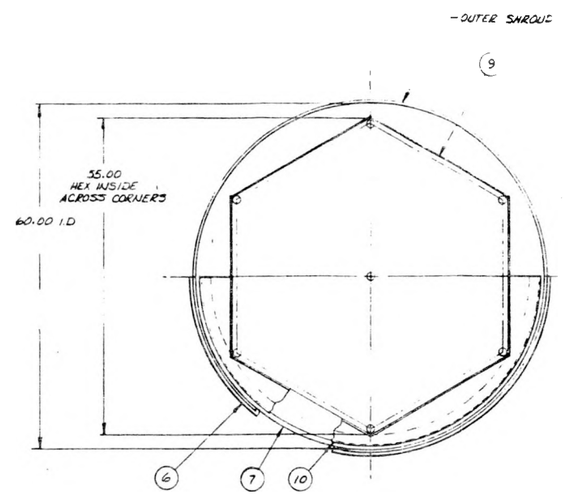

SECTION **A-A**
1/8 SCALE

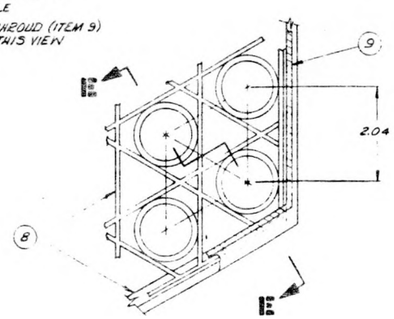

DETAIL **D**
FULL SCALE

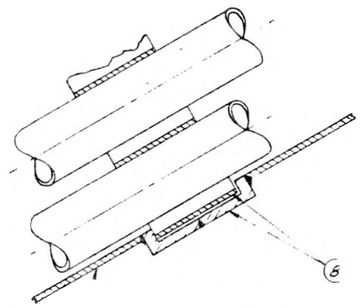

SECTION **E-E**

Fig. 2-70. New CAHE grid concept

ITEM	PART NO	DESCRIPTION	MATL/MATL SPEC
REQD/ASSEMBLY		PARTS LIST	

GENERAL ATOMIC COMPANY

TITLE GENERAL ARRANGEMENT BAYONET TUBE CAHE HTGR SCR

SIZE E | CODE IDENT NO. 32334 | DWG NO. 027041 | ISSUE A

SCALE NONE | QA | SHEET 2 OF 2

UNLESS OTHERWISE SPECIFIED DIMENSIONS ARE IN INCHES
NO BURRS OR SHARP EDGES
DIMENSIONS PER ANSI-Y-14.5
TOLERANCE
DECIMAL FRACTION ANGLE
XX ± ± ±
XXX ± ± ±
ALL MACHINED SURFACES
DO NOT SCALE PRINT

027041 11

2.22.2. Discussion

The plant layout criteria for the CACS controls portion of the BOPR manual was reviewed and updated. This effort included a review of the space requirements in the main control room and the physical dimensions and structural configuration of the control board. The CACWS was also reviewed, and the interfaces between the CACWS, the CACS controls, and other BOP systems were verified.

The control, instrumentation, and electrical portions of the CACS (NSSS) system description were prepared for each phase of CACS operation: initiation of the CACS by the plant protection system, warmup of the CAHE water loop to operating temperature and operation of the CACWS sequencing controller, starting of the auxiliary helium circulator, and subsequent cooling of the core by the combined CACWS, CAHE, and CACS control systems. This system description includes a discussion of the operation of the control system during each of these operational phases of the CACS and addresses the parameters displayed in the main control room for control of the CACS. Also discussed are those parameters, e.g., auxiliary circulator speed and CAHE water temperature, which are monitored and displayed in the main control room and in the data acquisition and processing system as part of the safety-related display instrumentation.

2.23. SAFETY-RELATED CONTROL AND INSTRUMENTATION (6032320100)

2.23.1. Scope

The scope of work for the safety-related control and instrumentation (C&I) system during this reporting period included support of the HTGR-SC/C baseline review meetings, resolution of critical issues, preparation of safety-related C&I requirements input to the BOPR document, and preparation of the safety-related C&I system description document, cost data, and instrument block diagrams.

2.23.2. Discussion

Previously the safety-related C&I system was called the plant protection system. This tended to cause confusion since "safety systems," "safety-related systems," and "systems important to safety" were included in one large system and there was no clear administrative separation of safety systems and non-safety systems. The addition of more safety-related systems and more systems important to safety to meet post Three Mile Island requirements led to further confusion. To resolve this difficulty, a new system organizational structure was formed. The safety-related C&I system is now organized into three functional systems: the plant protection system, the safety-related moisture monitor/detection equipment, and the special safety-related systems.

The plant protection system includes all the equipment from and including process sensors to the input terminal of actuation devices that directly control equipment required to protect the public health and safety by functioning to mitigate the consequences of design basis events. All plant protection system equipment is considered safety system equipment, and electrical equipment included in the system is Class 1E. The plant protection system is designed to satisfy the criteria of IEEE Standard 603-1980, "Criteria for Safety Systems for Nuclear Power Generating Stations."

The safety-related moisture monitor/detection equipment is by definition and function part of the plant protection system. However, owing to the unique characteristics of the safety-related moisture monitor/detection equipment, which includes a significant amount of auxiliary supporting features, it is treated as a separate system.

The special safety-related systems include all other safety-related C&I systems that are not safety systems but perform functions important to safety. These include systems that provide safety-related preventive features (e.g., operational interlocks), safety-related auxiliary control (e.g., remote shutdown area equipment), and safety-related monitoring (e.g., safety-related displays, post-accident monitoring, etc.). Because of their

various functions important to safety, the special safety-related systems are required to meet various industry and NRC requirements applicable to these specific functions.

Investigation of several critical issues continued during this reporting period. The addition of an auxiliary feedwater supply pump in the HTGR-SC/C design to improve feedwater availability and to enhance overall plant safety may now require a delay in the plant protection system initiation of the CACS at the detection of loss of feedwater flow. This delay may be required to allow time for the auxiliary feedwater pump to reestablish 15% feedwater flow. The impact of this delay on the plant protection system design is now under investigation, and a detailed design basis analysis will need to be performed before the delay can be incorporated in the plant protection system design.

The safety-related C&I system description document has been updated to include the present state of the design and to reflect the organization of the overall system into three component systems. A brief summary of the functional description of safty-related C&I systems is given below.

2.23.2.1. Plant Protection System. The plant protection system senses process variables to detect abnormal plant conditions and provides inputs to actuation devices that directly control equipment required to mitigate the consequences of design basis events to protect the public health and safety. The plant protection system provides these functions through the subsystems described below.

Reactor Trip System

This system limits the damage to fuel coatings and preserves the integrity of the primary coolant barrier by initiating a rapid reduction in reactor power following reactivity excursions, loss of adequate core cooling, and other events requiring a rapid reactor shutdown.

Steam Generator Isolation and Dump System

This system limits the quantity of water that can leak into the PCRV owing to a steam generator leak in order to limit damage to the fuel, to protect reactor vessel internals, and to protect the PCRV pressure boundary. This system is initiated by an automatic actuation signal from the safety-related moisture monitor/detection equipment or by a manual actuation signal. Upon initiation, the leaking steam generator is isolated and dumped. Steam from the steam generator dump is vented to the atmosphere until the dump is terminated by an additional plant protection system trip input to this subsystem.

Main Loop Shutdown System

This system limits the temperatures of the steam generator tubes in each of four main coolant loops to protect the primary coolant boundary following mismatches of the primary and secondary coolant flows.

CACS Initiation System

This system limits the damage to fuel coatings and preserves the integrity of the primary coolant barrier by initiating auxiliary core cooling following the loss of main loop cooling. Sequencing BOP components of the CACS is accomplished by the BOP-supplied engineered safety features actuation system.

CAHE Isolation System

This system limits the quantity of water that can leak into the PCRV due to a CAHE leak during CACS operation in order to limit damage to the fuel, to protect reactor vessel internals, and to protect the PCRV pressure boundary. This system also mitigates the consequences of primary coolant leaking into the CAHE secondary coolant due to a CAHE leak during CACS standby conditions. Upon initiation, the leaking CAHE is isolated.

The safety-parameter display system (SPDS) has been moved from the plant control system to the special safety-related system. The SPDS function is to assist control room personnel in evaluating the safety status of the plant and in detecting abnormal operating conditions. The SPDS is a continuous, dedicated display of a minimum set of plant parameters or derived variables from which the plant safety status can be assessed during normal operation, during shutdown, and during accident and post-accident conditions. Because of the flexibility required of the SPDS, a color cathode ray tube (CRT) is the display component of choice for the SPDS. At least one commercially available color CRT model which can meet the seismic qualification requirements of NRC Regulatory Guide 1.97 and IEEE Standard 497-1981 has been identified.

The present plant protection system conceptual design uses a 2-out-of-3 logic design. It has been suggested that a 2-out-of-4 logic design be considered to provide better availability and more on-line testing flexibility. The possible benefits of a 2-out-of-4 plant protection system logic design versus the increased costs of the fourth safety channel, the fourth Class 1E power source, and the additional division of plant protection system cabling are being studied.

The safety-related C&I system has major interfaces with the BOP for Class 1E power sources, control room layout, remote shutdown area layout, containment building isolation actuation devices, the CACS start sequencer, and other safety system actuation devices and actuated equipment. The BOP interfaces at this point in the conceptual design are as follows:

1. Plant protection system main superheater outlet valves.

2. Plant protection system main steam temperature sensor thermowells.

3. Plant protection system main steam pressure sensor taps.

4. Non-Class 1E ac power for control rod holding power.

5. Class 1E ac uninterruptible power system (UPS) for plant protection system channels.

6. Plant protection system feedwater block and trim valves.

7. Plant protection system steam generator atmospheric dump valves.

8. Plant protection system (NSS supplied) feedwater flow sensors.

8. Main control room and remote shutdown area to house safety-related C&I equipment.

10. Plant protection system CACS start sequencer.

11. Class 1E 480-Vac UPS for safety-related moisture monitor/ detection equipment.

12. Area in reactor containment building to house safety-related moisture monitor/detection equipment.

Containment Isolation System

This system limits the pressure buildup in the containment due to secondary stem steam leaks in order to preserve the integrity of the containment building. The containment isolation system also limits release of radioactivity from the containment if the primary coolant boundary should fail. Sequencing the isolation of the containment is accomplished by the BOP-supplied engineered safeguards features actuation system (ESFAS).

2.23.2.2. Safety-Related Moisture Monitor/Detection Equipment.

Main Loops (Moisture Monitoring)

This system samples the primary coolant from each main loop, measures high moisture content in each loop due to inleakage, and provides signals to

(1) the steam generator isolation and dump system for isolation and dump of the appropriate steam generator and (2) the reactor trip system to trip the reactor on detection of high moisture level.

CACS Loops (Moisture Detection)*

This system detects conditions which indicate a leak between the CACWS and the primary coolant (helium) system when auxiliary cooling water pressure is lower than that of the PCRV helium (during CACS standby) or higher than that of the PCRV helium (CACS pressurized cooldown, CACS cooling during depressurized conditions, or at those times when the CACS is being tested).

2.23.2.2. Special Safety-Related Systems. Special safety-related systems generally include safety-related preventive features, safety-related systems that monitor plant protection system status, safety-related systems that monitor the safe operation of the plant under normal operating and accident conditions, and safety-related controls that allow control of reactor shutdown and cooling from a remote shutdown area.

The functions of the special safety-related systems are described below.

PCRV Pressure Relief Block Valve Closure Interlock

This special safety-related system prevents the simultaneous closure of both PCRV relief block valves to ensure that at least one PCRV relief valve is always available to protect the PCRV and primary coolant boundary.

*Moisture detection in the CACS loops is currently specified as a plant protection system requirement. Further analysis is required to determine whether this conservative position is necessary.

Control Rod Bank Withdrawal Interlock

This special safety-related system prevents the simultaneous withdrawal of multiple control rod banks in order to limit excessive reactivity addition rates.

Safety-Related Display Instrumentation (SRDI)

The SRDI displays all plant protection system channel readouts and status indications including status indications of plant protection system actuation devices and actuated equipment. The SRDI also includes status indications of plant preventive features and displays of plant parameters that are important to safety. In general the SRDI provides those displays which enable the reactor operator to perform equipment surveillance and plant condition monitoring necessary to determine that the plant is operating within a safe operating envelope during normal operations, that the plant is safely shut down, and that core cooling and fission product barrier integrity is maintained during normal shutdown and following the occurrence of a design basis event (DBE). The SRDI provides information that may allow the reactor operator to take manual actions which are important to safety, but the plant protection system and plant design is such that there are no manually controlled actions necessary to activate the plant protection system and perform the plant protection system safety functions.

Post-Accident Monitoring (PAM) Instrumentation

The function of the PAM instrumentation is to indicate plant variables that are required by the control room operating personnel during accident situations to (1) provide information required to permit the operator to take preplanned manual actions to accomplish safe plant shutdown; (2) determine whether reactor trip, engineered safety feature systems, and other systems important to safety are performing their intended functons (i.e., reactivity control, core cooling, maintaining reactor coolant system integrity, and maintaining containment integrity); and (3) provide information to the operators that will enable them to determine the potential for causing a

gross breach of the barriers to radioactivity release and to determine if a gross breach of a barrier has occurred. In addition to the above, the PAM instrumentation indicates plant variables that provide information on the operation of plant safety systems and other systems important to safety that are required by the control room operating personnel during an accident to (1) furnish data regarding the operation of plant systems in order that the operator can make appropriate decisions as to their use and (2) provide information regarding the release of radioactive materials to allow for early indication of the need to initiate action necessary to protect the public and to allow estimation of the magnitude of any impending threat. The PAM instrumentation includes a subset of SRDI parameters plus additional parameters such as site radiological or site meteorological parameters. The PAM function is provided by redundant computer-driven CRT displays. These displays are also provided for display at the Technical Support Center and other Emergency Response Facilities.

Safety Parameter Display System (SPDS)

The SPDS function is to assist control room personnel in evaluating the safety status of the plant and in detecting abnormal operating conditions. The SPDS is a continuous, dedicated display of a minimum set of plant parameters or derived variables from which the plant safety status can be assessed during normal operation, during shutdown, and during accident and post-accident conditions. The SPDS parameters are a subset of or are derived from the SRDI sensed parameters. The SPDS function is provided by redundant microprocessor-based CRT displays. The PAM system can also display the SPDS format.

Remote Shutdown Area Equipment

The remote shutdown area provides an area outside the main control room where special safety-related systems are located to permit a reactor operator to achieve and maintain a safe plant shutdown in the event that the main control room becomes uninhabitable. Special safety-related systems located in the remote shutdown area provide the capability to initiate reactor trip,

to establish and maintain core cooling using safety-system-actuated equipment, and to monitor that the former two functions have been achieved.

Core Performance Instrumentation (CPI)

The CPI provides the capability of monitoring that the plant Limiting Conditions for Operation (LCO's) are met. The actual integrated CPI function is provided by the plant data acquisition and process (DAP) system. The special safety-related systems provide, through interfaces, a large portion of the plant parameters necessary for the plant DAP to provide the CPI function.

Initial design cost input data for the safety-related C&I system have been developed. Cost data from the previous design have been revised to reflect the increased costs to qualify Class 1E safety systems and some special safety-related system electrical equipment to IEEE Standard 323-974 and NUREG-0588 requirements and the increased costs of additional safety-related systems to meet NRC Regulatory Guide 1.97 and NUREG-0696 requirements. Also, the increased cost of a CAHE leak detection system has been accounted for. The cost of microprocessor-based and computer-based systems has been reduced to reflect recent technological advances.

Instrument block diagrams to reflect the present plant protection system conceptual design are under development. The outcome of the study of 2-out-of-3 plant protection system versus 2-out-of-4 plant protection system logic may require extensive later revisions in the system instrument block diagrams if 2-out-of-4 logic is required as a design change.

2.24. PLANT CONTROL SYSTEM (6032330100)

2.24.1. Scope

The scope of work for the plant control system during this reporting period included support of the HTGR-SC/C baseline review meetings, preparation of the plant control system requirements input to the BOPR document,

and preparation of the plant control system description document, cost data, and instrument block diagrams.

2.24.2. Discussion

The plant control system is organized into two functional systems: the plant control system and the main control room

The plant control system is an integrated system that includes the instrumentation and equipment associated with the monitoring and control of the NSS. Included in this system are the overall plant control loops that maintain rated steam conditions during normal operation and systems that provide protection for certain incidents that could otherwise result in the need for plant protection system action.

The main control room consists of the control room consoles and boards. This system also defines some general instrumentation and control equipment requirements for the plant control system, such as human factors, color coding, equipment layout, and enclosure dimensions.

The plant control system has major interfaces with the BOP for non-Class IE power sources, control room layout, HVAC system capacity, process sensors, and turbine-generator and process steam controllers. The BOP interfaces at this point in the conceptual design are as follows:

1. An area in the plant control building to house plant control system signal conditioning equipment.

2. Main steam temperature sensors and thermowells (two per loop).

3. Feedwater flow sensors (each loop).

4. Turbine-generator and process steam controllers.

5. Non-Class 1E, 120 Vac, uninterruptible instrumentation and control power.

6. A plant control building HVAC system to remove heat generated by the instrumentation and control system.

The plant control system description document has been updated to include the present state of the design. A brief summary of the functional description of the plant control system is given below.

Plant Control System

This system provides for safe plant operation and high plant availability. The system is designed to regulate reactor power and to control the pressure and temperature of steam delivered to the turbine-generators, to the process steam user, or to the bypass system during startup, shutdown, or standby operation. The system has the capability of automatic load following over a range of rates of change.

In addition to accommodating plant system perturbations resulting from normal load changes, the plant control system handles conditions imposed on the system during loop trip, reactor trip, turbine-generator trip, boiler feed-pump loss, electrical load rejection, or loss of process steam demand. Under these conditions adjustments are made to reactor power, feedwater flow, and helium flow at predetermined rates to minimize temperature transients imposed on the steam generator and reactor components. The plant control system receives reactor trip signals from the plant protection system and produces an automatic transition to the shutdown cooling mode, initiated by ramping feedwater flow to a predetermined level and by subsequent shutoff of one of the feedwater pumps.

An additional function of the plant control system is to provide protection of major equipment components, protection against certain incidents that could result in plant control system action, and protection against

prolonged plant unavailability. This function includes certain actions required as a result of failure of an active NSSS component. Failure of this function will not jeopardize public health or safety.

A simplified overview diagram of the plant control system is shown in Fig. 2-71.

Main Control Room

The main control room provides the plant with continuous power production controls operated from a centralized control and monitoring station. The design provides for a control operator's console that meets the above requirement, together with associated boards and consoles for control and monitoring of other plant systems. The main control room, in conjunction with the other portions of the NSS instrumentation and control system, enables operators to monitor and control the NSS during normal, upset, and emergency conditions. The system is designed to provide safe plant operation and high plant availability.

The conceptual main control room arrangement is shown in Fig. 2-72. The majority of the plant operational control is contained in a compact U-shaped array of vertical control boards surrounding a C-shaped center console. The vertical control board array contains control and instruments for the safety-related control and instrumentation systems, reserve shutdown system, primary and secondary coolant loops, plant control, NSS support systems, steam turbine, and turbine-generator. The center console contains video information and alarm displays, as well as sufficient additional control and indication equipment to enable a console operator and one additional operator to operate the plant under normal, upset, and emergency operating conditions.

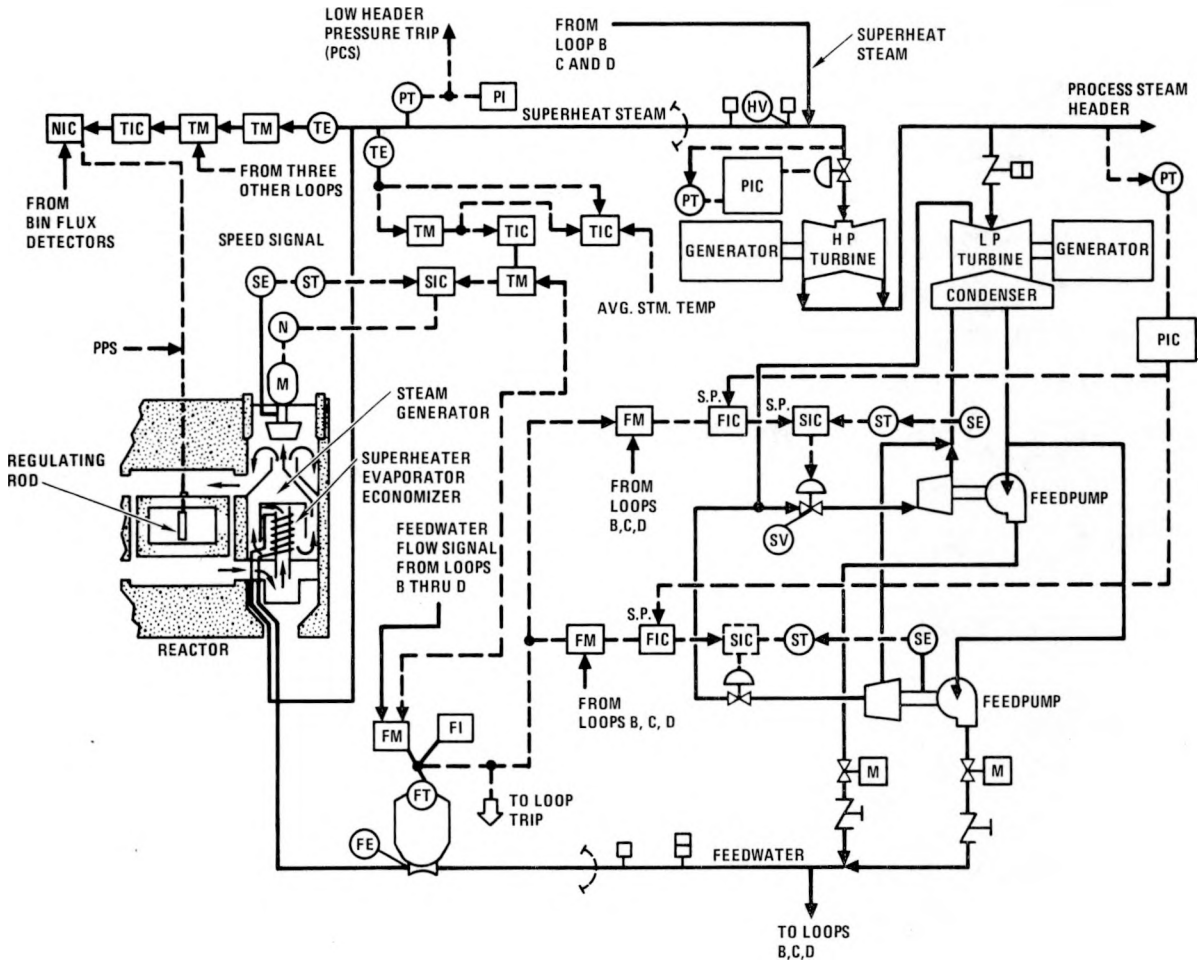

Fig. 2-71. Plant control system simplified overview diagram

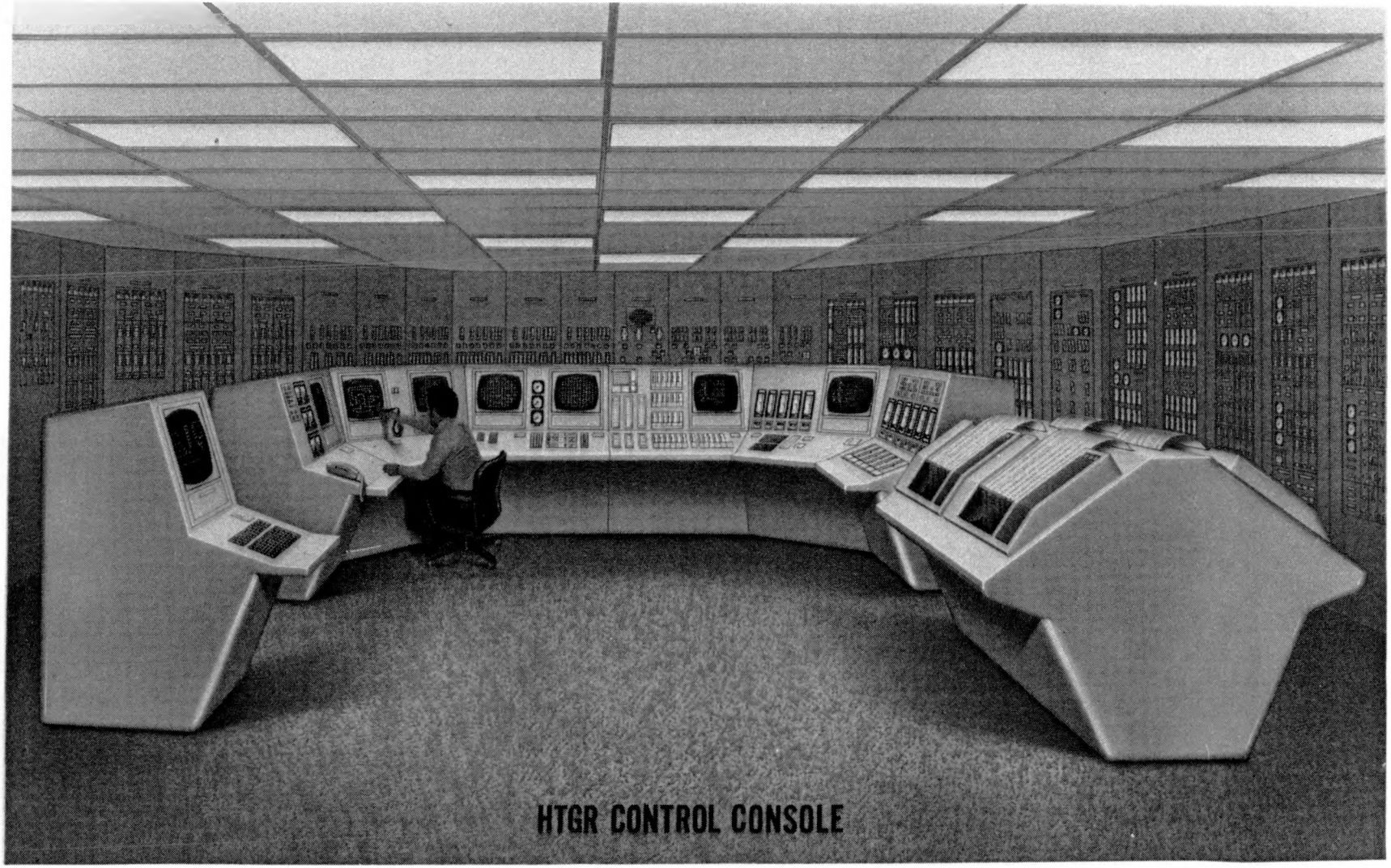

Fig. 2-72. HTGR control console conceptual design

REFERENCES

2-1. Mears, L., "Functional Specification, HTGR-Steam Cycle Cogeneration Reference Plant," Gas Cooled Reactor Associates Report PTR-1.0, January 27, 1982.

2-2. Lewis, J. H., and R. K. Wise, "Safety/Licensing Assessment of the 2240-MW(t) HTGR Steam Cycle Cogeneration Plant," DOE Report GA-A16457, GA Technologies, September 1981.

2-3. "HTGR Applications Program Semiannual Report for the Period April 1, 1981 through September 30, 1981," DOE Report GA-16538, GA Technologies, to be published.

2-4. "Design Responses Spectra for Nuclear Power Plants," U.S. NRC Regulatory Guide 1.6, Rev. 1, December 1973.

2-5. Lysner, J., et al., "Flush - A Computer Program for Approximate 3-D Analysis of Soil-Structural Interaction Problems," Earthquake Engineering Research Center Report EERC 75-30, November 1975.

2-6. Hurn, E., "HTGR Steam Generator Design Guide," GA Report GA-A16627, to be issued.

2-7. Hurn, E., "MK IV-A 570-MW(t) Steam Generator Design Basis," GA Technologies, unpublished data.

3. MONOLITHIC 1170-MW(t) HTGR-PH

3.1. SYSTEM PERFORMANCE (6042131001)

3.1.1. Scope

The scope of this task is to perform an evaluation study of plant parameters (and cost-of-product) to determine economic improvement trends.

3.1.2. Discussion

A study was made to identify primary system parameter trends that lead to improved economics. The parameters studied were those associated with the nuclear heat source (NHS) of the 1170-MW(t) HTGR-PH plant. The plant was a nuclear-heated chemical process plant that produces hydrogen by steam reforming of methane. Both an 850°C (1562°F) reactor outlet temperature indirect cycle configuration and a 950°C (1742°F) reactor outlet temperature direct cycle configuration were considered. The basis for assessing economic trends was minimum cost of product, i.e., the minimum cost of owning and operating the plant per pound of hydrogen produced.

Figures 3-1 and 3-2 are schematic diagrams of the indirect and direct cycle configurations, respectively. The figures show the major elements of the plant (NHS, BOPR, and process plant) and the major components in the NHS and BOPR scope of supply. The process plant is treated as a "black box."

Tables 3-1 and 3-2 list the NHS parameters for the indirect cycle configuration and the direct cycle configuration, respectively. These parameters define the base case plant and its cost-of-product, which serve as the focal point for assessing the economic trends associated with variations in selected primary system parameters. The parameters identified as having

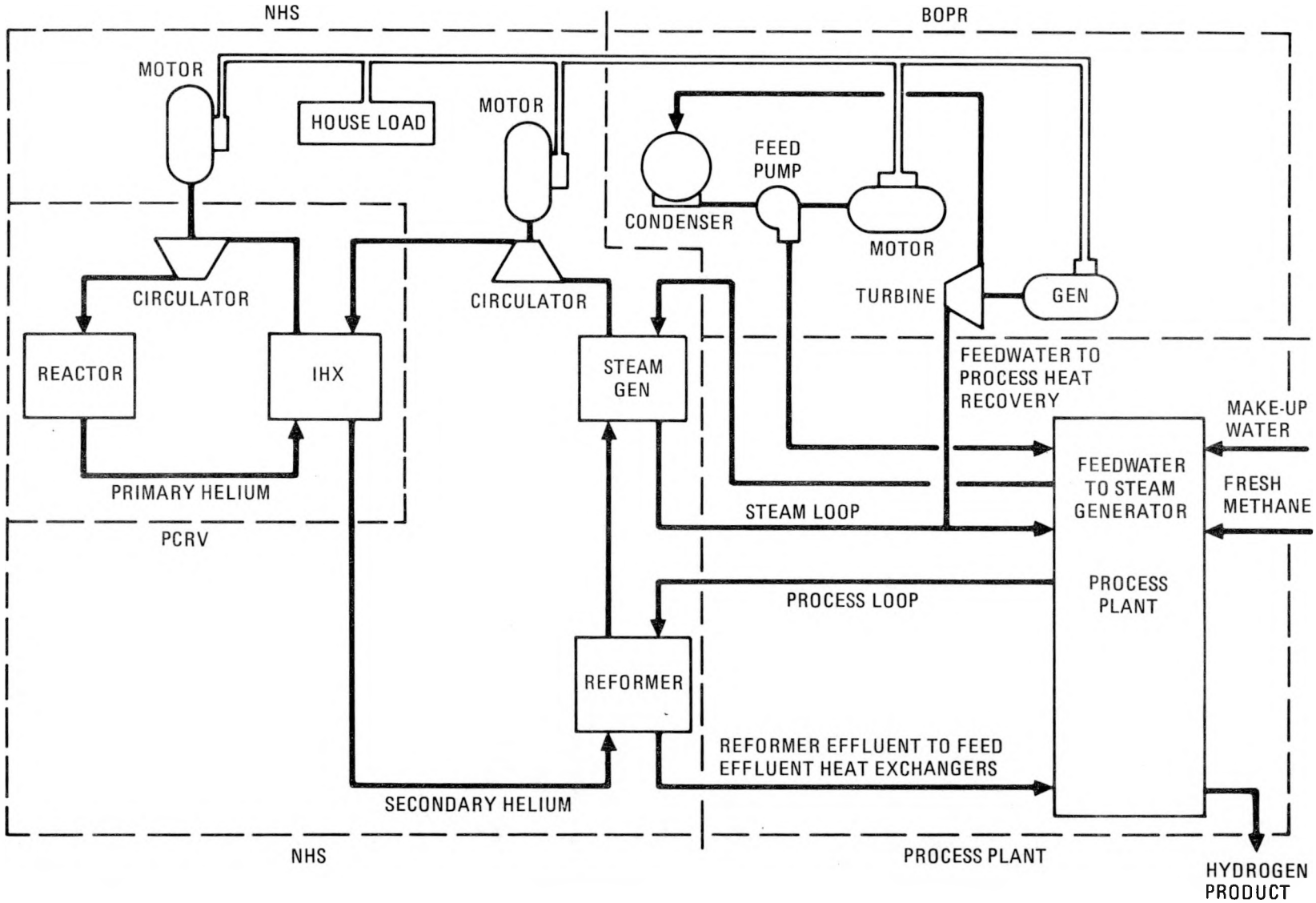

Fig. 3-1. Schematic diagram of indirect cycle HTGR-PH

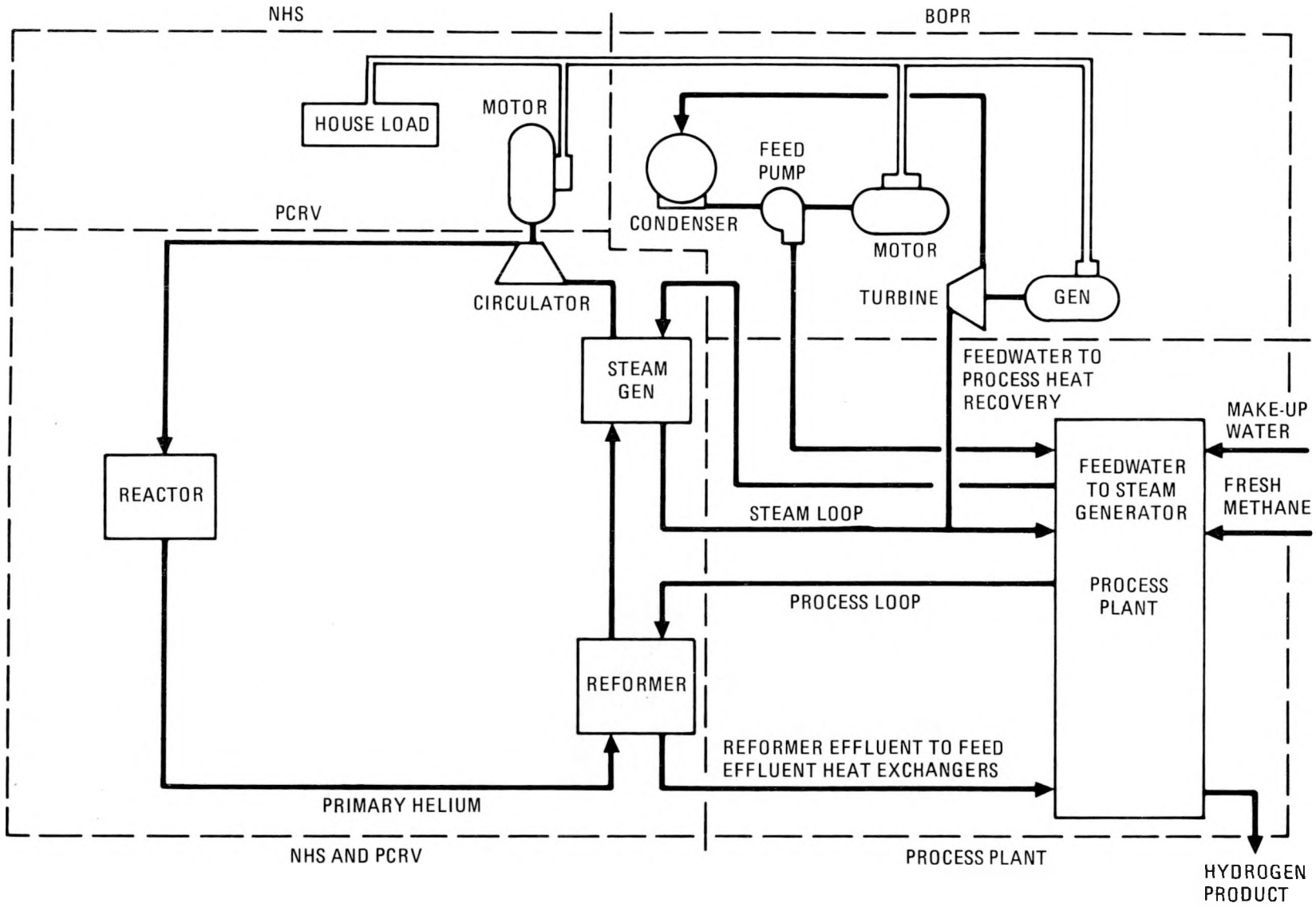

Fig. 3-2. Schematic diagram of direct cycle HTGR-PH

TABLE 3-1
PRIMARY SYSTEM AND SECONDARY SYSTEM PARAMETERS
FOR INDIRECT CYCLE HTGR-PH PLANT

Primary System	
Reactor core power [MW(t)]	1170
Circulator return power [MW(t)]	35.8
Heat losses [MW(t)]	10.1
IHX power [MW(t)]	1196
Core power density (W/cm^3)	6.6
Flow rate [kg/s (lb/hr)]	533 (4,230,000)
Reactor inlet pressure [MPa (psia)]	4.97 (721)
Reactor inlet temperature [°C (°F)]	427 (801)
Reactor outlet pressure [MPa (psia)]	4.90 (711)
Reactor outlet temperature [°C (°F)]	850 (1562)
IHX inlet pressure [MPa (psia)]	4.89 (709)
IHX inlet temperature [°C (°F)]	845 (1553)
IHX outlet pressure [MPa (psia)]	4.82 (699)
IHX outlet temperature [°c (°F)]	415 (779)
Circulator inlet pressure [MPa (psia)]	4.82 (699)
Circulator inlet temperature [°C (°F)]	415 (779)
Circulator outlet pressure [MPa (psia)]	5.00 (725)
Circulator outlet temperature [°C (°F)]	428 (802)
Secondary System	
IHX power [MW(t)]	1196
Circulator return power [MW(t)]	34.8
Heat losses [MW(t)]	13.3
Reformer thermal power [MW(t)]	506
Steam generator thermal power [MW(t)]	711
Flow rate [kg/s (lb/hr)]	512 (4,063,500)
IHX inlet pressure [MPa (psia)]	4.98 (722)
IHX inlet temperature [°C (°F)]	343 (649)
IHX outlet pressure [MPa (psia)]	4.89 (709)
IHX outlet temperature [°C (°F)]	793 (1459)
Reformer inlet pressure [MPa (psia)]	4.85 (703)
Reformer inlet temperature [°C (°F)]	792 (1458)
Reformer outlet pressure [MPa (psia)]	4.81 (698)
Reformer outlet temperature [°C (°F)]	601 (1114)
Steam generator inlet pressure [MPa (psia)]	4.81 (698)
Steam generator inlet temperature [°C (°F)]	600
Steam generator outlet pressure [MPa (psia)]	4.79 (695)
Steam generator outlet temperature [°c (°F)]	332 (630)
Circulator inlet pressure [MPa (psia)]	4.79 (695)
Circulator inlet temperature [°C (°F)]	331 (628)
Circulator outlet pressure [MPa (psia)]	5.00 (725)
Circulator outlet temperature [°C (°F)]	344 (651)
Process Side	
Reformer inlet pressure [MPa (psia)]	2.15 (312)
Reformer inlet temperature [°C (°F)]	538 (1000)
Reformer outlet pressure [MPa (psia)]	1.59 (231)
Reformer outlet temperature [°C (°F)]	727 (1341)
Steam/Water Side	
Steam generator inlet pressure [MPa (psia)]	19.8 (2872)
Steam generator inlet temperature [°C (°F)]	290 (554)
Steam generator outlet pressure [MPa (psia)]	17.2 (2495)
Steam generator outlet temperature [°C (°F)]	510 (950)

TABLE 3-2
PRIMARY SYSTEM PARAMETERS FOR DIRECT CYCLE HTGR-PH PLANT

Primary System	
Reactor core power [MW(t)]	1170
Circulator return power [MW(t)]	57.0
Heat losses [MW(t)]	11.0
IHX power [MW(t)]	1216
Core power density (W/cm^3)	6.6
Flow rate [kg/s (lb/hr)]	500 (3,968,300)
Reactor inlet pressure [MPa (psia)]	4.80 (696)
Reactor inlet temperature [°C (°F)]	500 (932)
Reactor outlet pressure [MPa (psia)]	4.69 (680)
Reactor outlet temperature [°C (°F)]	950 (1742)
Circulator inlet pressure [MPa (psia)]	4.54 (658)
Circulator inlet temperature [°C (°F)]	479 (894)
Circulator outlet pressure [MPa (psia)]	4.80 (696)
Circulator outlet temperature [°C (°F)]	501 (934)
Reformer inlet pressure [MPa (psia)]	4.69 (680)
Reformer inlet temperature [°C (°F)]	947 (1737)
Reformer outlet pressure [MPa (psia)]	4.61 (669)
Reformer outlet temperature [°C (°F)]	695 (1283)
Steam generator inlet pressure [MPa (psia)]	4.61 (669)
Steam generator inlet temperature [°C (°F)]	692 (1278)
Steam generator outlet pressure [MPa (psia)]	4.54 (658)
Steam generator outlet temperature [°C (°F)]	479 (894)
Process Side	
Reformer inlet pressure [MPa (psia)]	4.95 (718)
Reformer inlet temperature [°C (°F)]	538 (1000)
Reformer outlet pressure [MPa (psia)]	4.45 (645)
Reformer outlet temperature [°C (°F)]	632[a] (1170)
Steam/Water Side	
Steam generator inlet pressure [MPa (psia)]	20.0 (2900)
Steam generator inlet temperature [°C (°F)]	260 (500)
Steam generator outlet pressure [MPa (psia)]	17.2 (2495)
Steam generator outlet temperature [°C (°F)]	566 (1051)

potential for improved economics are primary system operating pressure, reactor inlet temperature, and core power density.

The economic trends were established in terms of percent deviation from the base case value of cost-of-product versus the parameter value. Improved economics usually occur when a change in a parameter results in a benefit from an increase in product output which is not offset by the increase in the plant capital cost needed to achieve the higher output. The economic trends for the indirect cycle configuration are given in Fig. 3-3 through 3-5. These figures indicate how the cost-of-product and product rate (product output) vary with the variations in the parameter values. The figures also show that there is limited potential for improved economics. For example, an increase in primary system pressure from 5.0 to 6.0 MPa (725 to 870 psia) results in only a 1% decrease in cost-of-product. The same economic trends are expected for the direct cycle configuration when considering the same primary system parameters, i.e., limited potential for improvement. This conclusion is based on qualitative assessment because a cost/benefit simulation of the direct cycle configuration is not currently available.

Based on the resultant limited potential for economic improvement, it was concluded that the existing plant parameters (Ref. 3-1) are close enough to optimum so as not to merit a change.

3.2. SAFETY STUDIES (6042130700)

3.2.1. Scope

The scope of this task is to perform a probability risk assessment of the indirect cycle HTGR-PH plant concept in support of safety licensing.

3.2.2. Discussion

Combustible releases, which may form potentially explosive mixtures with air, can accidentally occur in the process plants. Releases originating in the reformer area are characteristic of the HTGR-PH concept.

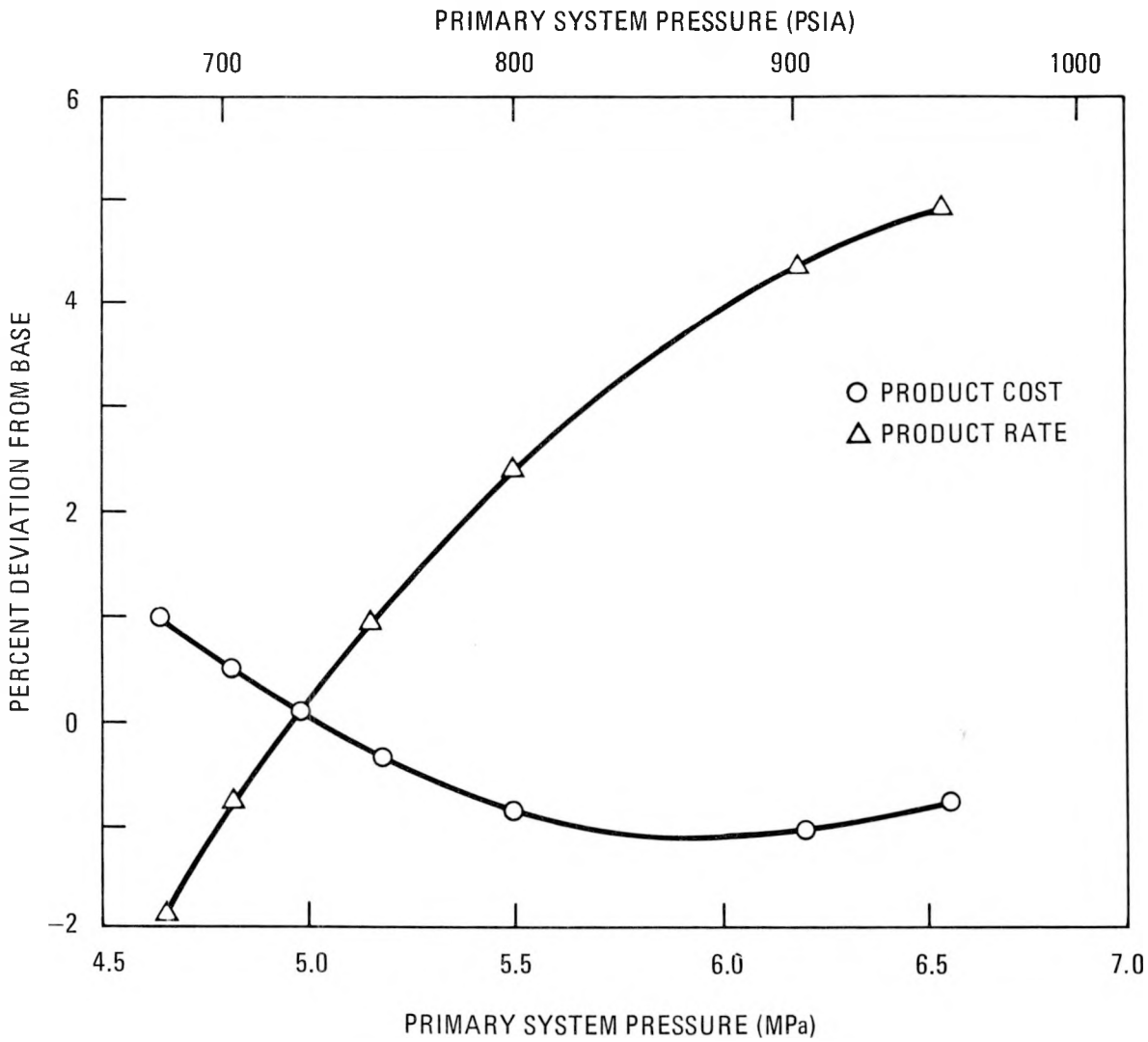

Fig. 3-3. Cost-of-product versus primary system pressure for indirect cycle HTGR-PH

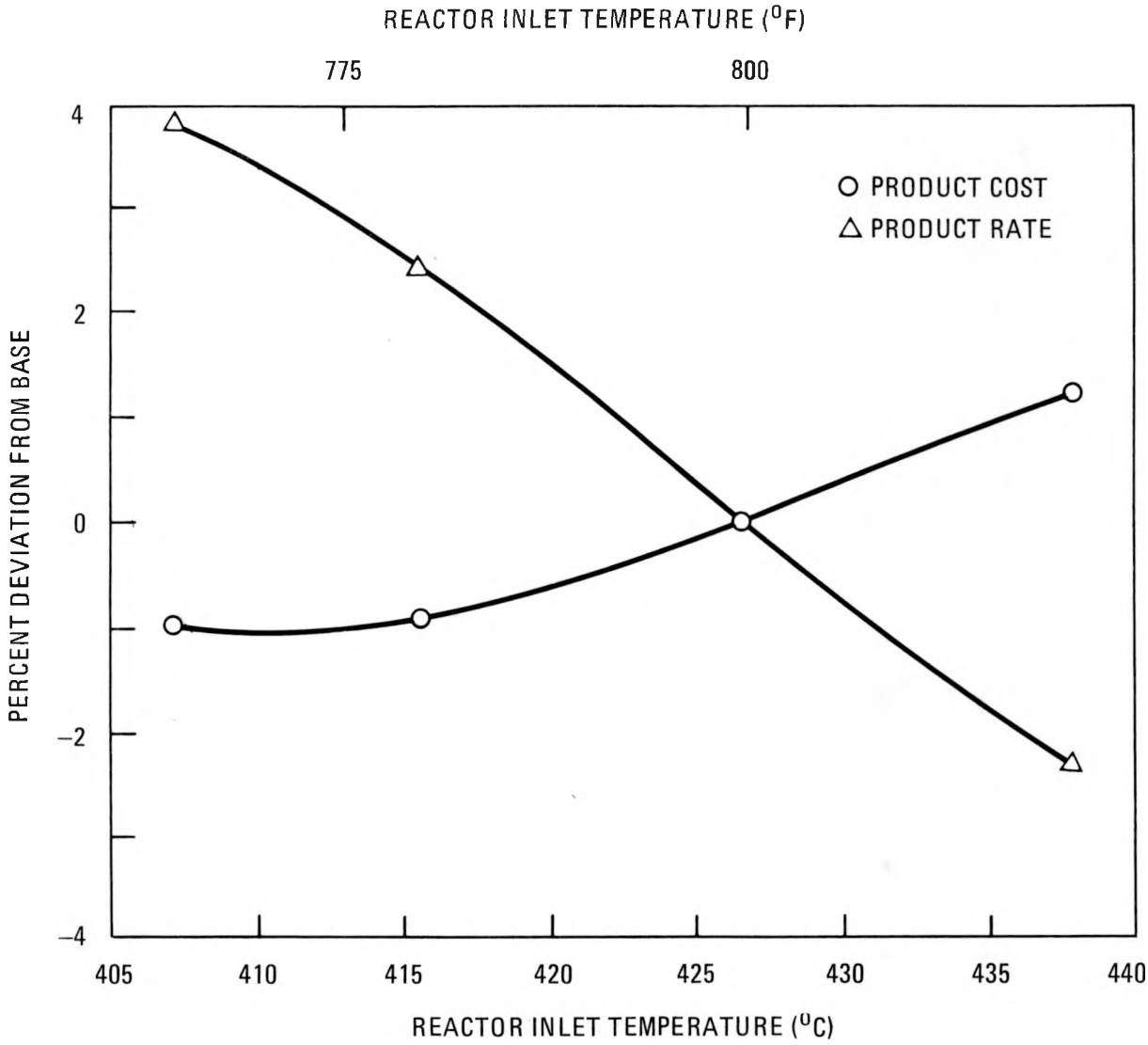

Fig. 3-4. Cost-of-product versus reactor inlet temperature for indirect cycle HTGR-PH

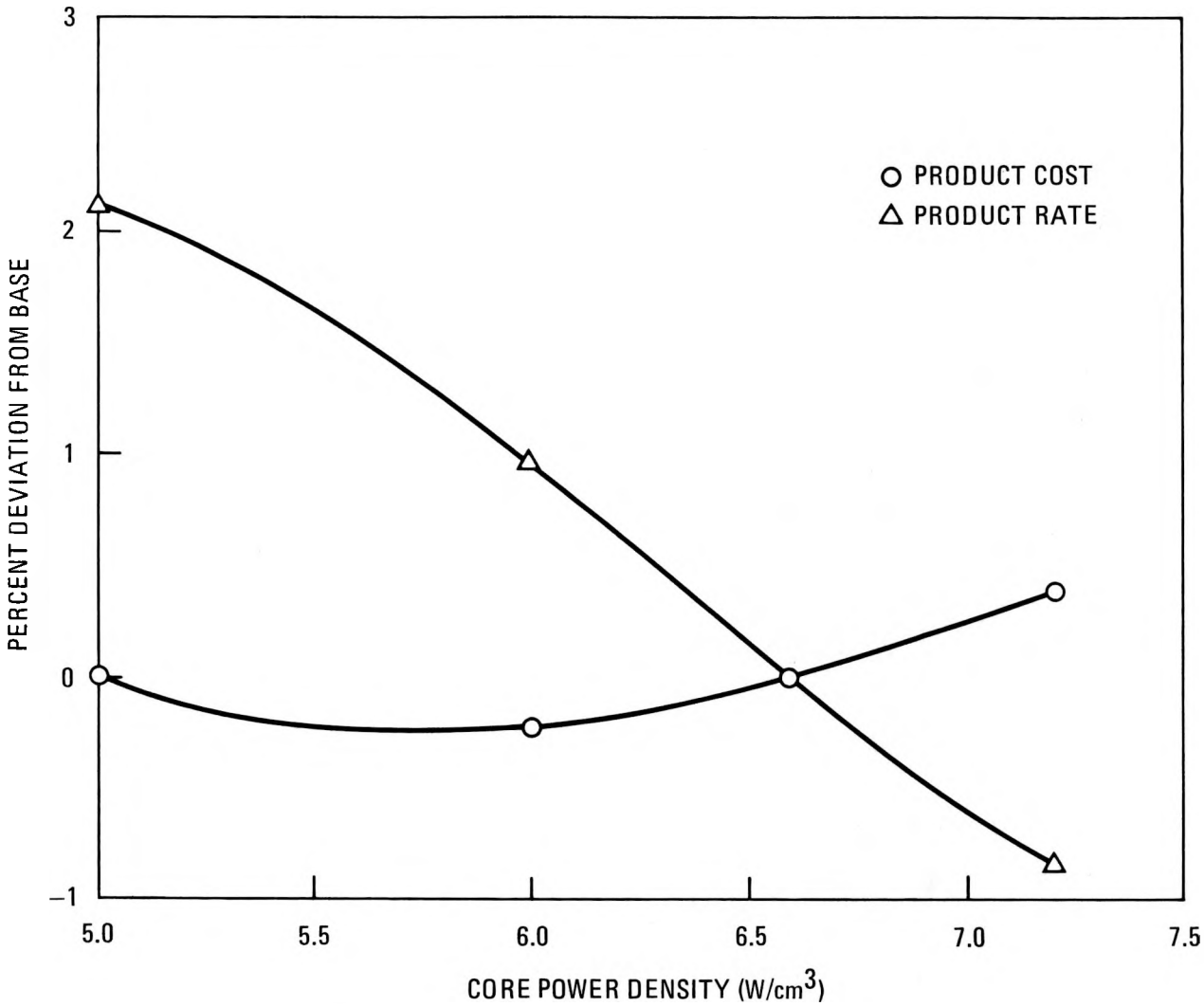

Fig. 3-5. Cost-of-product versus core power density for indirect cycle HTGR-PH

There are no regulatory guides for the explosions of process gases in or near nuclear power reactors. However, Regulatory Guide 1.91 (Ref. 3-2) for evaluation of explosions on transportation routes contains a regulatory framework which is instructive in planning for the licensing of a process heat reactor. Nevertheless, this regulatory guide is generally very conservative, and the licensing of an HTGR for process heat applications must depend on more detailed calculations to establish the safety associated with the handling of process gases.

One of the options in this regulatory guide is to show that the probability of explosions near the nuclear plant is less than 10^{-7}/yr and thereby justify the exclusion of the analysis of these explosions. For a process heat reactor, the frequencies of possible explosions are much higher than this, and therefore the effects of these explosions must be examined.

The propagation of blast waves is dealt with in the regulatory guide by a formula which is based upon the TNT equivalence concept for point explosions at ground level. This approach appears to be very conservative for clouds of combustible gases. Specific calculations on air mixing of the release must therefore be used in design basis accidents (DBAs) with appropriate and identifiable conservatism.

This regulatory guide also conservatively chooses 6.9 kPa (1 psi) as the limiting incident pressure which will cause no significant damage to critical structures and components. In some cases, the pressure transient of 20.6 kPa (3 psi) resulting from tornadoes as specified in Regulatory Guide 1.76 (Ref. 3-3) has been used as the acceptable limit for overpressure. Furthermore, damage from the blast waves of very short duration cannot be compared with that from the relatively long-duration pressure load of a tornado. Structures can therefore withstand higher pressures than 20.6 kPa (3 psi) without a failure which would impair the function of safety-class equipment within the structure. A typical HTGR concrete containment, for example, can sustain a blast pressure of about 700 kPa (100 psi) for a few milliseconds while still retaining its safety function. Other nuclear

safety related (NSR) structures may not have as high a resistance to external overpressure transients. However, these structures can withstand a lower pressure blast transient.

Another feature of Regulatory Guide 1.76 is that it assumes that all NSR structures must retain their function. A rule associated with fission product release is more suitable, as seen in other regulatory guides (e.g., Ref. 3-4), for judging the satisfactory performance of the structure. For example, the loss of one cooling structure is not necessarily prohibitive if the release of radioactivity can still be restricted.

The overall results of this probabilistic risk assessment study of the indirect cycle HTGR-PH concept is that VCEs initiated by compressor failure in the reformer train pose an additional small risk to the public that is similar to the already small risk associated with a normal HTGR-SC plant. The presence of combustible gases in the indirect cycle therefore does not appear to pose an undue hazard to the public, but further work is needed to extend the preliminary study.

3.3. LICENSING (6042130200)

3.3.1. Scope

The scope of this task consists of providing guidance and support on matters related to regulatory requirements.

3.3.2. Discussion

Because the relatively low level of effort on the monolithic plant study has not required specific licensing input, activity has been restricted to review of program documents and plans.

3.4. HTGR-PH INTERMEDIATE HEAT EXCHANGER (6042132100)

3.4.1. Scope

The primary objective of this task for FY-82 is to study the straight tube heat exchanger concept and a helically wound tube arrangement for the same application and determine their relative advantages and disadvantages. Additional subtasks are (1) to develop an appropriate steam generator size for the 950°C (1742°F) HTGR-PH plant and (2) to complete residual tasks from the prior design efforts on the disk-and-ring heat exchanger involving two design problem areas that could influence the viability of the design.

3.4.2. Discussion

3.4.2.1. IHX Problem Areas. Two problem areas identified during the previous reporting period are (1) tube bundle vertical support and (2) expansion joint design.

Tube Bundle Vertical Support

Axial pressure loads on the tubes caused excessive stress in the thermal expansion offsets at the cold end of the tubes and excessive creep buckling loads at the hot ends. To counteract these pressure loads, the bundle outer shroud has been employed with a flexible link at the cold end. The shroud expands thermally, causing the tubes to be in tension. By this means, the tube thermal offsets can be eliminated, the differential expansion between tubes being accommodated by the axial tensile loads. The concept uses the outer shroud supported by the hot tubesheet or by structures to nearly common support members. The shroud, in turn, supports a flexible link at the cold end in the form of a ring that is free to deflect. This supports the floating head, which includes the cold tubesheet.

Expansion Joints

The HTGR-PH IHX is designed for several modes of operation. These include shutdown, normal steady-state operation, and an emergency mode where the secondary loop flow has ceased. These together with other operational modes impose different thermal loads on the tubes and other structural members within the IHX assembly.

The bulk of the IHX, i.e., tubes, tubesheets, floating head, shrouds, etc., is supported from the lower end. As the temperature of the unit increases, the upper end and floating head increase in height. During normal operation the floating head will rise about 89 mm (3-1/2 in.) relative to the cold position. A worst case situation, a secondary loop shutdown with a hot soak, can cause the floating head to rise up to 254 mm (10 in.).

An expansion joint was designed based on the following assumptions: (1) no full pressure across the walls of the expansion joint, (2) walls to be maintained within the elastic range of the material, and (3) a hot soak to be limited to 2 hr.

A bellows joint was designed which is supplied by buffer helium to assure that the pressure differential across the walls is maintained to be no greater than 34 kPa (50 psi). Slip ring seals are used to restrict the flow of buffer helium leaking into the secondary loop upon loss of secondary loop pressure. Thermal insulation maintains the material temperature close to the primary helium temperature during normal operation. The flow passage for the primary helium has been reduced in diameter to 787 mm (31 in.). Strict attention to the design of the entry and exit sections should limit the pressure loss to a reasonable value.

It appears that this expansion joint design will fulfill the requirements. The safety and licensing problem of requiring a buffer helium system is to be studied, but early indications are that a static storage system will be acceptable. In-service-inspection problems will require further attention.

3.4.2.2. Helical Versus Straight Tube IHX. The question of whether the straight tube reference design IHX is optimum for this application or if a helically coiled tube bundle, similar to that designed for the steam generators, would be better was addressed. The study primarily considered the tube bundle diameter, since this significantly affects the diameter and the cost of the PCRV. Subjective consideration was also given to the number and size of tubes, helix angles, and tube stress and support problems. The results of the study indicate that, based strictly on thermal sizing, a helical IHX could be designed which would be nearly similar to the reference disk-and-donut straight tube design in diameter and considerably smaller in length. However, the design is not considered practical, since it would involve very steep helix angles and a great many small tubes. To approach the size of the straight tube heat exchanger, the helix angles must approach 90 deg, which, of course, simply straightens the tubes so that the helical geometry disappears. Decreasing the helix angle to usable values such as 30 deg increases the bundle diameter by about 300 mm (1 ft) if the same number and size of tubes [14,000, 12.7-mm (0.5-in.) O.D.] are used as in the reference design IHX. Numerous problems would be encountered, however, in attempting to construct suitable tube support plates drilled with 14,000 holes on angles even as shallow as 30 deg. In addition, the concept of threading this many tubes may not be practical. The seismic and thermal expansion stresses imposed on the support plates, which will have very small ligaments (due to the small tube pitch and the addition of wear protection devices in each hole), will not allow the tube pitch to approach the low values required for the small diameter of the straight tube IHX.

Increasing the tube size, the number of tubes, and the pitch-to-diameter ratio contributes to increasing the bundle diameter and length. Using a more practical number of larger tubes [4000, 25.4-mm (1.0-in.) O.D.] pitched according to steam generator design procedures [38.1 mm (1.5 in.)] will increase the diameter of the bundle by approximately 610 mm (2 ft) and the length by about 760 mm (5-1/2 ft) over the reference design and will result in quite steep (35-deg) helix angles. The steepness of the helix angle contributes to the difficulties in drilling the plates accurately, designing and installing wear protection devices, and threading the tubes

through the plates. The steeper angles do tend to reduce the tube-to-plate differential thermal expansion stresses ("bear-hug" stresses), but the reduction is significant only at really steep angles (greater than 45 deg).

Thus, it is concluded that the use of the straight tube design lends itself better to the IHX application, where minimizing bundle diameter is important and a length limit, determined by the core cavity, has not been reached.

3.5. HTGR-PH VESSEL DESIGN DEVELOPMENT (6042131100)

3.5.1. Scope

The objective of this task is to identify potential PCRV cost reduction areas and provide vessel inputs for plant parameter optimization for the following 1170-MW(t) plants:

- Indirect cycle PCRV [850°C (1562°F)].
- Direct cycle PCRV [950°C (1742°F)].
- Secondary loop PCPV [850°C (1562°F)].

3.5.2. Discussion

During this reporting period, technical support was provided to reduce the high-cost areas of the vessel.

The diameter for the indirect and direct cycle PCRVs and the secondary loop PCPV can be reduced by increasing the existing concrete [4482-MPa (6500-psi)] and linear tendon [11.1-MN (2478-kip)] capacities to 5516 MPa (8000 psi) and 13.3 MN (3000 kips), respectively. Further reduction in PCRV diameter is possible by reducing the number of reformer or steam generator cavities in the direct cycle plant or relocating the fuel transfer chute in the indirect cycle plant. The PCPV diameter can be reduced if only two cavities instead of three are used. The heights of the vessels in all of

the above three cases cannot be reduced, since they are governed by the respective component heights.

Table 3-3 shows the various PCRV and PCPV diameter reductions that can be achieved by increasing the concrete and tendon strength and also reducing or relocating the penetrations or cavities. It is noted that there would be little change in the PCRV diameter and height even if the maximum cavity pressures were to increase from 5.34 MPa (776 psig) to 6.21 MPa (900 psig). This results from readjusting the cavity locations to meet the additional ligament requirements and rearranging the linear prestressing tendons in the concrete ligaments of the PCRV and PCPV.

The above PCRV and PCPV sizing is preconceptual and is based on past experience with PCRV sizing. Because of the complexity of the design, it is essential to verify the sizes by later performing two-dimensional analyses and top head tendon layouts. Representative sketches of the reference PCRV and PCPV top head plan are shown in Figs. 3-6 through 3-8.

REFERENCES

3-1. "HTGR-SC/C Semiannual Progress Report for the Period Ending September 30, 1981," DOE Report GA-A16538, GA Technologies, to be issued.

3-2. "Evaluation of Explosions Postulated to Occur on Transportation Routes Near Nuclear Power Plants," Regulatory Guide 1.91, U.S. Nuclear Regulatory Commission, Revision 1, February 1978.

3-3. "Design Basis Tornado for Nuclear Power Plant," Regulatory Guide 1.76, U.S. Atomic Energy Commission, April 1974.

3-4. "General Site Suitability Criteria for Nuclear Power Stations," Regulatory Guide 4.7, U.S. Atomic Energy Commission, September 1974.

TABLE 3-3
VESSEL SIZE OPTIMIZATION FOR DIRECT AND INDIRECT CYCLE 1170-MW(t) HTGR-PH PLANTS

Plant Description	Diameter/Height MCP = 5.34 MPa (776 psi) Diameter [m (ft)]	Diameter/Height MCP = 5.34 MPa (776 psi) Height [m (ft)]	Diameter/Height MCP = 6.21 MPa (900 psi) Diameter [m (ft)]	Diameter/Height MCP = 6.21 MPa (900 psi) Height [m (ft)]	Factors Responsible for Optimization
Indirect cycle PCRV [850°C (1562°F) (Fig. 3-6)	26.52 (87.0)[a]	27.58 (90.5)	26.52 (87.0)	28.65 (94.0)	44.82-MPa (6500-psi) concrete and 11.1-MN (2478-kip) tendons.
	24.99 (82.0)	27.58 (90.5)	24.99 (82.0)	27.58 (90.5)	55.16-MPa (8000-psi) concrete and 13.3-MN (3000-kip) tendons.
	24.38 (80.0)	27.58 (90.5)	24.38 (80.0)	27.58 (90.5)	55.16-MPa (8000-psi) concrete, 13.3-MN (3000-kip) tendons, and location of plenum hoist and elevator drive and fuel transfer pens at 0 deg instead of 180 deg.
Direct cycle PCRV [950°C (1742°F)] (Fig. 3-7)	32.92 (108.0)[a]	28.04 (92.0)	33.22 (109.0)	29.41 (96.5)	44.82-MPa (6500-psi) concrete and 11.1-MN (2478-kip) tendons.
	34.70 (104.0)	28.04 (92.0)	32.92 (108.0)	28.04 (92.0)	55.16-MPa (8000-psi) concrete and 13.3-MN (3000-kip) tendons.
	31.09 (102.0)	28.04 (92.0)	32.31 (106.0)	28.04 (92.0)	55.16-MPa (8000-psi) concrete, 13.3-MN (3000-kip) tendons, and location of plenum hoist and elevator drive and fuel transfer pens at 0 deg instead of 180 deg.
	28.35 (93.0)	28.04 (92.0)	28.96 (95.0)	28.04 (92.0)	55.16-MPa (8000-psi) concrete, 13.3-MN (3000-kip) tendons and fewer cavities (reformer and steam generator located in the same cavity).
PCPV [850°C (1562°F)] (Fig. 3-8)	15.85 (52.0)[a]	25.60 (84.0)	16.46 (54.0)	25.60 (84.0)	44.82-MPa (6500-psi) concrete and 11.1-MN (2478-kip) tendons.
	15.54 (51.0)	25.60 (84.0)	15.85 (52.0)	25.60 (84.0)	55.16-MPa (8000-psi) concrete and 13.3-MN (3000-kip) tendons.
	13.72 (45.0)	25.60 (84.0)	13.72 (45.0)	25.60 (84.0)	55.16-MPa (8000-psi) concrete, 13.3-MN (3000-kip) tendons, and fewer cavities (two reformers only with steam generator cavity outside PCPV)

[a] Denotes reference plant.

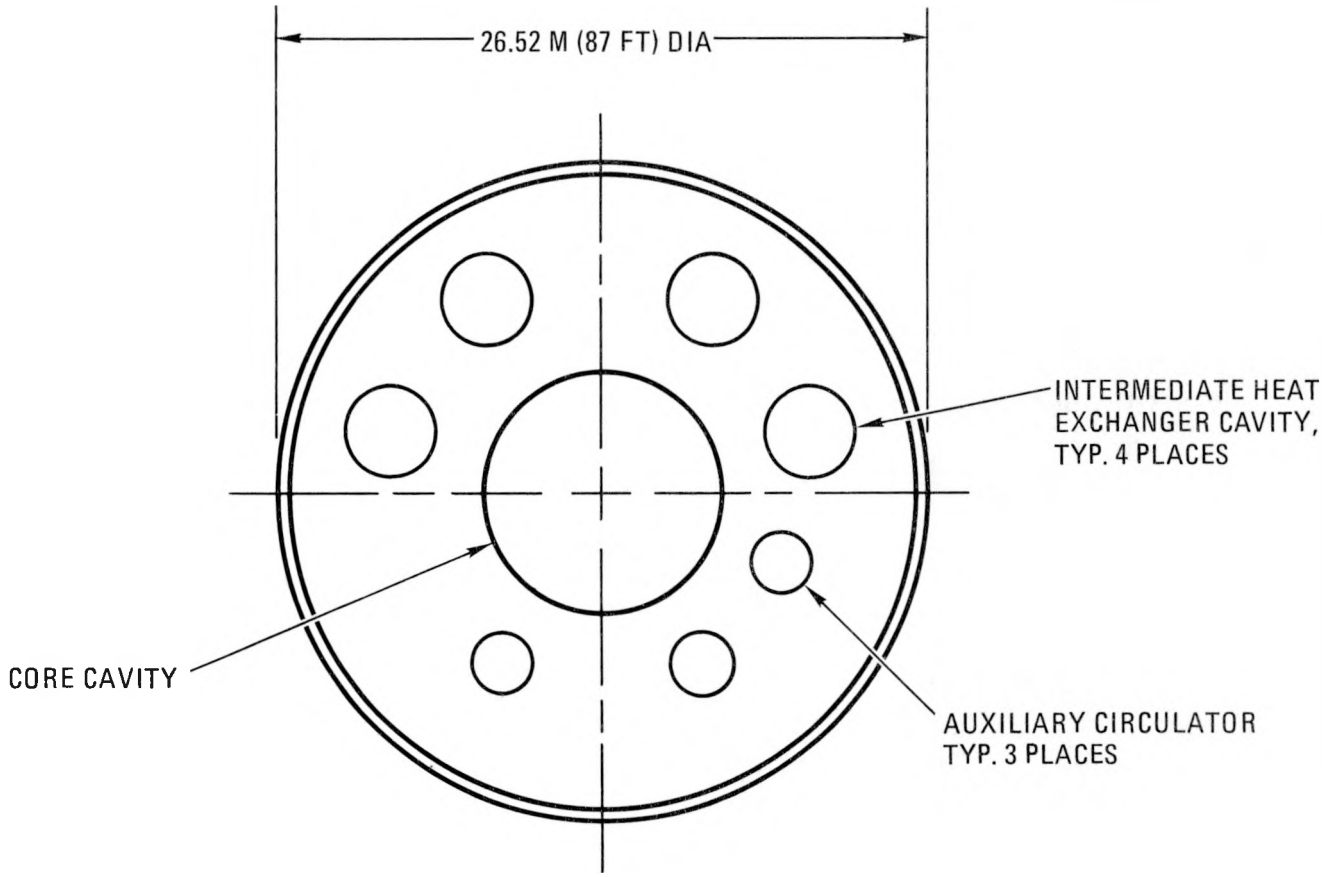

Fig. 3-6. PCRV top head plan for 950°C (1742°F) indirect cycle HTGR-PH

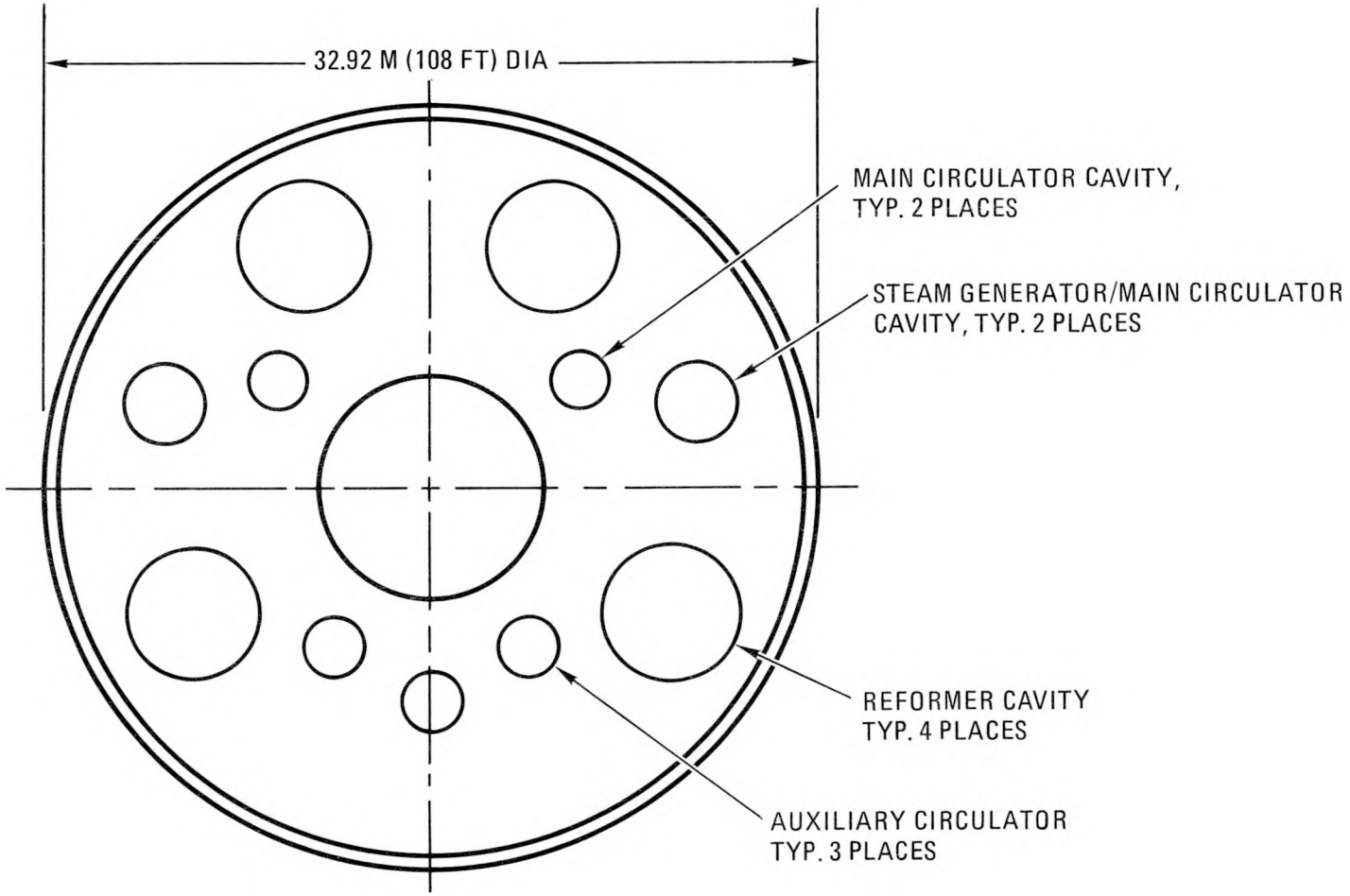

Fig. 3-7. PCRV top head plan for 950°C (1742°F) direct cycle HTGR-PH

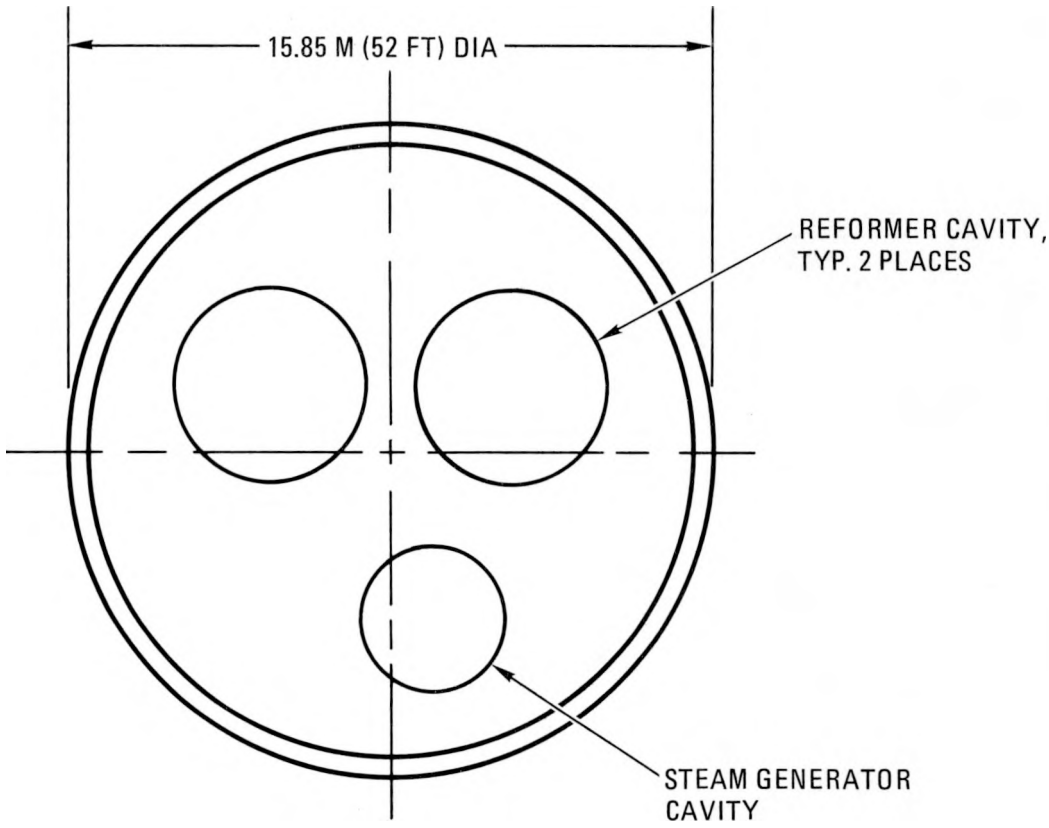

Fig. 3-8. PCVP top head plan for 850°C (1562°F) secondary loop HTGR-PH

4. HTGR MODULAR REACTOR SYSTEM PROCESS HEAT

4.1. SYSTEMS PERFORMANCE (6053010100)

4.1.1. Scope

The scope of this task is to establish the nuclear heat source (NHS) performance of the HTGR modular reactor system/process heat (HTGR-MRS/PH) at 100% power.

4.1.2. Discussion

Establishing the NHS performance required considerable coordination between GA and the General Electric Company to attain common conditions at the NHS/process plant interface. General Electric has the lead for the over-all program and is directly responsible for the process plant.

Figure 4-1 is a simplified heat-mass balance diagram for the NHS. The total NHS output is 252.5 MW(t). This value is based on a reactor power of 250 MW(t), NHS heat losses of 1.2 MW(t), and a circulator return power (heat addition) of 3.7 MW(t) for an overall NHS efficiency of 99.5%. The net thermal outputs from the reformer and from the steam generator are 139.5 MW(t) and 113.0 MW(t), respectively. These values and the values of process side pressure and temperature at the inlets and outlets of the heat exchangers are consistent with the process plant requirements. Table 4-1 gives the details of the NHS heat and mass balance and the NHS parameters.

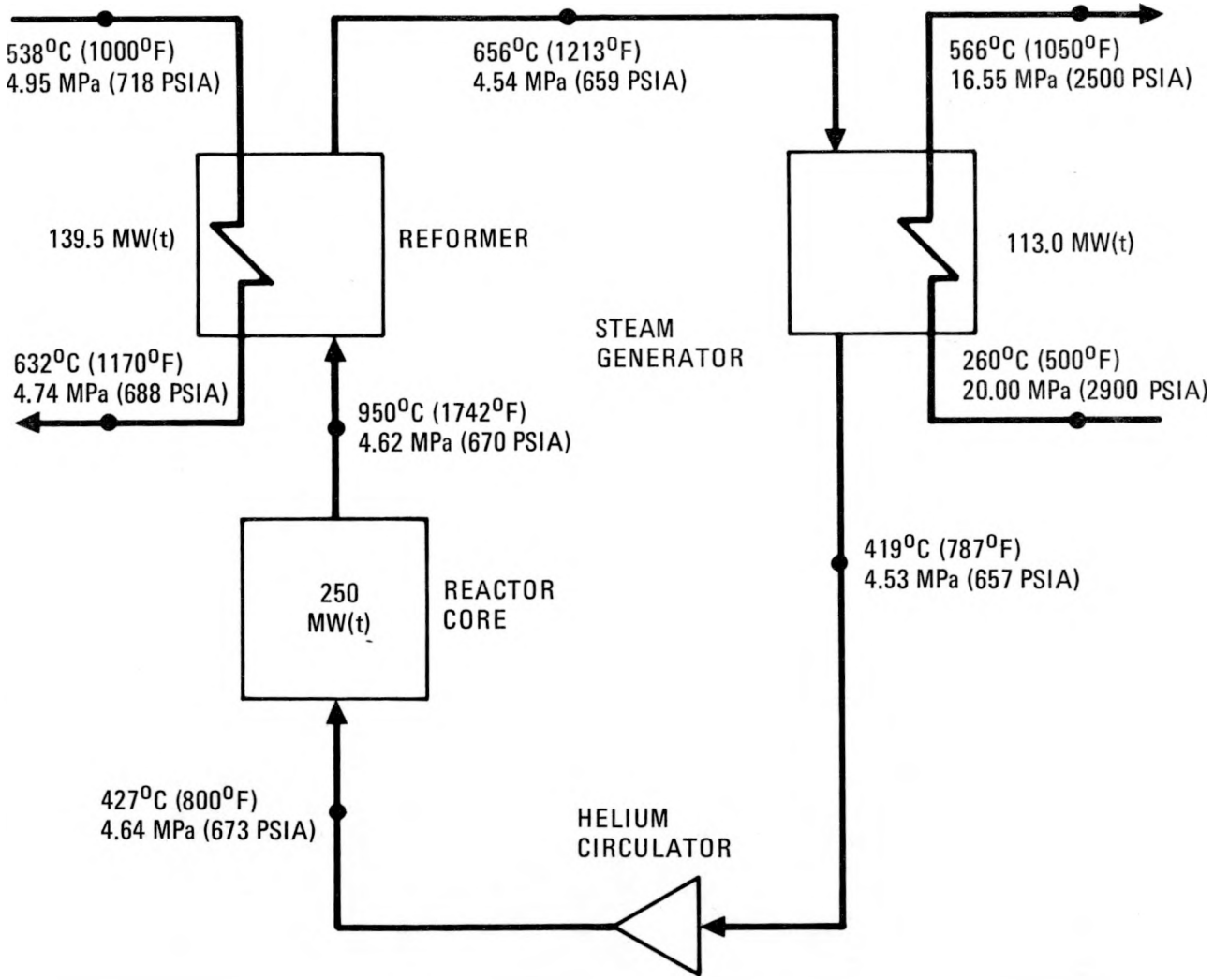

Fig. 4-1. HTGR-MRS/PH plant heat and mass balance

TABLE 4-1
MRS PLANT PARAMETERS

Heat balance	
Reactor power, MW(t)	250
Heat losses	1.2
Circulator return power, MW(t)	3.7
Power to process plant, MW(t)	139.5
Electricity generating plant, MW(t)	113.0
Parameters	
Primary system	
Flow rate, kg/s (lb/hr)	91.9 (729,300)
Core	
Inlet temperature, °C (°F)	427 (800)
Inlet pressure, MPa (psia)	4.63 (672)
Outlet temperature, °C (°F)	950 (1742)
Outlet pressure, MPa (psia)	4.62 (670)
Reformer	
Inlet temperature, °C (°F)	949 (1741)
Inlet pressure, MPa (psia)	4.62 (670)
Outlet temperature, °C (°F)	656 (1213)
Outlet pressure, MPa (psia)	4.56 (661)
Steam generator	
Inlet temperature, °C (°F)	656 (1213)
Inlet pressure, MPa (psia)	4.54 (659)
Outlet temperature, °C (°F)	419 (787)
Outlet pressure, MPa (psia)	4.53 (657)
Circulator	
Inlet temperature, °C (°F)	419 (787)
Inlet pressure, MPa (psia)	4.53 (657)
Outlet temperature, °C (°F)	427 (801)
Outlet pressure, MPa (psia)	4.64 (673)
Process plant	
Reformer	
Inlet temperature, °C (°F)	538 (1000)
Inlet pressure, MPa (psia)	4.95 (718)
Outlet temperature, °C (°F)	632 (1170)
Outlet pressure, MPa (psia)	4.74 (688)
Electricity generating plant	
Steam generator	
Inlet temperature, °C (°F)	260 (500)
Inlet pressure, MPa (psia)	20.0 (2900)
Outlet temperature, °C (°F)	566 (1050)
Outlet pressure, MPa (psia)	17.2 (2500)

4.2. DECAY HEAT REMOVAL (6053010200)

4.2.1. Scope

The scope of this task is to define and evaluate a decay heat removal system concept for the HTGR-MRS/PH plant.

4.2.2. Discussion

4.2.2.1. Introduction. Definition of the HTGR-MRS/PH design and decay heat requirements has been progressing over the past several months. Figure 4-2 shows the current reactor vessel design, and Fig. 4-3 shows the vessel cooling coil concept being considered in decay heat removal studies (Ref. 4-1). The following summary describes the results to date in the area of decay heat removal.

The decay heat removal configuration proposed for the HTGR-MRS/PH is as follows:

1. One main cooling system (MCS), nonsafety grade.

2. One redundant (two independent 100% loops) vessel cooling system (VCS), safety grade.

The proposed configuration contains one circulator with a main motor and an independently powered pony motor with 100% capacity for depressurized cooldown. Because there is only one circulator, no check valve is required on the primary coolant side. A valve located near the bottom of the steam generator allows the helium to bypass the steam generator during VCS operation.

The major criteria that establish decay heat removal requirements for the MRS-PH are discussed below together with key initiating events that establish VCS performance requirements. The decay heat removal system configuration is discussed to outline the systems and their sequence of

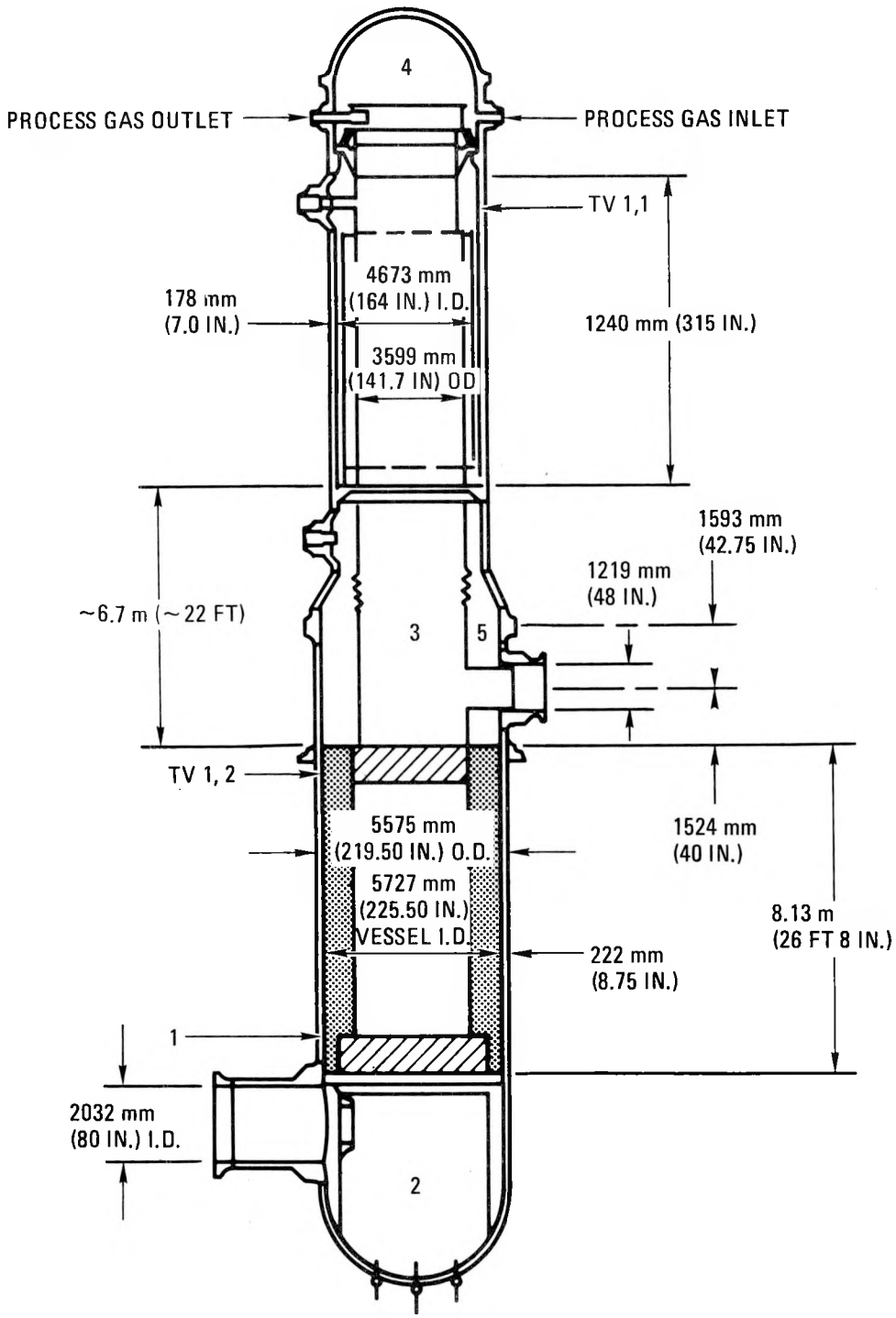

Fig. 4-2. Reactor vessel design (Ref. 4-1)

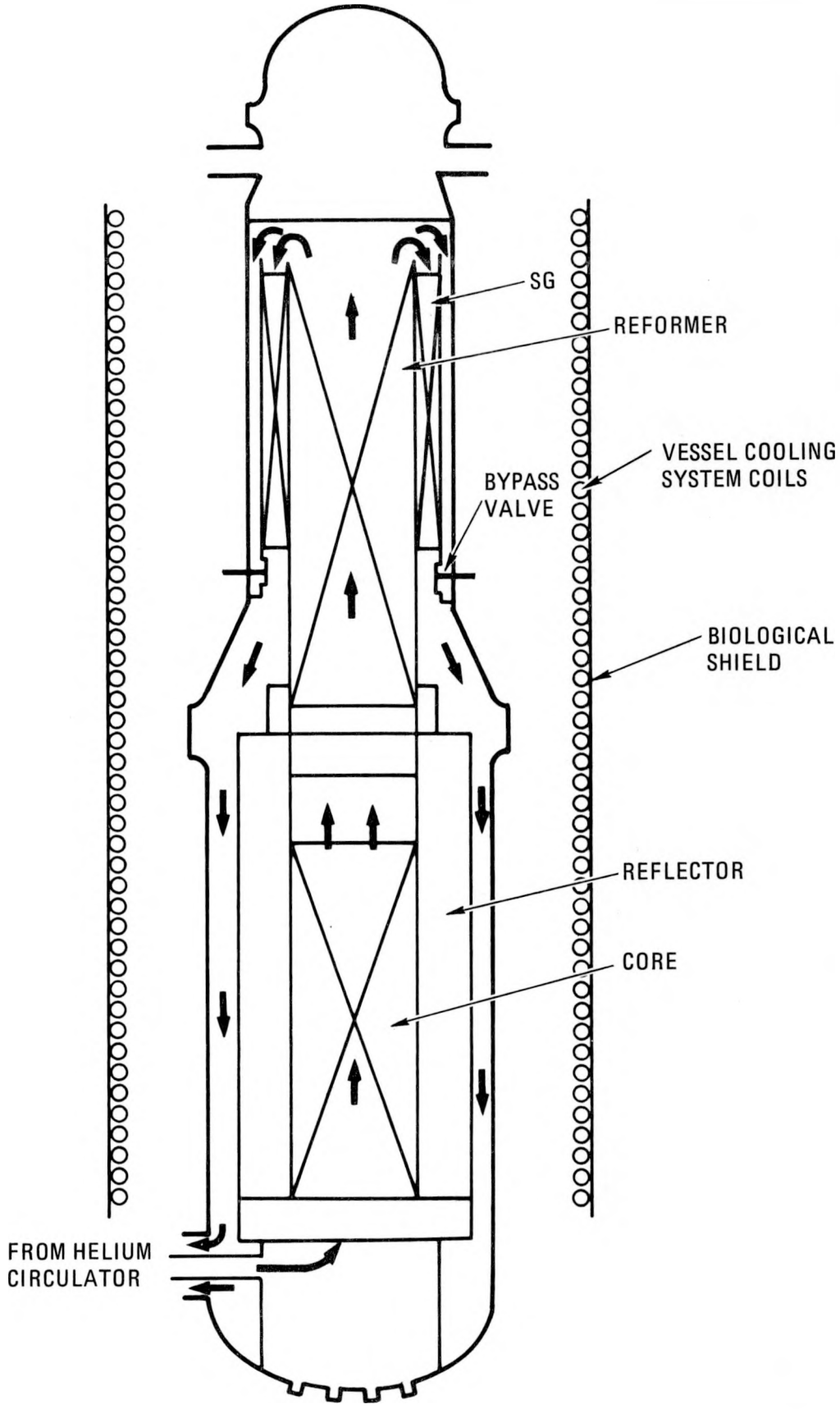

Fig. 4-3. Vessel cooling coil concept (Ref. 4-1)

operation, and a summary is presented of the transient analyses that have been performed to date. The discussions include a parameter study of normal (forced circulation) decay heat removal; natural circulation core cooling with decay heat removal by the MCS; a parameter study of natural circulation core cooling with decay heat removal by the VCS; and a parameter study of natural circulation core cooling with decay heat removal provided by a flow of air over the outside surface of the vessel.

4.2.2.2. Criteria. The primary guiding criteria applicable to decay heat removal are General Design Criterion 34 (Residual Heat Removal), General Design Criterion 35 (Emergency Core Cooling), and 10CFR50, paragraph 50.46 (Acceptance Criterion for Emergency Core Cooling Systems for Light Water Nuclear Power Reactors). Additionally, it is desired to satisfy the reliability goal for frequency of unrestrained core heatup of less than 10^{-4} per reactor year and the plant conditions (PC-1 to PC-5) which allow given consequences for events of given frequencies. (Note: It is unclear whether the criterion of 10^{-4}/reactor year will have to be met for loss of convective cooling, since the consequences of such an event are much less for the small HTGR than for the LWR core melt accident upon which the criterion is based.) The intent of Criterion 34 is to protect the integrity of the core and the coolant pressure boundary for pressurized decay heat removal assuming a single failure. Criterion 35 addresses loss of coolant (depressurized) cooldown. Due to the unique nature of gas cooling, one system (the CACS), which is single-failure-proof, is designed to satisfy the intent of both of these criteria for the large HTGR (Ref. 4-2). A similar approach using one system should be possible for small reactors providing that the system can meet the intent of these two criteria both pressurized and depressurized.

The following criteria based on Ref. 4-2 therefore establish the primary requirements for decay heat removal by the VCS.

Criterion 34 - Vessel Cooling System

A system shall be provided to remove fission product decay heat and other residual heat from the core at a rate such that specified acceptable limits of the fuel and other components within the primary coolant system boundary are not exceeded. The system, in conjunction with the protection and reactivity control systems, shall be capable of removing heat at a rate sufficient to prevent any damage that could inhibit effective core cooling following the loss of main loop cooling in conjunction with any anticipated operating occurrence or postulated accident, including a design basis depressurization accident (DBDA).

Suitable redundancy in components and features, and suitable interconnections, leak detection, and isolation capabilities, shall be provided to assure that for on-site electric power system operation (assuming off-site power is not available) and for off-site power system operation (assuming on-site power is not available), the system safety function can be accomplished assuming a single failure.

Criterion 35 - (Unnecessary, Intent Included in Restatement of Criterion 34 Above)

"Specified acceptable limits" discussed in Criterion 34 is addressed by means of the Plant Conditions which allow more severe consequences for less frequent events. A complete assessment of a full range of initiating events is beyond the current scope of this study. However, based upon a preliminary assessment of the frequency of key events that require VCS operation [loss of main cooling system (pressurized), loss of main cooling system during refueling, and DBDA], the following minimum performance requirements are proposed for the VCS:

Loss of MCS (pressurized). Maintain PC-2 (upset) conditions.

Loss of MCS (refueling). Maintain PC-2 (upset) conditions.

DBDA. Maintain PC-5 (faulted) conditions. This includes but is not limited to requirements to do the following:

- Maintain coolable core geometry and reactivity control.
- Maintain long-term heat removal.
- Prevent rapid, thermally induced fuel particle failure from propagating to a significant volume of the core.

4.2.2.3. Configuration.

Main Cooling System (MCS)

The MCS normally cools the core following reactor trip. The HTGR-MRS/PH secondary system is expected to employ standard components similar to those shown in Fig. 4-4. The system is, in general, not safety class. However, the single steam generator and the steam generator isolation valves and steam generator dump system are safety class components. To increase the MCS core cooling reliability, feedwater heater bypasses and redundant pumps are recommended as shown in Fig. 4-4.

If the steam generator is available for decay heat removal, forced primary coolant flow can be maintained pressurized or depressurized by either the main motor or the pony motor. If the circulator is not operational, core cooling can be induced by natural circulation (pressurized) across the steam generator coils through the circulator. The MCS is used in the forced convection mode to cool the core during refueling. In all cases, the reformer is isolated on the secondary side and is not used for decay heat removal.

Vessel Cooling System (VCS)

The VCS is used if the MCS is not available (see Figs. 4-3 and 4-5). The VCS is composed of redundant, alternating cooling coils that are mounted

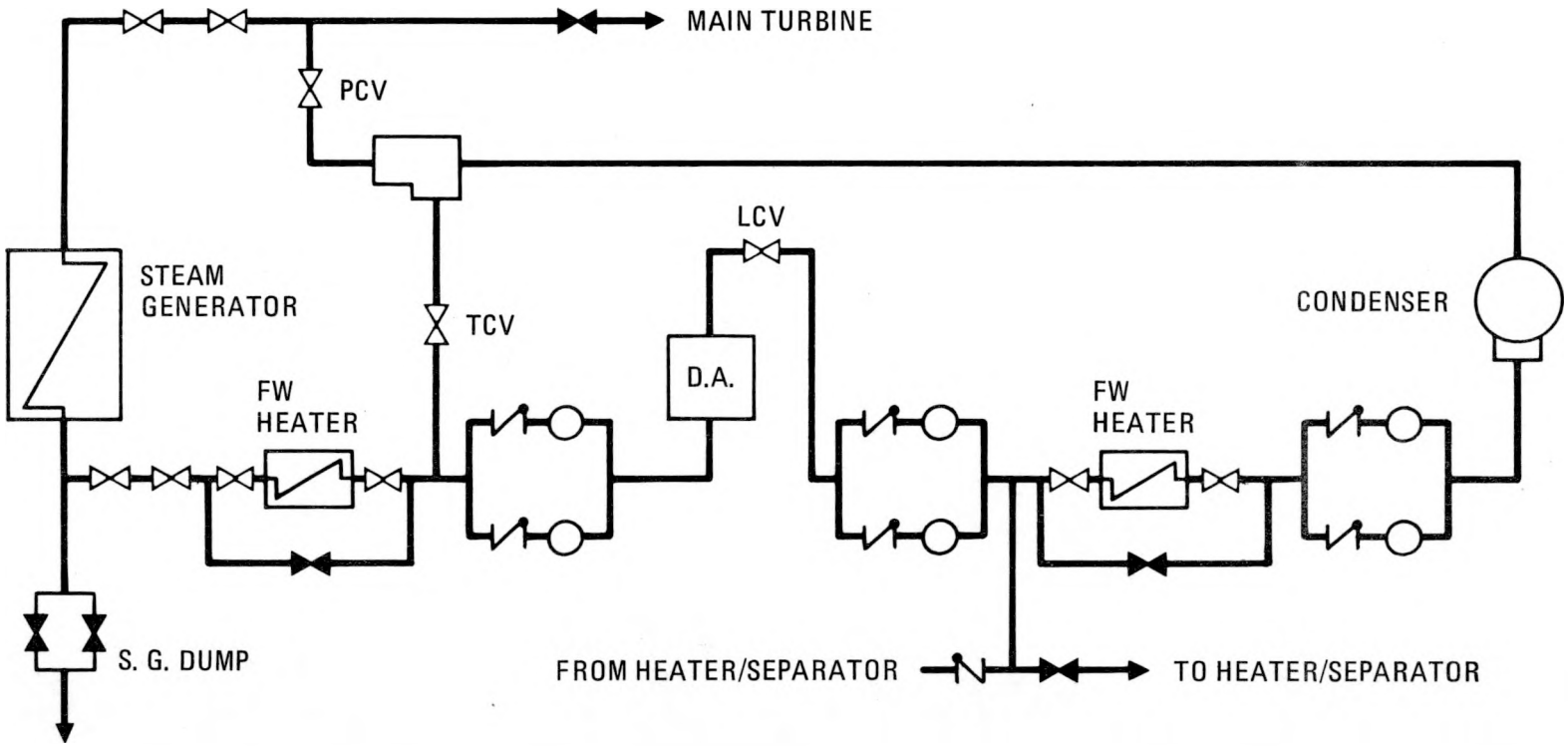

Fig. 4-4. HTGR-MRS/PH main cooling system shutdown cooling

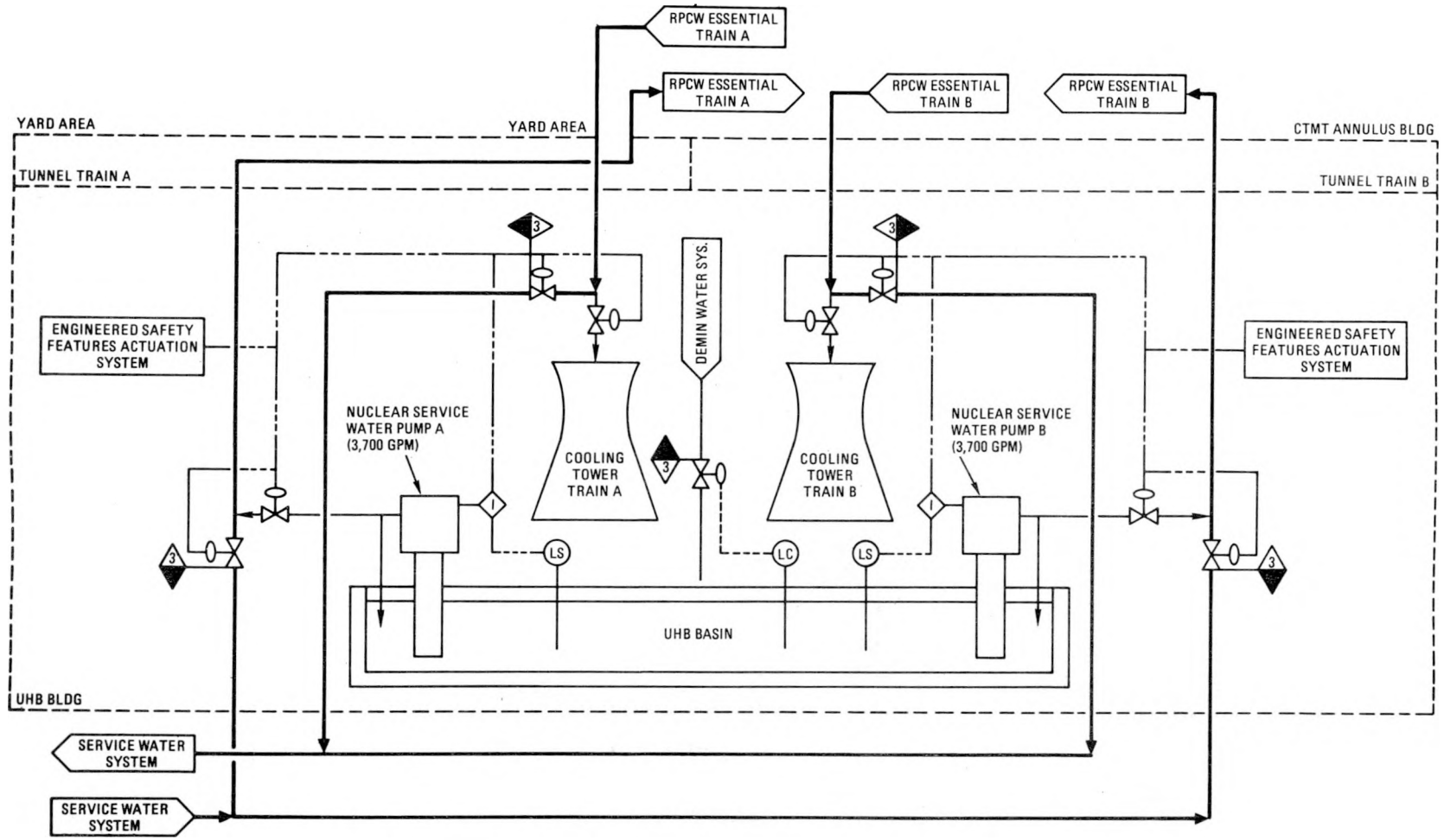

Fig. 4-5. Ultimate heat sink configuration for redundant VCS's (Note: VCS "A" cooling coils replace the liner cooling system loop associated with RPCW train A; VCS "B" is associated with train B in a similar manner (Ref. 4-3).

on the containment liner which is backed by a biological shield as shown in the sketch in Fig. 4-3.

For pressurized cooldown the coils cool the vessel (primarily by radiation), which in turn cools the primary coolant forming a relatively cool "cold leg" for induced natural-circulation cooling of the core. The primary coolant flow path along the upper vessel wall is located near the bottom of the steam generator. During normal forced cooling operation, these valves remain in the closed position.

For depressurized cooldown following a depressurization accident and loss of the MCS and circulator, heat is removed from the core radially by conduction and radiation. This is expected to be somewhat augmented by natural circulation due to the back pressure provided by the closed individual confinements.

The ultimate heat sink configuration shown in Fig. 4-5 is being utilized for preliminary reliability studies. A more complete description of this system and its operation is contained in Ref. 4-3.

The VCS is intended to be designed for both pressurized and loss-of-coolant (depressurized) cooldown so that one system satisfies the intent of both General Design Criterion 34 and General Design Criterion 35, as the CACS does for the large HTGR. Two independent (100% each) loops (minimum)* are provided to satisfy the single failure criterion, assuming neither loop is involved in the initiating event.

4.2.2.4. Sequence of Operation. For pressurized or depressurized core cooldown, the MCS is the first line of defense and uses the secondary coolant configuration described previously and shown in Fig. 4-4. The sequence of cooling system operation is somewhat different on the primary side,

---

*Note: Other combinations such as three 50% loops may be more desirable for reliability and availability, particularly for commercial-size plants (i.e., eight modules).

however, depending on whether the reactor is pressurized or depressurized. In all cases the reformer is isolated on the secondary side and is not utilized for decay heat removal.

Pressurized

The lines of defense for core cooling are as follows:

- Forced: MCS, main circulator motor.
- Forced: MCS, pony motor.
- Natural circulation: MCS (through steam generator).
- Natural circulation: VCS (through bypass).

Depressurized

- Forced: MCS, main circulator motor.
- Forced: MCS, pony motor.
- Conduction and radiation to VCS augmented by natural circulation.

Note: MCS cooling in either the forced or natural circulation mode requires that the steam generator be available and secondary coolant flow plus an ultimate heat sink be maintained. If any of these items are unavailable, the next line of defense is the VCS.

4.2.2.5. Performance Transients. To determine the transient design requirements on the various components comprising the HTGR-MRS/PH under various modes of core cooling and to suggest alternate design strategies, several key decay heat removal transients have been simulated. These include normal reactor trip using the MCS and forced circulation core cooling, natural circulation core cooling using the MCS, and natural circulation core cooling using the VCS. Additionally, a potential mode of vessel (and consequently also core) cooling using a forced flow of air over the exterior of the vessel was analyzed. These cases were analyzed by modifying an existing

GA computer code, NATCIR, to accommodate the HTGR-MRS/PH configuration. The design and simulation were evolving as these cases were analyzed; therefore, comparison between cases may not always be meaningful. The HTGR-MRS/PH design analyzed is primarily that presented at the summary review meeting held January 26, 1982, at General Electric, Sunnyvale (Ref. 4-1). The basic vessel configuration is shown in Fig. 4-2.

Forced Circulation Core Cooling with Decay Heat Removal by MCS (Cases 1A, 1B, and 1C)

This transient (Ref. 4-4) is simulated by the following sequence of events. At time 0^- the reactor is at the steady state shown in Fig. 4-6 and has been operating at that steady state for an extended period of time. At time 0^+ the reactor is tripped and the circulator is run back at 1/2% per second to a lower speed. The reformer secondary is isolated at the time of reactor trip, and this is simulated as an adiabatic boundary condition at the inside surface of the reformer tubes. The steam generator feedwater flow is run back beginning at time 0^+. The steam generator tube temperature response is a simulation boundary condition and has been estimated for preliminary HTGR-MRS/PH core cooling studies from FSV actual and simulated transient data. The estimated transient response of the vessel internals for the above sequence of events is shown in Figs. 4-7A through 4-7G. (Locations of temperatures indicated by numbers on Figs. 4-7B and 4-7E are shown in Fig. 4-2.) For this base case (Case 1A) the final circulator speed is 15%. All temperatures and pressures decrease following reactor trip with the exception of the reformer tube and helium outlet temperatures, which approach the core outlet temperature. The steam generator upper bundle tube temperatures may also increase somewhat, but this is not currently simulated. To determine whether the reformer tube temperature peak could be reduced by an increased flow of helium following reactor trip, two additional cases were analyzed for which the circulator speed following coastdown was 25% (Case 1B) and 35% (Case 1C). A comparison of the peak values of the major parameters simulated for these cases is shown in Table 4-2. The steady-state condition is the peak value of all parameters shown, except

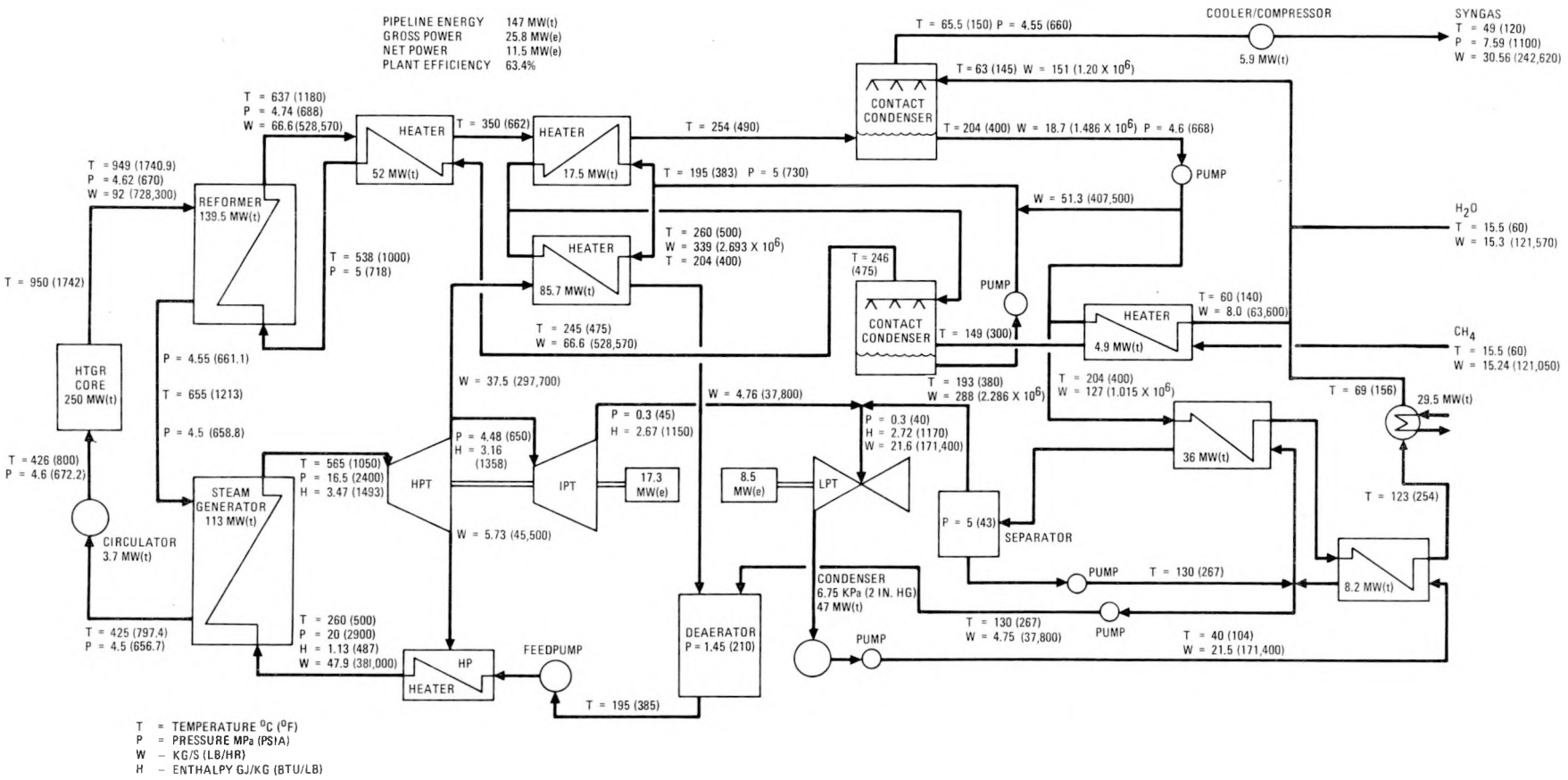

Fig. 4-6. Modular HTGR-R plant heat balance

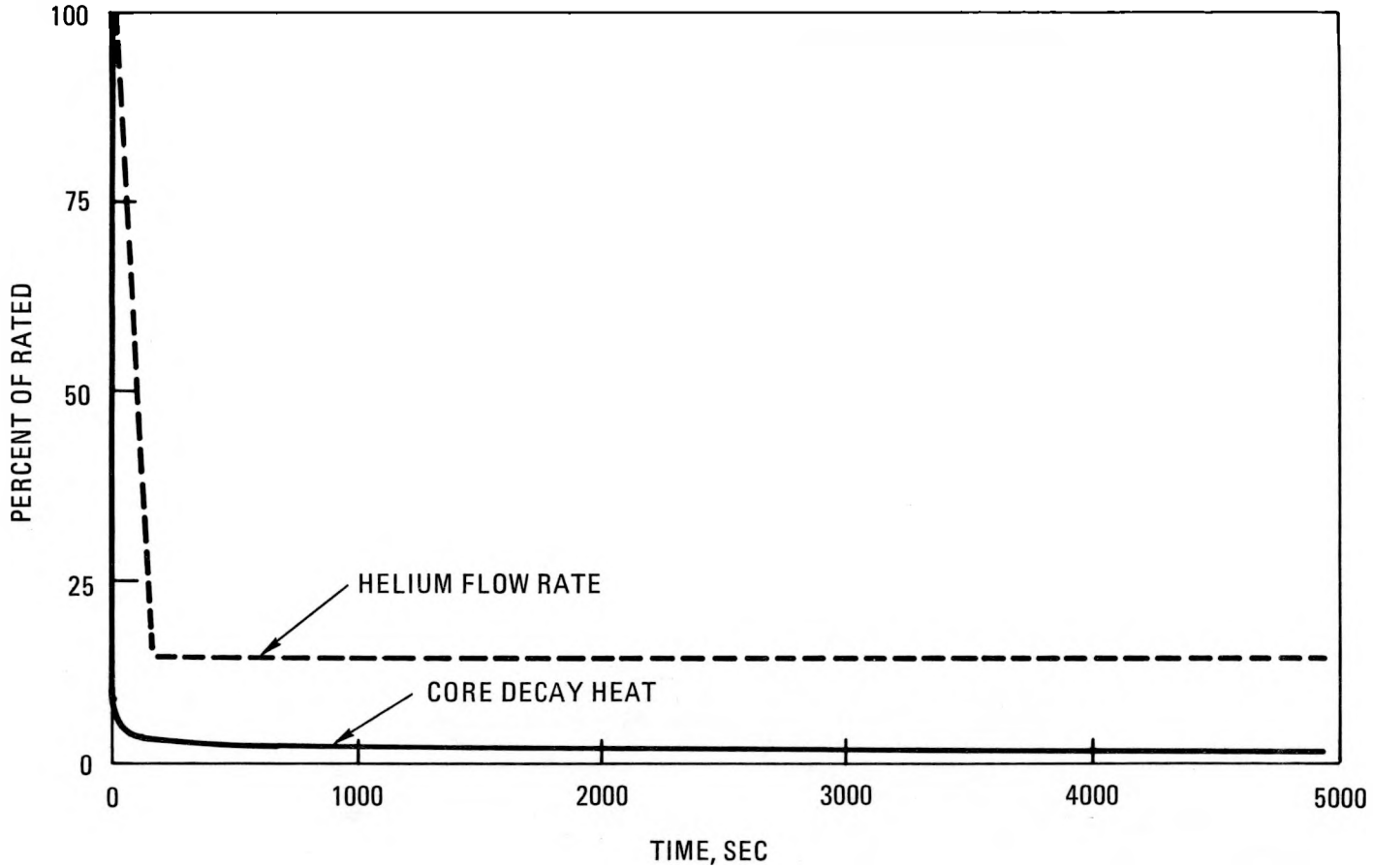

Fig. 4-7A. Normal reactor trip using MCS; circulator speed = 15%

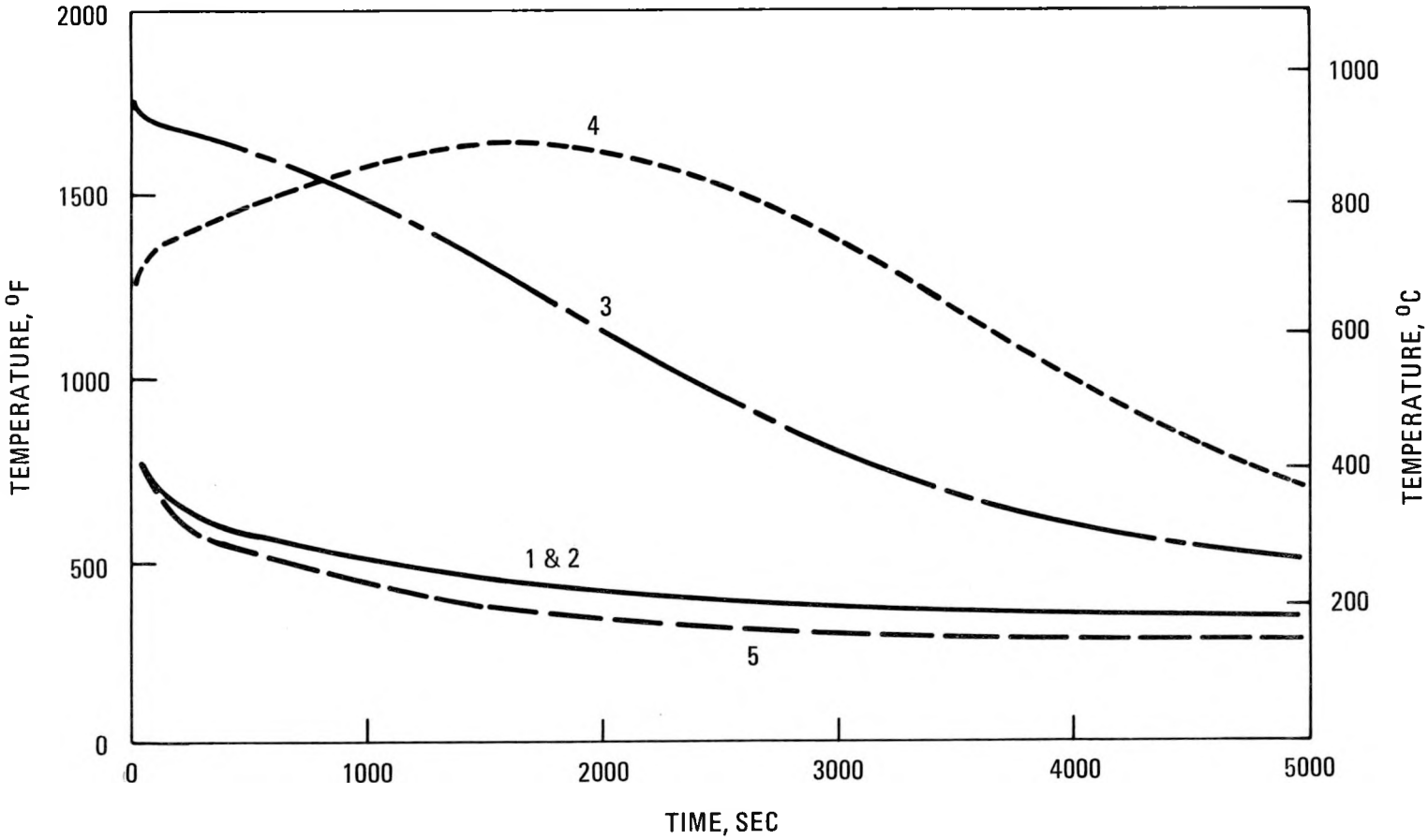

Fig. 4-7B. Helium temperatures

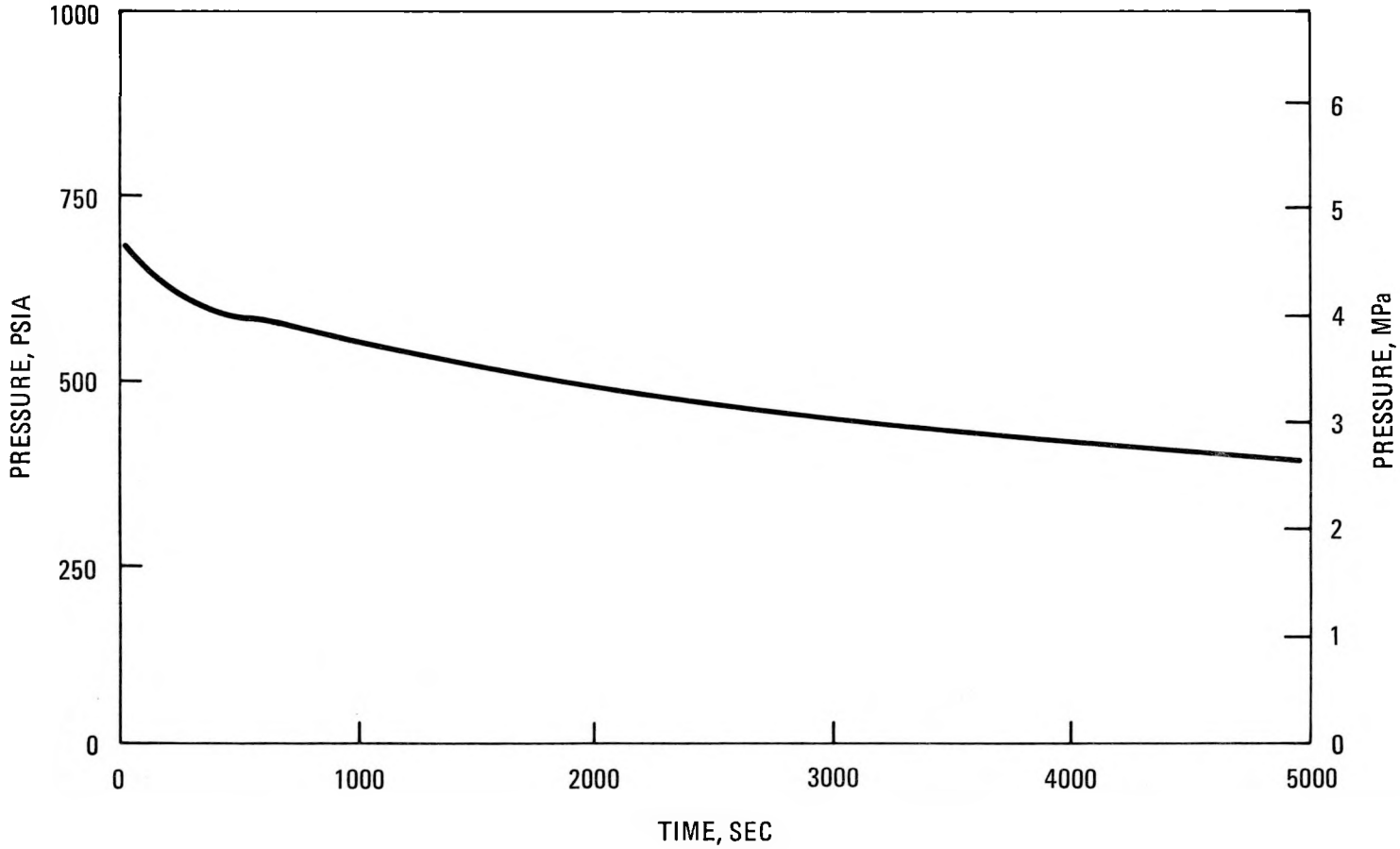

Fig. 4-7C. Pressure

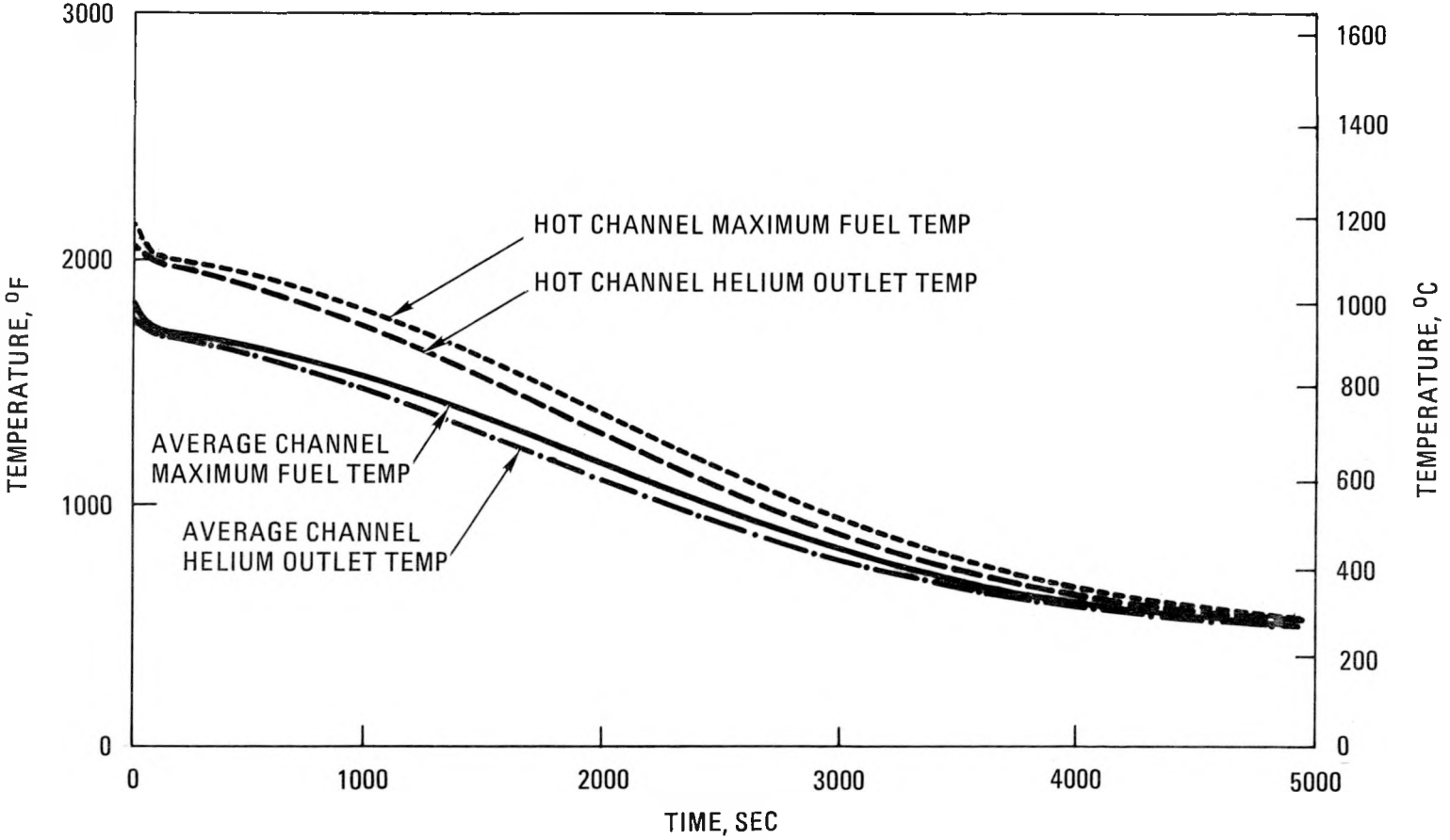

Fig. 4-7D. Core temperatures

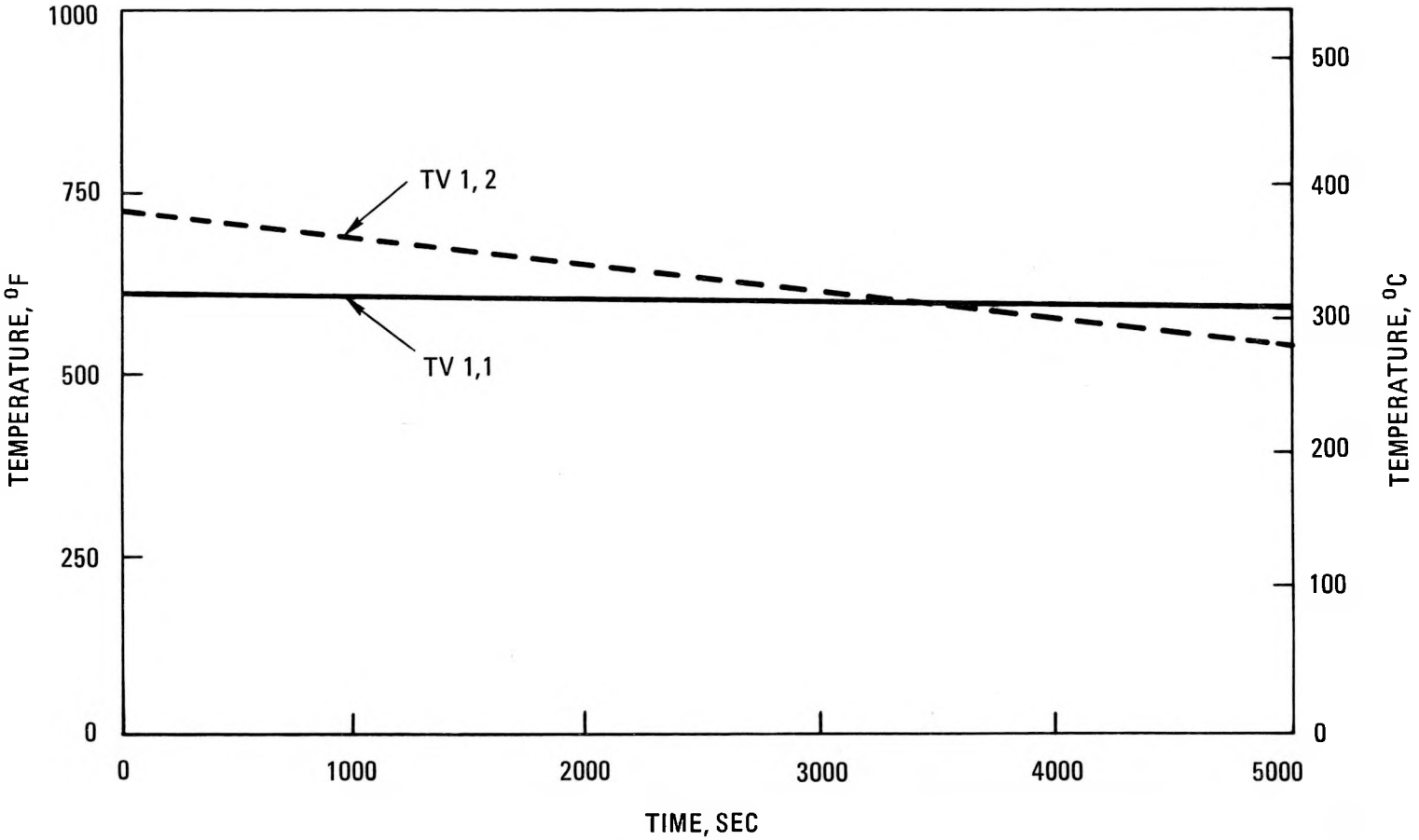

Fig. 4-7E. Vessel temperatures

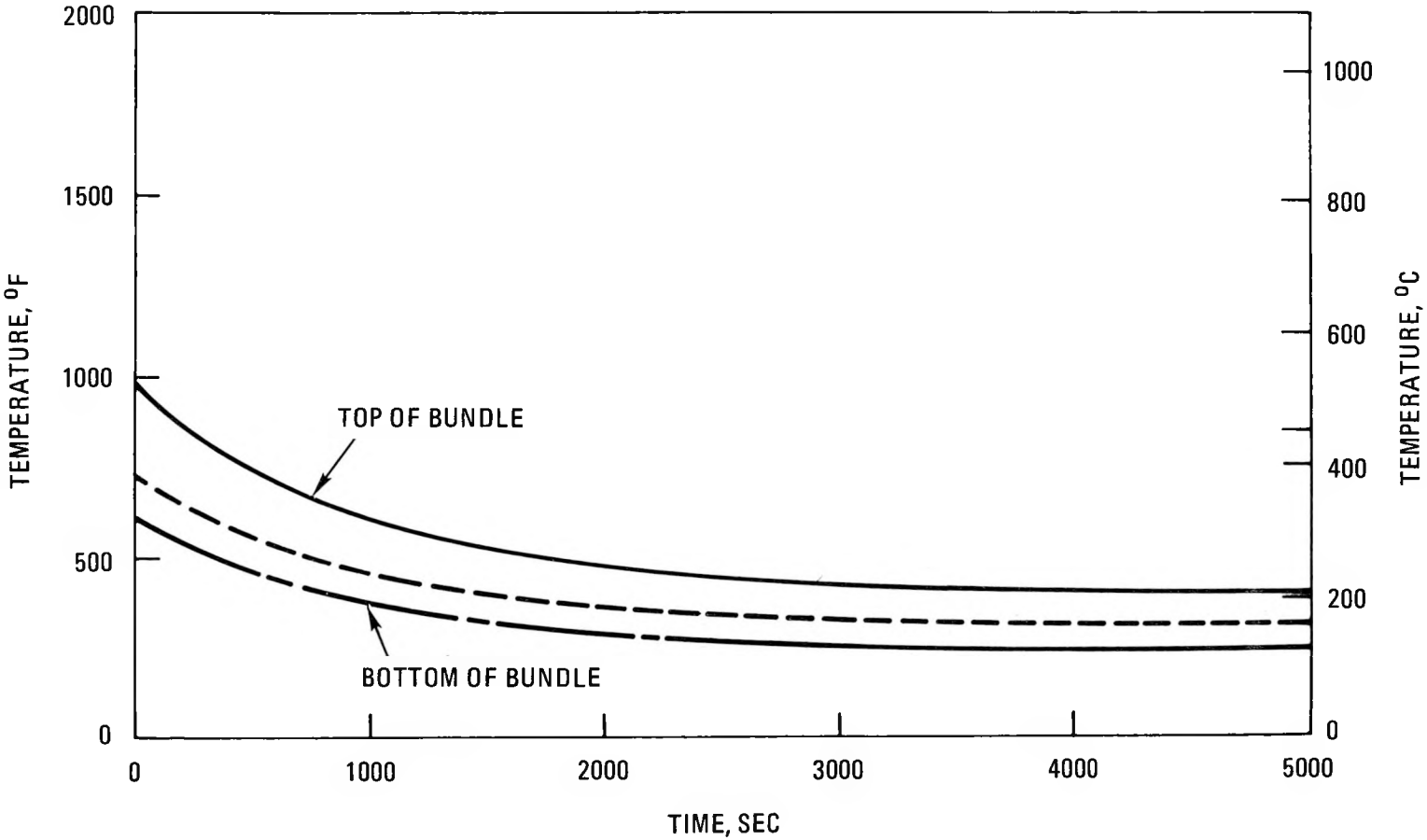

Fig. 4-7F. Steam generator tube temperatures (simulation inputs)

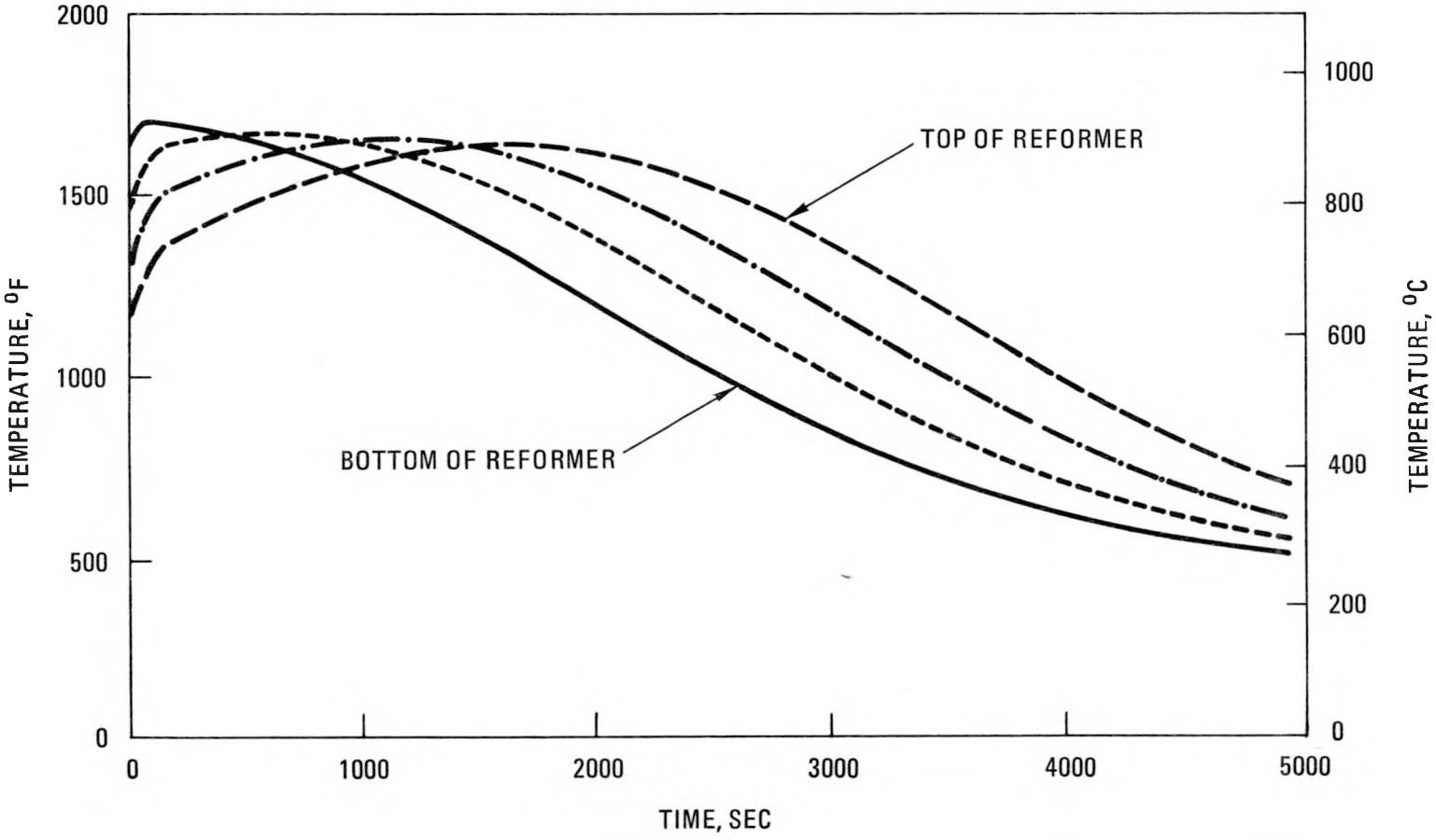

Fig. 4-7G. Reformer tube temperatures

TABLE 4-2
NORMAL REACTOR TRIP (MAIN COOLING SYSTEM, FORCED CIRCULATION)

	Normal (100%) Operation	1A	1B	1C
Circulator speed, % of rated	100	15	25	35
Maximum helium pressure, MPa (psia)	4.63 (672)	4.63 (672)	4.63 (672)	4.63 (672)
Maximum vessel midwall temperature, °C (°F)	382 (720)	382 (720)	382 (720)	382 (720)
Maximum core helium inlet temperature, °C (°F)	426.6 (800)	426.6 (800)	426.6 (800)	426.6 (800)
Maximum core average helium outlet temperature, °C (°F)	950 (1742)	950 (1742)	950 (1742)	950 (1742)
Maximum reformer helium outlet temperature, °C (°F)	656 (1213)	893 (1640)	882 (1620)	877 (1610)

for temperatures associated with the reformer. Figures 4-8 and 4-9 show the reformer tube temperature response for the additional cases. The increased helium flow rate can be seen to only slightly reduce the peak reformer tube and helium outlet temperatures at the expense of a more rapid thermal cycling of the reformer tubes. To lessen the differential thermal expansion design requirements of the reformer, a 15% circulator speed was selected for forced circulation core cooling on the MCS.

Natural Circulation Core Cooling with Decay Heat Removal by MCS (Case 2)

This transient is simulated by the following sequence of events. As previously, the reactor is initially at the operating condition shown in Fig. 4-6. At time 0^+ the reactor is tripped and electric power is assumed to be lost to drive the circulator so that the circulator begins to coast down. This is simulated by decreasing the circulator speed from 100% to 0% in 60 sec. A sensitivity study was performed to determine whether a bypass valve around the circulator would be required for natural circulation decay heat removal, and it was determined that a valve was not required (see information under next subheading). Pressure losses through the circulator annulus have been estimated from test data on a 1/3-scale model air flow test of the Del Marva circulator. The reformer is not used for decay heat removal and is isolated on the secondary side, as for the previous cases discussed. Secondary coolant (water) flow is maintained to the steam generator so that it ultimately floods out. The steam generator tube temperature, as stated previously, is a simulation boundary condition and has been estimated from other transient data. The estimated transient response of the vessel internals for the above sequence of events is shown in Figs. 4-10A through 4-10G. A summary of the key parameters is contained in Table 4-3 along with other natural circulation cases discussed below. As for the forced circulation MCS case already discussed, the steady-state condition is the peak value of all parameters except the reformer helium outlet temperature (and a small increase in the core exit temperature). Additionally, the reformer helium outlet temperature is about 55°C (100°F) hotter than that

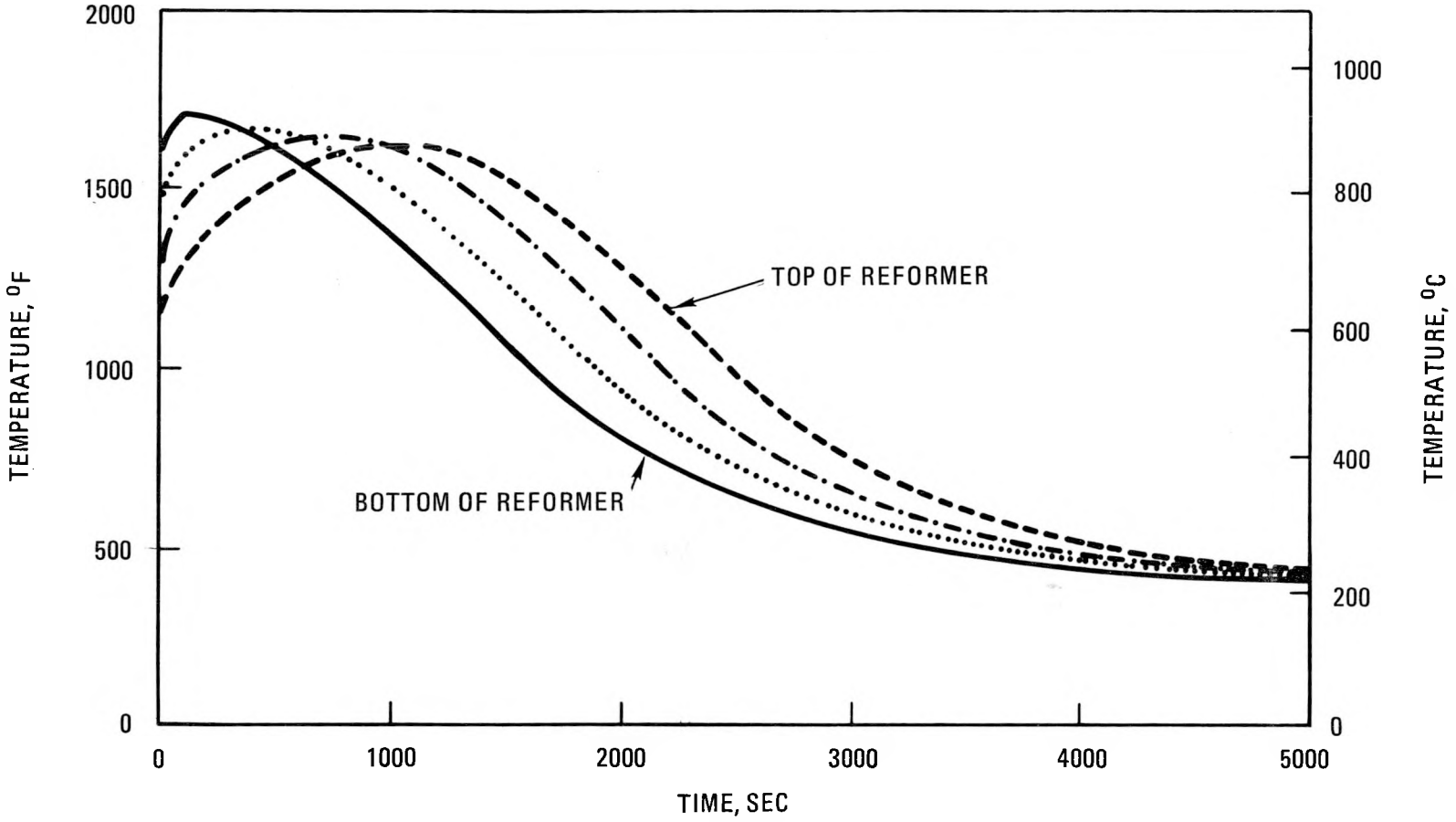

Fig. 4-8. Normal reactor trip using MCS; circulator speed = 25%

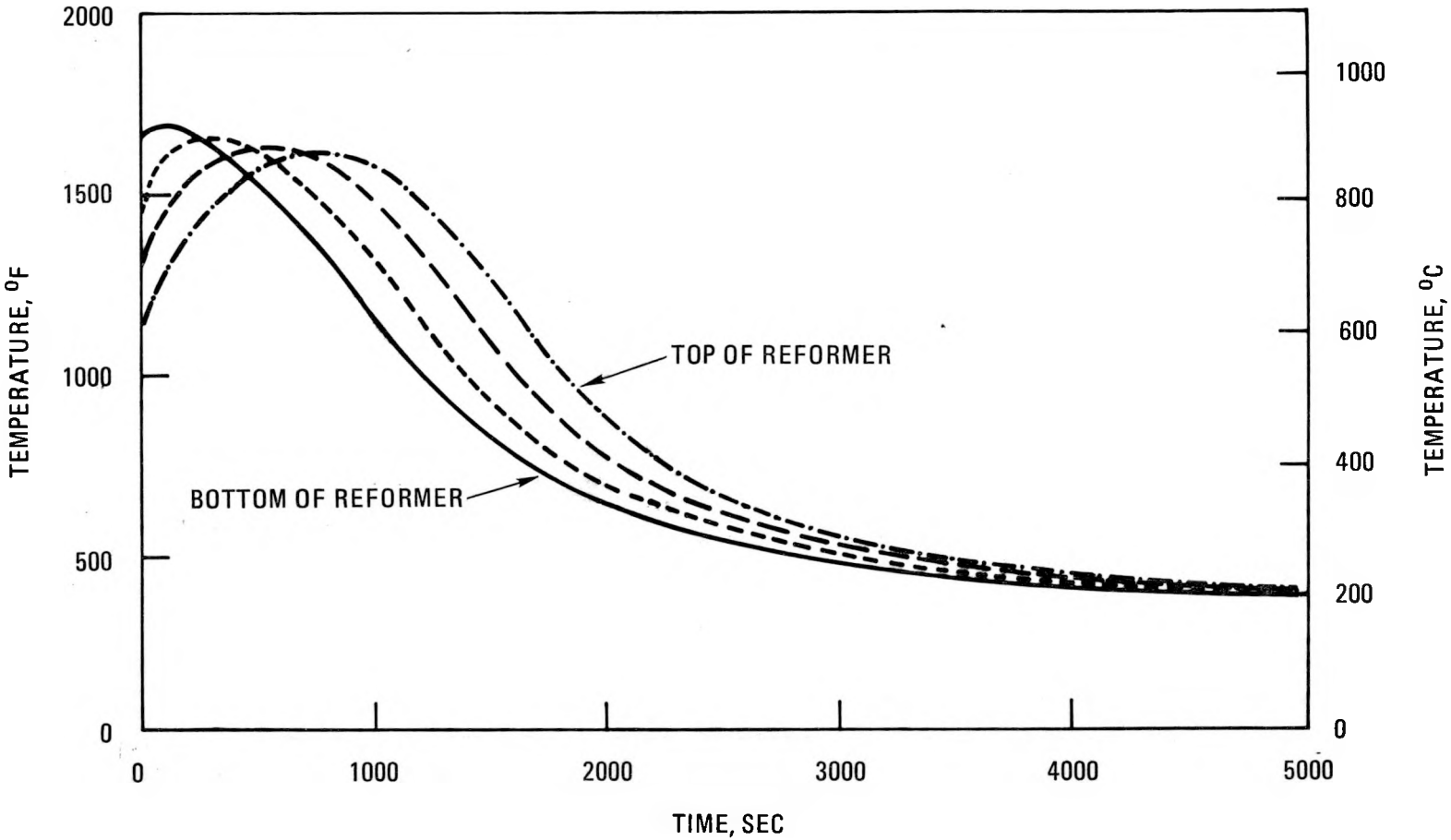

Fig. 4-9. Normal reactor trip using MCS; circulator speed = 35%

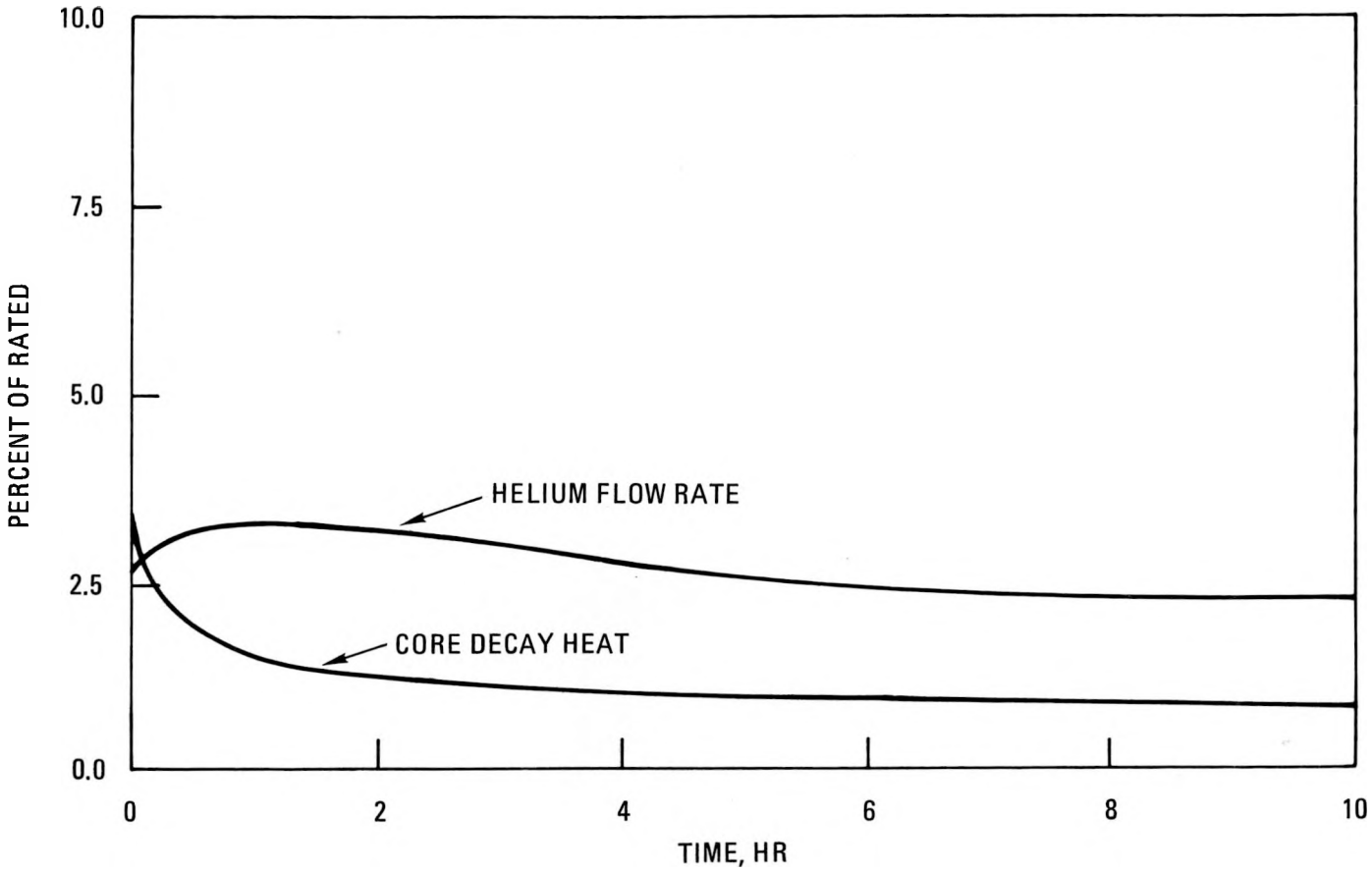

Fig. 4-10A. Natural circulation decay heat removal using MCS

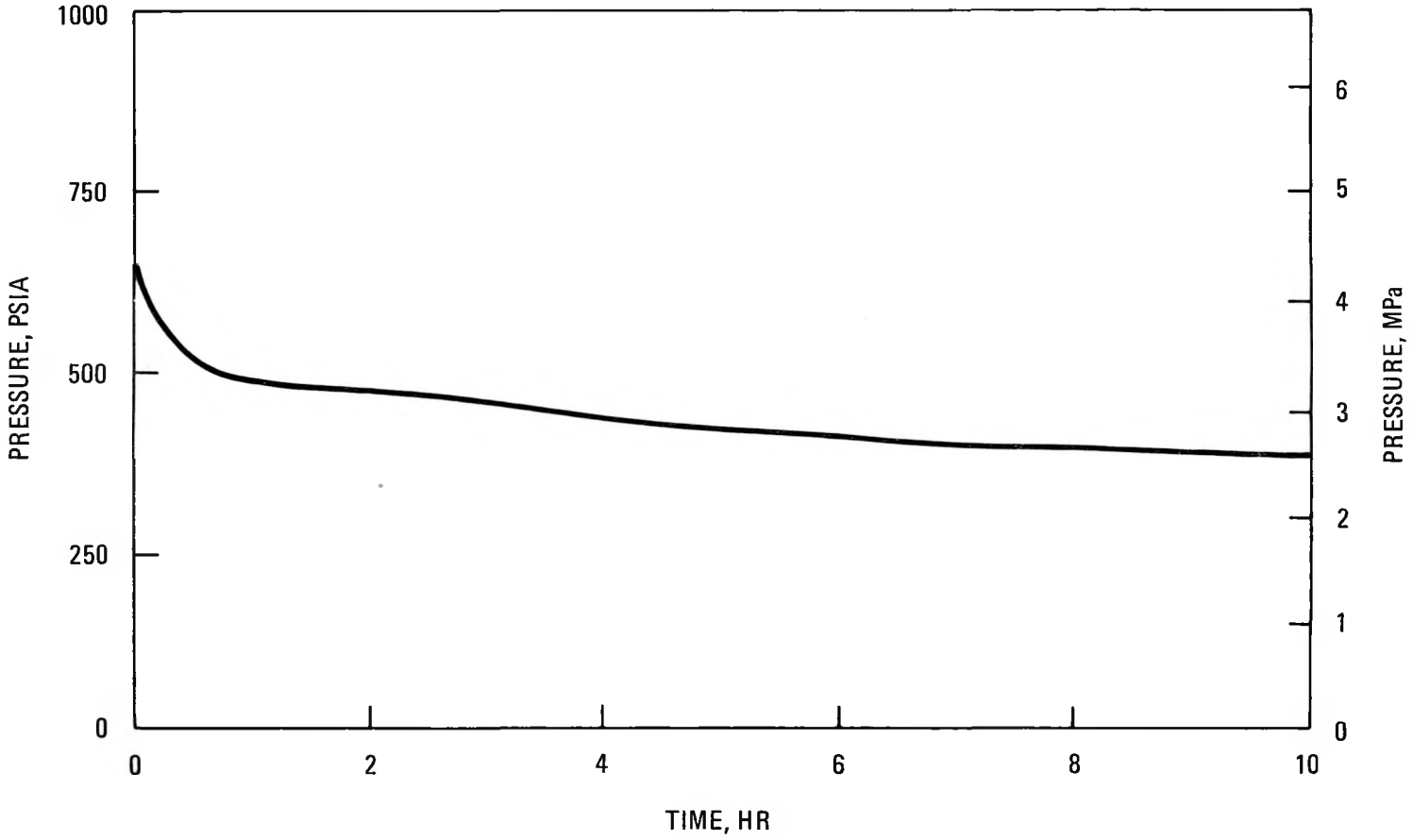

Fig. 4-10B. Pressure

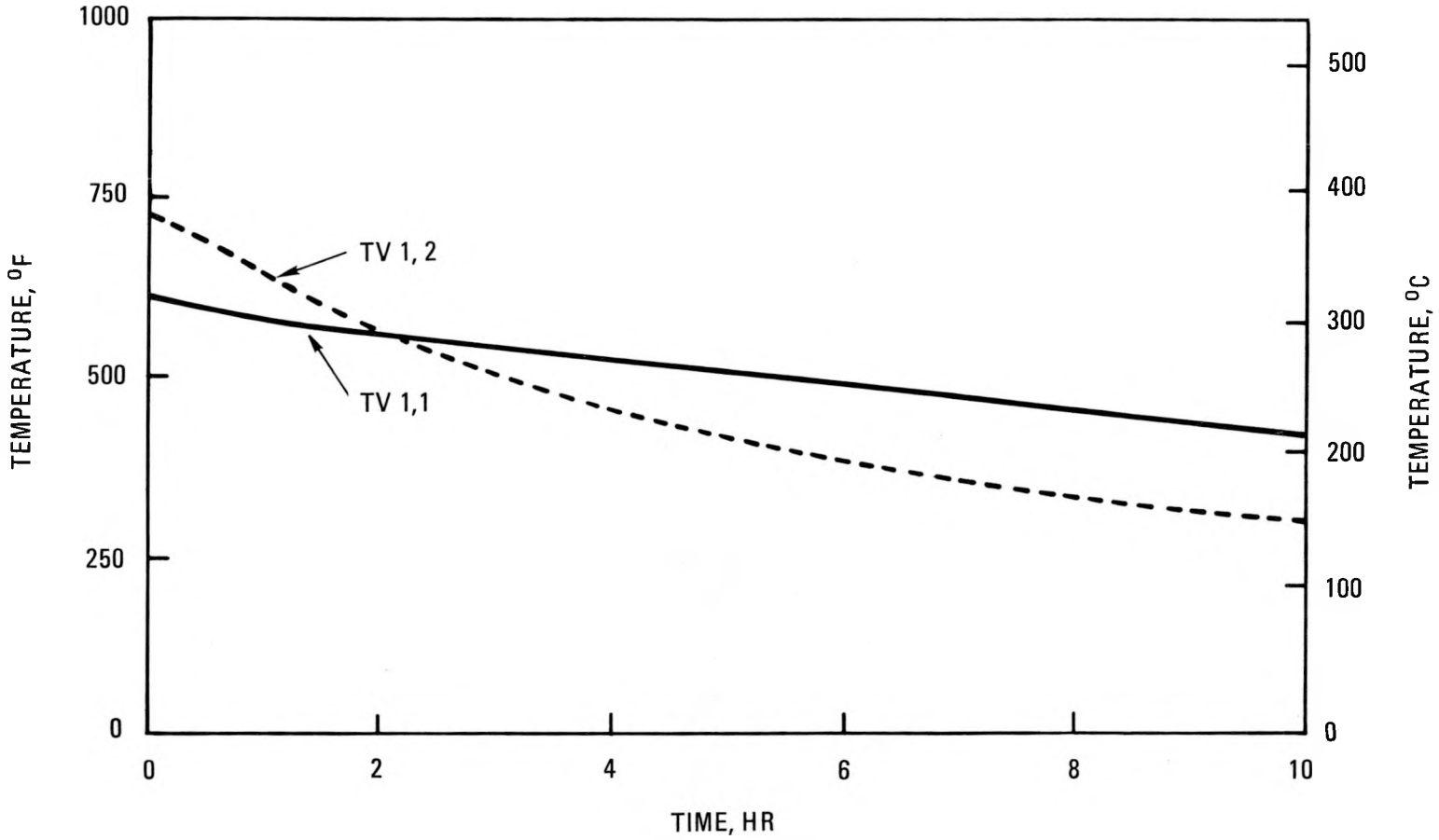

Fig. 4-10C. Vessel temperatures

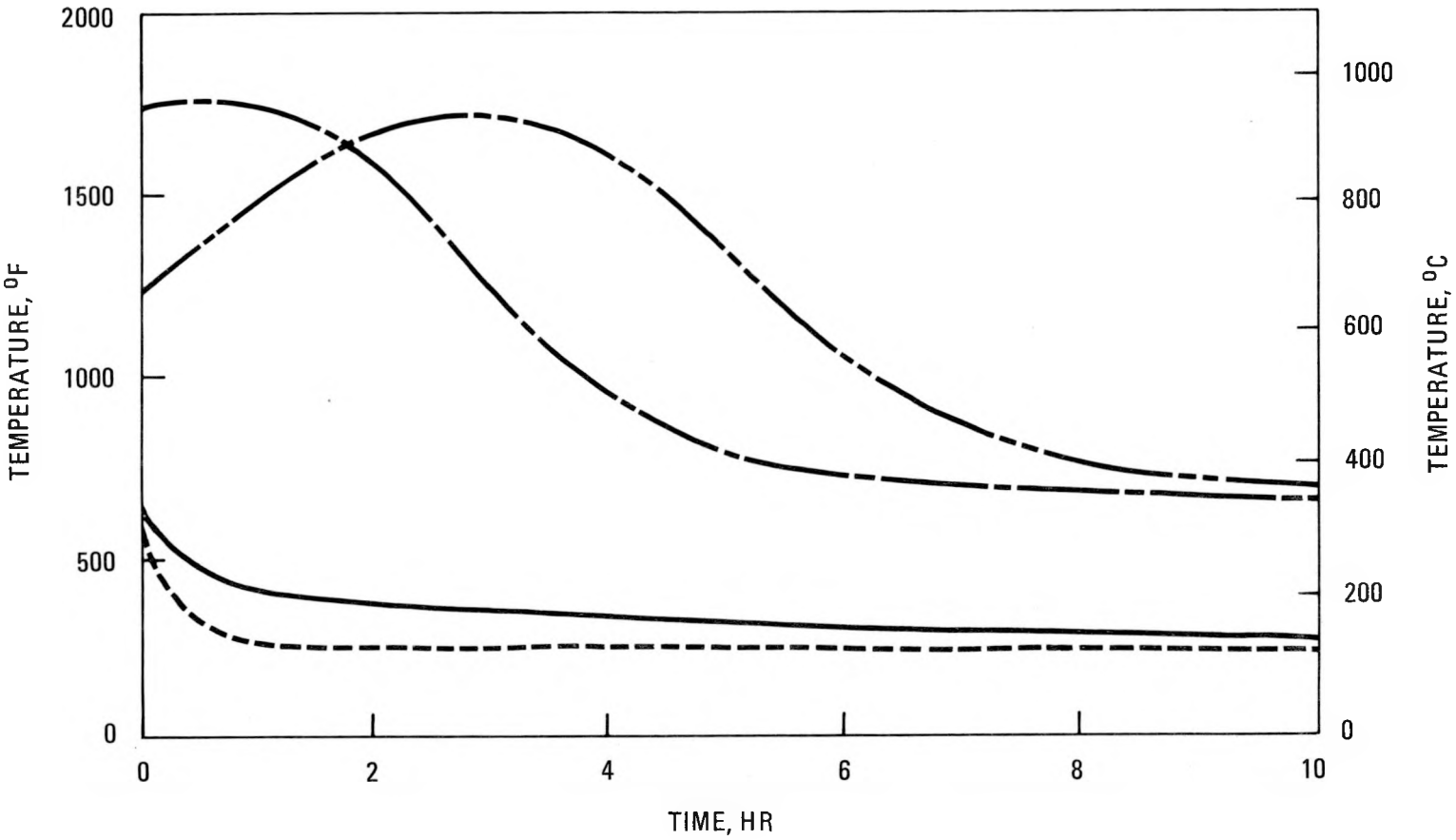

Fig. 4-10D. Helium temperatures

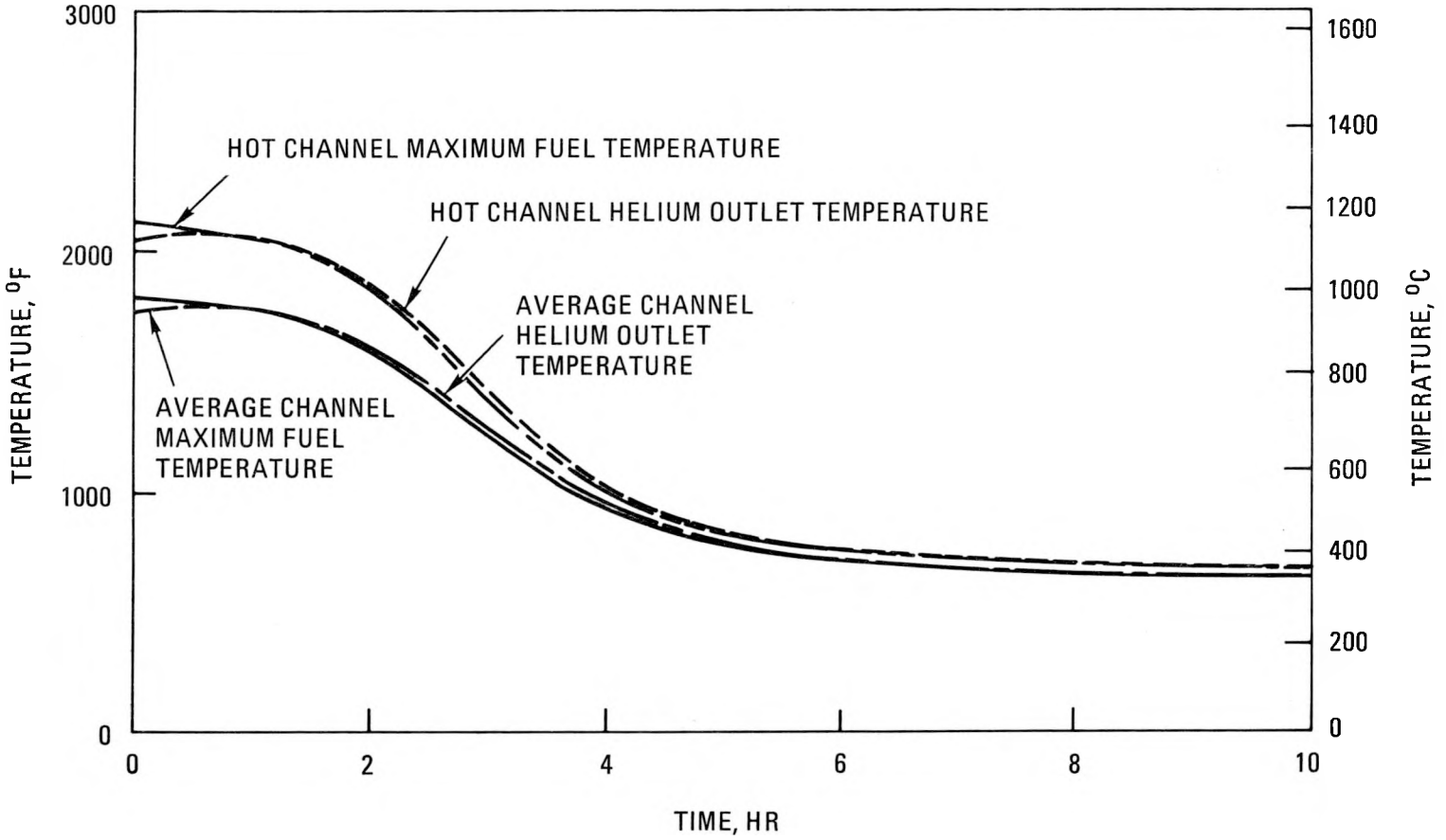

Fig. 4-10E. Core temperatures

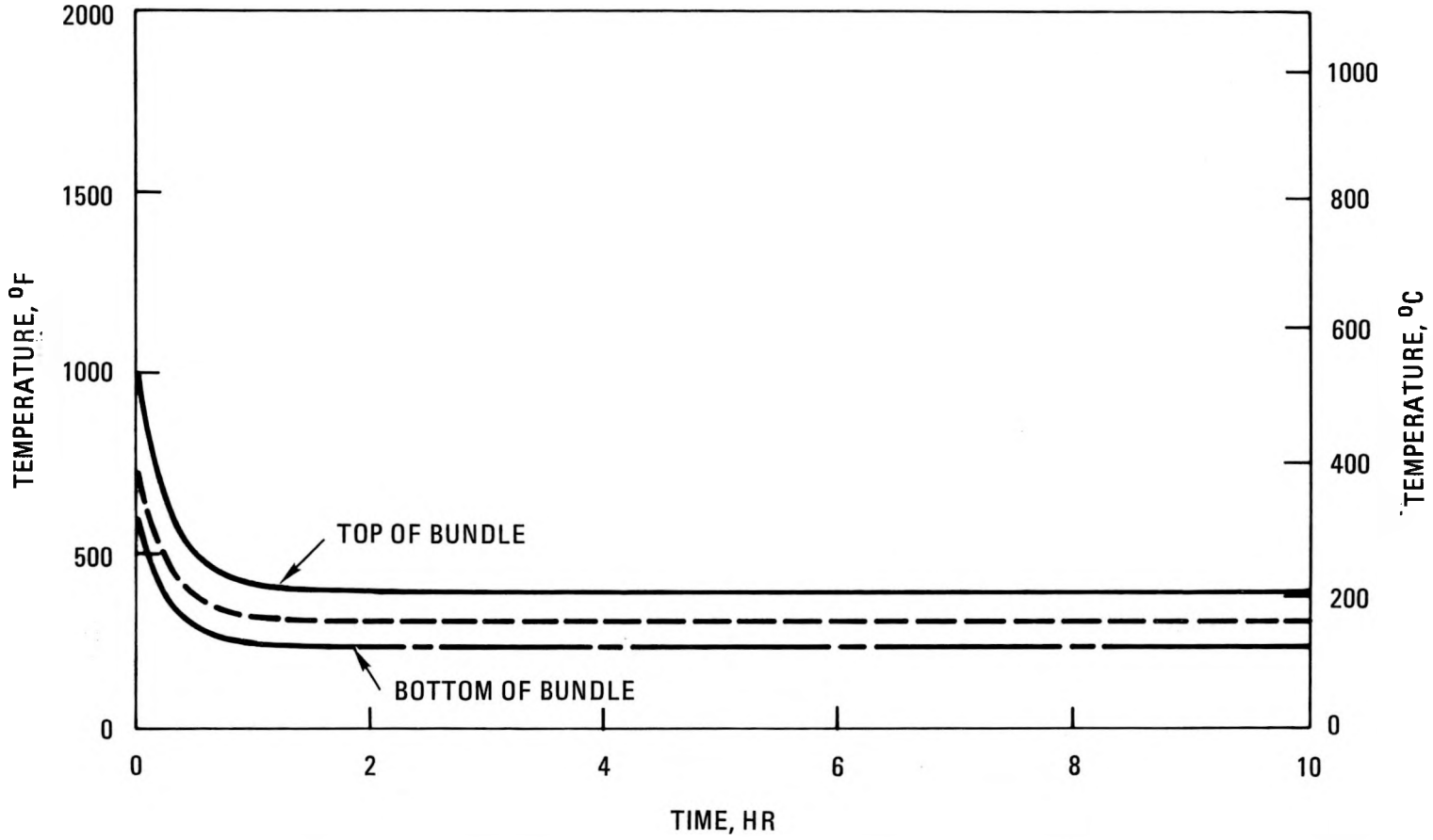

Fig. 4-10F. Steam generator tube temperatures

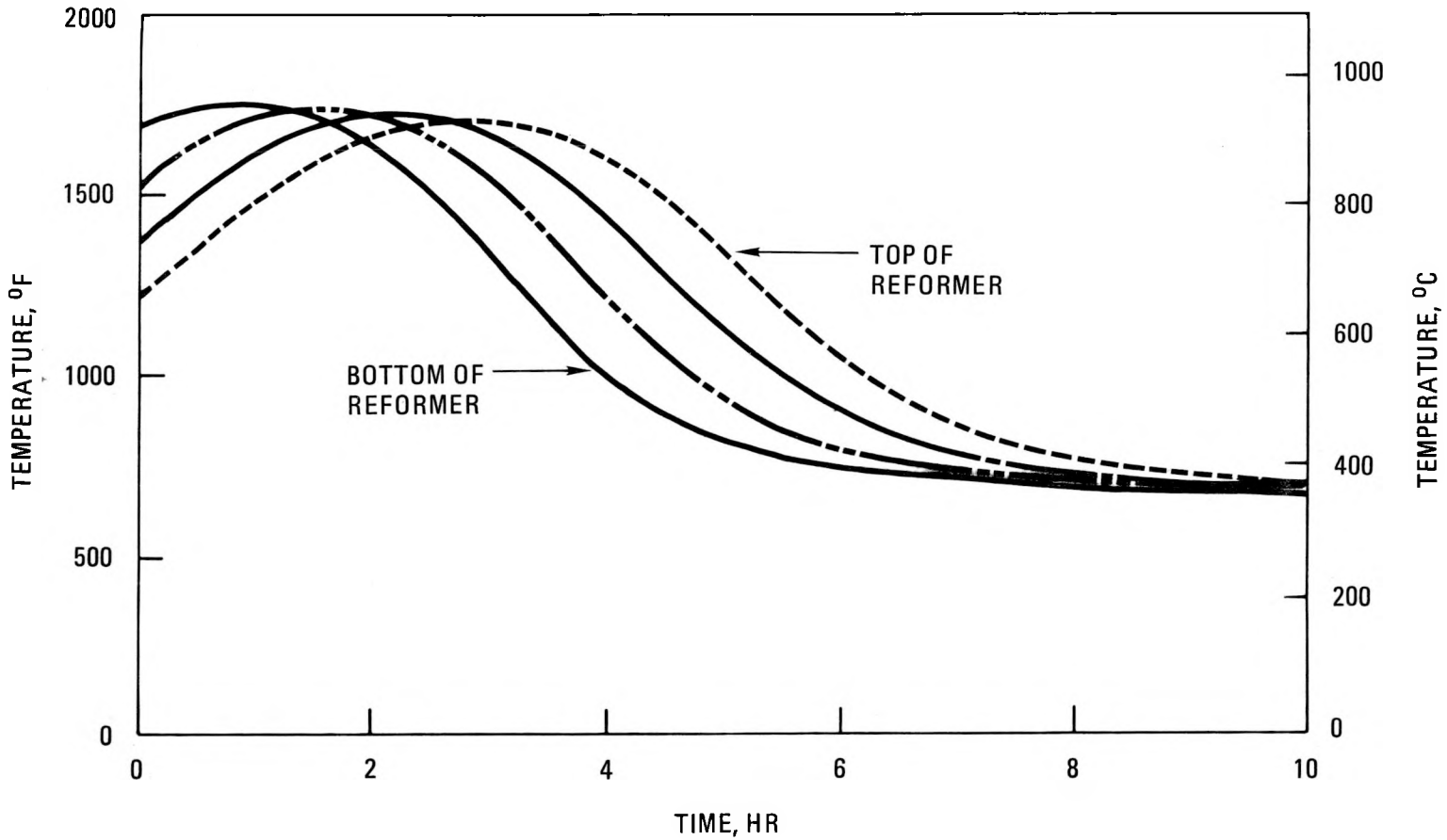

Fig. 4-10G. Reformer tube temperatures

TABLE 4-3
NATURAL CIRCULATION CORE COOLING (CASE 2: MAIN COOLING SYSTEM; CASES 3A THROUGH 3D: VESSEL COOLING SYSTEM)

	Normal 100% Operation	Case 2	Case 3A [76.2-mm (3-in.) top, 50.3-mm (2-in.) bottom]	Case 3B [152-mm (6-in.) top, 76-mm (3-in.) bottom]	Case 3C (Case 3A but with locked rotor)	Case 3D (Case 3A but with circulator bypass)
Natural circulation helium flow induced (at 7 hr, % of rated)	--	2.4	1.08	1.00	1.03	1.14
Maximum helium pressure, MPa (psia)	4.63 (672)	4.63 (672)	5.68 (825)	6.2 (900)	5.68 (825)	5.68 (825)
Maximum vessel midwall temperature, °C (°F)	382 (720)	382 (720)	468 (875)	413 (775)	469 (875)	476 (890)
Maximum core helium inlet temperature, °C (°F)	426 (800)	426 (800)	538 (1000)	643 (1190)	538 (1000)	549 (1020)
Maximum core average helium outlet temperature, °C (°F)	950 (1742)	960 (1760)	1010 (1850)	1052 (1925)	1038 (1900)	987 (1800)
Maximum reformer helium outlet temperature, °C (°F)	656 (1213)	938 (1720)	982 (1800)	1049 (1920)	1004 (1840)	960 (1760)

calculated for forced circulation cooling, and the rate of core cooldown is considerably slower.

Natural Circulation Core Cooling with Decay Heat Removal by VCS (Cases 3A through 3D)

This transient (Ref. 4-1) is simulated by the following sequence of events. The reactor is initially at the operating condition shown in Fig. 4-6. At time 0^+ the reactor is tripped and electric power is assumed to be lost to drive the circulator. This is simulated by ramping down the circulator speed as described above. The reformer is isolated on the secondary side, as previously. The steam generator is assumed not to be available for decay heat removal because of a tube leak or a secondary system malfunction. This was simulated, following circulator coastdown, by conservatively assuming that the isolated steam generator induces no additional helium flow. Instead, flow was calculated only through the steam generator outer annular bypass (along the vessel walls). The steam generator bypass valve is opened following circulator coastdown to allow flow to pass through this annulus. Decay heat is removed by conduction through the walls of the vessel and radiation to the VCS cooling coils. The relatively cooler vessel walls cool the helium primary coolant, forming an outer annular "cold leg" for induced natural circulation core cooling. The "hot leg" is formed in the central section of the vessel with heat input from the reactor core.

Since this case is an important condition in determining vessel design requirements, several significant parameters were varied to determine their impact on the maximum calculated vessel temperature and pressure. The base case (Case 3A) analyzed was for a 76-mm (3-in.) helium upper annular gap (steam generator bypass) and a 51-mm (2-in.) lower annular gap (core elevation), through a "freewheeling" circulator. Sensitivity of peak temperatures and pressure to a variation in the heat transfer to the vessel was investigated (Case 3B) by increasing the upper annular gap to 152 mm (6 in.) and the lower gap to 76 mm (3 in.). Sensitivity of peak temperatures and pressure to variations in the primary loop flow resistance was investigated

by varying the circulator flow resistance from a relatively high value estimated for a locked rotor condition (Case 3C) to a relatively low value estimated for a bypass valve around the circulator (Case 3D). For all cases heat is removed from the vessel by radiation from the outside surface of the vessel to the VCS cooling coils, which are maintained at about 93°C (200°F). The estimated transient response of key simulated parameters for the above sequence of events is shown in Figs. 4-11A through 4-11E. A summary of the key parameters is contained in Table 4-3. Based upon these results it was concluded that natural circulation cooling by an external set of cooling coils is feasible for vessel design limits of ~454°C (~850°F) and 6.2 MPa (900 psia), that some design flexibility existed (tradeoff between vessel design temperature and pressure) by changing the helium annulus size, and that natural circulation cooling is relatively insensitive to the circulator flow resistance so that a bypass valve around the circulator is not required. As a result of this study, an upper helium annular gap of 127 mm (5 in.) and a lower gap of 76.2 mm (3 in.) were selected for future analyses.

These results are for an early version of the simulation. Effects which should lower the calculated peak vessel temperature and pressure have subsequently been included in the simulation. These effects include calculation of parallel-induced natural circulation flow through both the steam generator and the annular bypass, a more complete simulation of the surface area of the vessel available for decay heat removal, and inclusion of a smaller though significant heat transfer mechanism (other than radiation) from the outside surface of the vessel, namely free convection to the surrounding air. Updated transients with these effects will be reported in the next semiannual report.

Natural Circulation Core Cooling with Decay Heat Removal by External Air Flow over Outside of Vessel (Cases 4A through 4D)

An alternate method of cooling the vessel by forcing a flow of air over the outside surface was investigated to determine the feasibility of such a concept (Ref. 4-5) and to further reduce the probability of unrestrained

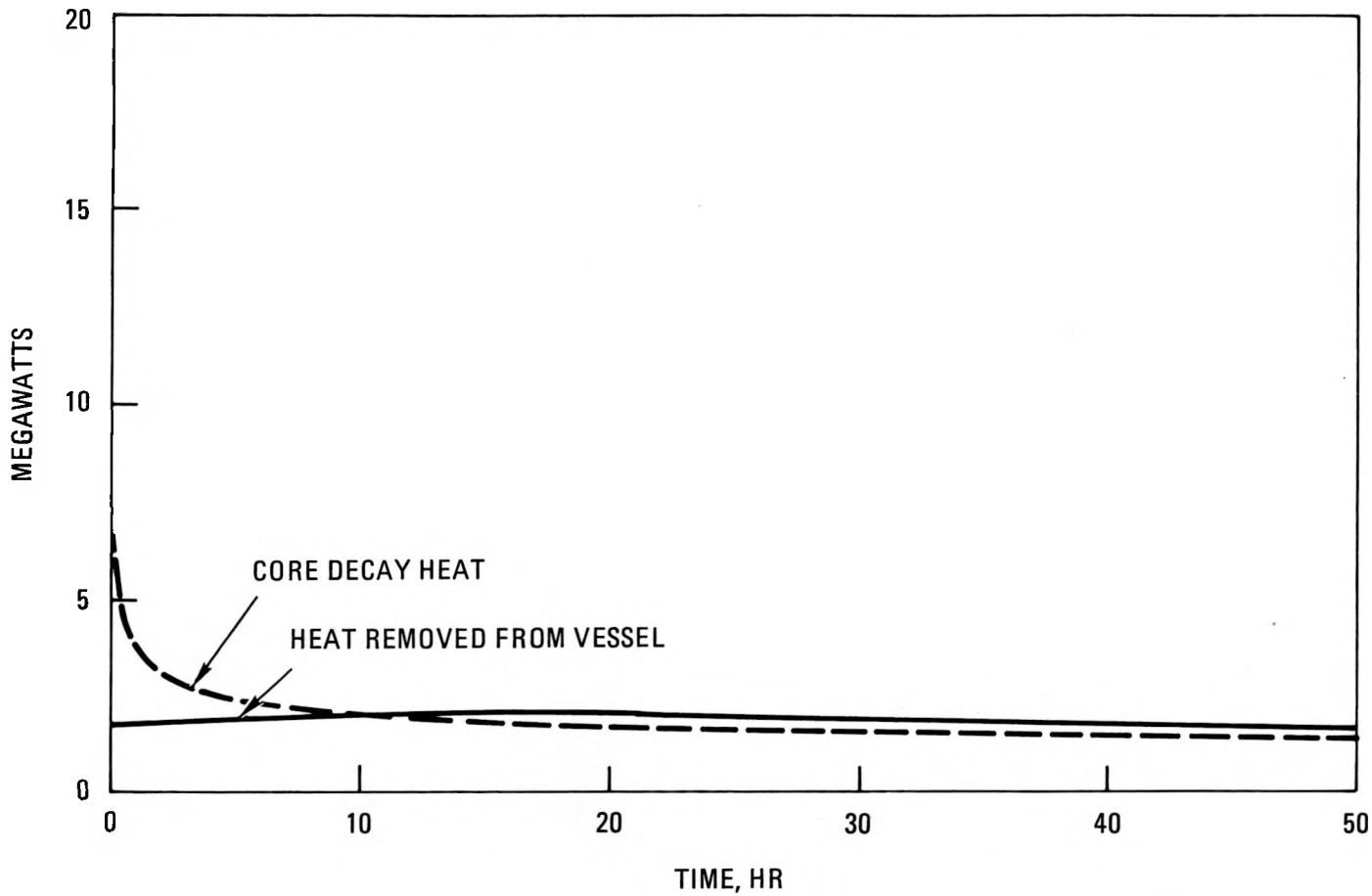

Fig. 4-11A. Natural circulation decay heat removal using VCS

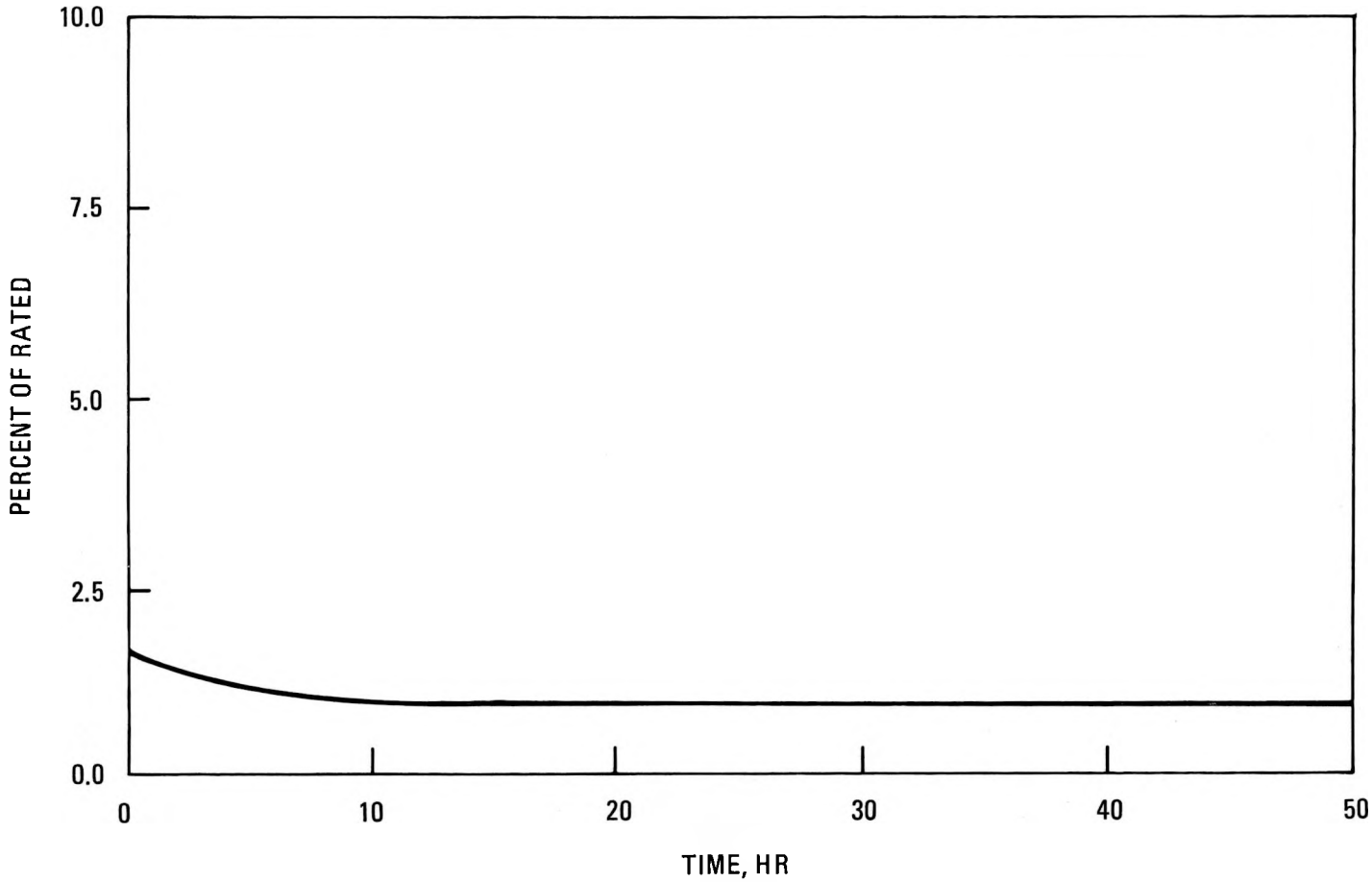

Fig. 4-11B. Helium flow

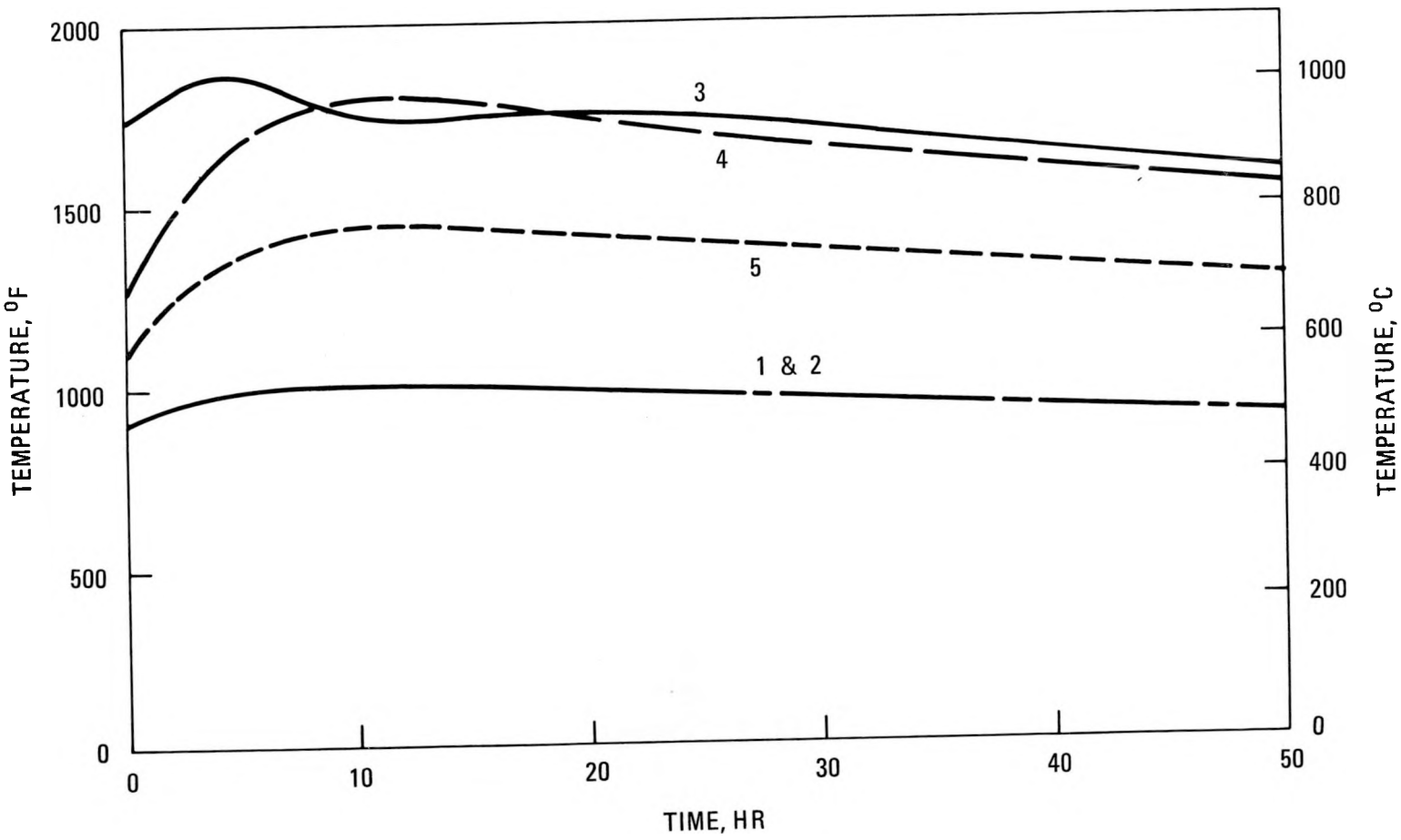

Fig. 4-11C. Helium temperatures

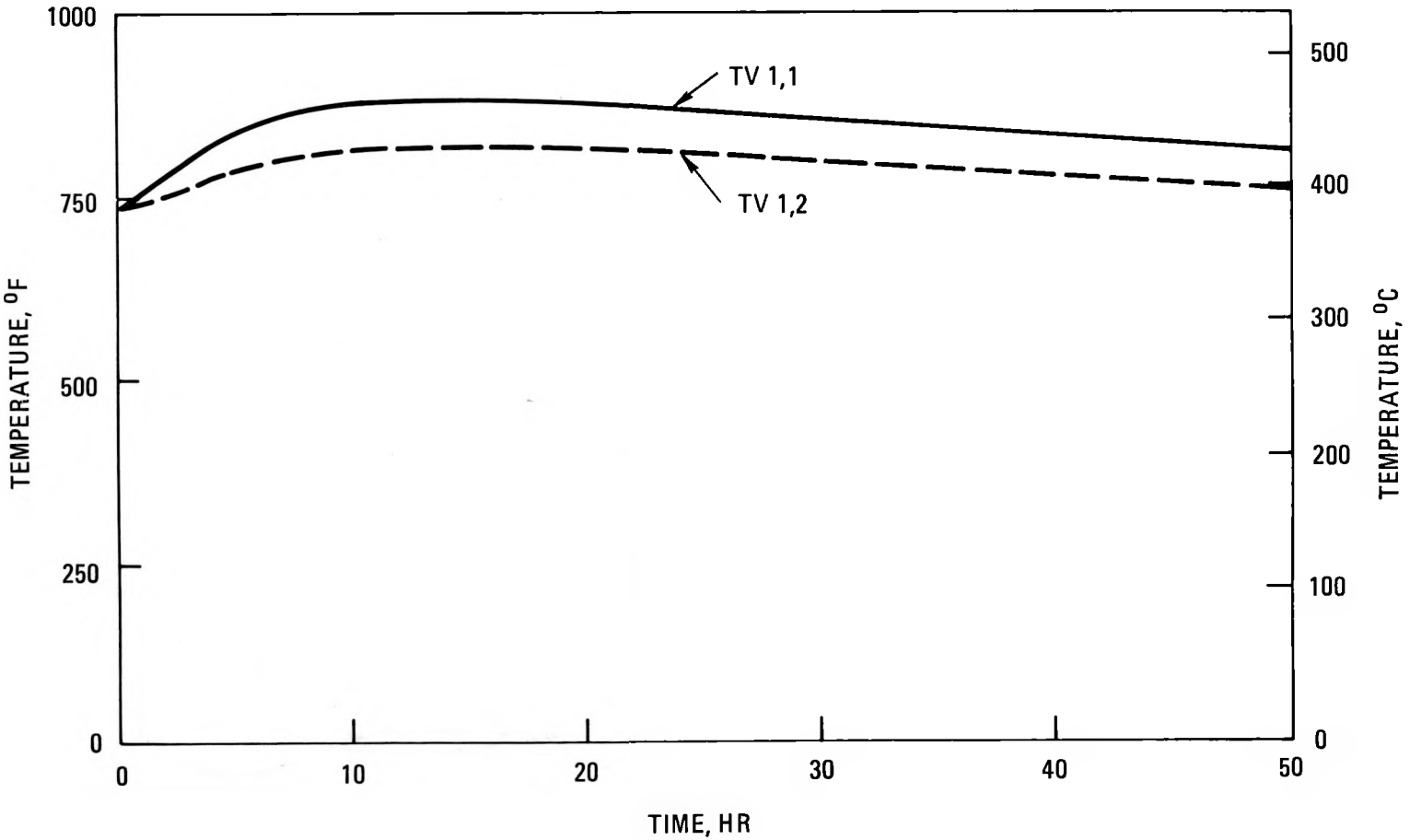

Fig. 4-11D. Vessel temperatures

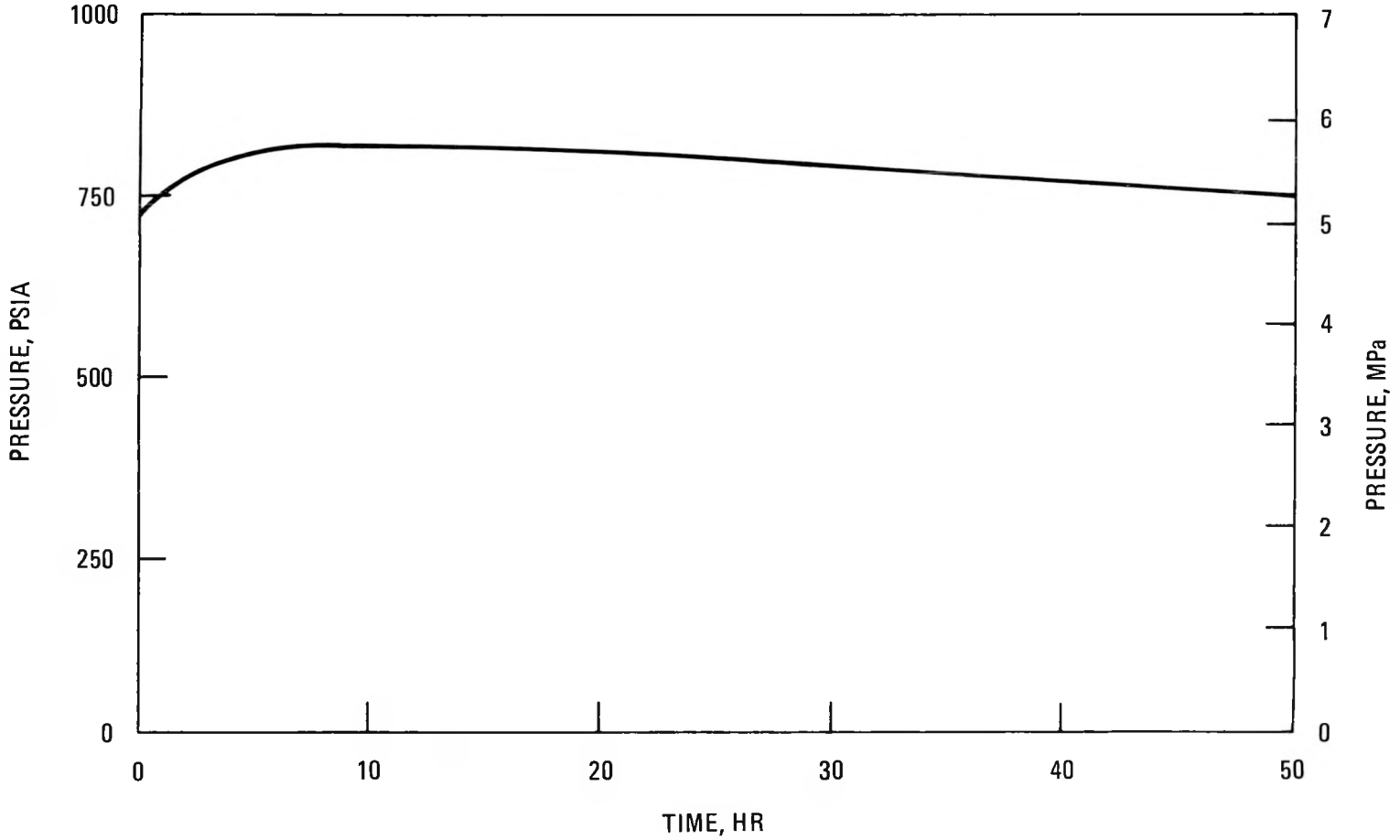

Fig. 4-11E. Pressure

core heatup. The sequence of events for this transient is identical to that for natural circulation cooling by the VCS except that the forced air cooling system replaces the VCS cooling coils.

To scope the air flow requirements, a supply of 38°C (100°F) air was assumed to be available. The annular confinement geometry shown in Fig. 4-12 was used for analysis. Heat transfer from the outside of the vessel is primarily by forced convection to the air and radiation to the surrounding cooler surfaces within the containment for the air flow rates required to maintain the vessel design conditions. This was bounded by considering heat transfer by convection only (from the nominal exterior surface of the vessel) as a minimum heat removal and then doubling the nominal surface area of the vessel to estimate the maximum heat transfer for both radiation and convection. Typical results for this sequence of events are shown in Figs. 4-13A through 4-13H for nominal vessel surface area and an air flow rate of 315 kg/s (2.5×10^6 lb/hr). For this transient, parallel primary coolant flow through the steam generator and bypass is incorporated into the simulation. This enables a transient estimate to be made of the steam generator tube temperatures and indicates a peak tube temperature of ~954°C (~1750°F) (Fig. 4-3). Peak vessel midwall temperatures and air outlet temperature as a function of the air flow rate bounded by nominal and 2σ nominal vessel surface area are shown in Fig. 4-14. The current estimated core heatup probability for the HTGR-MRS/PH reactor is 3×10^{-4}/module year, but the safety consequences of such an event are negligible (Ref. 4-1). The addition of a nonsafety class forced air cooling system is one possible alternative to reduce this probability to less than 10^{-4}/module year, if this is required. Forced air cooling differs from cooling by using water cooling coils. Based on the above results, such a concept is feasible with the current confinement geometry for air flow rates of about 201.5 kg/s (1.6×10^6 lb/hr) with the air outlet temperature not exceeding ~65°C (~150°F).

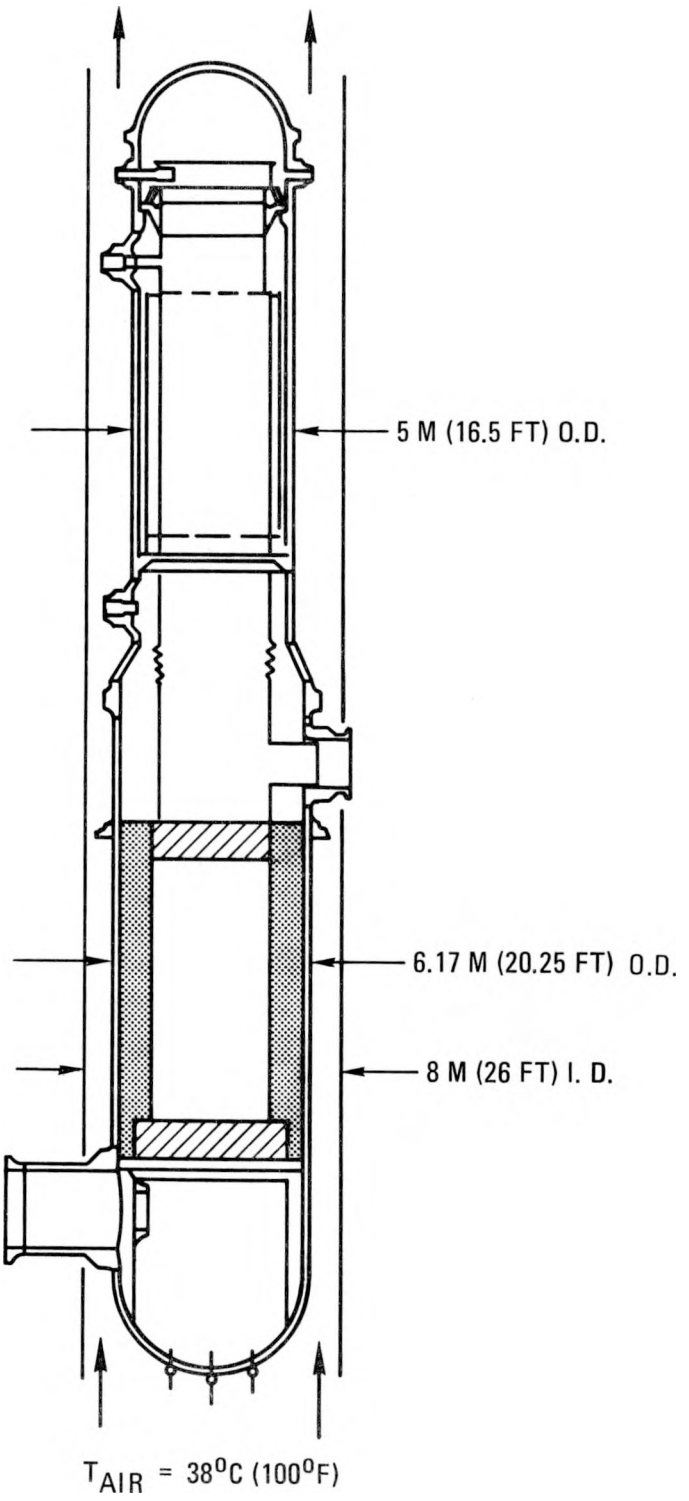

Fig. 4-12. External air cooling annular geometry

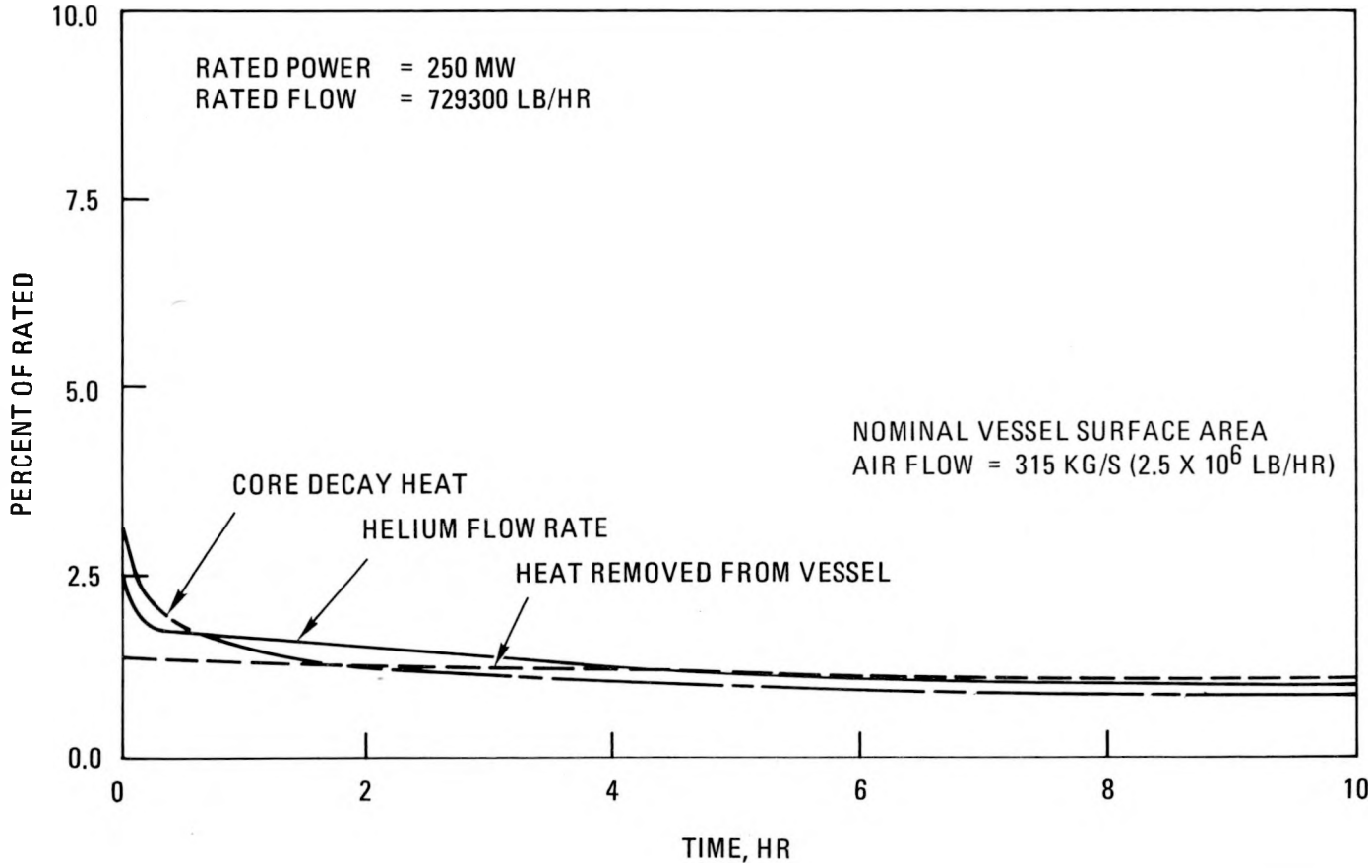

Fig. 4-13A. Natural circulation decay heat removal via flow of air over outside surface of vessel

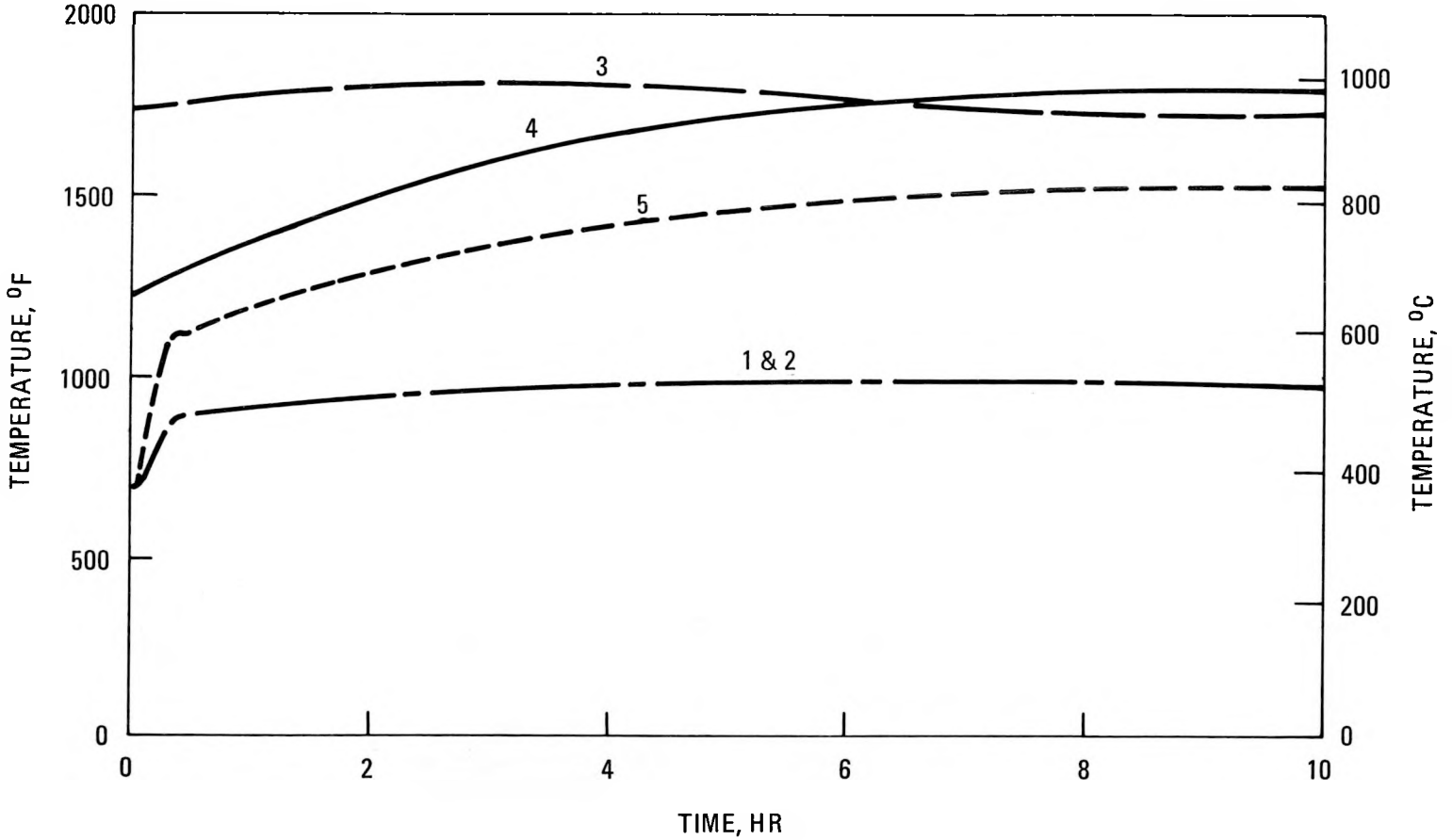

Fig. 4-13B. Helium temperatures

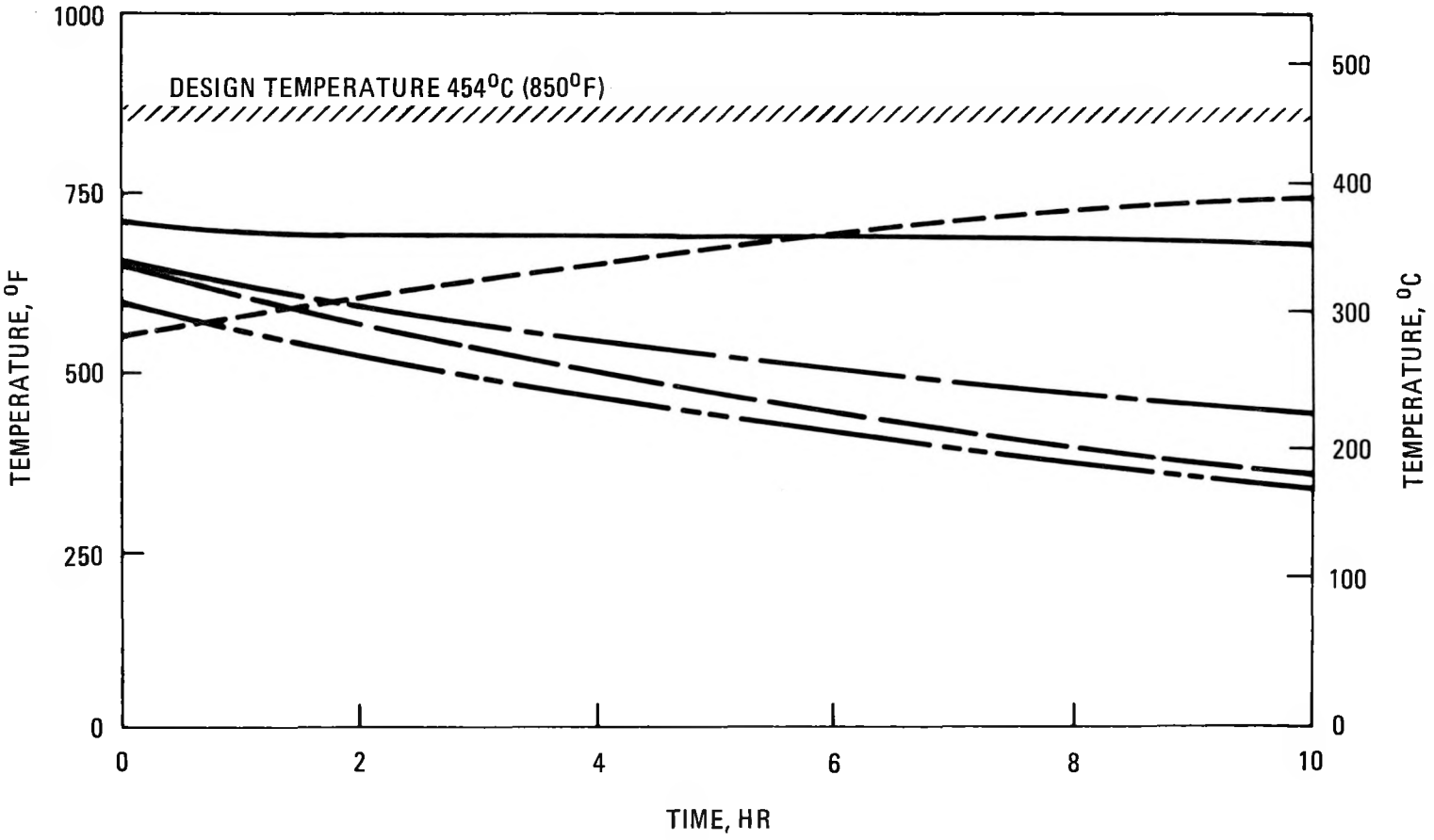

Fig. 4-13C. Vessel temperatures

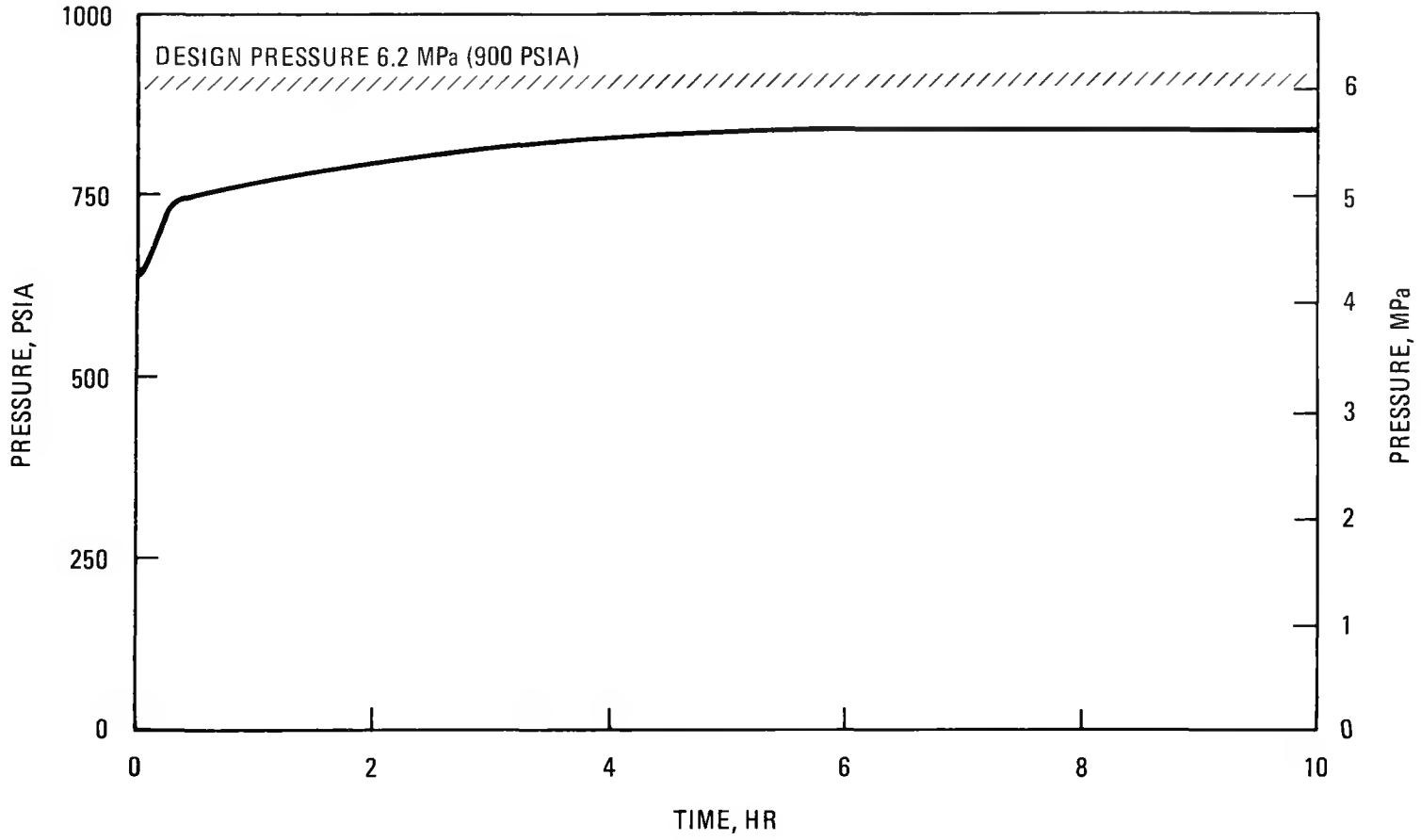

Fig. 4-13D. Pressure

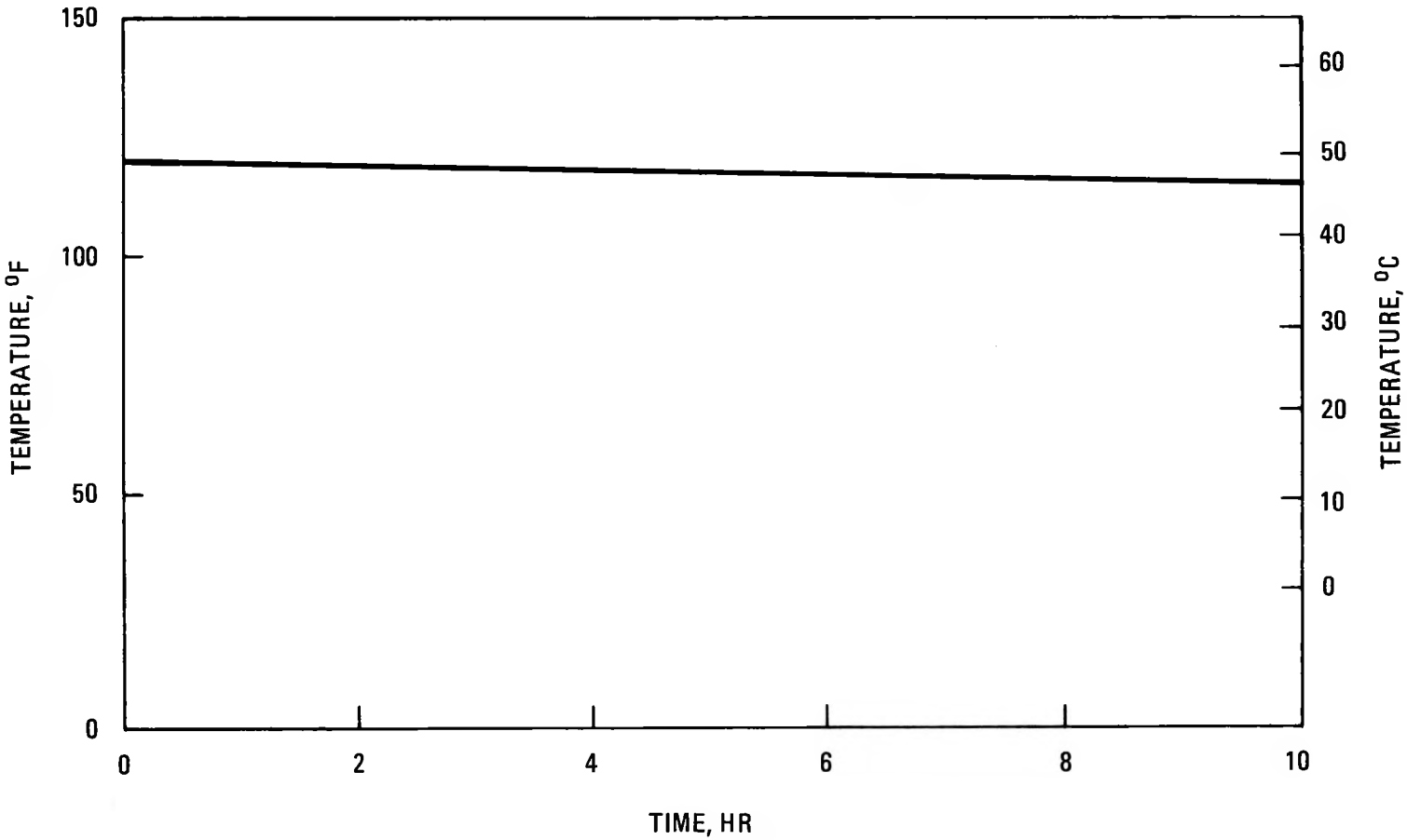

Fig. 4-13E. Air outlet temperature

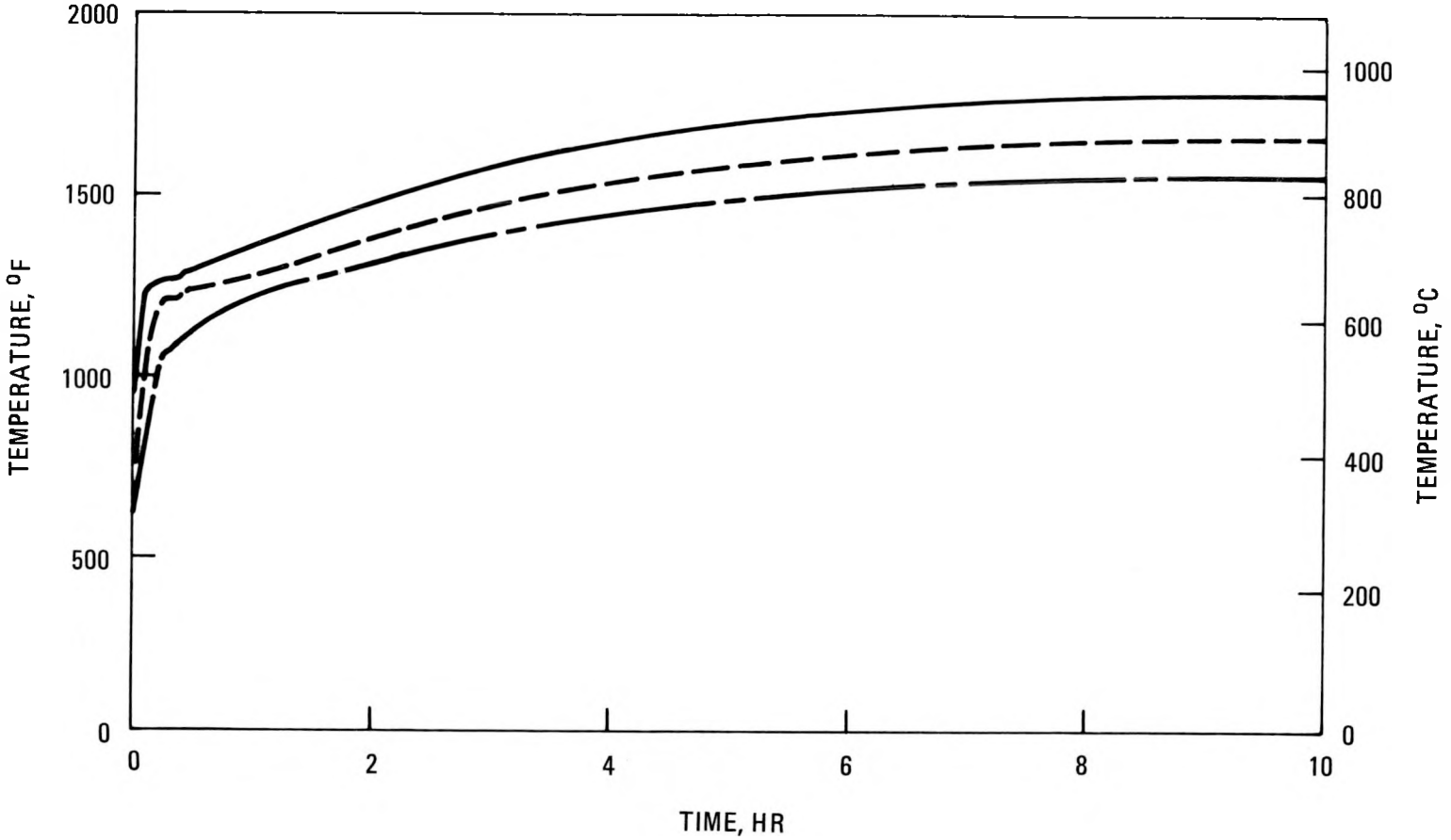

Fig. 4-13F. Steam generator tube temperatures

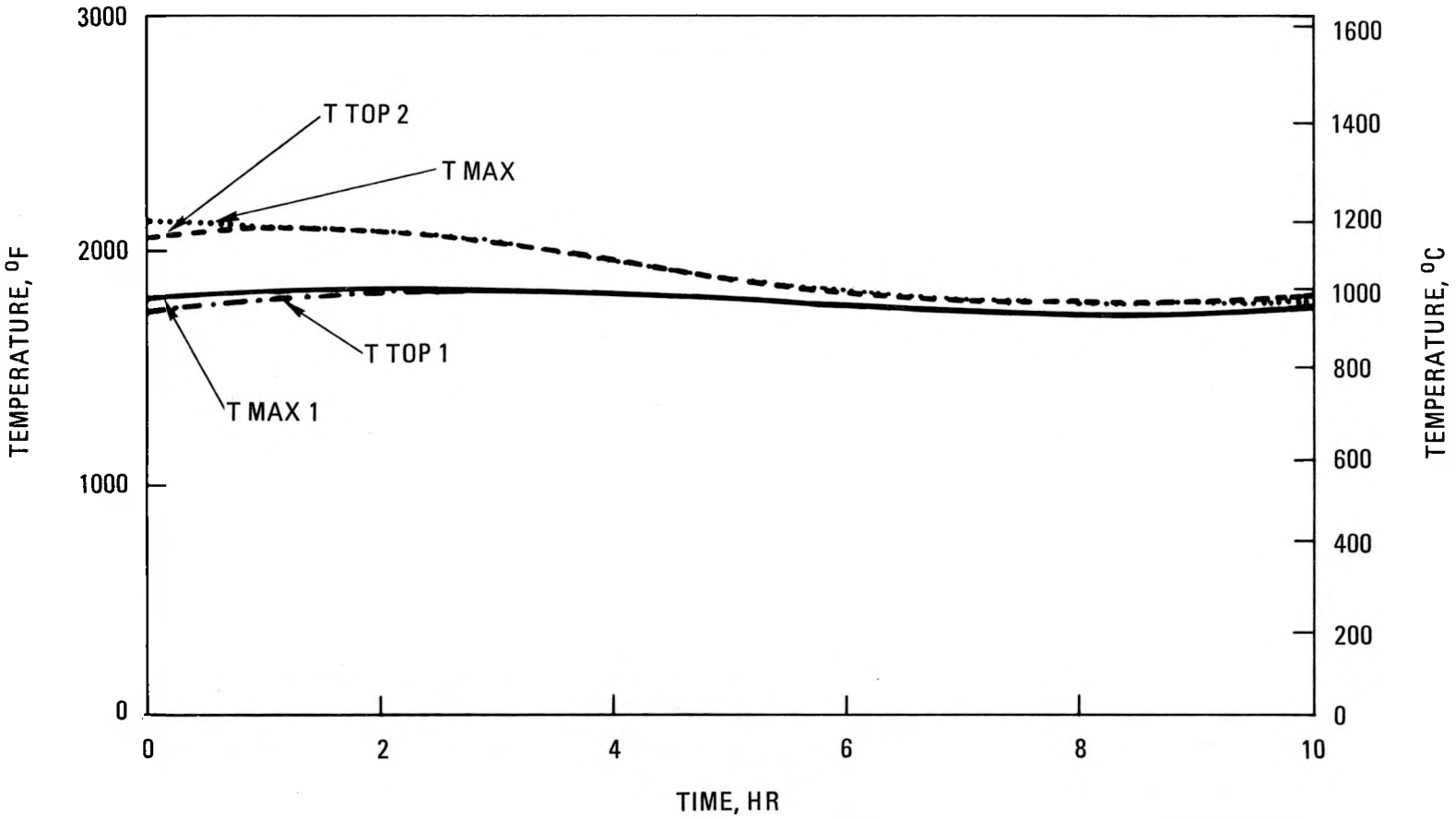

Fig. 4-13G. Core temperatures

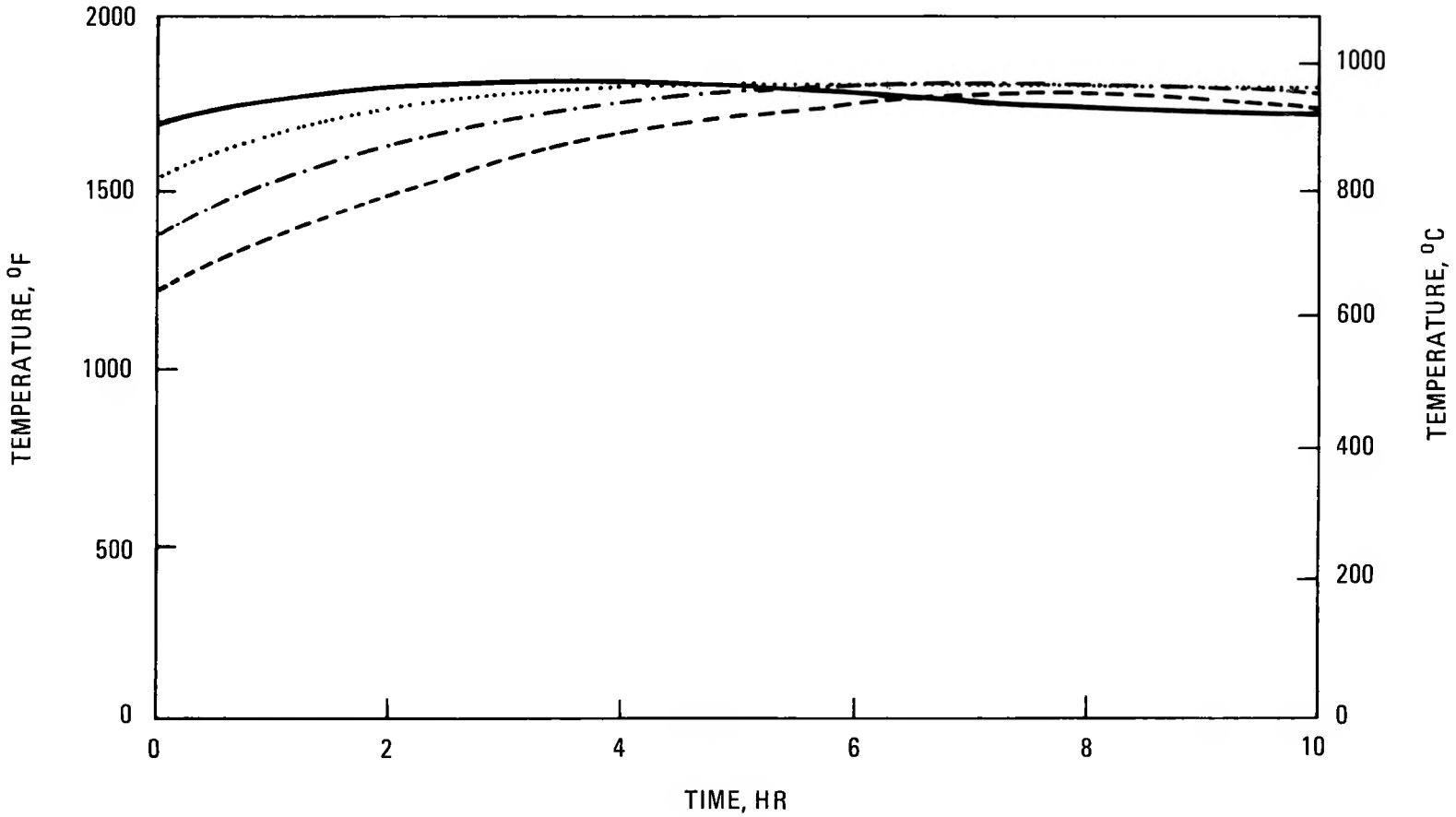

Fig. 4-13H. Reformer tube temperatures

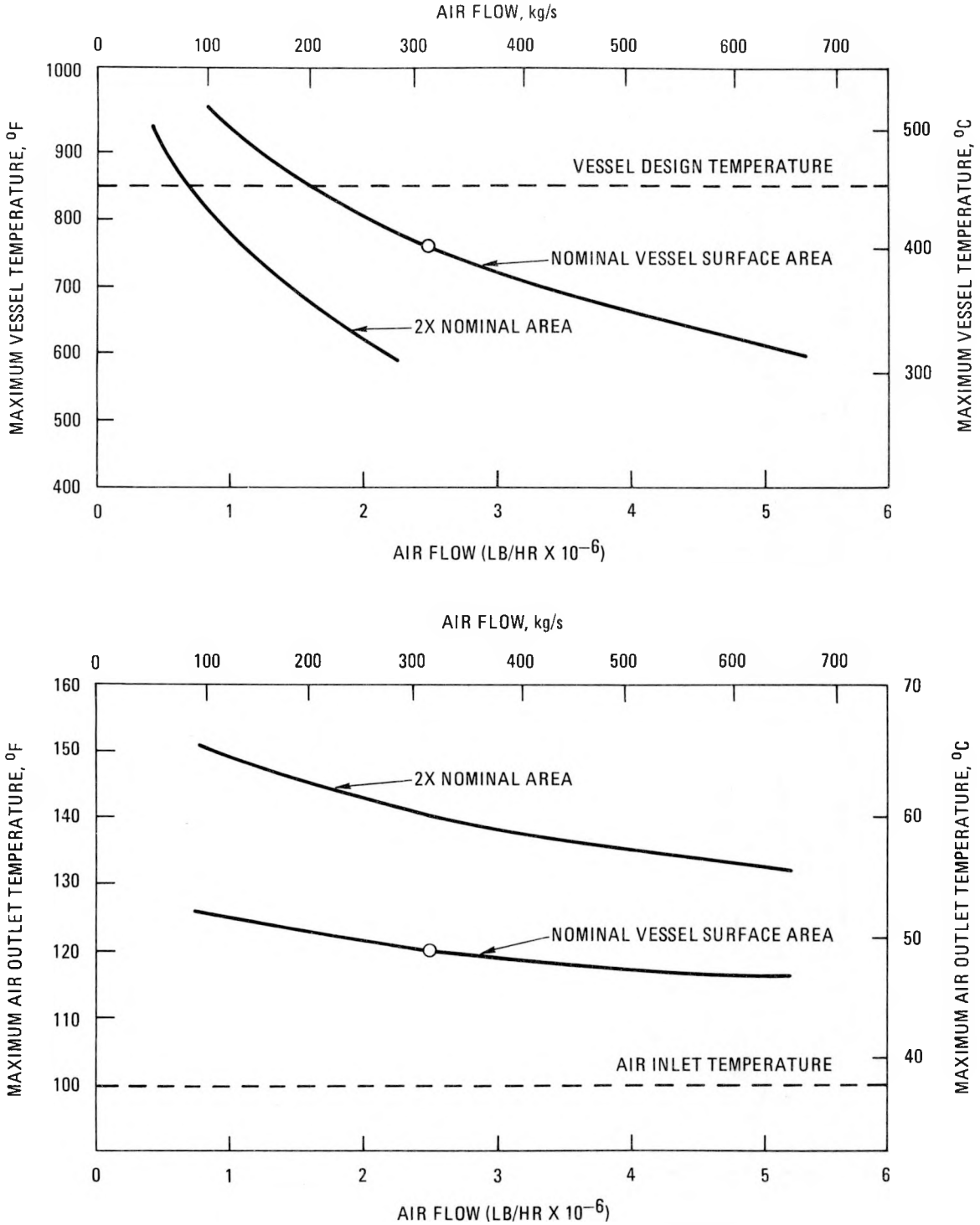

Fig. 4-14. External air flow parameters

4.3. SAFETY STUDIES (6053020001)

4.3.1. Scope

The scope of this task is to (1) investigate the consequences of loss of forced main loop cooling (LOFC) on the reactor core and (2) perform a preliminary reliability analysis of the core cooling for the 250-MW(t) HTGR-MRS/PH plant.

4.3.2. Discussion

4.3.2.1. LOFC Accident. In the accident sequence after LOFC for a 250-MW(t) HTGR-MRS/PH, natural circulation of helium develops through the steam generator or, if the steam generator fails, through a bypass using the VCS as a heat sink. These two modes of natural convection mechanisms would successfully remove the afterheat without damaging any reactor component. However, if both fail before the main loop can be restored, core heatup cannot be avoided.

The present studies investigated the depressurized core heatup accident with various natural or forced convection modes with prior cooldown and with or without vessel cooling. Core heatup studies were performed for the 250-MW(t) modular VHTR. CORCON (Ref. 4-6) and SORS (Ref. 4-7) models for the modular reactor were developed to calculate the transient reactor internal temperatures and the fission product release.

The base study case assumed an immediate depressurization after LOFC and reactor trip. CORCON results showed that the peak core temperatures reach a value of ~1980°C (~3600°F) about 30 hr into the accident, as seen in Fig. 4-15. The peak core temperature is fairly insensitive to the vessel-cavity cooling, as seen in Fig. 4-16. With or without vessel-cavity cooling, most active core temperatures exceed the melting point of the control rod [1371°C (2500°F)]. However, relocation of control rods in the side reflector region would avoid control rod melting, as the temperatures there are substantially lower (see Fig. 4-16).

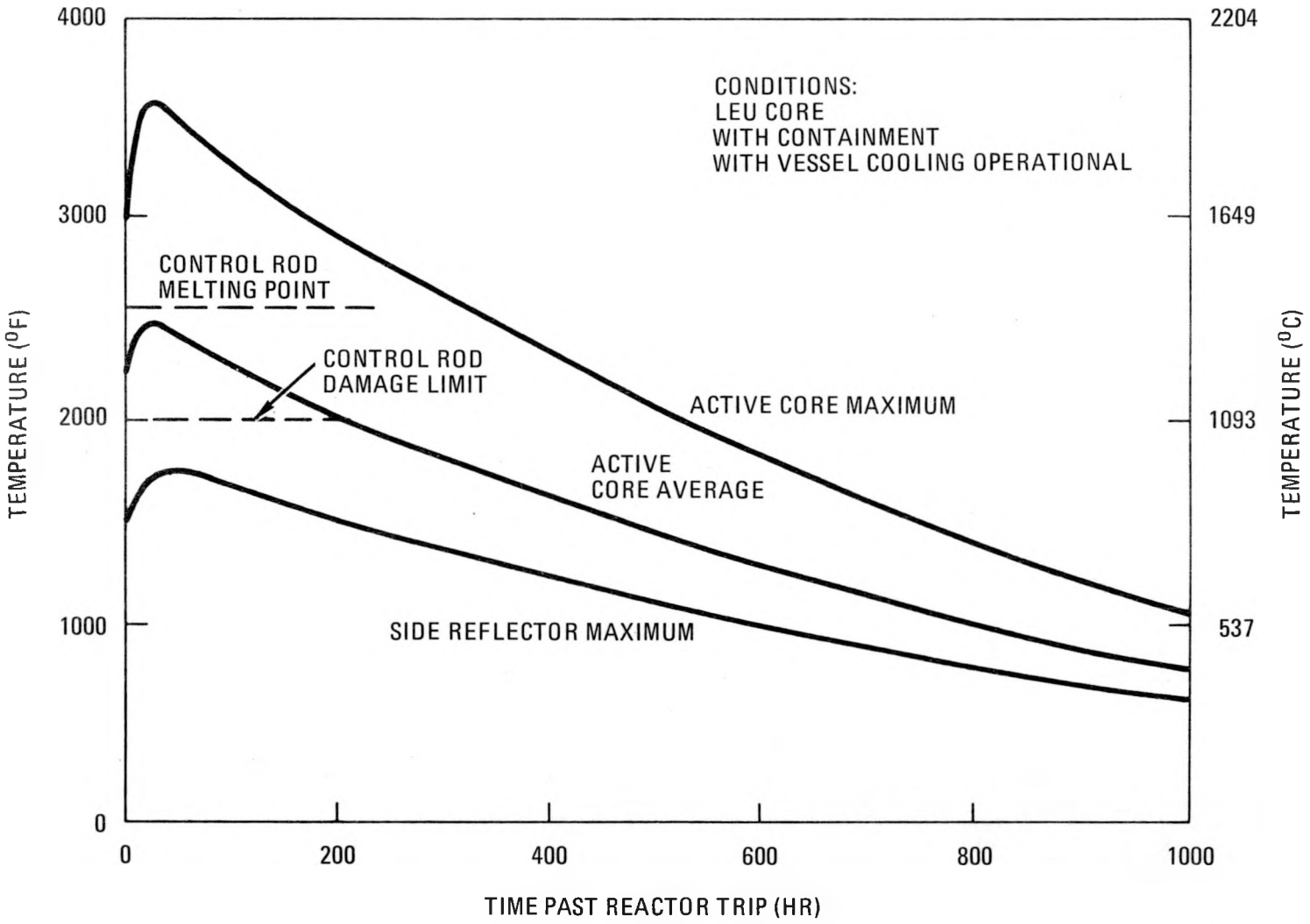

Fig. 4-15. Core temperatures for 250-MW(t) VHTR core heatup accident

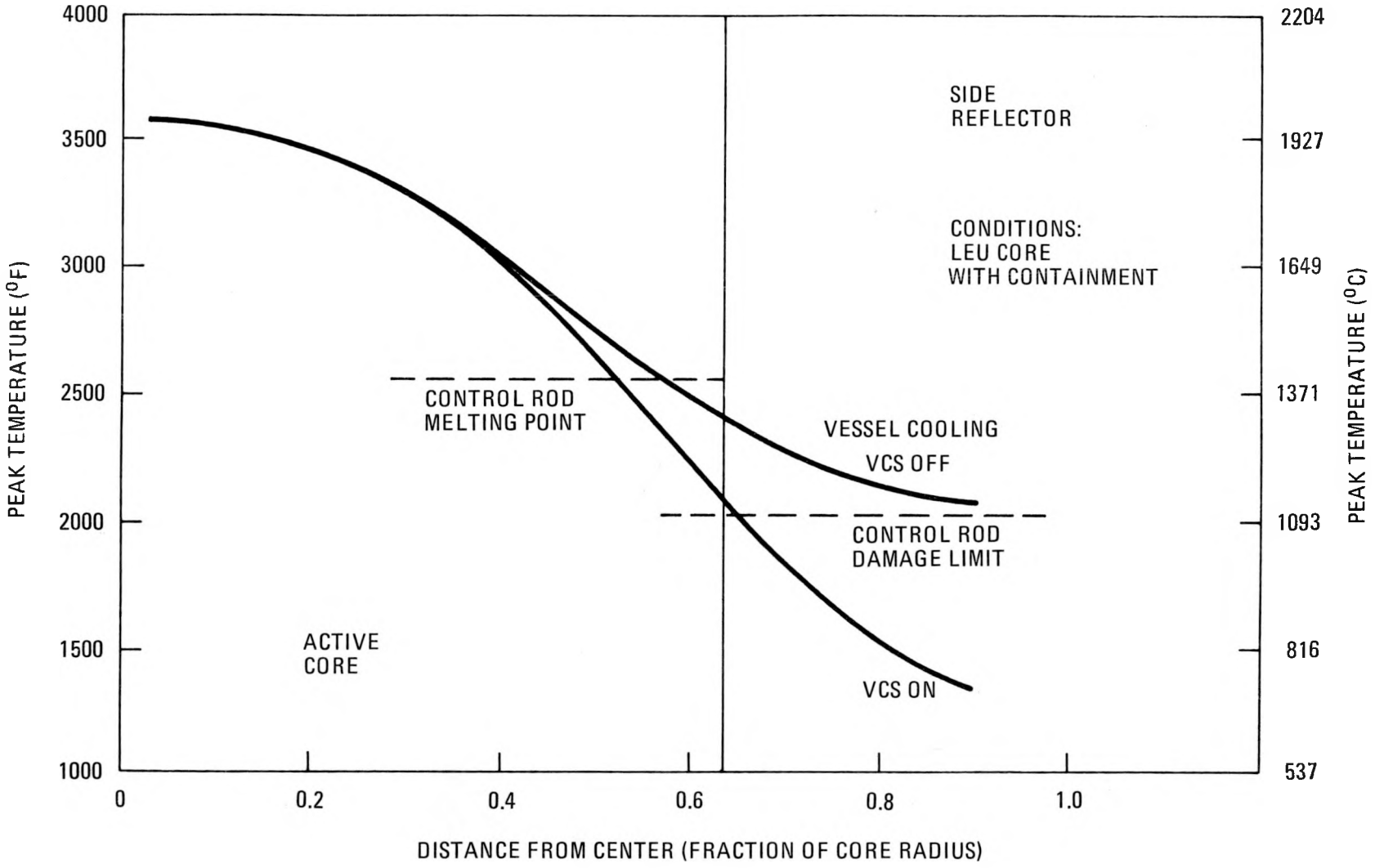

Fig. 4-16. Peak temperature versus radial distance for 250-MW(t) VHTR core heatup

SORS results showed that the maximum fuel failure fraction in the core is about 1% during the depressurized core heatup accident. Figure 4-17 shows the rate of release of fission products from the core. The release curve for Kr-85 represents essentially the fuel failure rate, as there is little attenuation by retention and decay. The slow rate of fuel failure results in significant reduction by decay of short-lived isotopes such as I-131.

With the vessel-cavity cooling system operating, the reactor vessel temperature during the core heatup accident peaks at about 427°C (800°F), which is below the 454°C (850°F) design limit. Without vessel-cavity cooling, the maximum vessel temperature would reach a much higher peak: in excess of 1038°C (1900°F) with vessel depressurization and 649°C (1200°F) without vessel depressurization.

The second study case considered natural circulation cooldown after LOFC and reactor trip. Initial conditions of natural circulation cooling using the VCS as a heat sink were based on Ref. 4-8 for termination of cooldown (or initiation of depressurization), which varies from 0 to 16 days. CORCON results are presented in Fig. 4-18. The first set of data points are those obtained in the base study case. It is seen that the core and vessel temperatures reach a lower peak with longer prior cooldown. Therefore, 15 days of prior cooldown is needed to avoid vessel damage, while 16 days is about the shortest time of prior cooldown to avoid control rod damage or other damage to the reactor.

The third study case considered core heatup under refueling conditions. Forced circulation cooldown for 2 days under slightly subatmospheric pressure was assumed. Temperatures obtained from CORCON are lower than those with natural circulation cooldown (at 2 days) because forced circulation cooldown is more effective in lowering the initial core and helium temperatures. However, the 2-day forced circulation cooldown is not long enough to avoid component damage. The peak vessel temperature is far above the damage limit without vessel-cavity cooling.

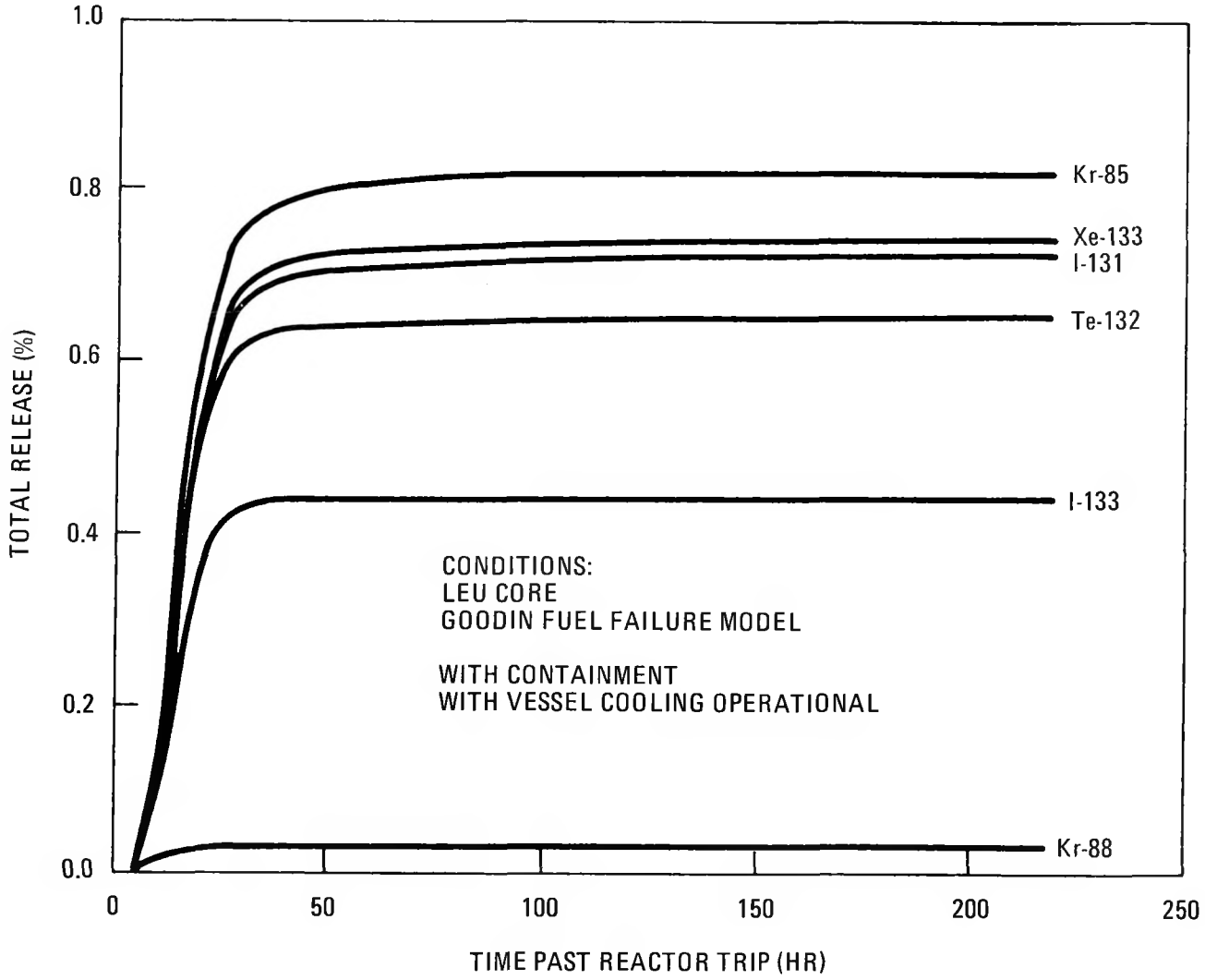

Fig. 4-17. Release of volatile isotopes during 250-MW(t) VHTR core heatup accident

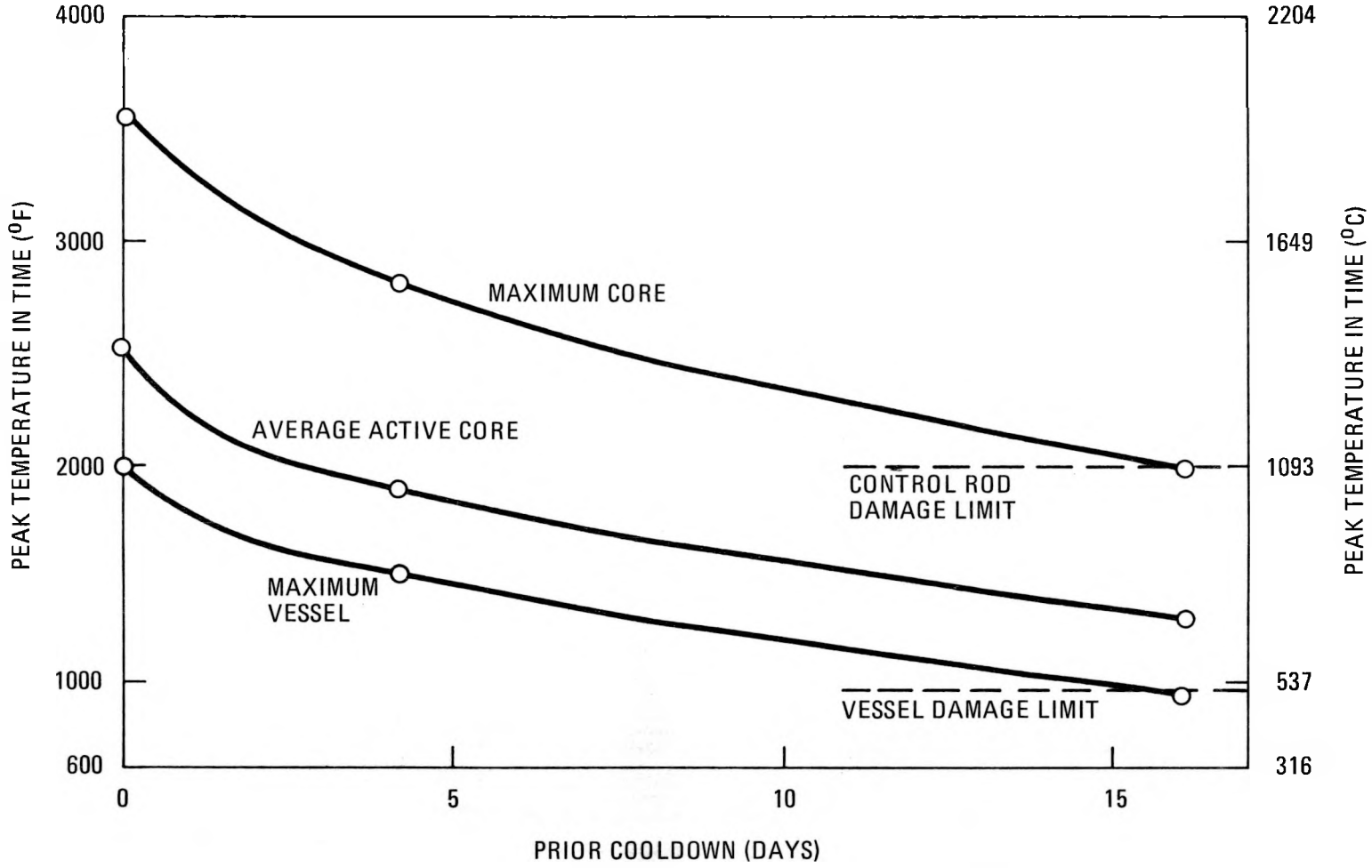

Fig. 4-18. Depressurized core heatup of 250-MW(t) modular VHTR with natural circulation cooldown prior to accident

4.3.2.2. Preliminary Reliability Analysis. A preliminary reliability analysis of core cooling for the HTGR-MRS/PH was completed. The study was based upon plant response to a loss of main loop cooling, since in studies of the large plant this initiating event dominated those sequences of events that lead to an eventual loss of core cooling.

Results of the study are summarized below:

Event	Median Frequency Per Reactor Yr
Cooling with VCS required	0.30
VCS steam generator bypass valves fail to open	5.4×10^{-5}
VCS fails to run until no longer needed	2.2×10^{-4}

Assumptions

This study of cooling reliability has been based only on a single initiating event, loss of main loop cooling. It must be borne in mind when assessing these results that other initiating events exist that can add to frequency of loss of core cooling. Furthermore, for the purposes of this study, a loss of core cooling has been defined as any cooling loss leading to control rod damage. A full spectrum of consequences would be expected dependent upon several factors such as the duration of the cooling loss. While work in this area is proceeding, it is not currently possible to quantify reliability at this level of detail. Finally, because of the preliminary stage of the system design, several other areas noted below have large uncertainties. Nevertheless, this study has already provided valuable guidance in the definition of modular reactor cooling systems by illustrating expected areas of strength and weakness in the concept.

System Description

Core cooling for the 250-MW(t) process heat modular reactor system is provided by two systems: the main loop cooling system and the VCS.

Major components of the main loop cooling system are shown in Fig. 4-19. Internal to the reactor pressure vessel is a single electric-motor-driven helium circulator with a reserve electric motor drive (pony motor) suitable for shutdown cooling. Circulating helium removes core heat through the reformer located in a central duct and then down through a single steam generator located in the annular region surrounding the central duct. For shutdown cooling, only the steam generator is used for heat removal. In addition to normal heat transport paths in the balance of plant, provision is made for once-through water cooling of the steam generators.

The VCS consists of two redundant cooling loops as shown in Fig. 4-20. Each loop is capable of removing 100% of the core heat following reactor shutdown. Each loop consists of:

1. A series of cooling coils wound about the inner face (nearest to the reactor pressure vessel) of the biological shield.

2. Two 100% capacity circulating water pumps, one normally running, the other in standby.

3. One pressurizer/relief valve system.

4. One 100% capacity heat exchanger cooled by either the service water system or one of the two redundant loops of the nuclear service water system.

Reliability of Core Cooling

A complete probabilistic risk assessment requires reviewing a full spectrum of initiating events potentially leading to plant damage. However,

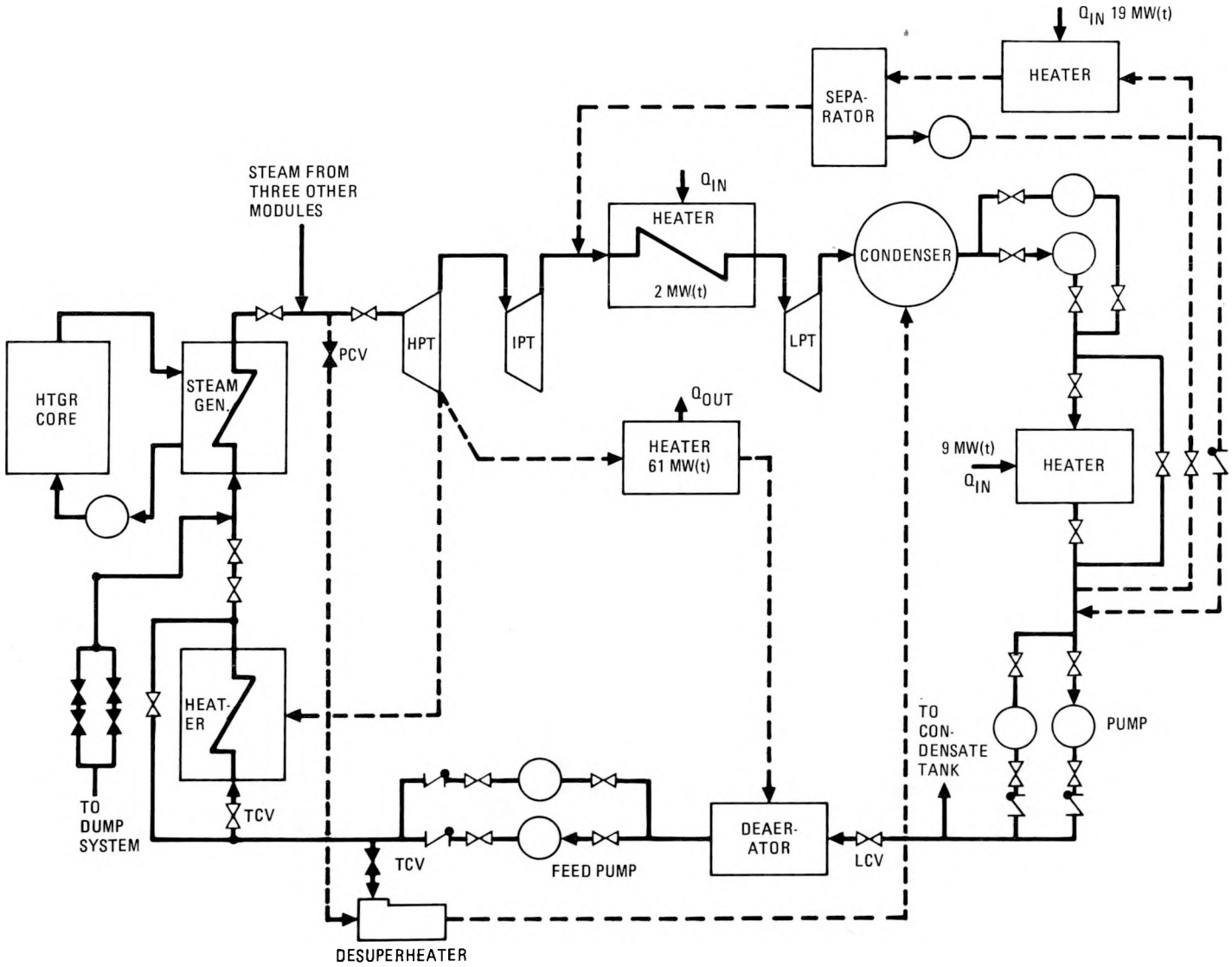

Fig. 4-19. Main loop cooling system

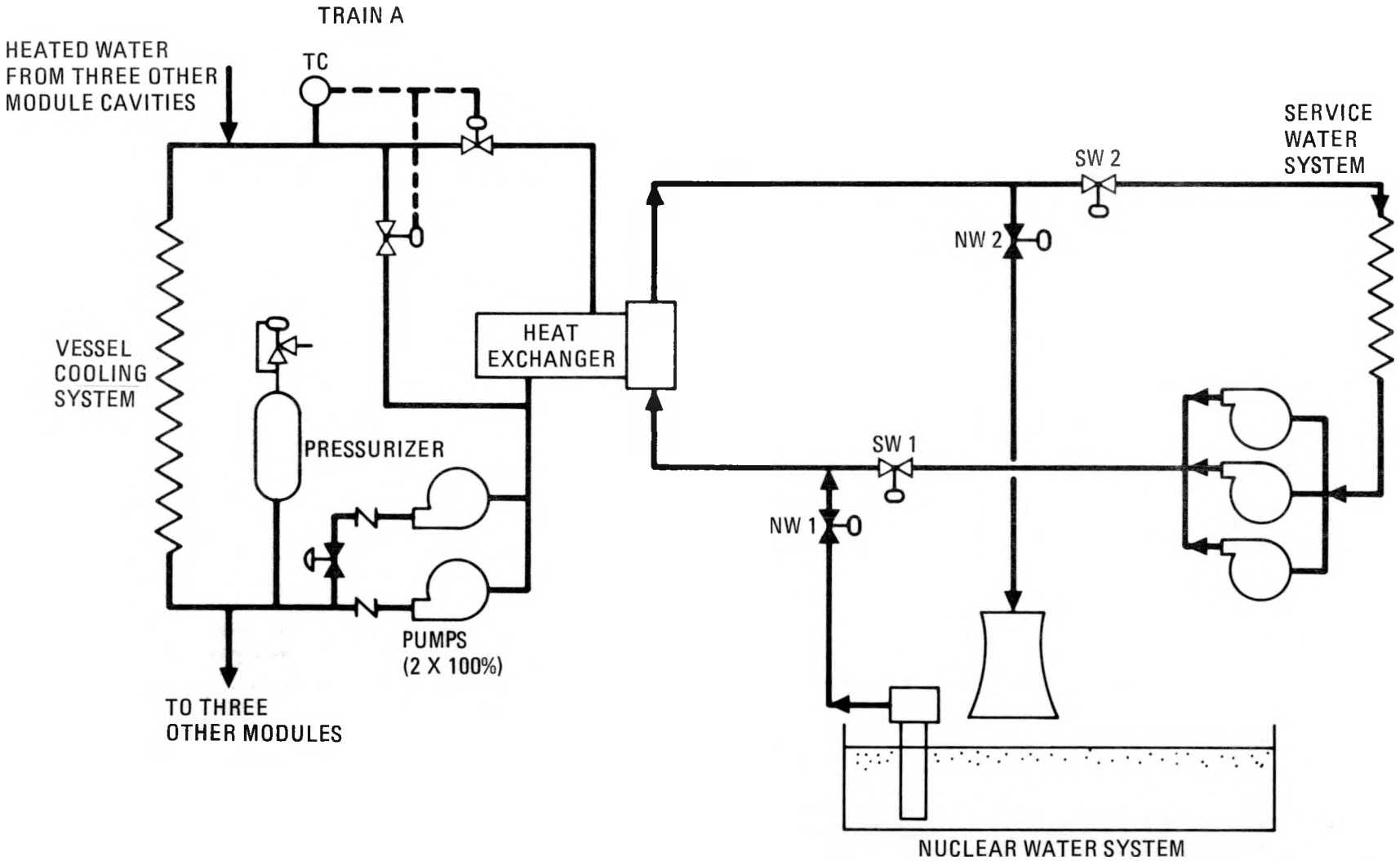

Fig. 4-20. Proposed VCS

previous work on the large HTGR has shown a loss of the main loop cooling system to be the dominating contributor to overall plant risk. Therefore, as a preliminary effort toward a full risk assessment and to provide design guidance in the formation stages of the modular reactor system development, core cooling reliability following a loss of the main loop cooling system was evaluated. The event tree used in the assessment is shown in Fig. 4-21.

For each event of the event tree, a fault tree was constructed to identify the factors contributing to the event frequency of occurrence. For example, Fig. 4-22 shows the fault tree constructed to evaluate the frequency of loss of main loop cooling (event No. 1).

Areas requiring further study include:

1. Interdependency between main and pony motor drives on the helium circulator (circulator failure frequency).

2. Allowable water ingress rate before the steam generator must be dumped (steam generator dump frequency).

3. VCS redundancy when more than one module is on site.

4. Heatup rates when the primary system is pressurized but all secondary cooling is lost.

5. VCS performance with the bypass valve shut.

6. System interdependencies when more than one reactor module is on site.

7. Probability and consequence of failure to shut down the reactor following a loss of main loop cooling.

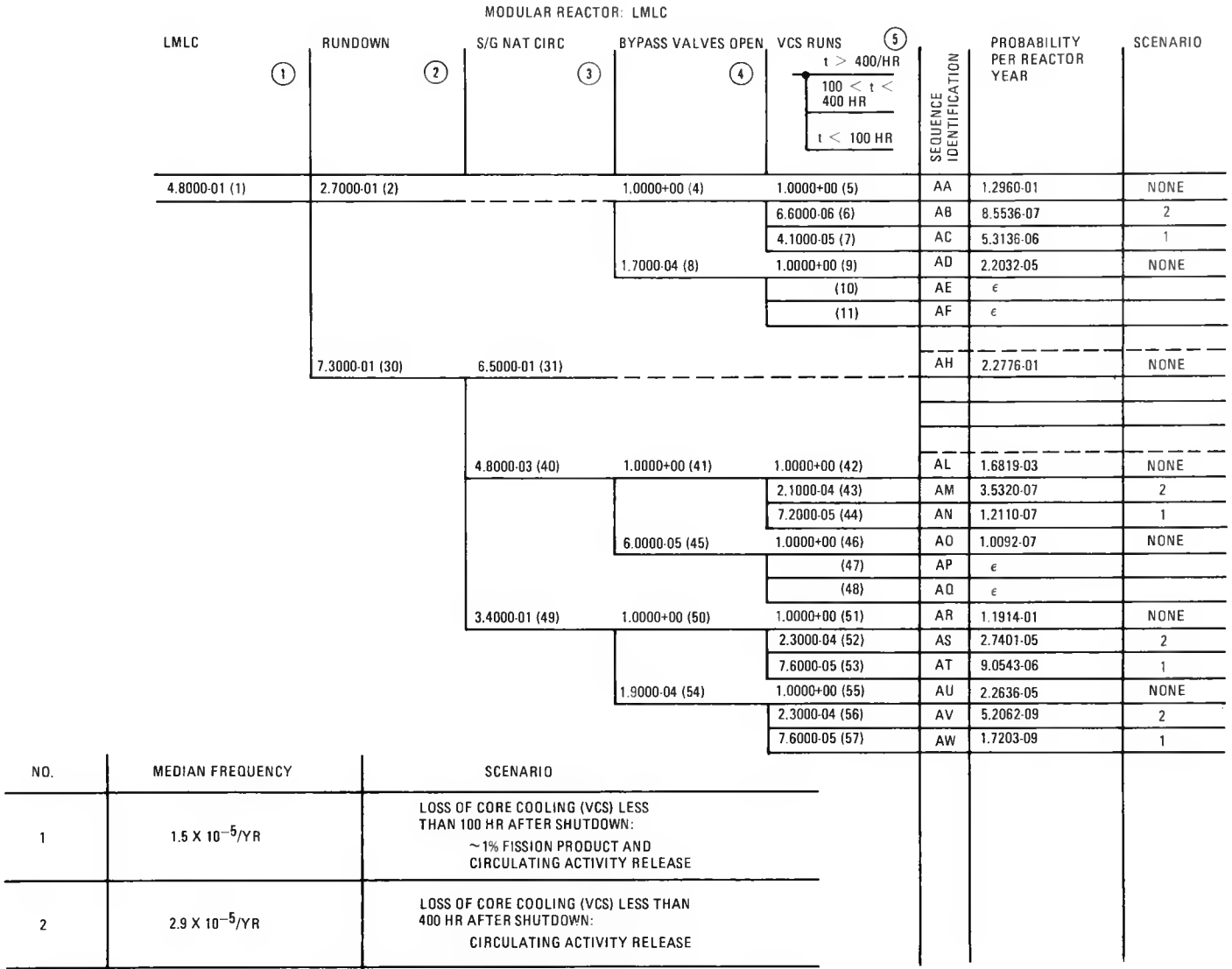

Fig. 4-21. Loss of main loop cooling event tree

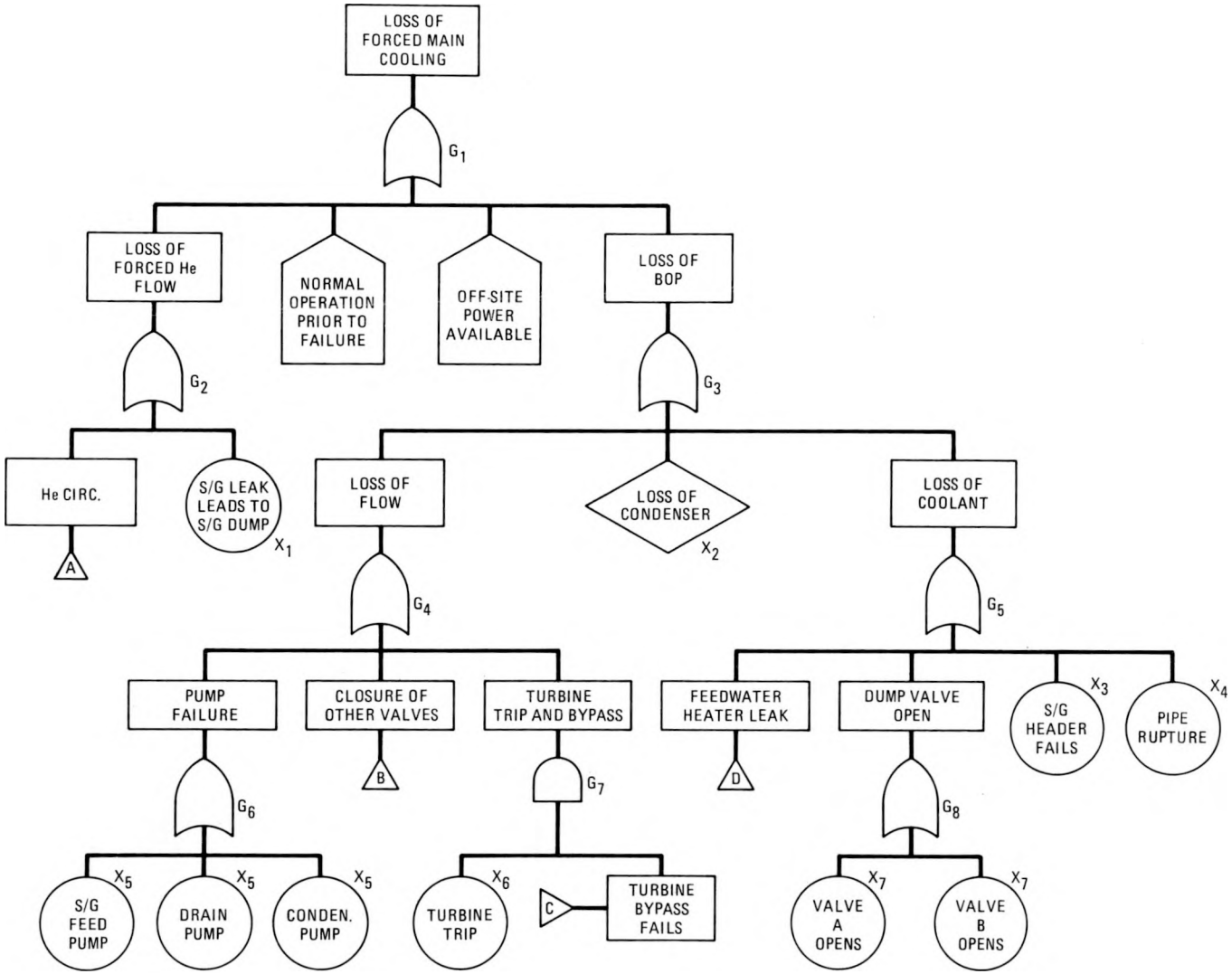

Fig. 4-22. Fault tree for Event 1, loss of main loop cooling (sheet 1 of 5)

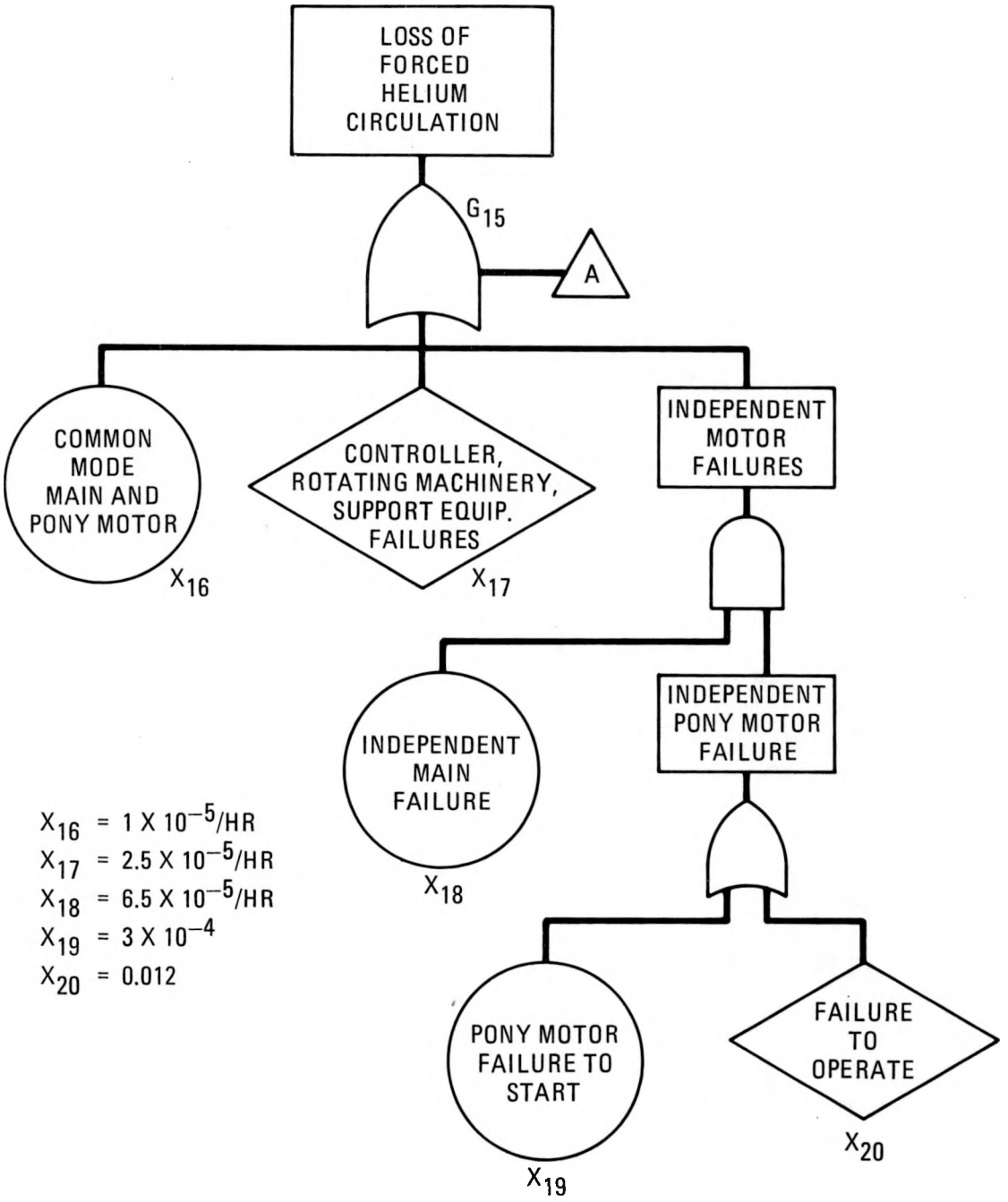

Fig. 4-22. Fault tree for Event 1, loss of main loop cooling (sheet 2 of 5)

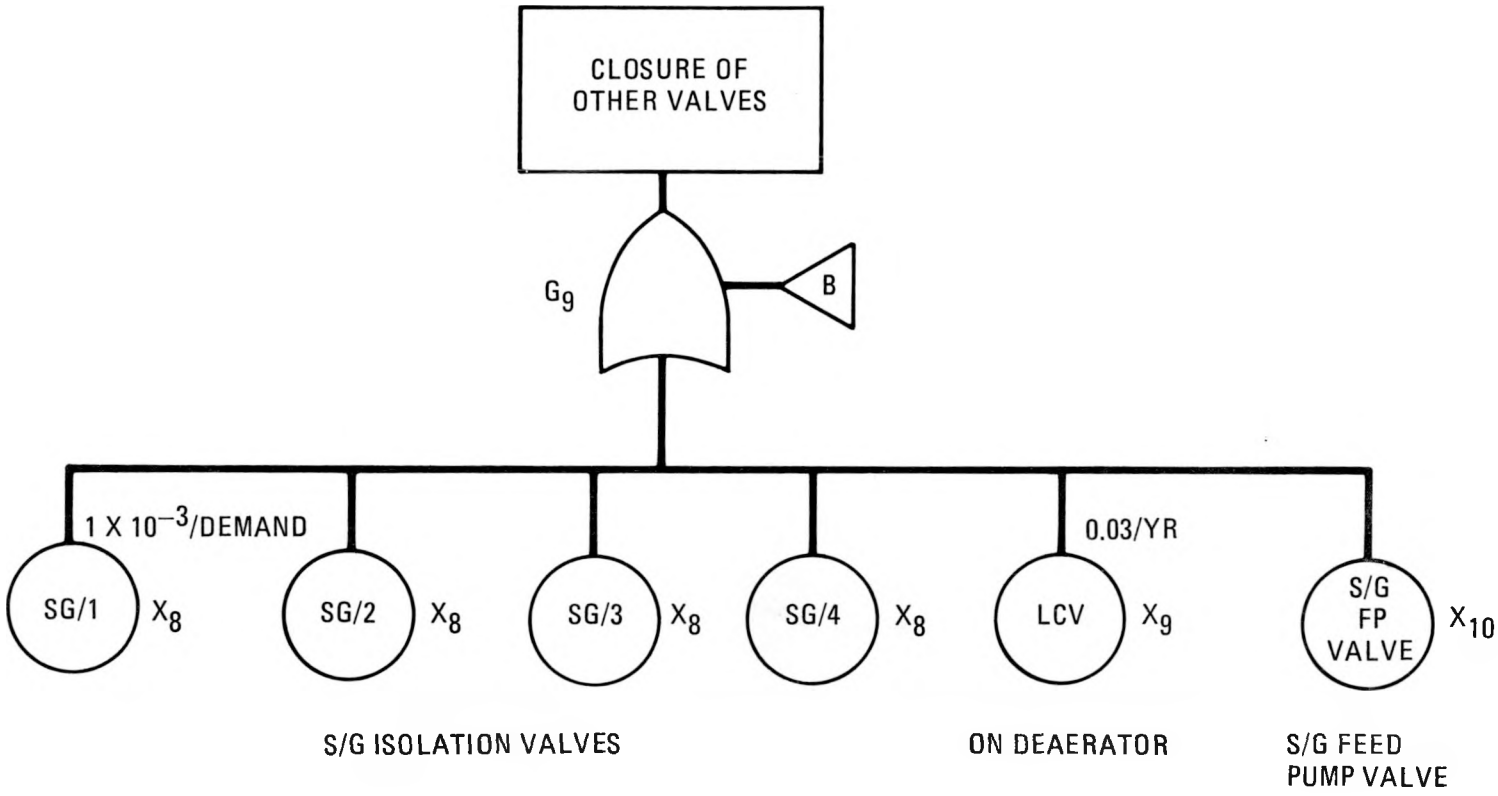

Fig. 4-22. Fault tree for Event 1, loss of main loop cooling (sheet 3 of 5)

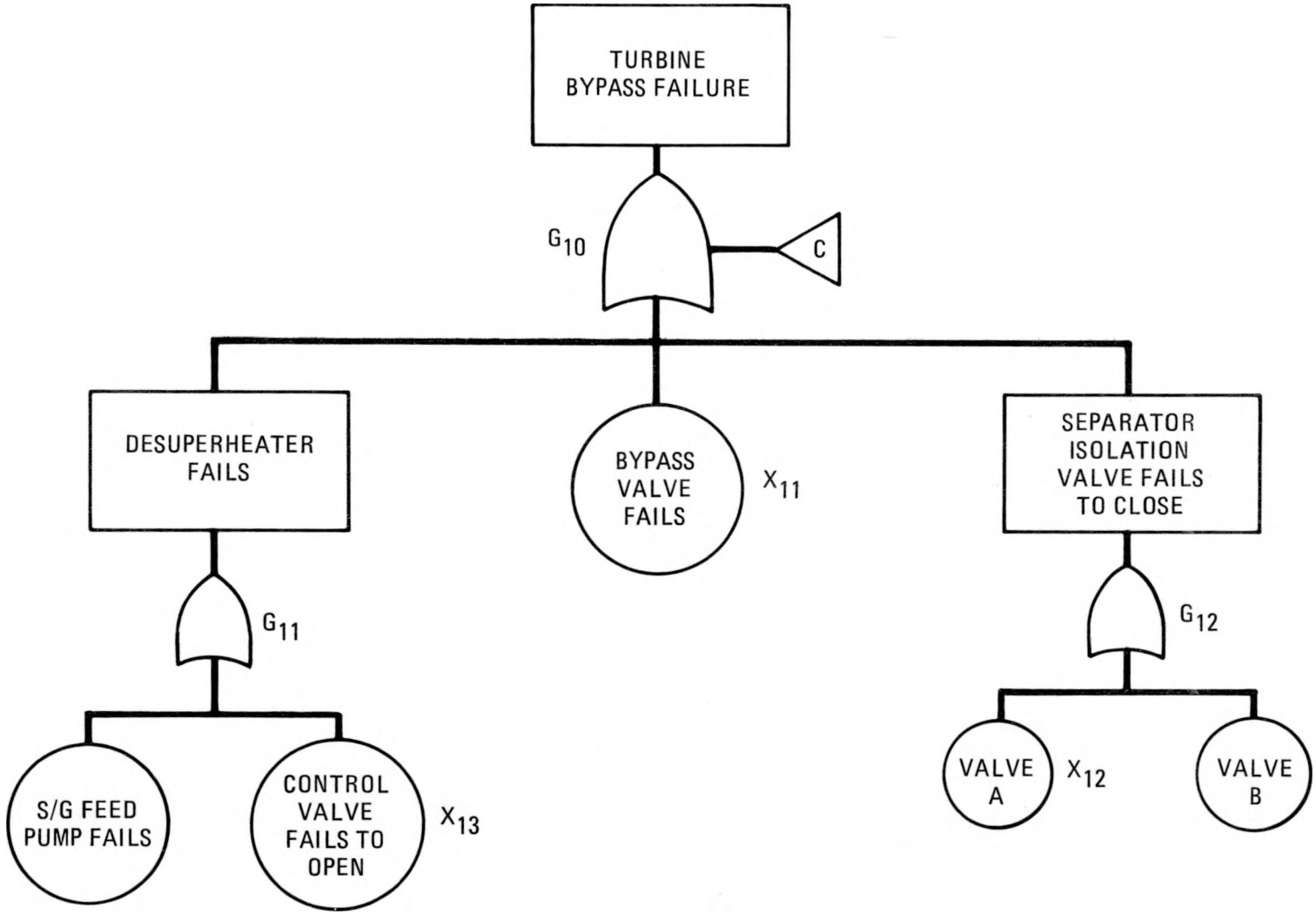

Fig. 4-22. Fault tree for Event 1, loss of main loop cooling (sheet 4 of 5)

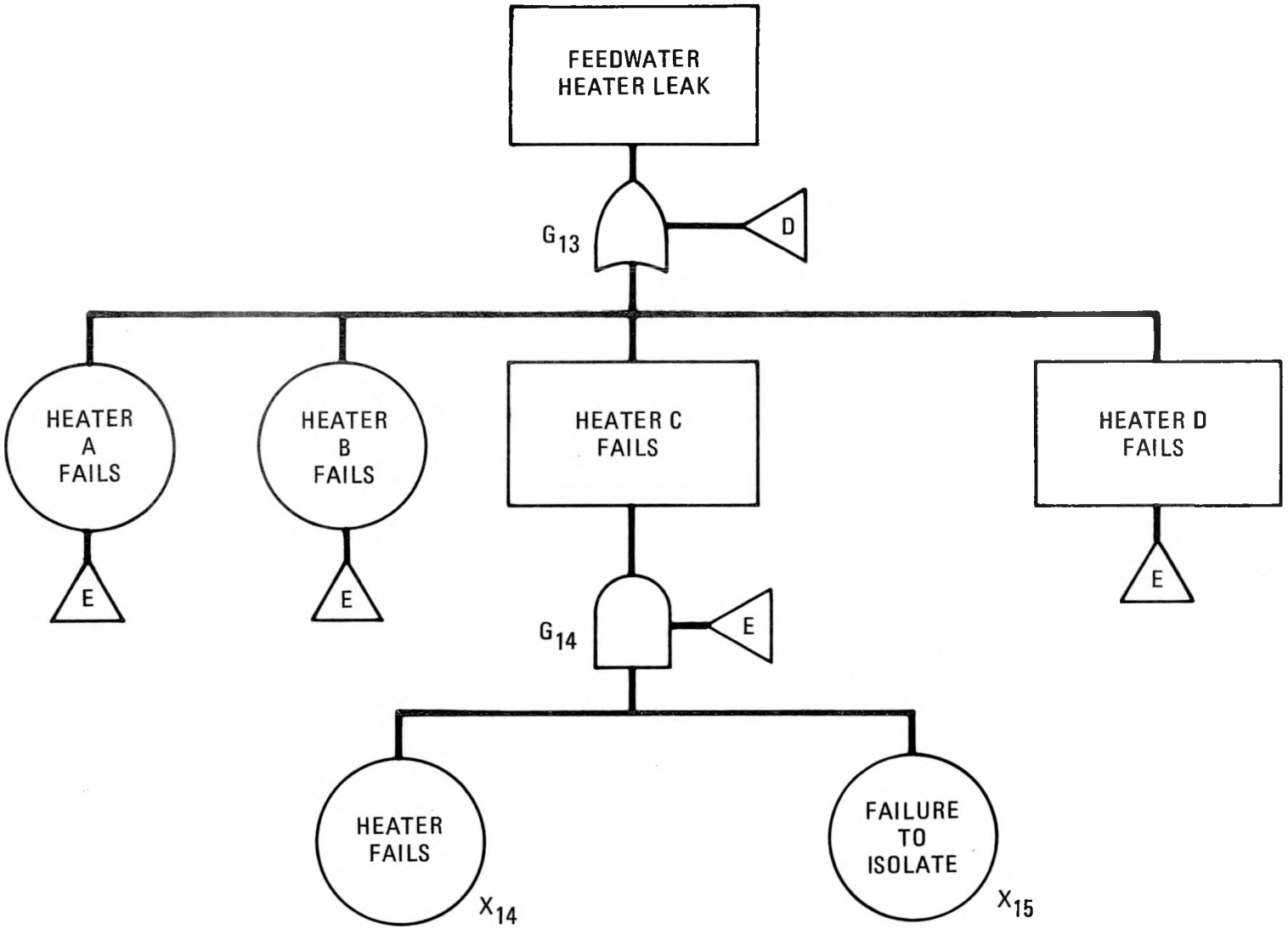

Fig. 4-22. Fault tree for Event 1, loss of main loop cooling (sheet 5 of 5)

4.4. LICENSING (6053040001)

4.4.1. Scope

The licensing activity consists of providing guidance and support on matters related to regulatory requirements.

4.4.2. Discussion

Several proposals for modular reactor cooling systems were reviewed and comments were provided to the designers. Licensing concurred that redundant, safety-related VCS's would meet requirements provided that adequate cooling capability is demonstrated.

A review of available design information on this concept revealed a number of characteristics that present potentially significant licensing problems. These include:

1. The unproven ability of the cooling systems to maintain component conditions within prescribed limits for certain event sequences.

2. Introduction of the rod drop accident for the HTGR.

3. The unproven ability to incorporate two adequate, diverse reactivity control systems.

4. The effects of steam generator or reformer leaks.

5. The potential for a large primary coolant blowdown area.

A proposal by Bechtel to use a confinement rather than a containment was reviewed and comments were provided to the Project Office.

4.5. HTGR-MRS/PH CORE NUCLEAR DESIGN (6053030100)

4.5.1. Scope

The scope of this task is to develop and evaluate core nuclear design and performance for the 250-MW(t) HTGR-MRS/PH.

4.5.2. Discussion

Acceptable preliminary core designs have been developed for a small 250-MW(t) HTGR with a 950°C (1742°F) helium outlet temperature to be used in multiple unit plants for process heat applications. The initial fuel cycle would be based on LEU/Th fuel and 4-yr batch loading. The reactor would be switched at some later time to a fuel cycle based on HEU/Th fuel with a batch residence time of 4 or 5 yr. The HEU/Th fuel provides significant fuel cycle cost and core performance advantages.

A governing feature of the fuel cycles considered for the HTGR-MRS/PH has been the 4- to 5-yr fuel residence time consistent with the reformer lifetime. Reactivity constraints limit the LEU/Th fuel cycle to a maximum cycle length of 4 yr. The HEU/Th fuel cycle, however, can be extended to a lifetime of about 5 yr without imposing severe problems associated with controlling the high initial excess reactivity. Both 5-yr and 4-yr HEU/Th fuel cycles were evaluated in the scoping studies. The latter offers a fall-back design option should more detailed studies reveal potential problems. A shorter fuel residence time, for the same C/Th ratio, requires less initial excess reactivity and offers greater flexibility for the zoning of fuel to achieve optimum power distributions.

Another important consideration in core design is the implicit relationship between the cycle length and the core inlet gas temperature. In general, a longer cycle length, and therefore a heavier fuel loading, limits the steepness of the axial fuel zoning and of the corresponding power profile because of fuel packing constraints. This poses a restriction on the maximum allowable core temperature rise (core ΔT) if the peak fuel

temperature in each fuel zone is to be held below a certain design limit. Since the exit gas temperature of 950°C (1742°F) is fixed, a lower core ΔT implies a higher inlet gas temperature. The inlet gas temperature, which is also the temperature that the HTGR-MRS/PH pressure vessel would experience, considerably influences the design and cost of the vessel. Before the cost sensitivity of the vessel design to the inlet gas temperature was quantified, a preliminary target of about 350°C (662°F) was set for the inlet gas temperature. Preliminary physics and thermal calculations showed that this would be feasible if the cycle length were reduced to about 3 yr. For a 3-yr batch-loaded LEU/Th fuel cycle (C/Th = 600), with 4 axial and 4 radial zones, a core ΔT of 600°C (1080°F) could be achieved while maintaining peak fuel centerline temperatures below the acceptable limit. A 3-yr cycle introduces fuel cycle cost penalties, however, and would fall short of the goal of achieving a 4- to 5-yr core lifetime.

Subsequently, the data made available on the pressure vessel costs versus inlet temperatures clearly showed that the cost impact of higher inlet temperatures becomes marked only at inlet temperatures beyond about 425°C (800°F). A core ΔT of 525°C (945°F) was therefore adopted for the reference HTGR-MRS/PH design. For the HEU/Th cycle, the present study shows that a core ΔT of 575°C (1035°F) could be acceptable.

4.5.2.1. Core Description. The HTGR-MRS/PH is designed to operate at a nominal thermal power level of 250 MW and a corresponding power density of 4.1 W/cm^3. The core consists of 85 columns of hexagonally shaped fuel blocks arranged in a roughly circular shape (Fig. 4-23) to fit into a core cavity having an inside diameter of 3.5 m (11.5 ft). Each fuel column consists of individual fuel blocks stacked eight high. Major core design parameters are summarized in Table 4-4.

The fuel blocks are of the 10-row type. The control blocks that make up 19 of the 85 columns in the core are of a modified design with a single central control rod hole having a diameter of 101 mm (4 in.). The fuel block handling procedure utilizes the four dowel pin positions rather than

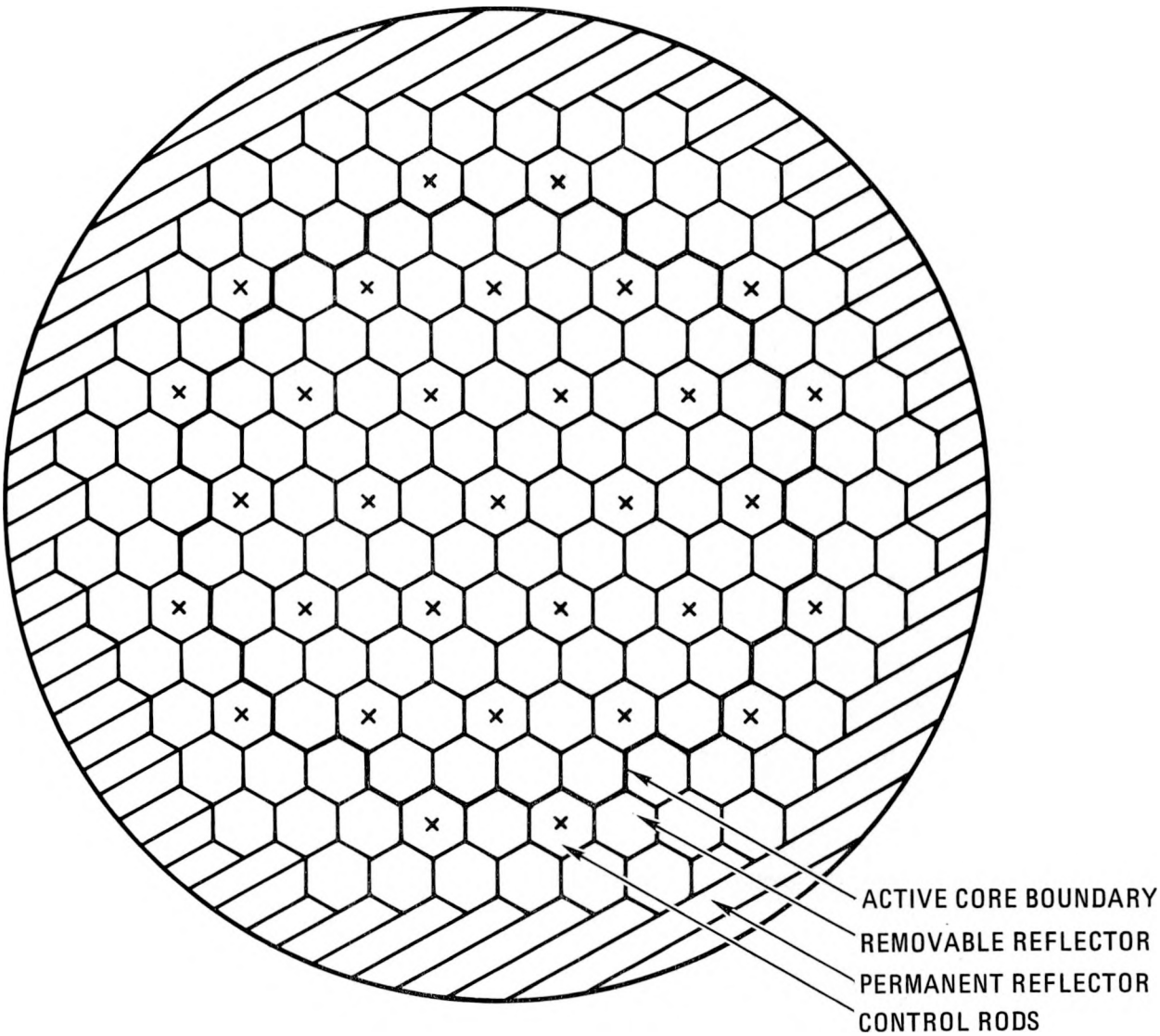

Fig. 4-23. Core layout for the 250-MW(t) HTGR-MRS/PH

TABLE 4-4
BASIC CORE PARAMETERS (HTGR-MRS/PH)

Thermal:	Power	250 MW(t)
	Power density	4.1 W/cm^3
	Outlet temp	950°C (1742°F)
	Core ΔT	525°C (945°F) [575°C (1035°F) for HEU cycle]
	Power/flow	2730 J/kg (344 W-hr/lbm)
	P-inlet	5 MPa (725 psia)
Fuel cycle:	Fuel	HEU/Th or LEU/Th
	Refueling	5-yr (HEU) or 4-yr (LEU/Th) Batch loading
	C/Th ratio	225 for HEU/Th, 600 for LEU/Th
Core layout:	85 columns, 8 blocks high (Fig. 4-23)	
Core dimensions:	Active core reflectors	Height 6.34 m (20.8 ft), diameter 3.5 m (11.5 ft) Side 1 m (3.28 ft), 1.2 m (4 ft), Top, 1.2 m (4 ft) Bottom
Block design:	66 columns of 10-row blocks	
	19 columns of modified 10-row blocks each with a central 101-mm (4-in.) hole to accommodate single control rods	

the central fuel handling hole of the conventional block design. Elimination of the handling hole in the standard blocks allows for a slightly larger number of fuel pins. Table 4-5 gives a summary of the preliminary fuel block parameters.

The fuel material consists of TRISO coated UCO fissile kernels and TRISO coated ThO_2 fertile kernels. The particles are bonded with graphite filler into 12.6-mm (0.49-m) diameter fuel rods. Particle descriptions are given in Tables 4-6 and 4-7.

Reactivity control is accomplished by single control rods (rather than by the conventional rod pairs) inserted from below into the 31 core and reflector locations shown in Fig. 4-23.

4.5.2.2. Power Distribution and Fuel Zoning Studies. Optimal core compositions were determined with the zero-dimensional GARGOYLE code. Radial and axial zoning of the uranium, thorium, and lumped burnable poison was then studied with the one-dimensional GASP code for both HEU/Th and LEU/Th cycles. The GASP code adjusts fuel concentrations by zone to achieve zone average power densities, including provision for stability with burnup. Radial power distributions were optimized to achieve approximately equal power peaks in all zones. Three radial zoning prescriptions were studied. The first, a three-zone combination of 19, 36, and 30 columns, was carried over from earlier HEU/Th cycle studies, but was consequently dropped in favor of four-zone layouts to reduce the peaking. Four-zone combinations of 19-18-24-24 or 19-18-18-30 columns were then adopted.

Table 4-8A gives the basic details and results of the radial zoning calculations for HEU/Th cycles for 5-yr and 4-yr residence times. The power factors listed express ratios of zone-average to core-average power densities, and the loading factors are the zone-to-core average concentration ratios required to produce the specified zone power distributions. At the bottom of the table it is seen that the four-zone design decreases the radial power peaking by about 7% relative to the three-zone combination.

TABLE 4-5
FUEL ELEMENT PARAMETERS (10-ROW DESIGN)

	Standard	Control
Length of fuel element, mm (in.)	793 (31.2)	793 (31.2)
Distance across flats, mm (in.)	360 (14.17)	360 (14.17)
Number of fuel holes	222	198
Number of coolant holes		
Large holes	102	90
Medium holes	6	6
Effective flow basis	105.3	93.3
Area basis	106.8	94.8
Hole diameters, mm (in.)		
Fuel holes	127 (0.5)	127 (0.5)
Large coolant hole	159 (0.62)	159 (0.62)
Medium coolant hole	127 (0.5)	127 (0.5)
Control rod	--	--
Pitches, mm (in.)		
Coolant - coolant	326 (1.28)	326 (1.28)
Coolant - fuel	188 (0.74)	188 (0.74)
Fuel - fuel	188 (0.74)	188 (0.74)
Web thickness, mm (in.)		
Coolant - coolant	167 (0.66)	167 (0.66)
Coolant - fuel	4.5 (0.18)	4.5 (0.18)
Fuel - fuel	6.1 (0.24)	6.1 (0.24)
Fuel rod diameter, mm (in.)	12.6 (0.5)	12.7 (0.5)
Fuel rod length, mm (in.)	63 (2.48)	63 (2.48)
Fuel stack height, mm (in.)	712.5 (28.0)	712.5 (28.0)

TABLE 4-6
PARTICLE SYSTEM FOR HEU/Th FUEL

	Particle Descriptions	
	Particle 1	Particle 2
Grain diameter	5.00000+02	2.00000+02
Coating thicknesses		
Buffer	8.00000+01	1.00000+02
Inner pyrolytic	3.50000+01	3.00000+01
Silicon carbide	3.50000+01	3.50000+01
Outer pyrolytic	4.00000+01	3.50000+01
Coating thickness/grain diameter	3.80000-01	1.00000+00
Densities (g/cm^3)		
Grain	9.80000+00	1.13000+01
Buffer	1.00000+00	1.00000+00
Inner pyrolytic	1.90000+00	1.90000+00
Silicon carbide	3.20000+00	3.20000+00
Outer pyrolytic	1.87000+00	1.87000+00
Total particle	3.36161+00	2.31569+00
For separability	3.85533+00	2.51664+00
Volume fractions		
Grain	1.83426-01	3.70370-02
Buffer	2.38449-01	2.59259-01
Inner pyrolytic	1.48973-01	1.54333-01
Silicon carbide	1.80467-01	2.38616-01
Outer pyrolytic	2.48685-01	3.10755-01
Atom ratio in grain		
Thorium	1.00000+00	0.00000
Uranium	0.00000	1.00000+00
Carbon	0.00000	2.00000+00
Oxygen	2.00000+00	0.00000
Enrichment		
U-233		0.00000
U-234		7.42293-03
U-235		9.31892-01
U-236		2.81597-03
U-238		5.78695-02
Heavy metal atom density in grain	2.23551-02	2.62573-02
Heavy metal atom density in particle	4.10052-03	9.72494-04
Graphite atom density in grain	0.00000	5.25147-02

TABLE 4-7
PARTICLE SYSTEM FOR LEU/Th FUEL

	Particle Descriptions	
	Particle 1	Particle 2
Grain diameter	500.0	350.0
Coating thicknesses		
Buffer	80.0	115.0
Inner pyrolytic	35.0	35.0
Silicon carbide	35.0	35.0
Outer pyrolytic	40.0	40.0
Coating thickness/grain diameter	0.3800	0.6429
Densities (g/cm^3)		
Grain	9.80	11.0
Buffer	1.00	1.00
Inner pyrolytic	1.90	1.90
Silicon carbide	3.20	3.20
Outer pyrolytic	1.87	1.87
Total particle	3.362	2.637
For separability	3.855	2.922
Volume fractions		
Grain	0.1834	0.0837
Buffer	0.2384	0.2973
Inner pyrolytic	0.1490	0.1553
Silicon carbide	0.1805	0.1926
Outer pyrolytic	0.2487	0.2710
Atom ratio in grain		
Thorium	1.00	0.00
Uranium	0.00	1.00
Carbon	0.00	0.30
Oxygen	2.00	1.70
Enrichment		
U-235		0.200000
U-238		0.800000
Heavy metal atom density in grain	2.23551-02	2.46996-02
Heavy metal atom density in particle	4.10052-03	2.06835-03
Graphite atom density in grain	0.00000	7.40987-03

TABLE 4-8A
RADIAL ZONING CALCULATIONS FOR VHTR MODULAR-CORE DESIGNS USING HEU/Th FUEL

Fuel Type/Residence	HEU/5 Yr	HEU/5 Yr	HEU/4 Yr
Core-average C/Th	200	225	250
Core-average C/U	2970	2860	3560
Number of radial zones	3	4	4
Number of fuel columns			
Zone 1	19	19	19
Zone 2	36	18	18
Zone 3	30	24	24
Zone 4	--	24	24
Power factor			
Zone 1	1.174	1.118	1.092
Zone 2	1.070	1.075	1.058
Zone 3	0.806	1.065	1.051
Zone 4	--	0.786	0.833
Th loading factor			
Zone 1	0.977	1.004	0.997
Zone 2	0.973	0.959	0.959
Zone 3	1.047	0.967	0.963
Zone 4	--	1.061	1.069
U loading factor			
Zone 1	0.981	0.934	0.907
Zone 2	1.141	1.045	1.013
Zone 3	0.842	1.243	1.204
Zone 4	--	0.775	0.860
Power peaking factor[a]			
Zone 1	1.243	1.171	1.142
Zone 2	1.242	1.169	1.144
Zone 3	1.229	1.162	1.149
Zone 4	--	1.126	1.157

[a]Fuel-only zoned, without burnup.

For the four-zone cases, comparing the 5-yr and 4-yr loading results indicates only slightly lower power zoning requirements and radial power peaking factors for the lighter loaded 4-yr design. Figure 4-24 compares the radial power profiles for the HEU design with the 19-18-24-24 layouts (fuel-only zoned, no burnable poison).

Results of radial zoning calculations for the LEU/Th cycles are given in Table 4-8B. Again, the heavier loading (4-yr design) is seen to yield slightly higher power peaks (unburned) than the 3-yr loading. Changing the zoning scheme (a six-column shift from zone 3 to zone 4) increases the power peaking a few percent. Compared to the similarly zoned HEU 4-yr design (last column in Table 4-7), the second LEU 4-yr design requires less severe power zoning and yields about 8% lower power peaking (for these unpoisoned, unburned core studies). This case is the reference selected for the two-dimensional studies described in Section 6. Figure 4-25 compares the radial power profiles corresponding to the Table 4-8B loadings; the radial power variations are seen to be less than that shown in Fig. 4-24 for the HEU loadings.

The GASP code also was used for the axial power zoning, but in this case, iterations were carried out with thermal-flow calculations (using the code BACH) to obtain axial power distributions that equalize the zone peak fuel temperatures. The eight-block stack of fuel elements in the columns is divided into several zones. In theory, the finer the zoning (larger number of zones), the lower the temperature peaks; however, effects of zone-to-zone neutron spectral differences give extra power peaking to diminish the advantages of many zones. Also, the required power factors for small first zones (bottom zone in upflow core) require loading factors beyond fuel-rod packing limitations. The resulting optimum axial zoning thus involves trade-offs between performance (core power and coolant temperature rise) and fuel residence (which determines heavy metal loadings). A four-zone scheme was found acceptable for a light loading (3-yr residence core), but the 4-yr and 5-yr loadings require three-zone combinations; two zones would be used for lower specifications on core coolant temperature rise.

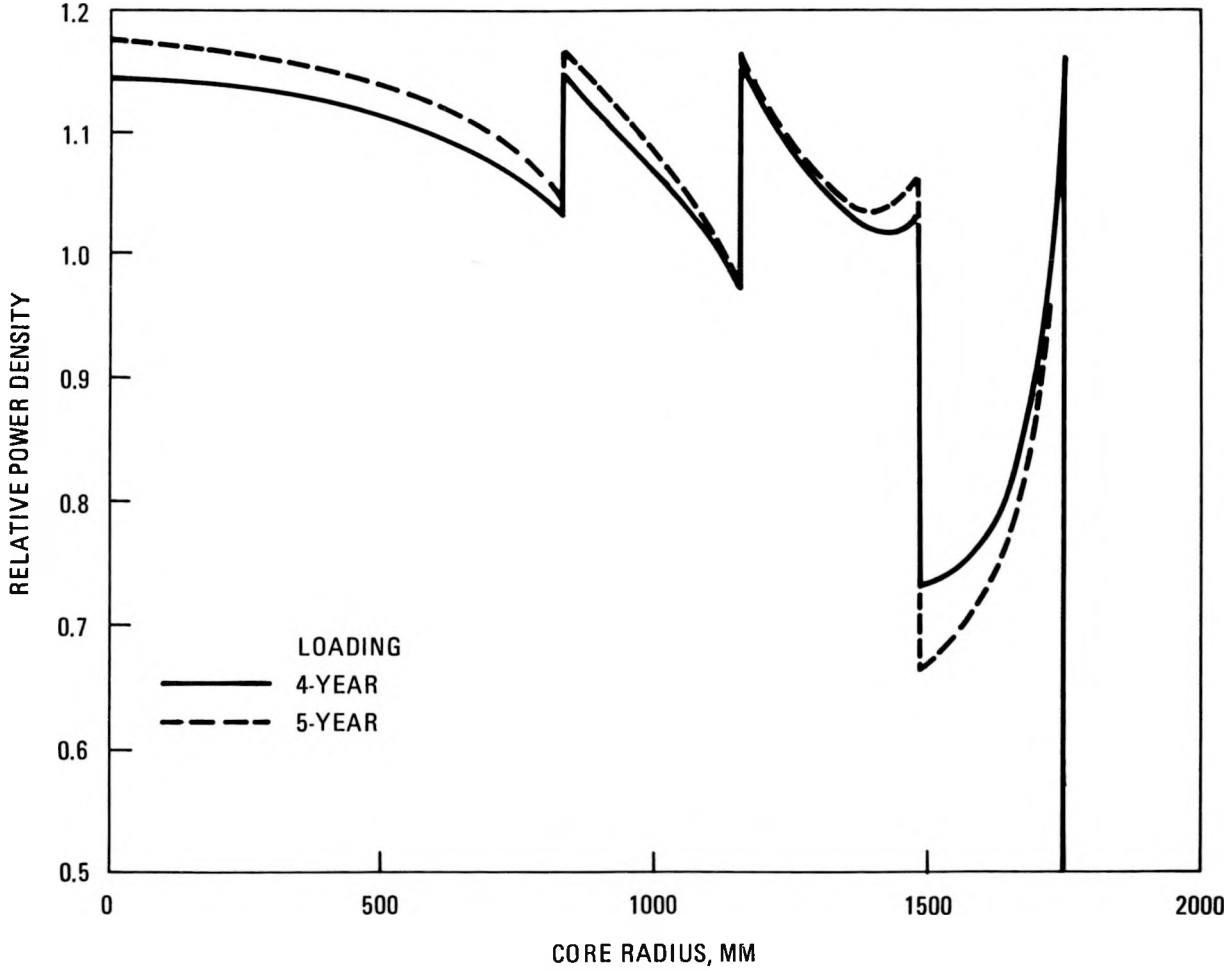

Fig. 4-24. Radial power profiles for HEU modular VHTR cores

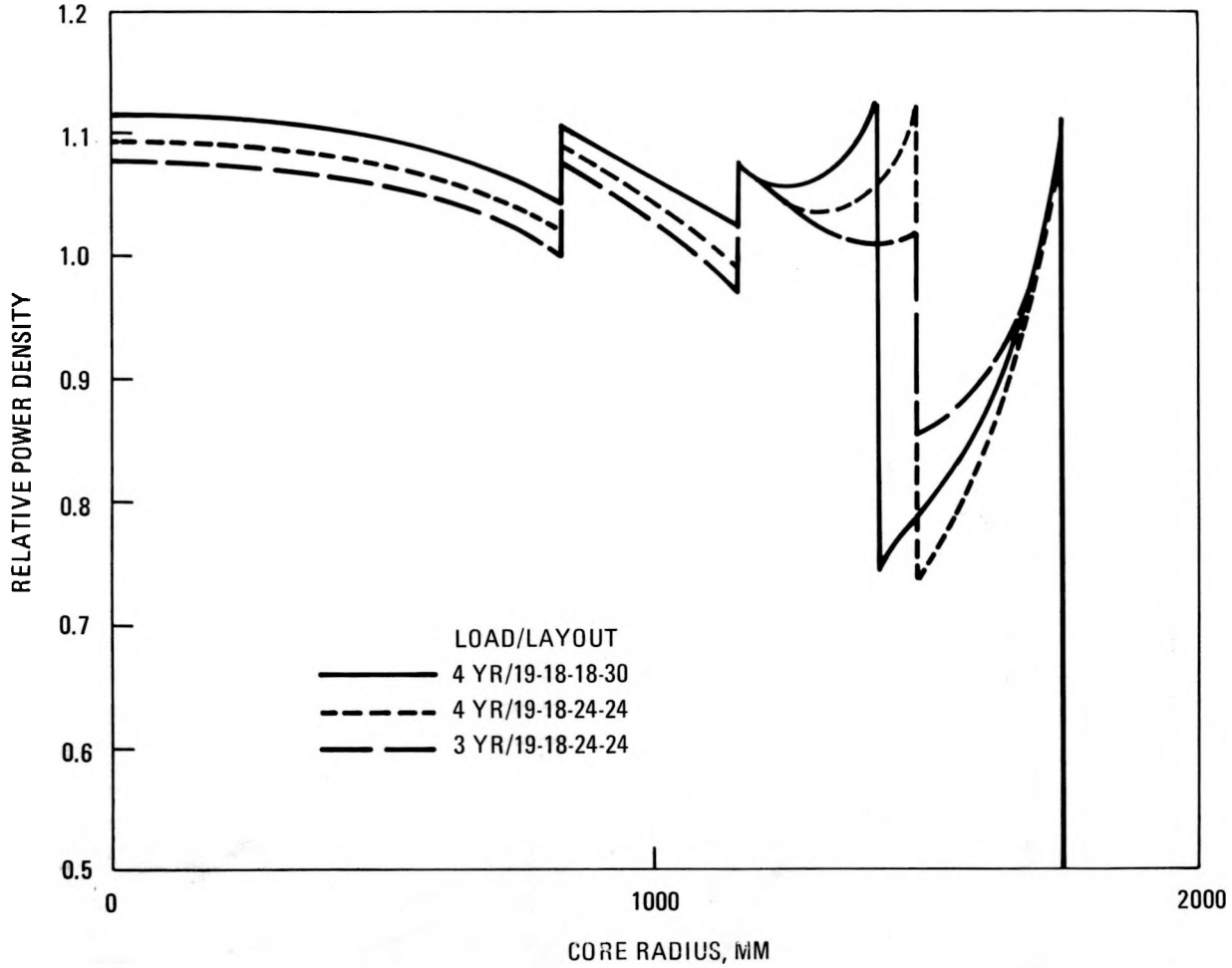

Fig. 4-25. Radial power profiles for LEU modular VHTR cores

TABLE 4-8B
RADIAL ZONING CALCULATIONS FOR VHTR MODULAR-CORE
DESIGNS USING LEU/TH FUEL

Fuel Type/Residence	LEU/3 Yr	LEU/4 Yr	LEU/4 Yr
Core-average C/Th	600	600	600
Core-average C/U	890	575	575
Number of radial zones	4	4	4
Number of fuel columns			
Zone 1	19	19	19
Zone 2	18	18	18
Zone 3	24	24	18
Zone 4	24	24	30
Power factor			
Zone 1	1.042	1.059	1.080
Zone 2	1.021	1.038	1.058
Zone 3	1.025	1.053	1.066
Zone 4	0.926	0.872	0.875
Th loading factor			
Zone 1	1.153	1.138	1.117
Zone 2	1.045	0.979	0.958
Zone 3	0.901	0.885	0.914
Zone 4	0.945	1.021	1.003
U loading factor			
Zone 1	0.933	1.006	1.059
Zone 2	1.005	1.079	1.126
Zone 3	1.116	1.169	1.176
Zone 4	0.933	0.766	0.781
Power peaking factor[a]			
Zone 1	1.075	1.090	1.112
Zone 2	1.074	1.089	1.103
Zone 3	1.075	1.070	1.119
Zone 4	1.077	1.085	1.106

[a]Fuel-only zoned, without burnup.

Table 4-9 lists the GASP results for axial zoning of two 5-yr loadings and a 4-yr HEU/Th loading with various axial zoning schemes. The previous process heat HTGR studies involved a 3-2-3 axial scheme, which when optimized requires unattainable fuel rod packing. Even the 4-4 scheme adopted for steam-cycle designs gives excessive packing for a 5-yr loading with an average C/Th ratio of 200. A 5-3, two-zone combination could be used to accommodate the C/Th = 200 loading, 5-yr residence. Increasing the C/Th to 225 (lighter loading) for the 5-yr designs allows for a four-block first zone, and here a 4-2-2, three-zone scheme is adopted. A 4-yr design, with a C/Th = 250 loading, also is readily accommodated by the 4-2-2 scheme.

Table 4-10 gives the results of several BACH (thermal-flow) calculations for the Table 4-9 HEU-fueled cores. The first three cases differ only in zoning scheme, and it is seen that, relative to a three-zone scheme, the two-zone schemes yield temperature peaks about 20°C (36°F) higher for the average fuel and for the assumed hottest-channel fuel. Increasing the coolant-temperature rise by 25°C (45°F) does not affect the average-channel fuel temperature [same core outlet of 950°C (1742°F)], but increases the hot-channel fuel temperature by about 20°C (36°F) for the 5-3 scheme and by 12°C (22°F) for a 4-2-2 scheme.

The last two columns in Table 4-10 compare 5-yr and 4-yr loading HEU designs using the same axial zoning scheme and power splits; here little difference is seen in the calculated peak fuel temperatures. Figure 4-26 shows the typical axial power and temperature profiles for a 4-2-2 zoned HEU core.

Results of GASP calculations for 3-yr and 4-yr LEU modular core axial zonings are given in Table 4-11. An initial case with the lighter 3-yr loading was run to ascertain the advantage of an eight-zone scheme (block-by-block zoning); here a first-zone power factor of 2.00 does not yield equalized zone-temperature peaks but already requires zone-1 loading in excess of the 50% packing fraction limits. A four-zone 2-2-2-2 scheme is easily optimized with the 3-yr loading.

TABLE 4-9
AXIAL ZONING CALCULATIONS FOR HEU/TH-FUELED VHTR
MODULAR CORE DESIGNS

Batch-loading fuel residence, yr	5	5	5	5	4
Core-average loading					
C/Th	200	200	200	225	250
C/U	2967	2967	2967	2860	3050
Average fuel rod packing (for 200/500 particles)					
Th, %	34.50	34.50	34.50	30.76	27.84
U, %	9.81	9.81	9.81	9.51	8.24
Axial zoning scheme (blocks/zone)	3-2-3	4-4	5-3	4-2-2	4-2-2
Zone-to-column power ratio					
Zone 1	1.500	1.400	1.250	1.413	1.413
Zone 2	1.000	0.600	0.583	0.804	0.804
Zone 3	0.500	--	--	0.371	0.371
Thorium loading factor					
Zone 1	1.269	1.217	1.141	1.225	1.243
Zone 2	0.998	0.783	0.766	0.926	0.921
Zone 3	0.730	--	--	0.625	0.593
Uranium loading factor					
Zone 1	1.547	1.414	1.251	1.432	1.425
Zone 2	0.886	0.586	0.582	0.732	0.734
Zone 3	0.730	--	--	0.404	0.416
Maximum fuel-rod packing[a]					
Th, %	42.4	40.6	38.1	36.4	33.5
U, %	18.9	17.2	15.2	16.9	14.6
Total, %	61.3	57.8	53.3	53.3	48.1

[a]For Zone 1 with factors for highest-loading radial zone (in four-zone design).

TABLE 4-10
SUMMARY OF THERMAL-FLOW CALCULATIONS FOR HEU/TH-FUELED MODULAR CORE DESIGNS

Fuel residence time, yr	5	5	5	5	5	5	4
Core-average loading							
C/Th	200	200	200	200	225	225	250
C/U	2967	2967	2967	2967	2859	2859	3050
Coolant ΔT (T-out = 950)	475	475	475	525	550	575	575
Axial zoning scheme	3-2-3	4-4	5-3	5-3	4-2-2	4-2-2	4-2-2
Power factor							
Zone 1	1.50	1.40	1.25	1.25	1.41	1.41	1.41
Zone 2	1.00	0.60	0.58	0.58	0.80	0.80	0.80
Zone 3	0.50	--	--	--	0.37	0.37	0.37
Zone 1 fuel-rod packing, %[a]	59.0	55.9	51.6	51.6	52.3	52.3	46.3
Peak fuel temperature for average channel, °C							
Zone 1	950	1022	1023	1022	1002	1000	1002
Zone 2	983	1009	1015	1018	998	998	996
Zone 3	1003	--	--	--	996	998	997
Peak fuel temperature for radial P/A = 1.250, °C							
Zone 1	1086	1178	1180	1197	1182	1190	1193
Zone 2	1131	1167	1175	1198	1181	1193	1191
Zone 3	1160	--	--	--	1182	1195	1193

[a]Without accounting for radial zoning factors.

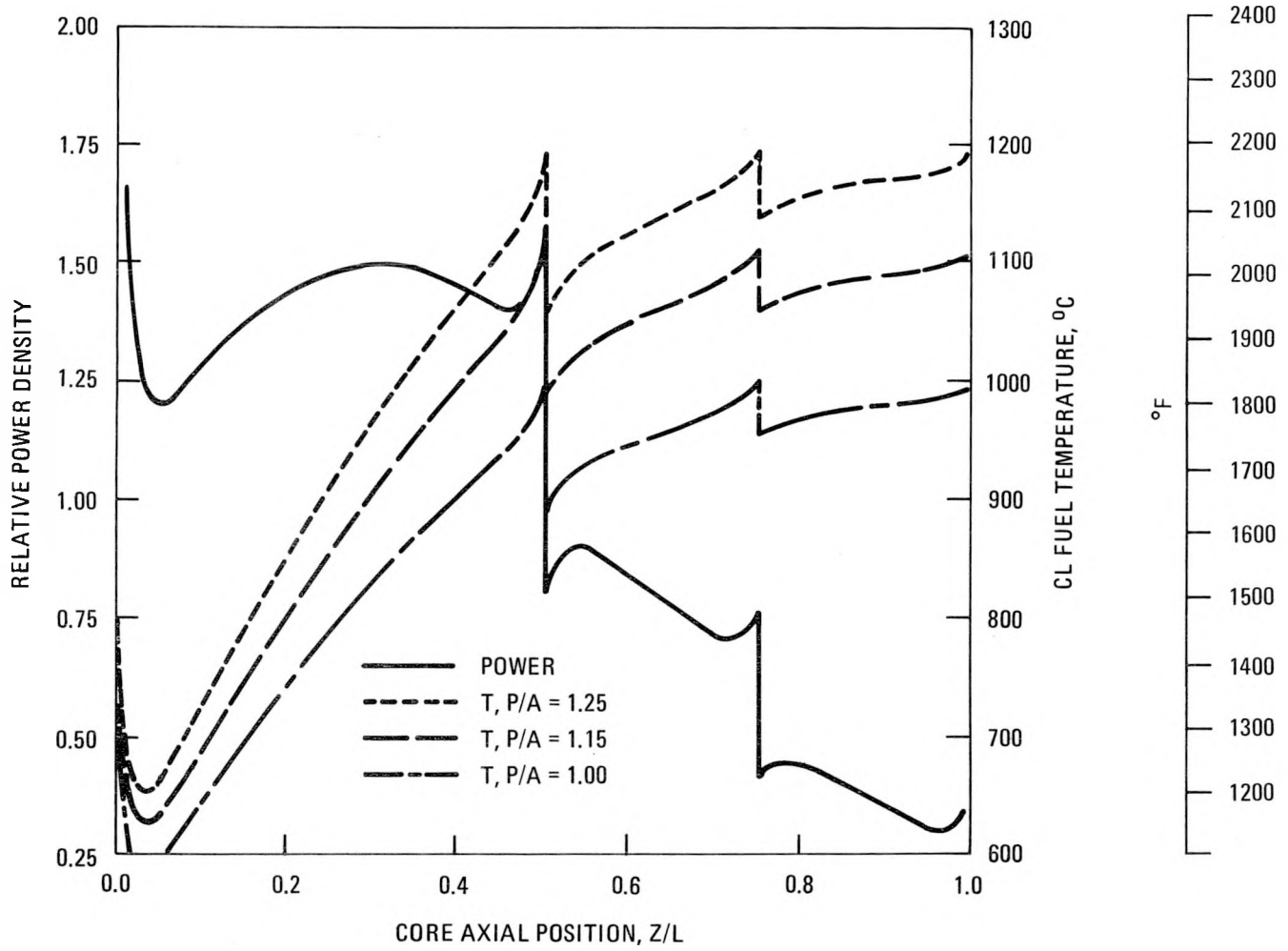

Fig. 4-26. Axial power and temperature profiles for HEU modular VHTR

TABLE 4-11
AXIAL ZONING CALCULATIONS FOR LEU/TH-FUELED VHTR MODULAR CORE DESIGNS

Batch-loading residence, yr	3	3	4	4
Core-average loading				
Th	600	600	600	600
U	890	890	575	575
Average fuel-rod packing (for 350/500 particles)				
Th, %	12.01	12.01	12.77	12.77
U, %	16.06	16.06	24.60	24.60
Axial zoning scheme	8-zone[a]	2-2-2-2	3-2-3	4-2-2
Zone-to-column power ratio				
Zone 1	2.000	1.832	1.538	1.321
Zone 2	1.640	1.201	1.014	0.885
Zone 3 (7)	(0.400)	0.651	0.449	0.473
Zone 4 (8)	(0.270)	0.310	--	--
Thorium loading factors				
Zone 1	0.842	1.008	0.758	0.908
Zone 2	1.165	1.258	1.346	1.220
Zone 3 (4)	(1.241)	1.049	1.014	0.964
Zone 4 (8)	(0.521)	0.684	--	--
Uranium loading factors				
Zone 1	2.854	2.322	1.928	1.528
Zone 2	1.776	0.926	0.663	0.616
Zone 3 (4)	(0.748)	0.470	0.288	--
Zone 4 (8)	(0.255)	0.281	--	0.328
Maximum fuel-rod packing (including maximum axial and radial zoning effects)				
Th, %	9.1	10.8	8.6	9.9
U, %	51.2	42.4	55.4	42.7
Total, %	60.3	53.2	64.0	52.6

[a]One zone per block.

The 4-yr LEU/Th core design requires a 54% increase in uranium loading (relative to the 3-yr core with the same C/Th ratio) and therefore cannot be optimized within the packing restraint. Therefore, a 4-2-2 three-zone scheme was finally adopted, giving a maximum zone-1 fuel-rod packing of about 53% (axial plus radial factors included).

Table 4-12 lists the results of several BACH calculations using the axial power distributions from the LEU-core GASP calculations. The unoptimized, eight-zone, 3-yr design gives peak temperatures about the same as from the four-zone (2-2-2-2) scheme; with a one-block first zone, the heavy fissile concentrations provide power and temperature peaks at the bottom of the zone (next to the reflector). For the two four-zone studies, the increase of coolant ΔT from 575° to 600°C (1035° to 1080°F) again has little effect on the average-fuel temperature peaks, but increases the hot-channel temperature peaks by about 4°C (7°F). Thus, it appears that the coarser the axial zoning, the higher the impact on fuel peak temperatures from decreasing the core-inlet helium temperature.

The 4-yr cases in Table 4-12 reveal that the rearrangements in three zones from 3-2-3 to 4-2-2 schemes would increase average and hot-channel fuel peak temperatures on the order of 10°C (18°F) because of the different in-zone power distributions and zone-end power peaking. With the adopted 4-yr LEU/Th loading and necessary 4-2-2 axial zoning scheme, it appears that a coolant rise of 575°C (1035°F) will yield fuel hot-spot temperatures in excess of 1200°C (2192°F) (and also instability of power zoning with burnup). Thus, a 50°C (90°F) lower ΔT of 525°C (945°F) [T-inlet = 423°C (797°F)] was adopted for the final case studied. The lower core ΔT reduces the peak temperatures by about 20°C (36°F) (for the assumed worst radial peaking factor of 1.25), revealing a consistent factor of 0.40 relating peak temperature change to ΔT change for the three-zone scheme.

Figure 4-27 shows the axial power and temperature profiles for the final case, the 4-yr LEU/Th core with a 4-2-2 axial zoning and core inlet temperature of 425°C (797°F). Comparison of power shapes with the Fig. 4-26

TABLE 4-12
SUMMARY OF THERMAL-FLOW CALCULATIONS FOR LEU/Th-FUELED MODULAR CORE DESIGNS

Fuel-residence time, yr	3	3	3	4	4	4
Core-average loading						
C/Th	600	600	600	600	600	600
C/U	890	890	890	575	575	575
Coolant ΔT, °C (T-out = 950)	575	575	600	575	575	575
Axial zoning scheme	8-zone	2-2-2-2	2-2-2-2	3-2-3	4-2-2	4-2-2
Power factors						
Zone 1 (1)	(2.00)	1.83	1.83	1.50	1.32	1.32
Zone 2 (2)	(1.64)	1.20	1.20	1.00	0.88	0.88
Zone 3 (6)	(0.40)	0.65	0.65	0.50	0.47	0.47
Zone 4 (8)	(0.27)	0.31	0.31	--	--	--
Zone 1 fuel-rod packing, %	56	49.4	49.4	55.7	48.7	48.7
Peak fuel temperature for average channel, °C						
Zone 1 (1)	(939)	991	988	994	1006	1010
Zone 2 (4)	(954)	989	987	996	1009	1008
Zone 3 (6)	(971)	987	987	1005	1007	1004
Zone 4 (8)	(983)	981	982	--	--	--
Peak fuel temperature for radial P/A = 1.25, °C						
Zone 1	(1154)	1180	1184	1181	1197	1180
Zone 2 (4)	(1136)	1181	1186	1187	1205	1182
Zone 3 (6)	(1164)	1183	1181	1204	1207	1180
Zone 4 (8)	(1181)	1180	1189	--	--	--

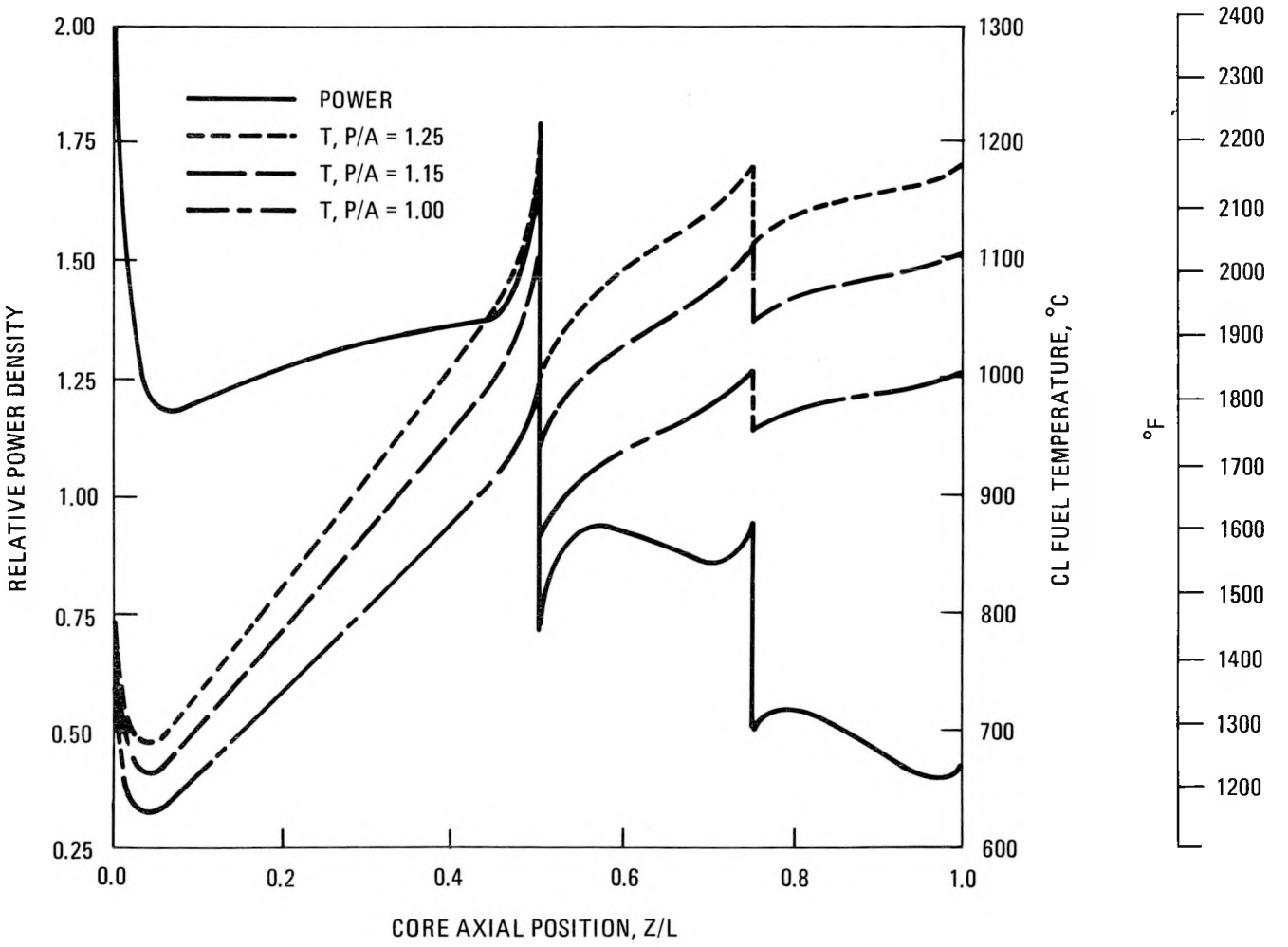

Fig. 4-27. Axial profiles for 4-yr LEU modular VHTR

curve for HEU fuel shows higher peak-to-average power spikes within zones for the LEU loadings.

4.5.2.3. Burnable Poison Zoning. The GASP code also provides for the zoning of burnable poison (boron-10) required to provide manageable excess reactivity throughout the cycle. The boron distributions calculated to retain the zone power splits achieved for the fuel zoning come out roughly proportional to the zone fissile concentrations. Maintaining the zone power distributions during burnout of the boron requires selective lumping of self-shielding of the poison; the lumping prescriptions are also calculated by GASP but can be refigured readily to vary the desired burnout rate. For HTGR-MRS batch loadings, the long residence requirements and high initial reactivity of the fuel require heavy poison loadings (about 12% absorption at start of cycle in boron) and heavy shielding to prevent early burnout.

Table 4-13 lists input and output parameters for the zoning of poison in the 5-yr HEU core design. Cases 1 and 2 are radial zoning with different poison contents and burnout rates. Doubling the burnout half-life from 860 to 1750 days is accomplished by increasing the self-shielding of the loaded poison but maintaining about the same initial absorption in boron. The longer half-life prescription is seen to reduce the peak reactivity rise during burnout while giving a still acceptable boron absorption fraction at the end of the 5-yr burn. The last column gives the results for an axial zoning of burnable poison for the same core but with a lower initial boron loading and with a faster burnout rate that results in greater reactivity swings in the cycle. Notice should be taken of the fairly uniform boron shielding factors obtained for the HEU-fueled loadings, an effect which contributes to equalizing the real burnout rates for boron by zone and to maintaining stability of the zone power factors.

Results of poison radial zoning for the 3-yr LEU design and axial poison zoning for the 4-yr design are given in Table 4-14. The two radial cases represent the same fuel loading but different poison lumping for the same unburned reactivity excess. The longer-lived (greater poison shielding

TABLE 4-13
BURNABLE POISON ZONING AND BURNUP CALCULATIONS
FOR HEU/TH-FUELED MODULAR CORE DESIGN

Fuel residence time, yr	5	5	5
Loading-average			
C/Th	225	225	225
C/U	2860	2860	2860
GASP and FEVER geometry	Radial	Radial	Axial
Zoning scheme	19-18-24-24	19-18-24-24	4-2-2
GASP zoning calculation			
k_{eff} fuel-only zoned	1.2205	1.2205	1.2133
k_{eff} for poison search	1.0015	1.0150	1.0400
Homogeneous B-10 concentration (10^{-7} a/b-cm)			
Zone 1	8.522	7.891	9.740
Zone 2	9.460	8.760	5.109
Zone 3	11.096	10.180	2.925
Zone 4	7.462	6.909	--
Half-life, days, for poison burnout	860	1750	343
Poison lumping self-shielding factors at beginning of cycle			
Zone 1	0.408	0.286	0.712
Zone 2	0.445	0.311	0.667
Zone 3	0.496	0.344	0.722
Zone 4	0.438	0.307	--
Results of FEVER calculation			
k_{eff}			
Day-0	1.0245	1.0401	1.0635
6 days	0.9995	1.0139	1.0376
1 year	1.0068	1.0006	1.0712
2 years	1.0423	1.0171	1.0927
3 years	1.0637	1.0414	1.0800
4 years	1.0492	1.0419	1.0541
5 years	1.0133	1.0130	1.0093
Fractional absorption in boron, %			
Day-0	14.90	13.95	11.46
1/2 year	13.12	12.83	8.54
1 year	11.25	11.70	5.95
2 years	6.63	8.43	2.25
3 years	2.57	4.26	0.65
4 years	0.68	1.34	0.15
5 years	0.13	0.29	0.03
Maximum peak/average power factor	1.168	1.167	2.309

TABLE 4-14
BURNABLE POISON ZONING AND BURNUP CALCULATIONS
FOR LEU/TH-FUELED MODULAR CORE DESIGN

Fuel residence time, yr			
Loading-average	3	3	4
C/Th	600	600	600
C/U	890	890	575
GASP and FEVER geometry	Radial	Radial	Axial
Zoning scheme	19-18-24-24	19-18-24-24	4-2-2
GASP zoning calculations			
k_{eff} fuel-only zoned	1.2232	1.2332	1.2097
k_{eff} for poison search	1.0500	1.0050	1.0503
Homogeneous B-10 concentration (10^{-7} a/b-cm)			
Zone 1	4.742	4.742	9.778
Zone 2	4.973	4.973	4.063
Zone 3	5.374	5.374	2.264
Zone 4	4.618	4.618	--
Half-life, days, for poison burnout	151	270	407
Poison lumping self-shielding factors at beginning of cycle			
Zone 1	0.856	0.640	0.739
Zone 2	0.900	0.672	0.553
Zone 3	0.947	0.707	0.544
Zone 4	0.887	0.662	--
Results of FEVER calculation			
k_{eff}			
Day-0	1.0792	1.0801	1.0765
6 days	1.0502	1.0490	1.0496
1 year	1.0997	1.0766	1.0517
2 years	1.0600	1.0543	1.0366
3 years	1.0027	1.0028	1.0066
4 years	--	--	0.9742
Fractional absorption in boron, %			
Day-0	12.18	12.16	10.15
1/2 year	6.03	7.73	7.39
1 year	2.81	4.42	5.25
2 years	0.49	0.96	2.14
3 years	0.06	0.14	0.93
4 years	--	--	0.36
Maximum peak/average power factor	1.131	1.132	2.750

case again flattens out the reactivity swing, but in this case the initial k was perhaps too high.

The various results shown in Tables 4-13 and 4-14 indicate the potential for shaping the reactivity variation during the fuel residence and accommodate control rod requirements and conditions by varying the shielding prescriptions for the burnable poison.

4.5.2.4. Burnup Stability of Power Profiles. Axial power profiles at three time points are shown in Fig. 4-28. In terms of impact on fuel temperatures, the variances in axial power profiles shown would probably increase the hot-channel fuel temperature peak by about +20°C (+36°F).

Figure 4-29 plots the radial power distributions derived for four time points from radial-geometry one-dimensional burnup (FEVER) calculations for the 5-yr HEU/Th loading. Although the zonal power distributions shift about during the burnup, the maximum radial power peaking does not exceed by more than a few percent the initial-zoning peak factor of about 1.17. For the axial temperature distribution calculations, a higher factor of 1.25 was selected to account for other perturbations during the cycle, such as from the insertion of control rods.

The axial power profiles for the optimum zoning and for the extreme variances at 1-1/2 and 4 yr are plotted in Fig. 4-30. These show greater within-zone changes of power shape than those for the HEU design in Fig. 4-28. Figure 4-31 plots the fuel centerline axial temperature profiles calculated using the Fig. 4-30 power profiles. Thus, the relative instability for the LEU axial power shapes with burnup contributes about +60°C (+108°F) to the maximum fuel temperature to be experienced during the cycle. Much of axial power-shape variation is attributable to the uneven burnout rates for the burnable poison. Adjustments to the burnable poison prescriptions would reduced the observed variances in power and temperature peaking.

Radial power profiles as a function of burnup for the 3-yr batch-loading LEU cores are plotted in Fig. 4-32. Here a progressive reduction in

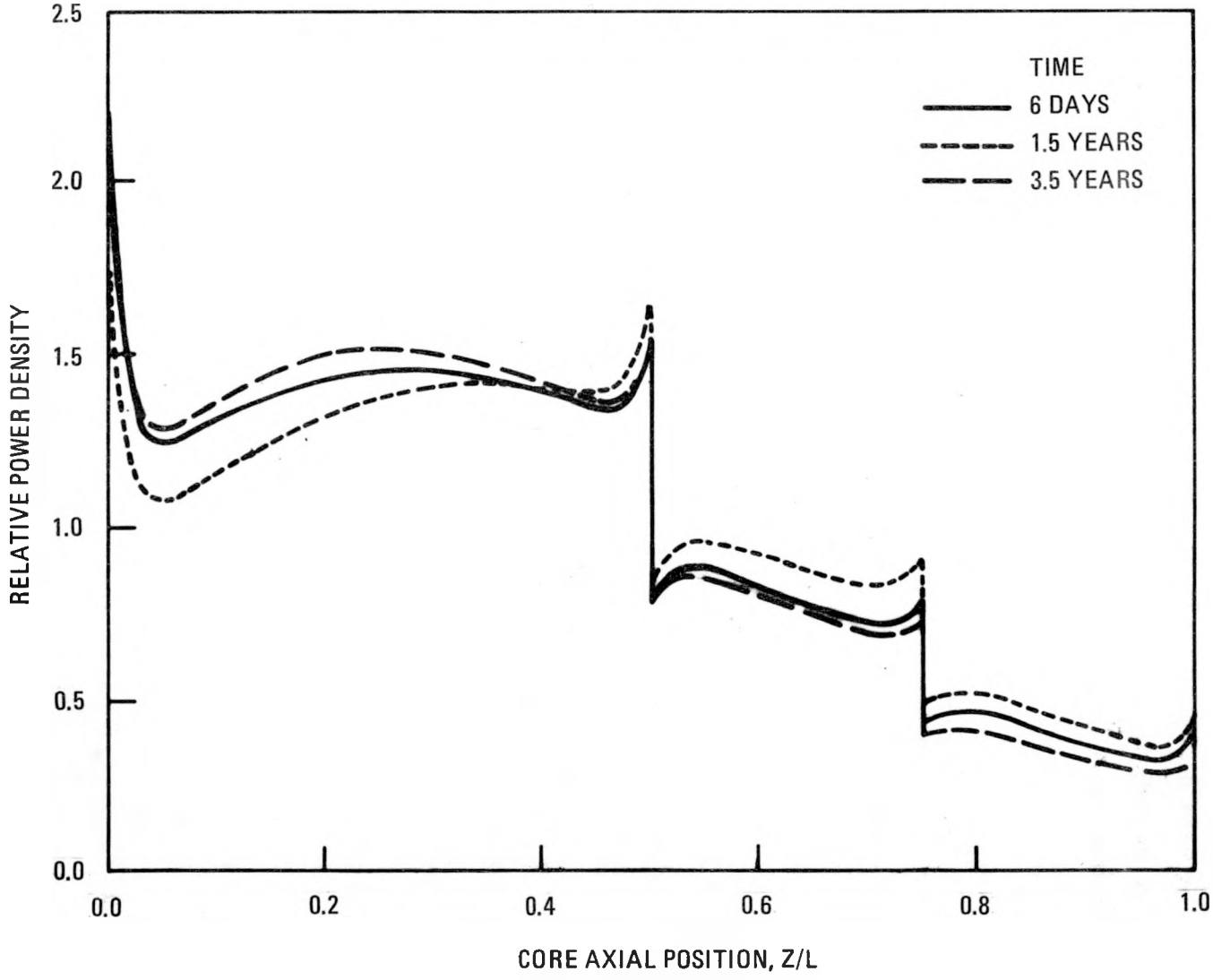

Fig. 4-28. Axial power shapes for HEU VHTR during cycle

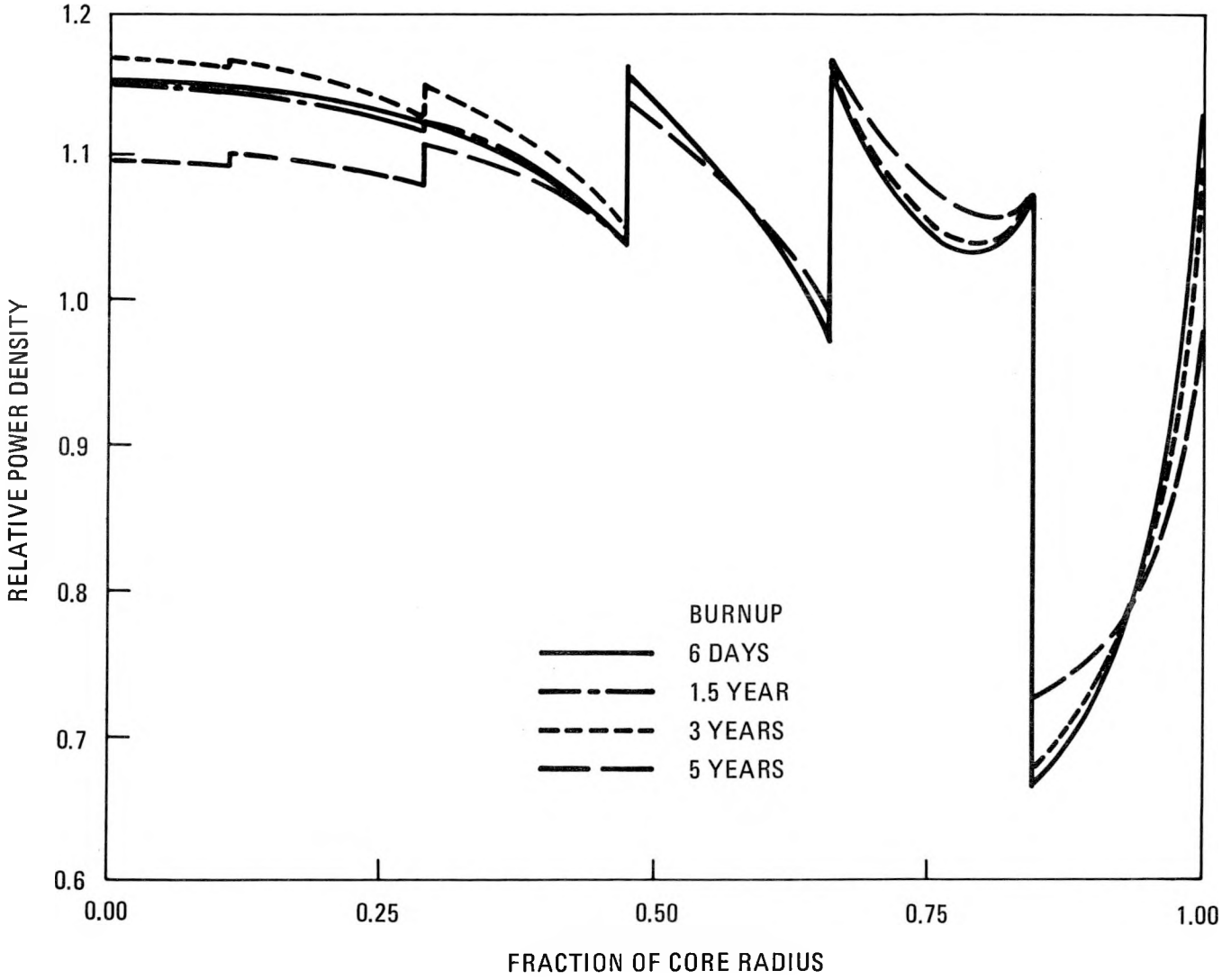

Fig. 4-29. Time variation of radial power profile for HEU VHTR

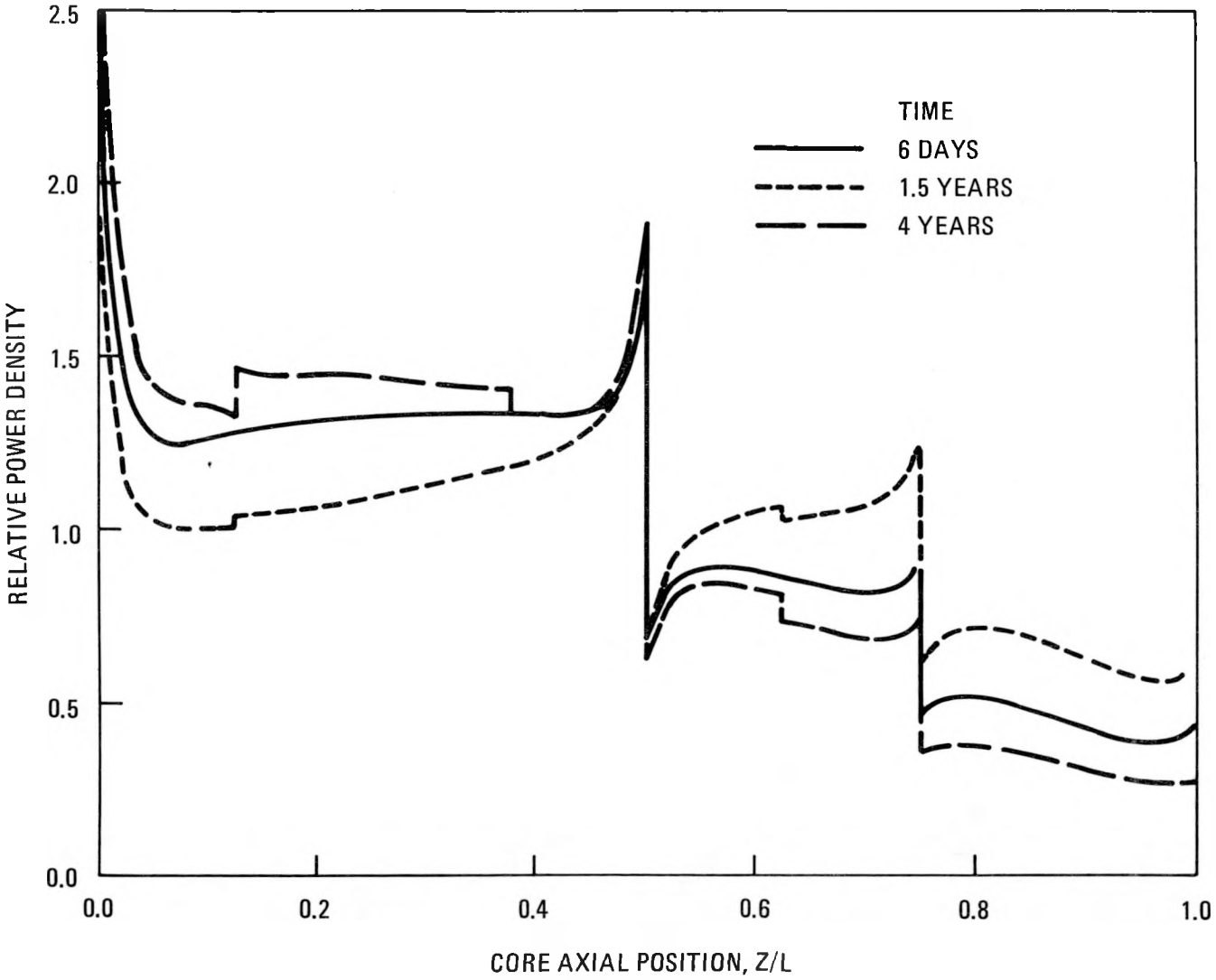

Fig. 4-30. Axial power shapes for LEU VHTR during cycle

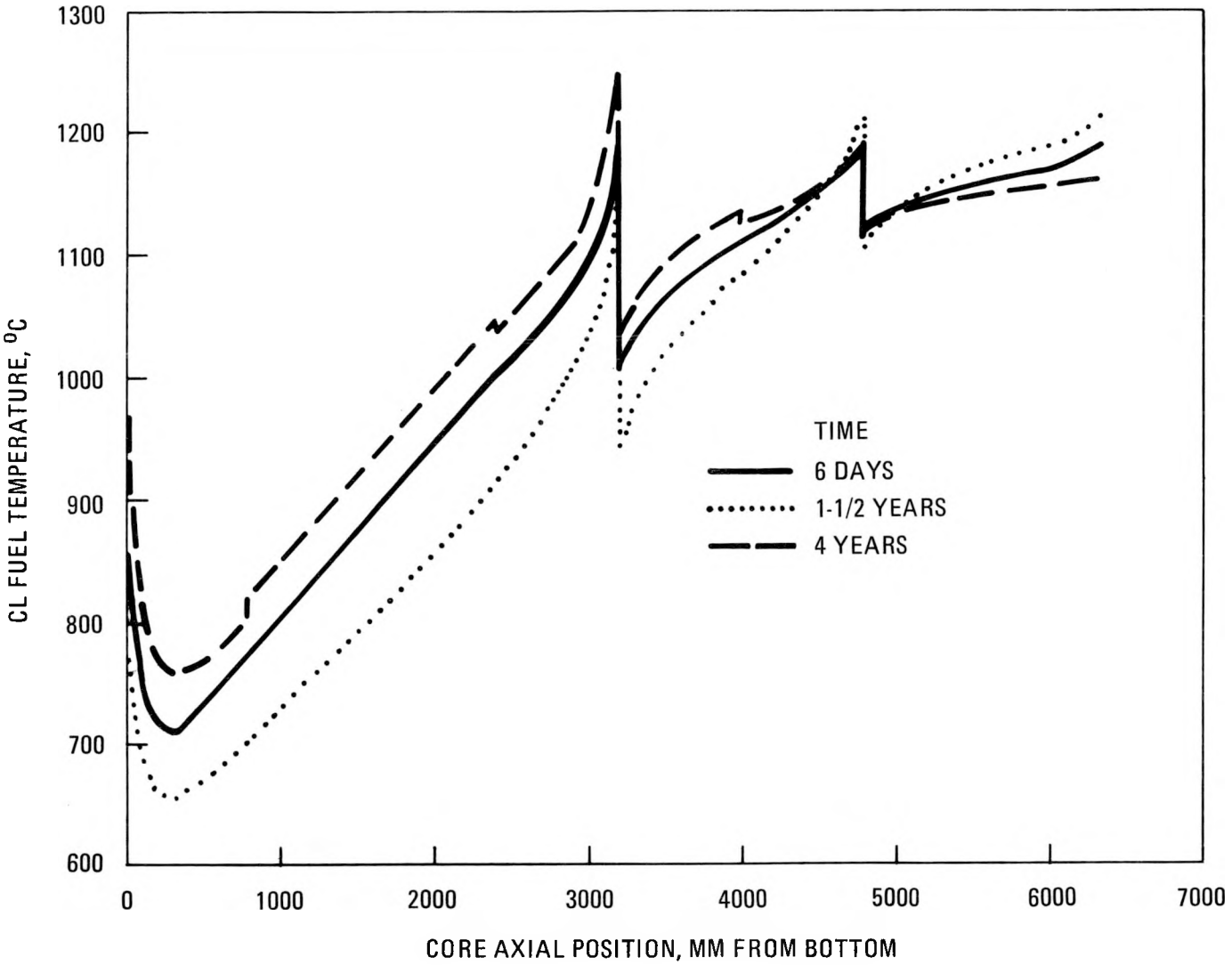

Fig. 4-31. Axial temperature for LEU VHTR during burnup

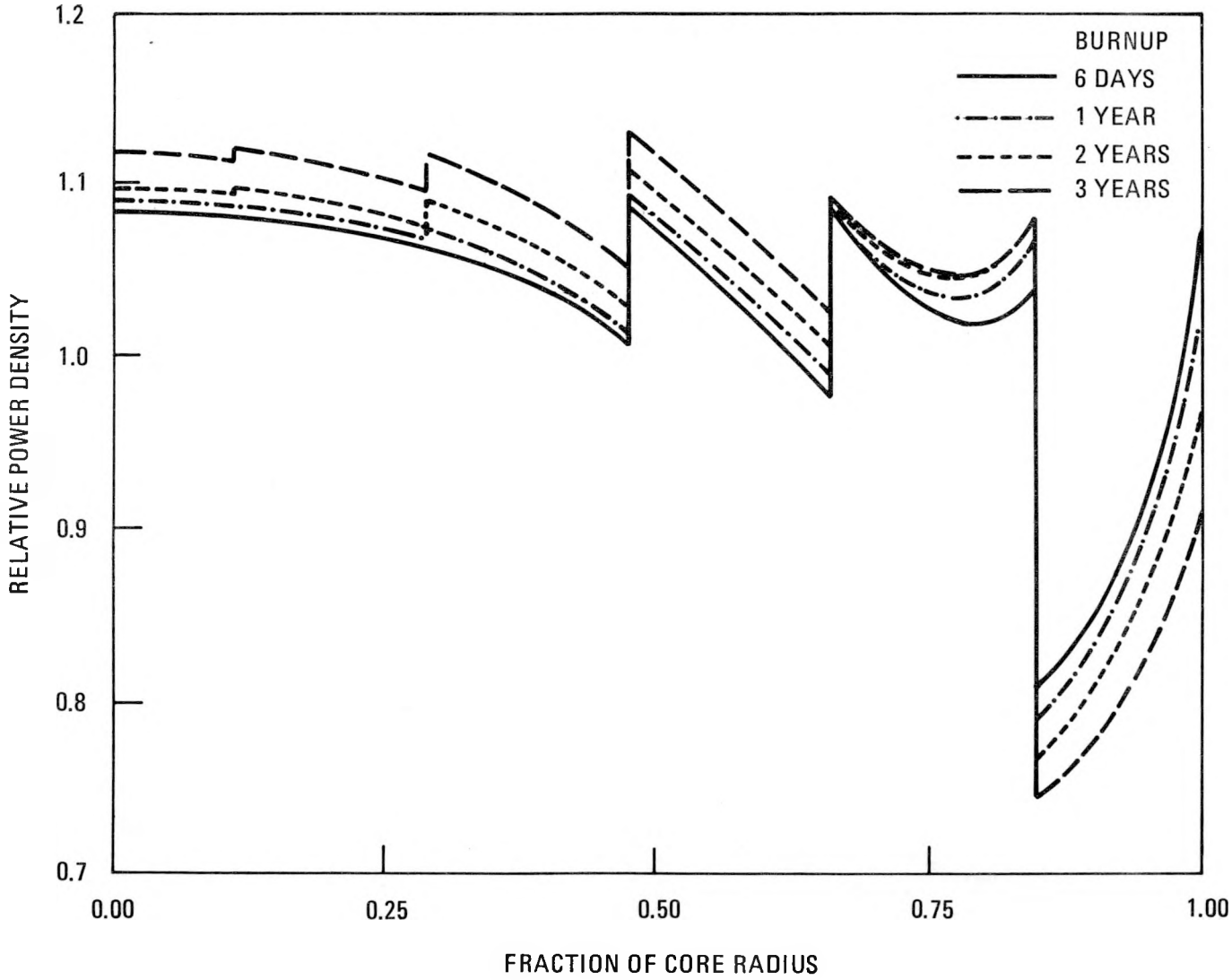

Fig. 4-32. Time variation of radial power profile for LEU VHTR

the outermost-zone average power density with time is seen. The maximum radial power peaking factor increases about 4% over the cycle, from 1.09 unburned to 1.14 after 3 yr. The 4-yr LEU core would probably give higher initial peaking and another percent or two increase for the added year of burnup.

4.5.2.5. Two-Dimensional Burnup and Control Worth Study. To study the reactivity worth obtainable with the proposed control rod layout, a two-dimensional whole-core GAUGE model was set up following the geometry of Fig. 4-23 for the reference LEU/Th cycle case. The radial fuel zoning was obtained from GASP and is given in Table 4-8 (last column). The GAUGE code's burnable poison search routine was used to determine a radial zoning of lumped B-10 poison that gave a multiplication factor of 1.04 for the fresh unrodded core.

The variation of k_{eff} with burnup over the 4-yr core life is shown in Fig. 4-33 with and without the lumped burnable poison included.

Rod worths were calculated by homogenizing the control poison over the single hexagonal blocks in which individual control rods are located, using self-shielding factors obtained from DTFX one-dimensional transport theory cell calculation for this geometry.

The worths of individual banks of control rods are given below for the fresh core at operating temperature with no xenon:

Case	k_{eff}	$\Delta\rho_{bank}$
Unrodded	1.0439	--
12 reflector rods in	1.0062	0.03596
Reflector rods + 6 outer core rods in	0.9744	0.03240
Reflector rods + 12 outer core rods in	0.9381	0.03967
Fully rodded (above case + central 7 rods)	0.8210	0.1521

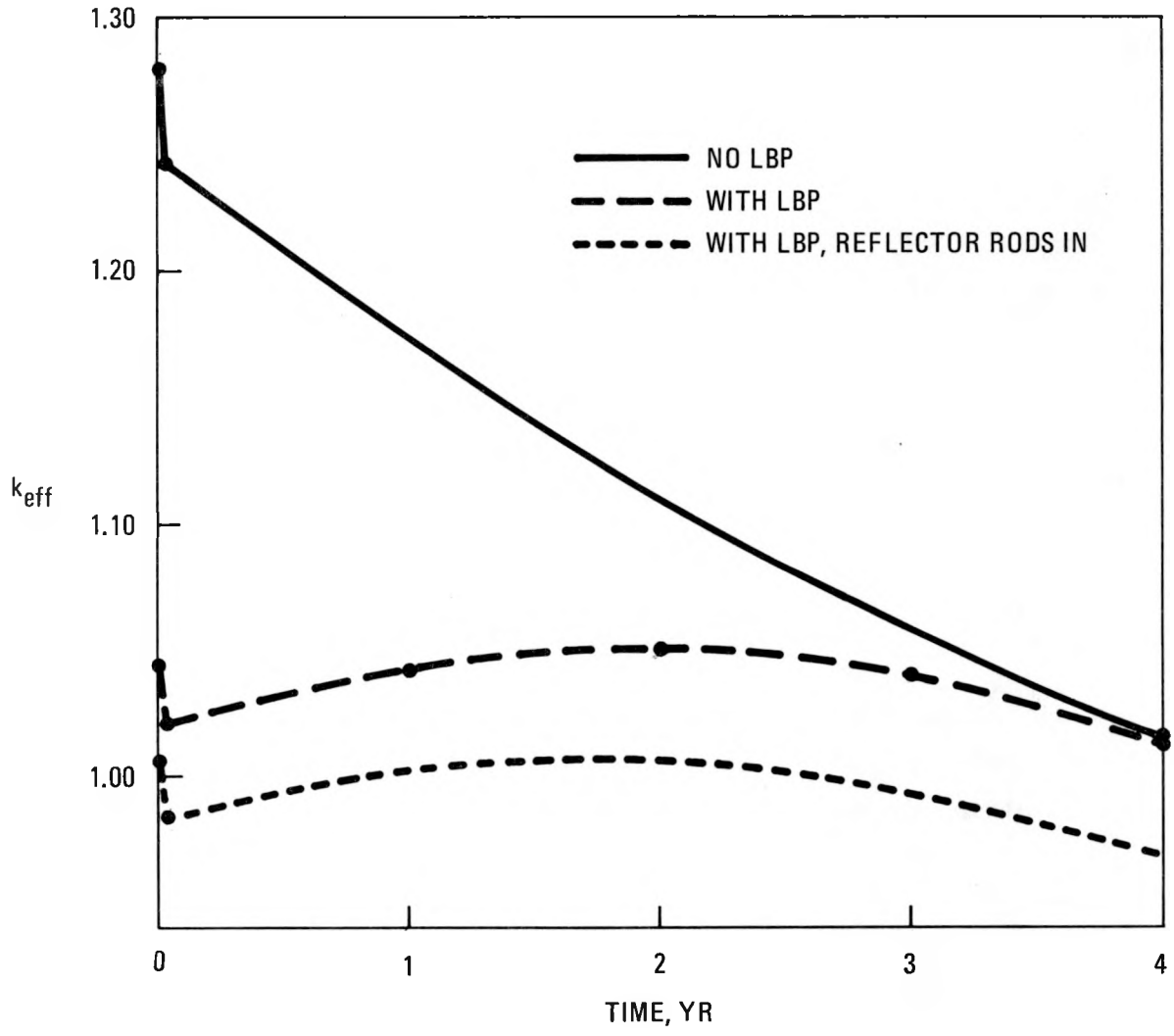

Fig. 4-33. GAUGE model burnup results (HTGR-MRS/PH)

These results indicate that the total number of rods provided is adequate to keep the core shut down. In addition, the fact that the worth of the 12 reflector rods is about 0.04 Δk suggests that the operating cycle can be handled with only these rods, with the remaining rods being used only for cold shutdown and during the rise to power. A burnup calculation in which the reflector rods were fully inserted throughout the 4-yr is also shown in Fig. 4-33 and confirms this possibility. If this strategy is adopted, the radial zoning specified should be modified to account for the effect of the poisoned reflector. A different radial zoning could enhance the reactivity worth of the reflector rods.

Table 4-15 summarizes the requirements of the general design criteria for control systems contained in 10CFR50, Appendix A. Criteria 20 through 29 are applicable. On the basis of these requirements, three preliminary criteria for the HTGR-MRS/PH control system design have been selected:

1. One system for long-term cold shutdown control rods.
2. Secondary system - hot shutdown capability only.
3. Different control mechanisms for diversity.

Three possible control rod systems that satisfy these criteria are listed in Table 4-16. These systems are also consistent with the concept of controlling the reactor by reflector rods at full power as suggested above. In System A, the reflector rods use a different type of rod drive mechanism. They could also be of a different size or absorber type design if required to satisfy the diversity requirement, although this has not been assumed in the reactivity worth calculations. Since some of the reflector rods may still be fully inserted during power operation, the six outermost in-core control rods are combined with the reflector rod for the scram function. The location of the outer in-core rods is such that they are not expected to reach limiting temperatures during a core heatup accident. The reflector rods provide a hot shutdown capability, and the in-core rods are used only for startup and cold shutdown.

TABLE 4-15
GENERAL DESIGN CRITERIA FOR CONTROL SYSTEMS
(10CFR50, APPENDIX A)

20. Automatic operation to prevent fuel damage.
21. Reliable and testable, no loss of function on single failure.
22. Redundant operation.
23. Fail-safe operation.
24. Separation of protection and control to ensure protective function reliability.
25. Operation with any single malfunction (not including rod dropout).
26. Two independent systems required:
    - Different design principles.
    - One system must use control rods and ensure fuel design limits not exceeded.
    - One system capable of cold shutdown.
    - Second system capable of controlling normal power operation.
27. Combined systems capability to prevent fuel damage under all accident conditions.
28. Limit rate and amount of reactivity insertion.
29. High reliability of operation.

TABLE 4-16
HTGR-MRS/PH CONTROL SYSTEM ALTERNATIVES

System	Primary System	Secondary System	Comments
A	19 in-core rods	12 reflector rods	Different drive systems Outer six in-core rods combined with reflector rods for immediate scram function
B	19 in-core plus 12 reflector rods	Reserve shutdown system (RSS) hoppers	Equivalent to FSV system; number and location of RSS channels to be determined Top entry backup system
C	19 in-core plus 12 reflector rods	12-18 reflector rods	Different drive systems Spacing of vessel penetrations a concern

System B is analogous to that of the FSV HTGR. The control at power is still by reflector rods, but all drive mechanisms are of the same design. A reserve shutdown system (RSS) mounted above the core discharges B_4C pellets into channels in selected fuel columns to provide a diverse shutdown system. A design in which the RSS is installed within the top reflector blocks appears feasible but has not been evaluated in detail.

System C is essentially the same as System B, with additional reflector rods taking the place of the RSS hoppers. However, it is not clear if it would be possible to design the pressure vessel penetrations as close together as would be required to have a control rod in almost every reflector column.

The reactivity worths of the three systems are summarized in Table 4-17. The worths of the reflector rods may be enhanced if the fuel is rezoned consistent with the consumption of reflector control.

System A would be the simplest and most economical and is the preferred concept at present.

The temperature defect inferred from MICROX calculations is around 0.08 Δk, so the total set of rods should be adequate for cold shutdown. The maximum worths of stuck rods have not yet been studied.

Power distribution data from the GAUGE calculation are given in Figs. 4-34 and 4-35. Since the modular HTGR is a batch core and does not use seven-column reload regions or orifice valves, the tabulation of region peaking factors and tilts usually given for HTGR cores is not appropriate. Figure 4-34 gives the ratio of power in individual columns to the core average power, an indication of the gross radial power shape. Figure 4-35 gives the pointwise peak-to-core-average powers in each column. These data are the two-dimensional equivalent of the radial power distribution given in Fig. 4-25 except that the GAUGE results include lumped burnable poison. The tendency seen in both Figs. 4-34 and 4-35 is for the power to shift to the center with burnup, which suggests that the zoning is not optimal for

TABLE 4-17
HTGR-MRS/PH CONTROL SYSTEM WORTHS

Control System	k_{eff} Hot	k_{eff} Cold
Unrodded	1.044	1.131
System A		
19 in-core rods	0.868	0.955
12 reflector rods[a]	1.006	1.095
12 reflector rods plus 6 in-core rods	0.974	1.062
System B		
19 in-core, 12 reflector rods	0.821	0.906
RSS hoppers	TBD	TBD
System C		
19 in-core, 12 reflector rods	0.821	0.906
12-18 reflector rods[a]	0.99 - 1.01	1.08 - 1.10

[a]Reactivity worth of reflector rods to be enhanced by rezoning fuel.

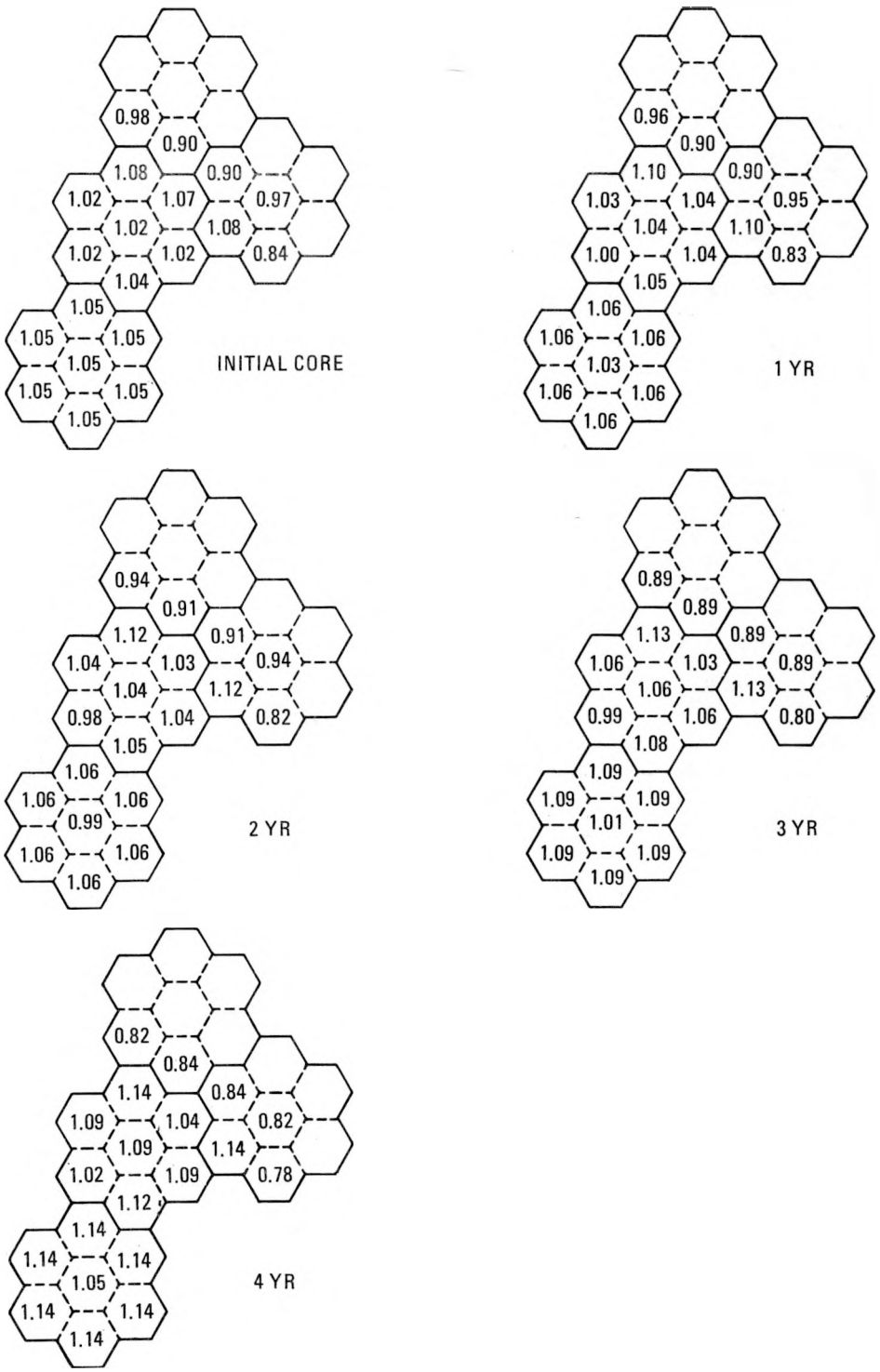

Fig. 4-34. LEU/Th reference case column peaking factors (column/core avg.), radially zoned fuel and LBP, unrodded burnup

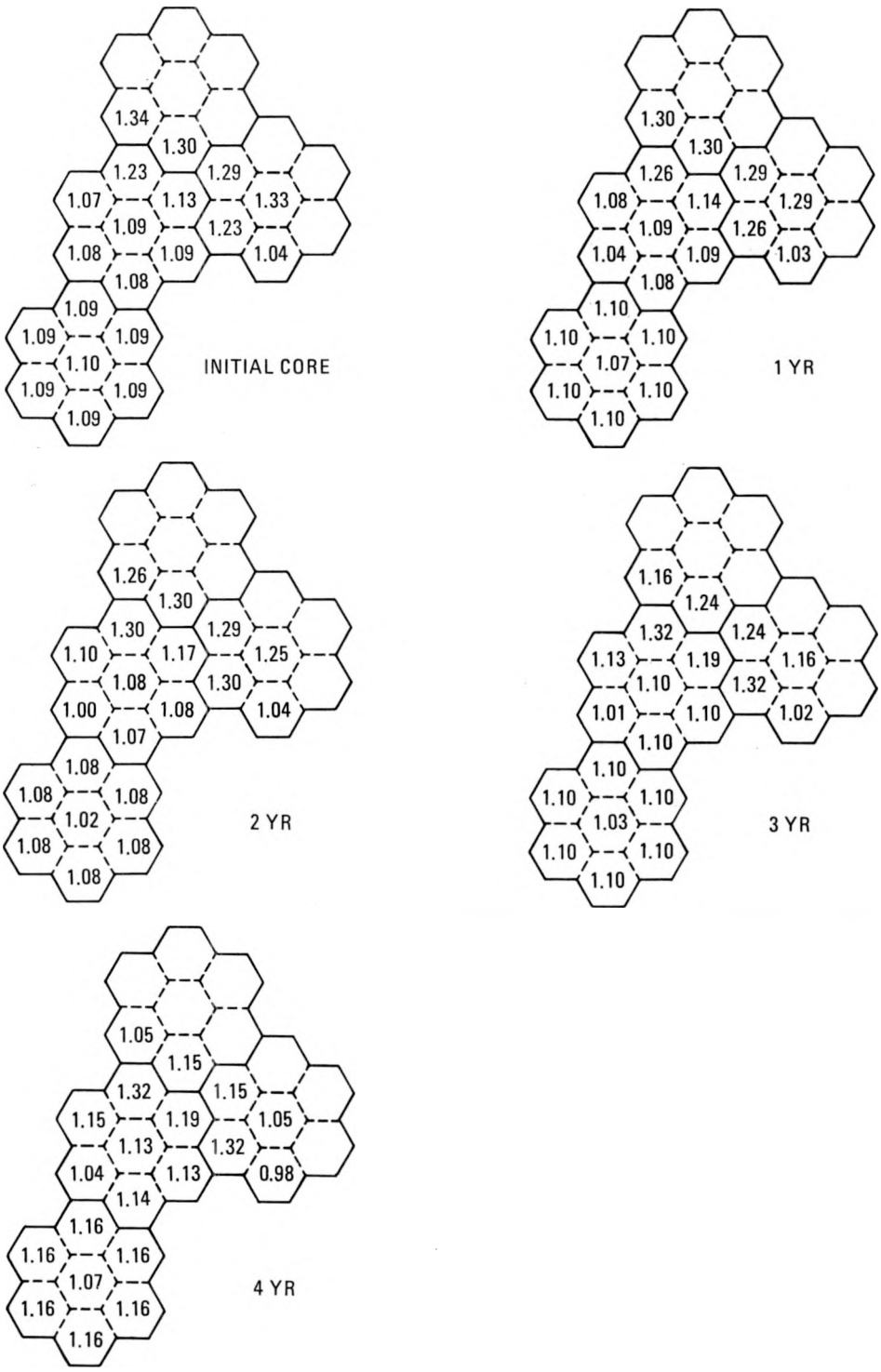

Fig. 4-35. LEU/Th reference case pointwise peaking factors by column (local peak/core avg.), radially zoned fuel and LBP, unrodded burnup

stability. Note that these burnup calculations are for an unrodded core. Control by reflector rods would diminish the observed power shift to the center, since the center would be preferentially burned at the start of the 4 yr and the power shifted to the outer columns as the rods are withdrawn. The zoning scheme required for reflector control therefore might not be too different from that of the present case.

4.5.2.6. Fuel Cycle Costs. Levelized fuel cycle costs (levelizing periods 15 and 30 yr) were calculated using the GACOST code for the LEU/Th and HEU/Th reference designs. The economic and resource assumptions, shown in Table 4-18, were the same as those currently used for the large HTGR designs. However, two different inflation rates (0% and 6%) and correspondingly two consistent sets of economic assumptions were used. Also, costs were calculated for either assuming the throwaway fuel cycle mode or taking credit for all discharged fissile uranium. Results are shown in Table 4-19.

4.6. REACTOR INTERNALS DESIGN (6053030200)

4.6.1. Scope

The scope of this task is to establish the core and reactor internals configuration for the HTGR-MRS/PH.

4.6.2. Discussion

The preliminary core physics design for the 250-MW(t) HTGR-MRS/PH was presented in Section 1 and was used as the basis for the reactor internals design study. The HTGR-MRS/PH uses a batch-loaded upflow core consisting of 85 fuel and control columns eight rows high. Basic core parameters are listed in Table 4-20, and plan and elevation views of the core and reactor internals are shown in Fig. 4-36.

The fuel elements for the HTGR-MRS/PH are 10-row elements similar to the FSV element design, the major difference being that an alternate fuel handling scheme is used in the HTGR-MRS/PH enabling slightly more fuel to be

TABLE 4-18
ECONOMIC, RESOURCE, AND HANDLING ASSUMPTIONS

Capacity factor	70%
Tails assay	0.2%
Startup date	1/1995
Base inflation rate	6%/0%
Real escalation rate	7.1%/1%
Ore inflation and scarcity	9.2%/3%
Working capital rate	15.3%/8.3%
Discount rate	10.5%/4.3%
Base date for fuel costs	1/1995
Base date for handling costs	1/1980
Fuel costs	
Conversion ($/kg)	6.0
Enrichment ($/kg)	6.0
U_3O_8 [$/kg ($/lb)]	88.2 (40.0)
U-233/U-235 parity ratio	1.10
Handling costs ($/FE)	
Fabrication	6380
Spent fuel shipping	3000
Waste (AFR + disposal)	6100
Reprocessing	7070
Processed waste	1250

TABLE 4-19

15- AND 30-YR LEVELIZED FUEL CYCLE COSTS [$/GJ ($/MBtu)] FOR THE 4-YR LEU/Th AND 5-YR HEU/Th BATCH-FUELED 250-MW(t) VHTR

	0-15 Yr		0-30 Yr	
Inflation rate	0%	6%	0%	6%
4-Yr LEU/Th				
Throwaway	2.12 (2.24)	6.07 (6.41)	2.39 (2.53)	8.52 (8.57)
U-credit	1.51 (1.59)	4.49 (4.74)	1.69 (1.78)	5.87 (6.19)
5-Yr HEU/Th				
Throwaway	1.68 (1.77)	4.95 (5.23)	1.89 (2.00)	6.59 (6.96)
U-credit	0.95 (1.29)	3.75 (3.96)	1.37 (1.45)	4.89 (5.16)

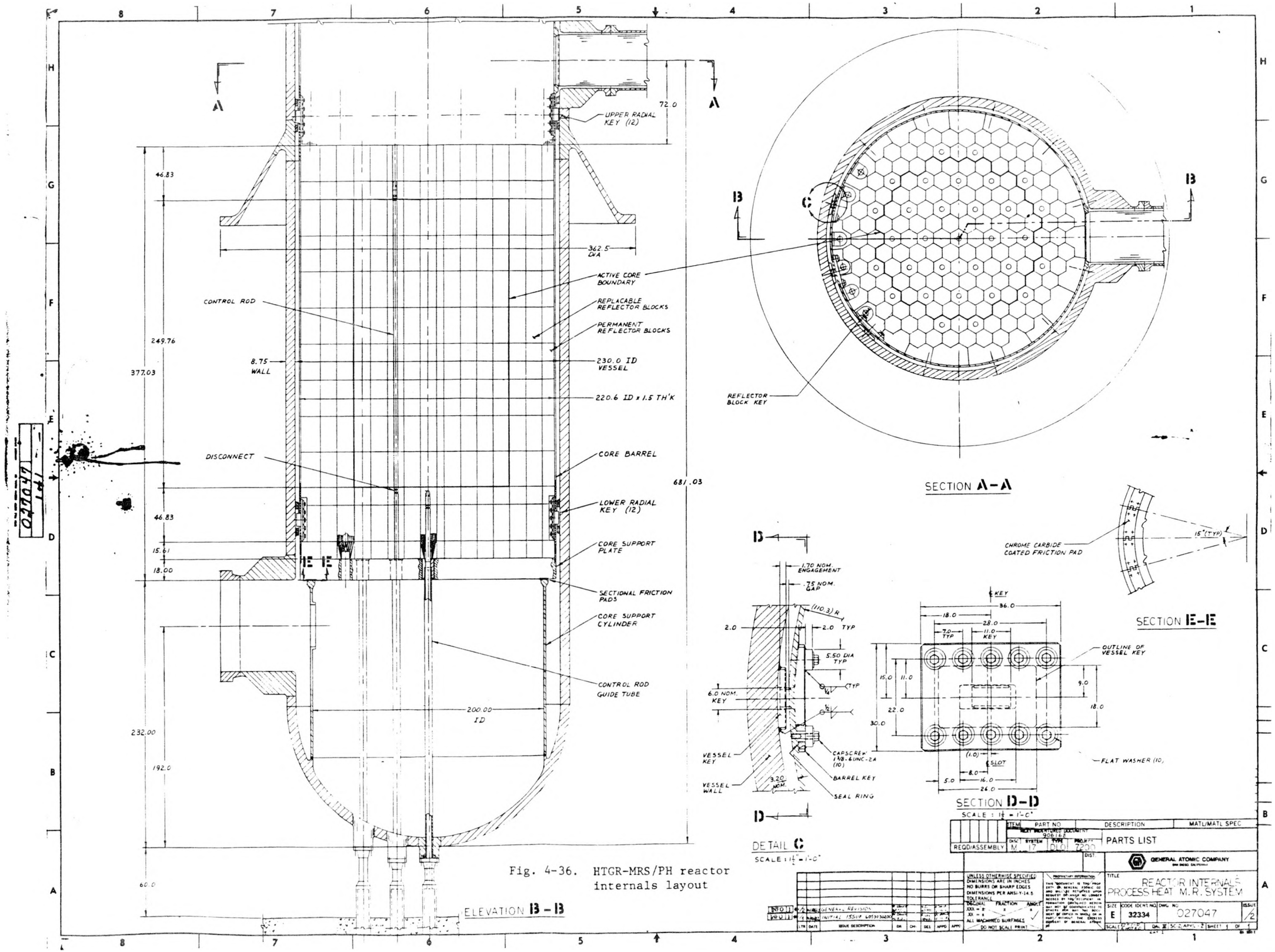

Fig. 4-36. HTGR-MRS/PH reactor internals layout

ITEM	PART NO.	DESCRIPTION	MAT'L/MATL SPEC.
REQD/ASSEMBLY	GENERAL ATOMICS PROPRIETARY DOCUMENT 906182 DWG. SYSTEM M 17 TYPE D101 PROJECT 7200	PARTS LIST	
	DIST.	GENERAL ATOMIC COMPANY	

UNLESS OTHERWISE SPECIFIED DIMENSIONS ARE IN INCHES. NO BURRS OR SHARP EDGES. DIMENSIONS PER ANSI-Y-14.5. TOLERANCE: DECIMAL XXX = ± FRACTION ANGLE XX = ± ALL MACHINED SURFACES. DO NOT SCALE PRINT.

PROPRIETARY INFORMATION: THIS DOCUMENT IS THE PROPERTY OF GENERAL ATOMIC CO. AND SHALL BE RETURNED UPON REQUEST OR WHEN NO LONGER NEEDED BY THE RECIPIENT. THE INFORMATION CONTAINED HEREIN SHALL NOT BE COMMUNICATED TO OTHERS NOR SHALL THIS BODY NOR ANY PART OF COPIED IN WHOLE OR IN PART WITHOUT THE EXPRESS CONSENT OF GENERAL ATOMIC.

LTR	DATE	ISSUE DESCRIPTION	DR	CH	DES	APPD	APPD
INFO		GENERAL REVISION					
NEW		INITIAL ISSUE 605303400					

TITLE: REACTOR INTERNALS PROCESS HEAT M.R. SYSTEM

SIZE	CODE IDENT NO.	DWG. NO.	ISSUE
E	32334	027047	1/2

SCALE: NONE | DO NOT SCALE PRINT | SHEET 1 OF 1

TABLE 4-20
MRS BASIC CORE PARAMETERS[a]

Thermal	
Power	250 MW(t)
Power density	4.1 W/cm^3
Outlet temperature	950°C (1742°F)
Core ΔT	525°C (977°F)
Inlet pressure	5.0 MPa (725 psi)
Fuel cycle	
Fuel	LEU/Th
Refueling	4-yr, batch loading
C/Th ratio	600
Core layout	
85 columns, 8 blocks high	
Core dimensions[b]	
Active core	Height 6.34 m (20 ft 9 in.), diameter 3.5 m (11 ft 5 in.)
Reflectors	1 m (3 ft 3 in.) side, 1.2 m (3 ft 11 in.) top, 1.2 m (3 ft 11 in.) bottom
Block design	
66 columns of 10-row blocks	
19 columns of modified 10-row blocks, each with a central 101.6-mm (4-in.) hole to accommodate single control rods	

[a]From Ref. 4-9.
[b]Dimensions approximate. Refer to Fig. 4-36 for current dimensions.

loaded into each block. Control elements are similar to the fuel elements except that the control elements contain a single, central 101-mm, (4-in.) diameter hole for control rod passage. No special provisions for sealing the element ends are required and none are provided.

The fuel and control elements constitute the active core. Radially, the active core is surrounded by two rings of replaceable reflector elements, which are in turn surrounded by a permanent reflector region for a total radial reflector thickness of approximately 1016 mm (40 in.) [The radial reflector is 965 mm (38 in.) thick at its thinnest section.] Axially, the active core is surrounded by top and bottom reflectors, each approximately 1219 mm (48 in.) thick and each made up of one layer of full-height elements and one layer of half-height elements. The half-height elements are located nearest the core and will contain boron shield pins. It is anticipated that either the top reflector elements will be keyed together radially or some other form of top column constraint will be employed.

The entire core and permanent side reflector assembly is contained within a core barrel and is supported by a steel core support plate, which in turn is supported from the pressure vessel lower head by a steel core support cylinder. The core support plate and the core support cylinder were sized for normal operating loads and for various abnormal events.

The permanent side reflector will, as a minimum, be keyed to the core barrel at the top. Additional keying along the entire height of the permanent side reflector may be required for seismic restraint of the core.

Scoping calculations for the seismic design of the HTGR-MRS/PH internals were done assuming an equivalent static seismic load of 1.5 g in the horizontal and vertical directions. The vertical natural frequency of the core support plate was calculated assuming that the total mass it supports was distributed in the plate. The resulting natural frequency was found to be about 23 Hz. The maximum seismic deflection of the plate is about

1.27 mm (0.05 in.), and the maximum seismic stress in the plate is about 21.37 MPa (3100 psi). Both the stress and the deflection are well within their respective allowable ranges.

The fundamental frequency of lateral vibrations of the core was calculated using a simplified model to be 10 to 12 Hz in the absence of lateral restraint other than that provided by the core support cylinder. The actual frequency might be much less than this. Since this is the amplified range of seismic motions, it is felt that additional lateral restraint of the core is required. Further evidence of the need for lateral restraint comes from analyses which showed that, in the absence of lateral restraint, the core support cylinder would yield during an SSE, possibly allowing the core to damage the pressure vessel. Lateral restraint of the core is therefore incorporated by providing radial keys at the top and bottom of the core barrel.

4.7. REFUELING AND CONTROL ROD DRIVES (6053050100)

4.7.1. Scope

This task includes scoping studies in the areas of control rod drives and refueling together with appropriate input to various project documents and presentations.

4.7.2. Discussion

4.7.2.1. Refueling System. The axial arrangement of the reformer mounted above the reactor vessel virtually prohibits fuel handling from above the core by conventional refueling equipment.

In the early stages of the task, consideration was given to removal of the reformer in order to gain access to the core for refueling. This approach was based on the premise that the frequency of reformer removal would coincide with that of refueling outage.

In addition to the questionable validity of the premise, two significant problem areas resulted in the top entry approach being abandoned. First, the need to maintain a helium atmosphere over the core and to prevent dilution of the gas during removal of the reformer necessitates some form of large isolation valve interposed between the reactor vessel and the reformer. Second, once removal of the reformer has been effected, shielding is required to provide protection for personnel during removal of fuel elements from the core. Figures 4-37, 4-38, and 4-39 indicate methods considered for meeting these problems.

The alternative method proposed, and generally accepted as a reference concept, was to obtain entry to the core through a horizontal penetration located between the reformer and the reactor core as shown in Fig. 4-40. The combined fuel element and hoist height in the early concepts necessitated an excessively large penetration in the vessel. Two methods were studied in an attempt to minimize the size of the opening. The first tilted the element into a horizontal position for withdrawal. The second, and preferred, method raises the element into alignment with the fuel handling machine while maintaining the element in a vertical attitude (see Fig. 4-40).

The penetration for the fuel handling machine extends through the concrete shield wall, at which point it is sealed by a bolted closure. A removable plug within the penetration provides both a closure for the aperture in the flow boundary shroud and biological shielding for protection of personnel on the refueling floor. The plug also restricts ingress of air during replacement of the penetration closure with an isolation valve and vice versa.

The fuel handling machine consists of a pair concentric sleeves, which telescope together within a shielded housing. The outer end of the inner tube carries an arm that can be moved through a limited arc about a vertical axis. The length of the arm is such that by rotation of the arm about its pivot, coupled with lateral displacement of the inner sleeve, complete

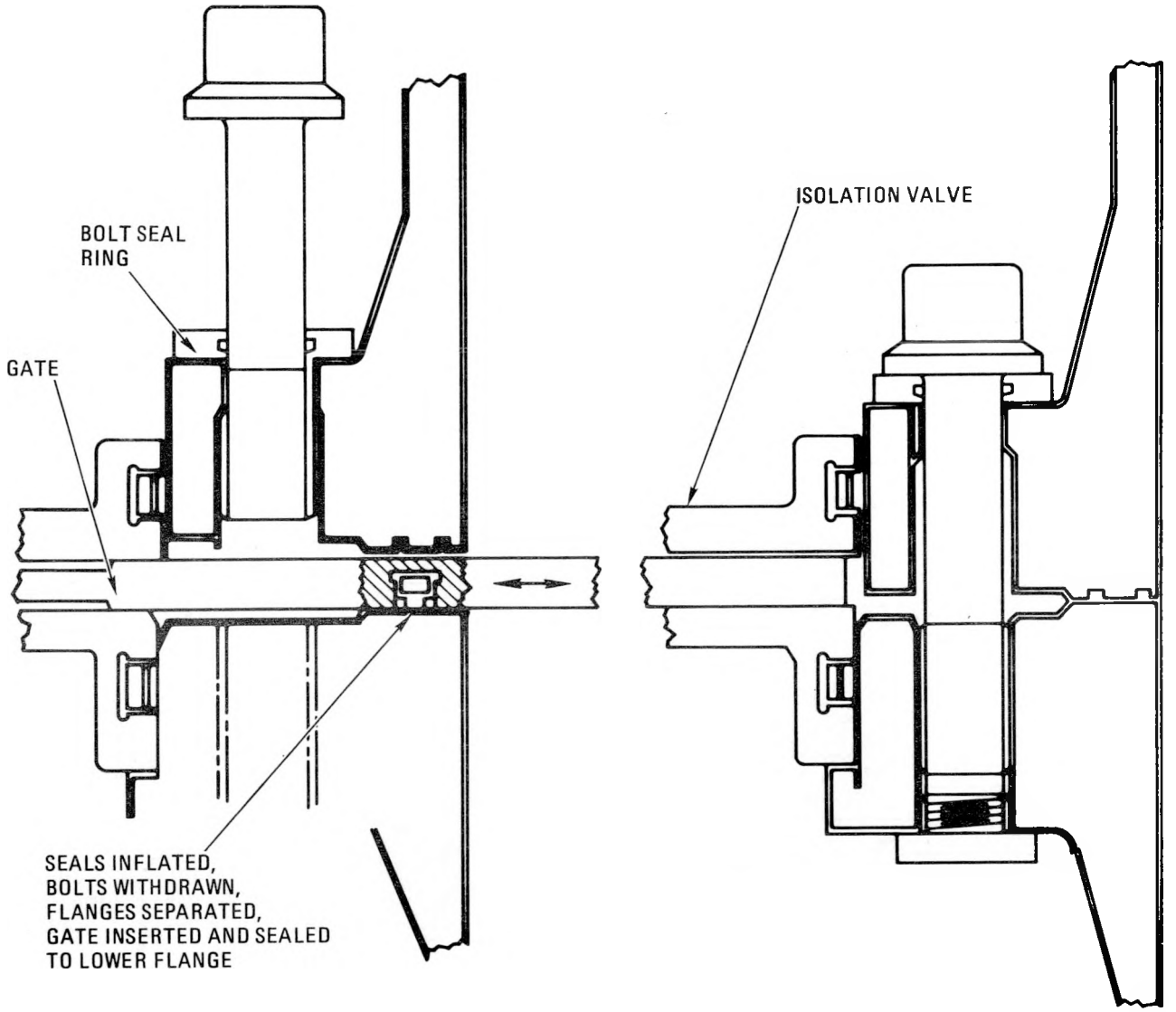

Fig. 4-37. Fuel servicing concept, MRS direct cycle

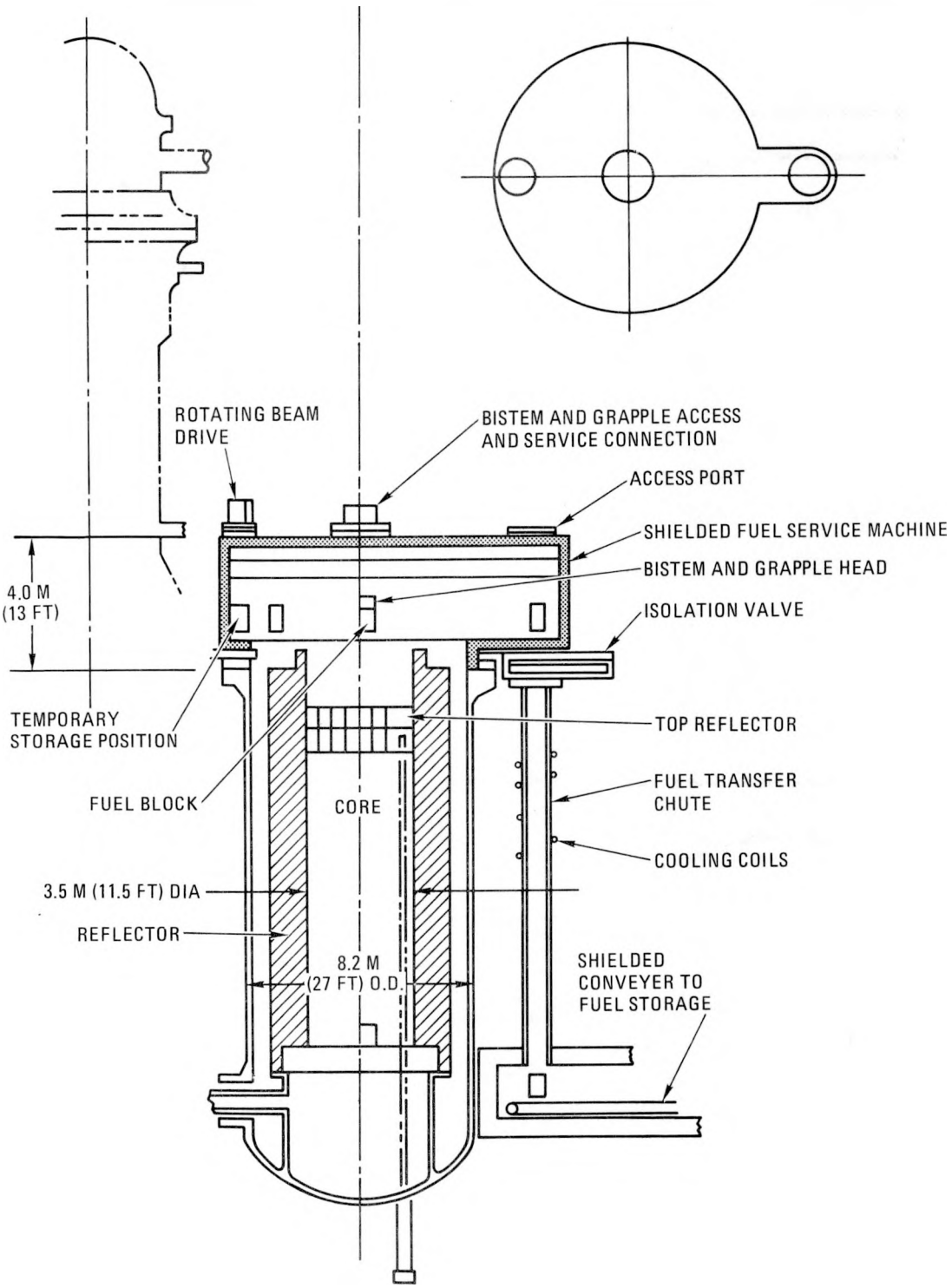

Fig. 4-38. Fuel servicing concept, MRS direct cycle

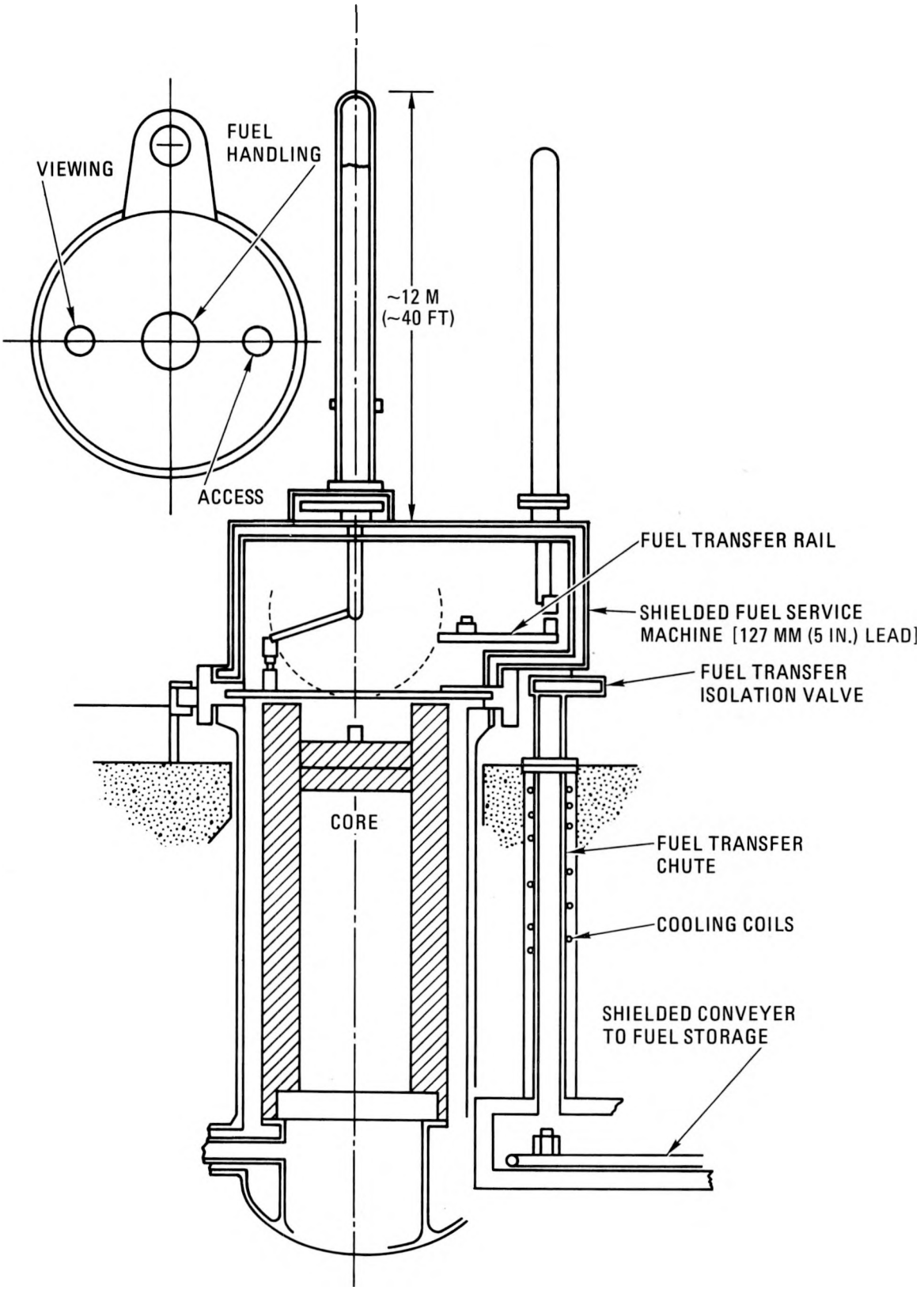

Fig. 4-39. Fuel servicing concept, MRS direct cycle

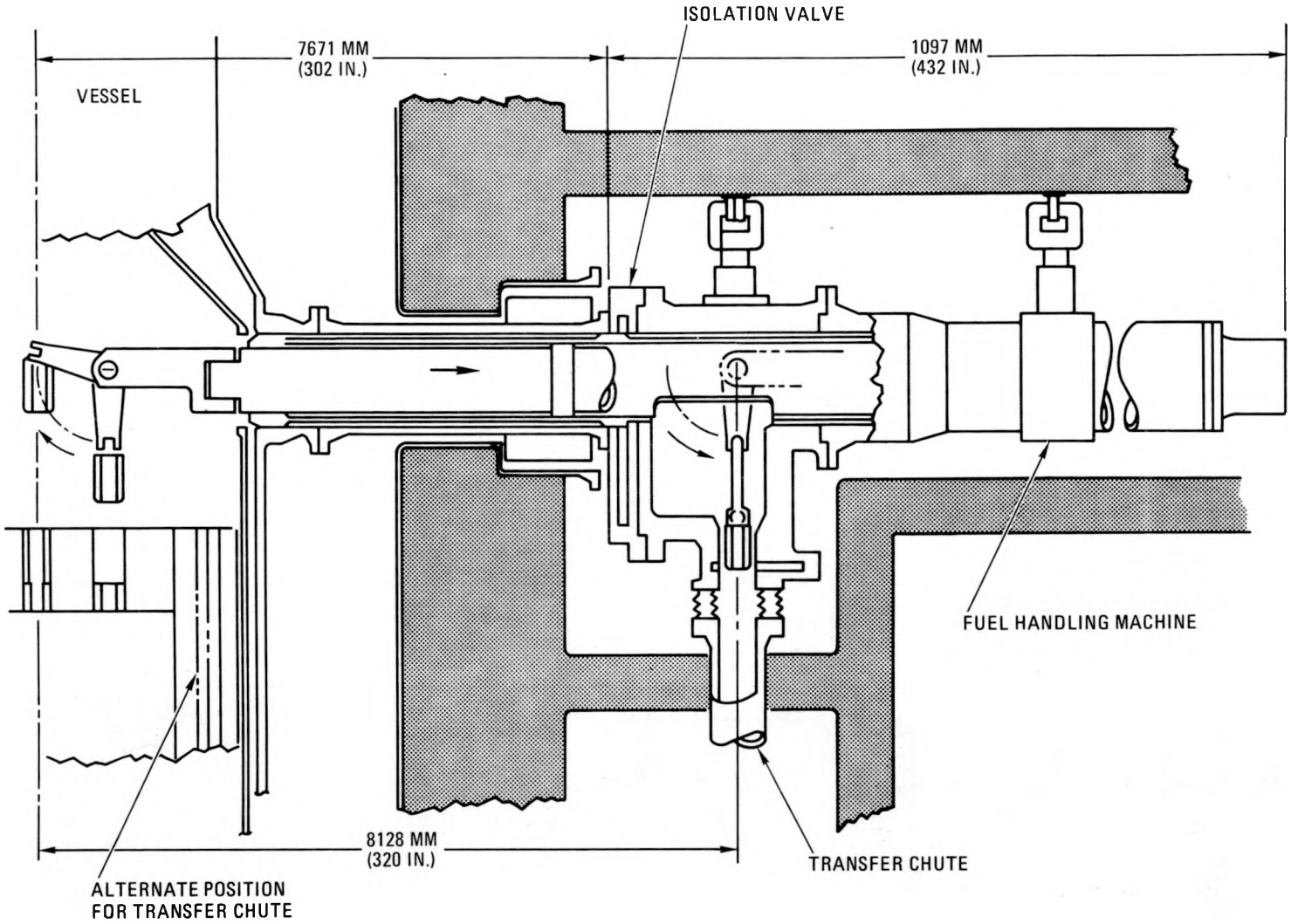

Fig. 4-40. Reference fuel servicing concept, MRS direct cycle

coverage of the entire core and removable reflector can be achieved as shown in Fig. 4-41.

A second arm, rotatable about a horizontal pivot, incorporates a hoist device, the purpose of which is to raise and lower a fuel element grapple the full depth of the core. When removing a fuel element, the arm is locked in a vertical attitude with the grapple directly under the pivot point. When the element has been fully raised, the grapple engages a slotted section of the arm. Rotation of the arm then raises the grapple and fuel element assembly to a position within the envelope of the vessel penetration, at the same time maintaining the element in a vertical position.

Both the inner and outer sleeves are next retracted into a cavity in the fuel handling machine where the arm and grapple can be returned to a vertical position directly over a transfer chute. The element is then lowered downward through the transfer chute onto a conveyor, and from there to a storage area.

New fuel and reflector elements are handled in a reverse sequence with appropriate stations for inspection and orientation.

The fuel handling machine is moved between each modular reactor on a set of rails, suitable leveling and elevation adjustment devices being provided to align the machine with individual reactor penetrations.

The arrangement where the transfer chute is located outside the shield wall (see Fig. 4-37) has been adopted as the reference concept for initial costing. However, an alternate arrangement has been considered whereby the transfer passage is provided by a vertical passage through the side reflector and a penetration in the bottom of the reactor vessel. The passage in the reflector would normally be filled by individual graphite plugs removable by the fuel handling machine and stored within the vessel prior to the start of refueling.

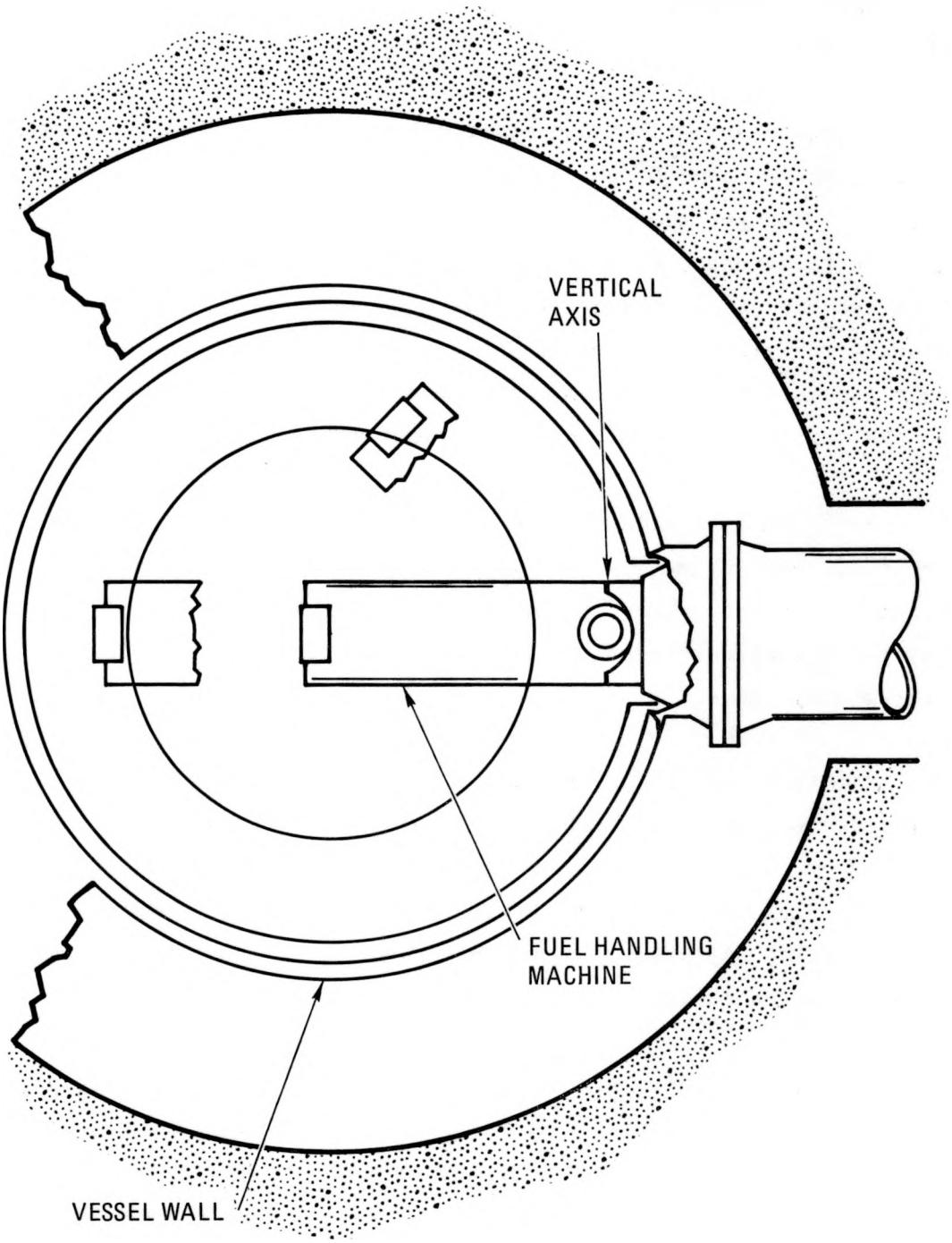

Fig. 4-41. Plan view of fuel handling machine

A preliminary estimate was made of the time required to replace the entire inventory of fuel elements, the top reflector elements and the inner row of side reflector elements, a total of 1149 elements. The total time, including pre-and post-operations, was estimated at twenty-three 24-hr days.

No attempt has been made to accelerate the refueling process since there is apparently no need to do so.

4.7.2.2. Control Rod Drive System. The reactor is controlled by an arrangement of control rods and shutdown rods, the actuating mechanisms for which are located below the reactor vessel. The cavity in which the mechanisms are located is shielded to provide adequate radiation protection for personnel during reactor shutdown. Personnel access to this equipment is possible only after reactor shutdown.

It is intended that, where appropriate, the design of the drive mechanism for the primary control rods will follow that already developed for the Peach Bottom HTGR. This reactor also featured bottom-mounted drives.

The basic difference between the drives for the HTGR-MRS/PH and those for the Peach Bottom reactor is that the rod travel in the former is longer by a factor of three. In order to minimize the head room below the reactor vessel required to accommodate the rod travel, the proposed drive features an offset arrangement shown schematically in Fig. 4-42.

A supplementary feature has been studied that would provide, in effect, a gravity scram capability for driving the rods upward into the core. The device to accomplish this motion can be described as a counterbalance weight supported by a secondary ball screw. The weight is constrained against rotation so that when released and allowed to free fall, the screw is caused to rotate. The secondary screw is coupled to the primary screw that activates the control rod, causing the primary screw to rotate in the direction of rod insertion. In this mode, the main power unit is uncoupled from the

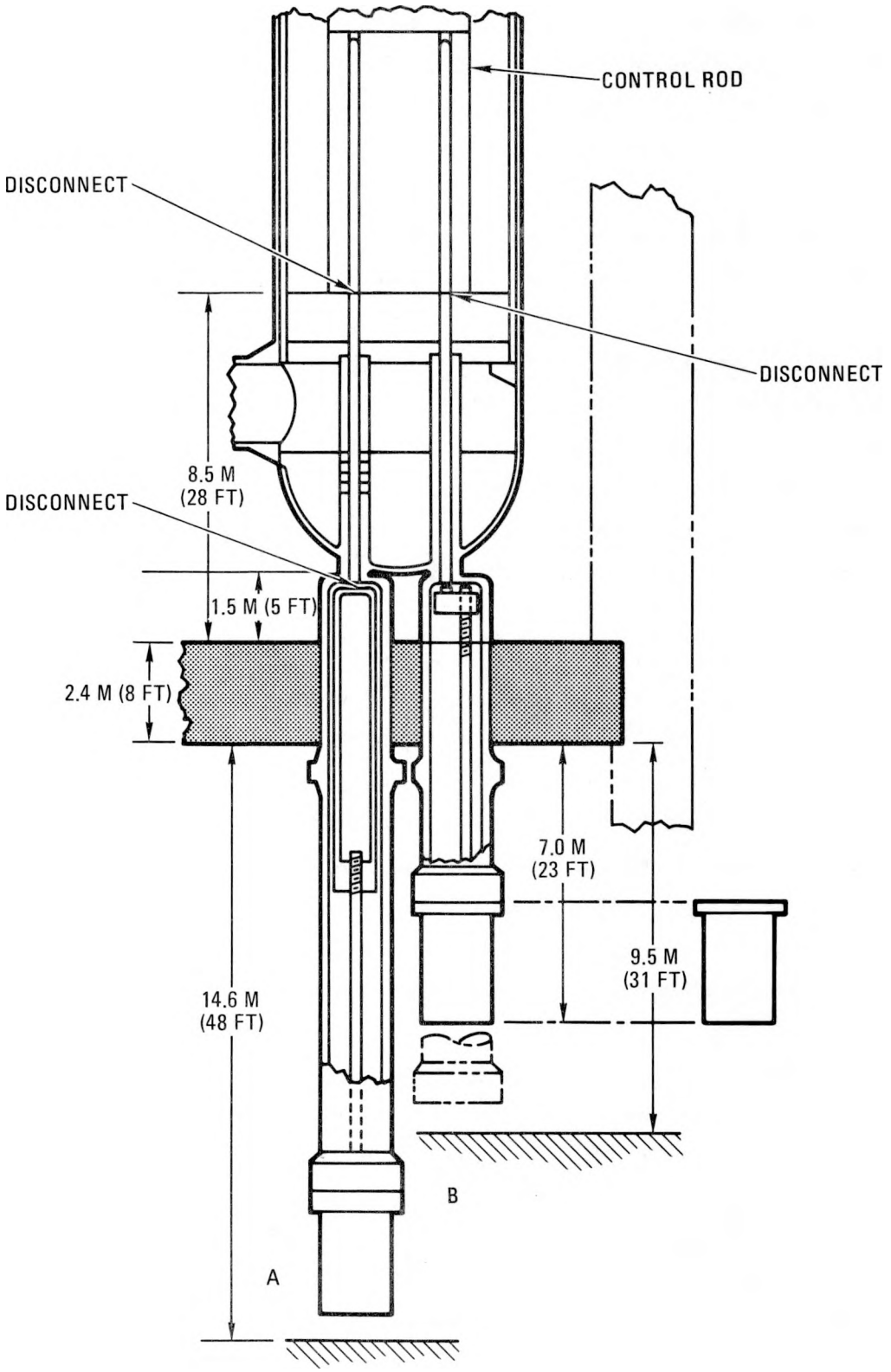

Fig. 4-42. Alternate control rod drive arrangement

ball screw by means of an intermediate clutch. The mechanism which decelerates the rod at end of travel remains engaged at all times.

A concept for a proposed reserve shutdown system is shown in Figs. 4-43 and 4-44. Absorber material is stored in hoppers formed within the thickness of the top reflector. The material, in spherical or granular form, is released from below the core into channels within the core and is eventually removed into a cask for disposal. Reloading is performed by the fuel handling machine prior to repressurization and startup.

4.8. HELIUM CIRCULATOR DESIGN (6053050200)

4.8.1. Scope

This task includes design effort required to establish the optimum circulator configuration for this application and to define the circulator envelope, aerodynamic performance, drive motor concept, and installation into the steel vessel. Part of this task is to provide pertinent circulator parameters to Cost Development for cost estimating. Maintenance and inspection requirements are also to be defined.

4.8.2. Discussion

The objective of this circulator design study was to investigate possible circulator concepts and to define the preferred circulator concept, including the motor drive arrangement.

The primary coolant system for the 250-MW(t) HTGR-MRS/PH plant uses a single helium circulator to circulate and control the helium flow that transfers the heat from the core to the reformer and the steam generator.

The circulator interfaces with the primary closure flange that is part of the main reactor vessel. The entire circulator assembly is supported at

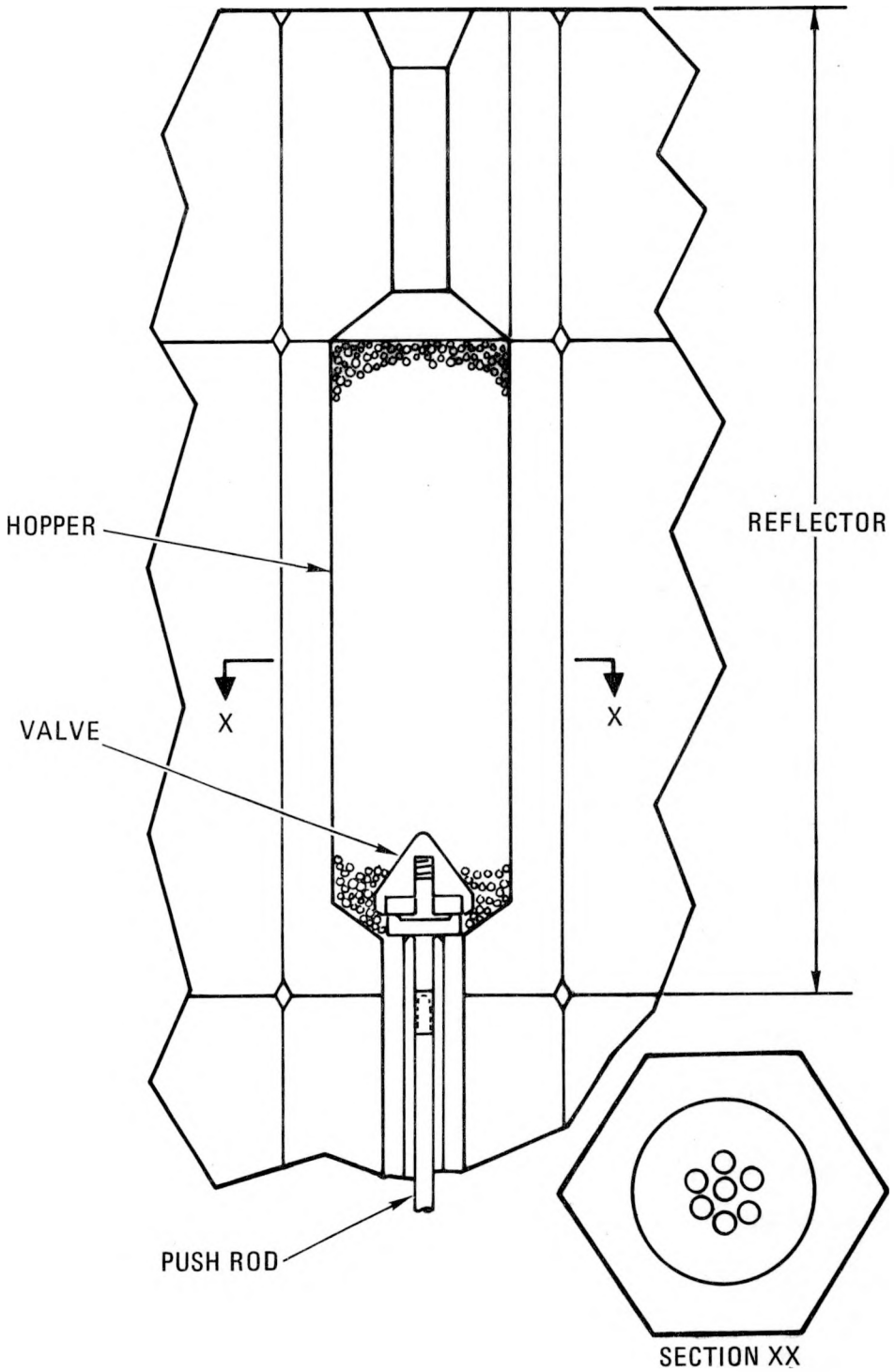

Fig. 4-43. Reserve shutdown concept

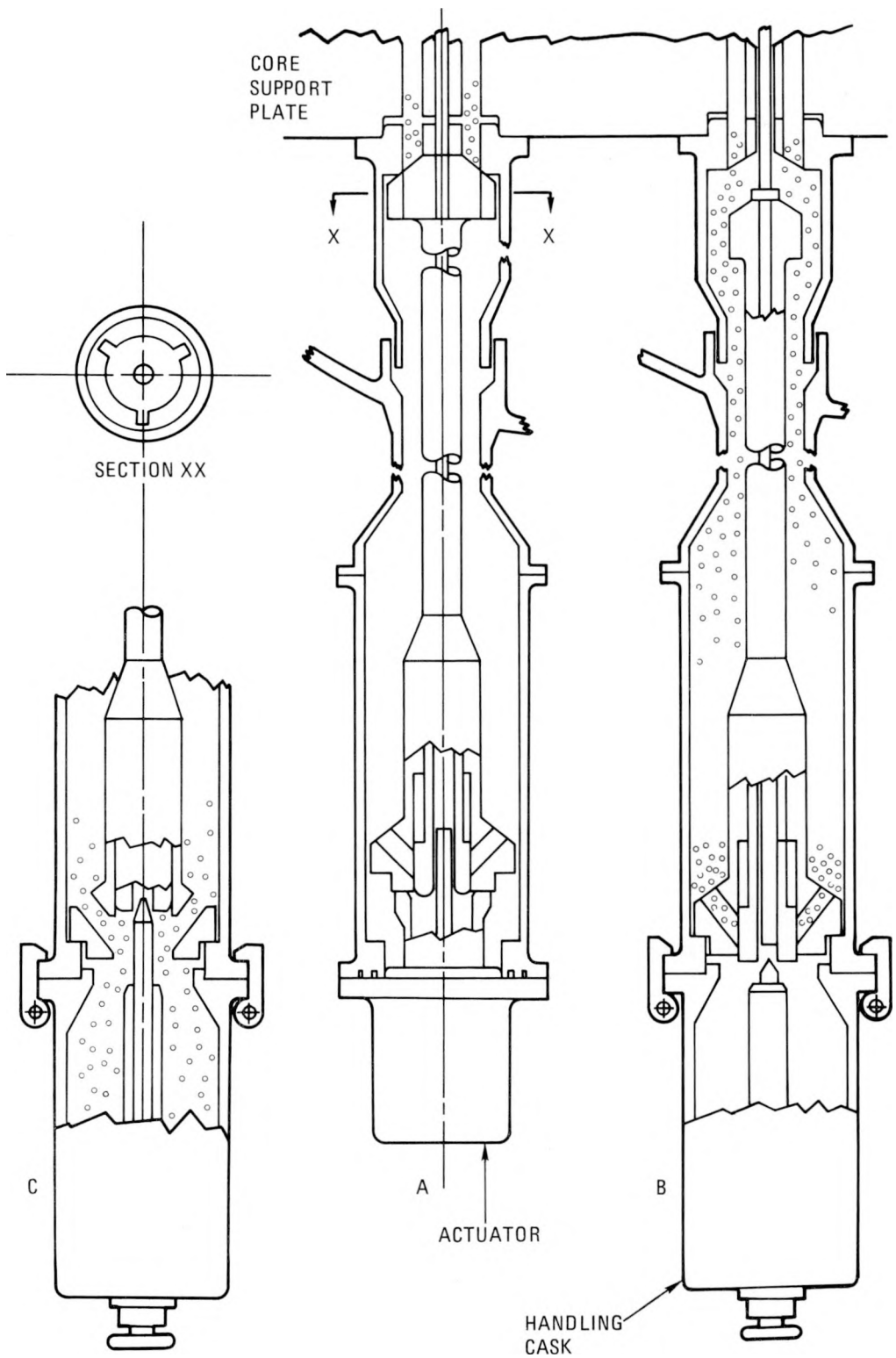

Fig. 4-44. Details of reserve shutdown system

this flange. The circulator discharge duct interfaces with the core inlet plenum that is internal to the reactor vessel.

On the basis of large reactor studies, a variable speed electric motor has been selected for the circulator drive. Evaluation was made of the following possible circulator compressor types:

1. Single-stage centrifugal flow. The single-stage centrifugal flow compressor matches fairly well the drive rotating speed of 3600 rpm. However, it results in a relatively large circulator impeller and diffuser as well as in parallel (nonconcentric) inlet and discharge ducting. The configuration (see Fig. 4-45) requires relatively large dome closures as well as large-diameter pipe weldments to the reactor vessel.

2. Single-stage axial flow. For a single-stage axial flow design with a minimum specific speed of N_S = 215.6 required for reasonable efficiency, the driver speed would need to be at least 7570 rpm. The motor for this rotating speed and about a 4100-kW (5500-hp) rating were considered to require considerable development, and this concept was discontinued.

3. Two-stage axial flow. The two-stage axial flow circulator offers a very compact arrangement and simple circulator ducting. The overall arrangement of the two-stage axial flow circulator is shown in Fig. 4-46. The 4500-rpm operating speed yields good stage efficiencies. A synchronous motor with a solid rotor presents no feasibility problems in this speed range. Several 15-MW motors for boiler feed pump drive application are currently in operation at 5500 rpm.

This study concluded that the preferred concept is the two-stage axial unit, shown in more detail in Fig. 4-47. The adiabatic efficiency of the two-stage unit with same-stage specific speed is higher than for the

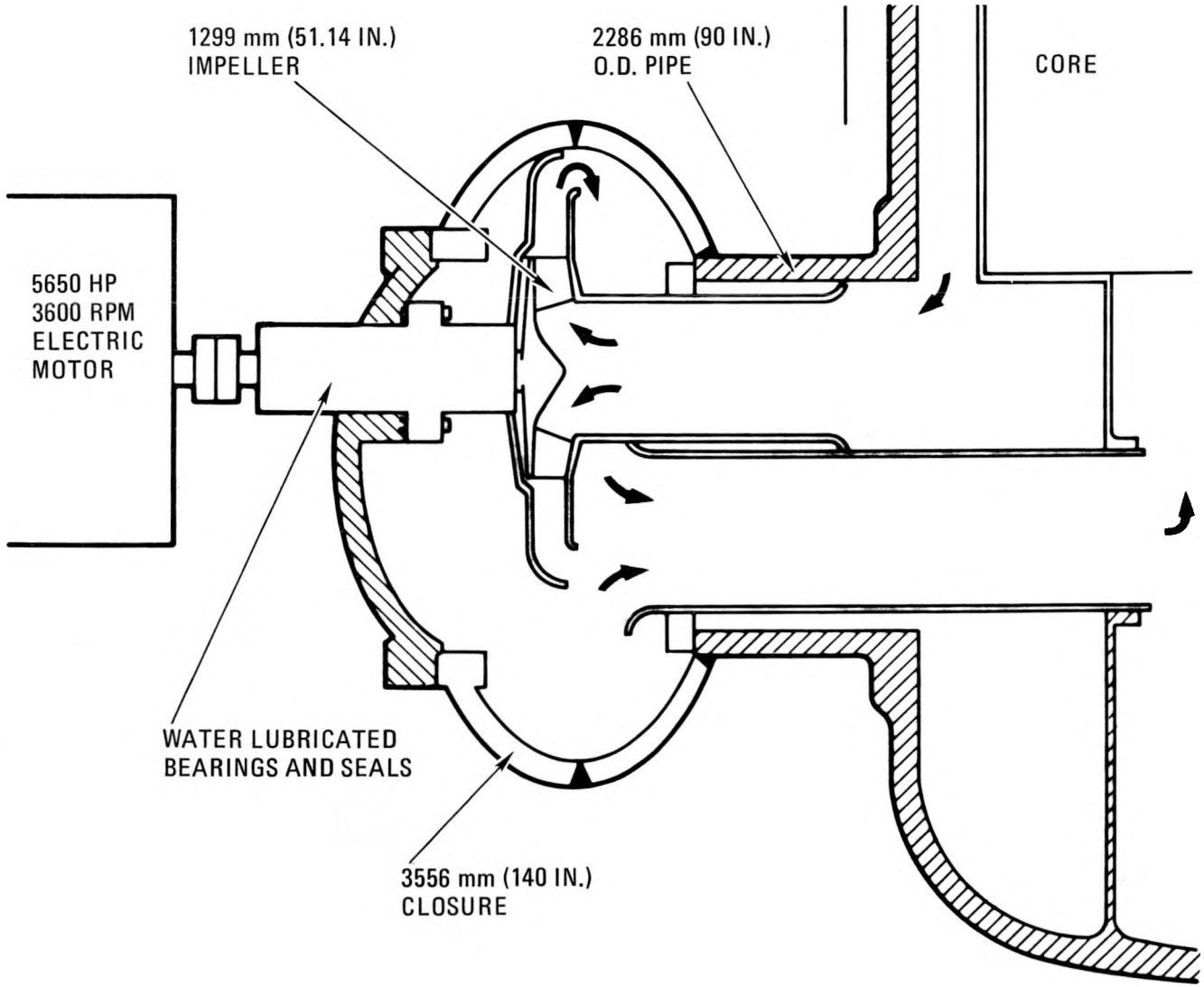

Fig. 4-45. Single-stage centrifugal flow circulator concept

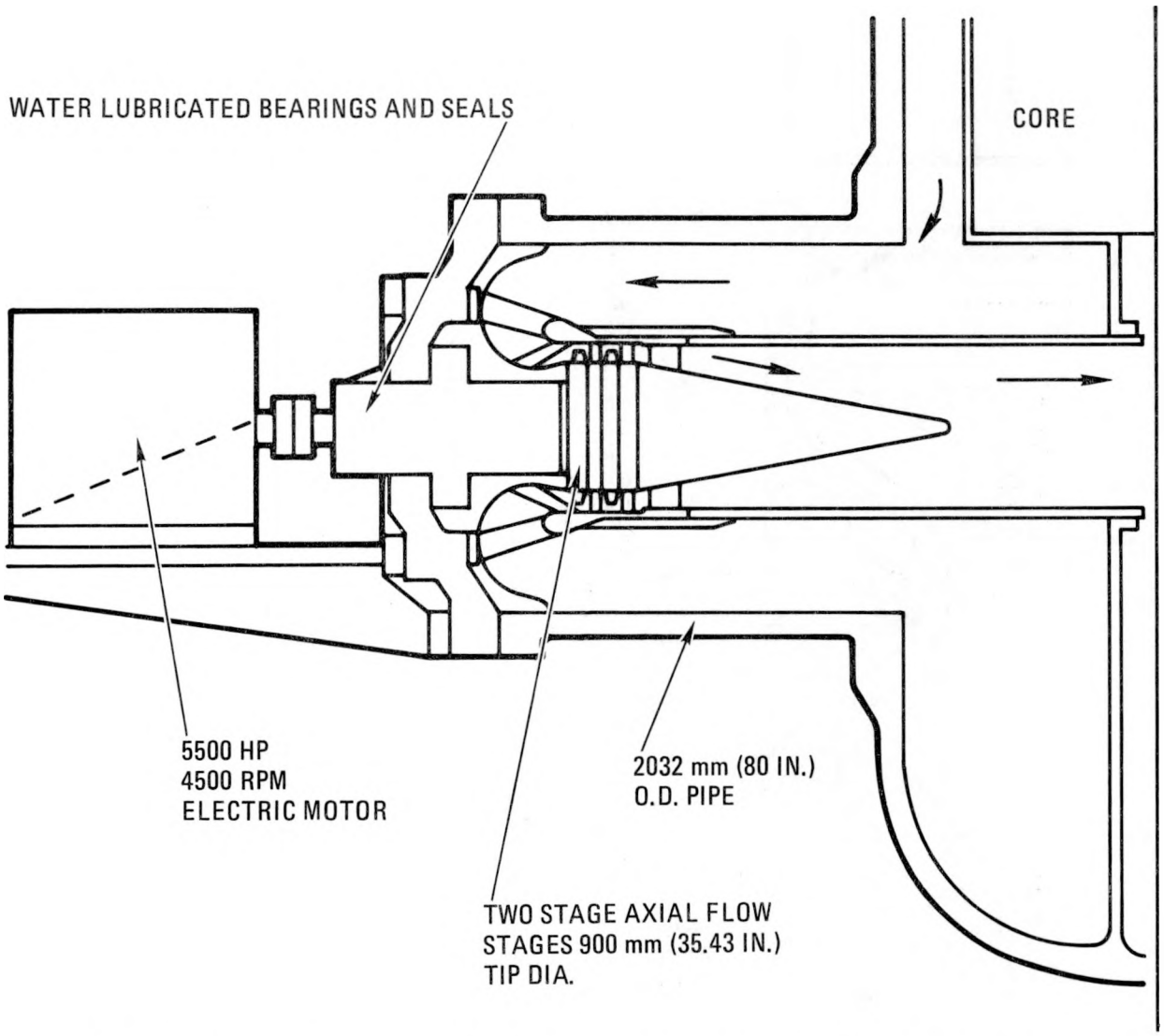

Fig. 4-46. Two-stage axial flow compressor circulator concept

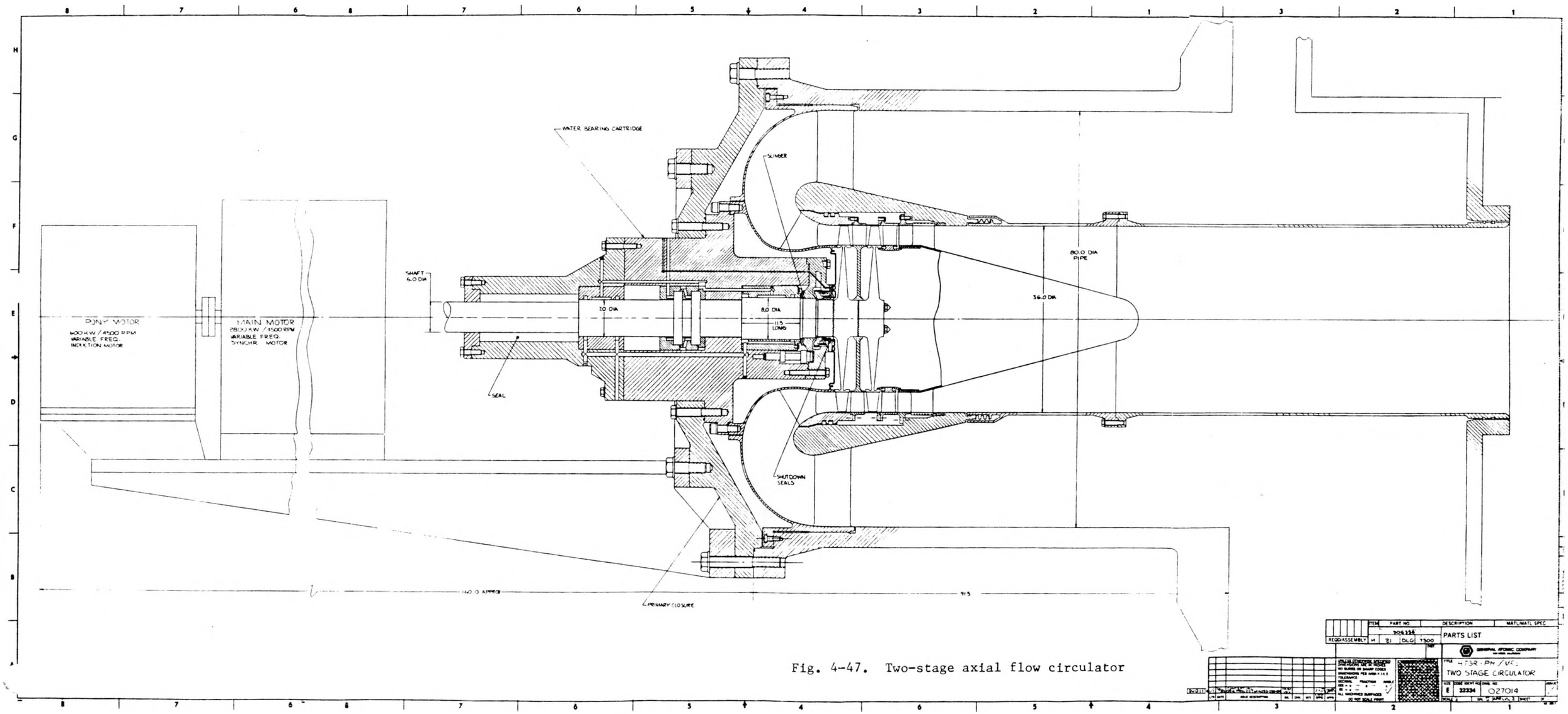

Fig. 4-47. Two-stage axial flow circulator

single-stage because of utilization of the dynamic head at the first stage discharge; i.e., the diffuser loss is distributed over the work performed by two stages rather than one. The tip diameter of each impeller is 900 mm (35.43 in.). The aerodynamic shaft power is 3930 kW (5266 hp) at 4500 rpm. The effect of rotating speed on maximum achievable compressor efficiency is shown in Fig. 4-48. As shown, the optimum rpm would have been higher than the 4500 rpm selected. However, the selection of a higher rpm would have resulted in a more difficult motor design. The 4500-rpm motor has already been considered and investigated for the large HTGR circulator drive application and found to be within the existing technology.

The circulator rotor is supported on two water-lubricated radial bearings. Axial thrust is taken by the motor bearing system, which consists of one double-acting thrust bearing and two radial bearings, all oil lubricated. A diagram of the bearing and seal service system for the circulator is shown in Fig. 4-49. The system employed here is basically the same as that used in the 2240-MW(t) HTGR except that it is applied to a horizontal shaft configuration and is approximately 50% lower in flow capacity.

The circulator main motor is a variable speed synchronous type with a solid-state variable frequency power supply. The motor is fully enclosed and is internally air cooled with air-to-water heat exchangers mounted inside the motor enclosures. The drive motor is coupled to the circulator rotor via a solid shaft.

The water bearings, helium/water seal, and the circulator impellers will be designed for 40-yr life with no maintenance required. The high-pressure water seal that is located outboard has an estimated life of 4 to 6 yr. It will be designed for easy replacement requiring no motor removal or loss of motor-circulator alignment via utilization of a shaft spool piece that is removed prior to seal assembly replacement. The interval between cleanup and check of the electric motor bearings and water coolers will be 6 yr or more. At refueling time, the circulator will be removed for cleanup and inspection of the impeller and bearings. This interval may be doubled if the first inspection shows low deposits on blades or bearing passages.

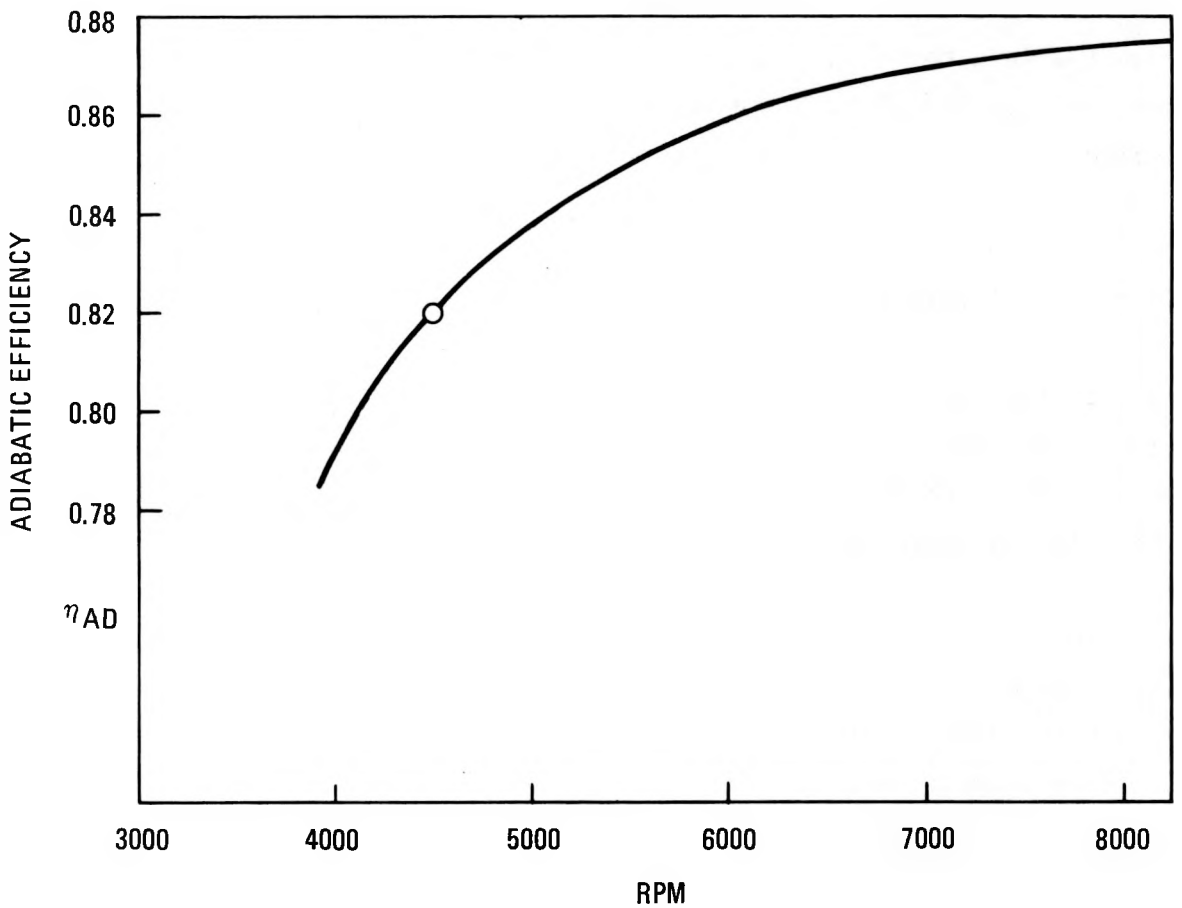

Fig. 4-48. Estimated maximum adiabatic efficiency versus rpm for various two-stage axial flow designs

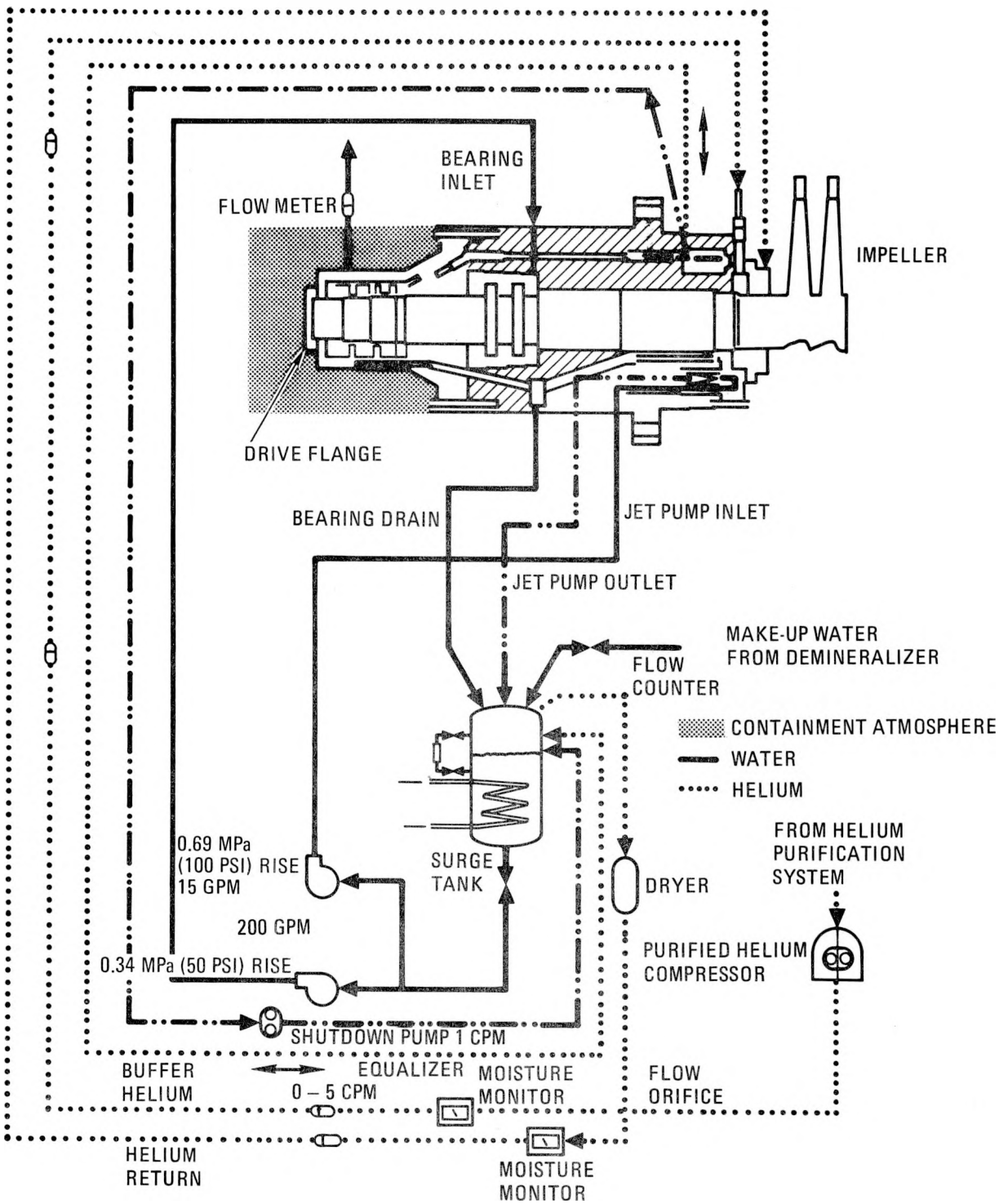

Fig. 4-49. Circulator bearing and seal service system

REFERENCES

4-1. "Reforming MRS - January 26 Ground Rule Meeting Minutes," unpublished data, General Electric Company, February 8, 1982.

4-2. Orvis, D. D., and P. H. Raabe, "Interpretation of General Design Criteria for High-Temperature Gas-Cooled Reactors," DOE Report GA-A15255, GA Technologies, January 1980.

4-3. "2240 MW(t) HTGR-Steam Cycle Conceptual Design Status Report," prepared for the Gas Cooled Reactor Associates by United Engineers and Constructors, May 1, 1979.

4-4. "Reforming MRS - March 18, 1982, Technical Coordination Meeting Minutes," unpublished data, General Electric Company, March 18, 1982.

4-5. "Reforming MRS - April 4, 1982, Technical Coordination Meeting Minutes," unpublished data, General Electric Company.

4-6. Schwartztrauber, K. E., and F. A. Silady, "CORCON: A Program for Analysis of HTGR Core Heatup Transients," GA Technologies Report GA-A12868, July 15, 1974.

4-7. Swartz, M. H., D. B. Sedgley, and M. M. Mendonca, "SORS: Computer Program for Analyzing Fission Project Release from HTGR Cores During Transient Temperature Excursions," GA Technologies Report GA-A12462, April 15, 1974.

4-8. "Minutes of MRS Groundrule Meeting, GE-Sunnyvale," unpublished data, GA Technologies, January 26, 1982.

4-9. Seth, S., and A. Hess, "Preliminary Core Designs for the LEU and HEU Fueled Small Modular VHTR," unpublished data, GA Technologies, February 2, 1982.

5. HTGR-SETS AND APPLICATIONS DEVELOPMENT STUDIES

5.1. SETS APPLICATIONS STUDY (6051020001)

5.1.1. Scope

- To document recommended design changes for improving the cost and performance of long-distance energy transmission pipeline systems developed in FY-81.
- To prepare plant performance for selected refinery applications.
- To document appropriate draft input to the HTGR-SETS screening report.

5.1.2. Discussion

This task concludes the technical portion of the screening phase for the HTGR-SETS system. It includes a continuation of FY-81 work to prepare a conceptual design and to provide cost estimates for an HTGR of approximately 750°C (1382°F) reactor outlet temperature capable of storing and/or transporting all or part of the reactor energy using molten nitrate salt as a sensible energy medium. Selected applications for utilizing the high-quality heat from the molten salt have been evaluated, and capital and product cost estimates have been provided. The study is being coordinated by GCRA, involves the participation of GA and UE&C, and will culminate in an HTGR-SETS screening report in CY-82. The SETS applications presently being documented include (1) an on-site base load and peaking electric generation system, (2) a process steam cogeneration application (to be provided by GCRA), (3) an oil shale recovery application, and (4) three possible oil refinery scenarios in which the SETS capabilities to provide multiple energy services are investigated. Technical details of items 3 and 4 and

the GA contributions to the GCRA study are included in this section. The preparation of cost and economic data is proceeding.

5.1.2.1. Oil Shale Recovery Applications Study. As reported in previous studies (Ref. 5-1), the indirect Paraho AGR process appears particularly suited to SETS because (1) a substantial portion of its energy requirement is derived outside the retort with a gas-fired heater that can be replaced with a molten salt heat exchanger, (2) the retorting temperature of 482° to 510°C (900° to 950°F) is consistent with molten salt technology, and (3) the siting flexibility of the SETS concept permits a remote NHS serving widely separated retorts to be considered. Figure 5-1 is a diagram of the indirect Paraho AGR process including a SETS hookup. During operation, crushed raw shale is fed continuously to the retort at the top and descends through the retort as a moving bed. As it moves, it is heated to pyrolysis temperatures by a rising stream of heated gas. The oil and gas produced are swept up through the bed to collecting tubes and out of the retort to product separation equipment. After the oil is separated, the off-gas is split into recycle and product gas streams. The recycled off-gas streams are split further into reheating and cooling gas streams. The reheating gas is heated up to pyrolysis temperatures in a molten salt heat exchanger and is reinjected into the middle of the retort. The cooling gas is first reduced in temperature in a conventional cooler, then is reinjected through the bottom of the retort to recover energy from the spent shale before discharge. The reinjected gases provide all the heat for the retorting process, and no combustion occurs in the retort vessel itself.

The crude shale oil product that is separated from the off-gas stream has a high nitrogen content and a high pour point, which makes it unsuitable as a refinery feedstock. Therefore, appropriate shale oil upgrading facilities were included in this study. Figure 5-2 schematically portrays the overall process plant complex.

Available data (Ref. 5-2) indicate that the indirect Paraho process is carried out with the injected recycle gas heating medium at 704°C (1300°F),

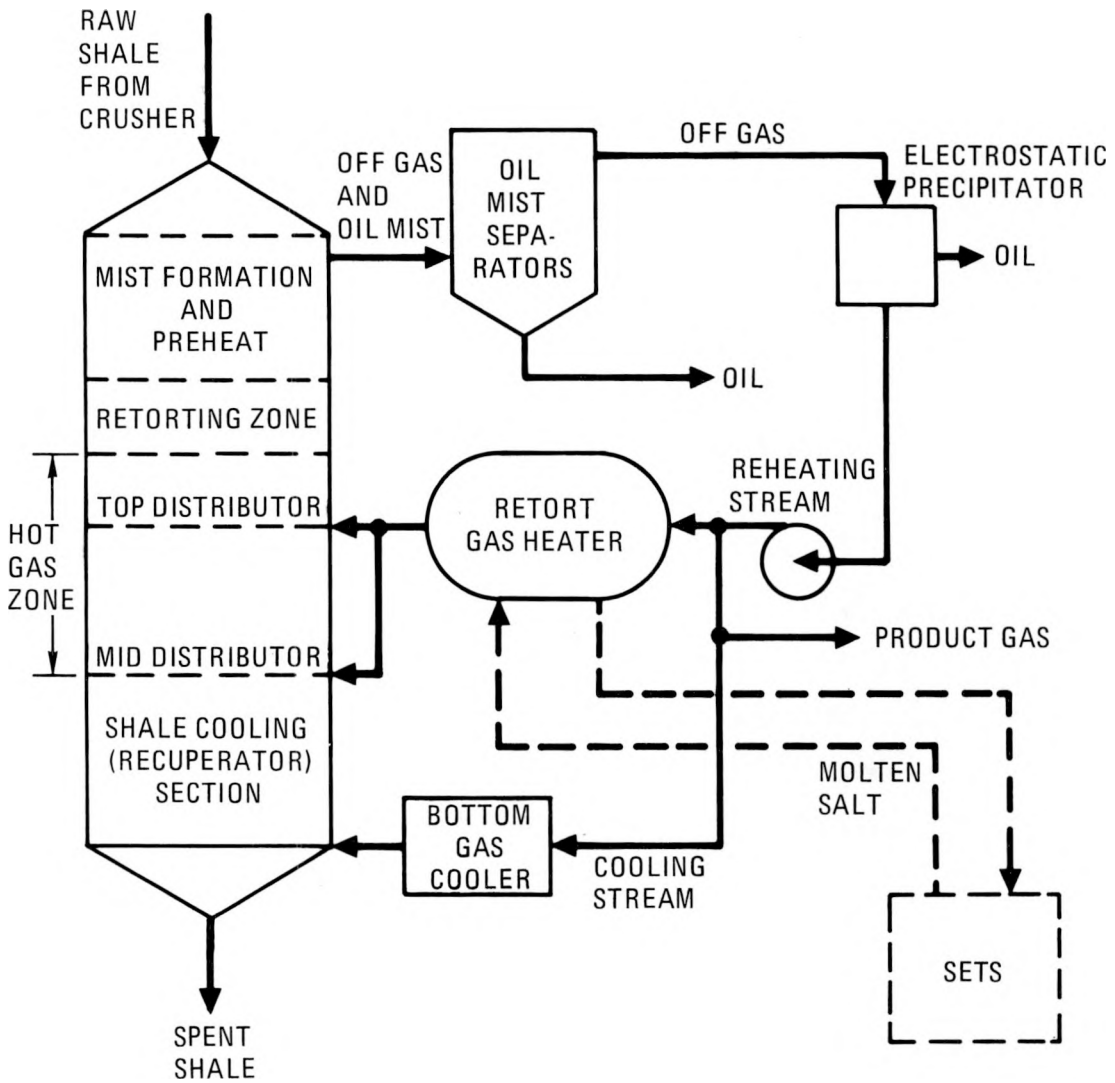

Fig. 5-1. Indirect Paraho oil shale retorting process serviced by SETS

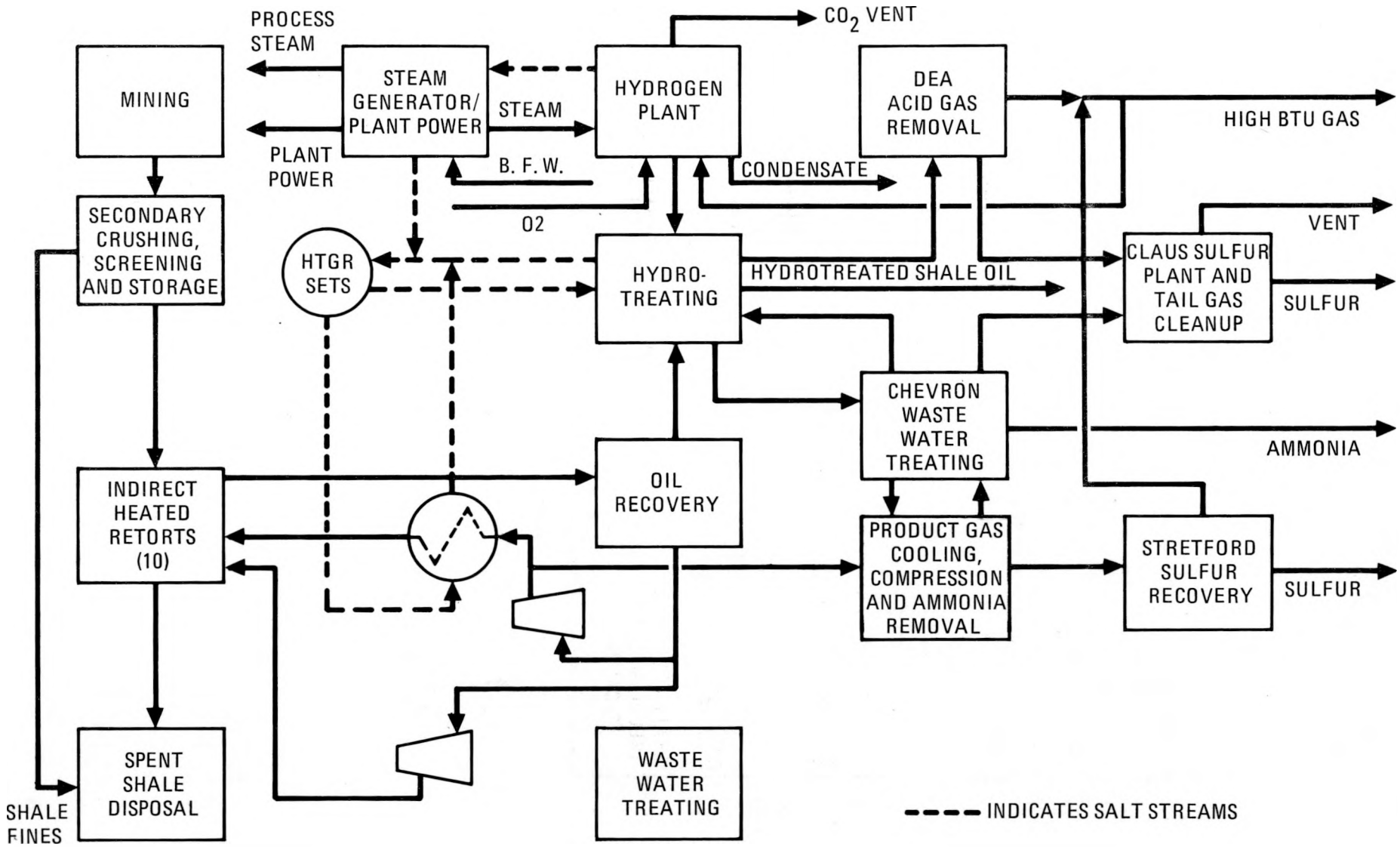

Fig. 5-2. Schematic process flow diagram for indirect Paraho AGR oil shale facility with HTGR-SETS heat source

even though the retorting process itself requires only that the shale be heated to 454° to 510°C (850° to 950°F). This study attempted to span this temperature range by comparing the following three cases:

Case Reference	Retorting Temperature [°C (°F)]	Recycle Gas Temperature [°C (°F)]
Fossil	510 (950)	704 (1300)
HTGR-SETS low temperature	454 (859)	510 (950)
HTGR-SETS high temperature	510 (950)	538 (1000)

Oil yield data as a function of temperature (see Fig. 5-3) were used to correlate retorting temperature with shale oil yield. The oil shale used had a Fischer assay* yield of 0.117 m^3/Mg (28 gal/ton) in all cases.

All cases were sized to yield the same quantity of crude shale oil, 0.0767 m^3/s (41,683 BBL/D). Based on information presented in Ref. 5-3, this crude shale oil yielded 0.0829 m^3/s (45,042 BBL/D) of synthetic crude after hydrotreating. The gas yield was assumed to be the same in all cases (500 scf/ton), proportional to the mass of shale required to yield the required crude shale oil.

The lengths of the retorts were recalculated based on the new temperature differences. Since the variations in the feed rates per retort were small, the total number of retorts was kept constant and the 7.5% flow variations were assumed to be within the normal tolerances for the equipment. However, retort lengths were adjusted for the smaller temperature difference and the increase in heat loads.

All equipment for handling the increase in gas flow through the retort and all gas treating equipment were resized to compensate for the lower

*Fischer assay is a standardized method of retorting oil shales to assess their oil content. In actual practice, yields range from about 80% to above 100% of the Fischer assay values because of differences between commercial retorting methods and the Fischer assay retorting.

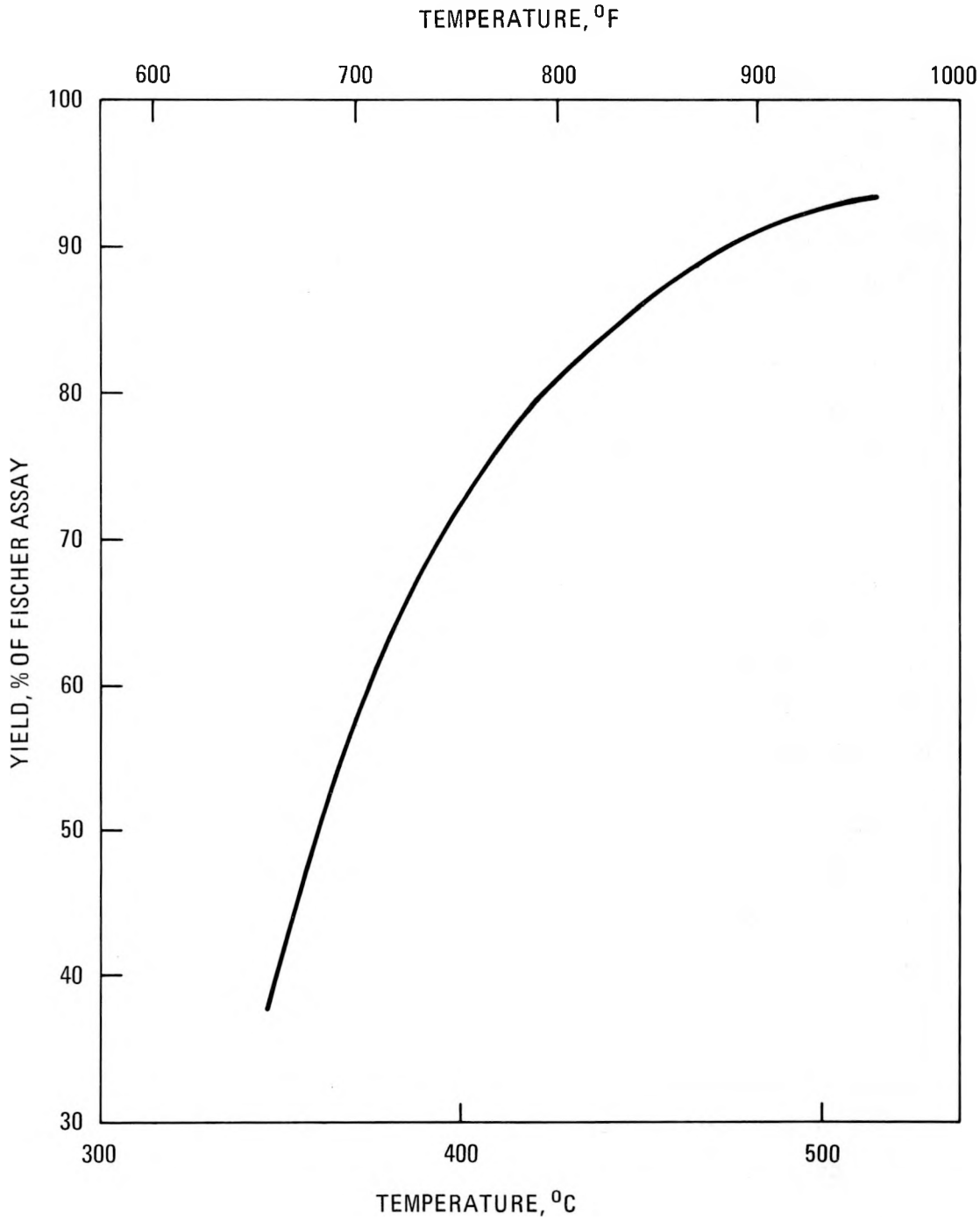

Fig. 5-3. Correlation of oil yield data as a function of temperature (Ref. 5-3)

temperature differences. Table 5-1, which is based on data from Refs. 5-4 and 5-5, summarizes all of these adjustments.

The HTGR-SETS was integrated by delivering hot salt at 566°C (1050°F) to the shale oil services. Tables 5-2 and 5-3 show the overall heat and product balances.

5.1.2.2. Refinery Repowering Studies. Prior applications studies have not fully exploited SETS capabilities for delivering high-grade process heat. Instead, SETS has been evaluated as a potential alternative to the HTGR-SC/C for producing process steam and electricity. In these earlier studies, SETS' relatively high capital costs and pumping power requirements prevented it from gaining a significant economic advantage over its competition in all such applications except those requiring remote siting of the reactor. While it was recognized that the economic posture of SETS might be improved if some or all of the high-temperature molten salt could be used directly as a process heating medium, definition of a suitable reference process could not be accomplished within the scope of the previous SETS studies (Ref. 5-1).

Repowering a large oil refinery was selected as the reference application for the FY-82 studies for the following reasons:

1. A large oil refinery typically requires electricity and process steam in large quantities, essentially on a base-loaded basis.

2. The combined duty of the process heaters is large, and the process conditions are generally compatible with the utilization of SETS-supplied molten salt as a heating medium.

3. Refinery complexes are often sited near other large users of process heat, steam, and electricity, permitting consideration of larger-capacity SETS plants with attendant economies of scale.

TABLE 5-1
RETORT PARAMETERS

Parameter	Fossil Case	HTGR-SETS Low-Temperature Case	HTGR-SETS High-Temperature Case
Shale feed, kg/s (tons/day)	704 (66,871)	757 (71,867)	704 (66,871)
Shale grade, m^3/Mg[a] (gal/ton)	0.117 (28)	0.117 (28)	0.117 (28)
Number of retorts	10	10	10
Retorting temperature, °C (°F)	510 (950)	454 (850)	510 (950)
Yield % of shale grade	93.5	87.0	93.5
Hot recycle gas temperature, °C (°F)	704 (1300)	510 (950)	538 (1000)
Hot recycle gas flow, kg/s (10^6 lb/hr)	190 (1.504)	308 (2.439)	281 (2.222)
Hot salt temperature, °C (°F)	--	538 (1000)	566 (1050)
Cold salt temperature, °C (°F)	--	--	--
Feed shale temperature, °C (°F)	25 (77)	25 (77)	25 (77)
Spent shale temperature, °C (°F)	177 (350)	177 (350)	177 (350)
Cold recycle gas temperature, °C (°F)	54 (130)	54 (130)	54 (130)
Cold recycle gas flow, kg/s (10^6 lb/hr)	208 (1.645)	243 (1.921)	208 (1.645)
Off-gas temperature,°C (°F)	138 (280)	138 (280)	138 (280)
Retort diameter, m (ft)	12.2 (40)	12.2 (40)	12.2 (40)
Heating section length, m (ft)	2.1 (7.04)	3.2 (10.45)	4.5 (14.9)
Cooling section length, m (ft)	4.2 (13.7)	3.9 (12.84)	4.2 (13.9)
Overall length, m (ft)	6.3 (20.74)	7.1 (23.29)	8.8 (28.8)
Ratio to fossil	1.0	1.12	1.39

[a] m^3/Mg = cubic meters of oil per 10^6 g.

TABLE 5-2
HEAT BALANCE SUMMARY

	Fossil Case	HTGR-SETS High-Temperature Case	HTGR-SETS Low-Temperature Case
Process heat			
Retort absorbed, MW(t)	319	319	319
Hydrotreating absorbed, MW(t)	10	10	10
Process steam, MW(t)	50	51	52
Electricity generated, MW(t) [MW(e)]	361 (139)	823 (317)	823 (317)
Process demand MW(t) [MW(e)]	361 (139)	588 (226)	608 (234)[a]
Excess, MW(e)	--	(91)	(83)

[a]Includes 195 MW(t) [75 MW(e)] for HTGR-SETS house load.

TABLE 5-3
PARAHO INDIRECT
PRODUCT BALANCE SUMMARY

	Fossil Case	HTGR-SETS Low-Temperature Case	HTGR-SETS High-Temperature Case
Shale quality, m^3/Mg[a] (gal/ton)	0.117 (28)	0.117 (28)	0.117 (28)
Feed shale, kg/s (tons/stream day)	704 (66,817)	757 (71,867)	704 (66,871)
Yield % of quality	93.5	87.0	93.5
Raw shale oil, MW (BBL/stream day)	3053 (41,683)	3053 (41,683)	3053 (41,683)
Hydrotreated oil products, MW (BBL/stream day)	3300 (45,042)	3300 (45,042)	3300 (45,042)
Gross product gas,[b] MW (BBL/stream day)	149 (2037)	174 (2382)	149 (2037)
Total gross products, MW (BBL/stream day)	3449 (47,079)	3474 (47,424)	3449 (47,079)
Purchased fuel, MW (BBL/stream day)	1156 (15,779)	204 (2780)	204 (2780)
Net product, MW (BBL/stream day)	2293 (31,300)	3270 (44,644)	3245 (44,299)
Ratio of net product to fossil-fired case	1.00	1.43	1.42

[a] Reformer feedstock deducted.

[b] m^3/Mg = cubic meters of oil per 10^6 g.

4. Industrial zones where such refinery complexes might be located are usually characterized by high population densities and site scarcity, creating strong incentives for remotely sited nuclear heat source facilities.

Since current user data for an existing refinery complex could not be obtained in time for this study, a hypothetical complex synthesized from refinery balances published in Ref. 5-6 was used as a basis for the study. This work was a joint effort between GA and UE&C, coordinated by GCRA.

The study initially focused on coupling a twin 1170-MW(t) HTGR-SETS nuclear heat source to a base-loaded electrical plant and to a 32-km (20-mi) long molten salt pipeline connecting the nuclear facility and the refinery. Figure 5-4 schematically illustrates the general concept and provides the overall energy balance used to guide UE&C balance-of-plant studies. Technical definition of the concept was completed. To the extent required to support conceptual cost estimates, economic analysis of this concept is under way.

5.1.2.3. SUPERSETS. Concurrent with the refinery repowering study, a conceptual extension of this refinery study is being made to explore the economy-of-scale incentives for a larger-capacity SETS facility. The resulting concept, identified as SUPERSETS, is a large-scale multiple-service energy park that can not only service the needs of the refinery discussed above but can also provide process steam and electricity to other industries near the refinery complex. The SUPERSETS facility combines the following elements at the energy park site:

1. Four 1170-MW(t) "slide-along" HTGR-SETS nuclear heat supply units.
2. A base-loaded electricity/process steam cogenerating station.
3. A molten salt heat transport and thermal storage facility.

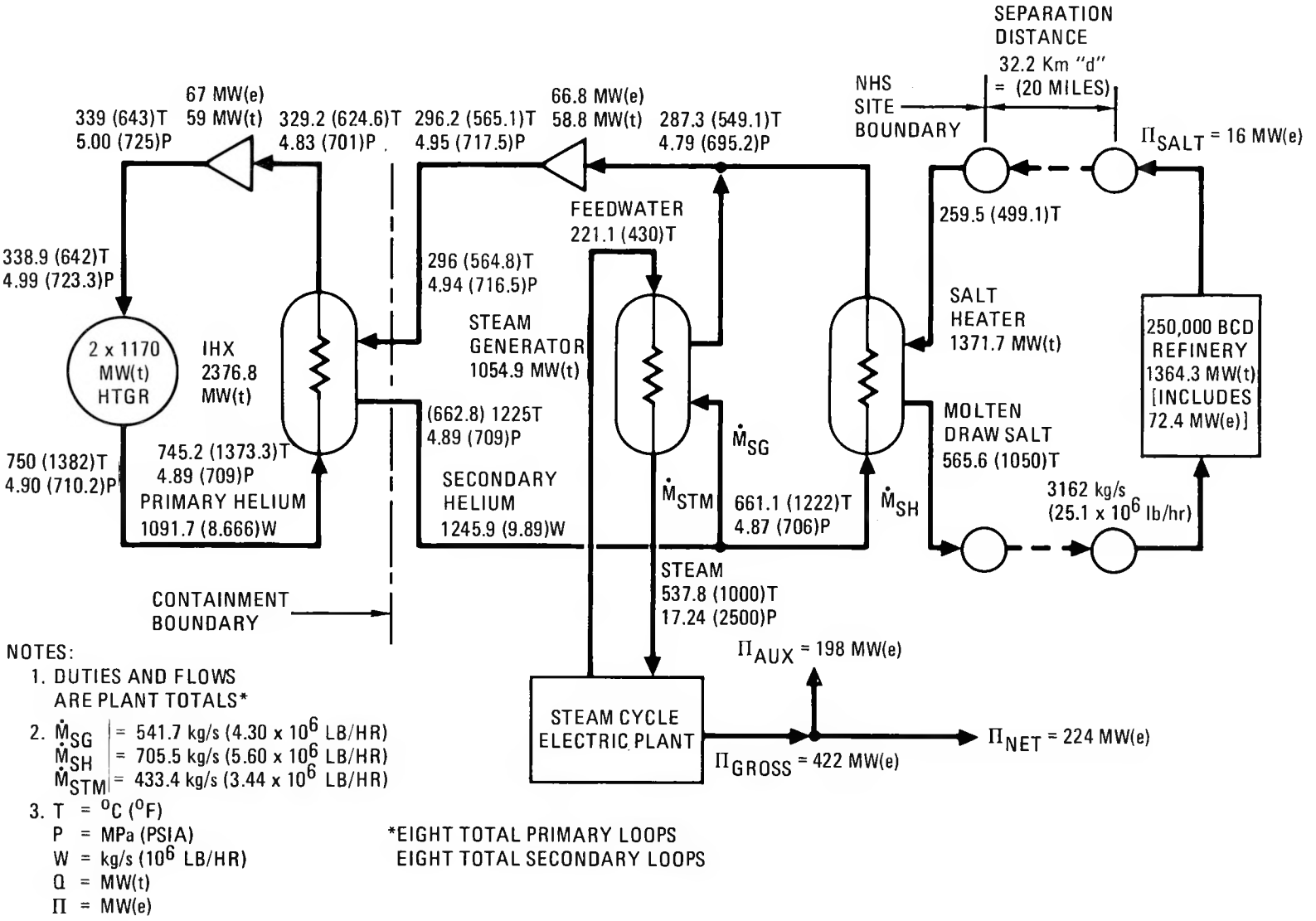

Fig. 5-4. HTGR-SETS twin plant refinery application flow diagram

4. A steam-driven peaking electrical power station in which the steam is generated with salt-heated boilers.

The large-capacity multiple-energy services, improved availability, and remote siting capability of the SUPERSETS concept are ideal for deployment in concentrated industrial areas such as the ship channel area located 16 km (10 mi) east of Houston, Texas. For the purposes of this study it was assumed that the SUPERSETS energy park is located at a site 32 km (20 mi) from a concentrated user complex on the Houston ship canal. Figure 5-5 shows a map of the area and lists the major users and their requirements. A review of the steam and electricity usage in this area indicates that an ample market should exist for the SUPERSETS output.

A heat balance and schematic diagram for the overall SUPERSETS energy park user arrangement is shown in Fig. 5-6. The SUPERSETS peaking electrical plant and thermal storage facility is sized to meet a peaking season daily profile of 1100 MW(e) for 8 hr. The daily profile assumed for off-season peaking operations is 700 MW(e) for 12 hr, which can be obtained through appropriate thermal storage capacity management without perturbing the operating conditions in the reactor plant or the external loops. With the resulting part-load efficiency, the peaking plant can produce approximately 1.53×10^6 MW(e)-hr of electricity during the 6-month off-peak season, compared with its full-load output of 1.60×10^6 MW(e)-hr developed during the peaking season. Figure 5-7 shows the role that can be assumed by these SUPERSETS outputs in the daily load profiles of the cognizant electrical utility. The load profiles are generalizations taken from 1982 projections for Houston Lighting & Power (HL&P).

Sufficient technical work has been completed on the SUPERSETS concept to support capital cost and economic analyses, which are currently in progress.

Industrial Plants			Nominal Energy Use	
Plant No.	Company	Major Fuel	Steam [kg/s (MM lb/hr)]	Electricity MW
12	Champion International	Gas	100.78 (0.8)	55
15	Diamond-Shamrock	Gas	163.76 (1.3)	250
16	Shell Oil	Gas	440.9 (3.5)	200
17	Tenneco	Gas	62.9 (0.5)	10
18	Rohm & Haas	Gas	81.88 (0.65)	30
19	Phillips Petroleum	Gas	151.47 (1.25)	31
20	Atlantic-Richfield Houston	Gas	214 (1.7)	100
21	Shell Chemical	Gas	126 (1.0)	10
22	Soltex Polymer	Gas	12.59 (0.1)	11
23	U.S. Industrial	Gas	56.68 (0.45)	50
24	Premier Petroleum	Gas	56.68 (0.45)	50
25	Ethyl Corporation	Gas	56.68 (0.45)	50
26	Olin Chemical	Gas	62.9 (0.5)	15
27	Texas Alkyls	Gas	N.A.	8
44	Atlantic-Richfield Channelview	Gas	12.59 (0.1)	100
45	Exxon	Oil	125.9 (1.0)	130
46	DuPont	Gas	75.58 (0.6)	21
47	Celanese	Gas	176.36 (1.4)	83
48	Oxirane	Gas	113.37 (0.9)	24
50	American Plant Food	Gas	37.79 (0.3)	1
51	Crown Central	Gas	50.39 (0.4)	7
	Total for Area		2185.69 (17.35)	1236

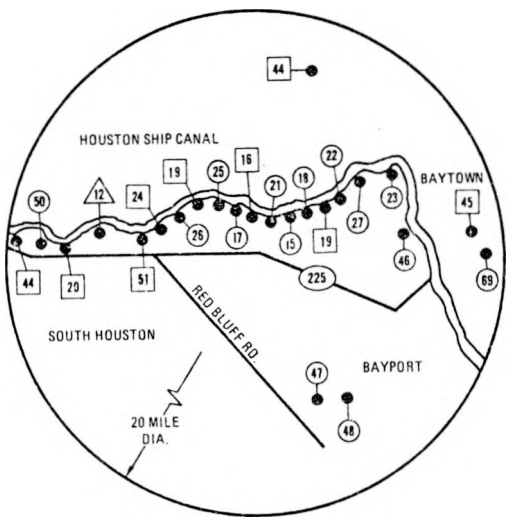

Fig. 5-5. Industrial steam and power concentrations in the Houston canal area (Ref. 5-6)

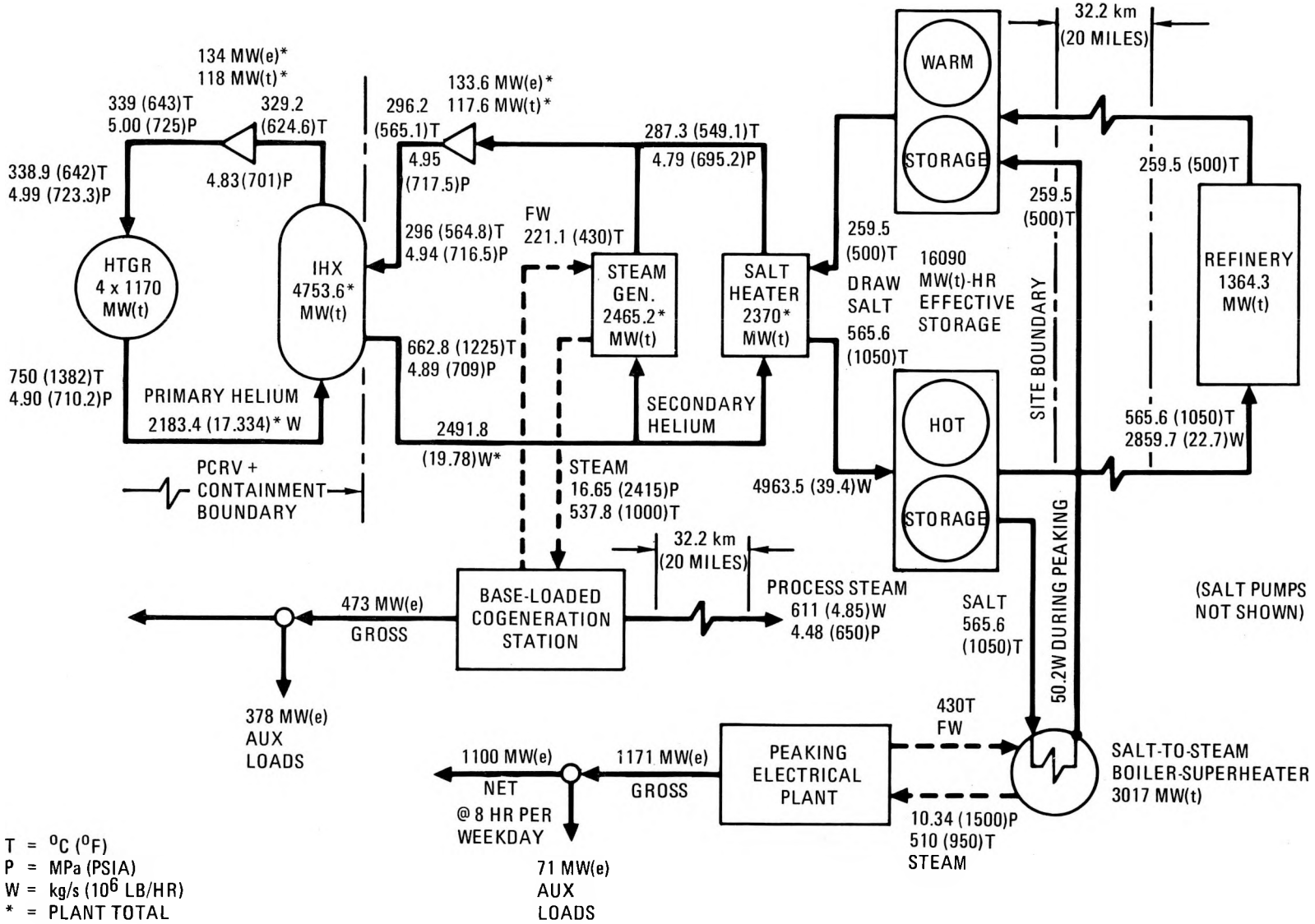

Fig. 5-6. SUPERSETS energy park heat balance and flow schematic

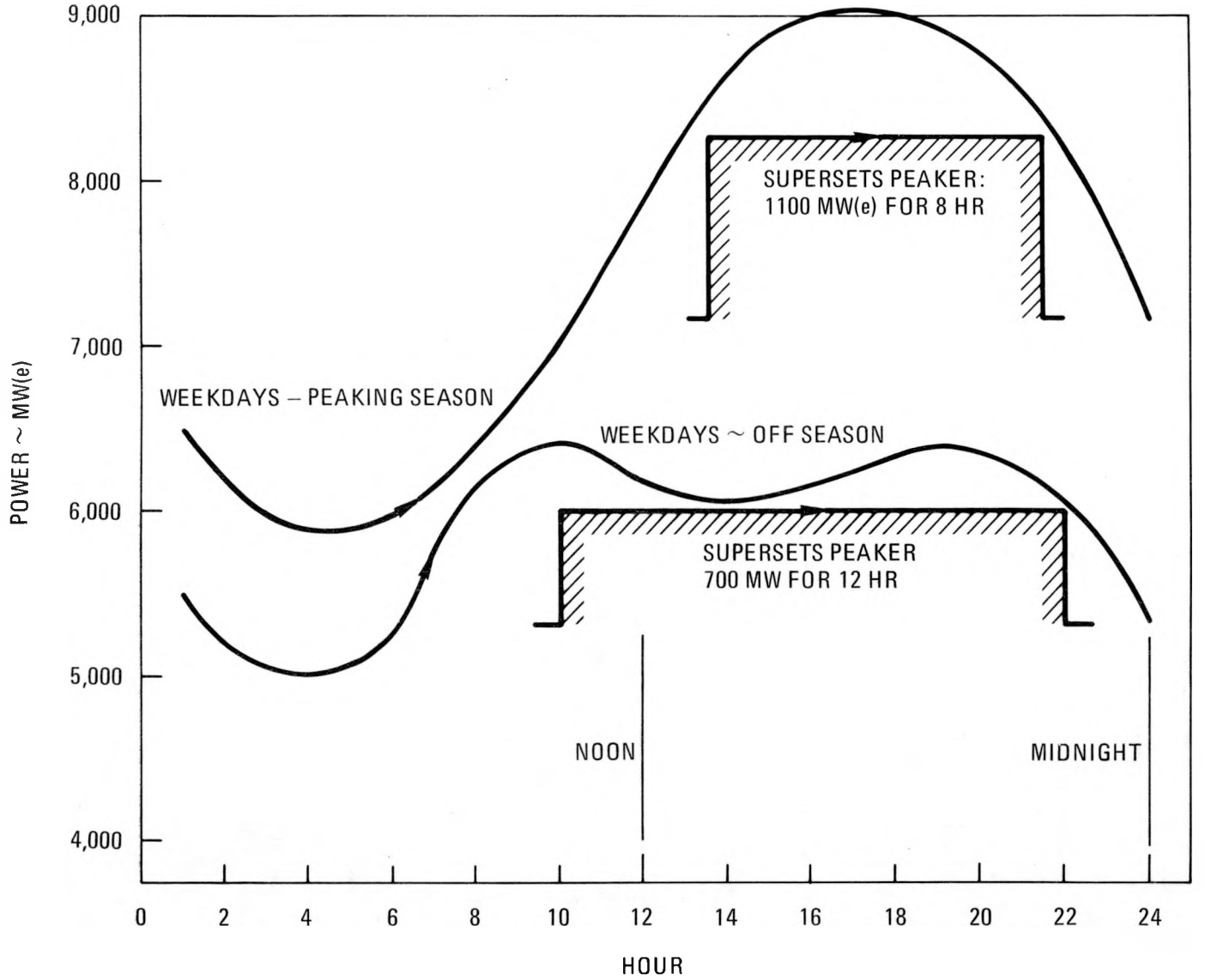

Fig. 5-7. Hypothetical fitups of SUPERSETS peaker output to representative utility load profiles

5.2. APPLICATION PROCESS DEVELOPMENT (600301300)

5.2.1. Scope

Work under this heading included the following:

- Study and assess above-ground retorting (AGR) processes in which the process energy is supplied by an HTGR-SC/C or an HTGR-PH/VHTR.

- Investigate water treatment and environmental impacts in heavy oil fields and the suitability of the treated water to meet HTGR HTGR steam-generator feedwater requirements.

- Perform conceptual design and evaluation of reboilers for treating recovered untreated process water from a heavy oil field, a tar sands field, and a typical chemical complex, and for rendering it suitable for use in the HTGR.

5.2.2. Discussion

5.2.2.1. AGR of Oil Shale. The Davy McKee study (Ref. 5-6) prepared under subcontract to GA in FY-81 describes an AGR process for oil shale using (1) a hot recycle gas at 704°C (1300°F), which is heated by secondary helium from an 1170-MW(t) HTGR-PH/VHTR plant, and (2) a conventional low-temperature 510°C (950°F) recycle gas heated by burning product gas and product oil.

Two shale AGR studies using the HTGR-SC/C plant to supply the energy to the process were initiated by GA during the present reporting period. The first study examined the possibility of integrating an HTGR-SC/C plant with the conventional low-temperature recycle gas AGR process for providing process heat instead of burning gas and product oil. The second AGR study concerned the retorting of shale with low-pressure superheated steam at 344 kPa/482°C (50 psia/900°F) using an HTGR-SC/C plant. The process of shale

retorting by steam was originally developed by the Marathon Oil Company of Denver. Presently, laboratory data alone are available from Marathon for this process.

An initial comparative assessment was made of the three concepts, i.e., of the two HTGR-SC/C plant applications and the HTGR-PH/VHTR plant applications.

AGR Using an HTGR-PH/VHTR - Indirect Retort Heating

This AGR process system uses secondary helium transported from an HTGR-PH/VHTR plant. A detailed description of this process is given in Ref. 5-6. A process plant feed of 688 kg/s (65,590 T/D) of prepared shale [pieces nominally measuring 9.5 mm x 76 mm (3/8 in. x 3 in.)] is fed into retorts, each rated at 69 kg/s (6,559 T/D) capacity. Each retort is a refractory-lined cylindrical vertical kiln. A brief description of the process follows.

The HTGR-PH/VHTR supplies hot helium at 801°C (1457°F) to the retorts and other processing units. The minimum helium return temperature to the HTGR-PH/VHTR is 327°C (620°F). The sensible heat of the helium provides all process heat (e.g., catalytic steam reforming for hydrogen production), process steam, and electric power. Included in the electric power demand are 85 MW(e) for nuclear in-house services such as helium circulators, lighting, reactor cooling, and other auxiliary duties.

The process block flow diagram with major process and energy flow data is shown in Fig. 5-8. In addition to raw shale feed, the plant requires about 384 mm^3/s (6,100 GPM) of raw water make-up. This facility produces 82 mm^3/s (45,042 BBL/D) of hydrotreated shale oil and 4.47 m^3/s (13.65 million SCFD) of high-Btu gas. The overall energy balance shows that about 58.2% of the input energy is recovered as shale oil and about 2.3% is recovered as high-Btu gas. The overall thermal efficiency of the plant is 61.6% based on 1.2×10^{-4} m^3/kg (29 GPT) shale with a Fischer assay of 92%.

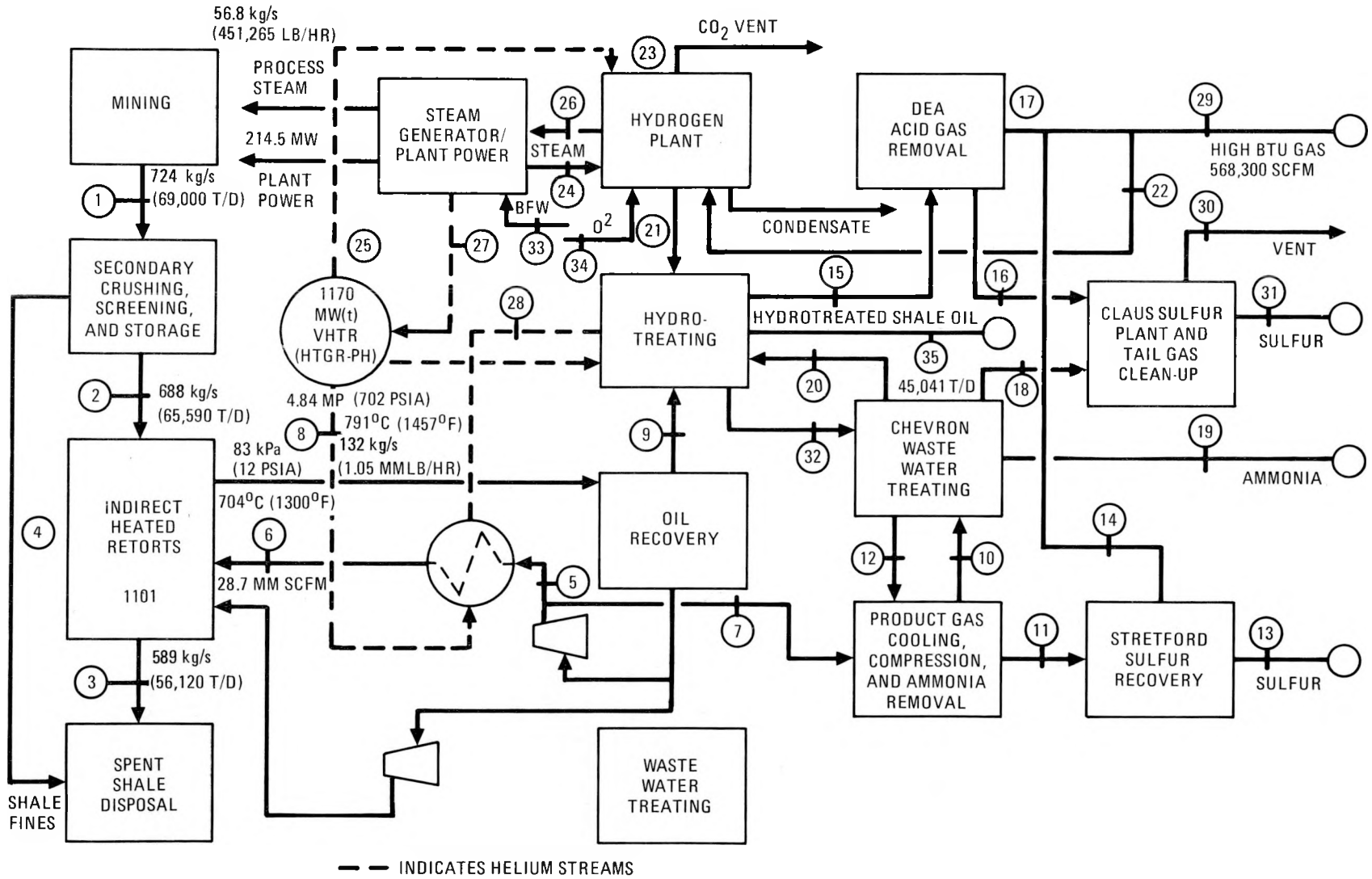

Fig. 5-8. Process flow diagram for high-temperature recycle gas shale retorting using an HTGR-PH plant

Low-Temperature Gas Retorting Using an HTGR-SC/C Plant - Indirect Retort Heating

The process block flow diagram for low-temperature gas retorting is shown in Fig. 5-9. Stream quantities and compositions for retorting 754 kg/s (71,867 T/D) are also shown in Fig. 5-9. One 1170-MW(t) HTGR-SC/C plant supplies all of the process heat and process steam required. Hydrogen is generated by steam reforming of retort product gas. The shale feed rate is 754 kg/s (71,867 T/D), and the net production of this facility is 0.082 m^3/s (44,604 BBL/D) of hydrotreated shale oil. All of the 5.5 m^3/s (16.8 MM SCFD) of product gas produced by this facility is used as fuel in the hydrogen plant. The overall energy balance shows that about 54.5% of the input energy is recovered as shale oil; thus, the overall plant thermal efficiency is 57.85%, based on 87% Fischer assay and 1.2×10^{-4} m^3/kg (28 GPT) shale feed.

The heat for retorting gas is supplied by high-temperature primary steam from the HTGR plant. The retort product gas is sent to gas cooling, compression, and NH_3 removal, followed by a Stretford sulfur recovery unit. Clean gas, supplemented with high-Btu gas from the DEA unit, feeds the hydrogen plant for the manufacture of H_2. The steam reformer is fired with 5.5 m^3/s (16.8 MM SCFD) of product gas and 8×10^{-4} m^3/s (438 BBL/D) of upgraded product oil. A Chevron hydrotreating unit is used to upgrade the crude shale oil to produce 0.083 m^3/s (45,042 BBL/D) of total product. Steam from the HTGR plant preheats the crude upstream of the reactors.

AGR with Direct Steam Heating

Marathon Oil Company has developed a shale retorting process using superheated water vapor (steam). The retorting experiments for this process were conducted in an 89-mm (3-1/2-in.) ID and a 38-mm (1-1/2-in. ID) tubular reactor that could be charged with 3.6 kg (8 lb) and 1 kg (2.2 lb) lots of crushed 6.3 mm (1/4 in.) x 8 mesh shale. Superheated steam was passed through the reactor at superficial velocities ranging from 5×10^{-3} to 1 m/s (1 to 200 ft/min) at temperatures from 371° to 510°C (700° to 950°F) and

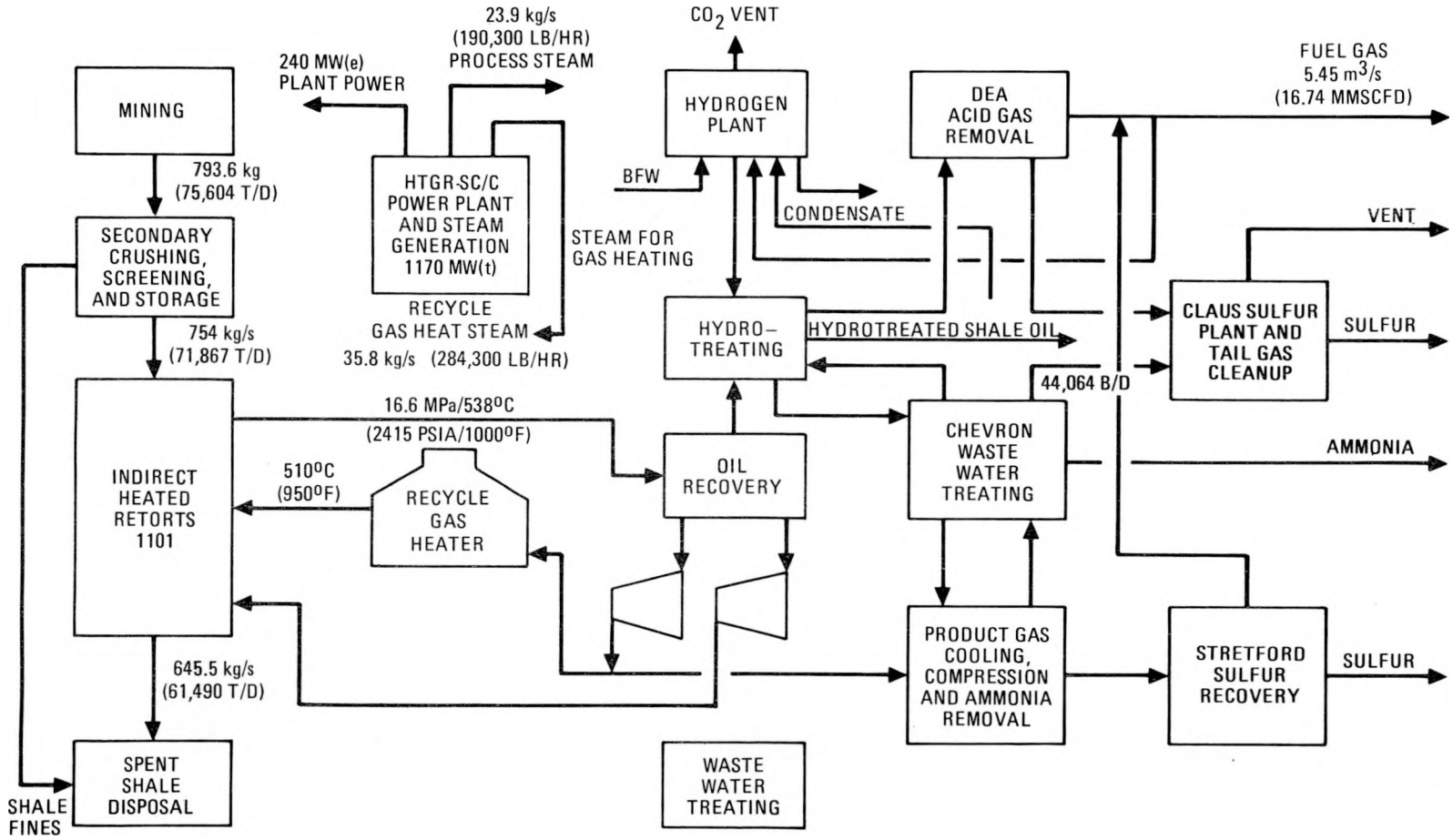

Fig. 5-9. Process block diagram for shale AGR with 510°C (950°F) recycle gas using an HTGR-SC/C plant

pressures from 13.8 to 565 kPa (2 to 82 psia.) Fischer assays ranged from 100% to 130% for the experimental parameters stated. Based on the results of the experimental studies, Marathon concluded that retorting of shale in the presence of superheated water vapor offered unique advantages: (1) increased yields of oil and gas, (2) lower retorting temperatures, (3) simplified oil recovery technology, (4) higher-quality product gases with increased hydrogen content, and (5) more environmentally acceptable retorted shales.

Figure 5-10 shows the process arrangement for this case. Superheated steam at 344 kPa/482°C (50 psia/900°F) is fed into the retort units. The products exiting the retort (shale oil mist and dry saturated steam require that retort exit steam be free of moisture) and off-gases are sent through an evaporator/condenser (EC) unit in which steam is condensed. The off-gases are passed on to a gas treatment system. Raw shale oil is separated from water in the water treatment plant; 734 kg/s (70,000 T/D) of shale are retorted in 105 mkg/s to 73 kg/s (10 to 7000 T/D) capacity retort modules, and 0.092 m^3/s (50,000 BBL/D) of raw shale oil are produced. The raw shale oil is then sent for processing in a hydrotreating unit as in the low-temperature gas retorting case.

Condensate exiting the condenser section of the EC unit is circulated through the evaporator section for condensing the incoming steam from the retort at 345 kPa (50 psia). Evaporator section entry water pressure is controlled so that the heat of vaporization of the incoming steam is fully recovered. The evaporator exit steam pressure is approximately 207 kPa (30 psia); the steam is compressed to about 483 kPa/240°C (70 psia/462°F) by a steam compressor. This steam is then heated to 482°C (900°F) by the primary steam from the HTGR plant in a separate heat exchanger unit and is used for retorting. About 5% of the condensate from the condenser unit is assumed lost through blowdown in the water treatment plant and is compensated for by steam raised from the sensible heat of the retorted shale. A separate spent shale heat exchanger unit or a built-in integral unit inside the retort can be used to generate this steam.

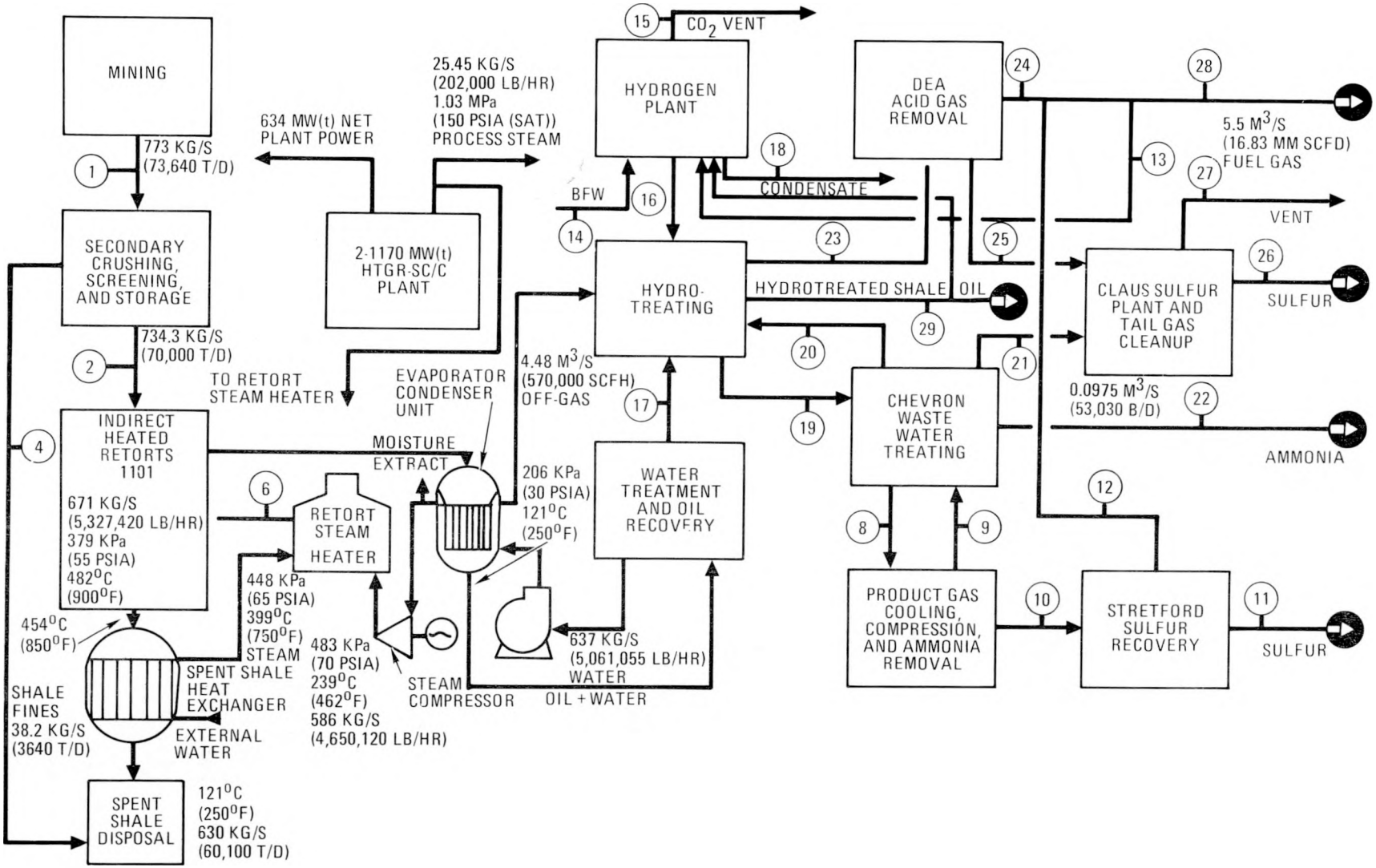

Fig. 5-10. Process flow diagram for shale AGR by steam using two 1170-MW(t) HTGR-SC/C plants

The product gas resulting from the steam shale retorting process is rich in hydrogen (about 50% by volume). About 5.5 m^3/s (16.8 MMSCFD) of product gas is produced from a feed of 734.8 kg/s (70,000 T/D) of shale and has a thermal power of approximately 170 MW(t). The hydrogen plant requires about 203 MW(t) high-temperature [>738°C (>1000°F)] heat (which could not be provided by the HTGR plant), and the entire product gas produced is used as fuel in the hydrogen plant. The balance heat is supplied by burning hydrogenerated product shale oil. The process heat for the hydrotreater unit is provided by HTGR primary steam.

Merits attributed to the steam retorting process by the Marathon Oil Company include:

- Water vapor retorting appreciably reduces the operating temperature, which is important for at least two reasons. First, it decreases the extent to which the inorganic mineral carbonates decompose, giving a more acceptable retorted shale for disposal, and second, it requires less heat energy for retorting.

- The carbon monoxide content is appreciably reduced. In fact, in some of the experiments it was below detection limits, again indicating that the shift reactions are proceeding to near equilibrium conditions.

- Shale oil recovery from the vapor phase is also greatly simplified since it co-condenses with the water vapor and forms an immiscible liquid phase that readily separates from the water. In commercial practice, this will simplify the oil recovery equipment, since a stable oil mist that seems to be characteristic of many other retorting processes does not seem to be a problem. Therefore, electrostatic precipitators will probably not be required. Another advantage is that the volume of gas being handled after the condensation is greatly reduced compared to processes which recycle gas or use air injection and internal combustion to supply heat.

Presently, the Marathon Oil Company is conducting a pilot plant operation on steam retorting of shale using Paraho facilities at Anvil Points. The results from this pilot plant would be more representative of a commercial operation than the data presented here, which are extrapolated from laboratory data. At this time, it is not known when the Anvil Points pilot plant results will be published.

Energy Requirements

Table 5-4 shows the energy requirements for the three shale retorting processes considered: (1) Davy McKee high-temperature gas, (2) conventional low-temperature gas, and (3) steam retorting processes. In the high-temperature gas case, all of the process heat is supplied by one 1170-MW(t) HTGR-PH/VHTR plant via secondary helium; 56.8 kg/s (451,265 lb/hr) of process steam is supplied as extraction steam from power turbines. The hydrogen plant is the major consumer of process steam [34.7 kg/s (276,000 lb/hr)]; 129-MW(e) electric power required for the process is cogenerated in the HTGR-PH plant. No surplus electric power is available for export sale.

The low-temperature gas retorting case shows a lower demand for process steam (from the HTGR plant) than the high-temperature gas case. This is due to significant amounts of internal steam generation from the fossil-fuel-fired reformer units. However, the electric power demand is higher in the low-temperature gas retorting case because of increases in shale feed load and off-gas volumes. Gas compression accounts for approximately 50% of the process electric power demand. The fossil-fuel-fired hydrogen plant has a higher thermal power demand than the HTGR-PH hydrogen plant. One 1170-MW(t) HTGR plant provides about 66% of the process thermal power requirement and 100% of the electric power requirement. A surplus of 77 MW(e) is available for export.

The thermal energy requirements of the steam retorting case closely parallel those for the low-temperature gas retorting case. The electric power demand in the steam retorting case is the highest [283 MW(e)] because

TABLE 5-4
ENERGY REQUIREMENTS FOR AGR PROCESSES

	Davy McKee High-Temperature Gas Process (HTGR-PH)	Low-Temperature Gas Retorting Process (HTGR-SC/C)	Steam Retorting Process (HTGR-SC/C)
Process Steam			
Pressure, MPa (psia)	1.03 (150) (dry sat.)	1.03 (150) (dry sat.)	1.03 (150) (dry sat.)
Flow rate, kg/s (lb/hr)	56.8 (451,265)	23.97 (190,300)	25.4 (202,000)
MW(t)	132	56[a]	68[a]
Heat of retort, MW(t)	319	319	319
Heat for hydrogen and hydrotreating plant, MW(t)	81	213[b]	215[b]
Process electric power equivalent, MW(t) [MW(e)]	338 (129)	427 (163)	741 (283)
Total, [MW(t)]	870	1015	1343

[a]Demand is shown lower because of process internal steam generation.
[b]Hydrotreating process heat is provided by HTGR primary steam; heat for H_2 plant is supplied by gas and oil.

of large-capacity steam compressors [~140 MW(e)] used in the process. The HTGR plant provides 66% of process thermal power requirements and all of the electric power requirements. Two 1170-MW(t) HTGR plants are used to supply thermal and electric power. A surplus electric power of 351 MW(e) is available for alternate use or export.

Heat Balances/Steam Cycle Arrangements

High-Temperature Gas Retorting Process. Figure 5-11 shows the heat cycle for the high-temperature gas retorting process as developed by Davy McKee. Details of the heat balance and heat loads at various points shown in Fig. 5-11 are given in Ref. 5-7.

Low-Temperature Gas Retorting Process. Figure 5-12 shows the heat balance and steam cycle arrangement for the low-temperature [510°C (950°F)] gas retorting case using one 1170-MW(t) HTGR plant. This process requires 319.37 MW (1,090 x 10^6 Btu/hr) to heat recycle gas from 138° to 485°C (280° to 905°F). The gas is heated to 388°C (730°F) in HX 1 and from 388°C to 510°C (730°F to 950°F) in HX 2. The heat exchangers were assumed to be located about 0.8 km (0.5 mi) from the reactor, and a 345-kPa (50-psi) pressure drop in transmission piping was estimated.

Also shown in Fig. 5-12 is the extraction of 24 kg/s (190,300 lb/hr) of steam at 1.1 MPa (160 psia) from T-G 2. This steam is for process use. Additionally, some steam from the HX 2 outlet is used in the hydrotreating process to heat fluid from 368° to 396°C (695° to 745°F).

Steam at the T-G 2 inlet is shown as 5.5 MPa/351°C (800 psia/665°F). It is throttled to those conditions after it leaves the heat exchangers in order to limit turbine exhaust moisture to the same level as in the straight steam cycle turbines, which have 16.6 MPa/538°C (2415 psia/1000°F) steam at the inlet.

T-G 2 would probably be located in the shale retorting plant. Its output of 151 MW(e) (generator terminals) falls slightly short of the specified

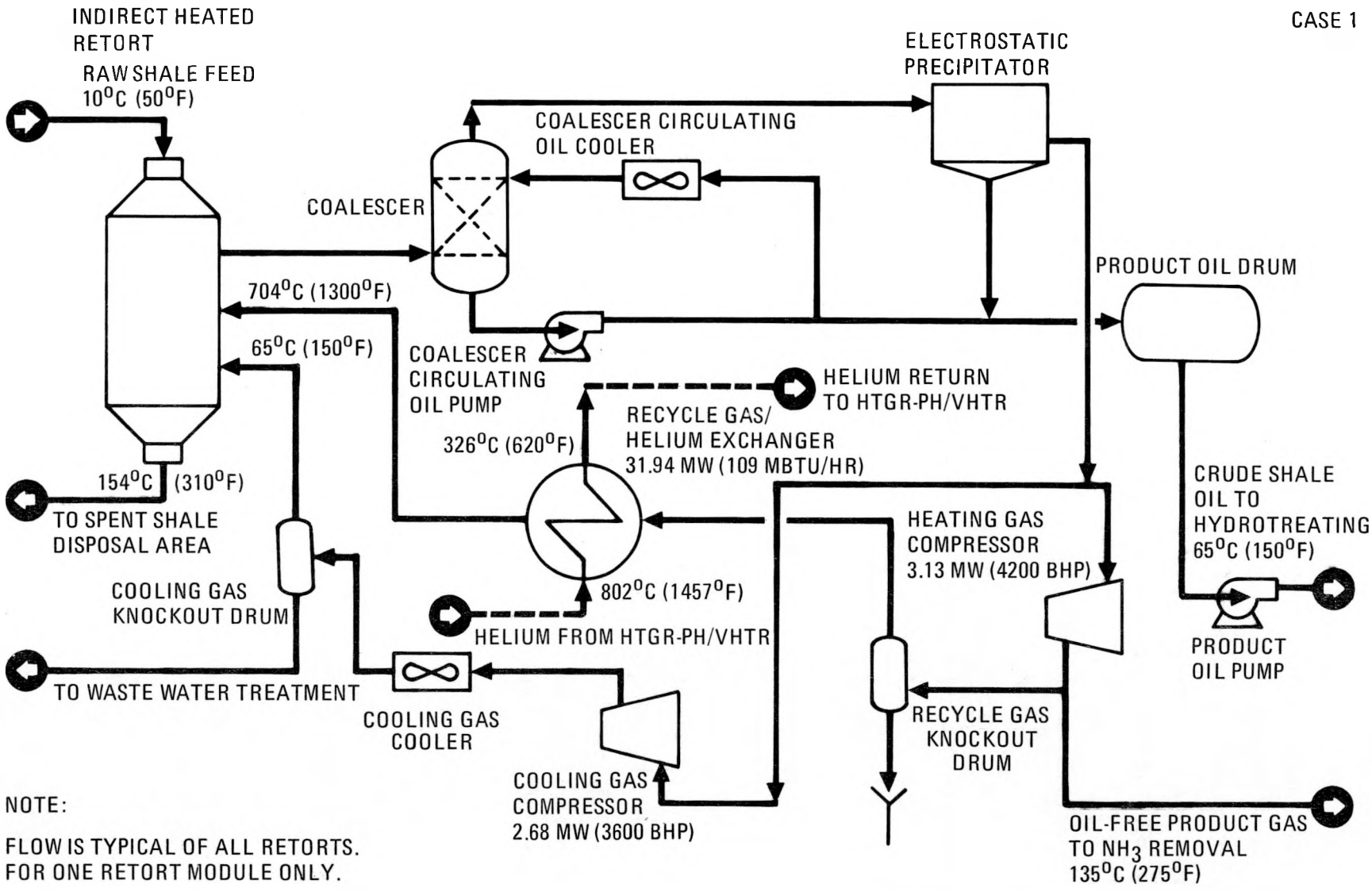

Fig. 5-11. Heat cycle for high-temperature gas retorting of shale with an HTGR-PH/VHTR

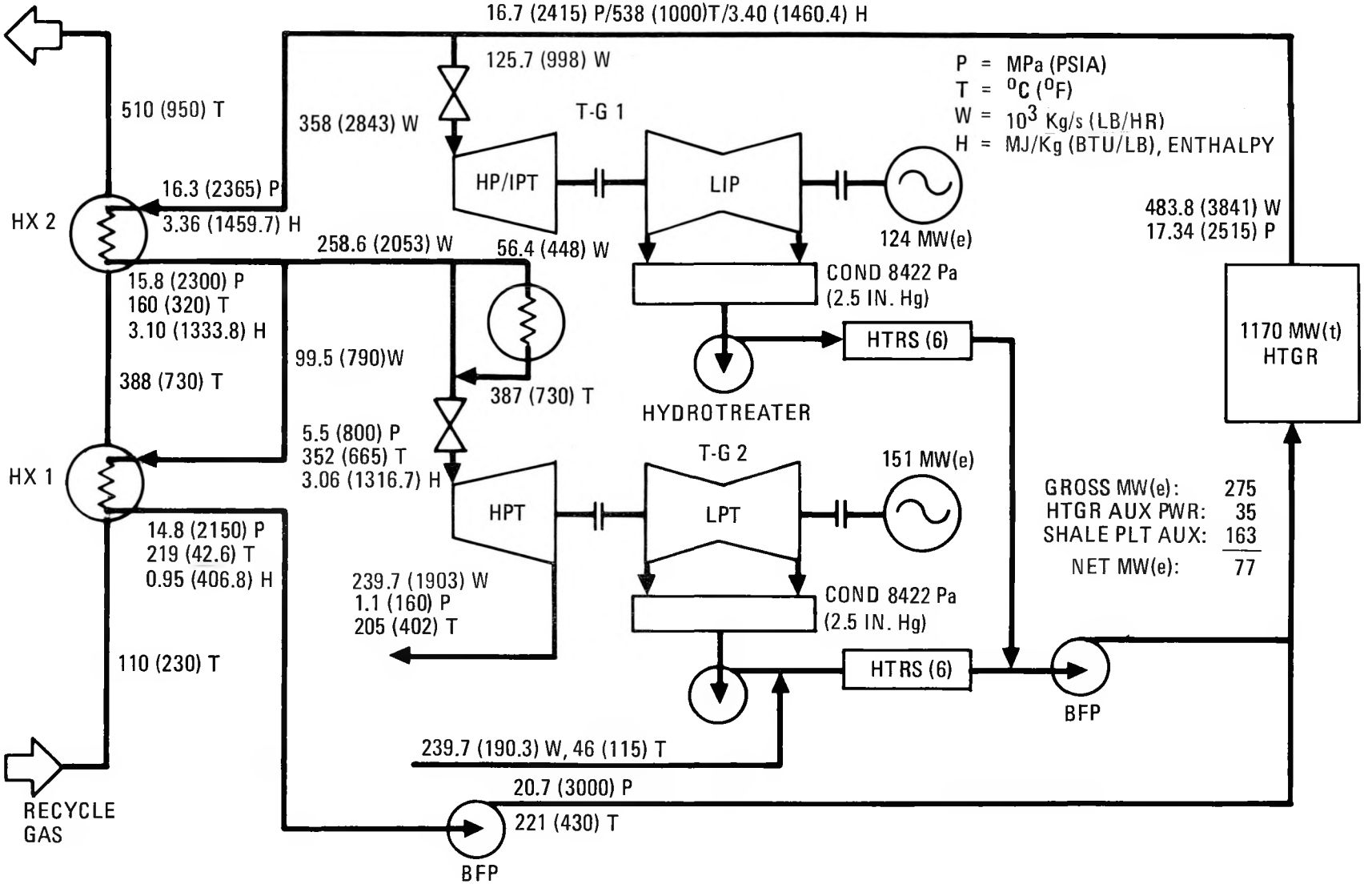

Fig. 5-12. 1170-MW(t) HTGR steam cycle for hot gas [510°C (950°F)] retorting of oil shale

163 MW(e) requirements of that plant. The output of T-G 1 [124 MW(e)] supplies the 35-MW(e) auxiliary load of the HTGR plant and 12 MW(e) supplies the 35-MW(e) auxiliary load of the HTGR plant and 12 MW(e) to the shale plant, leaving a surplus of about 177 MW(e).

HX 1 was arbitrarily selected to have a minimum pinch-point-temperature difference of about 14°C (25°F). Using the same pinch-point value, other heat exchanger alternatives for heating recycle gas were considered. These alternatives were based on the use of a single heat exchanger instead of a split design and used varying amounts of subcooling of the condensed steam. Figure 5-13 shows the maximum hot gas temperature available for a range of condensate drain temperatures up to the saturation temperature of 357°C (646°F). The maximum hot gas temperature available from complete condensation to the steam, without subcooling, is 493°C (920°F).

AGR with Superheated Steam

Figure 5-14 shows the steam cycle arrangement for shale retorting with steam. The process uses a secondary (retorting) steam loop with a steam compressor. Heat is transferred to the secondary (retorting) steam from the primary (HTGR) steam through shell and tube heat exchangers.

The secondary steam flows through heat exchangers HX 1 and HX 2 in series, which adds superheat to the secondary steam. On the primary side, 16.5 MPa, 534°C (2400 psig, 1000°F) steam is introduced into HX 2.

Some 86% of the primary steam from the outlet of HX 2 is supplied to a turbine for the production of power. As shown in Fig. 5-15, the 427°C (800°F) steam is reduced in pressure to about 5.5 MPa (800 psia) before expansion in T-G 2. This pressure reduction is made in order to limit exhaust moisture to the same level as is obtained from the HTGR-SC using 16.6 MPa/534°C (2415 psia/1000°F) steam and expanding to 8442 kPa (2.5 in.

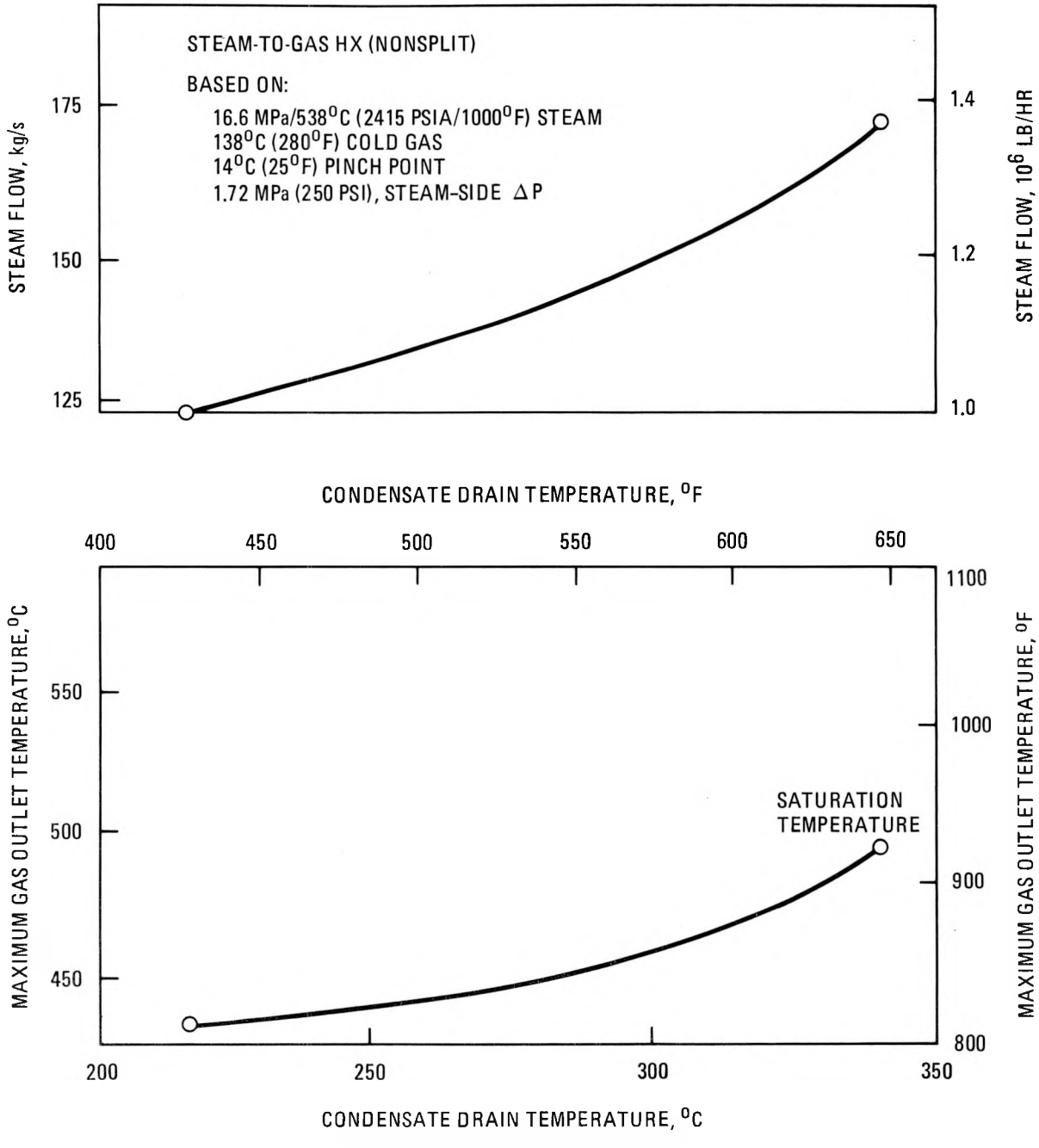

Fig. 5-13. Single heat exchanger alternative for gas heating with steam - low-temperature gas retorting process

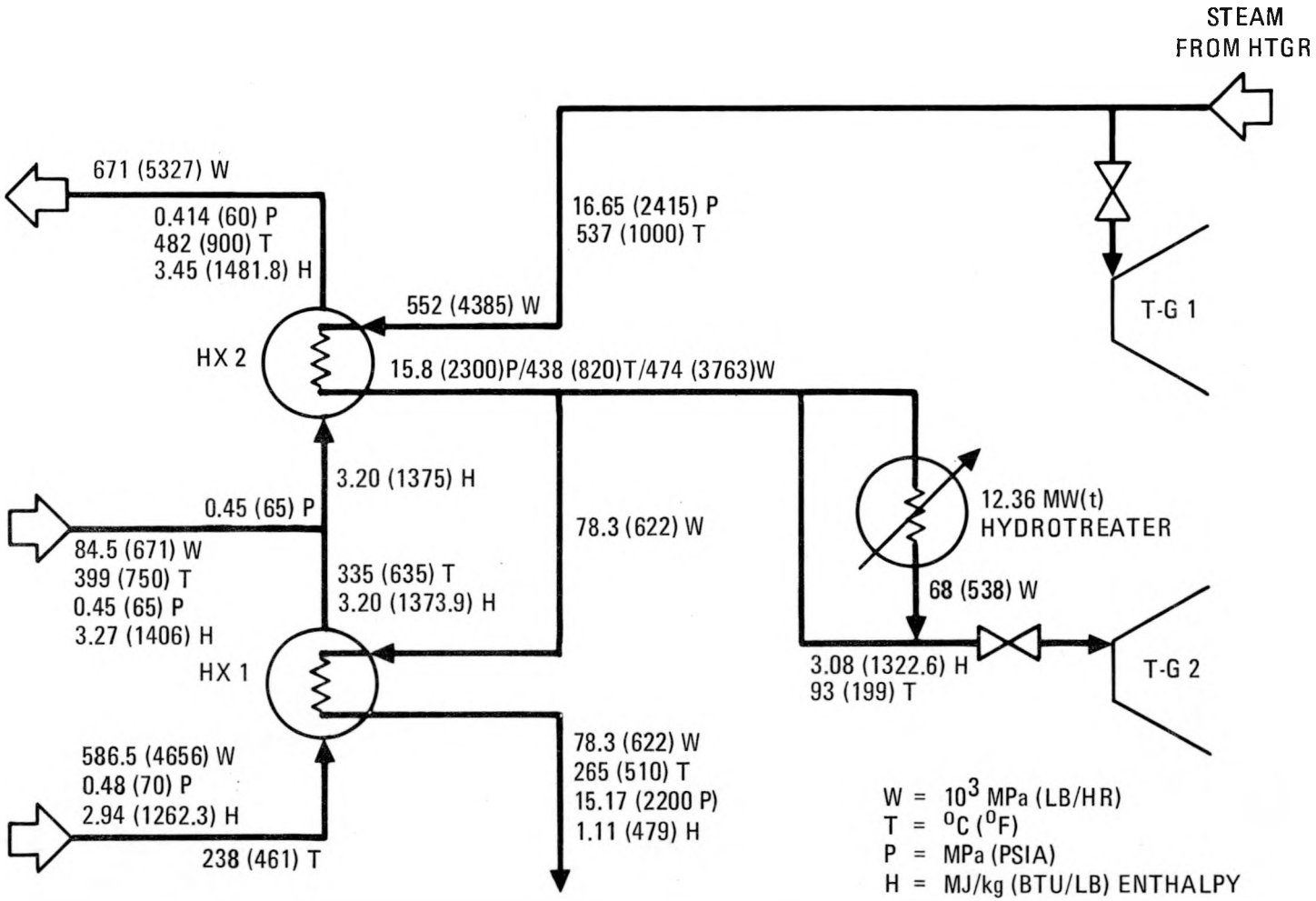

Fig. 5-14. Retort steam heating by HTGR primary system

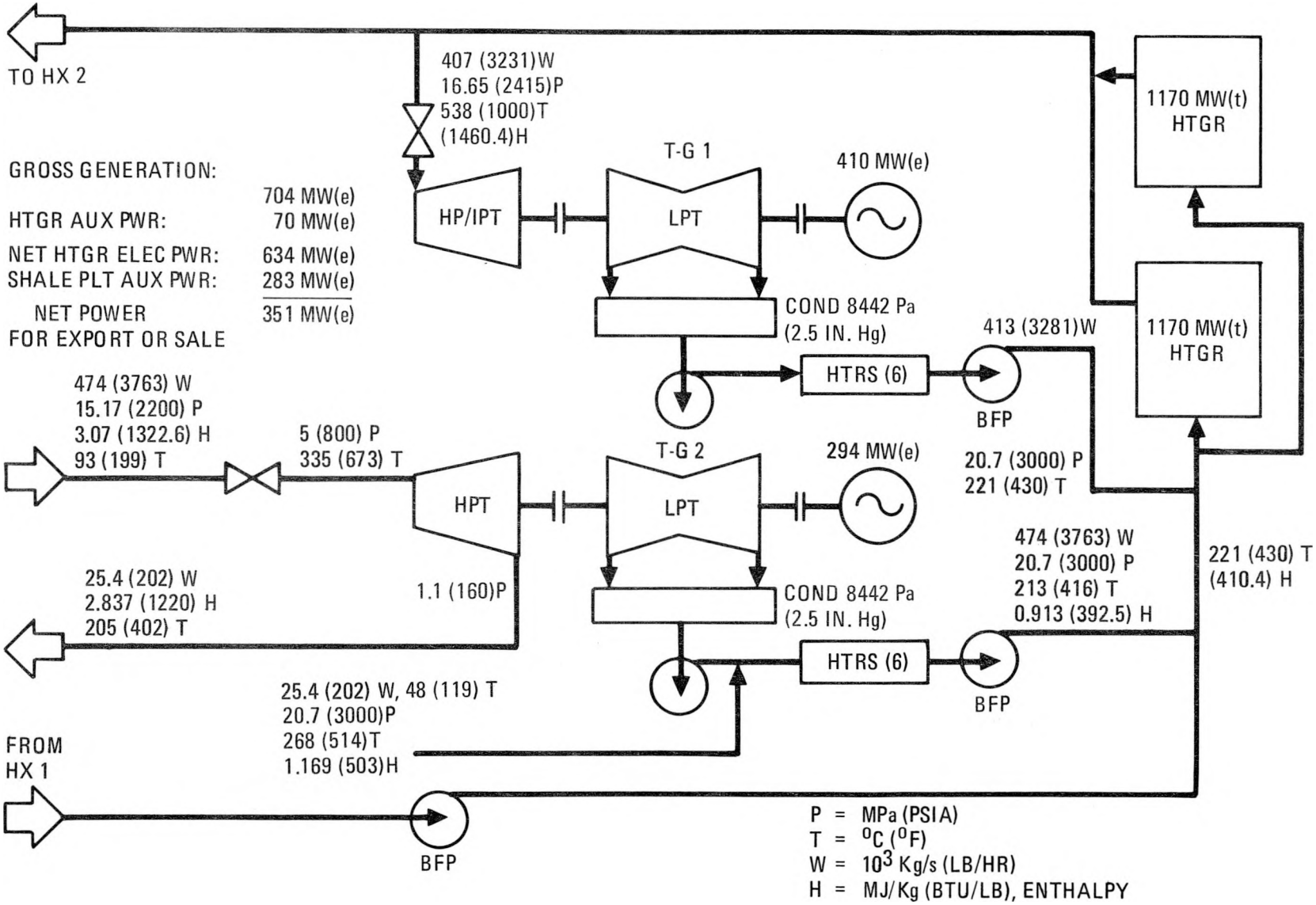

Fig. 5-15. Twin 1170-MW(t) HTGRs for shale retorting with steam

HgA) at the condenser.* Figure 5-15 also shows that two 1170-MW(t) reactors are used to provide sufficient primary steam for HX 2. If the size of the retorting plant were reduced about 10% from 2.1 mm^3/s (50,000 BBL/D), a single 1170-MW(t) reactor could furnish the required steam.

Figure 5-15 shows that with the twin 1170-MW(t) reactors the net electrical power generated is 634 MW(e). This net figure has considered all of the auxiliary electrical power requirements of the nuclear plant. After allotting approximately 283 MW(e) electric power for the process, a surplus of 351 MW(e) is available for export or sale.

Relative Assessment

Table 5-5 shows data for use in a relative assessment of the three processes considered. While a final assessment of these concepts cannot be made until completion of the task, the following observations are made from the data presented in Table 5-5 representing the present status.

The steam retorting process has the highest Fischer assay (100%). In fact, the Marathon Oil Company's laboratory data support a much higher Fischer assay (~120%) for the retort injection steam conditions used [345 kPa/482°C (50 psia/900°F)]. However, a 100% Fischer assay value was selected for a preliminary commercial plant operation. In the retorting process with recycle gas, the Fischer assay decreased with decreasing temperature of retorting.

The recycle gas needs to be heated up to 704°C (1300°F) in the HT gas retorting process as compared with 510°C (950°F) in the LT gas retorting

*As an alternative to throttling, it is possible to consider admitting the steam to the turbine at full pressure, raising the exhaust pressure to a level that would result in the same exhaust moisture as the throttling scheme. It was estimated that the required exhaust pressure would be near atmospheric. Exhaust steam temperature would thereby be around 110°C (215°F). That temperature would make a dry cooling tower or air-cooled condenser an interesting alternative to investigate.

TABLE 5-5
RELATIVE ASSESSMENT OF DAVY McKEE, LOW-TEMPERATURE GAS AND STEAM CASES

Description	Davy McKee High-Temperature Gas Case (HTGR-PH)	Low-Temperature Gas Case (HTGR-SC/C)	Steam Retort Case (HTGR-SC/C)
Retort Parameters			
Retorting medium temperature	704 (1300)	510 (950)	482 (900)
Temp of retorting, °C (°F)	510-538 (950-1000)	454 (850)	--
Shale grade, mm^3/kg (GPT)	1.21×10^{-4} (29)	1.17×10^{-4} (28)	1.25×10^{-4} (30)
Fischer assay, %	92	87	100
Feed and Yield Data			
Charge to retort, kg/s (T/D)	688 (65,590)	754 (71,867)	735 (70,000)
Shale oil yield, m^3/s (BBL/D)	0.083 (45,042)	0.0820 (44,604)[a]	0.097 (53,030)[a]
Product gas (net) m^3/s (SCFD 10^6) [mm^3/s (FOE BBL/D)]	4.47 (13.65) [3.5 (1900)]	5.5 (16.79)[b] [4.3 (2336)]	5.51 (16.83)[b] [4.3 (2342)]
Process Considerations, Qualitative			
Hydrotreating	Same	Same	Same
Hydrogen plant	Reformer heat supplied by VHTR	Heat supplied by product gas/oil or external fuel oil	Same as low-temperature gas case

[a]After allowing for part product oil for H_2 plant heat duty.
[b]Product gas used as fuel in H_2 plant.

TABLE 5-5 (Continued)

Description	Davy McKee High-Temperature Gas Case (HTGR-PH)	Low-Temperature Gas Case (HTGR-SC/C)	Steam Retort Case (HTGR-SC/C)
Process Considerations, Qualitative (Continued)			
Process status	Commercial size module operated	Unknown	Results available from lab experiments
Retort section length, m (ft)	6.7 (22) (ref.)	7.6 (25) (estimated)	Not sized
Retort medium heat load, MW(t)	319	319	319
Spent shale disposal, kg/s (T/D)	58[a] (56,120)	645 (61,490)	631 (60,100)
Energy Data			
Process electric power requirement, MW(e)	129	163	283
Process thermal power requirement, MW(t)	532	588	602
Plant Components			
Reactor	HTGR-PH (advanced technology)	HTGR-SC/C (available technology)	HTGR-SC/C (available technology)
Compressor	Gas	Gas	Steam
Evaporator/ condenser unit	Not required	Not required	Required
Spent shale HX	No	No	Yes

process and steam to 482°C (900°F) in the steam retorting process. The requirement of 704°C (1300°F) gas in the HT gas process will therefore have an impact in the selection of suitable materials for equipment construction and on the equipment cost.

The LT gas retorting process requires a higher feed load (~10% more) to yield the same amount of shale oil as the HT gas retorting process. The steam retorting process has the highest net oil yield [1.33×10^{-4} m^3/kg (0.76 BBL/T)], followed by the HT gas process [1.2×10^{-4} m^3/kg (0.71 BBL/T] and LT gas process [1.17×10^{-4} m^3/kg (0.67 BBL/T)], respectively, based on 1.25×10^{-4} m^3/kg (30 GPT) shale. The steam and LT gas retorting processes have approximately the same net yield of product gas [7.5×10^{-3} (240 SCF/T)], whereas the HT gas process has a slightly lower yield [6.5×10^{-3} m^3/kg (208 SCF/T)]. The product gas obtained from the steam retorting process has higher hydrogen content (50% by volume) as compared with the gas retorting processes (~34% by volume). The steam and LT gas processes consume all of the net product gas as fuel in the H_2 plant, whereas the product gas produced in the HT gas retorting process has to be used alternatively or exported.

The process heat for the reformer in the HT gas retorting process is provided by the HTGR-PH, while the LT gas and steam retorting processes provide the reformer process heat by burning product gas and hydrogenerated shale oil. The steam retorting process shows the highest energy requirement to produce hydrogenerated shale oil per ton of shale [19.2 kW/T, including the thermal equivalent of electric power] compared with 14.1 kW/T (LT) and 13.3 kW/T (HT) for the gas retorting processes on the same basis.

Regarding process equipment considerations, the steam retorting process requires large-volume high-power steam compressors [10 units, ~14 MW(e) each].

An important piece of equipment design involved in the steam shale retorting process is the evaporator/condenser unit. This unit has two-phase

flow on either side of the tubes, dry saturated 345-kPa (50-psia) steam condensing on the shell side and water boiling and producing dry saturated steam at 206 kPa (30 psia) on the tube side. The gas retorting processes do not require such complex equipment as the steam retorting process.

It is claimed in Ref. 5-7 that the electrostatic precipitators that are used in the gas retorting process are not required for the steam retorting process.

Tables 5-6 and 5-7 show overall plant (process + utility) thermal efficiency and process-only thermal efficiency, respectively. The plant thermal efficiency includes the effects due to utility plant size and available surplus energy. The process thermal efficiency includes only the energy required for the process from the utility plant.

The steam retorting process is shown to have the highest overall plant thermal efficiency, followed by the HT and LT gas retorting processes. This is primarily due to the large surplus electric power available from the HTGR plant. The difference between the HT and LT gas process overall plant thermal efficiencies is negligible. On the basis of process thermal efficiency, the HT gas process has the highest efficiency followed by the steam and LT gas retorting processes. The differences in the efficiencies are shown to be significant on this basis.

In terms of the utility plant, the LT gas process (and also the steam retorting process) uses an HTGR plant, which is an available technology, while the HT gas process requires an HTGR-PH/VHTR, an advanced technology.

Continuation of Work

A proposed scope of work for continuation of this task includes a critical comparison of the two gas AGR processes. Both technical and economic factors will be considered in the assessment to select one gas retorting

TABLE 5-6

RELATIVE ASSESSMENT OF THERMAL EFFICIENCY
(OVERALL PLANT)

Item	Davy McKee [MW(t)] (HTGR-PH)	LT Gas [MW(t)] (HTGR-SC/C)	Steam [MW(t)] (HTGR-SC/C)
Energy In			
Shale rock feed	4404	4825	4700
Power plant	1170	1170	2340
Subtotal	5574	5995	7040
Energy Out			
Shale oil	3299	3299	3884
Product gas	139	--	--
Electric power for export [equivalent Mw(t)]	--	202	919
Subtotal	3438	3468	4803
Thermal efficiency, %	3438/5574 = 61.68	3468/5995 = 57.85	4803/7040 = 68.0
Thermal efficiency normalized to 1.25×10^{-4} m^3/kg (30 GPT), %	63.72	62.34	68.0

TABLE 5-7

PROCESS THERMAL EFFICIENCY

Item	Davy McKee [MW(t)] (HTGR-PH)	LT Gas [MW(t)] (HTGR-SC/C)	Steam [MW(t)] (HTGR-SC/C)
Energy in			
Shale rock	4404	4825	4700
Process energy net Reqd (item IV, p. 2)	870	1015	1342
Subtotal	5274	5840	6042
Process output energy			
Shale oil	3299	3266	3884
Product gas	139	--	--
	3438	3266	3884
Overall efficiency	65%	56%	64%
Overall efficiency normalized to 1.25×10^{-4} m^3/kg (30 GPT)	67%	60%	64%

process for comparison with the steam retorting process. Also in need of evaluation are the advantages and limitations of the steam retorting process and the trade-off between increased product oil/product gas yields and additions of hardware such as evaporator/condenser units, large steam compressors, and spent shale heat exchangers. Interaction with the Marathon Oil Company will be pursued to develop and extend understanding of the steam retorting process for a commercial size operation.

A feasibility study of the steam retorting process without an evaporator/condenser unit is also envisaged. This could lead to the elimination of steam compressors used in the process and the saving of substantial electric power required to run the compressors.

5.2.2.2. Water Treatment Schemes and Environmental Impact in the Heavy Oil Fields of California. The Mittelhauser Corporation (El Toro, California) has studied water treatment schemes and environmental impact in the heavy oil fields of California that use steam flooding. The primary objective of its study was to examine the possible use of produced waters for generating superheated steam in the once-through steam generators of the HTGR or for generating dry saturated steam with reboilers, and to examine the system requirements of a suitable water treatment plant. Additional areas studied by Mittelhauser included information on various pollutants resulting from existing steam generator units and their impact, state and federal regulatory requirements, and the reduction in pollutant emissions that could be brought about by installing an 1170-MW(t) HTGR-SC/C plant.

Mittelhauser's major findings are summarized in the following paragraphs.

Water Treatment

The following table presents the boiler feedwater quality criteria and the respective general basis applicable to the existing conventional field boilers (once-through) used in the heavy oil fields.

Quality Criteria	Basis
Total hardness less than 1 ppm	Scale control within field steam generator
Free of suspended solids	Minimize potential reservoir plugging
Free of oil	Protect ion exchange resin
Total dissolved solids	Negligible impact

Hardness control is necessary to reduce the potential of scale deposits on the tube sheets within the boiler. These scale deposits would result in hot spots and rapid steam generator failure. Scale deposit potential is also minimized by controlling the steam quality from the generator. For the once-through units employed in field steaming operation, quality is controlled so as not to exceed a steam quality of 80% to 85%.

Suspended solids are removed from the boiler feedwater to essentially nondetectable levels to minimize the potential plugging of the reservoir. Total dissolved solids (TDS) are not a major boiler feedwater quality criterion as is found to be the case in conventional steam generation units located in power plants or industrial facilities. The reason for this lack of significance is the once-through nature of the steam generator and the low quality of the steam produced. However, TDS do impact upon the complexity of the water softening step within the treatment plant. As the produced water TDS exceed 3000 ppm, the ability of a sodium cycle ion exchange system to attain required hardness removals decreases sharply.

The basic treatment plant flowsheets for preparing boiler feedwater from produced waters in the major heavy oil fields in Kern County are similar. Specifically, the steps are oil-water separation, filtration, and softening. Each of these steps attains a quality criterion as discussed above. However, the actual applications vary significantly based upon

specific field locations and their produced water composition differences, fresh water availability and composition, and energy recovery concerns.

The selection of softener equipment in the heavy oil fields of Kern County is the most site-specific aspect of the treatment train. The Kern River fields of the east side of the valley produce much lower TDS and water hardness that is easier and cheaper to soften to the boiler feedwater quality criteria. These waters are successfully treated by a two-stage sodium-cycle softener. The first stage removes the bulk of the hardness while the second stage acts as a polisher. On the west side of the valley, the produced waters have extremely high TDS, varying from 5,000 ppm to 10,000 ppm. Sodium-cycle ion exchange softening for this water is complicated because of the high salinity that affects the reversibility of the ion exchange reaction. As a response to this situation, producers and equipment manufacturers are supplying either strong or weak acid resins as primary contacting units, with either weak acid or sodium cycle ion exchange vessels being used as polishing units.

The type of water treatment units being operated in the heavy oil fields by Kern County producers such as Getty, Texaco, Shell, Santa Fe Energy, and Union Oil are shown in Fig. 5-16.

At the present state of technology, the feasibility of dry saturated steam generation at the heavy oil production fields would preclude the reuse of produced waters within the water treatment plant. This inability to reuse produced water is based upon treatment economics and is a consistent conclusion for any location in the Kern County heavy oil fields. This is due to the high TDS found in the produced waters from any Kern County formation, ranging from 800 to 10,000 ppm. California aqueduct water has an average TDS level of 272 ppm.

Total feedwater demineralization is necessary to produce 17.24 MPa/738°C (2500 psi/1000°F) steam from the HTGR. Net demineralization costs are a function of both flow and composition of the treated water. Capital costs

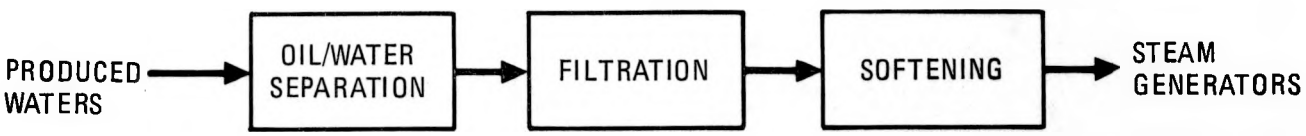

OIL WATER SEPARATION
- EXCLUSIVELY INDUCED AIR FLOTATION

FILTRATION
- DIATOMACEOUS EARTH FILTERS
- MULTIMEDIA (ANTHRACITE/GARNET) FILTERS

SOFTENING (ACTUAL APPLICATIONS IN KERN COUNTY)
- SODIUM SOFTENING
- TWO-STAGE SODIUM SOFTENING (ALSO WITH BLENDING WATER FRESH)
- TWO-STAGE SODIUM SOFTENING WITH WEAK-ACID POLISHING
- WEAK ACID WITH SODIUM CYCLE POLISHER
- TWO-STAGE WEAK ACID
- TWO-STAGE STRONG ACID WITH WEAK-ACID POLISHER

Fig. 5-16. Produced-water treatment methods for California heavy oil fields

are influenced more closely by flowrate, while system operating costs follow the influent composition. Boiler feedwater purity requirements can affect both capital and operating costs when American Boiler Manufacturing Association drum water specifications and energy conservation by blowdown minimization suggest a full-flow mixed-bed polisher.

Therefore, the treatment scheme for boiler feedwater treatment using the most cost-effective commercial technology would start with pumping 100% make-up water from the California aqueduct system through a filtration step.

Major system items include fresh water storage, demineralized water storage, deaeration equipment, and high-pressure boiler feedwater pumps feeding the 17.24-MPa (2500-psig) steam generators. A schematic of the treatment system is shown in Fig. 5-17. Since this system must economically assume full make-up of fresh water to the treatment system, a full-flow produced water treatment system must be included in the cost of the total water-related expenses for the steam generation package. The cost of the produced water system would depend upon the ultimate disposal source and criteria.

An important issue is the cost of incremental water now being assessed by the West Valley Water Authority. For new water requirements, the authority is assessing a first-time charge of $\$880/m^3$ per day plus 40 cents/m^3 ($140 per barrel per day plus 5.4 cents per barrel). This quote was to an existing operator, but if applicable for these flows the installation charge would be about $29 million and the annual cost to purchase the fresh water for the steam generator would be about $4 million.

Mittelhauser obtained a rough budget estimate from a major equipment supplier for the lines of water treatment equipment shown in Fig. 5-14. The purchase cost for a filtration, demineralization, and polishing boiler feedwater treatment system would be approximately $15 million. This cost would be for skid-mounted units ready for field installation. The installation

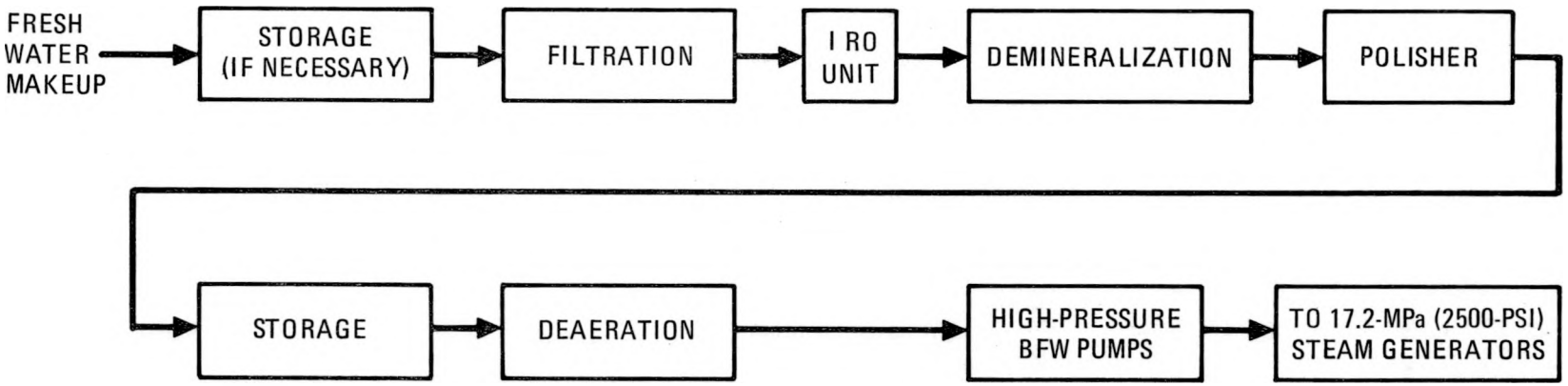

Fig. 5-17. Schematic treatment system for 378 kg/s (3 x 10^6 lb/hr) steam generation system

cost is dependent upon site characteristics such as access to utility connections, labor, materials, and heavy equipment. The operating cost for treating the California aqueduct water would likely be about 26 to 32 cents per m^3 ($1.00 to $1.20 per 1000 gal) of boiler feedwater produced.

Water Regulatory Issues

The effluent limitations that apply to onshore oil wells and agricultural or wildlife water use are shown in Table 5-8. No discharges above these limits will be allowed and the state may impose more stringent limitations than those listed.

In some cases, the effluent limitations will not be sufficient to protect or improve the water quality of the receiving waters. This will most frequently occur along heavily industrialized rivers, along streams with a pristine water quality, and in arid areas with low stream flows. In such cases, stricter controls may be required to achieve water quality standards.

The federal Clean Air Act sets the pattern for the state air laws and regulations. There are two federal regulations (standards) that may impact enhanced oil recovery (EOR) steam drive projects. These are New Source Performance Standards for fossil-fuel fired steam generators of more than 735.8 ngJ/s (250 million Btu/hr) heat input (40CFR60.4) and storage vessels for petroleum liquids (40CF60.110a). The steam generator standard regulates the emission of particulate pollutants, sulfur dioxide (SO_2), and nitrogen oxides (NO_x) from the facility. The applicable standards for these pollutants are shown below.

Particulates

- Contain particulate matter in excess of 43 nanograms/joule heat input (0.10 lb/million Btu) derived from fossil fuel or fossil fuel and wood residue.

TABLE 5-8
ENVIRONMENTAL PROTECTION AGENCY
EFFLUENT GUIDELINES AND STANDARDS FOR OFFSHORE OIL AND GAS EXTRACTION

(40CFR435; 40FR42543, September 15, 1975; amended by 41FR44942, October 13, 1976; revised by 44FR22069, April 13, 1979)

Subpart C-Onshore Subcategory

Effluent Limitation

There shall be no discharge of waste water pollutants into navigable waters from any source associated with production, field exploration, drilling, well completion, or well treatment (i.e., produced water, drilling muds, drill cuttings, and produced sand).

Subpart E-Agricultural and Wildlife Water Use

Effluent Limitation

(1) There shall be no discharge of waste pollutants into navigable waters from any source (other than produced water) associated with production, field exploration, drilling, well completion, or well treatment (i.e. drilling muds, drill cuttings, and produced sands).
(2) Produced water discharges shall not exceed the following daily maximum limitation:

Effluent Characteristics:	Effluent limitation (mg/l).
Oil and Grease:	35.

- Exhibit greater than 20% opacity except for one 6-min period per hour of not more than 27% opacity.

Sulfur Dioxide

- 340 nanograms/joule heat input (0.80 lb/million Btu) derived from liquid fossil fuel or liquid fossil fuel and wood residue.

- 520 nanograms/joule heat input (1.2 lb/million Btu) derived from solid fossil fuel or solid fossil fuel and wood residue.

Nitrogen Oxides

- 86 nanograms/joule heat input (0.20 lb/million Btu) derived from gaseous fossil fuel or gaseous fossil fuel and wood residue.

- 130 nanograms/joule heat input (0.30 lb/million Btu) derived from liquid fossil fuel or liquid fossil fuel and wood residue.

- 300 nanograms/joule heat input (0.70 lb/million Btu) derived from solid fossil fuel or solid fossil fuel and wood residue (except lignite or a solid fossil fuel containing 25 wt % or more of coal refuse).

There is current control technology available to treat the flue gases from a steam generator to these standards.

Air Emissions from Comparison of Coal, Oil, and HTGR Steam Generators

Table 5-9 presents the emissions for a coal-fired and an oil-fired power plant and compares these emissions with a tabulation of radioactive wastes produced by General Atomic's HTGR. The calculation basis is 1366 MW(t) for both the coal- and the oil-fired cases.

TABLE 5-9
ENVIRONMENTAL EFFLUENTS FROM LARGE CENTRAL
STEAM GENERATING FACILITIES

	Coal-Fired Power Plant[a]	Oil-Fired Power Plant[a]	General Atomic HTGR[b]
Air Emissions			
SO_2, TPY	1752	2260	--
NO_x, TPY	4445	4303	--
Particulates, kg/s (TPY)	0.0235 (818)	5.18×10^{-4} (18)	--
CO_2, TPY	3,603,000	2,460,400	--
Noble gases, Ci/yr	--	--	190
Iodine and particulates, Ci/yr	--	--	0.014
Solid Wastes			
Bottom ash, kg/s (TPY)	0.588 (20,460)	--	--
Flyash, kg/s (TPY)	2.32 (80,850)	0.05 (1789)	--
FGD wastes, kg/s (TPY)	1.10 (38,280)	1.59 (55,440)	--
Misc. radioactive material TPY,[c] Ci/yr	--	--	65 14500
Liquid Effluents			
Process water, kg/s (TPY)	19.3 (673,500)	19.3 (673,500)	(d)
Mixed fission products (no tritium), Ci/yr			0.004
Tritium, Ci/yr	--	--	0.0

[a]Calculations based upon 1366-MW(t) heat input and plant equipped with best available control technology.

[b]1170-MW(t) plant.

[c]Assumes a cubic meter weighs approximately one ton for calculation and comparison.

[d]Steam generation water treating equipment will have liquid wastes similar to those of a high-pressure coal- or oil-fired power plant.

For steam generator comparison purposes, the air and solid waste emissions show significant regulated pollutant reductions for the HTGR over the conventional fossil fuel units for conventional regulated pollutants.

5.2.2.3. Conceptual Reboiler Study. Process steam used in EOR operations and in the petrochemical industry is generally raised from water which contains substantial amounts of dissolved solids and impurities, and no specific treatment is given for their elimination. In the EOR fields, process steam is generated at 70% quality (dry) in order to hold the dissolved solids in solution, and possible scale formation on the boiler or tube surfaces is thereby inhibited. Treatment of such feedwater is expected to entail very high costs and sophisticated designs that are yet to be commercially deployed. ESSO (Canada) has a preliminary design for treating water in tar sands fields of Canada to generate process steam at dry saturated conditions. One way of using the untreated water (i.e., water containing dissolved solids) with an HTGR plant is to interpose a reboiler between the HTGR plant and the process plant.

Three steam conditions were selected for the conceptual reboiler design and are shown in Table 5-10. Case 1 shows the conditions in a heavy oil field, Case 2 in a tar sands field, and Case 3 in a typical chemical complex.

The work performed on the conceptual reboiler design included review of various configurations, selection of a reference configuration, design methodology and computer code work, fouling factor selection and its impact on reboiler design, material selection, dimensional reboiler sketches, and unit redundancy.

Conceptual Reboiler Sizing

Design Methodology and Computer Code. The economizer and superheater/desuperheater units were sized using standard correlations for heat transfer and pressure drop for the axial flow (flow parallel to the tubes) economizer

TABLE 5-10
REBOILER DESIGN PARAMETERS

Case	Application	Primary Steam Pressure [MPa (psia)] In/Out	Primary Steam Temp [°C (°F)] In/Out	Primary Steam Flowrate [kg/s (lb/hr)] In/Out	Secondary Steam Pressure MPa (psia) In/Out	Secondary Steam Temp [°C (°F)] In/Out	Secondary Steam Flowrate [kg/s (lb/hr)] In/Out
1	Heavy oil recovery	7.34/6.9 (1065/1000)	413/65.5 (776/150)	356 (2.83×10^6)	4.82/4.58 (700/665)	26.6/258 (80/497)[a]	386 (3.07×10^6)
2	Tar-sands recovery	16.65/15.86 (2415/2300)	538/93.3 (1000/200)	370 (2.94×10^6)	13.8/13.1 (2000/1900)	38/331 (100/629)[a]	444.7 (3.53×10^6)
3	Multi-purpose	6.9/6.2 (1000/900)	407/49 (765/120)	699 (5.55×10^6)	5.17/4.82 (750/700)	20/360 (68/680)	690 (5.48×10^6)

[a]Saturation temperature.

and cross flow (flow across the tube bank) superheater/desuperheater. The two-phase-flow kettle units were sized using the Heat Transfer Research Institute computer code RKH-1. This code is described in Ref. 5-8.

The RKH-1 code cannot directly include combined desuperheating and condensing. Therefore, the kettle configuration was developed by separately sizing the desuperheating and condensing portions and matching them togther. The code assumes saturation temperature entering the shell side because of the high internal recirculation flow. This assumption, however, results in some oversurfacing for the Case 2 kettle, which has 41°C (105°F) of subcooling at entry. The code calculates the shell inside diameter based on an input entrainment coefficient. For a moisture carryover of 1% (which is the driest condition attainable without using separators), a shell diameter of two times the bundle diameter was obtained for all cases.

Conceptual Arrangement. The conceptual reboiler arrangement for each of the three cases is shown in Figs. 5-18, 5-19, and 5-20. These sketches are based on clean units; however, with fouling included the number of shell/tube passes increases as shown in Tables 5-11, 5-12, and 5-13. These tables also show the thicknesses of major components, such as tube sheet, channel, shell, and nozzle sizes. The economizer sections are provided as separate units to obtain full counterflow-heat exchange benefits. Consequently, the diameter of the kettle is reduced by separating the economizer section, resulting in reduced tube sheet thermal stresses. U-tubes were selected for compactness, except for the superheater/desuperheater of Case 3, which required only one pass.

Reboiler Sizing and Modular Design. A tube outside diameter of 19 mm (3/4 in.) was selected, with pitches ranging from 25.4 to 26.9 mm (1 to 1.06 in.) for compactness. This allows for a minimum clearance of 6.35 mm (1/4 in.) between tubes as recommended by TEMA for cleaning.

The surface area was calculated both clean and with shell side fouling factors estimated from data given in Ref. 5-9. The fouling factor on the

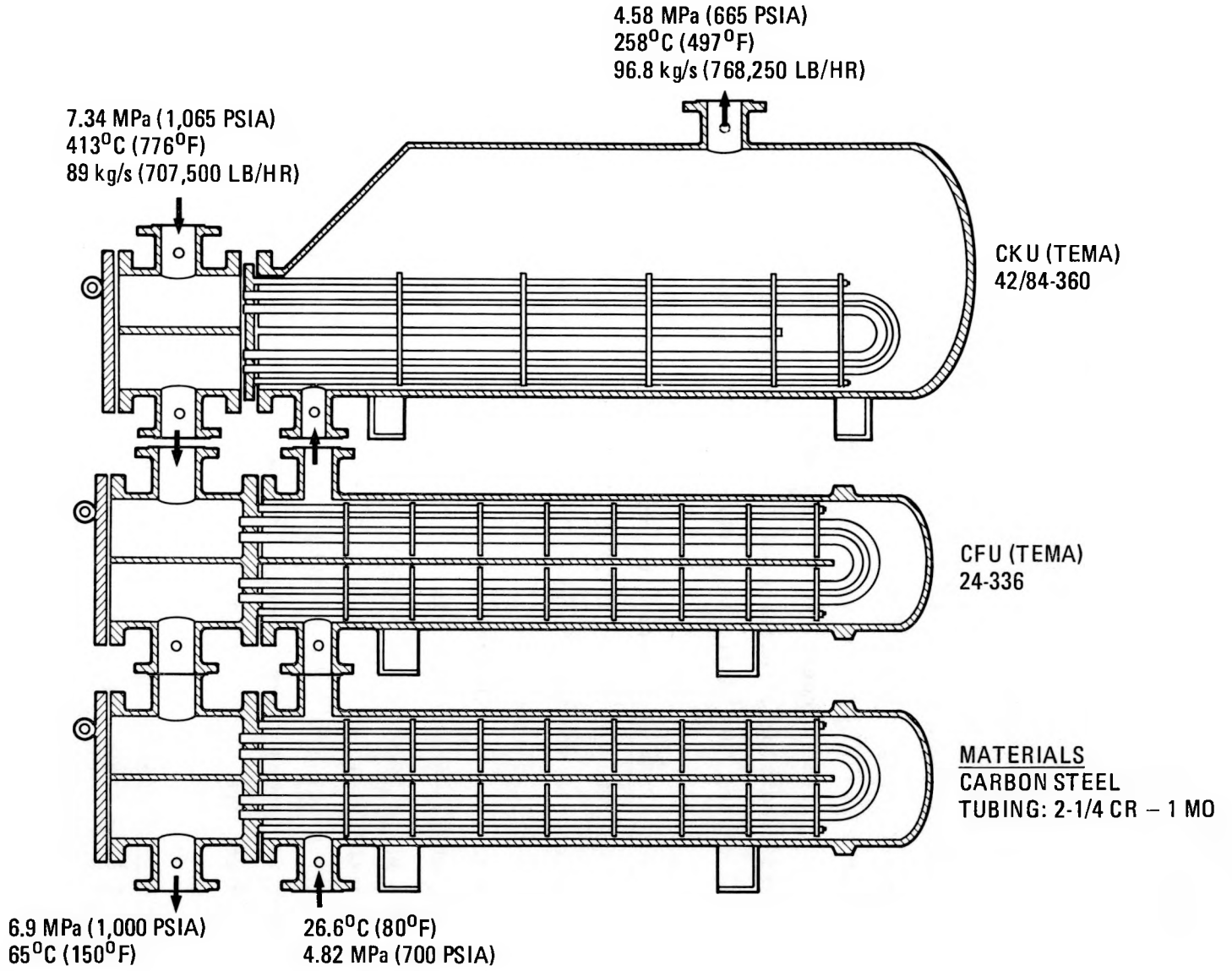

Fig. 5-18. Conceptual reboiler arrangement for Case 1 (heavy oil recovery) (one-quarter capacity, clean unit)

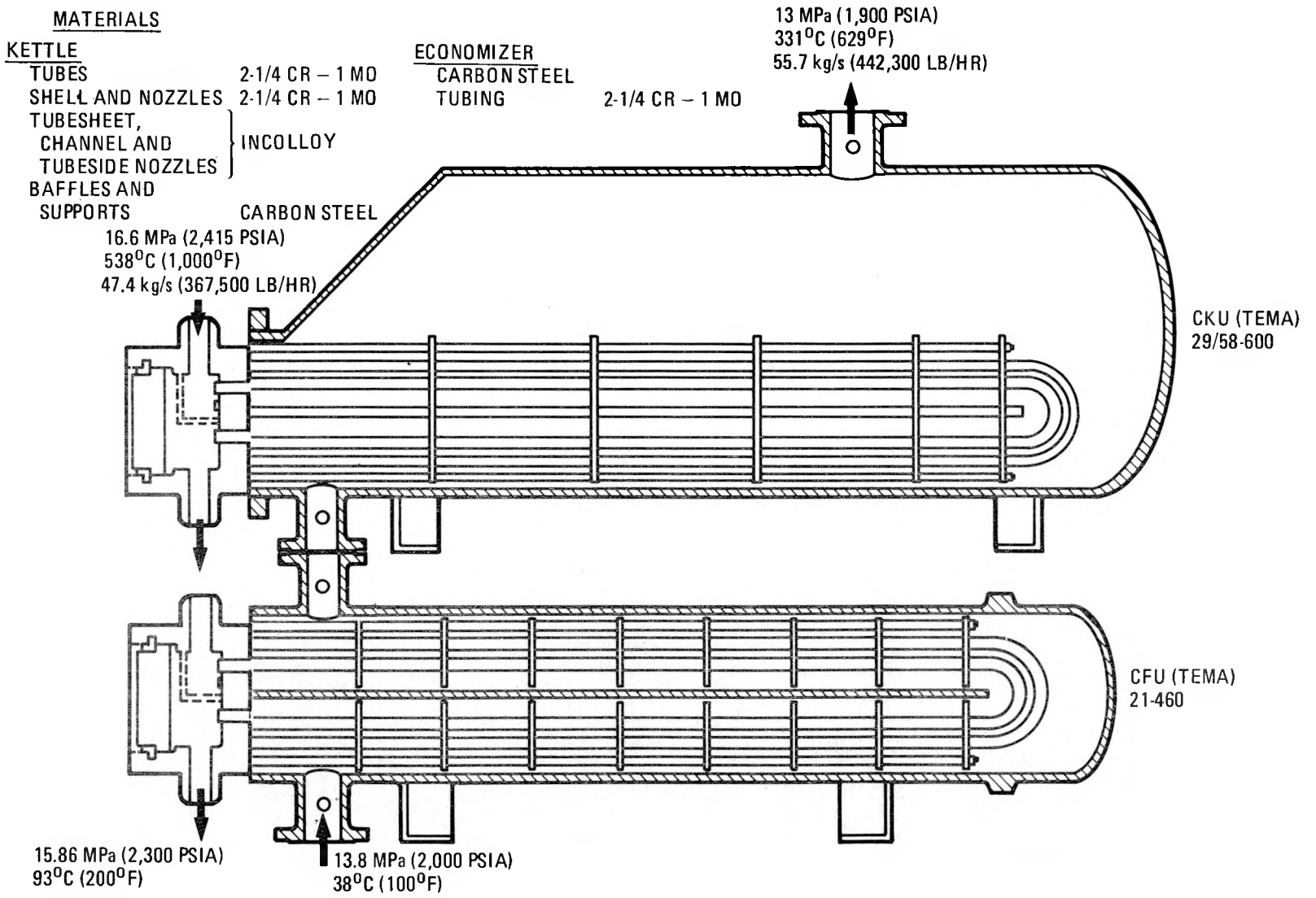

Fig. 5-19. Conceptual reboiler arrangement for Case 2 (tar sands recovery) (one-eighth capacity, clean unit)

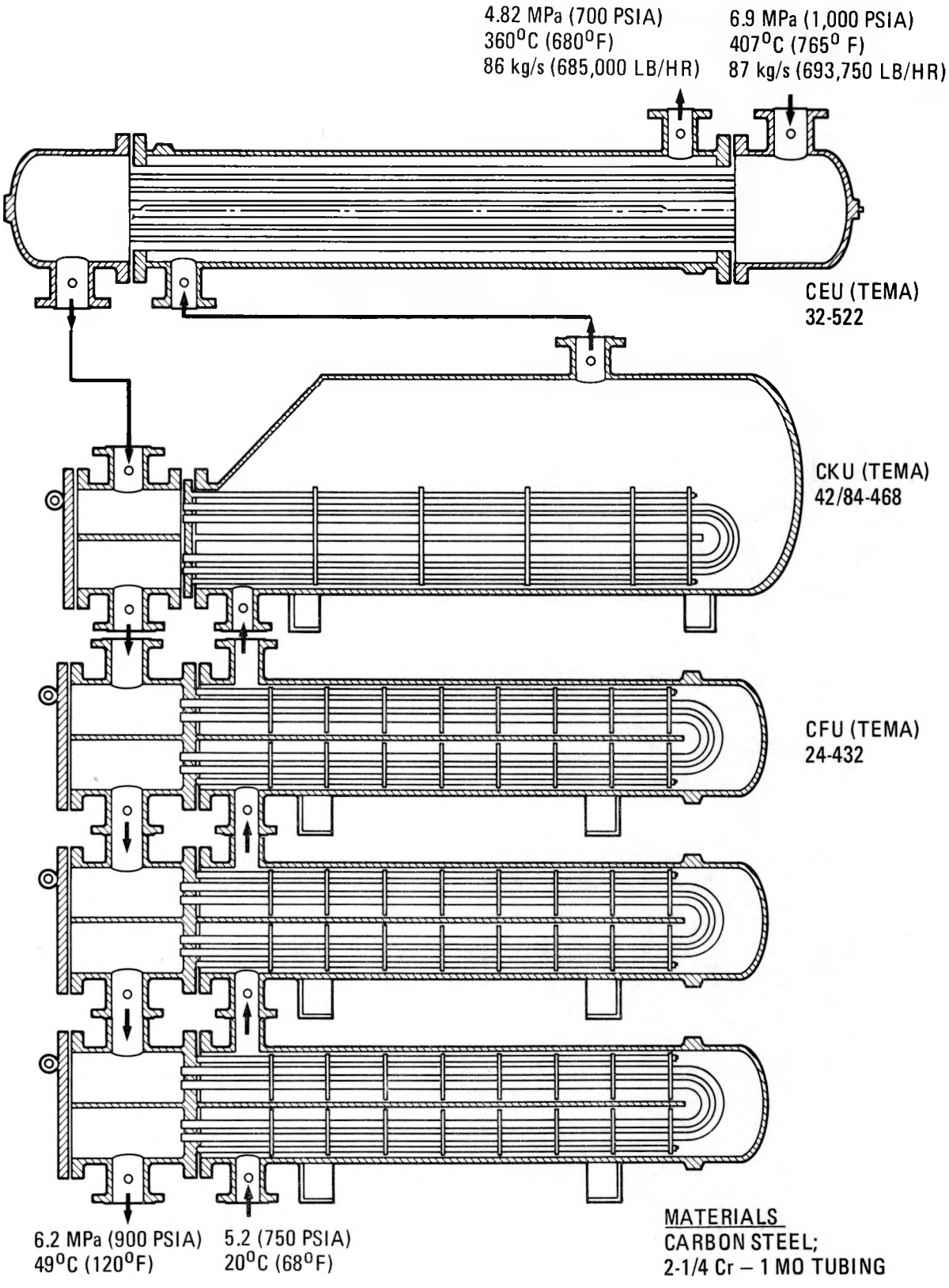

Fig. 5-20. Reboiler conceptual arrangement for Case 3 (multipurpose) (one-eighth capacity, clean unit)

TABLE 5-11
CASE 1 - CONCEPTUAL REBOILER DATA

	Kettle				Economizer			
Clean (C)/fouled (F)	C	F	C	F	C	F	C	F
No. units + spare	4 + 1	8 + 1	2 + 1	2 + 1	4 + 1	8 + 1	2 + 1	2 + 1
Diam, mm (in.)	1066/2100 (42/84)[a]	1066/2100 (42/84)	1524/3048 (60/120)	2159/4318 (85/170)	609 (24)	432 (17)	863 (34)	863 (34)
Length, m (ft)	9 (30)	13.7 (45)	9 (30)	13.7 (45)	8.5 (28)	13 (43)	8.5 (28)	13 (43)
Tube passes	2	4	2	4	4	6	4	6
Shell passes	1	1	1	1	4	6	4	6
Tubesheet thickness, mm (in.)	203 (8)	203 (8)	279 (11)	405 (16)	127 (5)	89 (3.5)	178 (7)	178 (7)
Channel/shell thickness, mm (in.)	44/57 (1-3/4 / 2-1/4)	44/57 (1-3/4 / 2-1/4)	63.5/82.5 (2-1/2 / 3-1/4)	89/114 (3-1/2 / 4-1/2)	25.4/19 (1/3/4)	19/12.7 (3/4 / 1/2)	38/25.4 (1-1/2 / 1)	38/25.4 (1-1/2 / 1)
Nozzle Diam, mm (in.)								
Shell in	203 (8)	152 (6)	305 (12)	305 (12)	203 (8)	152 (6)	305 (12)	305 (12)
Shell out	355 (14)	254 (10)	509 (20)	509 (20)	203 (8)	152 (60)	305 (12)	305 (12)
Tube in	305 (12)	203 (8)	406 (16)	406 (16)	254 (10)	152 (6)	355 (14)	355 (14)
Tube out	254 (10)	152 (6)	355 (14)	355 (14)	203 (8)	152 (6)	305 (12)	305 (12)
Surface area, m^2 (ft^2) including spare	3,530 (38,000)	9,522 (102,500)	4227 (45,500)	12,681 (136,500)	2,322 (25,000)	4,923 (53,000)	2,926 (31,500)	6,549 (70,500)

[a]Tube sheet/shell (typical).

TABLE 5-12
CASE 2 - CONCEPTUAL REBOILER DATA

Economizer							
Clean(C)/fouled (F)	F	C	F	C	F	C	F
No. units + spare	2 + 1	8 + 1	16 + 1	4 + 1	8 + 1	2 + 1	2 + 1
Diam, mm (in.)	2083/4166 (82/164)	533 (21)	381 (15)	762 (30)	533 (21)	1067 (42)	1067 (42)
Length, mm (ft)	17 (56)	11.6 (38)	10.7 (35)	11.6 (38)	10.7 (35)	1.6 (38)	10.7 (35)
Tube passes	4	2	6	2	6	2	6
Shell passes	1	2	6	2	6	2	6
Tubesheet thickness, mm (in.)	359 (22)[b]	203 (8)	152 (6)	305 (12)	203 (8)	381 (15)	381 (15)
Channel/shell thickness, mm (in.)	159/229 (6-1/4(b)/ 9)	51/38 (1-3/3 / 1-1/2)	32/32 (1-1/4 / 1-1/4)	64.57 (2-1/2 / 2-1/4)	44/38 (1-3/4 / 1-1/2)	95/83 (3-3/4 / 4-1/4)	95/83 (3-3/4 / 3-1/4)
Nozzle Diam, mm (in.)							
Shell in	406 (16)	152 (6)	102 (4)	203 (8)	152 (6)	305 (12)	305 (12)
Shell out	305 (12)	203 (8)	152 (6)	305 (12)	203 (8)	406 (16)	406 (16)
Tube in	406 (16)	203 (8)	152 (60	305 (12)	203 (8)	406 (16)	406 (16)
Tube out	406 (16)	152 (6)	102 (4)	203 (8)	152 (6)	305 (12)	305 (12)
Surface area, m^2 (ft^2) including spare	18,393 (198,000)	2,3220 (25,000)	6,0850 (65,500)	2,6010 (28,000)	6,410 (69,000)	3,112 (33,500)	8,593 (92,500)

Kettle						
Clean(C)/fouled (F)	C	F	C	F	C	F
No. units + spare	8 + 1	16 + 1	4 + 1	8 + 1	2 + 1	2 + 1
Diam, mm (in.)	737/1473 29/58[a]	737/1473 29/58	1041/2083 41/82	1041/2083 (41/82)	1473/4166 (82/164)	2083/4166 (82/164)
Length, mm (ft)	15.2 (50)	17 (56)	15.2 (50)	17 (56)	152 (50)	17 (56)
Tube passes	2	4	2	4	2	4
Shell passes	1	1	1	1	1	1
Tubesheet thickness, mm (in.)	330 (13)	330 (13)	305 (12)[b]	305 (12)[b]	381 (15)[b]	359 (22)[b]
Channel/shell thickness, mm (in.)	89/83 (3-1/2 / 3-1/4)	89/85 (3-1/2 / 3-1/3)	83/114 (3-1/3[b]/ 6-1/2)	114/165 (4-1/2[b]/ 6-1/2)	114/165 (4-1/2[b]/ 6-1/2)	159/229 (6-1/4[b]/ 9
Nozzle Diam, mm (in.)						
Shell in	203 (8)	152 (6)	305 (12)	203 (8)	406 (16)	406 (16)
Shell out	152 (6)	102 (4)	203 (8)	152 (6)	305 (12)	305 (12)
Tube in	203 (8)	152 (6)	305 (12)	203 (8)	406 (16)	406 (16)
Tube out	203 (8)	152 (6)	305 (12)	203 (8	406 (16)	406 (16)
Surface area, m^2 (ft^2) including spare	6,131 (66,000)	13,0050 (140,000)	6,828 (73,500)	13,7950 (148,500)	8,1750 (88,000)	18,393 (198,000)

[a]Tubesheet/shell (typical).
[b]Inco.

TABLE 5-13
CASE 3 - CONCEPTUAL DESIGN DATA

	Superheater						Kettle			
Clean (C)/fouled (F)	C	F	C	F	C	F	C	F	C	F
No. units + spare	8 + 1	24 + 1	4 + 1	12 + 1	2 + 1	2 + 1	8 + 1	24 + 1	4 + 1	12 + 1
Diam, mm (in.)	812 (32)	482 (19)	1,168 (46)	660 (26)	1,626 (64)	1,626 (64)	1066/2100 (42/84)[a]	1066/2100 (42/84)	1524/3048 (60/120)	1524/3048 (60/120)
Length, mm (ft)	13.3 (43.5)	17.7 (58)	13.3 (43.5)	17.7 (58)	13.3 (43.5)	17.7 (58)	11.9 (39)	15.8 (52)	11.9 (39)	15.8 (52)
Tube passes	1	1	1	1	1	1	2	6	2	6
Shell passes	1	1	1	1	1	1	1	1	1	1
Tubesheet, mm (in.)	127 (5)	76 (3)	178 (7)	102 (4)	25.4 (10)	154 (10)	203 (8)	203(8)	279 (11)	279 (11)
Channel/shell, mm (in.)	32/22.2 (1-1/4 / 7/8)	12.7/9.5 (1/2 / 3/8)	44/32 (1-3/4 / 1-1/4)	25/19 (1 / 3/4)	63.5/44 (2-1/2 / 1-3/4)	63.5/44 (2-1/2 / 1-3/4)	38/57 (1-1/2 / 2-1/4)	38/57 (1-1/2 / 2-1/4)	57/83 (2-1/4 / 3-1/4)	57/83 (2-1/4 / 3-1/4)
Nozzle Diam, mm (in.)										
Shell in	305 (12)	203 (8)	406 (16)	305 (12)	609 (24)	609 (24)	254 (10)	152 (6)	355 (14)	203 (8)
Shell out	406 (16)	203 (8)	609 (24)	305 (12)	762 (30)	762 (30)	305 (12)	203 (8)	406 (16)	305 (12)
Tube in	355 (14)	203 (8)	509 (20)	305 (12)	762 (30)	762 (30)	203 (8)	127 (5)	305 (12)	203 (8)
Tube out	254 (10)	152 (6)	355 (14)	203 (8)	609 (24)	609 (24)	254 (10)	152 (6)	355 (14)	203 (8)
Surface area, m^2 (ft^2)	5,8990 (63,500)	7,8500 (84,500)	6,549 (70,500)	8,175 (88,000)	7,850 (84,500)	10,451 (112,500)	8,035 (86,500)	29,726 (320,000)	8,918 (96,000	30,934 (333,000)

[a]Tubesheet/shell (typical)

shell side is dependent on the process water chemistry, which in turn is dependent on a specific site and process.

The impact of fouling on reboiler size and number of units is given in Tables 5-11, 5-12, and 5-13. Figure 5-21 graphically illustrates the significance of the fouling allowance on unit configuration for Case 1 conditions. The maximum-size units are obtained with two operating units plus one spare that allows for one unit to be out of service for cleaning and/or repair. At the other extreme, a minimum-size unit is based on the largest available standard flange. This results in a maximum number of units and in a spare unit having a small percentage of total surface area.

There can be a significant cost advantage with a relatively large number of standard-diameter units having a reduced fouling factor with a continuous maintenance operation. More data on the rate of fouling buildup are needed to design in this way; however, for purposes of developing a cost estimate on the reboilers, an intermediate selection of size and number of units was proposed. Thus, Case 1 and Case 2 have 8 units plus a spare, and Case 3 has 12 units plus a spare, all allowing for fouling.

Material Selection. Materials selected for the major components are shown on the concept sketches (Figs. 5-18, 5-19, and 5-20). Carbon steel is specified throughout, except for the kettle of Case 2, since maximum metal temperatures should not exceed 371°C (700°F). A corrosion allowance of 3.18 mm (1/8 in.) is included on all pressure parts, except tubes as recommended by TEMA. The Case 2 kettle has an Incoloy channel and tube sheet and a chromium-molybdenum shell. Tube material for all units is 2-1/4 Cr -1 Mo, which has satisfactory corrosion-resistant properties. A corrosion allowance of 1 mm (0.04 in.) or more exists in the tubing material depending on the excess material of the standard gage selected. Materials Engineering initially recommended using galvanized carbon steel tubing for Case 1 and Case 3 units. While galvanizing adds excellent anticorrosion properties to the tubing and can probably accrue substantial cost savings, several uncertainties and risk factors involved require further investigation.

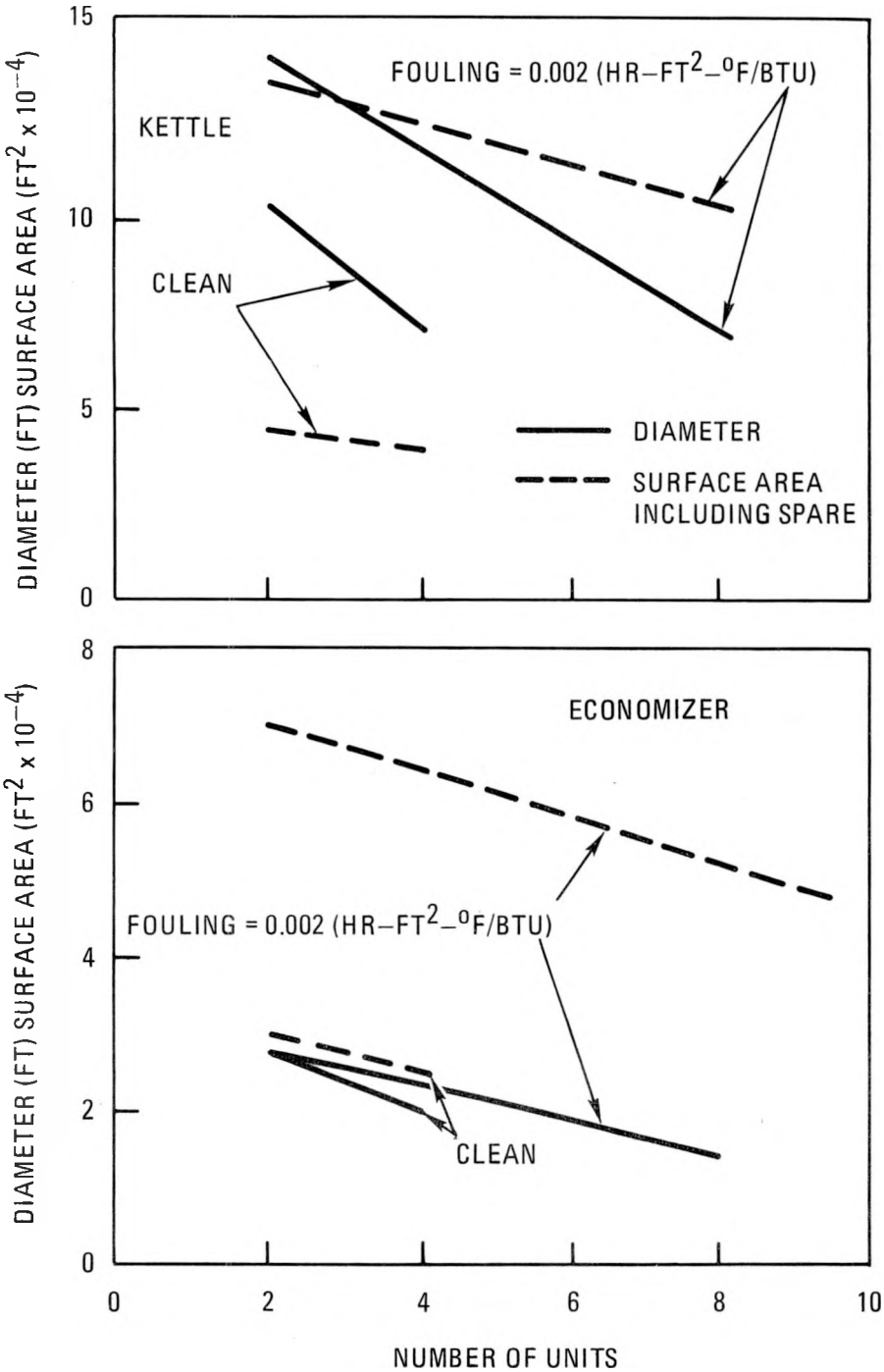

Fig. 5-21. Impact of fouling on unit size and number and surface area for Case 1

Specifically, during a postulated partial or full dry-out of the shell side of the kettle units and superheater unit (Case 3), a potential exists for the melting of zinc. Besides, industrial experiences have shown, in some cases, tubing damage due to the presence of pinholes in galvanized surfaces. Therefore, pending further understanding of the galvanizing process and its applicability for the current study, Materials Engineering recommended withholding galvanized tubing. Stainless steel Type 304 can be used as an alternate tubing material; however, because of potential chloride stress corrosion, stresses at the tube sheet and U-bends may be seriously compromised. Another good corrosion-resistant tubing material recommended by Materials Engineering was 9 Cr - 1 Mo.

Conceptual Reboiler Costs

Reboiler costs for each case were estimated for several materials of construction.

Tube costs for 2-1/4 Cr - 1 Mo and 9 Cr - 1 Mo were substituted for the carbon steel tube costs where required. These costs were taken from current tube vendor price catalogs. There were no adjustments made in the labor costs due to the use of different types of tube materials, as it was felt from prior experience that these costs would be insignificant in the overall cost. The galvanizing cost of the carbon steel tube was based on current market rates.

Table 5-14 shows reboiler cost estimates in thousands of January 1982 dollars, FOB point of manufacture, and are for the total quantity indicated (one spare unit is included). Cost estimates are shown for the same three tubing materials in all three cases. The materials are (1) galvanized CS for the economizer tubes, A210 GRC for the kettle tubes, and A213-T22 (2-1/4 Cr - 1 Mo) for the superheater tubes; (2) A213-T22 (2-1/4 Cr - 1 Mo) for all tubing; and (3) A199-T9 or A213-T9 (9 Cr - 1 Mo) for all tubing.

TABLE 5-14
REBOILER COST ESTIMATES
(Thousands of January 1982 Dollars)

	Economizer Tubing Galvanized CS; Kettle and Superheater Tubing 2-1/4 Cr - 1 Mo	Tubing 2-1/4 Cr - 1 Mo	Tubing 9 Cr - 1 Mo
Case 1 - Heavy Oil Recovery			
9 economizers	910.8	1077.6	1359.0
9 kettles	1734.0	1734.0	2277.6
Case 2 - Tar Sands Recovery			
9 economizers	3285.3	3484.6	3597.7
9 kettles	7719.4	7719.4	8534.4
Case 3 - Multipurpose			
13 economizers	1977.6	2596.3	3673.4
13 kettles	3707.9	3707.9	5453.1
13 superheaters	1364.1	1364.1	1827.1

5.3. SITE-SPECIFIC STUDIES

5.3.1. Scope

This task is to provide technical support for studying the application of the HTGR-SC/C to supply process energy for the Gulf refinery at Port Arthur, Texas, and Alliance, Texas.

The scope of work during this reporting period included the following:

- Provide support for studies on the use of reboilers versus feedwater treatment facilities and alternative backup power sources at Port Arthur.
- Evaluate the suitability of siting a nuclear plant within an acceptable steam transportation distance of the Gulf refinery at Port Arthur.
- Provide support for studies on reactor/refinery steam transportation piping; SETS transmission piping is also to be included for economic evaluation.
- Review and evaluate site suitability and licensing considerations (i.e., demographics and potential explosive hazards) for Port Arthur.

5.3.2. Discussion

5.3.2.1. Reboiler and Feedwater Study. A work scope was prepared for this subtask covering a study of reboilers versus no-reboilers as a source of process steam, with General Atomic being assigned the responsibility to (1) establish the chemistry of the feedwater required for reboilers, (2) select the location of the reboilers (in the HTGR plant or in the refinery), (3) size and cost the reboilers, and (4) calculate the differential plant output between the reboiler and the no-reboiler cases.

With respect to water chemistry for reboilers, literature sources were reviewed for recommendations, including a document by the ASME Research Committee on Water in Thermal Power Systems. Table 5-15 presents a consensus recommendation for maximum impurity allowances in steam, boiler water, and feedwater for the refinery application using a reboiler. The values given are considered to be on the conservative side of an acceptable range, considering that maintenance, repair, and replacement of the reboilers are probably not as difficult as on most steam generating equipment. However, the importance of plant availability was recognized in recommending feedwater conditions that will minimize outages and maintenance.

5.3.2.2. Backup Steam Supply Studies. As support for the studies of alternative backup steam sources, a matrix was prepared showing various combinations of HTGR's and fossil-fuel steam generators. The data compiled in Table 5-16 show the net kW(e) that could be generated above HTGR plant needs when either 30%, 70%, or 100% of the refinery steam needs are supplied by the HTGR plants. The matrix also shows the following fossil-fuel requirements for each combination:

- Total installed steam generating capacity.
- Steaming, on-line capacity.
- Hot standby capacity.
- Cold standby capacity.

An assumption used in the preparation of Table 5-16 is that the refinery requires for safety reasons an essentially noninterruptible source of steam equal to approximately 30% of total steam consumption. Another premise used is that a single reactor plant must have at least 100% fossil backup, because no reduction in refinery capability is permissible during reactor outages of significant duration, such as for refueling.

Calculations were made to determine the amount of steam contained in steam transmission lines of various length between the reactor plant and the refinery. Then the time was calculated for steam pressure to decay to

TABLE 5-15
REBOILER WATER QUALITY CONDITIONS FOR
SITE-SPECIFIC REFINING APPLICATION

Steam Quality	
Specific conductivity, μmho/cm	3-4
Total dissolved solids, ppm	0.030
Sodium, ppm	0.010
SiO_2, ppm	0.020
Boiler	
Specific conductivity, μmho/cm	1500 (max), 400 (nominal)
Total dissolved solids, ppm	2000 (max), 500 (nominal
Total suspended solids, ppm	50
Total alkalinity, ppm $CaCO_3$	150-200
Solution pH, 25°C (77°F)	9.5-10.5
Sulfite (SO_3), ppm	20-30
Phosphate (PO_4), ppm	30-70
Sodium/phosphate molar ratio	2.3
Sodium/phosphate molar ratio range	2.0-2.6
Silica (SiO_2), ppm	20
Feedwater	
Specific conductivity, μmho/cm	10
Total dissolved solids, ppm	15
Solution pH, 25°C (77°F)	7.5-10.0
Hardness, ppm $CaCO_3$	0.100
Silica (SiO_2), ppm	0.020
Chlorides (cl), ppm	0.300
Iron (Fe), ppm	0.020
Copper (Cu), ppm	0.015
Organics, ppm	0.500
Oxygen (O_2), ppm	0.007

TABLE 5-16
HTGR APPLICATION TO PORT ARTHUR REFINERY - ALTERNATIVE SCHEMES

	Number and Size of HTGR's										
	1 x 1170			2 x 1170		1 x 2240			2 x 2240		
HTGR steam to refinery, % of refinery required[a]	30	51[b]	30	70	100	30	70	97.5[b]	30	70	100
Refinery fossil steam generation, on line, %	70	49	70	30	0	70	30	2.5	70	30	0
Refinery backup fossil steam for safety, hot standby, %	0	0	0	10	40	0	10	37.5	0	10	40
Refinery backup fossil steam for availability, cold, %	40	61	10	0	0	40	70	70	10	0	0
Total installed fossil steam capacity, %	110	110	80	40	40	110	110	110	80	40	40
HTGR plant net MW(e)[c] (10-mi pipeline)	275	155	725	493	320	702	471	312	1579	1347	1174
MW for 1/2-mi pipeline	+ 6.6	+ 11.2	+ 6.6	+ 15.3	+ 21.9	+ 6.6	+ 15.3	+ 21.3	+ 6.6	+ 15.3	+ 21.9

[a] 100% refinery requirements = 674 kg/s (5,350,000 lb/hr).

[b] Maximum extraction with enough flow to an extracting turbine to heat condensate/feedwater.

[c] This is electrical power above HTGR auxiliary needs. Based on 16-km (10-mi) transmission line.

2.07 MPa (300 psia) in the pipeline following sudden loss of reactor-generated steam. These calculations were based on the pipe sizing that assumed that reactor-generated steam supplied 70% of refinery needs [1,698,000 kg/h (3,745,000 lb/hr)] at a transmission pipeline outlet pressure of 4.76 MPa (690 psia). As shown in Fig. 5-22, a 16.1-km (10-mi) pipeline has inventory to furnish steam for about 7.5 min before pressure decays to 2.07 MPa (300 psia). Of course, it is not likely that the refinery could continue to use steam at the full-flow rate with the supply pressure decreasing to less than half of rated value. It was concluded from this study that the pipeline inventory of steam provides little time to bring standby steam generating capacity on line following a sudden reactor outage.

As an additional possibility for a source of backup steam, a cursory assessment was made of the feasibility of a simple system using salt (draw salt or Hitec) as a heat storage medium from which steam at 4.65 MPa (675 psia) and 359°C (679°F) would be generated at full refinery flow for a 3-hr period either for shutdown of the refinery or to allow other sources of steam to be brought on line. In this scheme, live steam from the reactor was used as the charging source of heat energy to be put into the salt. The calculation showed that a very large inventory [approximately 40.8×10^6 kg (90×10^6 lb)] of salt is required. It was concluded that the cost of salt, storage tanks, and heat transfer equipment makes this scheme unattractive.

5.3.2.3. Port Arthur Site Suitability. As part of the Port Arthur site-specific study, an evaluation of site suitability is being made. Basically, the purpose is to determine if siting of a nuclear plant within an acceptable steam transportation distance of the Gulf Oil refinery is feasible given the various regulatory and environmental requirements to be met. Although the HTGR has low releases of radioactivity and is known to be environmentally benign, the Port Arthur application was recognized as having a combination of challenges not previously encountered in reactor siting. These challenges arise immediately from the proposition that the nuclear plant should be located near the refinery (preferably within a mile or two), which itself is situated adjacent to the edge of the city of Port Arthur.

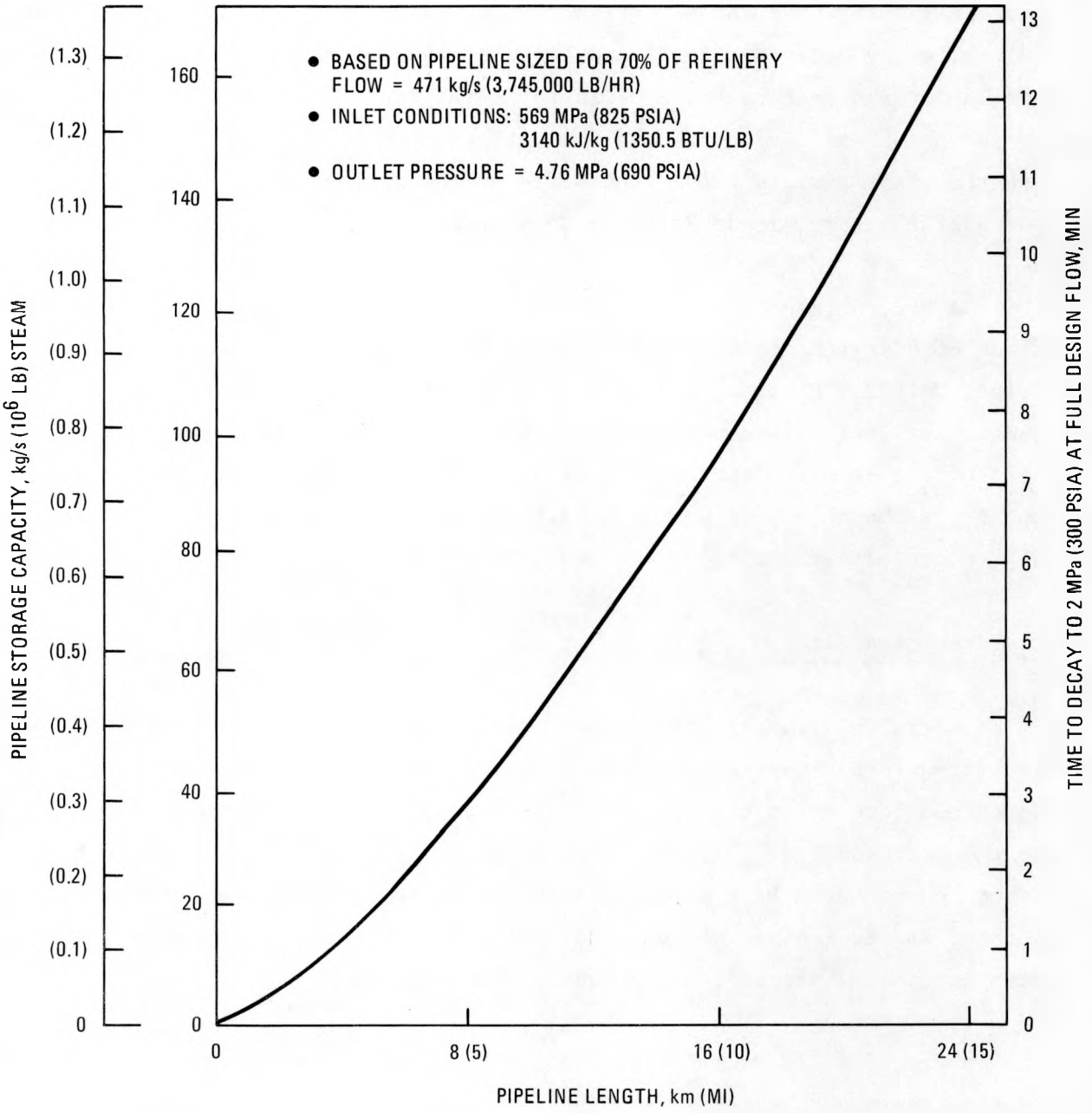

Fig. 5-22. Pipeline steam storage and pressure decay time

The Gulf refinery and other facilities in the general area of interest are served by railways, highways, a ship channel, a barge canal, and numerous pipelines carrying a variety of raw materials and products. The region is only slightly above sea level and has poor characteristics for a foundation. Available land area near the refinery is restricted because of the developed areas to the east and north and the wetlands to the west and south. These are the major factors being considered by the Siting/Environmental Task Force of the Port Arthur Refinery Cogeneration Alternatives Study.

GA has one member on the task force, which also includes representatives of GCRA (chairman), United Engineers & Constructors, Gulf States Utilities, Gulf Oil Houston, and Gulf Oil Refinery. This section of this report summarizes actions and decisions of the task force as they bear on the progress of the study. This section is limited to discussion of the nuclear option, although consideration of a coal-fired cogeneration plant is part of the overall study.

Proposed Sites

Initially, two potential sites identified in a previous study were under consideration. One of these, called the Texaco site, lies to the north and borders on the Gulf Oil refinery. The Texaco refinery lies a mile to the east and Arco Polymers plant a mile to the west. The site is bordered on the north by a major highway and on the east by a major local street. Several pipelines cross or run along the edge of the site. A tank farm is located across the highway to the northeast.

The second site, called the Gulf site, lies to the southwest of the Gulf refinery. Between are a highway, a railroad line, and a ship channel. The intracoastal canal borders the site on the south, a large tank farm lies to the north, and to the west are wetlands. A major pipeline alley enters the tank farm, and a natural gas pipeline runs along the eastern boundary.

From observations and map measurements, it was concluded that both the Gulf and the Texaco sites were sufficiently large to accommodate a nuclear

station. It was obvious that the local industrial hazards would be a major siting factor and that foundation construction and flood protection would have to be considered. Demographic considerations would have to account for the local worker populations.

Task Force Activities

Interaction of the task force members has been through personal contacts and communication. The meetings, which have been held to exchange information, to make data requirements known, and to make assignments for various activities, are summarized below:

Gulf Refinery, Dec. 7-8, 1981. The discussion included the topics of flood protection, seismicity, demography, external industrial hazards, and meteorology. GCRA, UE&C, and GA each presented their ideas on site and environmental requirements and data needs. It was agreed that major emphasis would have to be placed on evaluating the hazards arising from the industrial facilities, transportation routes, and pipelines. Population density and distribution with respect to the candidate sites were deemed important, as were the plant features of flood protection and foundation/seismic design. A conclusion was that a search for alternate sites within a distance of about 16 km (10 mi) from the refinery should be conducted.

Gulf States Utilities, Feb. 8-9, 1982. The Task Force ranked the two initial candidate sites and found the Gulf site to be preferred. Although information on pipelines (i.e., maps) had been provided by Gulf Oil, the need for more extensive data was again discussed. Hazards to be evaluated are those from toxic gases, explosives, and flammable gas clouds. Gas clouds arising from the release of heavier-than-air gases present a particularly difficult problem and are of major concern. A potential site to the west at Big Hill Dome was discussed, but because of the distance this was not considered to be a real alternative.

Gulf States Utilities, March 31-April 1, 1982. General Atomic presented a list of siting ground rules for consideration and UE&C reviewed its list of study parameters. A preliminary outline for the final report prepared by UE&C was also discussed. Additional data on pipelines were requested by GA and it was noted that data on ship and barge traffic were still to be provided by UE&C.

The potential alternate site at Big Hill Dome was discounted, but a more promising location to the northeast of Port Arthur was discussed. This is the site of the existing GSU Sabine Power Station near Bridge City, Texas. While more favorable from the standpoint of land area and fewer industrial hazards, a major consideration would be the length of the steam line [more than 16 km (10 mi)] and the potential difficulty of reaching the Gulf refinery by passing through or around Port Arthur. More investigation of the candidate site is to be conducted.

The suspected foundation problem was determined to have an engineering solution (though costly). It would consist of excavating to a depth estimated at 18 to 36 m (60 to 120 ft) and backfilling with an engineered backfill material. The River Bend nuclear plant near Baton Rouge, Louisiana, is an example of such a foundation.

It was also noted by the environmentalists that wetlands are excluded from site consideration because of Corps of Engineers restrictions on permanent construction. However, the opinion was expressed that a permit for a steam line could be obtained.

Preliminary Results

The Task Force has identified two potential sites, the preferred being the Gulf Oil site adjacent to the refinery. Demographic criteria being used in the evaluation are met, but the severity of the problem from external hazards, particularly pipeline breaks, has not been completely evaluated. Flood protection and foundation construction are major engineering challenges, but they are solvable. Effluent releases and off-site doses are not

believed to be a problem, but the rather large concentration of workers at the Gulf Oil refinery and the need for some minimum operating staff could present a unique situation for emergency planning.

The potential alternate site at the Sabine Power Station meets the demographic criteria and is removed from external hazards except possibly pipelines, which have not yet been evaluated. However, the economic penalty of pipeline length and routing may be severe.

5.3.2.4. Pipeline Transport Studies. The UE&C studies for both direct steam transmission and salt energy transmission systems (SETS) were performed by using a computer code for piping design. This code optimizes pipe size versus pressure drop/pumping power and also optimizes piping insulation thicknesses. For these studies the code included factors to approximate extra piping length needed by loops to absorb thermal expansion of the piping. The code also included factors to approximate the pressure drop in fittings and valves in addition to the fluid flow, pipe material, and unit cost parameters for the system. For the SETS systems, the input also included values for maximum pump head, based on selected pump performance data. The studies considered only the energy transmission systems per se and did not account for differences in cogenerated electric power, reactor plant auxiliary power requirements, reactor plant costs, cogeneration equipment costs, etc., between the alternatives evaluated. Consideration of process uses for heat, as opposed to process steam, and consideration of energy storage value for some applications were also excluded.

Because the conventional U-shaped expansion loops used in the UE&C design added large penalties in both the total length of piping required and in system pressure drops, this study examined alternative expansion bend designs. The use of material with higher allowable stresses for the hot salt piping was also examined. Total reactor plant and transport system costs and performance were considered and alternative heat cycles were developed, including cases for delivery of steam to the process plant at higher temperatures and pressures. For each alternative the net cost of energy delivered to the process plant, including credits for cogenerated

electric power, was estimated. Table 5-17 summarizes design, cost, and economic data both for the UE&C designs and for the improved designs, all based on a process plant 32-km (20-mi) transmission distance between the reactor plant and the process plant.

Data for seven transport system cases are tabulated:

Case 1. HTGR-SC/C, UE&C design, 6.2 MPa/377°C (900 psia/711°F)* steam inlet to pipeline, above ground, 4.48 MPa/1329°C (650 psia/672°F) process steam.

Case 2. HTGR-SC/C, GA design, 6.2 MPa/399°C (900 psia/750°F)** steam inlet to pipeline, above ground, 4.75 MPa/372°C (689 psia/702°F) process steam.

Case 3. HTGR-SC/C, GA design, 4.1 MPa/399°C (900 psia/750°F) steam inlet to pipeline, below ground, 4.75 MPa/372°C (689 psia/702°F) process steam.

Case 4. HTGR-SETS, UE&C design, 565°C (1050°F) supply/260°C (500°F) return drawsalt system, with generation of steam at the process plant and at 12.4 MPa/510°C (1800 psia/950°F), cogenerated electric power and production of 4.48/374°C (650 psia/705°F) process steam.

Case 5. HTGR-SETS, GA design, 565°C (1050°F)/supply 260°C (500°F) return drawsalt system, with generation of steam at the process plant and at 17.34 MPa/540°C (2515 psia/1005°F), cogenerated electric power and production of 4.48 MPa/355°C (650 psia/672°F) process steam.

Case 6. HTGR-SC/C, GA design, 17.34 MPa/540°C (2515 psia/1005°F) steam inlet to pipeline, 12.4 MPa/496°C (1800 psia/926°F) process steam, and

*Established by UE&C to obtain 4.5 MPa/357°C (650 psia/672°F) pipeline outlet conditions.

**Approximate cogeneration turbine-generator exhaust conditions.

TABLE 5-17
ECONOMIC DATA AND ENERGY COSTS

	Case 1 UE&C Design Above Ground 4.48 MPa (650 psia) Process Steam	Case 2 GA Design Above Ground 4.8 MPa (689 psia) Process Steam	Case 3 GA Design Below Ground 4.8 MPa (689 psia) Process Steam	Case 4 UE&C Design Below Ground 4.48 MPa (650 psia) Process Steam	Case 5 GA Design Below Ground 4.48 MPa (650 psia) Process Steam	Case 6 GA Design Below Ground 12.4 MPa (1800 psia) Process Steam	Case 7 GA Design Below Ground 12.4 MPa (1800 psia) Process Steam	Case 8 Standard Multi-purpose HTGR-SC/C	Case 9 Geismar, La. Petro-chemical Appl.	Case 10 Port Arthur, TX, Refinery Appl.
Reactor/Transmission System Data										
Reactor type and power, MW	170-MW(t) HTGR-SC/C	1170-MW(t) HTGR-SC/C	1170-MW(t) HTGR-SC/C	1170-MW(t) HTGR SETS	1170-MW(t) HTGR SETS	1170-MW(t) HTGR-SC/C	1170-MW(t) HTGR SETS	1170-MW(t) HTGR-SC/C	(3)1170-MW(t) HTGR-SC/C	(2)1170-MW(t) HTGR-SC/C
Transmission fluid	Steam	Steam	Steam	Draw Salt	Draw Salt	Steam	Draw Salt			
Transmission distance, km (mi)	32 (20)	32 (20)	32 (20)	32(20)	32(20)	32(20)	32(20)			
Flow rate, (10^6 lb/hr)	345 (2.74)	345 (2.74)	345 (2.74)	2535 (20.124)	2535 (20.124)	327 (2.72)	2535 (20.124)			
Inlet press./temp, MPa/°C (psia/°F)	6.2/317 (900/711)	6.2/399 (900/750)	6.2/399 (900/750)	0.68/565 (100/1050)	0.68/565 (100/1050)	17.3/540 (2515/1005)	0.68/565 (100/1050)			
Outlet press./temperaTURE (psia/°F)	4.48/355 (650/672)	4.75/372 (689/702)	4.75/372 (689/702)	0.68/250 (100/500)	0.68/250 (100/500)	1.38/45) (200/115)	0.68/250 (100/500)			
Pipeline/pumping power, MW	0.4	0.4	0.4	33.5	27.7	0.4	28			
Other house power, MW	36.1	36.1	36.1	90.0	90.0	36.1	90			
Gross electric power, MW	166.7	166.7	166.7	145.1	167.7	91.9	118			
Net electric power, MW	130.6	130.6	130.6	21.6	50.0	55.4	0	150	723	354
Steam power to process, MW	1002	1014	1014	1052	1036	1077	961	1000	2214	1926
Capital Costs $\$10^6$ (1/1/80)										
NSS	114.1	114.1	114.1	148.0	148.0	114.1	148.0	114.1	510.3	228.2
BOP	249.9	249.9	249.9	302.2	304.9	230.9	298.5	254.9	778.9	567.8
Pipeline	192.0	114.5	133.6	409.7	215.3	559.9	215.3	--	--	--
Indirects	144.8	144.8	144.8	152.3	153.3	142.0	151.1	143.0	446.7	269.2
Contingency	105.1	93.5	96.4	151.8	123.2	157.0	121.9	77.0	230.4	159.8
Total base capital cost and contingency	805.9	716.8	738.8	1164.0	944.7	1203.9	934.8	589.0	1766	1225
Annual Costs, $\$10^6$[a]										
Fixed charges	82.0	73.0	76.0	118.0	96.0	122.0	95.0	60.0	181.0	125.0
Fuel costs (LEU/Th)	30.0	30.0	30.0	30.0	30.0	30.0	30.0	30.0	90.0	60.0
O&H costs	25.0	25.0	25.0	25.0	25.0	25.0	25.0	25.0	75.0	50.0
Credit for electric power	(31.0)	(31.0)	(31.0)	(5.0)	(12.0)	(13.0)	--	(35.0)	(170.0)	(63.0)
Total annual costs	106.0	97.0	100.0	168.0	139.0	164.0	150.0	80.0	175.0	152.0
Energy Cost \$/GJ ($/10^6$ Btu delivered)	4.77 (5.04)	4.34 (4.58)	4.43 (4.69)	7.23 (7.63)	6.07 (6.41)	6.89 (7.27)	7.07 (7.46)	3.61 (3.81)	3.58 (3.78)	3.57 (3.77)

[a]Levelized over 30 yr. Plant owners' costs for salt inventory and regeneration not included.

cogeneration of electric power at reactor plant by feedwater heating extraction turbine-generator.

Case 7. HTGR-SETS, GA design, 565°C (1050°F)/supply 260°C (500°F) return drawsalt system, with generation of steam at 12.4 MPa/510°C (1800 psia/950°F) and cogeneration of electric power by an extraction/condensing turbine at the process plant end.

Data for three HTGR-SC/C applications with the reactor located adjacent to the process plant are also listed for comparison. Schematic diagrams of the seven transmission piping cases are shown in Figs. 5-23, 5-24, and 5-25.

Piping Expansion and Flexibility. The factors used by UE&C for additional piping length needed for piping flexibility are based on the use of conventional U-shaped loops. This resulted both in large factors for extra piping length and in a large number of elbows (which is significant to pressure drop and pumping power). Therefore, alternative flexibility arrangements were examined, including Z-shaped bends and a zigzag arrangement. The Z arrangements reduced the number of elbows to half those required for U bends (or less, with increased anchor spacing) and also somewhat reduced the total pipe length required. The zigzag arrangements showed even greater improvement compared with U bends, resulting in marked reductions in both the length of piping and number of bends required.

For the zigzag arrangements the use of 127-mm (5-in.) diam pipe bends instead of elbows, which reduces both pressure drop and bending stress intensification factors, appears to be advantageous. The reductions in the number of bends and total pipe length also permit the use of smaller diameter pipe while maintaining the same or lower pressure drop and pumping power. The zigzag arrangements may require somewhat greater right-of-way width than the U- or Z-bend arrangements for very high temperature pipes such as the hot salt supply line, but this appears to be within limits acceptable for most interplant tie-line applications. Figures 5-26 and 5-27 compare the U-bend designs with the zigzag designs for the hot salt and

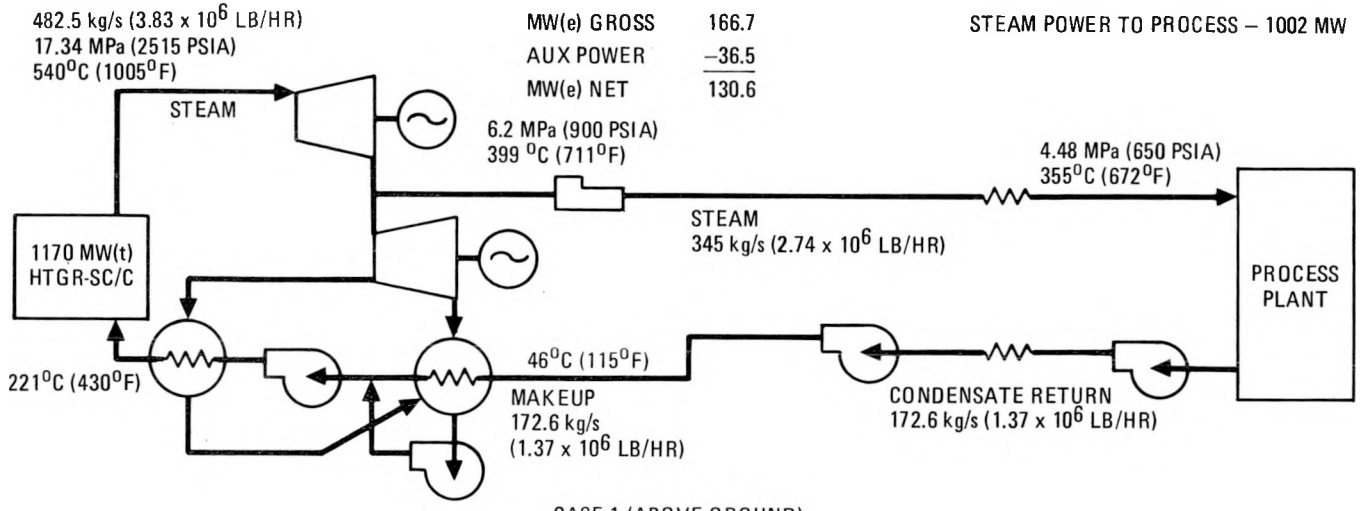

CASE 1 (ABOVE GROUND)
UE&C DESIGN, DIRECT STEAM TRANSMISSION FOR 4.45 MPa (650 PSIA) PROCESS STEAM

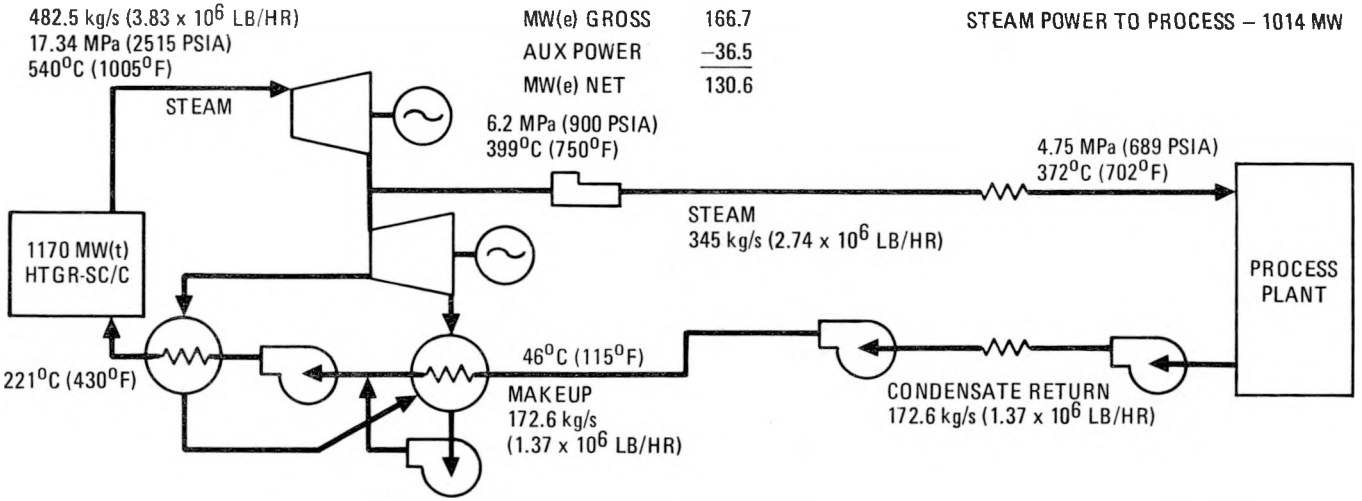

CASE 2 (ABOVE GROUND) AND CASE 3 (BELOW GROUND)
GA DESIGN, DIRECT STEAM TRANSMISSION FOR 4.45 MPa (650 PSIA) PROCESS STEAM

Fig. 5-23. Direct steam transmission for medium-pressure process steam

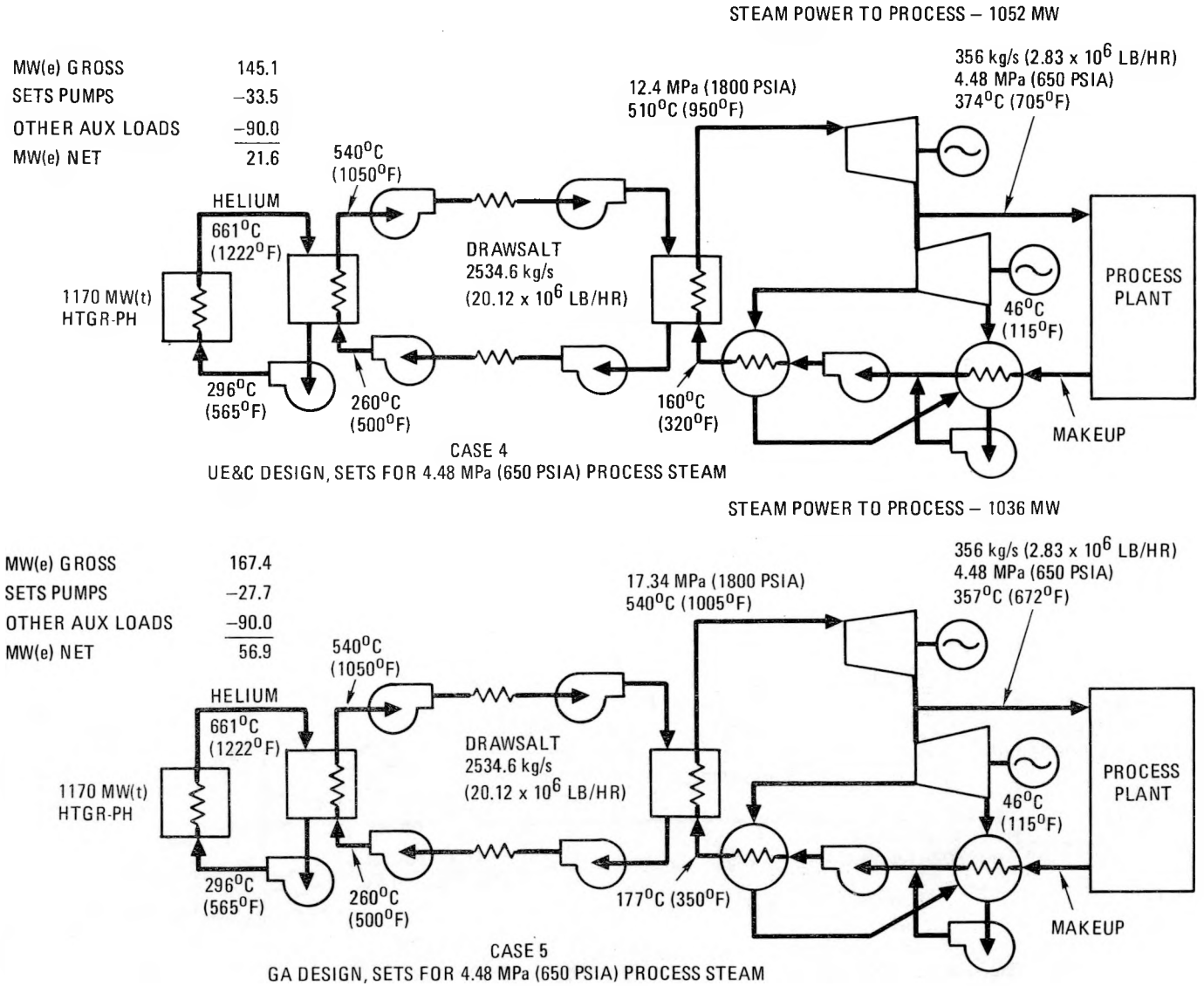

Fig. 5-24. SETS for medium pressure process steam

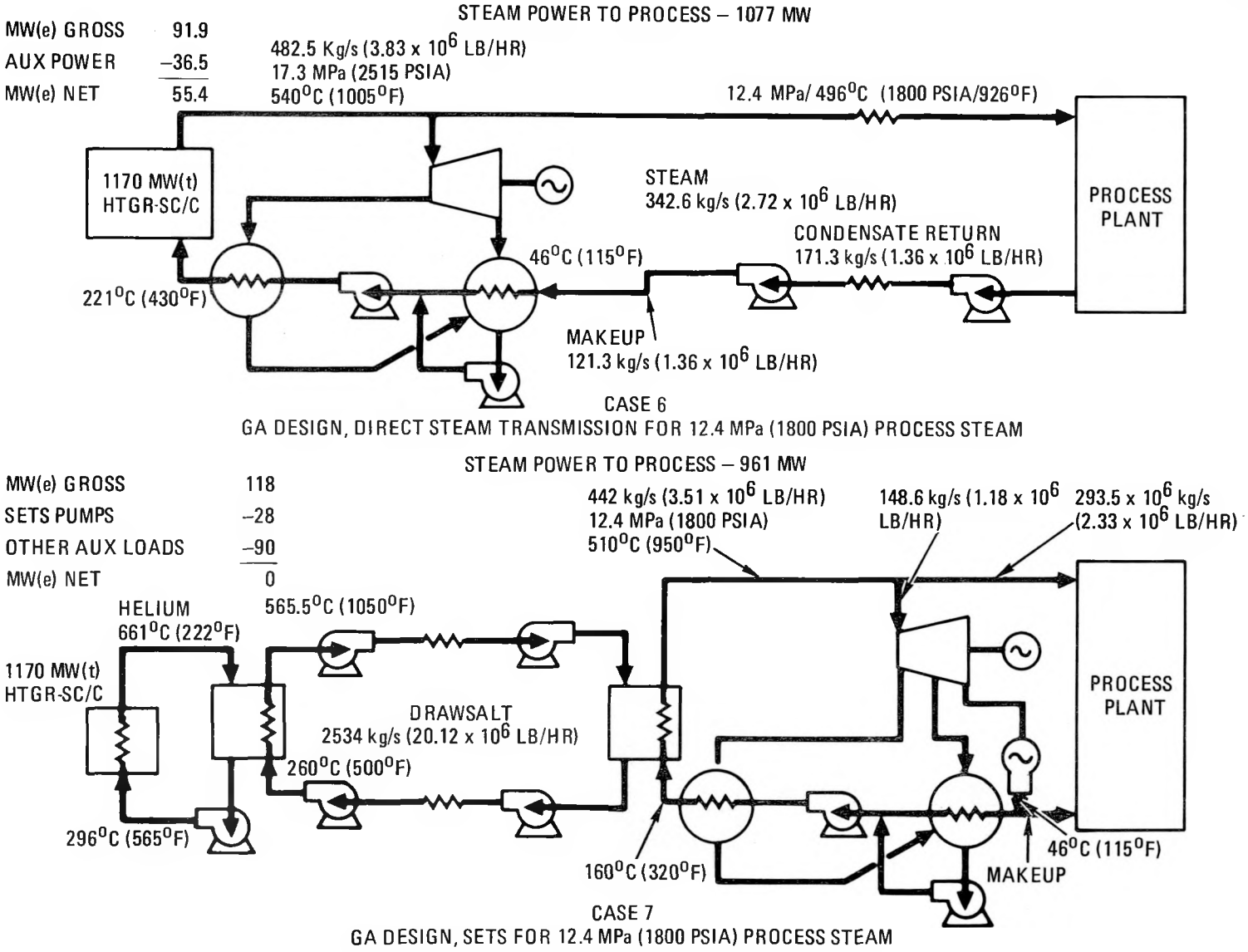

Fig. 5-25. Direct steam transmission and SETS for high-pressure process steam

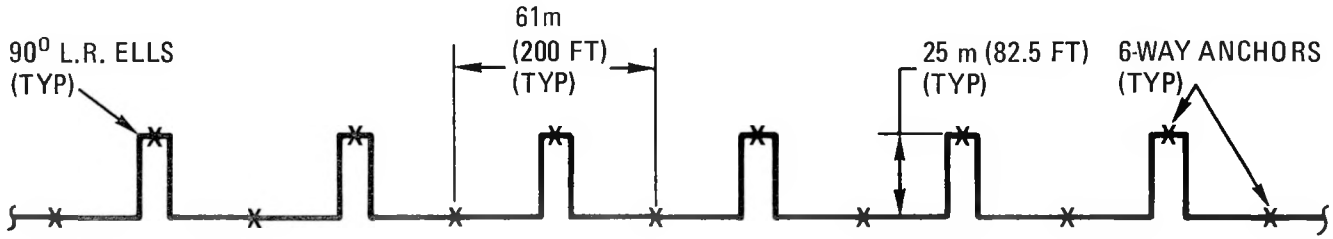

762 mm x 19 m (30 IN. O.D. x 0.762 IN.) 316H SS
(ANSI B31.1 LOW STRESS VALUES)

EXPANSION FACTOR	1.825
NUMBER OF 90-DEG ELLS	2112
PUMPING POWER	32.1 MW (GA CALCULATION)
TOTAL PIPE WEIGHT	20.8×10^6 kg (45.9×10^6 LB)

A. UE&C U-BEND DESIGN

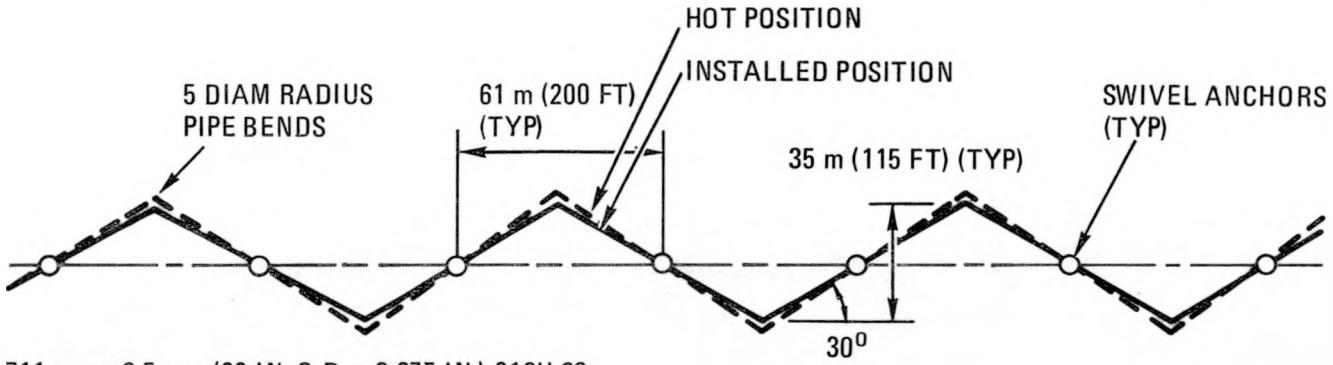

711 mm x 9.5 mm (28 IN. O.D. x 0.375 IN.) 316H SS
(ANSI B31.1 HIGH STRESS VALUES)

EXPANSION FACTOR	1.155
NUMBER OF 30-DEG BENDS	528
PUMPING POWER	20.5 MW
TOTAL PIPE WEIGHT	6.07×10^6 kg (13.4×10^6 LB)

B. GA ZIGZAG DESIGN

Fig. 5-26. Hot salt supply line expansion arrangements; 566°C (1050°F), 2.07 MPa (300 psia), 2.535×10^3 kg/s (20.124×10^6 lb/hr), 32-km (20-mi) transmission distance

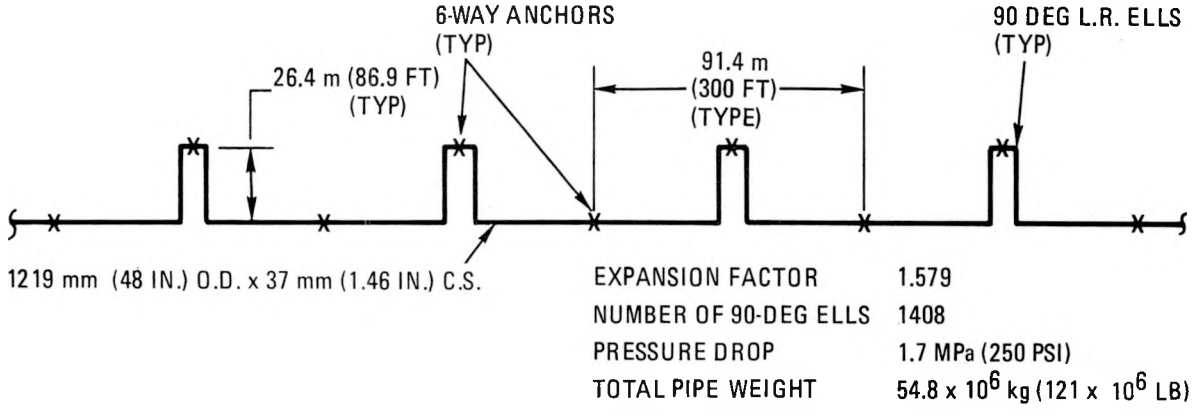

A. UE&C U-BEND DESIGN

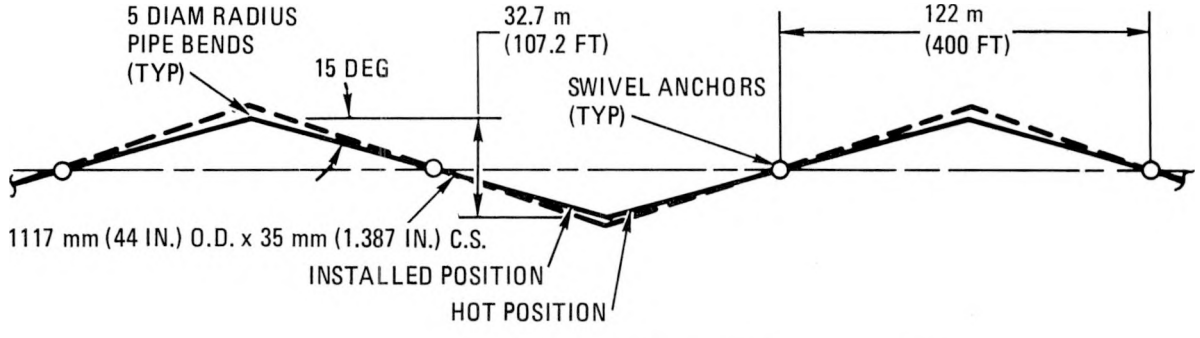

B. GA ZIGZAG DESIGN

Fig. 5-27. Steam transmission line expansion arrangements: 399°C/6.2 MPa (750°F/900 psia) inlet, 342.6 kg/s (2.72 x 10^6 lb/hr), 32-km 20-mi) transmission distance

direct steam transmission piping, respectively. The zigzag configurations shown are conservatively designed and further optimizations can be made.

Hot Salt Piping Material. The material selected by UE&C for the hot salt piping at 565°C (1050°F) is welded stainless steel ASTM A-312, type 316H. For this and other austenitic stainless materials, ANSI B31.1, Power Piping, lists alternative allowable stress values. Lower values are to be used where deformations may be critical, such as for valves and flanges, and higher values can be used for other applications, such as for pipe and fittings. UE&C conservatively used the lower stress values, but there appears to be no reason why the higher values should not be applicable, both for establishing pipe wall thickness and for expansion bending stresses. Alternative material selections such as type 316N or 347H SS should also be considered, as well as designing to ANSI B31.3, Petroleum Refinery and Chemical Plant Piping, as an alternative to ANSI B31.1. For this study the GA designs conform to ANSI B31.1 higher stress values. Table 5-18 lists code allowable stress values for some of the candidate materials.

Cost Estimates. Consistent capital cost estimates, based on the same unit cost data used by UE&C, were developed for the transmission piping systems for each of the seven cases studied. Transmission piping systems were treated as a subcontracted item per the UE&C estimates. Breakdowns of the transmission piping system estimates are given in Table 5-19. These were used, together with current NSSS and NHS estimates and conceptual estimates for balance-of-plant equipment and structures, to determine total plant plus transmission system capital costs. Indirect and contingency costs were included in accordance with current UE&C practice for FY-81 HTGR program estimates.

Economic Analysis. Economic analyses were performed on a utility ownership basis, using the revenue requirement method, to establish the net cost of energy delivered to the process plant for each of the seven cases. FY-81 HTGR program economic assumptions, shown in Tables 5-20 and 5-21, were used. Table 5-17 gives the economic data and the resulting energy costs for

TABLE 5-18
CODE ALLOWABLE STRESSES AT 565°C (1050°F)

	ANSI B31.1 (1980) [MPa (lb/in.^{2})]		ANSI B31.3 (1980) [MPa (lb/in.^{2})]
	Low Value	High Value	
A-312 tp 316H, seamless	72.4 (10,500)	100 (14,500)	100 (14,500)
A-312 tp 316H, welded	61.4 (8,900)[a]	84.8 (12,300)[a]	84.8 (12,300)[a]
A-312 tp 316N, seamless	84.14 (12,200)	103.4 (15,000)	--
A-312 tp 316N, welded	71.7 (10,400)[a]	92.4 (13,400)[a]	--
A-312 tp 347H, seamless	86.2 (12,500)	97.2 (14,100)	118 (17,100)
A-312 tp 347H, welded	73.1 (10,600)[a]	82.7 (12,000)[a]	100 (14,500)[a]
A-312 tp 304H, seamless	65.5 (9,500)	84.1 (12,200)	84.1 (12,200)
A-312 tp 304H, welded	55.8 (8,100)[a]	71.7 (10,400)[a]	71 (10,300)[a]

[a]Based on 0.85 weld efficiency.

TABLE 5-19
TRANSMISSION SYSTEM CAPITAL COSTS
(1/1/80 DOLLARS X 10^6)

	Case 1 Steam, UE&C Design Above Ground, 4.48 MPA (650 psia) Process Steam	Case 2 Steam, GA Design, Above Ground, 4.75 MPa (689 psia) Process Steam	Case 3 Steam, GA Design Below Ground, 4.75 MPa (689 psia) Process Steam	Case 4 SETS, UE&C Design, Below Ground, 4.48 MPa (650 psia) Process Steam	Case 5 SETS, GA Design, Below Ground, 4.48 MPa (650 psia) Process Steam	Case 6 Steam, GA Design, Below Ground, 12.4 MPa (1800 psia) Process Steam	Case 7 SETS, GA Design Below Ground, 12.4 MPa (1800 psia) Process Steam
Supply pipe	138.4	78.9	78.9	159.8	46.8	466.2	46.8
Return pipe	5.0	5.3	5.3	35.7	25.2	5.4	25.2
Insulation	18.1	10.9	10.9	18.4	12.1	26.4	12.1
Supports	17.7	11.6	3.0	5.2	3.3	3.0	3.3
Concrete encasement	-	-	24.0	42.4	26.8	24.7	26.8
Equipment rental	2.5	1.6	4.3	7.5	4.8	4.4	4.8
Pumps	0.1	0.1	0.1	49.1	40.7	0.1	40.7
Steam tracing	-	-	-	69.9	44.2	-	44.2
Subtotal	181.8	108.4	126.5	388.0	203.9	530.2	203.9
Subcontract indirects	10.2	6.1	7.1	21.7	11.4	29.7	11.4
Total	192.0	114.5	133.6	409.7	215.3	559.7	215.3

TABLE 5-20
ECONOMIC ASSUMPTIONS FOR HTGR PROGRAM

Region: northeast region near Wilmington, Delaware	
Commercial plant basis	Nth Plant
Capacity factor	70%
Base date for all costs	January 1980
Date of operation for all plants	January 1995
Investment life for all plants	30 yr
Electricity replacement power costs (January 1980 $)	40 mills/kW/hr
1995 fuel cost projections (January 1980 $)	
Coal, $/GJ ($/MBtu)	2.13 (2.25)
Oil, $/GJ ($/MBtu)	8.75 (9.25)
Natural gas, $/GJ ($/MBtu)	7.82 (8.25)
Uranium (U_3O_8), $/kg ($/lb)	88.2 (40)
Conversion (UF_6), $/kg ($/lb)	6 (2.72)
Separative work (0.2% tails)	120 $/SWU
Nuclear fuel cycle costs:	Based on detailed analysis at General Atomic

Operation and Maintenance Costs (January 1980 $)	Fixed (10^6 $/yr)	Variable [mills/kW(t)-hr]
HTGR-SC (SC/C)	12.0 (12.2)	0.45 (0.95)
HTGR-SETS	TBD	TBD
LWR	12.0	0.60
Coal electric (SC/C)	11.0 (11.2)	1.10 (1.60)
HTGR-PH (R)	TBD	TBD

Common Cost Factors - Utility-owned Facility	Constant Dollars (%)
Weighted cost of capital	4.3
Levelized fixed charge rate	8.3
Allowance for funds during construction	3.5

Real Escalation Rates	Base Inflation (%)	
Construction	6	1.00
O&M	6	1.00
Electric power	6	2.00
Fuel (all)	6	3.00

TABLE 5-21
REGULATED UTILITY
FINANCIAL ASSUMPTIONS
ASSUMING ZERO INFLATION RATE

	Percent
Capital Structure	
Debt	50
Preferred equity	15
Common equity	35
Financing Costs	
Bond yield	3.1
Preferred equity yield	4.1
Common equity yield	5.9
Weighted cost of capital	4.3
Property taxes and insurance	2.0
Effective tax rate	50.0
AFDC rate	3.5
Resulting fixed charge rate	8.3
Plant investment life, yr	30
Plant tax life, yr	20
Depreciation method	Accelerated SYD

the seven cases. For comparison, three cases are included for HTGR-SC/C applications with the reactor located adjacent to the process plant.

Transmission Cost Versus Distance Trends. The application studies listed in Table 5-17 assume a 32-km (20-mi) transmission distance between the reactor plant and process plant and assume that energy is required at the process plant in the form of steam. The UE&C studies assume that the steam is delivered at approximately 4.48 MPa/354°C (650 psia/670°F). For this review, cases assuming steam delivery at approximately 12.4 MPa/510°C (1800 psia/950°F) were also included. In addition, energy delivery costs at both pressure levels for distances between 0 and 64 km (0 and 40 mi) were estimated using pipeline costs scaled from the 32-km (20-mi) distance estimates (see Tables 5-22 and 5-23). Steam power tc process for each case was adjusted to account for changes in heat loss with transmission distance. The results are plotted in Fig. 5-28. For applications requiring process steam it appears that the economics favor direct transmission of steam from HTGR-SC/C plants over energy transmission from HTGR-SETS plants at distances up to 32 km (20 mi), even for applications requiring process steam at higher pressures and temperatures. The SETS system shows an advantage over direct steam transmission for higher pressure and temperature process steam at distances greater than 32 km (20 mi).

Conclusions and Recommendations. For both HTGR-SC/C and HTGR SETS plants, it appears that the economic penalties for remote location of the reactor can be substantially reduced from previous estimates by improvements in the design of the transmission systems. However, for long transmission distances, these penalties remain significant.

Additional studies should be performed to establish parameters for application of the HTGR-SETS and HTGR-SC/C plants. The HTGR-SETS appears to be most suitable for applications requiring heat, as opposed to process steam, and at higher temperature levels. For applications requiring process steam at moderate pressure/temperature levels and for higher pressure/temperature levels at transmission distances up to 32 km (20 mi), the HTGR-SC/C appears to have better economics, in part because of its greater

TABLE 5-22
HTGR-SC/C DIRECT STEAM TRANSMISSION ENERGY
COST VERSUS DISTANCE TRENDS

	4.75 MPa (689 psia), 0 km (0 mi)	4.75 MPa (689 psia), 16 km (10 mi)	4.75 MPa (689 psia), 32 km (20 mi)	4.75 MPa (689 psia), 48 km (30 mi)	4.75 MPa (689 psia), 64 km (40 mi)	12.4 MPa (1800 psia), 0 km (0 mi)	12.4 MPa (1800 psia), 16 km (10 mi)	12.4 MPa (1800 psia), 32 km (20 mi)	12.4 MPa (1800 psia), 48 km (30 mi)	12.4 MPa (1800 psia), 64 km (40 mi)
Capital Costs, 10^6 (1/1/80)										
NSS	114.1	114.1	114.1	114.1	114.1	114.1	114.1	114.1	114.1	114.1
BOP	249.9	249.9	249.9	249.9	249.9	230.9	230.9	230.9	230.9	230.9
Pipeline[a]	—	55.2	133.6	225.2	327.4	-	217.9	559.9	974.9	1446.4
Indirects	144.8	144.8	144.8	144.8	144.8	142.0	142.0	142.0	142.0	142.0
Contingency	76.3	84.6	96.4	110.1	125.4	73.1	105.7	157.0	219.3	240.0
Total	585.1	648.6	738.8	844.1	961.6	560.1	810.6	1203.9	1618.2	223.4
Annual Costs, 10^6										
Fixed charges	59.7	66.2	76.0	86.1	98.0	57.1	82.7	122.0	171.5	226.8
Fuel costs (LEU/Th)	30.0	30.0	30.0	30.0	30.0	30.0	30.0	30.0	30.0	30.0
O&M costs	25.0	25.0	25.0	25.0	25.0	25.0	25.0	25.0	25.0	25.0
Credit for electric power	(31.0)	(31.0)	(31.0)	(31.0)	(31.0)	(31.0)	(31.0)	(31.0)	(31.0)	(31.0)
Total annual costs	83.7	90.2	100.0	110.1	122.0	99.1	124.7	164.0	213.5	268.8
Steam power to process, 10^6 Btu/hr	3509	3483	3457	3421	3385	3745	3709	3976	3632	3592
Energy costs, $GJ ($/10^6 Btu delivered)	3.68 (3.89)	4.0 (4.22)	4.44 (4.69)	4.97 (5.25)	5.57 (5.88)	4.09 (4.32)	5.19 (5.48)	6.89 (7.27)	9.09 (9.59)	11.56 (12.20)

[a]Pipeline costs scaled from 32-km (20-mi) distance estimate, GA zigzag design.

TABLE 5-23
HTGR-SETS ENERGY COST VERSUS DISTANCE TRENDS

	4.48 MPa (650 psia), 0 km (0 mi)	4.48 MPa (650 psia), 16 km (10 mi)	4.48 MPa (650 psia), 32 km (20 mi)	4.48 MPa (650 psia), 48 km (30 mi)	4.48 MPa (650 psia), 64 km (40 mi)	12.4 MPa (1800 psia), 0 km (0 mi)	12.4 MPa (1800 psia), 16 km (10 mi)	12.4 MPa (1800 psia), 32 km (20 mi)	12.4 MPa (1800 psia), 48 km (30 mi)	12.4 MPa (1800 psia), 64 km (40 mi)
Capital Costs, 10^6 (1/1/80)										
NSS	148.0	148.0	148.0	148.0	148.0	148.0	148.0	148.0	148.0	148.0
BOP	304.9	304.9	304.9	304.9	304.9	298.5	298.5	298.5	298.5	298.5
Pipeline[a]	-	107.7	215.3	323.0	430.6	-	107.7	215.3	323.0	430.6
Indirects	153.3	153.3	153.3	153.3	153.3	151.1	151.1	151.1	151.1	151.1
Contingency	90.9	107.1	123.2	139.4	155.5	89.6	105.8	121.9	138.1	154.2
Total	697.1	821.0	944.7	1068.6	1192.3	687.2	811.1	934.8	1058.7	1182.4
Annual Costs, 10^6										
Fixed charges	71.1	83.7	96.0	109.0	121.6	70.1	82.7	95.0	108.0	120.6
Fuel costs (LEU/Th)	30.0	30.0	30.0	30.0	30.0	30.0	30.0	30.0	30.0	30.0
O&M costs	25.0	25.0	25.0	25.0	25.0	25.0	25.0	25.0	25.0	25.0
Credit for electric power	(12.0)	(12.0)	(12.0)	(12.0)	(12.0)	-	-	-	-	-
Total annual costs	114.1	126.7	139.0	152.0	164.6	125.1	137.7	150.0	163.0	175.6
Steam power to process (10^6 Btu/hr)	3536	3536	3536	3536	3536	3280	3280	3280	3280	3280
Energy costs ($/GJ ($10^6$ Btu delivered)	4.98 (5.26)	5.29 (5.85)	6.07 (6.41)	6.64 (7.01)	7.19 (7.59)	5.89 (6.22)	6.49 (6.85)	7.07 (7.46)	7.69 (8.11)	8.27 (8.37)

[a]Pipeline costs scaled from 32-km (20-mi) distance estimate, GA zigzag design.

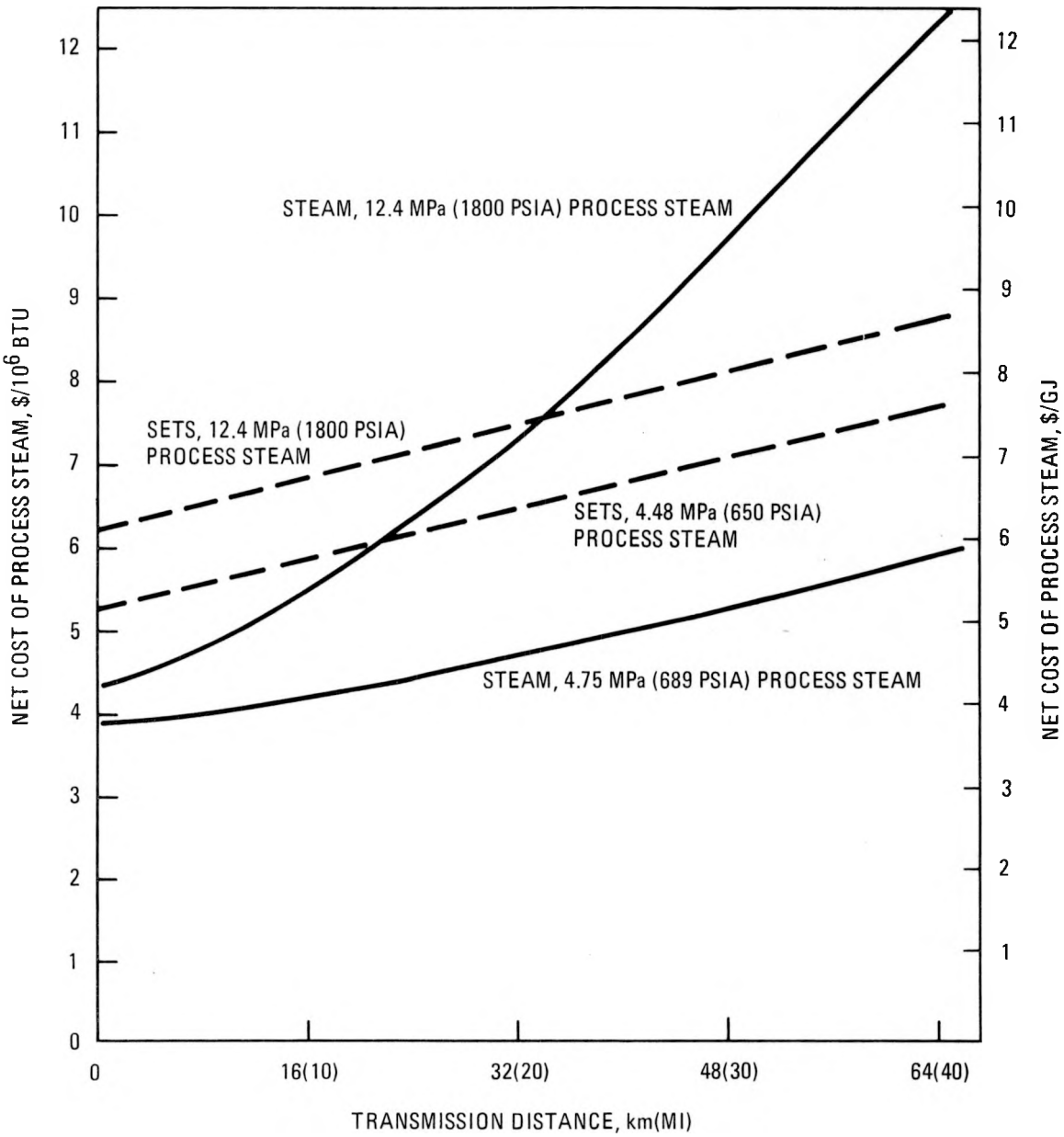

Fig. 5-28. Energy cost versus distance trends

potential for cogenerating electric power. Additional studies are needed to further optimize transmission system design and costs and to establish economics for both reactor types as functions of process heat conditions and transmission distances. Comparisons with the chemical heat pipe system should also be included.

The zigzag design for flexibility of the higher-temperature transmission piping developed during this review should be further studied. The design used for the bases considered here is not optimized, either for geometry of the bends or for pipe size versus pressure drop/pumping power economics. This arrangement appears to offer a very marked improvement over the U-bend or other designs commonly used and should be considered for further steam and SETS transmission piping studies and for other high-temperature piping applications where the geometry is suitable, such as in the HTGR-PH secondary helium system piping.

5.3.2.5. Demographic Evaluation. Four potential sites near Port Arthur have been surveyed using the SECPOP code (Ref. 5-10) for compliance with the population density criteria for Regulatory Guide 4-7 and the March 1981 NRC staff recommendations. (The SECPOP code determines the population in 22-1/2 degree sectors about a specified location from census input data.)

The table below contains the population density criteria that have been used for the demographic study of the Port Arthur sites. These criteria are taken from Regulatory Guide 4.7 and from the March 1981 staff recommendation.

NRC Guideline	Annular Distance [km/(mi)]	Maximum Density [persons/km^2 (mi^2)]
Regulatory Guide 4.7 (Ref. 5-11)	EAB-30	1295 (500)
March 1981 recommendation	EAB-2	647 (250) [1295 (500) in Northeast*]
(Ref. 5-12)	2-30	1295 (500) [1942 (750) in Northeast*]
	{No restriction beyond 25 km (20 mi) for plant size smaller than 900 MW(e) [600 MW(e)].}	

*Northeast: north of 39th parallel and east of 90th meridian.

These criteria have been applied to the results of SECPOP (Ref. 5-10) computer runs for locations at the Gulf Oil site, the Texaco site, the Big Hill Dome site, and the Bridge City site.

Results and Discussion

The following sites have been surveyed using the above population density criteria and the SECPOP code.

Site	Location Number	Latitude (North)	Longitude	Passed Criteria
Gulf Oil	1	29°49'50"	93°58'27"	Yes
	2	29°49'32"	93°58'29"	Yes
Texaco	3	29°52'35"	93°59'13"	No
	4	29°52'19"	93°59' 0"	No
Big Hill Dome	5	29°44'28"	94°15'39"	Yes
	6	29°45'47"	94°16'22"	Yes
Bridge City	7	30° 1'47"	93°52'52"	Yes
	8	30° 2'30"	93°53'39"	No

The consensus data input to the SECPOP code was from the 1970 census. In addition, for the Gulf site at location 1, preliminary 1980 census data for Jefferson County were used along with the estimated transient population. Again location 1 passed both criteria.

It is concluded that the Gulf Oil site (location 1) is acceptable for reactor siting based on population density criteria, and that possible alternative sites have been identified at Big Hill Dome to the west and near the Gulf States Utilities plant near Bridge City to the east.

External Explosion Hazard

A preliminary study was performed to characterize the hazards from external explosions at the Gulf Oil site near Port Arthur.

Additional information was formulated and requested to initiate the Port Arthur site location of the nuclear plant. As information became available, a cursory survey was made of the nearby [i.e., 8 km (5-mi) radius] industrial and transportation facilities.

Since the pipeline releases that are heavier than air pose the most severe hazard to the operability of NSR installations, the engulfment of those installations by combustible clouds was considered. Finally, a more detailed study was made in which several specific conditions of external explosion were studied for the various source types such as tank farms, tankers, trucks, and pipelines.

The cursory survey of the industrial and transportation facilities within the 8-km (5-mi) radius circle, centered at the nuclear plant site, indicated the potential sources for external explosions. Tanker and truck sources can be shown to produce explosions whose blasts do not exceed the 108-kPa (1-psig) peak pressure established by Regulatory Guide 1.91 for the NSR structures. Gasoline tank explosions containing a stoichiometric mixture of gasoline and air are also unable to produce shock waves exceeding 108 kPa (1 psig) at the reactor site. As far as pipeline leaks are concerned, the crude pipelines pose no hazards. The natural gas pipelines are able, under very restrictive cases (specific releases, explosion while en route, etc.), to produce impinging blasts exceeding a few psig at the reactor site as a consequence of detonation of accidental releases.

The analysis of releases from the pipelines for products is more involved. These releases are heavier than air and consequently more hazardous, since they move attached to the ground and hence have a potential for engulfing NSR structures. Moreover, due to the absence of lift, these releases may be treated as instantaneous or continuous, depending on the comparison between the release and transit (or travel) times. Further, contrary to the Waterford Plant FSAR, there is no design basis accident based on maximum releases and maximum amount of explosive material in the traveling cloud. The largest pressure or impulse on the NSR structure does not necessarily correspond to those maxima (e.g., Section 7 of Ref. 5-12), because the relative location between the exploding cloud and the reactor site is another parameter to be accounted for. Thus, explosions of small clouds in contact with NSR structures (i.e., impinging detonation waves) are more dangerous than distant explosions of large clouds (i.e., well-attenuated shock waves). Additional studies using PRA are planned to address the above-mentioned concerns to quantify the external hazards from pipelines carrying heavier-than-air combustible products.

The results obtained correspond to realistic, rather than probabilistic, calculations about the incident peak pressure on NSR installations as a consequence of external explosions following the release of combustible fluids.

Results of this analysis are summarized below:

1. Tanker Explosion. Explosion of a very large tanker containing a stoichiometric mixture [119,175 m^3 (750,000 BBL)] produces an impinging pressure for the blast, at the reactor site, below 108 (1 psig), satisfying Regulatory Guide 1.91.

2. Truck Explosion. Explosion of the total capacity of propane in a truck [(39.75 m^3 (10,000 gal)] produces an incident peak pressure blast at the reactor site below 108 kPa (1 psig), satisfying Regulatory Guide 1.91.

3. Tank Explosion. Explosion of a gasoline tank containing a stoichiometric mixture with air produces a blast with an incident peak pressure at the reactor site below 108 kPa (1 psig), satisfying Regulatory Guide 1.92.

4. Pipelines. The three types of pipelines in the vicinity of the nuclear plant site are the following:

   a. Crude. Too-distant and less-volatile fluid to be considered in comparison with other pipelines.

   b. Natural Gas. Since natural gas (essentially methane) is considered lighter than air, buoyant releases are produced as a consequence of pipeline leaks and the releases are not able to engulf NSR structures. Maximum (i.e., normally) reflected peak pressures due to detonation, while traveling, of natural gas releases do not exceed a few psig.

   c. Products. These fluids are heavier than air. Their releases are therefore able to engulf NSR structures, since they move attached to the ground. It can be concluded that during weather conditions for stability classes A, B, and C the accidentally released combustible clouds cannot engulf the NSR structures, but that they can possibly do so during stability class D. Consequently, detonation waves may impinge the NSR structures during stability classes E and F, and possibly D.

      The effect of distant detonations (i.e., blast) must still be investigated, but additional data to quantify the release range is still lacking.

The results appear to be conclusive for tankers, trucks, and tank releases and even for pipelines containing crude.

Potential explosions from natural gas releases from pipelines can never exceed a few psig on the reactor site and are of low probability (explosions while en route).

Potential explosions from accidental releases of pipelines carrying products must be analyzed using PRA in combination with additional results for the impact of blasts.

5.4. INTEGRATION OF AN HTGR INTO AN SRC-II COAL LIQUEFACTION PROCESS APPLICATION

5.4.1. Scope

The scope of this work was to investigate the technical and economic feasibility of using the HTGR-SC/C and HTGR-PH plant heat source to replace fossil energy in a SRC-II coal liquefaction process refinery.

5.4.2. Discussion

The studies performed by GA together with the Scientific Design Company during 1980-81 on using the HTGR as the primary heat source to replace fossil energy within a Solvent Refined Coal (SRC-II) liquefaction process plant were completed, and their results were reported in Refs. 5-4 and 5-5. These studies show that nuclear energy can replace essentially all fossil energy, increasing the yield of the process plant by the amount of oil equivalent to the nuclear reactor power used.

The HTGR-SC/C concept offers a more economic source of energy than coal gasification or an HTGR-PH system based on any foreseeable coal price. If coal prices reach \$4.20/GJ (\$4.34/10^6 Btu) or above, the HTGR-PH is shown to be a more economic energy source than coal.

Based on a constant coal refinery feed of 352 kg/s (33,500 TSD), with the HTGR-SC/C the refinery product is increased by 8% and with the HTGR-PH by 13% above the conventional coal-fed process used in this study. Product

cost using the HTGR-SC/C is ~14% lower than for the coal process, while the HTGR-PH product cost is ~5% higher.

It is also shown that the capital cost for the HTGR-SC/C integrated into the process system is ~15% higher than for the standard coal system studied. The HTGR-PH integrated capital cost is shown to be ~107% higher than for the coal system.

The use of an HTGR as a heat source increases the product per unit of coal consumed by 29% and extends the available coal resource significantly. In addition, because fossil fuels are reduced or eliminated, the release of carbon dioxide to the environment is reduced by a factor of 5; nitrogen oxides, carbon monoxide, and nonmethane hydrocarbons are almost completely eliminated, and total suspended particulates are reduced by ~36%.

The SRC-II liquefaction process, which liquefies coal by hydrogenating it to a liquid product in a solvent carrier, was used as the basic process for these application studies because of its viability as a leading synfuel process and the availability of relevant data.

The SRC-II coal liquefaction process has been modified in this study by the addition of a plant to produce transportation fuels from the normal SRC-II product. This integrated plant is identified as a coal refinery because its products are analogous to those produced by an oil refinery. The products obtained from the plant are motor gasoline, jet fuel, liquefied petroleum gas (LPG), butanes, substitute natural gas, and in one case synthesis gas. By-products from the refinery are sulphur and ammonia.

The coal refinery requires considerable steam and electric power consistent with that offered by the HTGR.

The studies reported in Refs. 5-4 and 5-5 included evaluation of single HTGR-SC/C or HTGR-PH units integrated into the 352-kg/s (33,500-TPSD) SRC-II refinery.

An HTGR-PH can produce 0.65 m^3 of oil per Mg of coal (3.7 barrels of product per ton of coal); a coal-fired plant produces 0.50 m^3 of oil per Mg of coal (2.8 BBL/T of coal). This means that the nuclear-based process provides 30% more oil from a given amount of coal than the coal-fired plant.

The capital costs of the HTGR-PH are such that a penalty exists for electricity production under the current economic ground rules. That is, the selling price for excess electricity is not sufficient to pay for that portion of the plant devoted to its production. Options open to improve this condition include (1) obtaining a price for salable electricity high enough to have zero effect on the cost of the refinery product, or (2) adjusting the size of the nuclear or fossil portion of the plant so that there is no excess electric power for sale.

The use of an HTGR-PH increases the amount of nuclear heat used by the process 41% over that delivered by an HTGR-SC/C. However, the HTGR-PH does not have an economic advantage over HTGR-SC/C or a coal-based plant with the SRC-II process adaptation chosen for study.

Under the ground rules established for this study, the modular HTGR sizes used were such that the production of by-product electricity accounted for 23% to 28% of the reactor power. Using these ground rules, the price obtained for the by-product electricity was insufficient to pay for the added investment required to produce the by-product electricity. In the case of multiple reactor installations, this added investment is not counterbalanced by an expected increase in availability.

Because of the lack of current data on the potential advantages of improved availability using multiple HTGR-SC/C and HTGR-PH heat sources, it is recommended that additional studies be made in this area. It is also recommended that the HTGR-SETS plant concept with heat storage be included in these availability studies. In addition, it is proposed that studies be performed to consider the process modes to reduce the capital cost and improve the economics of the refinery when integrated with an HTGR-PH plant.

REFERENCES

5-1. "HTGR Applications Program, Semiannual Report for the period April 1, 1981 through September 30, 1981," DOE Report GA-A16538, General Atomic Company, to be published.

5-2. Jones, J. B., Jr., "Technical Evaluation of the Paraho Process," Paraho Development Corporation, Grand Junction, Colorado, paper presented at the 11th Israel Conference on Mechanical Engineering Technion, Haifa, Israel, July 11-12, 1977.

5-3. Synthetic Fuels Data Handbook, 2nd ed., Cameron Engineers, Inc., Denver, Colorado, 1978.

5-4. Beskind, M. M., B. M. Doshi, and B. Juran, "Process Heat Applications of a High Temperature Gas-Cooled Nuclear Reactor," Scientific Design Company, November 1980.

5-5. Beskind, M. M., "Integration of a HTGR-SC/C in a SRC-II Refinery," Scientific Design Company, July 1981.

5-6. "Paraho Retorting of Oil Shale Using a Very High Temperature Reactor," Davy McKee Engineers & Constructors.

5-7. "Considerations for Retorting Oil Shales with Superheated Water Vapor," V. Dean Allred, Marathon Oil Company, Denver Research Center, Littleton, Colorado.

5-8. Heat Transfer Research Institute Computer Program RKH-1, March 1974.

5-9. Fraase, A. P., and M. N. Ozisik, Heat Exchanger Design, John Wiley & Sons, New York, 1965.

5-10. Environmental Protection Agency, Office of Radiation Programs version of U.S. Department of Commerce, Office of Telecommunications code described in Technical Memorandum 73-146.

5-11. "General Site Suitability Criteria for Nuclear Power Stations," Regulatory Guide 4.7, Rev. 1, U.S. Nuclear Regulatory Commission Office of Standards Development, Washington, D.C., November 1975.

5-12. Higgins, Patrick C., letter to Steering Group, Committee on Reactor Licensing and Safety, May 15, 1981.